AD

USAAVLABS TECHNICAL REPORT 66-77

COMPARISON OF THEORETICAL AND EXPERIMENTAL MODEL ROTOR BLADE VIBRATORY SHEAR FORCES

By

Lawrence J. Bain

October 1967

U. S. ARMY AVIATION MATERIEL LABORATORIES
FORT EUSTIS, VIRGINIA

CONTRACT DA 44-177,AMC-136(T)
UNITED AIRCRAFT CORPORATION
SIKORSKY AIRCRAFT DIVISION
STRATFORD, CONNECTICUT

Disclaimers

The findings in this report are not to be construed as an official Department of the Army position unless so designated by other authorized documents.

When Government drawings, specifications, or other data are used for any purpose other than in connection with a definitely related Government procurement operation, the United States Government thereby incurs no responsibility nor any obligation whatsoever; and the fact that the Government may have formulated, furnished, or in any way supplied the said drawings, specifications, or other data is not to be regarded by implication or otherwise as in any manner licensing the holder or any other person or corporation, or conveying any rights or permission, to manufacture, use, or sell any patented invention that may in any way be related thereto.

Disposition Instructions

Destroy this report when no longer needed. Do not return it to originator.

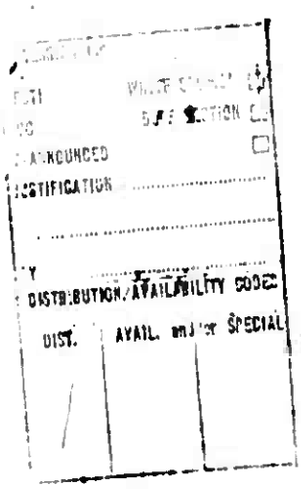

DEPARTMENT OF THE ARMY
U. S. ARMY AVIATION MATERIEL LABORATORIES
FORT EUSTIS, VIRGINIA 23604

This report has been reviewed by tbe U. S. Army Aviation Materiel Laboratories and is considered to be technicelly sound. It ie publisbed for the dissemination and application of the information conteined herein.

Task 1D121401A14203

Contract DA 44-177-AMC-136(T)

USAAVLABS Technical Report 66-77

October 1967

COMPARISON OF THEORETICAL AND EXPERIMENTAL MODEL ROTOR BLADE VIBRATORY SHEAR FORCES

SER-50419

by

Lawrence J. Bain

Prepared by

United Aircraft Corporation
Sikorsky Aircraft Division
Stratford, Connecticut

for

U. S. ARMY AVIATION MATERIEL LABORATORIES
FORT EUSTIS, VIRGINIA

SUMMARY

An investigation was undertaken to obtain quantitative measurements of the vibratory forcing functions from the blades of rotary wing aircraft in the flight speed range encompassing both pure and compound helicopter operation. These measurements were made using dynamically scaled model rotor blades mounted on a specially instrumented rotor head. Testing was accomplished in the United Aircraft Corporation's 18 foot subsonic wind tunnel within a range of equivalent forward speeds from 75 to 300 knots and within a range of full scale rotor lifts from zero to 40,000 pounds. In addition to rotor performance, the final data include ten harmonics of the orthogonal blade root shear forces, rotor blade bending moments, and rotor control loads.

It was concluded from the experimental work that:

1) High harmonics of vibratory shear forces can be measured at the blade root over a wide range of speeds and lifts.
2) Only the first harmonic of flatwise and edgewise shear force is significantly effected by the flapping trim condition of the rotor.
3) Elimination of lag damping may increase or decrease the edgewise shear force, depending on its proximity of the operating condition to a blade natural frequency.
4) Increasing forward speed causes an increase in both flatwise and edgewise shear forces, the latter becoming predominant at the highest forward speeds.
5) Increasing rotor lift at constant forward speed causes a gradual increase in the magnitude of the flatwise shear force harmonics.
6) The radial shear force first harmonic longitudinal component takes on values which can be significant, but the fundamental nature of this force is not well defined.

The experimental results were correlated at seven test points with a fully coupled aeroelastic analysis. The evaluation of this work led to the following conclusions:

1) The inclusion of wake-induced velocity effects in the theoretical method shifts the calculated flatwise shear forces in a direction which improves the correlation but has no significant effect on the calculated edgewise shear forces.
2) The overall degree of correlation is strongly influenced by the accuracy to which the blade natural frequencies are known, the continuity of the calculated induced velocity distribution, and the predictability of the edgewise rotor blade behavior.

FOREWORD

This program was sponsored by the U. S. Army Aviation Materiel Laboratories (formerly U. S. Army Transportation Research Command) Fort Eustis, Virginia, and was monitored by Mr. Joseph McGarvey.

The experimental and theoretical research program was carried out from May 1964 through November 1965. Assisting in this program was Mr. P. J. Arcidiacono of the United Aircraft Corporation Research Laboratories, who directed the development of the rotor head and the impedance analysis.

CONTENTS

ILLUSTRATIONS

SYMBOLS

Dimensional		Unit
A_{1s}	lateral cyclic pitch	degrees
B_{1s}	longitudinal cyclic pitch	degrees
c	blade chord	feet
D	rotor drag	pounds
L	rotor lift	pounds
Q	rotor torque	foot-pounds
r	radial distance to local blade station	feet
R	rotor radius	feet
V	forward speed	feet per second
V_k	forward speed	knots
α_s	shaft angle of attack	degrees
α	rotor angle of attack, $\alpha_s - B_{1s}$	degrees
θ	collective pitch	degrees
ρ	mass density of air	slugs per cubic foot
ψ	azimuth angle, measured from downwind position in direction of rotation	degrees
Ω	rotor angular velocity	radians per second

SYMBOLS

(continued)

Nondimensional

b	number of blades
C_D/σ	rotor drag coefficient-solidity ratio, $D/\pi R^2\rho(\Omega R)^2\sigma = D/R^3\rho\Omega^2 bc$
C_L/σ	rotor lift coefficient-solidity ratio, $L/\pi R^2\rho(\Omega R)^2\sigma = L/R^3\rho\Omega^2 bc$
C_Q/σ	rotor torque coefficient-solidity ratio, $Q/\pi R^2\rho(\Omega R)^2 R\sigma$
$M_{(x, \psi)}$	Mach number at radius station x and azimuth position ψ .
x	radius station, r/R
μ	advance ratio, $V/\Omega R$
σ	rotor solidity, $bc/\pi R$

Note: All Fourier series coefficients for shear forces and rotor blade flapping and lagging motions are based on the assumption of a positive series; i.e.,

$$f(t) = AO + A1\cos\Omega t + A\,2\cos 2\Omega t + - - - + AN\cos N\Omega t + - - -$$
$$+ B1\sin\Omega t + B\,2\sin 2\Omega t + - - - + BN\sin N\Omega t + - - -$$

where AN = Nth harmonic cosine coefficient

BN = Nth harmonic sine coefficient

N = harmonic order

INTRODUCTION

As continual improvements have been made in the performance characteristics of rotary wing aircraft, attention to the problems of vibratory loading and associated structural fatigue has increased. The achievement of low fuselage vibration levels and subsequent improvement in aircraft component life and crew efficiency requires, however, a detailed knowledge of the origin of the forces which excite the fuselage. Prior to the start of this investigation, the cause-effect relationship between vibratory loading and fuselage response was not well defined. Previous studies, such as Reference 1, have presented rotor blade vibratory airloads and stresses, and successful attempts have been made to measure vibratory loads by instrumenting the rotor shaft, as in Reference 2. None of these studies, however, have reached the source of fuselage forced response; that is, the vibratory forces fed into the fuselage from the rotor blades at the blade root.

It was not considered feasible to design and fabricate a rotor head which could be instrumented to measure these vibratory forces until two conflicting objectives were resolved. First, maximum sensitivity had to be achieved so that higher harmonics of the loads could be accurately measured; second, the stress in the structural components of such a rotor head had to be minimized to reduce the probability of failure. The development of the semiconductor strain gage effectively closed the gap between these two objectives, thus making possible a detailed investigation of rotor blade vibratory root shear forces.

The purpose of the present investigation was to obtain quantitative measurements of the vibratory forcing functions from blades of rotary wing aircraft within the flight speed range encompassing both pure and compound helicopter operations. In addition, the degree of correlation between experimental results and theoretical calculations, including the effects of wake-induced velocities, was to be determined. The experimental data were to be obtained from wind tunnel tests of dynamically scaled model rotor blades mounted on a specially designed rotor head instrumented to measure flatwise, edgewise, and radial vibratory root shear forces.

The objective of this report is to present the experimentally obtained data and to place these data into a meaningful context by discussing, with specific examples, the effects of forward speed, rotor loading, lag damping, and flapping trim condition. The experimental results are correlated with a theory developed at Sikorsky Aircraft, described in Reference 3.

DESIGN DATA AND DESCRIPTION OF EQUIPMENT

ROTOR HEAD

The model rotor head was designed to utilize semiconductor strain gages having a gage factor of approximately 100. The structural components of the head, namely, the upper and lower plates, are 7075-T6 aluminum alloy. A fail-safe mechanism with a safety factor of 20 was provided to prevent major damage in the event of failure in the instrumented section. Figure 1 (a) shows the basic rotor head with the installed semiconductor strain gages, and Figure 1 (b) shows the assembly of the head. The pitch control horns are adaptable to pitch-flap coupling ratios of zero and unity, but the present investigation was conducted entirely in the $\delta_3=0$ configuration. Figure 2 is a schematic diagram showing the force and moment conventions and the location of the strain gages.

CALIBRATION

The model rotor head instrumentation was statically calibrated to determine primary slopes, interaction constants, and temperature compensation factors. In the course of this work it was found that to obtain a satisfactory calibration matrix, it was necessary to include measurements of the tangential moment on the instrumented section caused by the lag damper reaction and the edgewise shear force. The resolution of the shear force measurements based on the static calibrations and the noise level of the data acquisition system was determined to be:

Flatwise ± 0.17 pound

Edgewise ± 0.12 pound

Radial ± 0.05 pound

The repeatability of the shear forces determined during the wind tunnel testing and the magnitude of the calibration matrix elements resulted in a final shear force accuracy of ± 0.2 pound in all three directions. The flatwise and edgewise shear force strain gage circuits were each composed of two active and two dummy gages wired to measure the total shear force and to cancel bending in the instrumented section caused by the shear force. The radial shear force circuit was composed of four active gages in the Poisson arrangement. This circuit also measured the total shear force and cancelled bending. The tangential moment circuit was composed

of two active and two dummy gages to measure the bending moment on the upper instrumented section. All of the dummy gages were mounted on the unstressed center section of the upper plate.

ROTOR BLADES

The model rotor blades were untwisted, 9-foot diameter, 2.69-inch chord with an NACA 0012 airfoil section, and were dynamically scaled in flatwise, edgewise, and torsional stiffness properties from the Sikorsky S-56 (CH-37) main rotor blades.* With the specially instrumented, four-bladed rotor head, the rotor solidity is 0.0634. Figure 3 shows the components of a model blade and a fully assembled blade. The model spar was built up of laminations of fiber glass and paper. Trailing edge pockets were composed of balsa wood ribs covered with magnesium and were bonded to the spar. Figure 4 shows the blade spanwise mass and stiffness distributions, and Figure 5 shows the flatwise, edgewise, and torsional natural frequencies of the blade as functions of rotor speed.

The development of the fiber glass model blades evolved from dynamically scaled model rotor blades made of aluminum, used in studies such as Reference 4. These metal blades were designed to operate at full scale tip speeds, but the investigation of rotor behavior at high forward speeds necessitated the development of blades which would retain their dynamic similarity while operating at reduced tip speeds. The reduced speeds resulted from the desire to simulate forward speeds higher than the wind tunnel limit of 175 knots. Reference 5 describes the development of this type of blade using reduced-stiffness spars of fiber glass-paper laminate construction. The various scaling ratios, listed in Table III, are taken from reference 5. The stiffness of the composite spars is scaled in the flatwise, edgewise, and torsional directions from full scale values. The resulting stiffnesses are reduced from those of the aluminum model blades by a factor of 5.5, so that the reduced experimental velocities are $1/\sqrt{5.5}$ times the full scale velocities. For example, at an actual tunnel speed of 100 knots, the fiber glass rotor blades are dynamically similar to the full scale blades operating at $100\sqrt{5.5}$ or 235 knots, and this speed is referred to as the equivalent forward speed.

---

* The full scale S-56 main rotor blades are twisted -8 degrees

WIND TUNNEL

Testing was conducted in the United Aircraft Corporation's large subsonic wind tunnel. This is an atmospheric-density, closed-return tunnel powered by a 9000-horsepower motor and having a maximum speed of approximately 175 knots. The test section is octagonal in cross section, 18 feet across the opposite flats. Remotely controlled air exchangers are employed to maintain constant stagnation temperature during operation. Figure 6 is an artist's drawing depicting the general arrangement of the tunnel.

HELICOPTER ROTOR TEST RIG

The helicopter rotor test rig (HRTR) is equipped with a six-component strain gaged balance and is powered by a variable frequency electric motor rated at 375 horsepower at 6000 rpm. Figure 7 (a) shows an overall view of the HRTR mounted in the wind tunnel, and Figure 7 (b) shows the details of the hub and swash plate area. The coincident flapping and lagging hinges are located at the 5.6 percent radius station. Lagging motion is restrained by rotary viscous dampers having a nominal damping factor of 1.9 foot-pound-second for a lag motion amplitude of 1 degree. This value represents 55 percent critical damping. The model dampers have an adjustable damping feature which permits the selection of any desired damping factor within a moderate range determined by the working fluid in the damper. The dampers were set to the above value by calibrating them in a special calibration fixture which operates the damper at a specified frequency and amplitude and records the resulting torque output. The damper was adjusted in small increments until the proper combination of frequency, amplitude and torque was reached. There was a small phase difference between the application of the force to the damper and the minimum force output indicating the presence of spring force in the damper. This was taken into account in the calibration so the value stated above represents the pure damping output. Rotary transformers are used to sense flapping and lagging motion. A conventional swash plate is driven by three precision electric actuators. Collective and cyclic pitch are remotely set from a servo system in the wind tunnel control room, and the yaw table of the wind tunnel provides variation in shaft angle of attack.

The HRTR drive motor is supported by frictionless hydrostatic oil bearings. The motor case is restrained from rotation by a strain gage torque beam to measure rotor torque. Axial displacement of the motor-shaft system is limited by a strain gage thrust beam. The rotor head is supported by a four-component strain gage balance which was not used in

this test program, as this balance is sized for larger forces than were anticipated for this test. Electric signals are transmitted from the rotating system to the stationary system through a 100-channel slip ring assembly.

Dynamic data from the rotor test rig are recorded on a 20-channel EPSCO data acquisition system. Each channel is scanned 36 times per revolution for six revolutions. The information is received from the HRTR in analog form, digitized, and recorded on magnetic tape. These data are transmitted to an IBM 7094 data processing unit and reduced. The primary data reduction program reduces the performance data to dimensional and coefficient form in the wind and shaft axes systems. Tare forces and moments on the rotor hub, obtained with the blades removed, are subtracted from the measured data, so that the reduced performance data correspond to that from the rotor blades alone. Blade motions and bending moment data are reduced to average and peak-to-peak values. The secondary data reduction program performs a harmonic analysis on all 20 channels of information. The measured shear force and tangential moment data are further reduced to correct for calibration interactions and blades-off tares, and finally these data are corrected for the effects of hub flexibility, as discussed in the section on experimental procedures.

THEORETICAL METHOD

The theoretical method of Reference 3 was used to correlate the experimental data obtained in this program. This method is a fully coupled flatwise, edgewise, torsional aeroelastic analysis based on an extension of Myklestad's method for rotating beams. A variable inflow analysis, developed by the Cornell Aeronautical Laboratory, Inc. (CAL) and described in Reference 6, was combined with the blade aeroelastic analysis. The analytical procedure included an initial determination of flatwise and torsional rotor blade motion with a uniform inflow iteration to obtain required values of rotor lift and propulsive force. This information was used in the CAL analysis to obtain a distribution of induced velocity at ten radial blade stations and twenty-four azimuth locations. With this distribution, using the first flatwise shear force harmonic as a boundary condition, a second iteration was made on the rotor lift and propulsive force, which gave final values of blade motions and loadings.

SIGN CONVENTIONS

The sign convention used is that a positive sign indicates:

Measurement	Direction
Flatwise Shear Force	Upward
Edgewise Shear Force	In direction of rotor rotation
Radial Shear Force	Radially outward from rotor ℄
Flatwise Bending Moment	Upper surface in compression
Edgewise Bending Moment	Trailing edge in compression
Torsion Moment	Leading edge upward
θ	Leading edge upward
α_s	Rotor Shaft tilted downstream
A_{1_s}	Pitch reduction at ψ = 0 degrees
B_{1_s}	Pitch reduction at ψ = 90 degrees

EXPERIMENTAL PROCEDURE

HELICOPTER ROTOR TEST RIG IMPEDANCE

Since it is desirable to have vibratory shear force results which are independent of the particular rotor test rig employed, the measured shear forces must be corrected for the effects of the displacements of the hub, which induce extraneous forces in the instrumented section of the rotor head. These displacements are caused by the shear forces themselves; therefore, the correction factors must be determined from the test data in conjunction with predetermined properties of the rotor test rig.

The analytical background of this procedure is based on the fact that the deflections of the rotor hub can be predicted with a knowledge of the applied forces. Such deflections are determined by dividing the measured shear forces by an experimentally determined rotor hub impedance. The product of this quotient and the rotor blade impedance, determined analytically, yields the force induced on the blade by the hub motion. This force is then subtracted from the measured results to produce the final shear force, reflecting only the effects of the rotor blade loading and no effects of the supporting structure motion. The correction can be written in the form of a matrix equation, as follows:

$$\left\{\text{corrected shear force}\right\} = \left\{\text{measured shear force}\right\} - \left[\begin{matrix}\text{theoretical}\\ \text{blade impedance}\end{matrix}\right] \times \left[\begin{matrix}\text{experimental}\\ \text{HRTR impedance}\end{matrix}\right]^{-1} \times \left\{\begin{matrix}\text{measured}\\ \text{shear force}\end{matrix}\right\}$$

To determine the rotor test rig impedance, a special rotor head was fabricated which matched the weight of the one to be used in the wind tunnel testing. This head was mounted on the HRTR in the wind tunnel, and to it was attached an electromagnetic shaker with appropriate instrumentation to measure forces and displacements. By taking measurements over a range of excitation frequencies in the axial and in-plane directions, the variation of HRTR impedance and principal axes was determined within the range of frequencies to which the rig would be subjected during actual testing. For a rotor with "n" blades, the n^{th} harmonic of the flatwise root shear forces combine to produce an n/rev vertical excitation of the fuselage. The (n + 1) and (n - 1) harmonics of the flatwise root shears combine to form n/rev hub moments resulting in vibratory pitching and rolling moments of the airframe. The (n + 1) and (n - 1) harmonics of the edgewise root shear forces combine to form n/rev longitudinal and lateral in-plane forces at the rotor head. Since the

test rotor was a four-bladed configuration, only the third, fourth, fifth, seventh, eighth, and ninth shear force harmonics affected hub motions. Because in an "n" bladed rotor system only integer multiples of the $n\Omega$ frequency will be seen in the fixed system, the hub motion corrections were confined to the four-per-revolution and eight-per-revolution frequencies. The final test conditions were selected, whenever possible, so that the rotor speeds would correspond to frequencies away from those of low HRTR impedance, in order to minimize the correction factors on the measured data. The corrections of the shear forces based on this analysis were approximately 0.1 pound throughout the test, and the maximum correction was approximately 0.7 pound. It was determined prior to testing that the motion of the HRTR would not alter the rotor blade impedance characteristics by a significant amount, so that these characteristics were reduced to functions of rotor speed only. An example of the HRTR impedance matrix for a rotor speed of 636 rpm is given below.

	upstream direction		advancing blade direction	
	real	imaginary	real	imaginary
4 per rev.	- 1570 lb/in.	- 765 lb/in.	- 7050 lb/in.	- 2420 lb/in.
8 per rev.	- 3750 lb/in.	- 4920 lb/in.	- 4920 lb/in.	- 4750 lb/in.

The impedances in the rotor shaft direction were large enough to be considered infinite in comparison to the impedances shown in the above matrix.

WIND TUNNEL TESTING

The wind tunnel testing procedure was to set a desired rotor tip speed, shaft angle of attack, and tunnel speed and then to record data at each of a series of increasing collective pitch settings. The minimum value of collective pitch was that required for zero thrust; and at each collective pitch, longitudinal and lateral cyclic pitch were adjusted to eliminate first harmonic flapping in respect to the rotor shaft. This cyclic pitch condition was defined as trimmed. For some test conditions, the cyclic pitch values were set to yield longitudinal first harmonic flapping of -4 degrees (forward), while holding the lateral flapping at zero to determine the influence of out-of-trim flapping on the vibratory shear forces. The maximum collective pitch was determined by the limiting vibratory stress amplitude on the rotor head or blades. The tested rotor operating conditions are shown in Figure 8 and Table I. In the remainder of the report these conditions are referred to by the nominal advance ratio values, 0.2, 0.3, 0.4, 0.5, 0.7, and 1.0.

EXPERIMENTAL RESULTS

Table I is a listing of each test point in this program. Shaft and rotor angle of attack, non-dimensionalized thrust and torque, nominal collective pitch, and flapping and lagging motion are listed for each advance ratio. The flapping and lagging motion harmonic amplitudes are printed to three decimal places since the reproduction of the table was done directly from the test data through the data processing unit, but these amplitudes are only accurate to one decimal place or 0.1 degree.

The complete test results are presented in the appendices, and the most significant of these are presented again and discussed in the following section.

The first through tenth harmonic orthogonal components of flatwise and edgewise vibratory shear force obtained in the wind tunnel tests are presented in Appendix I. The flatwise force coefficients are shown as functions of rotor lift coefficient-solidity ratio, and the edgewise force coefficients as functions of rotor torque coefficient-solidity ratio. These data are grouped by advance ratio, each group covering a range of shaft angle of attack.

The first through fourth harmonic orthogonal components of radial shear force are presented in Appendix II. The first harmonic cosine coefficient is shown as a function of rotor angle of attack for constant collective pitch at eack advance ratio. The variation of this coefficient with changes in trim and lag damping is indicated by flagged and double flagged symbols, respectively. None of the other harmonic coefficients of radial shear force reached magnitudes approaching those of the first cosine harmonic, instead, they were approximately one pound or 0.3 percent of the steady radial load. The radial shear force harmonics above the fourth did not exceed the one pound level at any test point and are not presented. The remaining radial shear force coefficients are given as functions of rotor lift coefficient-solidity ratio.

Flatwise rotor blade bending moments were measured at four radial stations on the blade at 21, 33, 47, and 64 percent radius. Throughout the range of test conditions, the flatwise moment at the inboard station, 21 percent radius, was consistently the largest measured moment. This fact is substantiated in the following section of the report. The radial locations of the largest measured edgewise and torsional moments are also verified in that section. Part (a) of the figures in Appendix III gives the one-half peak-to-peak values of the flatwise moment at 0.21R as it varies with rotor angle of attack for constant collective pitch and

advance ratio. A flatwise moment of 21 inch-pounds at this radial station on the blade corresponds to a stress of 10,000 psi on an equivalent rotor blade made of aluminum; i.e., it has the same unit strain. Edgewise bending moments were measured at 21, 33, and 47 percent radial stations on the blade. The location of the maximum measured value varied between the inboard and outboard stations within the range of test conditions. Part (b) of the figures in Appendix III presents the one-half peak-to-peak edgewise moment at the 21 percent station as a function of rotor angle of attack for constant collective pitch and advance ratio. An edgewise moment of 56 inch-pounds at this station on the blade corresponds to 10,000 psi edgewise stress on an equivalent aluminum blade. Part (c) of the same set of figures is a plot of the moments measured in the edgewise direction at the 47 percent radial station, with 29 inch-pounds giving the equivalent of 10,000 psi stress. The rotor blade torsional moment was measured at the 17.5, 38, and 90 percent radial stations. The inboard moment was largest at all test points, and its one-half peak-to-peak value is presented in part (d) of the figures of Appendix III in a manner identical to that of the other blade moments. A 35 inch-pound torsional moment at the 17.5 percent radial station corresponds to 10,000 psi on the equivalent aluminum blade. The change in each of the three blade bending moments resulting from out-of-trim operation is indicated by the flagged symbols on the plots for the advance ratio of 0.2. The change resulting from elimination of lag damping is indicated by double-flagged symbols on the plots for advance ratios 0.2 and 0.5.

Rotor control loads were measured on the push rod for the instrumented blade. The one-half peak-to-peak values of this load are presented in Appendix IV in a form identical to that of the blade bending moments.

EVALUATION OF EXPERIMENTAL RESULTS

OUT-OF-TRIM OPERATION

The effect of out-of-trim operation of the flatwise and edgewise vibratory shear forces can be seen by comparing parts (a) and (b) of Figure 9, which are taken directly from Appendix I. The only force harmonic which is significantly altered by adjusting the first harmonic flapping with respect to the shaft to -4 degrees in the longitudinal direction is the first harmonic, which produces a pitching moment in the fixed system of coordinates. In particular, the amplitude of the first harmonic shear in both the flatwise and edgewise directions takes on a value on the order of double that of trimmed operation. This behavior is what would be expected since a one per revolution forcing function is being introduced in the system. Figure 9 also shows that the phase of the first harmonic shear force becomes less sensitive to changes in rotor lift when the rotor is taken out-of-trim. The effect on the cosine compcnent of the first radial shear force harmonic is not well defined, but the points in Figure 60 of Appendix II indicate that this component is generally increased by operation out-of-trim. The data in Figure 85 of Appendix III reveal that the principal effect of out-of-trim operation on blade bending moments is an increase in the one-half peak-to-peak flatwise moment approximately equivalent tc that resulting from a 2-degree increase in collective pitch or roughly a 7500-pound increase in full-scale rotor lift. However, the edgewise and torsional moments are not significantly altered. It should be noted that because of the flapping and lagging motion of the blades, the blade bending, and the variation of the blade pitch over the rotor disk; the axis system in which the blade bending moments are measured is being continually displaced in both translational and rotational directions with respect to the axis system in which the root shear forces are measured. As a result, there is a large interaction between events occuring in any one direction of the blade axis system and the three directions of the shear force axis system. This effect is seen above where operation out-of-trim caused a change in the edgewise shear force with no significant change in the edgewise blade bending moment.

EFFECT OF LAG DAMPING

The effect of lag damping on the vibratory shear forces and blade moments must be evaluated in light of the proximity of the rotor operating condition to an edgewise blade natural frequency. For this reason two rotor speeds are considered. At the advance ratio of 0.2, the first edgewise bending frequency is very nearly three per revolution, whereas

at the higher advance ratio , 0.5, at which the rotor tip speed is reduced, the first edgewise bending frequency is farther removed from a resonance point, as shown in Figure 5. Comparing parts (a) and (b) of Figure 10, which is taken directly from Appendix 1, it is seen that removal of the lag damping at the condition near the edgewise natural frequency results in an increase in the edgewise shear force harmonics shown, particularly the third; which displays an increase in maximum amplitude of about 25 percent. Removal of lag damping at the other condition results in a decrease in the edgewise shears, as seen by comparing parts (a) and (b) of Figure 11. The third harmonic amplitude decreases 20 percent at C_Q/σ =0.005 for this case. The remaining shear force harmonics for these four test conditions, given in Appendix I, show that the edgewise force harmonics above the fourth behave essentially the same as those shown in Figures 10 and 11 and that the flatwise shear force increases with the removal of lag damping at both rotor speeds. The latter effect results from the increase in flatwise blade bending moments discussed below. The effect of lag damping on the radial shear force is not clearly indicated by the data taken from μ =0.2, but Figure 63 of Appendix II for μ =0.5 shows a definite pattern in which the first cosine harmonic is initially reduced but later reverses as the collective pitch is increased and eventually increases at the higher collective pitches.

The data in Appendix III show that removal of lag damping results in a slight increase in flatwise and torsional blade bending moments at both rotor speeds. This moment increase is largest at the high collective pitch settings and is essentially zero at the low settings. This effect is a result of the fact that, experimentally, more longitudinal cyclic pitch was required to maintain the rotor in a trimmed condition when the lag damping was removed than with full lag damping. It is not clear why this additional cyclic pitch is necessary, but the effect is consistent throughout the test. The edgewise bending moments at the inboard radial station are increased at both rotor speeds by an amount equivalent to a one degree increase in collective pitch or an increase in full scale lift of approximately 4000 pounds. At the outboard station the increment in edgewise moment due to the removal of lag damping is much larger at the higher rotor speed than it is at the lower speed. The increase at the lower speed at this station is of the same order of magnitude as the increases on the inboard station. This is seen in Figure 12, which is a plot of data extracted from Appendix IV. This effect of rotor speed on the edgewise response to changes in lag damping, is related to the effects of the rotor operating condition's being near an edgewise natural frequency, already discussed in connection with the edgewise shear force. It would be expected that the removal or reduction of lag damping at rotor speeds

remote from an edgewise natural frequency would cause a reduction rather than an increase in the edgewise bending moments because the restraining load on the blade root is reduced. For the rotor speed in question, however, Figure 5 shows that the test point is not sufficiently removed from the critical speed to preclude the presence of resonant excitation effects. The trend of reduction in edgewise bending moment and shear force with changes in rotor speed away from the critical value is clear, nevertheless, and for an advance ratio of 0.7, Figure 12 shows edgewise moments which are considerably lower than those measured with full lag damping.

EFFECT OF FORWARD SPEED

Figure 13 shows the effect of forward speed on the flatwise and edgewise shear forces. The amplitudes of the second through tenth harmonic coefficients, derived from the data presented in Appendix I, are presented as functions of advance ratio for a constant rotor lift coefficient - solidity ratio of 0.035 and a shaft angle of attack of -4 degrees with the rotor trimmed to zero flapping with respect to the shaft. The shear force amplitudes are nondimensionalized by the lift per blade to provide an indication of the magnitude of the vibratory loads relative to the steady loading on the rotor. The flatwise vibratory loading shows a general increase with forward speed in all harmonics. In some harmonics, particularly the third and fourth, the increase is very rapid as the advance ratio exceeds 0.5. The same pattern is evident in the edgewise vibratory loading, with the third and fourth harmonics again reaching very large values at $\mu = 0.7$. This flatwise and edgewise shear force response stems directly from the change in the behavior of the rotor blade in the edgewise direction as the forward speed is increased. This change is discussed below. The effect of forward speed on the first cosine harmonic of the radial shear force can be assessed from Figures 60 through 64 in Appendix II. In general, increasing forward speed causes this shear component to change from a nose down pitching moment component to a nose up component. The magnitude of this shear force was not anticipated and the cause of the measured behavior could not be determined without an extensive analytical effort, beyond the scope of the present study.

Figure 14 presents the one-half peak-to-peak blade bending moments as functions of advance ratio. The test points, listed in Table II, included those for $\alpha_s = -4$ degrees for $\mu = 0.2$, 0.4, 0.5, and 0.7, and for $\mu = 0.3$ with $C_L/\sigma = 0.062$. The lift coefficient-solidity ratios are not constant for these five points but decrease with forward speed, as would be the case in compound helicopter operation, from

C_L/σ = 0.071 at μ = 0.2 to C_L/σ = 0.032 at μ = 0.7. The results shown represent a more realistic situation as compared, for instance, to the case with a constant C_L/σ equal to 0.032. The blade moments in all three directions increase with advance ratio. The edgewise and torsional moments are strongly influenced by the forward speed above the 0.5 advance ratio. It is notable that the maximum flatwise bending moment occurs at the inboard radial station throughout the forward speed range as does the maximum torsional moment, while the edgewise moment shifts from the inboard end of the blade to the outboard end as the forward speed is increased. The time histories of these moments can be seen in Figures 18, 21, 22, 23, and 24; and it is evident that the shift of the maximum edgewise bending moment station is a result of the change in the participation of edgewise bending modes. At the low advance ratios the first elastic mode predominates, but as the speed is increased additional modes become significant so the station of maximum bending moment is changed accordingly. It should also be noted that with the flatwise stiffness distribution given in Figure 4, the maximum bending stress tends to occur at the 64 percent radial station, which is in accord with flight measurements.

The time histories of the flatwise, edgewise, and radial shear forces at the same five test points are shown in Figures 15, 16, and 17; from them the change in harmonic content with forward speed can be observed. As the advance ratio is increased from 0.2 to 0.4, the first harmonic predominates in all three directions with some high harmonics of small amplitude appearing in no definite pattern. Above 0.4, all of the forces are predominately fourth harmonic. This effect would cause a change in the fuselage forcing functions from a steady moment at the low speeds to a four per revolution excitation at the high speeds. The cause of this variation of shear force harmonic content can be determined from the points in question shown in Figures 18 through 24, which present the azimuthal plots of blade bending moments at all seven points listed in Table II. The striking feature in these plots is the character of the edgewise bending moment at the high advance ratios. Essentially, it is composed of the fourth harmonic with an amplitude on the outboard station reaching 20 inch-pounds. Since the flatwise bending moment does not exhibit the same character, it can be concluded that at the 0.7 advance ratio the shear forces are primarily influenced by the edgewise blade bending through the mechanism of the displacement of the blade axis system from the shear force axes system.

Looking now at the change in harmonic content of the blade bending moments with forward speed in Figures 18, 21, 22, 23, and 24, the edgewise moment is seen to be essentially third harmonic at the lower

advance ratios as would be expected because of the nearness of the rotor speed to the edgewise natural frequency point. At the higher advance ratios, however, the rotor speed is reduced and moves away from the critical speed, but does not closely approach the four per revolution natural frequency. Therefore, the edgewise behavior at these high advance ratios cannot be categorically attributed to resonant excitation. The list of lag motion harmonics in Table I for the $\mu = 0.7$ data point shows a fourth harmonic amplitude larger than any others but the first, and a comparison in Table I with the lower speed points reveals that the first harmonic lag motion dominates all other harmonics in amplitude. Although the magnitudes being compared are on the borderline of the measuring system accuracy, an aerodynamic source of the high speed edgewise behavior is implied; but this has not been positively determined. It was observed during testing that removal of the lag damping at the high forward speeds resulted in a reduction of the fourth harmonic magnitude and in an increase in the third harmonic magnitude of the edgewise blade response. It should also be noted that the test data at $\mu = 1.0$ show the same effect: a large fourth harmonic with lag damping and a shift toward the third harmonic with reduced lag damping, even though the rotor speed is 15 percent lower at this condition than it is in the $\mu = 0.7$ condition. Investigation of this phenomenon is impeded by the shortage of experimental dynamic data at high forward speeds and by the complexity of the actual lag damper behavior. While the moment output is nominally pure damping linearly related to the velocity, as discussed in the section entitled "Helicopter Rotor Test Rig"; there is some spring content which varies in a complex manner with frequency and amplitude. The exact determination of these characteristics is beyond the scope of the present study. In this program, the structural limitations of the special rotor head precluded extensive data taking at the high advance ratios because of the very large vibratory forces involved. Designing for such large forces would have reduced measuring accuracy at lower values of advance ratio, μ.

The torsional moment in Figures 18 through 21 is essentially first harmonic in character at the low forward speeds, reflecting the cyclic pitch input. At the higher speeds, appearing first at an advance ratio of 0.4, the torsional moment has an increasing content of high harmonics, particularly at the inboard stations. At the two highest advance ratios, 0.5 and 0.7, presented in Figures 23 and 24, the eighth harmonic response can be traced to the proximity of a natural frequency at 580 rpm. The harmonic content of the flatwise bending moments is difficult to visualize because of the effects of high seventh, eighth, ninth, and tenth airload harmonics at all forward speeds. It is apparent, however, from Figures 18 through 24, that the third and fourth harmonics

show a large increase with increasing forward speed relative to the increases that take place in the high harmonics. None of this is attributable to resonant excitation of flatwise modes, but coupling with edgewise blade response undoubtedly contributes to this part of the flatwise response, particularly since both the collective and cyclic pitch settings are high under these conditions; i.e., θ = 12 degrees, B_{1s}=13.7 degrees at μ = 0.7 .

EFFECT OF ROTOR LIFT

Figures 25, 26, and 27 present the time histories of the flatwise, edgewise, and radial shear forces at a constant advance ratio of 0.3 for a range of rotor lift under trimmed conditions. A phase change in the first harmonic is readily apparent in all three components. In addition, the initail reduction and subsequent increase in this harmonic can be seen by comparing the middle load conditions with the high and low conditions. This comparison also reveals that the magnitude of the higher harmonics changes very little over the range of lift. It should be noted that the lowest equivalent forward speed in this program was approximately 75 knots, and due to the variation of wake-induced velocity effects with forward speed the results discussed herein cannot generally be extrapolated to lower speeds.

The correlation between rotor thrust level and vibratory loading is shown in Figure 28. The amplitudes of the flatwise and edgewise shear force harmonics, obtained from Figure 50 of Appendix I, are presented as functions of rotor lift coefficient - solidity ratio at an advance ratio of 0.3 and a shaft angle of attack of -4 degrees. The amplitudes are nondimensionalized by the lift per blade, and data for C_L/σ below 0.04 are not plotted in order to avoid the distortion that takes place as the lift goes to zero. The low flatwise harmonics show an increase as the rotor lift increases. Except for the seventh and tenth, the harmonics above the fourth remain low throughout the range of lift. The rotor speed at this advance ratio, μ = 0.3, yields an operating condition close to the seven per revolution natural frequency of the third flatwise blade bending mode and the ten per revolution natural frequency of the fourth flatwise mode, explaining the departure of the seventh and tenth harmonics from the pattern of the others. Looking at the harmonics of flapping motion for μ = 0.3 and α_s= -4 degrees, it is seen that the amplitudes of second, third, and fourth harmonic flapping increase with rotor lift. It is this effect which produces the increase in the flatwise shear force second, third, and fourth harmonics seen in Figure 28. The correlation between the rotor thrust level and the nondimensional edgewise shear force harmonic amplitudes is similar to that of the flatwise case for the

low harmonics although it is not as marked. The edgewise amplitudes above the fourth harmonic remain low throughout the lift range and do not exhibit even the small increase at the highest lift that was seen in the flatwise harmonic amplitudes.

The vibratory shear forces data presented in Figures 9, 10, 11, 13, 15, 17, and 25 through 28 are taken from only a very small number of the test conditions included in Appendix I. Sufficient information is given in Table I and Appendix I to enable the reader to replot the data of any of the 116 test conditions in any of the forms used herein and to evaluate specific operating conditions in more detail.

CORRELATION OF THEORY AND EXPERIMENT

The experimental data for the seven test points listed in Table II were correlated with the theoretical method of Reference 3.

Figures 29 through 35 present the measured and calculated shear force harmonic amplitudes. In Figures 29, 32, 33, and 35, the results of uniform inflow computations are also shown. In comparing the measured flatwise shear force harmonic amplitudes with the calculated variable inflow values, the second and fifth harmonics show the most consistent difference among the seven subject points. In all cases, except at $\mu = 0.7$, it was found that the fourth and/or fifth harmonic of induced velocity on the inboard segment of the blade, as computed in the variable inflow analysis, was higher than any other harmonics above the second. The effect of this on blade response can also be seen in the calculated flatwise blade bending moments at $\mu = 0.3, 0.4, 0.5$, shown in Figure 36. In the case of a large second harmonic difference, it was found that the calculated rotor wake produced a flatwise loading on the outboard portion of the blade which was essentially composed of a two per revolution load. This resulted in a blade flapping motion in which the primary component was second harmonic. For example, examination of the flapping coefficients given in Table I for the $\mu = 0.5$ point reveals a second harmonic magnitude of 0.8 degrees as opposed to the calculated value of 1.3 degrees.

Looking in particular at the $\mu = 0.2$ case, the flatwise bending moment presented in Figure 37 shows a sharp peak at the 165-degree azimuth in the calculated values that are present, but is greatly attenuated in the measured values. The cause of this peak was traced to the representation of the rotor wake, in which a tip vortex from one blade is passing under the inboard end of the following blade. Since the circulation is assumed to be concentrated at the vortex core, a rapid increase in induced velocity is felt by the blade, and the high peak in bending moment results. In the physical case with a finite vortex core, the increase in induced velocity is more gradual and the blade response is less drastic, as seen from the measured results in Figure 37. It was analytically determined that a peak such as that given by the calculations would cause an increase in the magnitudes of all harmonics, and it is seen that a downward shift of the calculated shear force harmonics in Figure 29 would yield a much better correlation in every harmonic. As the forward speed and rotor lift are increased and the wake is washed away from the rotor, this peaking effect is diminished as the subject vortex passes under the aft part of the rotor.

The remaining significant differences in the measured and calculated flatwise shear forces are in the seventh harmonic at $\mu = 0.2$ and the fourth harmonic at $\mu = 0.7$, as shown in Figures 29 and 35, respectively. The latter difference stems from the fact that the large fourth harmonic edgewise blade bending discussed earlier in conjunction with the measured shear force data is not predicted in the computations, even though the flatwise blade bending moment correlation is not unreasonable, as seen in Figure 37. The magnitude of the computed seventh harmonic at the low speed is a result of a resonant excitation of the third flatwise bending mode of the blade caused by a seventh harmonic-induced velocity component over the inboard blade segments having a value nearly equal to the steady induced velocity.

The flatwise shear force harmonics calculated with the assumption of uniform inflow show a steady decrease in magnitude as the harmonic order is increased. The measured results, however, do not follow this pattern, and it is evident that without the higher harmonic excitation provided by a variation in induced velocities, there is no possibility of accurately predicting the harmonic content of the vibratory shear forces. At the high advance ratio, $\mu = 0.7$, the difference between the uniform and variable inflow results is very small, but the analysis of wake-induced velocities used in this program was not developed for use at high speed. Therefore, the similarity of the two results does not necessarily imply that the effects of wake-induced velocities can be neglected at high speeds. Figure 39a, which shows the measured and calculated flatwise shear forces as functions of azimuth position, verifies that an accurate knowledge of harmonics is the key to vibratory shear force analysis.

Comparison of the measured values of edgewise shear force harmonic coefficients with the calculated variable inflow values, Figures 29 and 32 through 35, reveals a steady decrease in the degree of correlation as forward speed is increased. This is primarily evident in the low harmonics, where the measured values display a magnitude increase not matched by the theoretical values. The agreement of the higher harmonics is better, but only to the extent that both calculated and measured values remain small. It was shown earlier that all the harmonics of edgewise shear force tend to increase with forward speed, but no such trend is evident in the calculations. This absence, then, is the major deficiency in the edgewise shear force analysis. Since the nature of the blade edgewise behavior at the high advance ratios is not well understood because of the undefined effects of such things as the lag dampers and the blade counterweights, and even though calculated results compare favorably at an advance ratio as high as 0.5, as seen in Figure 38, very little can be said about the correlation of edgewise shear forces.

The results presented do, however, highlight the need for additional theoretical and experimental analyses of rotor behavior at high forward speeds.

The uniform inflow results and the comparative time histories of the edgewise shear forces, Figure 39b, add nothing to the understanding of the problem at hand. There is no significant difference between the uniform and variable inflow results, and both results differ from the measured values to a large extent. The induced velocity analysis does not account for variations of in-plane velocities, but whether or not the inclusion of these would effect the degree of correlation of the edgewise shear forces could not be determined within the scope of this investigation.

With respect to the overall correlation effort, it is felt that although there is considerable room for improvement, the results are encouraging in view of the fact that it has been impossible to even attempt such a correlation in the past for lack of detailed experimental data. The deficiencies in the flatwise shear force calculations clearly point to the areas in which improvements should be made. Namely, the especially restrictive comparison by harmonics demands that the wake-induced velocities be free of sudden large variations and that the rotor blade natural frequencies be well defined through the high modes. In addition, the strong influence of the aeroelastic behavior of the rotor blade in the edgewise direction necessitates a fundamental understanding of this behavior before a better degree of correlation can be achieved at high speeds.

CONCLUSIONS

The results of the experimental investigation of the vibratory shear forces generated by an individual helicopter rotor blade of a four bladed rotor system led to the following principal conclusions:

1) The harmonic content of vibratory shear forces can be accurately determined over a wide range of forward speeds and rotor lifts through the use of high sensitivity semiconductor strain gages.

2) The trim condition of the rotor exerts a strong influence on the amplitude and phase of the first harmonic flatwise and edgewise shear forces, but has no appreciable effect on other harmonics. The change in amplitude of the first harmonic forces is proportional to the amount of out-of-trim flapping. The trim condition exhibited no well defined effect on radial shear forces.

3) Removal of linear viscous lag damping results in a slight increase in the flatwise shear force and either an increase or a decrease in the edgewise shear force, depending on the nearness of the rotor speed to a rotor blade edgewise natural frequency.

4) Increasing forward speed over a range of from 75 to 300 knots results in a gradual increase in the flatwise shear force. The edgewise shear force remains essentially constant from 75 to 175 knots and then increases rapidly from 175 to 300 knots, becoming the predominate force at the highest speeds. At forward speeds above 200 knots, the edgewise bending of the blade dominates the shear forces in all three directions to result in a significant change in the harmonic content of the shear forces over the total speed range.

5) Increasing the rotor lift at constant forward speed produces a gradual increase in the flatwise vibratory shear force. A similar effect takes place in the edgewise shear force, but it is confined to the low harmonics.

6) The longitudinal first harmonic component of the radial shear force can take on values having a magnitude equal to those of the other shear forces under high rotor lift conditions at low forward speeds and under low rotor lift conditions at high forward speeds. The fundamental nature and significance of the radial shear force could not be determined within the scope of this investigation.

The comparison of experimental results and theoretical results obtained with a fully coupled aeroelastic analysis led to the following

principal conclusions:

1) The inclusion of the effects of wake-induced velocities alters the theoretcial results in a direction which improves the correlation of the flatwise shear forces.

2) The natural frequencies of the rotor blade must be well defined through the high harmonic range, because the use of wake-induced velocities in the theoretical analysis necessarily introduces high harmonic forcing functions which excite a response in the blade that can be directly reflected in the vibratory shear force harmonics.

3) The theoretical distribution of induced velocities must be free of singular points having velocities greater by an order of magnitude than the surrounding points, because the singular points tend to introduce errors in all the harmonics of a force under consideration.

4) The deterioration of the degree of correlation of edgewise shear forces with increasing forward speed indicates the need for an improved theoretical and experimental definition of edgewise rotor blade aeroelastic behavior.

5) The inclusion of wake-induced velocities has no significant effect on the degree of correlation of edgewise shear forces.

RECOMMENDATIONS

A more complete understanding of the origin of fuselage excitation requires additional research in the following areas:

1) The existing model rotor should be tested through the low speed range in a wind tunnel having a larger cross section than that of the tunnel used in this investigation. Such a test will provide not only an indication of the magnitude of the effects of the tunnel-rotor diameter ratio (2:1 in this program) on the vibratory shear forces, but will also provide supplementary data at forward speeds below those evaluated herein.

2) A new rotor head having strengthened instrumented sections and fitted with the existing fiber glass blades should be tested to provide more data at forward speeds in the vicinity of 300 knots. Theoretical analyses should be made in conjunction with this experimental work so that specific questions can be answered, such as those arising in connection with the dominance of the edgewise rotor blade bending over the vibratory shear forces.

BIBLIOGRAPHY

1. Scheiman, J., A Tabulation of Helicopter Rotor Blade Differential Pressures, Stresses, and Motions as Measured in Flight, NASA TM X-952, March 1964.

2. Gabel, R., In-Flight Measurement of Steady and Oscillatory Rotor Shaft Loads, CAL/TRECOM Symposium, Buffalo, New York, June 1963.

3. Carlson, R., and Hilzinger, K., Analysis and Correlation of Helicopter Rotor Blade Response in a Variable Inflow Environment, USAAVLABS Technical Report 65-51, September 1965. (Sikorsky Engineering Report 50405).

4. Rabbott, J. P., Jr., Comparison of Theoretical and Experimental Model Helicopter Rotor Performance in Forward Flight, TCREC Technical Report 61-103, July 1961. (Sikorsky Engineering Report 50129).

5. Fradenburgh, E. A., and Kiely, E. F., Development of Dynamic Model Rotor Blades for High Speed Helicopter Research, Symposium on Aeroelastic and Dynamic Modeling Technology, Wright-Patterson Air Force Base, Ohio, September 1963.

6. Piziali, R. A., and DuWaldt, F. A., A Method for Computing Rotary Wing Airload Distributions in Forward Flight, TCREC Technical Report 62-44, July 1962. (Cornell Aeronautical Laboratories Report BB-1495-S-1).

TABLE I FLAPPING AND LAGGING MOTIONS AS FOURIER COEFFICIENTS, DEG.

ADVANCE RATIO = 0.181

ALPHA S = 0 CL/SIG = -0.000 THETA = -1
CG/SIG = 0.0001 ALPHA C = -0.1

FLAPPING						LAGGING					
A0	-0.142					A0	-3.321				
A1	-0.174	B1	0.071			A1	0.076	B1	-0.033		
A2	0.098	B2	-0.186			A2	-0.004	B2	0.008		
A3	0.042	B3	-0.026			A3	-0.005	B3	-0.005		
A4	0.043	B4	0.031			A4	0.005	B4	0.004		
A5	-0.011	B5	-0.009			A5	-0.004	B5	-0.004		
A6	0.004	B6	-0.009			A6	0.007	B6	-0.		
A7	0.002	B7	-0.003			A7	-0.007	B7	0.001		
A8	0.006	B8	0.			A8	0.005	B8	-0.005		
A9	0.002	B9	0.005			A9	-0.001	B9	0.004		
A10	0.004	B10	-0.004			A10	-0.00[illegible]	B10	-0.005		

ALPHA S = 0 CL/SIG = 0.038 THETA = 2
CG/SIG = 0.0002 ALPHA C = -1.0

FLAPPING						LAGGING					
A0	1.953					A0	-3.497				
A1	-0.124	B1	0.129			A1	0.003	B1	-0.028		
A2	-0.067	B2	-0.050			A2	-0.007	B2	0.006		
A3	0.107	B3	0.094			A3	0.002	B3	0.006		
A4	0.038	B4	0.052			A4	-0.003	B4	0.006		
A5	0.011	B5	-0.019			A5	0.002	B5	0.002		
A6	0.012	B6	-0.008			A6	-0.	B6	-0.		
A7	-0.011	B7	-0.024			A7	-0.001	B7	-0.001		
A8	0.012	B8	-0.006			A8	-0.004	B8	-0.		
A9	0.005	B9	-0.003			A9	-0.002	B9	0.001		
A10	0.006	B10	-0.004			A10	-0.002	B10	-0.		

ALPHA S = 0 CL/SIG = 0.044 THETA = 4
CG/SIG = 0.0009 ALPHA C = -2.0

FLAPPING						LAGGING					
A0	3.436					A0	-3.431				
A1	-0.082	B1	0.086			A1	-0.034	B1	-0.021		
A2	-0.171	B2	0.015			A2	-0.012	B2	0.006		
A3	0.141	B3	-0.137			A3	0.008	B3	0.008		
A4	0.043	B4	0.071			A4	-0.007	B4	0.008		
A5	0.029	B5	-0.030			A5	0.002	B5	-0.		
A6	0.022	B6	-0.008			A6	-0.002	B6	-0.002		
A7	0.014	B7	-0.030			A7	-0.	B7	-0.002		
A8	0.013	B8	-0.008			A8	-0.	B8	-0.		
A9	0.003	B9	-0.009			A9	-0.002	B9	-0.002		
A10	0.009	B10	-0.016			A10	0.002	B10	-0.001		

ALPH S = 0 CL/SIG = 0.085 THETA = 6
CG/SIG = 0.0025 ALPHA C = -3.1

FLAPPING						LAGGING					
A0	4.178					A0	-2.399				
A1	0.037	B1	0.035			A1	-0.148	B1	-0.008		
A2	-0.257	B2	0.038			A2	-0.008	B2	0.004		
A3	0.184	B3	-0.103			A3	0.016	B3	0.030		
A4	0.071	B4	0.074			A4	-0.008	B4	0.016		
A5	0.058	B5	-0.027			A5	0.008	B5	0.003		
A6	0.037	B6	-0.016			A6	0.004	B6	-0.001		
A7	0.038	B7	-0.028			A7	0.002	B7	-0.004		
A8	0.021	B8	-0.009			A8	0.004	B8	-0.		
A9	0.007	B9	-0.008			A9	-0.001	B9	0.003		
A10	0.009	B10	-0.024			A10	-0.001	B10	-0.001		

ALPHA S = -4 CL/SIG = 0.002 THETA = 1
CG/SIG = 0.0001 ALPHA C = -4.3

FLAPPING						LAGGING					
A0	-0.					A0	-C.				
A1	-0.	B1	-0.			A1	-0.	B1	-0.		
A2	-0.	B2	-0.			A2	-0.	B2	-0.		
A3	-0.	B3	-0.			A3	-0.	B3	-0.		
A4	-0.	B4	-0.			A4	-0.	B4	-0.		
A5	-0.	B5	-0.			A5	-0.	B5	-0.		
A6	-0.	B6	-0.			A6	-0.	B6	-0.		
A7	-0.	B7	-0.			A7	-0.	B7	-0.		
A8	-0.	B8	-0.			A8	-0.	B8	-0.		
A9	-0.	B9	-0.			A9	-0.	B9	-0.		
A10	-0.	B10	-0.			A10	-0.	B10	-0.		

ALPHA S = -4 CL/SIG = 0.021 THETA = 2
CG/SIG = 0.0003 ALPHA C = -4.8

FLAPPING						LAGGING					
A0	-0.					A0	-0.				
A1	-0.	B1	-0.			A1	-0.	B1	-0.		
A2	-0.	B2	-0.			A2	-0.	B2	-0.		
A3	-0.	B3	-0.			A3	-0.	B3	-0.		
A4	-0.	B4	-0.			A4	-0.	B4	-0.		
A5	-0.	B5	-0.			A5	-0.	B5	-0.		
A6	-0.	B6	-0.			A6	-0.	B6	-0.		
A7	-0.	B7	-0.			A7	-0.	B7	-0.		
A8	-0.	B8	-0.			A8	-0.	B8	-0.		
A9	-0.	B9	-0.			A9	-0.	B9	-0.		
A10	-0.	B10	-0.			A10	-0.	B10	-0.		

ALPHA S = -4 CL/SIG = 0.044 THETA = 4
CG/SIG = 0.0010 ALPHA C = -5.9

FLAPPING						LAGGING					
A0	-0.					A0	-0.				
A1	-0.	B1	-0.			A1	-0.	B1	-0.		
A2	-0.	B2	-0.			A2	-0.	B2	-0.		
A3	-0.	B3	-0.			A3	-0.	B3	-0.		
A4	-0.	B4	-0.			A4	-0.	B4	-0.		
A5	-0.	B5	-0.			A5	-0.	B5	-0.		
A6	-0.	B6	-0.			A6	-0.	B6	-0.		
A7	-0.	B7	-0.			A7	-0.	B7	-0.		
A8	-0.	B8	-0.			A8	-0.	B8	-0.		
A9	-0.	B9	-0.			A9	-0.	B9	-0.		
A10	-0.	B10	-0.			A10	-0.	B10	-0.		

ALPHA S = -4 CL/SIG = 0.071 THETA = 6
CG/SIG = 0.0024 ALPHA C = -6.9

FLAPPING						LAGGING					
A0	-0.					A0	-0.				
A1	-0.	B1	-0.			A1	-0.	B1	-0.		
A2	-0.	B2	-0.			A2	-0.	B2	-0.		
A3	-0.	B3	-0.			A3	-0.	B3	-0.		
A4	-0.	B4	-0.			A4	-0.	B4	-0.		
A5	-0.	B5	-0.			A5	-0.	B5	-0.		
A6	-0.	B6	-0.			A6	-0.	B6	-0.		
A7	-0.	B7	-0.			A7	-0.	B7	-0.		
A8	-0.	B8	-0.			A8	-0.	B8	-0.		
A9	-0.	B9	-0.			A9	-0.	B9	-0.		
A10	-0.	B10	-0.			A10	-0.	B10	-0.		

ALPHA S = -4 CL/SIG = 0.087 THETA = 8
CG/SIG = 0.0047 ALPHA C = -8.2

FLAPPING						LAGGING					
A0	-0.					A0	-0.				
A1	-0.	B1	-0.			A1	-0.	B1	-0.		
A2	-0.	B2	-0.			A2	-0.	B2	-0.		
A3	-0.	B3	-0.			A3	-0.	B3	-0.		
A4	-0.	B4	-0.			A4	-0.	B4	-0.		
A5	-0.	B5	-0.			A5	-0.	B5	-0.		
A6	-0.	B6	-0.			A6	-0.	B6	-0.		
A7	-0.	B7	-0.			A7	-0.	B7	-0.		
A8	-0.	B8	-0.			A8	-0.	B8	-0.		
A9	-0.	B9	-0.			A9	-0.	B9	-0.		
A10	-0.	B10	-0.			A10	-0.	B10	-0.		

NOTE: COEFFICIENTS ARE ALL LISTED AS -0. WHEN NO BLADE MOTION DATA WAS OBTAINED DUE TO INSTRUMENTATION DIFFICULTIES.

TABLE I CONTINUED.

ADVANCE RATIO = 0.18

ALPHA S = -4 CL/SIG = 0.897 THETA = 10
CQ/SIG = 0.0081 ALPHA C = -9.1

PLAPPING		LAGGING	
A0 -0.		A0 -0.	
A1 -0.	B1 -0.	A1 -0.	B1 -0.
A2 -0.	B2 -0.	A2 -0.	B2 -0.
A3 -0.	B3 -0.	A3 -0.	B3 -0.
A4 -0.	B4 -0.	A4 -0.	B4 -0.
A5 -0.	B5 -0.	A5 -0.	B5 -0.
A6 -0.	B6 -0.	A6 -0.	B6 -0.
A7 -0.	B7 -0.	A7 -0.	B7 -0.
A8 -0.	B8 -0.	A8 -0.	B8 -0.
A9 -0.	B9 -0.	A9 -0.	B9 -0.
A10-0.	B10-0.	A10-0.	B10-0.

ALPHA S = -8 CL/SIG = 0.004 THETA = 2
CQ/SIG = 0.0001 ALPHA C = -8.7

PLAPPING		LAGGING	
A0 -0.		A0 -0.	
A1 -0.	B1 -0.	A1 -0.	B1 -0.
A2 -0.	B2 -0.	A2 -0.	B2 -0.
A3 -0.	B3 -0.	A3 -0.	B3 -0.
A4 -0.	B4 -0.	A4 -0.	B4 -0.
A5 -0.	B5 -0.	A5 -0.	B5 -0.
A6 -0.	B6 -0.	A6 -0.	B6 -0.
A7 -0.	B7 -0.	A7 -0.	B7 -0.
A8 -0.	B8 -0.	A8 -0.	B8 -0.
A9 -0.	B9 -0.	A9 -0.	B9 -0.
A10-0.	B10-0.	A10-0.	B10-0.

ALPHA S = -8 CL/SIG = 0.032 THETA = 4
CQ/SIG = 0.0010 ALPHA C = -9.4

PLAPPING		LAGGING	
A0 -0.		A0 -0.	
A1 -0.	B1 -0.	A1 -0.	B1 -0.
A2 -0.	B2 -0.	A2 -0.	B2 -0.
A3 -0.	B3 -0.	A3 -0.	B3 -0.
A4 -0.	B4 -0.	A4 -0.	B4 -0.
A5 -0.	B5 -0.	A5 -0.	B5 -0.
A6 -0.	B6 -0.	A6 -0.	B6 -0.
A7 -0.	B7 -0.	A7 -0.	B7 -0.
A8 -0.	B8 -0.	A8 -0.	B8 -0.
A9 -0.	B9 -0.	A9 -0.	B9 -0.
A10-0.	B10-0.	A10-0.	B10-0.

ALPHA S = -8 CL/SIG = 0.057 THETA = 6
CQ/SIG = 0.0024 ALPHA C = -10.9

PLAPPING		LAGGING	
A0 -0.		A0 -0.	
A1 -0.	B1 -0.	A1 -0.	B1 -0.
A2 -0.	B2 -0.	A2 -0.	B2 -0.
A3 -0.	B3 -0.	A3 -0.	B3 -0.
A4 -0.	B4 -0.	A4 -0.	B4 -0.
A5 -0.	B5 -0.	A5 -0.	B5 -0.
A6 -0.	B6 -0.	A6 -0.	B6 -0.
A7 -0.	B7 -0.	A7 -0.	B7 -0.
A8 -0.	B8 -0.	A8 -0.	B8 -0.
A9 -0.	B9 -0.	A9 -0.	B9 -0.
A10-0.	B10-0.	A10-0.	B10-0.

ALPHA S = -8 CL/SIG = 0.078 THETA = 8
CQ/SIG = 0.0044 ALPHA C = -11.8

PLAPPING		LAGGING	
A0 -0.		A0 -0.	
A1 -0.	B1 -0.	A2 -0.	B1 -0.
A2 -0.	B2 -0.	A2 -0.	B -0.
A3 -0.	B3 -0.	A3 -0.	B -0.
A4 -0.	B4 -0.	A4 -0.	B -0.
A5 -0.	B5 -0.	A5 -0.	B5 -0.
A6 -0.	B6 -0.	A6 -0.	B6 -0.
A7 -0.	B7 -0.	A7 -0.	B7 -0.
A8 -0.	B8 -0.	A8 -0.	B8 -0.
A9 -0.	B9 -0.	A9 -0.	B9 -0.
A10-0.	B10-0.	A10-0.	B10-0.

ALPHA S = -8 CL/SIG = 0.089 THETA = 10
CQ/SIG = 0.0074 ALPHA C = -13.5

PLAPPING		LAGGING	
A0 -0.		A0 -0.	
A1 -0.	B1 -0.	A1 -0.	B1 -0.
A2 -0.	B2 -0.	A2 -0.	B2 -0.
A3 -0.	B3 -0.	A3 -0.	B3 -0.
A4 -0.	B4 -0.	A4 -0.	B4 -0.
A5 -0.	B5 -0.	A5 -0.	B5 -0.
A6 -0.	B6 -0.	A6 -0.	B6 -0.
A7 -0.	B7 -0.	A7 -0.	B7 -0.
A8 -0.	B8 -0.	A8 -0.	B8 -0.
A9 -0.	B9 -0.	A9 -0.	B9 -0.
A10-0.	B10-0.	A10-0.	B10-0.

ALPHA S = -8 CL/SIG = 0.092 THETA = 11
CQ/SIG = 0.0089 ALPHA C = -13.9

PLAPPING		LAGGING	
A0 -0.		A0 -0.	
A1 -0.	B1 -0.	A1 -0.	B1 -0.
A2 -0.	B2 -0.	A1 -0.	B2 -0.
A3 -0.	B3 -0.	A3 -0.	B3 -0.
A4 -0.	B4 -0.	A4 -0.	B4 -0.
A5 -0.	B5 -0.	A5 -0.	B5 -0.
A6 -0.	B6 -0.	A6 -0.	B6 -0.
A7 -0.	B7 -0.	A7 -0.	B7 -0.
A8 -0.	B8 -0.	A8 -0.	B8 -0.
A9 -0.	B9 -0.	A9 -0.	B9 -0.
A10-0.	B10-0.	A10-0.	B10-0.

OUT-OF-TRIM

ALPHA S = 0 CL/SIG = -0.007 THETA = 0
CQ/SIG = 0.0000 ALPHA C = -4.9

PLAPPING			LAGGING		
A0 -0.288			A0 0.043		
A1 4.278	B1 0.329		A1 0.028	B1 -0.006	
A2 0.891	B2 -0.228		A2 0.009	B2 -0.012	
A3 0.039	B3 -0.058		A3 -0.	B3 -0.003	
A4 0.040	B4 0.028		B4 0.004	B4 -0.003	
A5 -0.004	B5 -0.010		A0 0.001	B5 -0.	
A6 0.007	B6 -0.008		B6 -0.001	B6 -0.	
A7 -0.004	B7 0.009		A7 -0.	B7 0.001	
A8 0.001	B8 0.004		A8 -0.	B6 -0.001	
A9 0.003	C9 0.003		A9 -0.	B9 -0.001	
A10-0.003	B10 0.002		A20 0.001	B10-0.	

OUT-OF-TRIM

ALPHA S = C CL/SIG = 0.021 THETA = 2
CQ/SIG = 0.0004 ALPHA C = -3.0

PLAPPING			LAGGING		
A0 1.2A2			A0 0.099		
A1 4.160	B1 0.213		A1 0.018	B1 -0.034	
A2 -0.878	B2 -0.086		A2 0.008	B2 -0.019	
A3 0.074	B3 -0.047		A3 -0.001	B3 -0.002	
B4 0.049	B4 0.044		A4 0.001	B4 -0.003	
A5 0.017	B5 -0.028		A5 0.002	B5 -0.002	
AA 0.017	B4 -0.009		AA 0.001	BA -0.001	
A7 0.003	B7 -0.013		A7 -0.	B7 -0.001	
A8 0.009	B8 -0.		A8 0.001	B8 -0.	
A9 0.007	C9 -0.001		A9 0.002	B9 -0.001	
A10 0.001	B10 0.002		A10 0.002	B10-0.	

TABLE I CONTINUED.

ADVANCE RATIO = 0.191

OUT-OF-TRIM

ALPHA S = 0 CL/SIG = 0.047 THETA = 4
CD/SIG = 0.0012 ALPHA C = -0.2

FLAPPING				LAGGING			
A0	2.922			A0	0.249		
A1	4.152	B1	0.184	A1	0.005	B1	-0.089
A2	-0.222	B2	-0.057	A2	0.008	B2	-0.012
A3	0.124	B3	-0.121	A3	0.010	B3	0.009
A4	0.080	B4	0.078	A4	-0.002	B4	-0.001
A5	0.050	B5	-0.057	A5	0.003	B5	0.002
A6	0.021	B6	-0.004	A6	-0.001	B6	0.002
A7	0.015	B7	-0.030	A7	-0.001	B7	0.002
A8	0.014	B8	-0.002	A8	0.001	B8	-0.
A9	-0.001	B9	-0.005	A9	-0.002	B9	-0.005
A10	0.008	B10	-0.025	A10	0.001	B10	-0.001

ZERO LAG DAMPING

ALPHA S = -4 CL/SIG = 0.025 THETA = 2
CD/SIG = 0.0004 ALPHA C = -5.0

FLAPPING				LAGGING			
A0	1.777			A0	0.100		
A1	0.101	B1	-0.159	A1	0.058	B1	-0.025
A2	-0.140	B2	-0.130	A2	0.001	B2	0.001
A3	0.125	B3	-0.089	A3	0.008	B3	0.007
A4	0.040	B4	0.049	A4	-0.001	B4	-0.001
A5	0.018	B5	-0.014	A5	0.002	B5	-0.
A6	0.022	B6	0.009	A6	0.001	B6	-0.002
A7	0.011	B7	-0.034	A7	0.001	B7	-0.001
A8	0.011	B8	0.007	A8	0.001	B8	-0.
A9	0.014	B9	0.005	A9	-0.	B9	-0.002
A10	-0.017	B10	-0.014	A10	-0.	B10	-0.

ZERO LAG DAMPING

ALPHA S = -4 CL/SIG = 0.089 THETA = 8
CD/SIG = 0.0048 ALPHA C = -8.0

FLAPPING				LAGGING			
A0	9.140			A0	2.505		
A1	0.044	B1	-0.092	A1	-0.275	B1	0.175
A2	-0.842	B2	-0.155	A2	-0.410	B2	0.057
A3	0.295	B3	-0.070	A3	0.074	B3	0.088
A4	0.188	B4	0.120	A4	-0.005	B4	0.012
A5	0.096	B5	-0.055	A5	0.011	B5	0.004
A6	-0.085	B6	0.055	A6	0.008	B6	0.002
A7	0.017	B7	-0.108	A7	0.012	B7	-0.007
A8	0.015	B8	-0.003	A8	0.000	B8	0.005
A9	0.016	B9	0.020	A9	0.001	B9	-0.001
A10	0.013	B10	-0.058	A10	-0.	B10	-0.005

OUT-OF-TRIM

ALPHA S = 0 CL/SIG = 0.071 THETA = 6
CD/SIG = 0.0025 ALPHA C = -7.2

FLAPPING				LAGGING			
A0	4.084			A0	0.915		
A1	4.207	B1	0.199	A1	-0.048	B1	-0.110
A2	-0.345	B2	-0.084	A2	0.012	B2	-0.009
A3	0.187	B3	-0.129	A3	0.015	B3	0.005
A4	0.091	B4	0.118	A4	-0.006	B4	0.005
A5	0.052	B5	-0.031	A5	0.007	B5	0.002
A6	0.040	B6	0.008	A6	0.002	B6	0.001
A7	0.010	B7	-0.029	A7	0.003	B7	0.002
A8	0.021	B8	-0.008	A8	-0.	B8	-0.002
A9	0.005	B9	-0.002	A9	-0.001	B9	-0.001
A10	-0.	B10	-0.040	A10	-0.	B10	-0.

ZERO LAG DAMPING

ALPHA S = -4 CL/SIG = 0.048 THETA = 4
CD/SIG = 0.0012 ALPHA C = -9.1

FLAPPING				LAGGING			
A0	5.597			A0	0.505		
A1	0.212	B1	-0.074	A1	-0.024	B1	-0.003
A2	-0.285	B2	-0.038	A2	-0.009	B2	0.009
A3	0.194	B3	-0.128	A3	0.024	B3	0.025
A4	0.054	B4	0.079	A4	-0.004	B4	0.001
A5	0.051	B5	-0.029	A5	0.003	B5	0.003
A6	0.015	B6	0.002	A6	0.001	B6	-0.001
A7	0.024	B7	-0.052	A7	0.005	B7	-0.002
A8	0.025	B8	-0.009	A8	0.003	B8	0.001
A9	0.017	B9	-0.004	A9	-0.001	B9	-0.
A10	-0.008	B10	-0.044	A10	-0.	B10	-0.

ZERO LAG DAMPING

ALPHA S = -4 CL/SIG = -0.004 THETA = 0
CD/SIG = 0.0001 ALPHA C = -4.0

FLAPPING				LAGGING			
A0	0.098			A0	-0.103		
A1	0.213	B1	0.078	A1	0.002	B1	-0.058
A2	0.060	B2	-0.205	A2	-0.001	B2	-0.002
A3	0.060	B3	-0.039	A3	-0.002	B3	0.003
A4	0.039	B4	0.026	A4	0.001	B4	-0.001
A5	0.003	B5	-0.012	A5	0.002	B5	-0.
A6	0.008	B6	-0.007	A6	0.002	B6	-0.001
A7	-0.005	B7	-0.004	A7	0.001	B7	0.001
A8	0.009	B8	-0.004	A8	-0.	B8	-0.
A9	0.007	B9	0.005	A9	0.001	B9	-0.
A10	-0.010	B10	0.014	A10	0.002	B10	-0.001

ZERO LAG DAMPING

ALPHA S = -4 CL/SIG = 0.075 THETA = 8
CD/SIG = 0.002A ALPHA C = -9.7

FLAPPING				LAGGING			
A0	5.037			A0	1.294		
A1	0.189	B1	-0.094	A1	-0.129	B1	0.095
A2	-0.452	B2	0.012	A2	-0.007	B2	0.010
A3	0.245	B3	-0.110	A3	0.048	B3	0.050
A4	0.107	B4	0.105	A4	-0.005	A4	0.009
A5	0.077	B5	-0.020	A5	0.008	B5	0.002
A6	0.049	B6	0.020	AA	0.007	B6	0.002
A7	0.004	B7	-0.044	A7	0.009	B7	-0.004
A8	0.021	B8	0.034	A8	0.005	B8	0.002
A9	0.009	B9	-0.001	A9	-0.	B9	-0.001
A10	-0.001	B10	-0.04A	A10	-0.005	B10	-0.001

TABLE I CONTINUED.

ADVANCE RATIO = 0.283

ALPHA S = 8 CL/SIG = -0.023 THETA = -2
CQ/SIG = 0.0008 ALPHA C = 0.9

	FLAPPING			LAGGING		
A0	-0.424			A0	2.334	
A1	-0.457	B1	-0.067	A1	0.093	B1	-0.063
A2	0.239	B2	-0.324	A2	-0.009	B2	0.007
A3	0.092	B3	0.016	A3	-0.001	B3	0.005
A4	0.077	B4	0.025	B4	0.003	B4	-0.002
A5	-0.010	B5	0.010	A3	-0.001	B3	0.001
A6	0.014	B6	-0.018	B4	-0.001	B6	-0.
A7	-0.	B7	0.053	A7	0.001	B7	-0.
A8	-0.	B8	0.003	A8	-0.	B8	0.001
A9	0.011	B9	-0.	A9	-0.002	B9	-0.001
A10	0.002	B10	0.031	A10	0.001	B10	-0.001

ALPHA S = 8 CL/SIG = -0.007 THETA = 0
CQ/SIG = 0.0007 ALPHA C = -0.9

	FLAPPING			LAGGING		
A0	0.432			B4	2.517	
A1	-0.247	B1	0.588	A1	0.079	B1	-0.870
A2	0.134	B2	-0.297	A2	-0.003	B3	-0.002
A3	0.894	B3	-0.040	A3	0.005	B3	0.004
A4	0.073	B4	0.044	B4	0.003	B4	-0.001
A5	-0.011	B5	0.003	A5	-0.	B3	-0.001
AA	0.015	BA	-0.013	B4	-0.	B4	-0.002
A7	-0.007	B7	0.048	A7	-0.	B7	-0.001
A8	-0.004	B8	0.001	A8	0.001	B8	-0.001
A9	0.011	B9	-0.002	A9	0.001	B9	0.001
A10	0.008	B10	0.033	A10	0.001	B10	-0.001

ALPHA S = 8 CL/SIG = 0.015 THETA = 2
CQ/SIG = 0.0008 ALPHA C = -2.4

	FLAPPING			LAGGING		
A0	1.638			B4	2.925	
A1	-0.224	B1	-0.141	A1	0.034	B1	-0.058
A2	0.089	B2	-0.240	A2	-0.001	B2	0.004
A3	0.893	B3	-0.093	A3	0.007	B3	-0.
A4	0.058	B4	0.040	A4	0.001	B4	0.002
A5	-0.005	B5	-0.007	A5	-0.	B5	0.001
AA	0.012	BA	-0.016	AA	-0.001	B6	-0.003
A7	-0.008	B7	0.094	A7	-0.001	B7	-0.001
A8	-0.009	B8	0.000	A8	0.002	B4	0.001
A9	0.004	B9	0.003	A9	-0.	B9	0.001
A10	-0.009	B10	0.026	A10	-0.	B10	-0.

ALPHA S = 8 CL/SIG = 0.040 THETA = 4
CQ/SIG = 0.0015 ALPHA C = -5.9

	FLAPPING			LAGGING		
A0	3.078			A0	2.431	
A1	-0.540	B1	0.134	A1	-0.043	61	-0.014
A2	-0.212	B2	-0.177	A2	-0.005	B2	0.018
A3	0.065	B5	-0.155	A5	0.011	B5	0.006
A4	0.050	B4	0.049	A4	-0.002	B4	0.008
B5	0.017	B3	-0.011	A5	0.002	B3	0.001
AA	0.022	B6	-0.002	B4	-0.	BA	-0.001
A7	-0.031	B7	0.071	A7	-0.001	F7	-0.
A8	-0.017	B8	0.006	A8	0.001	A8	-0.
A9	-0.002	B9	0.00A	A9	-0.	B9	0.001
A10	-0.017	B10	0.023	A10	-0.	B10	-0.

ALPHA S = 8 CL/SIG = 0.069 THETA = 6
CQ/SIG = 0.0031 ALPHA C = -5.2

	FLAPPING			LAGGING		
A0	4.814			B4	3.290	
A1	-0.345	B1	0.090	A2	-0.131	61	0.041
A2	-0.414	B2	-0.576	A2	-0.003	B2	0.033
A3	0.093	B5	-0.153	A3	0.033	B5	0.009
A4	0.042	B4	0.000	A4	-0.	B4	0.01A
A5	0.022	B5	-0.005	A3	0.003	B5	0.009
A6	0.031	BA	0.008	B4	-0.005	B4	-0.001
A7	-0.006	B7	0.102	A7	0.001	B7	-0.
A8	-0.012	A8	0.008	A8	0.005	B9	-0.001
A9	0.002	B9	-0.	A9	0.001	B9	0.003
A10	0.010	B10	0.019	A10	0.001	B10	0.002

ALPHA S = 8 CL/SIG = 0.045 THETA = 8
CQ/SIG = 0.0056 ALPHA C = -4.8

	FLAPPING			LAGGING		
A0	4.497			A0	4.531	
A1	-0.318	61	-0.108	A1	-0.283	B1	0.159
A2	-0.397	A7	-0.585	A2	-0.004	B2	0.050
A5	0.218	A5	-0.182	A3	0.035	B5	-0.00A
A4	0.049	A4	0.090	A4	0.004	B4	0.024
A9	0.079	B5	-0.034	A3	0.006	B5	0.007
A6	0.068	BA	0.041	A6	-0.	BA	-0.001
A7	-0.060	A7	0.053	A7	-0.001	A7	-0.003
A8	-0.03A	A8	-0.014	A8	0.001	B8	0.007
A9	-0.008	B9	-0.023	A9	-0.001	A9	0.00A
A10	0.015	B10	-0.006	A10	0.002	B10	0.002

ALPHA E = 0 CL/SIG = 0.074 THETA = 10
CQ/SIG = 0.0083 ALPHA C = -8.0

	FLAPPING			LAGGING		
A0	3.064			B4	4.063	
A1	-0.231	B1	-0.034	A1	-0.433	B1	0.381
A2	-0.774	B2	-0.604	A2	-0.013	B2	0.079
A3	0.318	65	-0.127	A3	0.041	B3	-0.01A
A4	0.191	34	0.052	B4	0.013	B4	0.015
A5	-0.033	B5	-0.05A	A3	0.006	B5	-0.001
B4	0.003	BA	-0.004	B4	-0.004	00	0.001
A7	-0.034	B7	0.153	A7	-0.003	B7	0.007
A8	-0.001	B8	-0.009	A8	0.003	B8	0.004
A9	-0.010	B9	0.007	A9	0.005	B8	0.002
B50	-0.033	B10	-0.025	A10	-0.	B50	-0.004

ALPHA S = -4 CL/SIG = -0.002 THETA = 1
CQ/SIG = 0.0001 ALPHA C = -4.6

	FLAPPING			LAGGING		
A0	-0.583			A0	2.629	
A1	-0.332	B1	-0.019	A1	0.088	B1	-0.PPP
A2	0.133	B2	-0.288	A2	-0.	B2	-0.
A3	0.873	A3	-0.033	A3	-0.001	B3	0.003
A4	0.082	B4	-0.001	A4	0.006	B4	-0.001
A3	0.00A	B5	0.004	A6	0.002	B5	-0.
AA	0.011	BA	-0.017	B4	-0.	B4	-0.
A7	0.001	B7	0.038	A7	-0.	B7	-0.
A8	0.002	B6	-0.001	A8	0.001	B8	-0.
A9	0.013	B9	-0.001	A9	0.001	B9	0.001
a10	0.	B10	0.038	650	-0.005	B10	-0.

ALPHA S = -4 CL/SIG = 0.019 THETA = 2
CQ/SIG = 0.0004 ALPHA C = -4.8

	FLAPPING			LAGGING		
A0	0.845			A8	2.AB8	
A1	-0.392	61	-0.C99	A1	0.043	61	-0.047
A2	0.004	B2	-0.227	A2	-0.002	B2	0.001
A3	0.883	B5	-0.089	A5	0.002	B3	-0.001
A4	0.079	B4	0.01A	A4	0.005	B4	-0.902
A5	-0.006	B5	-0.001	A5	0.005	B5	-0.
AA	0.014	BA	-0.013	AA	-0.	AA	0.001
A7	-0.015	B7	0.059	A7	0.001	B7	-0.
A8	-0.003	B8	-0.	A8	-0.	B8	-0.
A9	0.010	B9	0.003	A9	-0.	B9	-0.001
A10	-0.010	B10	0.055	A10	0.001	B10	-0.

TABLE I CONTINUED.

ADVANCE RATIO = 0.265

ALPHA S = -8 CL/SIG = 0.041 THETA = 4
CQ/SIG = 0.0011 ALPHA C = -8.5

	FLAPPING				LAGGING			
A0	1.461			A0	2.787			
A1	-0.558	B1	-0.065	A1	0.015	B1	-0.024
A2	-0.159	B2	-0.100	A2	-0.001	B2	-0.
A3	0.115	B3	-0.156	A3	0.005	B3	-0.001
A4	0.082	B4	0.041	A4	0.001	B4	0.004
A5	-0.008	B5	-0.015	A5	0.001	B5	-0.002
A6	0.024	B6	-0.004	A6	0.001	B6	0.001
A7	-0.027	B7	0.019	A7	0.001	B7	-0.
A8	-0.005	B8	0.004	A8	-0.	B8	-0.
A9	0.007	B9	0.005	A9	0.002	B9	-0.
A10	-0.010	B10	0.008	A10	-0.001	B10	0.001

ALPHA S = -4 CL/SIG = 0.062 THETA = 6
CQ/SIG = 0.0022 ALPHA C = -7.9

	FLAPPING				LAGGING			
A0	3.074			A0	5.500			
A1	-0.427	B1	-0.080	A1	-0.046	B1	0.018
A2	-0.575	B2	-0.152	A2	-0.004	B2	0.012
A3	0.151	B3	-0.198	A3	0.015	B3	0.006
A4	0.058	B4	0.080	A4	-0.002	B4	0.007
A5	0.004	B5	-0.015	A5	-0.	B5	0.005
A6	0.015	B6	0.007	A6	-0.	B6	-0.
A7	-0.045	B7	0.051	A7	0.001	B7	-0.
A8	-0.021	B8	0.007	A8	0.002	B8	-0.001
A9	-0.025	B9	0.010	A9	0.001	B9	-0.001
A10	-0.007	B10	0.044	A10	-0.001	B10	0.002

ALPHA S = -4 CL/SIG = 0.077 THETA = 8
CQ/SIG = 0.0042 ALPHA C = -10.0

	FLAPPING				LAGGING			
A0	5.969			A0	9.281			
A1	-0.255	B1	0.044	A1	-0.147	B1	0.046
A2	-0.958	B2	-0.216	A2	-0.	B2	0.029
A3	0.157	B3	-0.151	A3	0.044	B3	7.014
A4	0.051	B4	0.141	A4	-0.008	B4	0.018
A5	0.010	B5	0.005	A5	0.002	B5	0.007
A6	-0.002	B6	0.041	A6	0.001	B6	0.001
A7	-0.046	B7	0.052	A7	-0.002	B7	-0.
A8	-0.026	B8	-0.007	A8	-0.001	B8	0.001
A9	-0.001	B9	0.00	A9	0.002	B9	0.005
A10	-0.017	B10	0.030	A10	0.001	B10	0.002

ALPHA S = -4 CL/SIG = 0.087 THETA = 10
CQ/SIG = 0.0074 ALPHA C = -11.4

	FLAPPING				LAGGING			
A0	4.414			A0	5.904			
A1	-0.228	B1	0.003	A1	-0.520	B1	0.214
A2	-0.724	B2	-0.499	A2	-0.009	B2	0.047
A3	0.271	B3	-0.168	A3	0.022	B3	-0.001
A4	0.085	B4	0.215	A4	0.005	B4	0.054
A5	0.017	B5	0.047	A5	0.009	B5	0.012
A6	0.055	B6	0.034	A6	-0.005	B6	-0.001
A7	-0.075	B7	0.071	A7	-0.004	B7	0.004
A8	-0.055	B8	-0.009	A8	0.001	B8	0.005
A9	-0.001	B9	0.024	A9	-0.001	B9	0.001
A10	-0.041	B10	0.017	A10	-0.001	B10	-0.002

ALPHA S = -8 CL/SIG = -0.009 THETA = 2
CQ/SIG = -0.0001 ALPHA C = -8.9

	FLAPPING				LAGGING			
A0	-0.118			A0	0.536			
A1	0.065	B1	0.178	A1	0.008	B1	-0.054
A2	0.029	B2	-0.264	A2	0.005	B2	0.006
A3	0.082	B3	-0.044	A3	-0.005	B3	0.006
A4	0.091	B4	-0.018	A4	0.009	B4	-0.004
A5	0.010	B5	0.017	A5	0.002	B5	0.005
A6	0.012	B6	-0.002	A6	-0.002	B6	-0.
A7	-0.005	B7	0.028	A7	-0.001	B7	-0.
A8	-0.	B8	-0.002	A8	0.001	B8	-0.
A9	0.015	B9	-0.008	A9	0.002	B9	-0.
A10	-0.005	B10	0.027	A10	-0.	B10	-0.001

ALPHA S = -8 CL/SIG = 0.016 THETA = 4
CQ/SIG = 0.0007 ALPHA C = -10.6

	FLAPPING				LAGGING			
A0	0.854			A0	0.727			
A1	0.227	B1	0.175	A1	0.035	B1	-0.045
A2	-0.017	B2	-0.245	A2	-0.012	B2	0.004
A3	0.091	B3	-0.138	A3	0.005	B3	-0.004
A4	0.002	B4	-0.002	A4	0.002	B4	-0.001
A5	0.014	A5	0.014	A5	0.005	B5	-0.
A6	0.018	B6	0.002	A6	0.002	B6	-0.
A7	-0.017	B7	0.029	A7	-0.	B7	-0.001
A8	-0.	B8	-0.001	A8	-0.	B8	-0.
A9	0.007	B9	0.006	A5	-0.	B9	0.001
A10	-0.004	B10	0.010	A10	0.001	B10	0.001

TABLE I CONTINUED.

ADVANCE RATIO = 0.283

ALPHA S = -8 CL/SIG = 0.039 THETA = 6
CO/SIG = 0.0021 ALPHA C = -11.5

FLAPPING				LAGGING			
A0	2.238			A0	1.272		
A1	-0.010	B1	0.399	A1	0.003	B1	-0.015
A2	-0.295	B2	-0.164	A2	-0.	B2	0.002
A3	0.127	B3	-0.199	A3	0.008	B3	0.002
A4	0.087	B4	0.022	A4	0.002	B4	0.002
A5	0.022	B5	-0.	A5	0.003	B5	0.001
A6	0.017	B6	0.008	A6	-0.	B6	-0.001
A7	-0.019	B7	0.031	A7	-0.	B7	0.002
A8	-0.001	B8	0.003	A8	-0.	B8	0.001
A9	0.006	B9	0.006	A9	-0.	B9	0.001
A10	-0.002	B10	0.020	A10	0.001	B10	-0.

ALPHA S = -8 CL/SIG = 0.059 THETA = 8
CO/SIG = 0.0038 ALPHA C = -13.3

FLAPPING				LAGGING			
A0	3.369			A0	2.225		
A1	0.244	B1	0.186	A1	-0.381	B1	0.012
A2	-0.473	B2	-0.183	A2	-0.010	B2	0.012
A3	0.174	B3	-0.223	A3	0.017	B3	0.010
A4	0.083	B4	0.067	A4	-0.	B4	0.007
A5	0.032	B5	0.010	A5	0.003	B5	0.002
A6	0.017	B6	0.015	A6	0.002	B6	-0.003
A7	-0.022	B7	0.026	A7	-0.001	B7	-0.
A8	-0.	B8	0.005	A8	0.001	B8	-0.
A9	0.005	B9	0.007	A9	-0.002	B9	0.001
A10	-0.015	B10	0.025	A10	-0.	B10	0.002

ALPHA S = -8 CL/SIG = 0.069 THETA = 10
CO/SIG = 0.0061 ALPHA C = -14.8

FLAPPING				LAGGING			
A0	4.269			A0	3.523		
A1	0.309	B1	0.125	A1	-0.215	B1	0.092
A2	-0.652	B2	-0.352	A2	-0.011	B2	0.028
A3	0.223	B3	-0.216	A3	0.051	B3	0.025
A4	0.060	B4	0.105	A4	-0.006	B4	0.016
A5	0.025	B5	0.032	A5	-0.	B5	0.008
A6	-0.005	B6	0.040	A6	0.003	B6	0.005
A7	-0.029	B7	0.037	A7	-0.001	B7	0.004
A8	0.002	B8	0.007	A8	-0.001	B8	0.002
A9	0.007	B9	0.014	A9	-0.	B9	0.004
A10	-0.021	B10	0.028	A10	0.001	B10	0.002

ALPHA S = -8 CL/SIG = 0.078 THETA = 11
CO/SIG = 0.0079 ALPHA C = -15.7

FLAPPING				LAGGING			
A0	4.634			A0	4.314		
A1	0.410	B1	0.183	A1	-0.302	B1	0.150
A2	-0.762	B2	-0.505	A2	-0.010	B2	0.051
A3	0.280	B3	-0.195	A3	0.054	B3	0.018
A4	0.078	B4	0.119	A4	-0.009	B4	0.024
A5	0.048	B5	0.062	A5	0.003	B5	0.017
A6	-0.012	B6	0.061	A6	-0.	B6	0.004
A7	-0.022	B7	0.005	A7	0.001	B7	0.003
A8	0.001	B8	-0.009	A8	-0.	B8	0.004
A9	0.007	B9	-0.	A9	-0.003	B9	0.003
A10	-0.007	B10	0.006	A10	0.001	B10	-0.

TABLE I CONTINUED.

ADVANCE RATIO = 0.389

ALPHA S = 4 CL/SIG = -0.004 THETA = -4
CC/SIG = 0.0003 ALAMA C = 4.8

FLAPPING				LAGGING			
A0	0.128			A0	2.333		
A1	0.057	B1	0.021	A1	0.048	B1	-0.07A
A2	0.427	B2	-0.535	A2	-0.013	B2	0.014
A3	0.032	B3	0.085	A3	0.030	B3	0.00A
A4	0.30E	B4	0.031	A4	-0.001	B4	-0.002
A5	-0.0A3	B5	0.072	A5	0.002	B5	-0.001
A6	-0.026	B6	0.015	A6	0.001	B6	-0.002
A7	-0.04C	B7	0.022	A7	-0.	B7	-0.
A8	-0.01C	B8	-0.008	A8	0.001	B8	0.001
A9	0.005	B9	-0.	A9	-0.002	B9	-0.
A10	-0.04E	B10	0.031	A10	0.002	B10	-0.

ALAMA S = 4 CL/SIG = 0.017 THETA = -2
CC/SIG = -0.0004 ALAMA C = 3.0

FLAPPING				LAGGING			
A0	1.166			A0	2.187		
A1	-0.088	B1	-0.003	A1	0.080	B1	-0.083
A2	0.244	B2	-0.515	A2	-0.012	B2	0.004
A3	0.050	B3	-0.043	A3	0.009	B3	0.002
A4	0.124	B4	0.025	A4	0.001	B4	-0.004
A5	-0.028	B5	0.056	A5	0.001	B5	-0.002
A6	-0.037	B6	0.017	A6	0.003	B6	-0.
A7	-0.002	B7	0.021	A7	0.002	B7	-0.
A8	-0.004	B8	0.005	A8	-0.	B8	0.002
A9	0.005	B9	0.005	A9	-0.	B9	-0.
A10	-0.043	B10	0.022	A10	-0.	B10	-0.

ALAMA S = 4 CL/SIG = 0.035 THETA = 0
CO/SIG = -0.0006 ALAMA C = 1.2

FLAPPING				LAGGING			
A0	2.131			A0	2.089		
A1	0.046	B1	-0.132	A1	0.02A	B1	-0.047
A2	-0.030	B2	-0.446	A2	-0.011	B2	0.006
A3	0.051	B3	-0.135	A3	0.016	B3	-0.011
A4	0.134	B4	0.010	A4	0.005	B4	-0.002
A5	-0.018	B5	0.051	A5	0.003	B3	-0.
A6	-0.023	B6	0.025	A6	0.001	B6	0.001
A7	0.004	B7	0.011	A7	-0.001	B7	0.001
A8	0.003	B8	0.001	A8	-0.	B8	0.001
A9	0.008	B9	0.010	A9	-0.003	B9	-0.002
A10	-0.020	B10	0.02A	A10	-0.	B10	-0.

ALPHA S = 4 CL/SIG = 0.053 THETA = 2
CG/SIG = -0.0002 ALPHA C = -0.5

FLAPPING				LAGGING			
A0	3.17C			A0	2.2C0		
A1	-0.28E	B1	-0.120	A1	-0.025	B1	-0.053
A2	-0.291	B2	-0.405	A2	-0.005	B2	0.028
A3	0.018	B3	-0.256	A3	0.029	B2	-0.011
A4	0.118	B4	0.053	A4	0.007	B4	-0.
A5	-0.01E	B5	0.028	A5	0.002	B5	-0.001
AA	-0.00S	B6	0.026	B6	-0.001	B6	0.001
A7	-0.01S	B7	0.014	A7	0.003	B7	0.002
A8	0.00S	B8	0.016	A8	-0.	B8	-0.
A9	0.01C	B9	0.005	A6	-0.B02	B6	-0.002
A10	-0.021	B10	0.021	A10	-0.	B10	-0.001

ALAMA S = 4 CL/SIG = 0.060 THETA = 2
CC/SIG = 0.0002 ALAMA C = -1.7

FLAPPING				LAGGING			
A0	3.543			A0	2.515		
A1	-0.023	B1	-0.158	A1	-0.075	B1	-0.028
A2	-0.420	B2	-0.421	A2	-0.	B2	0.039
A2	0.051	B3	-0.327	A3	0.028	B3	-0.016
A4	0.141	B4	0.090	A4	0.006	B4	0.009
A3	0.012	B3	0.014	A8	0.002	B5	0.002
A6	0.013	B6	0.047	A6	-0.	B4	0.003
A7	-0.012	B7	0.026	A7	0.003	S7	-0.001
A8	0.004	B8	0.017	A8	-0.004	B6	-0.0C1
A9	-0.	B9	0.021	A9	-0.001	B6	-0.003
A10	-0.024	B10	0.040	A10	-0.	B10	-0.001

ALAMA S = 0 CL/SIG = 0.002 THETA = -1
CO/SIG = 0.0002 ALAMA C = -0.7

FLAPPING				LAGGING			
A0	0.390			A0	2.527		
A1	-0.043	B1	-0.140	A1	0.084	B1	-0.071
A2	0.190	B2	-0.507	A2	-0.007	B2	0.036
A3	0.078	B3	-0.022	A3	0.003	B3	0.C01
A4	0.108	A4	-0.004	A4	0.003	B4	-0.007
A5	-0.008	B5	0.055	A3	0.002	B5	-0.001
AA	-0.018	B6	0.002	A6	0.001	B6	-0.
A7	0.004	B7	0.040	A7	-0.	B7	-0.001
A8	-0.008	B8	0.003	A8	-0.	B6	-0.
A6	0.008	B6	0.002	A9	-0.001	B6	-0.002
A10	-0.029	B10	0.046	A10	0.001	B10	-0.

ALPHA S = 0 CL/SIG = 0.010 THETA = 0
CG/SIG = 0.0001 ALAMA C = -1.9

FLAPPING				LAGGING			
A0	0.82E			A0	2.510		
A1	0.13C	B1	-0.064	A1	0.071	B1	-0.075
A2	0.115	B2	-0.474	A2	-0.005	B2	0.005
A3	0.08E	B3	-0.088	A2	0.004	B3	0.001
A4	C.09E	B4	0.004	A4	0.002	B4	-0.001
A5	-0.013	B5	0.054	A5	0.002	B5	0.001
A6	+0.02E	B6	0.004	A6	0.001	B6	-0.
A7	0.004	B7	0.036	A7	-0.	B7	-0.001
A8	+0.00S	B8	0.004	A8	-0.	B8	0.001
A9	C.00S	B5	0.002	A6	-0.001	B6	-0.001
A10	+0.025	B10	0.038	A10	0.003	B10	-0.001

ALAMA S = 0 CL/SIC 0.031 THETA = 2
CO/SIG = 0.0003 ALAMA C = -3.2

FLAPPING				LAGGING			
A0	1.663			A0	2.575		
A1	-0.160	B1	-0.183	A1	0.020	B1	-0.046
A2	-0.08A	B2	-0.438	A2	0.002	B2	0.005
A3	0.064	B3	-0.203	A3	0.011	B3	-0.008
A4	0.120	B4	0.011	A4	0.006	B4	0.002
A5	0.00A	B5	0.046	A5	-0.	B5	0.001
A6	-0.014	B6	0.016	A6	0.001	B6	-0.002
A7	0.008	B7	0.034	A7	-0.002	B7	0.001
B8	-0.007	B8	0.018	A8	0.001	B8	0.002
A9	-0.003	B9	0.016	A6	-0.004	B6	-0.002
B10	-0.038	B10	0.017	A10	0.002	B10	-0.

ALAMA S = 0 CL/SIG = 0.047 THETA = 4
CO/SIG = 0.0010 ALAMA C = -5.1

FLAPPING				LAGGING			
A0	2.834			A0	2.921		
A1	-0.045	B1	-0.173	A1	-0.040	A1	-0.037
A2	-0.304	B2	-0.402	A2	-0.004	B2	0.022
A3	0.100	B3	-0.300	A2	0.024	B3	-0.012
A4	0.104	B4	0.045	A4	0.003	B4	0.006
A5	0.025	B5	0.035	A5	-0.	B5	0.001
A6	-0.001	B6	0.034	AA	-0.002	B6	0.002
A7	0.003	B7	0.038	A7	0.001	B7	-0.
A8	-0.004	B8	0.024	A8	-0.002	B8	0.001
A6	-0.008	B6	0.018	A9	-0.001	B9	0.001
A10	-0.048	B10	0.010	A10	0.002	B10	0.002

TABLE I CONTINUED.

ADVANCE RATIO = 0.500

ALPHA S = 0 CL/SIG = 0.065 THETA = 6
CQ/SIG = 0.0026 ALPHA C = -7.1

FLAPPING						LAGGING					
A0	3.925					A0	5.755				
A1	-0.017	B1	0.284			A1	-0.115	B1	0.031		
A2	-0.567	B2	-0.515			A2	0.006	B2	0.025		
A3	0.193	B3	-0.452			A3	0.055	B3	-0.016		
A4	0.144	B4	0.113			A4	0.004	B4	0.018		
A5	0.042	B5	0.056			A5	0.001	B5	0.004		
A6	0.021	B6	0.070			A6	-0.001	B6	0.001		
A7	0.023	B7	0.022			A7	0.005	B7	-0.001		
A8	-0.022	B8	0.042			A8	0.001	B8	0.001		
A9	-0.033	B9	0.042			A9	-0.001	B9	-0.002		
A10	-0.026	B10	0.021			A10	0.001	B10	-0.001		

ALPHA S = -4 CL/SIG = 0.046 THETA = 6
CQ/SIG = 0.0022 ALPHA C = -9.5

FLAPPING						LAGGING					
A0	2.754					A0	3.575				
A1	-0.276	B1	-0.147			A1	-0.054	B1	0.001		
A2	-0.442	B2	-0.389			A2	0.001	B2	0.009		
A3	0.181	B3	-0.385			A3	0.026	B3	-0.008		
A4	0.124	B4	0.048			A4	0.008	B4	0.005		
A5	0.027	B5	0.026			A5	-0.	B5	-0.		
A6	-0.009	B6	0.014			A6	-0.002	B6	-0.		
A7	0.051	B7	0.004			A7	0.002	B7	-0.		
A8	0.015	B8	0.012			A8	-0.001	B8	-0.002		
A9	-0.008	B9	0.020			A9	0.001	B9	-0.		
A10	-0.018	B10	-0.015			A10	-0.001	B10	-0.001		

ALPHA S = -4 CL/SIG = 0.006 THETA = 2
CQ/SIG = 0.0004 ALPHA C = -6.0

FLAPPING						LAGGING					
A0	0.666					A0	2.716				
A1	-0.088	B1	-0.077			A1	0.085	B1	-0.050		
A2	-0.007	B2	-0.450			A2	0.015	B2	-0.015		
A3	0.084	B3	-0.508			A3	-0.	B3	-0.002		
A4	0.093	B4	-0.028			A4	0.004	B4	0.001		
A5	-0.004	B5	0.048			A5	0.001	B5	-0.005		
A6	-0.025	B6	-0.001			A6	0.002	B6	0.001		
A7	0.001	B7	0.059			A7	-0.	B7	0.002		
A8	-0.006	B8	0.011			A8	0.001	B8	0.001		
A9	0.007	B9	0.009			A9	-0.001	B9	-0.001		
A10	-0.029	B10	0.010			A10	0.001	B10	-0.		

ALPHA S = -4 CL/SIG = 0.060 THETA = 8
CQ/SIG = 0.0041 ALPHA C = -11.5

FLAPPING						LAGGING					
A0	5.540					A0	4.562				
A1	-0.081	B1	-0.019			A1	-0.144	B1	0.057		
A2	-0.675	B2	-0.501			A2	0.007	B2	0.020		
A3	0.248	B3	0.502			A3	0.049	B3	-0.019		
A4	0.104	B4	0.107			A4	0.002	B4	0.017		
A5	0.052	B5	0.020			A5	0.001	B5	0.005		
A6	0.006	B6	0.046			A6	-0.	B6	0.001		
A7	0.067	B7	0.007			A7	0.002	B7	-0.002		
A8	0.007	B8	0.040			A8	0.004	B8	-0.002		
A9	-0.022	B9	0.027			A9	0.001	B9	-0.001		
A10	0.017	B10	0.018			A10	0.001	B10	-0.		

ALPHA S = -4 CL/SIG = 0.025 THETA = 4
CQ/SIG = 0.0010 ALPHA C = -7.9

FLAPPING						LAGGING					
A0	1.607					A0	2.913				
A1	-0.109	B1	0.075			A1	0.029	B1	-0.042		
A2	-0.173	B2	-0.350			A2	0.006	B2	0.003		
A3	0.115	B3	-0.220			A3	0.008	B3	-0.009		
A4	0.128	B4	-0.014			A4	0.005	B4	0.001		
A5	0.021	B5	0.026			A5	0.002	B5	-0.003		
A6	-0.009	B6	-0.004			A6	0.001	B6	-0.		
A7	0.018	B7	0.019			A7	-0.	B7	0.001		
A8	-0.001	B8	0.014			A8	-0.002	B6	-0.002		
A9	-0.004	B9	0.012			A9	-0.001	B9	0.001		
A10	-0.029	B10	0.008			A10	-0.	B10	0.001		

ALPHA S = -8 CL/SIG = -0.009 THETA = 4
CQ/SIG = 0.0003 ALPHA C = -10.6

FLAPPING						LAGGING					
A0	-0.019					A0	2.755				
A1	-0.082	B1	-0.128			A1	0.043	B1	-0.054		
A2	-0.124	B2	-0.540			A2	-0.005	B2	-0.017		
A3	0.160	B3	-0.154			A3	-0.002	B3	-0.003		
A4	0.073	B4	-0.015			A4	0.010	B4	0.001		
A5	0.018	B5	0.021			A5	0.004	B5	-0.		
A6	-0.004	B6	0.005			A6	-0.	B6	0.001		
A7	0.014	B7	0.021			A7	0.001	B7	0.001		
A8	0.001	B8	0.006			A8	0.001	B8	0.001		
A9	0.005	B9	0.006			A9	0.001	B9	0.001		
A10	-0.016	B10	0.014			A10	-0.001	B10	-0.		

TABLE I CONTINUED.

ADVANCE RATIO = 0.389

ALPHA S = -8 CL/SIG = 0.018 THETA = 6
CO/SIG = 0.0015 ALPHA C = -12.6

FLAPPING				LAGGING			
A0	0.983			A0	3.267		
A1	0.127	B1	-0.088	A1	0.025	B1	-0.027
A2	-0.294	B2	-0.311	A2	0.001	B2	0.005
A3	0.111	B3	-0.253	A3	0.007	B3	-0.010
A4	0.093	B4	-0.006	A4	0.008	B4	0.004
A5	0.044	B5	0.006	A5	0.002	B5	-0.
A6	0.001	B6	0.006	A6	-0.001	B6	-0.001
A7	0.025	B7	0.008	A7	0.001	B7	0.001
A8	0.004	B8	0.007	A8	-0.	B8	-0.001
A9	0.005	B9	0.009	A9	0.001	B9	0.001
A10	-0.008	B10	0.008	A10	0.001	B10	-0.

ALPHA S = -8 CL/SIG = 0.027 THETA = 7
CO/SIG = 0.0022 ALPHA C = -13.5

FLAPPING				LAGGING			
A0	1.454			A0	3.675		
A1	0.056	B1	-0.077	A1	-0.012	B1	-0.010
A2	-0.393	B2	-0.314	A2	-0.006	B2	-0.003
A3	0.125	B3	-0.309	A3	0.008	B3	-0.008
A4	0.100	B4	-0.007	A4	0.009	B4	0.003
A5	0.047	B5	0.004	A5	0.002	B5	0.001
A6	0.007	B6	0.010	A6	0.002	B6	0.001
A7	0.020	B7	-0.009	A7	-0.	B7	-0.
A8	0.006	B8	0.007	A8	-0.002	B8	-0.001
A9	-0.001	B9	0.006	A9	0.001	B9	0.001
A10	-0.011	B10	0.005	A10	-0.	B10	-0.

ALPHA S = -8 CL/SIG = 0.038 THETA = 8
CO/SIG = 0.0032 ALPHA C = -14.6

FLAPPING				LAGGING			
A0	2.073			A0	4.209		
A1	-0.037	B1	-0.145	A1	-0.067	B1	0.011
A2	-0.535	B2	-0.320	A2	-0.	B2	0.008
A3	0.170	B3	-0.378	A3	0.021	B3	-0.010
A4	0.095	B4	0.013	A4	0.009	B4	0.009
A5	0.061	B5	0.006	A5	0.001	B5	0.001
A6	0.003	B6	0.014	A6	-0.	B6	-0.
A7	0.029	B7	-0.002	A7	-0.	B7	-0.001
A8	0.008	B8	0.013	A8	-0.	B8	-0.001
A9	-0.	B9	0.010	A9	-0.001	B9	0.002
A10	0.001	B10	-0.001	A10	0.001	B10	-0.001

ALPHA S = -8 CL/SIG = 0.046 THETA = 9
CO/SIG = 0.0042 ALPHA C = -15.1

FLAPPING				LAGGING			
A0	2.304			A0	4.707		
A1	-0.009	B1	-0.223	A1	-0.114	B1	0.038
A2	-0.437	B2	-0.363	A2	-0.002	B2	0.005
A3	0.203	B3	-0.440	A3	0.035	B3	-0.015
A4	0.104	B4	0.027	A4	0.009	B4	0.012
A5	0.077	B5	-0.005	A5	0.001	B5	0.003
A6	0.007	B6	0.024	A6	-0.	B6	0.001
A7	0.030	B7	-0.012	A7	0.001	B7	-0.002
A8	0.005	B8	0.013	A8	0.001	B8	-0.002
A9	-0.003	B9	0.008	A9	-0.001	B9	-0.
A10	0.007	B10	0.003	A10	0.001	B10	0.001

TABLE I CONTINUED.

ADVANCE RATIO = 0.488

ALPPA S = 0 CL/SIG = 0.003 THETA = -2
CO/SIG = 0.0001 ALPHA C = 0.8

FLAPPING				LAGGING			
A0	0.163			A0	2.615		
A1	-0.348	B1	-0.079	A1	0.132	B1	-0.110
A2	0.385	B2	-0.600	A2	-0.015	B2	0.005
A3	0.084	B3	0.028	A3	0.009	B3	0.002
A4	0.014	A6	0.040	A4	0.007	B4	-0.001
A5	-0.014	B5	0.057	A5	0.002	B5	-0.002
A6	-0.043	B6	0.055	A6	0.002	B6	0.001
A7	-0.021	B7	0.051	A7	0.005	B7	-0.002
A8	-0.027	B8	-0.004	A8	0.002	B8	-0.
A9	-0.014	B9	-0.011	A9	0.004	B5	0.006
A10	-0.009	B10	-0.019	A10	-0.001	B10	0.002

ALPPA S = 0 CL/SIG = 0.015 THETA = 0
CO/SIG = 0.0000 ALPHA C = -1.6

FLAPPING				LAGGING			
A0	0.783			A0	2.546		
A1	-0.048	B1	0.020	A1	0.110	B1	-0.114
A2	0.144	B2	-0.646	A2	-0.007	B2	0.008
A3	0.054	B5	-0.119	A3	0.009	B5	-0.007
A4	0.053	B4	-0.004	A4	0.012	A6	0.002
A5	0.010	B3	0.842	A5	0.002	B9	0.001
A6	-0.003	B6	0.002	A6	-0.001	A6	0.002
A7	0.003	B7	0.022	A7	0.002	B7	-0.002
A8	-0.013	B8	-0.002	A8	0.001	A6	0.001
A5	-0.002	B9	-0.005	A5	0.005	B9	0.003
A10	-0.003	B10	0.010	A10	-0.	B10	0.001

ALPPA S = 0 CL/SIG = 0.053 THETA = 2
CO/SIG = 0.0001 ALPHA C = -3.5

FLAPPING				LAGGING			
A0	1.726			A0	2.337		
A1	-0.486	B1	0.087	A1	0.035	B1	-0.108
A2	-0.115	B2	-0.620	A2	-0.	B2	0.011
A3	0.012	B3	-0.307	A5	0.011	B5	-0.026
A6	0.000	A6	-0.060	A4	0.023	B4	0.004
A5	0.024	B3	0.027	A5	0.004	B5	-0.
A6	-0.007	B6	0.053	A6	0.002	A6	0.002
A7	-0.050	B7	0.028	A7	0.001	B7	-0.001
A8	-0.014	B8	0.002	A8	0.003	B8	0.001
A9	-0.003	B9	0.001	A9	0.001	B5	-0.
A10	-0.018	B10	0.017	A10	0.001	B10	-0.

ALPPA S = 0 CL/SIG = 0.044 THETA = 4
CO/SIG = 0.0008 ALPHA C = -5.8

FLAPPING				LAGGING			
A0	2.373			A0	2.727		
A1	-0.582	B1	0.160	A1	0.005	B1	-0.081
A2	-0.343	B2	-0.998	A2	0.005	B2	0.015
A3	-0.001	B5	-0.448	A5	0.016	B5	-0.044
A4	0.053	B4	-0.000	A6	0.030	B4	0.007
A3	0.024	B3	-0.012	A5	0.001	B3	-0.001
A6	-0.001	B6	0.011	A6	0.002	B6	-0.
A7	-0.031	B7	5.014	A7	0.002	B7	-0.002
A8	-0.010	B8	0.001	A8	0.002	B8	0.003
A9	-0.004	B4	0.011	A9	0.005	B5	0.005
A10	-0.031	B10	0.012	A10	0.001	B10	0.001

ALPHA 3 = 0 CL/SIG = 0.056 THETA = 6
CO/SIG = 0.0022 ALPHA C = -7.5

FLAPPING				LAGGING			
A0	5.034			A0	5.416		
A1	-0.070	B1	-0.027	A3	-0.094	B1	-0.017
A2	-0.560	B2	-0.615	A2	0.017	B2	0.055
A3	0.024	B3	-0.095	A5	0.048	B5	-0.060
A4	0.152	B4	-0.044	B4	0.051	A6	0.018
A3	0.043	B5	-0.048	A3	0.001	B5	-0.
A6	0.011	B6	0.044	A6	0.002	B6	-0.004
A7	-0.070	B7	-0.044	A7	-0.	B7	-0.007
A8	0.010	B8	-0.	A8	-0.007	B8	-0.
A5	0.006	B5	0.018	A9	0.001	B5	0.001
A10	-0.018	B10	0.008	A30	0.002	B10	-0.

ALPPA S = 0 CL/SIG = 0.070 THETA = 8
CO/SIG = 0.0042 ALPHA C = -9.6

FLAPPING				LAGGING			
A0	3.873			A0	4.285		
A1	-0.360	B1	0.036	A1	-0.228	B1	0.093
A2	-0.845	B2	-0.695	A2	0.029	B2	0.038
A3	0.078	B5	-0.771	A5	0.081	B5	-0.093
A4	0.224	B4	-0.007	A6	0.044	B4	0.012
A5	0.050	B5	-0.042	A5	0.010	B5	-0.
A6	0.041	B6	0.042	A6	0.006	B6	-0.003
A7	-0.061	B7	-0.075	A7	-0.005	B7	-0.010
A8	0.026	B8	0.011	A8	-0.010	B8	-0.
A5	-0.001	B9	0.015	A9	0.001	B9	-0.003
A10	-0.024	B10	-0.022	A10	-0.	B10	-0.003

ALPPA S = 6 CL/SIG = 0.088 THETA = 10
CO/SIG = 0.0064 ALPHA C = -11.7

FLAPPING				LAGGING			
A0	4.284			A0	5.401		
A1	0.014	B1	-0.054	A1	-0.538	B1	0.163
A2	-1.044	B2	-0.828	A8	0.031	B2	0.077
A5	0.237	B5	-0.815	A5	0.105	B3	-0.059
A6	0.277	B4	0.074	A4	0.031	B4	0.025
A5	0.070	B5	-0.022	A5	0.018	B5	0.015
A6	8.024	B6	0.077	A6	0.015	B6	0.002
A7	0.016	B7	-0.146	A7	0.003	B7	-0.017
A8	0.057	B8	0.033	A8	-0.009	B8	-0.007
A9	-0.003	B5	0.018	A5	0.003	B9	-0.006
A10	-0.021	B10	-0.045	A10	-0.001	B10	-0.001

ALPPA S = 0 CL/SIG = 0.085 THETA = 11
CO/SIG = 0.0077 ALPHA C = -12.8

FLAPPING				LAGGING			
A0	4.553			A0	9.074		
A1	-0.468	B1	-0.001	A1	-0.426	B1	0.225
A2	-1.146	B2	-0.929	A2	0.055	B2	0.095
A3	0.563	B5	-0.854	A5	0.125	B5	-0.110
A4	0.285	A6	0.158	A6	0.053	A6	0.035
A3	0.075	B5	0.001	A6	0.027	B5	0.016
A6	0.002	B6	0.047	A6	0.020	B6	-0.002
A7	0.075	B7	-0.251	A7	0.004	B7	-0.025
A8	0.057	B8	0.029	A5	-0.010	B8	-0.014
A5	-0.013	B5	0.010	A9	0.007	B9	-0.001
A10	-0.014	B10	-0.055	A10	0.001	B10	0.001

ALPHA 3 = -4 CL/SIG = -0.008 THETA = 0
CO/SIG = 0.0001 ALPHA C = -4.0

FLAPPING				LAGGING			
A0	-0.616			A0	2.565		
A1	-0.440	B1	0.009	A1	0.135	B1	-0.116
A2	0.510	B2	-0.588	A2	-0.002	B2	0.001
A3	0.084	B3	0.035	A3	0.004	B5	-0.003
A4	-0.025	B4	0.030	A4	0.009	A6	0.001
A5	0.050	B5	0.035	A5	0.002	B5	0.001
A6	-0.020	A6	0.001	A6	0.001	A6	0.001
A7	0.089	B7	0.025	A7	0.001	B7	-0.
A8	-0.005	B8	0.014	A8	-0.	B8	-0.
A5	0.001	B9	-0.005	A5	-0.	B5	-0.
A10	0.022	B10	0.055	A10	-0.	B10	0.001

TABLE I CONTINUED.

ADVANCE RATIO = 0.488

ALPHA S = -4 CL/SIG = 0.003 THETA = 2
CD/SIG = 0.0004 ALPHA C = -3.9

FLAPPING				LAGGING			
A0	0.114			A0	2.373		
A1	-0.234	B1	0.131	A1	0.117	B1	-0.109
A2	0.095	B2	-0.939	A2	-0.003	B2	0.003
A3	0.07C	B3	-0.097	A3	0.001	B3	-0.010
A4	0.01A	B4	-0.013	A4	0.014	B4	0.002
A5	0.043	B5	0.021	A5	-0.001	B5	0.002
A6	-0.014	B6	0.021	A6	0.001	B6	0.004
A7	0.09A	B7	-0.004	A7	0.001	B7	-0.003
A8	-0.002	B8	0.008	A8	0.002	B8	-0.
A9	0.002	B9	0.004	A9	-0.001	B9	0.001
A10	0.013	B10	0.021	A10	-0.001	B10	-0.001

ALPHA S = -4 CL/SIG = 0.020 THETA = 4
CD/SIG = 0.0009 ALPHA C = -7.9

FLAPPING				LAGGING			
A0	0.898			A0	2.730		
A1	-0.193	B1	-0.010	A1	0.069	B1	-0.079
A2	0.129	B2	-0.494	A2	0.003	B2	0.001
A3	0.049	B3	-0.247	A3	0.009	B3	-0.023
A4	0.049	B4	-0.050	A4	0.018	B4	0.003
A5	0.03C	B5	-0.012	A5	0.002	B5	-0.
A6	-0.004	B6	-0.009	A6	-0.	B6	0.002
A7	0.042	B7	-0.029	A7	0.002	B7	-0.001
A8	0.012	B8	0.007	A8	0.001	B8	-0.001
A9	0.007	B9	0.008	A9	0.001	B9	0.002
A10	0.003	B10	0.032	A10	-0.	B10	-0.

ALPHA S = -4 CL/SIG = 0.039 THETA = 6
CD/SIG = 0.0019 ALPHA C = -9.9

FLAPPING				LAGGING			
A0	1.73A			A0	3.133		
A1	-0.397	B1	-0.039	A1	-0.003	B1	-0.046
A2	-0.383	B2	-0.474	A2	0.007	B2	0.004
A3	0.032	B3	-0.472	A3	0.014	B3	-0.048
A4	0.122	B4	-0.076	A4	0.028	B4	0.007
A5	0.061	B5	-0.043	A5	0.002	B5	-0.
A6	0.007	B6	0.007	A6	0.003	B6	-0.003
A7	-0.011	B7	-0.039	A7	-0.002	B7	-0.002
A8	0.013	B8	0.008	A8	-0.002	B8	-0.
A9	0.006	B9	0.013	A9	-0.001	B9	0.002
A10	-0.019	B10	0.018	A10	0.002	B10	-0.001

ALPHA S = -4 CL/SIG = 0.048 THETA = 8
CD/SIG = 0.0034 ALPHA C = -11.9

FLAPPING				LAGGING			
A0	2.3A8			A0	3.950		
A1	-0.244	B1	0.011	A1	-0.094	B1	0.011
A2	-0.925	B2	-0.927	A2	0.017	B2	0.019
A3	0.109	B3	-0.627	A3	0.048	B3	-0.094
A4	0.199	B4	-0.033	A4	0.032	B4	0.019
A5	0.09G	B5	-0.068	A5	0.009	B5	-0.002
A6	0.039	B6	0.036	A6	0.003	B6	-0.
A7	-0.032	B7	-0.071	A7	-0.004	B7	-0.007
A8	0.01A	B8	0.009	A8	-0.003	B8	0.001
A9	0.006	B9	0.019	A9	-0.002	B9	0.001
A10	-0.01E	B10	0.008	A10	0.002	B10	-0.

ALPHA S = -4 CL/SIG = 0.061 THETA = 10
CD/SIG = 0.0093 ALPHA C = -14.1

FLAPPING				LAGGING			
A0	3.186			A0	4.932		
A1	-0.262	B1	0.048	A1	-0.231	B1	0.097
A2	-0.893	B2	-0.829	A2	0.027	B2	0.060
A3	0.199	B3	-0.801	A3	0.081	B3	-0.093
A4	0.227	B4	-0.010	A4	0.046	B4	0.023
A5	0.130	B5	-0.068	A5	0.019	B5	-0.002
A6	0.040	B6	0.082	A6	-0.010	B6	-0.006
A7	-0.033	B7	-0.231	A7	-0.001	B7	-0.012
A8	0.040	B8	0.023	A8	-0.007	B8	-0.008
A9	-0.	B9	0.034	A9	0.009	B9	-0.003
A10	-0.024	B10	-0.007	A10	0.004	B10	-0.001

ALPHA S = -4 CL/SIG = 0.070 THETA = 12
CD/SIG = 0.0080 ALPHA C = -15.6

FLAPPING				LAGGING			
A0	3.391			A0	6.219		
A1	-0.128	B1	-0.017	A1	-0.381	B1	0.17[illegible]
A2	-1.139	B2	-0.831	A2	0.023	B2	0.054
A3	0.313	B3	-0.921	A3	0.110	B3	-0.099
A4	0.272	B4	0.086	A4	0.034	B4	0.039
A5	0.148	B5	-0.043	A5	0.023	B5	0.015
A6	0.023	B6	0.096	A6	0.012	B6	-0.005
A7	0.024	B7	-0.198	A7	0.006	B7	-0.019
A8	0.042	B8	0.033	A8	-0.003	B8	-0.012
A9	-0.011	B9	0.026	A9	0.006	B9	-0.005
A10	-0.009	B10	-0.033	A10	0.002	B10	-0.003

ALPHA S = -4 CL/SIG = 0.073 THETA = 13
CD/SIG = 0.0099 ALPHA C = -16.8

FLAPPING				LAGGING			
A0	3.72[illegible]			A0	7.009		
A1	-0.114	B1	-0.002	A1	-0.433	B1	0.217
A2	-1.24G	B2	-0.971	A2	0.026	B2	0.0A7
A3	0.425	B3	-0.932	A3	0.123	B3	-0.102
A4	0.263	B4	0.168	A4	0.039	B4	0.048
A5	0.137	B5	-0.023	A5	0.033	B5	0.023
AA	-0.004	BA	0.106	A6	0.018	B6	-0.
A7	0.09C	B7	-0.299	A7	0.009	B7	-0.022
A8	0.033	B8	0.038	A8	-0.010	B8	-0.010
A9	-0.017	B9	0.017	A9	0.013	B9	0.001
A10	0.006	B10	-0.031	A10	0.006	B10	-0.002

ALPHA S = -8 CL/SIG = -0.006 THETA = 4
CD/SIG = 0.0000 ALPHA C = -10.4

FLAPPING				LAGGING			
A0	-0.319			A0	-2.339		
A1	-0.177	B1	0.193	A1	0.091	B1	-0.098
A2	-0.011	B2	-0.889	A2	-0.001	B2	-0.008
A3	0.101	B3	-0.216	A3	0.007	B3	-0.009
A4	0.043	B4	0.003	A4	0.010	B4	-0.001
A5	0.029	B5	-0.009	A5	0.003	B5	0.002
A6	-0.020	B6	-0.018	A6	0.002	B6	0.001
A7	0.004	B7	0.061	A7	0.004	B7	0.001
A8	0.010	B8	0.007	A8	-0.	B8	-0.001
A9	0.011	B9	0.008	A9	-0.009	B9	0.002
A10	0.019	B10	0.021	A10	0.001	B10	-0.001

ALPHA S = -8 CL/SIG = 0.010 THETA = 6
CD/SIG = 0.0011 ALPHA C = -12.2

FLAPPING				LAGGING			
A0	0.331			A0	-1.A01		
A1	-0.241	B1	0.028	A1	0.060	B1	-0.070
A2	-0.232	B2	-0.373	A2	-0.	B2	-0.007
A3	0.007	B3	-0.260	A3	0.004	B3	-0.019
A4	0.073	B4	-0.037	A4	0.314	B4	-0.002
A5	0.038	B5	-0.027	A5	0.009	B5	-0.002
A6	0.003	B6	-0.024	A6	0.002	B6	-0.
A7	0.049	B7	0.00[illegible]	A7	0.003	B7	0.001
A8	0.011	B8	0.008	A8	0.002	B8	0.001
A9	0.010	B9	0.007	A9	-0.	B9	0.002
A10	0.011	B10	0.018	A10	0.001	B10	0.001

TABLE I CONTINUED.

ADVANCE RATIO = 0.400

ALPHA S = -8 CL/SIG = 0.021 THETA = 8
CD/SIG = 0.0023 ALPHA C = -14.8

FLAPPING				LAGGING			
A0	1.036			A0	-1.154		
A1	0.151	B1	0.076	A1	0.010	B1	-0.046
A2	-0.463	B2	-0.328	A2	0.002	B2	0.001
A3	0.107	B3	-0.433	A3	0.022	B3	-0.042
A4	0.123	B4	-0.049	A4	0.022	B4	0.033
A5	0.073	B5	-0.050	A5	0.004	B5	-0.033
A6	0.012	B6	0.002	A6	-0.001	B6	-0.003
A7	0.013	B7	-0.	A7	0.001	B7	-0.002
A8	0.017	B8	0.003	A8	-0.001	B8	0.003
A9	0.013	B9	0.011	A9	0.001	B9	0.001
A10	-0.002	B10	0.011	A10	0.002	B10	0.001

ALPHA S = -8 CL/SIG = 0.062 THETA = 14
CD/SIG = 0.0056 ALPHA C = -19.8

FLAPPING				LAGGING			
A0	2.825			A0	2.428		
A1	-0.401	B1	0.027	A1	-0.340	B1	0.127
A2	-1.267	B2	-0.896	A2	-0.	B2	0.027
A3	0.414	B3	-0.993	A3	0.073	B3	-0.848
A4	0.225	B4	0.095	A4	0.045	B4	0.041
A5	0.102	B5	-0.024	A5	0.022	B5	0.004
A6	-0.017	B6	0.067	A6	0.010	B6	-0.001
A7	0.070	B7	-0.125	A7	0.010	B7	0.011
A8	0.024	B8	0.048	A8	-0.008	B8	0.008
A9	-0.	B9	0.011	A9	0.008	B9	0.005
A10	0.019	B10	0.010	A10	0.002	B10	0.001

ZERO LAG DAMPING

ALPHA S = -4 CL/SIG = 0.022 THETA = 6
CD/SIG = 0.0017 ALPHA C = -10.8

FLAPPING				LAGGING			
A0	1.483			A0	0.787		
A1	0.134	B1	0.026	A1	0.011	B1	-0.069
A2	-0.542	B2	-0.479	A2	0.014	B2	0.011
A3	0.045	B3	-0.486	A3	0.012	B3	-0.081
A4	0.125	B4	-0.121	A4	0.026	B4	0.008
A5	0.059	B5	-0.044	A5	0.002	B5	-0.007
A6	0.018	B6	0.002	A6	-0.	B6	-0.002
A7	-0.645	B7	-0.008	A7	-0.002	B7	-0.003
A8	0.022	B8	0.207	A8	0.002	B8	0.002
A9	0.010	B9	0.011	A9	0.003	B9	0.003
B10	0.091	B10	0.017	A10	0.002	B10	0.001

ALPHA S = -8 CL/SIG = 0.039 THETA = 10
CD/SIG = 0.0043 ALPHA C = -16.1

FLAPPING				LAGGING			
A0	2.036			A0	-0.221		
A1	-0.475	B1	0.058	A1	-0.078	B1	0.026
A2	-0.727	B2	-0.390	A2	0.009	B2	0.009
A3	0.152	B3	-0.869	A3	0.036	B3	-0.058
A4	0.165	B4	-0.037	A4	0.030	B4	0.016
A5	0.112	B5	-0.076	A5	0.012	B5	-0.003
A6	0.044	B6	0.020	A6	0.004	B6	-0.002
A7	0.004	B7	-0.054	A7	-0.	B7	-0.003
A8	0.021	B8	0.014	A8	0.003	B8	-0.002
A9	0.008	B9	0.014	A9	0.003	B9	0.004
A10	-0.002	B10	0.010	A10	0.002	B10	0.001

ZERO LAG DAMPING

ALPHA S = -4 CL/SIG = -0.007 THETA = 2
CD/SIG = 0.0002 ALPHA C = -6.6

FLAPPING				LAGGING			
A0	0.132			A0	0.036		
A1	0.440	B1	-0.213	A2	0.115	B1	-0.118
A2	0.003	B2	-0.547	A2	0.001	B2	-0.004
A3	0.093	B3	-0.093	A8	-0.014	B3	-0.020
A4	0.025	B4	-0.013	B6	0.010	B4	-0.
A5	0.016	B5	0.011	A6	0.002	B5	0.001
A6	-0.022	B6	-0.012	A8	0.003	B6	-0.
A7	0.072	B7	-0.058	A7	0.002	B7	-0.
A8	0.004	B8	0.014	A6	-0.	B8	-0.003
A9	0.004	B9	-0.002	A9	-0.002	B9	0.003
A10	0.017	B10	0.007	A20	-0.	B10	-0.001

ZERO LAG DAMPING

ALPHA S = -4 CL/SIG = 0.035 THETA = 8
CD/SIG = 0.0029 ALPHA C = -12.9

FLAPPING				LAGGING			
A0	2.456			A0	1.509		
A1	0.326	B1	0.178	A1	-0.469	B1	0.005
A2	-0.844	B2	-0.396	A2	0.032	B2	0.050
A3	0.014	B3	-0.700	A8	0.034	B3	-0.116
A4	0.232	B4	-0.244	B4	0.036	B4	0.014
A5	0.076	B5	-0.043	A6	0.006	B5	-0.009
A6	0.006	B6	0.021	A8	-0.003	B6	-0.006
A7	-0.071	B7	-0.014	A7	-0.007	B7	-0.002
A8	0.020	B8	-0.006	A6	-0.002	A8	0.006
A9	0.010	B9	0.016	A9	0.004	B9	0.002
A10	-0.002	B10	0.023	A20	0.001	B10	0.001

ALPHA S = -8 CL/SIG = 0.050 THETA = 12
CD/SIG = 0.0067 ALPHA C = -18.2

FLAPPING				LAGGING			
A0	2.808			A0	0.998		
A1	-0.270	B1	0.102	A1	-0.197	B1	0.076
A2	-0.968	B2	-0.589	A2	0.006	B2	0.015
A3	0.241	B3	-0.812	A3	0.044	B3	-0.040
A4	0.172	B4	-0.003	A4	0.037	B4	0.022
A5	0.148	B5	-0.072	A5	0.016	B5	-0.001
A6	0.025	B6	0.044	A6	-0.	B6	-0.003
A7	-0.021	B7	-0.085	A7	0.001	B7	-0.005
A8	0.020	B8	0.020	A8	-0.005	B8	-0.004
A9	0.006	B9	0.017	A9	0.015	B9	-0.
A10	0.003	B10	0.016	A10	0.012	B10	0.001

ZERO LAG DAMPING

ALPHA S = -4 CL/SIG = 0.010 THETA = 4
CD/SIG = 0.0009 ALPHA C = -8.4

FLAPPING				LAGGING			
A0	1.013			A0	0.359		
A1	-0.050	B1	-0.049	A1	0.071	B1	-0.096
A2	-0.269	B2	-0.519	A2	0.008	B2	-0.
A3	0.043	B5	-0.284	A3	-0.008	B5	-0.042
A4	0.058	B4	-0.073	A4	0.014	B4	0.001
A5	0.043	B5	-0.023	A5	0.002	B5	-0.001
A6	-0.003	B6	-0.017	A6	-0.	B6	0.001
A7	0.049	B7	-0.050	A7	0.001	B7	-0.002
A8	0.008	B8	0.006	A8	-0.001	B8	-0.002
A9	0.006	B9	0.006	A9	-0.	B9	0.003
A10	0.014	B10	0.010	A10	0.001	B10	-0.001

ZERO LAG DAMPING

ALPHA S = -4 CL/SIG = 0.051 THETA = 10
CD/SIG = 0.0049 ALPHA C = -14.6

FLAPPING				LAGGING			
A0	3.090			A0	2.590		
A1	0.151	B1	-0.020	A1	-0.248	B1	0.126
A2	-0.976	B2	-0.624	A2	0.042	B2	0.061
A3	0.153	B3	-0.806	A3	0.120	B3	-0.156
A4	0.251	B4	-0.043	A4	0.050	B4	0.022
A5	0.089	B5	-0.097	A5	0.010	B5	-0.013
A6	0.033	B6	0.032	A6	-0.004	B6	-0.014
A7	-0.101	B7	-0.056	A7	-0.012	B7	-0.008
A8	0.036	B8	0.001	A8	-0.009	B8	0.007
A9	0.008	B9	0.020	A9	0.006	B9	-0.
A10	-0.005	B10	0.016	A10	-0.	B10	0.002

TABLE I CONTINUED.

ADVANCE RATIO = 0.085

ALPHA 3 = 4 CL/SIG = 0.008 THETA = -7
CO/BIO = -0.0002 ALPHA C = 7.1

FLAPPING				LAGGING			
A0	-0.037			A0	-0.		
A1	0.826	B1	0.087	A1	-0.	B1	-0.
A2	6.702	B2	-1.468	A2	-0.	B2	-0.
A3	-0.028	B3	0.103	A3	-0.	B3	-0.
A4	-0.06C	BA	0.086	A4	-0.	BA	-0.
A9	0.112	B2	-0.020	A2	-0.	B9	-0.
A6	-0.004	B6	-0.016	A4	-0.	B6	-0.
A7	0.54A	B7	-0.097	A7	-0.	B7	-0.
4B	0.813	BB	0.03A	A4	-0.	BB	-0.
A9	-0.00[illegible]	B9	0.019	A9	-0.	B9	-0.
A10	-0.008	B10	0.009	A10	-0.	B10	-0.

ALPHA 3 = 4 CL/BIG = 0.015 THETA = -6
CO/3IG = -0.0004 ALPHA C = 9.9

FLAPPING				LAGGING			
AC	0.208			A0	-0.		
A1	-0.112	B1	-0.125	A1	-0.	B1	-0.
A2	0.220	B2	-1.418	A2	-0.	B2	-0.
A3	-0.047	B9	-0.008	4B	-0.	B9	-0.
AA	-0.093	BA	0.081	A4	-C.	B4	-0.
A2	0.113	B9	-0.071	AS	-0.	B9	-0.
AA	0.013	BA	-0.018	A4	-0.	B6	-0.
A7	0.02A	B7	-0.097	A7	-0.	B7	-0.
A8	0.018	BB	0.045	A0	-0.	BB	-0.
A9	-0.002	B9	0.014	A9	-0.	B9	-0.
A10	-0.00A	B10	0.012	A10	-0.	B10	-0.

ALPHA 9 = 4 CL/3IG = 0.021 THETA = -4
CO/3IG = -0.000A ALPHA C = 3.7

FLAPPING				LAGGING			
A0	0.443			A0	-0.		
41	-0.002	B1	-0.092	A1	-0.	B1	-0.
A2	0.209	B2	-1.332	42	-0.	B2	-0.
A3	-0.048	B3	-0.20A	A2	-0.	B3	-0.
A4	-0.098	B4	0.010	A4	-0.	B4	-0.
A9	0.079	B2	-0.031	A9	-0.	B5	-0.
A4	-0.021	BA	-0.009	AA	-0.	BA	-0.
A7	0.012	B7	-0.099	AT	-0.	B7	-0.
A8	0.010	BA	0.011	A8	-0.	BB	-0.
A9	-0.010	B9	0.009	A9	-0.	B9	-0.
A10	-0.018	B10	-0.001	A10	-0.	B10	-0.

ALPHA 5 = 4 CL/3IG = 0.031 THETA = -2
CO/3IG = -0.0007 ALPHA C = 1.4

FLAPPING				LAGGING			
A0	1.093			A0	-0.		
A1	0.110	B1	0.003	A1	-0.	B1	-0.
A2	-0.10A	B2	-1.222	A2	-0.	B2	-0.
A3	-0.094	B3	-0.390	A3	-0.	B3	-0.
A4	-0.024	B4	-0.098	A4	-0.	BA	-0.
A2	C.083	B9	-0.021	A9	-0.	B9	-0.
A6	-0.021	BA	0.001	A6	-0.	BA	-0.
A7	0.013	B7	-0.068	A7	-0.	B7	-0.
A8	-0.012	BB	0.019	A8	-0.	BB	-0.
A2	-0.012	B9	0.008	A9	-0.	B9	-0.
A10	-0.013	B10	0.008	A10	-0.	B10	-0.

ALPHA 3 = 4 CL/2IG = 0.059 THETA = 0
CO/5IG = -0.0009 ALPHA C = -0.8

FLAPPINC				LAGGING			
AC	1.A04			A0	-0.		
A1	0.087	B1	0.109	A1	-0.	B1	-0.
A2	-0.421	B2	-1.198	A2	-0.	B2	-0.
A2	-0.18A	B3	-0.009	AS	-0.	B9	-0.
A4	-0.098	B4	-0.210	A4	-0.	BA	-0.
A2	0.07A	B2	-0.025	AS	-0.	B9	-0.
A6	-0.026	BA	-0.028	A4	-0.	BA	-0.
A7	0.094	B7	-0.078	A7	-0.	B7	-0.
A8	0.003	BB	0.028	A8	-0.	BB	-0.
A9	-0.004	B9	0.017	A9	-0.	B9	-0.
A10	-0.002	B10	0.011	A10	-0.	B10	-0.

ALPH4 3 = 4 CL/3IC = 0.030 THETA = 2
CO/9IG = -0.00J1 4LPHA C = -3.1

FLAPPINC				LAGGING			
A0	2.04A			A0	-0.		
A1	0.080	81	0.062	41	-0.	B1	-0.
A2	-0.449	B2	-1.022	A2	-0.	B2	-0.
A2	-0.249	03	-0.489	A3	-0.	B3	-0.
A4	-0.0A0	B4	-0.221	A4	-0.	B4	-0.
A2	0.04A	B3	-0.032	A2	-0.	B3	-0.
AA	-0.029	B6	-0.042	4A	-0.	BA	-0.
A7	0.039	B7	-0.0A4	A7	-0.	B7	-0.
A8	0.010	BB	0.002	A8	-0.	BB	-0.
49	0.001	B9	0.012	49	-0.	B9	-0.
410	-0.002	B10	0.009	A10	-0.	B10	-0.

ALPHA 5 = 4 CL/3IG = 0.022 THETA = 4
CO/EIG = 0.0009 ALPHA C = -9.3

FLAPPING				LAGGING			
A0	2.252			A0	-0.		
A1	0.22A	B1	-0.0A6	A1	-0.	B1	-0.
A2	-0.92A	B2	-0.987	A2	-0.	B2	-0.
A3	-0.299	B2	-0.084	AS	-0.	B9	-0.
A4	-0.022	B4	-0.568	A4	-0.	BA	-0.
A9	0.044	B9	-0.022	A9	-0.	B9	-0.
A6	-0.001	B6	-0.098	A6	-0.	B6	-0.
A7	0.093	B7	-0.052	A7	-0.	27	-0.
A8	0.029	BB	-0.010	A0	-0.	BB	-0.
A9	0.00A	B9	0.007	A9	-0.	B9	-0.
A10	0.013	B10	-0.009	A10	-0.	B10	-0.

ALPHA 3 = 4 CL/2IG = 0.0A2 THETA = A
CO/3IG = 0.0020 ALPHA C = -7.6

FLAPPING				LAGGING			
A0	2.764			A0	-0.		
A1	0.056	B1	-0.041	A1	-0.	B1	-0.
A2	-1.259	B2	-1.092	A2	-0.	B2	-0.
A3	-0.251	B3	-1.008	A8	-0.	B9	-0.
AA	0.193	BA	-0.598	A4	-0.	A4	-0.
A2	-0.021	B2	0.017	AS	-0.	B9	-0.
A6	-0.012	B6	-0.031	A6	-0.	B6	-0.
A7	-0.057	B7	0.026	A7	-0.	B7	-0.
A8	0.012	BB	-0.056	A8	-0.	BB	-0.
A9	0.003	B9	-0.020	A9	-0.	B9	-0.
A10	0.006	B10	-0.02A	A10	-0.	B10	-0.

ALPHA 3 = 0 CL/3IC = 0.00A THETA = -2
CO/3IG = 0.0009 ALPHA C = -0.4

FLAPPING				LAGGING			
A0	0.107			A0	-0.		
A1	0.221	B1	0.04A	A1	-0.	B1	-0.
A2	0.292	B2	-1.071	A2	-0.	B2	-0.
A3	0.05A	B2	-0.098	A3	-0.	B3	-0.
AA	-0.122	B4	0.015	A4	-0.	B4	-0.
A2	0.169	B2	0.002	A2	-0.	B5	-0.
AA	-0.	B6	0.023	A6	-0.	BA	-0.
A7	0.041	B7	-0.088	A7	-0.	B7	-0.
A8	-0.003	BB	0.027	A8	-0.	BB	-0.
A9	-0.019	B9	0.312	A9	-0.	B9	-0.
A10	-0.007	B10	-0.002	A10	-0.	B10	-0.

TABLE I CONTINUED.

ADVANCE RATIO = 0.003

ALPHA S = 0 CL/SIG = 0.01A THETA = 0
CQ/SIG = 0.0005 ALPHA C = -2.5

	FLAPPING			LAGGING		
A0	0.435			A0	-0.	
A1	-0.107	B1	-0.014	A1	-0.	B1 -0.
A2	-0.025	B2	-0.971	A2	-0.	B2 -0.
A3	-0.052	B3	-0.352	A3	-0.	B3 -0.
A4	-0.024	B4	-0.098	A4	-0.	B4 -0.
A5	0.1A1	B5	-0.040	A5	-0.	B5 -0.
A6	-0.001	B6	0.006	A6	-0.	B6 -0.
A7	0.045	B7	-0.008	A7	-0.	B7 -0.
A8	-0.005	B8	0.029	A8	-0.	B8 -0.
A9	-0.009	B9	0.013	A9	-0.	B9 -0.
A10	-0.011	B10	-0.001	A10	-0.	B10 -0.

ALPHA S = 0 CL/SIG = 0.01A THETA = 2
CQ/SIG = 0.0005 ALPHA C = -4.7

	FLAPPING			LAGGING		
A0	0.908			A0	-0.	
A1	0.157	B1	0.001	A1	-0.	B1 -0.
A2	-0.200	B2	-0.020	A2	-0.	B2 -0.
A3	-0.007	B3	-0.097	A3	-0.	B3 -0.
A4	-0.047	B4	-0.190	A4	-0.	B4 -0.
A5	0.154	B5	-0.050	A5	-0.	B5 -0.
A6	0.005	B6	-0.005	A6	-0.	B6 -0.
A7	0.057	B7	-0.050	A7	-0.	B7 -0.
A8	-0.002	B8	0.017	A8	-0.	B8 -0.
A9	-0.002	B9	0.000	A9	-0.	B9 -0.
A10	-0.005	B10	-0.001	A10	-0.	B10 -0.

ALPHA S = 0 CL/SIG = 0.020 THETA = 4
CQ/SIG = 0.0008 ALPHA C = -7.0

	FLAPPING			LAGGING		
A0	1.492			A0	-0.	
A1	-0.095	B1	-0.149	A1	-0.	B1 -0.
A2	-0.557	B2	-0.726	A2	-0.	B2 -0.
A3	-0.007	B3	-0.115	A3	-0.	B3 -0.
A4	0.081	B4	-0.262	A4	-0.	B4 -0.
A5	0.064	B5	-0.058	A5	-0.	B5 -0.
A6	-0.001	B6	-0.009	A6	-0.	B6 -0.
A7	0.034	B7	-0.004	A7	-0.	B7 -0.
A8	-0.005	B8	-0.001	A8	-0.	B8 -0.
A9	-0.008	B9	-0.002	A9	-0.	B9 -0.
A10	-0.008	B10	-0.006	A10	-0.	B10 -0.

ALPHA S = 0 CL/SIG = 0.040 THETA = 8
CQ/SIG = 0.0017 ALPHA C = -9.4

	FLAPPING			LAGGING		
A0	1.781			A0	-0.	
A1	-0.028	B1	-0.007	A1	-0.	B1 -0.
A2	-0.795	B2	-0.055	A2	-0.	B2 -0.
A3	-0.181	B3	-0.782	A3	-0.	B3 -0.
A4	0.095	B4	-0.329	A4	-0.	B4 -0.
A5	0.057	B5	-0.098	A5	-0.	B5 -0.
A6	0.017	B6	-0.057	A6	-0.	B6 -0.
A7	0.005	B7	0.016	A7	-0.	B7 -0.
A8	0.009	B8	-0.018	A8	-0.	B8 -0.
A9	-0.004	B9	-0.003	A9	-0.	B9 -0.
A10	-0.002	B10	-0.000	A10	-0.	B10 -0.

ALPHA S = 0 CL/SIG = 0.040 THETA = 8
CQ/SIG = 0.0020 ALPHA C = -11.5

	FLAPPING			LAGGING		
A0	2.157			A0	-0.	
A1	-0.051	B1	-0.095	A1	-0.	B1 -0.
A2	-1.155	B2	-0.358	A2	-0.	B2 -0.
A3	-0.515	B3	-1.058	A3	-0.	B3 -0.
A4	0.088	B4	-0.078	A4	-0.	B4 -0.
A5	-0.027	B5	-0.078	A5	-0.	B5 -0.
A6	0.058	B6	-0.086	A6	-0.	B6 -0.
A7	0.006	B7	0.050	A7	-0.	B7 -0.
A8	0.039	B8	-0.050	A8	-0.	B8 -0.
A9	0.024	B9	-0.010	A9	-0.	B9 -0.
A10	0.014	B10	-0.011	A10	-0.	B10 -0.

ALPHA S = 0 CL/SIG = 0.049 THETA = 9
CQ/SIG = 0.0035 ALPHA C = -15.7

	FLAPPING			LAGGING		
A0	3.390			A0	-0.	
A1	-0.324	B1	-0.174	A1	-0.	B1 -0.
A2	-1.58A	B2	-0.A84	A2	-0.	B2 -0.
A3	-0.245	B3	-1.195	A3	-0.	B3 -0.
A4	0.145	B4	-0.590	A4	-0.	B4 -0.
A5	-0.055	B5	-0.059	A5	-0.	B5 -0.
A6	0.014	B6	-0.086	A6	-0.	B6 -0.
A7	-0.010	B7	0.074	A7	-0.	B7 -0.
A8	0.050	B8	-0.082	A8	-0.	B8 -0.
A9	0.034	B9	-0.011	A9	-0.	B9 -0.
A10	0.01A	B10	-0.012	A10	-0.	B10 -0.

TABLE I CONTINUED.

ADVANCE RATIO = 0.883

ALPHA S = -4 CL/SIG = -0.007 THETA = 2
CG/SIG = 0.0003 ALPHA C = -6.4

	FLAPPING			LAGGING		
A0	-0.047			A0	-0.034	
A1	-0.294	B1	0.090	A1	0.138	B1	-0.124
A2	0.144	B2	-0.550	A2	-0.	B2	0.002
A3	0.112	B3	-0.047	A3	0.009	B3	-0.014
A4	-0.046	B4	-0.003	A4	0.025	B4	-0.018
A5	0.132	B5	-0.018	A5	0.004	B5	0.004
A6	-0.002	B6	0.016	A6	0.004	B6	-0.
A7	0.011	B7	-0.083	A7	0.002	B7	-0.001
A8	0.024	B8	0.019	A8	-0.	B8	0.002
A9	0.005	B9	0.011	A9	0.004	B9	0.003
A10	0.007	B10	-0.001	A10	-0.002	B10	-0.

ALPHA S = -4 CL/SIG = 0.001 THETA = 4
CG/SIG = 0.0006 ALPHA C = -8.A

	FLAPPING			LAGGING		
A0	0.339			A0	0.055	
A1	-0.117	B1	0.025	A1	0.111	B1	-0.110
A2	-0.142	B2	-0.439	A2	0.013	B2	0.003
A3	0.044	B3	-0.228	A3	0.010	B3	-0.024
A4	-0.034	B4	-0.040	A4	0.034	B4	-0.025
A5	0.088	B5	-0.032	A5	0.004	B5	0.001
A6	-0.055	B6	0.005	A6	0.005	B6	0.001
A7	0.014	B7	-0.040	A7	0.002	B7	-0.002
A8	0.021	B8	0.004	A8	0.004	B8	0.001
A9	0.006	B9	0.008	A9	0.001	B9	-0.
A10	0.005	B10	-0.008	A10	-0.005	B10	-0.001

ALPHA S = -4 CL/SIG = 0.00A THETA = 6
CO/SIG = 0.0009 ALPHA C = -11.C

	FLAPPING			LAGGING		
A0	0.698			A0	0.198	
A1	0.213	B1	0.001	A1	0.073	B1	-0.106
A2	-0.382	B2	-0.371	A2	0.027	B2	0.008
A3	0.006	B3	-0.439	A3	0.00A	B3	-0.038
A4	0.011	B4	-0.150	A4	0.064	B4	-0.012
A5	0.039	B5	-0.064	A5	0.001	B5	-0.001
A6	-0.019	B6	-0.006	A6	0.002	B6	-0.
A7	-0.010	B7	-0.019	A7	-0.001	B7	0.002
A8	0.013	B8	-0.013	A8	0.005	B8	0.001
A9	0.013	B9	-0.003	A9	-0.	B9	0.006
A10	-0.001	B10	-0.009	A10	0.001	B10	-0.

ALPHA S = -4 CL/SIG = 0.014 THETA = 8
CG/SIG = 0.0016 ALPHA C = -13.2

	FLAPPING			LAGGING		
A0	1.16A			A0	C.514	
A1	0.132	B1	0.026	A1	0.318	B1	-0.085
A2	-0.A74	B2	-0.286	A2	0.034	B2	0.020
A3	-0.04A	B3	-0.706	A3	0.025	B3	-0.05A
A4	0.057	B4	-0.228	A4	0.109	B4	-0.006
A5	-0.024	B5	-0.050	A5	-0.005	B5	0.003
A6	-0.004	B6	-0.007	A6	-0.009	B6	0.003
A7	0.005	B7	0.044	A7	0.001	B7	0.003
A8	0.009	B8	-0.027	A8	0.007	B8	-0.003
A9	0.004	B9	-0.009	A9	-0.002	B9	0.004
A10	-0.01C	B10	-0.003	A10	-0.002	B10	-0.003

ALPHA S = -4 CL/SIG = 0.026 THETA = 10
CO/SIG = 0.0029 ALPHA C = -15.4

	FLAPPING			LAGGING		
A0	1.725			A0	1.110	
A1	-0.982	B1	0.024	A1	-0.074	B1	-0.056
A2	-1.032	B2	-0.827	A2	0.058	B2	0.029
A3	-0.171	B3	-0.996	A3	0.037	B3	-0.081
A4	0.111	B4	-0.279	A4	0.138	B4	-0.035
A5	-0.091	B5	-0.070	A5	-0.007	B5	-0.002
A6	0.014	B6	-0.017	A6	-0.012	B6	0.004
A7	-0.020	B7	0.073	A7	0.002	B7	0.004
A8	0.021	B8	-0.049	A8	-0.001	B8	-0.004
A9	0.005	B9	-0.008	A9	-0.003	B9	-0.001
A10	-0.005	B10	0.001	A10	0.001	B10	-0.002

ALPHA S = -4 CL/SIG = 0.032 THETA = 12
CO/SIG = 0.0042 ALPHA C = -17.7

	FLAPPING			LAGGING		
A0	1.829			A0	1.724	
A1	0.491	B1	0.218	A1	-0.159	B1	-0.065
A2	-1.288	B2	-0.219	A2	0.060	B2	0.037
A3	-0.199	B3	-1.234	A3	0.059	B3	-0.096
A4	0.184	B4	-0.259	A4	0.150	B4	-0.028
A5	-0.136	B5	-0.096	A5	-0.010	B5	-0.008
A6	0.034	B6	-0.008	A6	-0.015	B6	0.005
A7	-0.037	B7	0.105	A7	0.001	B7	0.007
A8	0.031	B8	-0.044	A8	-0.	B8	-0.005
A9	0.006	B9	0.003	A9	-0.003	B9	-0.004
A10	-0.009	B10	0.016	A10	0.001	B10	-0.

TABLE I CONCLUDED.

ADVANCE RATIO = 0.995

ALPHA S = 0 CL/SIG = -0.009 THETA = 4
CQ/SIG = -0.0007 ALPHA C = -8.1

FLAPPING				LAGGING			
A0	-0.349			A0	2.480		
A1	0.002	B1	0.140	A1	0.181	B1	-0.282
A2	-0.398	B2	-0.271	A2	0.067	B2	0.038
A3	0.213	B3	-0.383	A3	0.033	B3	-0.049
A4	0.032	B4	-0.250	A4	0.042	B4	-0.112
A5	0.048	B5	-0.125	A5	0.021	B5	-0.
A6	0.035	B6	0.108	A6	-0.009	B6	-0.004
A7	0.031	B7	0.019	A7	0.004	B7	-0.
A8	-0.063	B8	0.160	A8	-0.003	B8	0.009
A9	-0.018	B9	0.049	A9	0.006	B9	-0.001
A10	-0.017	B10	0.031	A10	0.003	B10	0.002

ALPHA S = 0 CL/SIG = -0.006 THETA = 6
CQ/SIG = -0.0014 ALPHA C = -10.5

FLAPPING				LAGGING			
A0	-0.266			A0	2.061		
A1	0.041	B1	-0.025	A1	0.125	B1	-0.327
A2	-0.601	B2	-0.013	A2	0.098	B2	0.048
A3	0.067	B3	-0.641	A3	0.053	B3	-0.087
A4	0.024	B4	-0.449	A4	-0.009	B4	-0.128
A5	0.446	B5	0.040	A5	0.031	B5	0.011
A6	0.090	B6	0.171	A6	0.001	B6	0.001
A7	0.100	B7	0.043	A7	0.007	B7	0.003
A8	0.006	B8	0.227	A8	-0.009	B8	0.002
A9	0.030	B9	0.079	A9	0.005	B9	-0.
A10	-0.	B10	0.062	A10	0.005	B10	0.004

ALPHA S = 0 CL/SIG = -0.004 THETA = 2
CQ/SIG = 0.0002 ALPHA C = -5.8

FLAPPING				LAGGING			
A0	-0.092			A0	2.944		
A1	-0.169	B1	-0.138	A1	0.204	B1	-0.253
A2	-0.296	B2	-0.603	A2	0.030	B2	0.035
A3	0.133	B3	-0.284	A3	0.008	B3	-0.035
A4	-0.057	B4	-0.110	A4	0.005	B4	-0.062
A5	0.347	B5	-0.344	A5	0.010	B5	-0.007
A6	0.082	B6	0.029	A6	-0.004	B6	-0.006
A7	0.025	B7	-0.019	A7	-0.	B7	-0.002
A8	0.047	B8	0.088	A8	-0.001	B8	-0.004
A9	0.005	B9	0.035	A9	0.003	B9	-0.003
A10	-0.002	B10	0.016	A10	0.002	B10	-0.001

ALPHA S = 0 CL/SIG = -0.002 THETA = 8
CQ/SIG = -0.0018 ALPHA C = -12.8

FLAPPING				LAGGING			
A0	-0.019			A0	1.868		
A1	0.082	B1	-0.118	A1	0.055	B1	-0.384
A2	-1.001	B2	0.058	A2	0.095	B2	0.061
A3	-0.121	B3	-0.857	A3	0.060	B3	-0.123
A4	-0.061	B4	-0.620	A4	0.029	B4	-0.136
A5	0.661	B5	0.276	A5	0.035	B5	0.014
A6	0.182	B6	0.161	A6	0.033	B6	0.003
A7	0.204	B7	0.014	A7	0.018	B7	-0.005
A8	0.021	B8	0.245	A8	-0.005	B8	0.007
A9	0.056	B9	0.072	A9	0.007	B9	0.006
A10	0.021	B10	0.069	A10	-0.001	B10	0.004

ALPHA S = 0 CL/SIG = 0.004 THETA = 0
CQ/SIG = 0.0007 ALPHA C = -3.4

FLAPPING				LAGGING			
A0	0.245			A0	3.183		
A1	-0.036	B1	-0.147	A1	0.233	B1	-0.224
A2	-0.084	B2	-1.140	A2	0.008	B2	0.030
A3	0.085	B3	-0.409	A3	-0.002	B3	-0.025
A4	-0.132	B4	0.063	A4	-0.026	B4	-0.037
A5	0.333	B5	-0.457	A5	0.004	B5	-0.005
A6	0.135	B6	0.021	A6	-0.007	B6	-0.004
A7	0.045	B7	-0.008	A7	-0.	B7	-0.001
A8	0.043	B8	0.103	A8	-0.001	B8	-0.001
A9	0.016	B9	0.033	A9	0.002	B9	-0.001
A10	0.005	B10	0.004	A10	-0.	B10	-0.001

TABLE II SHEAR FORCE HARMONIC COEFFICIENTS, LB.

ADVANCE RATIO = 0.191

ALPHA S = -4 ALPHA C = -6.9 THETA = 6
CL/SIG = 0.071 CD/SIG = -0.0041 CQ/SIG = 0.0024

	FLATWISE		EDGEWISE		RADIAL	
N	COSINE	SINE	COSINE	SINE	COSINE	SINE
1	0.5	0.9	1.8	1.1	-7.9	0.9
2	-0.6	0.0	-0.3	0.0	0.4	1.1
3	1.6	0.0	-0.5	-0.5	0.6	1.2
4	-0.2	0.3	0.2	-0.2	-0.5	0.4
5	0.3	0.1	0.0	-0.1	0.3	0.0
6	0.1	0.3	-0.1	0.2	-0.2	0.2
7	0.2	0.1	-0.5	0.0	0.0	-0.1
8	0.0	-0.1	-0.2	0.0	0.0	0.0
9	-0.1	0.0	-0.2	0.1	-0.1	-0.0
10	0.2	0.1	-0.1	0.2	-0.2	0.2

ADVANCE RATIO = 0.283

ALPHA S = -4 ALPHA C = -4.8 THETA = 2
CL/SIG = 0.019 CD/SIG = 0.0007 CQ/SIG = 0.0004

1	-0.4	-3.3	2.3	1.1	-2.3	1.6
2	0.3	-0.3	-0.2	0.3	0.1	-0.7
3	0.4	-0.1	-0.4	-0.3	-0.0	0.4
4	0.2	0.0	0.2	-0.2	-0.2	0.0
5	0.0	-0.0	-0.1	-0.0	-0.0	0.1
6	0.0	0.1	-0.0	-0.1	0.0	0.0
7	-0.3	-0.0	-0.0	-0.0	-0.0	0.0
8	0.0	0.0	-0.0	-0.0	0.0	0.0
9	-0.1	0.1	-0.0	-0.0	-0.1	0.0
10	-0.3	-0.1	0.2	0.1	-0.1	-0.1

ALPHA S = -4 ALPHA C = -6.5 THETA = 4
CL/SIG = 0.041 CD/SIG = -0.0008 CQ/SIG = 0.0011

1	-1.0	-2.3	0.5	-0.1	-1.2	0.1
2	-0.3	-0.3	-0.3	0.5	-0.0	-0.7
3	0.7	-0.2	0.0	0.2	-0.2	0.2
4	0.2	0.4	-0.2	0.1	-0.2	-0.1
5	0.1	-0.0	0.1	0.1	0.1	0.1
6	-0.0	0.1	0.0	-0.1	-0.0	0.0
7	-0.3	-0.1	-0.1	-0.0	-0.1	-0.0
8	0.0	-0.1	0.0	0.1	-0.1	-0.1
9	0.1	-0.2	-0.1	0.3	-0.2	-0.2
10	-0.3	-0.2	0.1	-0.0	-0.0	-0.1

ALPHA S = -4 ALPHA C = -7.9 THETA = 6
CL/SIG = 0.062 CD/SIG = -0.0029 CQ/SIG = 0.0022

1	-2.4	-1.0	-2.2	-0.3	-0.5	-0.2
2	-0.7	-0.6	0.0	0.9	-0.2	-0.9
3	1.4	-0.7	0.5	0.8	-0.5	-0.1
4	0.0	0.4	-0.2	-0.1	0.1	-0.2
5	0.3	-0.2	0.3	0.3	0.2	-0.1
6	0.0	0.1	0.0	0.0	-0.0	-0.1
7	-0.6	-0.2	0.2	-0.0	-0.0	-0.1
8	-0.1	-0.4	0.1	0.2	-0.2	-0.2
9	0.2	0.1	-0.3	-0.0	0.1	0.1
10	0.4	-0.3	0.1	0.0	-0.0	-0.0

TABLE II CONCLUDED

ADVANCE RATIO = 0.389

ALPHA S = -4 ALPHA C = -9.5 THETA = 6
CL/SIC = 0.046 CD/SIG = -0.0018 CQ/SIG = 0.0022

	FLATWISE		EDGEWISE		RADIAL	
N	COSINE	SINE	COSINE	SINE	COSINE	SINE
1	-2.1	-1.5	-0.5	-0.2	-0.6	-0.2
2	-1.2	-1.8	-0.6	-1.2	0.0	1.0
3	1.0	-1.4	-0.9	0.5	0.8	0.5
4	0.7	0.3	-0.2	-0.4	-0.3	0.3
5	0.2	0.0	0.0	-0.3	0.4	0.2
6	-0.2	0.2	-0.2	0.1	-0.1	-0.1
7	0.2	0.3	0.1	0.1	-0.3	-0.1
8	-0.4	0.1	-0.1	-0.2	0.2	-0.1
9	-0.2	0.3	-0.2	-0.2	0.0	0.3
10	0.0	0.1	-0.1	-0.1	0.0	-0.0

ADVANCE RATIO = 0.488

ALPHA S = -4 ALPHA C = -11.9 THETA = 8
CL/SIC = 0.048 CD/SIC = -0.0024 CQ/SIG = 0.0034

1	-0.5	-0.2	0.0	0.4	0.2	-0.3
2	-1.3	-2.4	-0.9	-1.5	0.5	1.4
3	0.0	-2.6	-1.3	1.2	0.6	0.3
4	0.6	-1.0	-0.7	-1.0	-0.3	0.5
5	0.4	-0.2	-0.1	0.0	0.4	-0.1
6	-0.2	0.2	0.0	0.3	-0.1	-0.0
7	0.3	-1.1	-0.3	-0.2	0.1	1.0
8	0.1	0.4	0.3	0.3	-0.4	-0.2
9	-0.2	0.3	0.0	0.3	0.1	-0.7
10	-0.3	-0.1	0.0	0.0	0.2	-0.2

ADVANCE RATIO = 0.683

ALPHA S = -4 ALPHA C = -17.7 THETA = 12
CL/SIC = 0.032 CD/SIC = 0.0033 CQ/SIC = 0.0042

1	2.0	0.0	2.0	0.0	-1.0	-0.7
2	-2.9	-2.4	-2.9	2.4	2.3	1.1
3	-2.0	-2.7	-2.0	2.7	2.2	-1.0
4	-4.3	-4.3	-4.3	4.3	4.6	2.9
5	0.3	0.0	0.0	0.3	0.3	-1.3
6	1.0	-0.1	1.0	-0.1	-0.7	0.1
7	0.0	0.4	0.0	0.4	0.1	0.3
8	0.4	-0.9	0.4	-0.8	-0.6	0.4
9	0.3	0.2	0.3	0.3	-0.1	-0.1
0	0.8	0.3	0.8	0.3	-0.4	-0.0

TABLE III - SCALING RATIOS

Model linear dimension = 1/S x full scale linear dimension

Subscript m - model
Subscript fs - full scale

Parameter	Full Scale Blade
Radius & other linear dimensions R_m/R_{fs}	$1/S$
Areas- A_m/A_{fs}	$1/S^2$
Mass per unit length m_m/m_{fs}	$1/S^2$
Total mass $M_{b_m}/M_{b_{fs}}$	$1/S^3$
Stiffness $EI_{xx_m}/EI_{xx_{fs}}$, etc.	$1/S^5$
Angular velocity Ω_m/Ω_{fs}	$\sqrt{S}$
Linear velocities $(\Omega R)_m/(\Omega R)_{fs}$	$1/\sqrt{S}$
Mach number M_m/M_{fs}	$1/\sqrt{S}$
Froude number $(\Omega^2 R/g)_m/(\Omega^2 R/g)_{fs}$	1
Reynolds number RN_m/RN_{fs}	$1/S^{\frac{3}{2}}$
Output forces F_m/F_{fs}	$1/S^3$
Output moments $Mom._m/Mom._{fs}$	$1/S^4$
Output elastic strains ϵ_m/ϵ_{fs}	1
Natural frequencies ω_m/ω_{fs}	$\sqrt{S}$

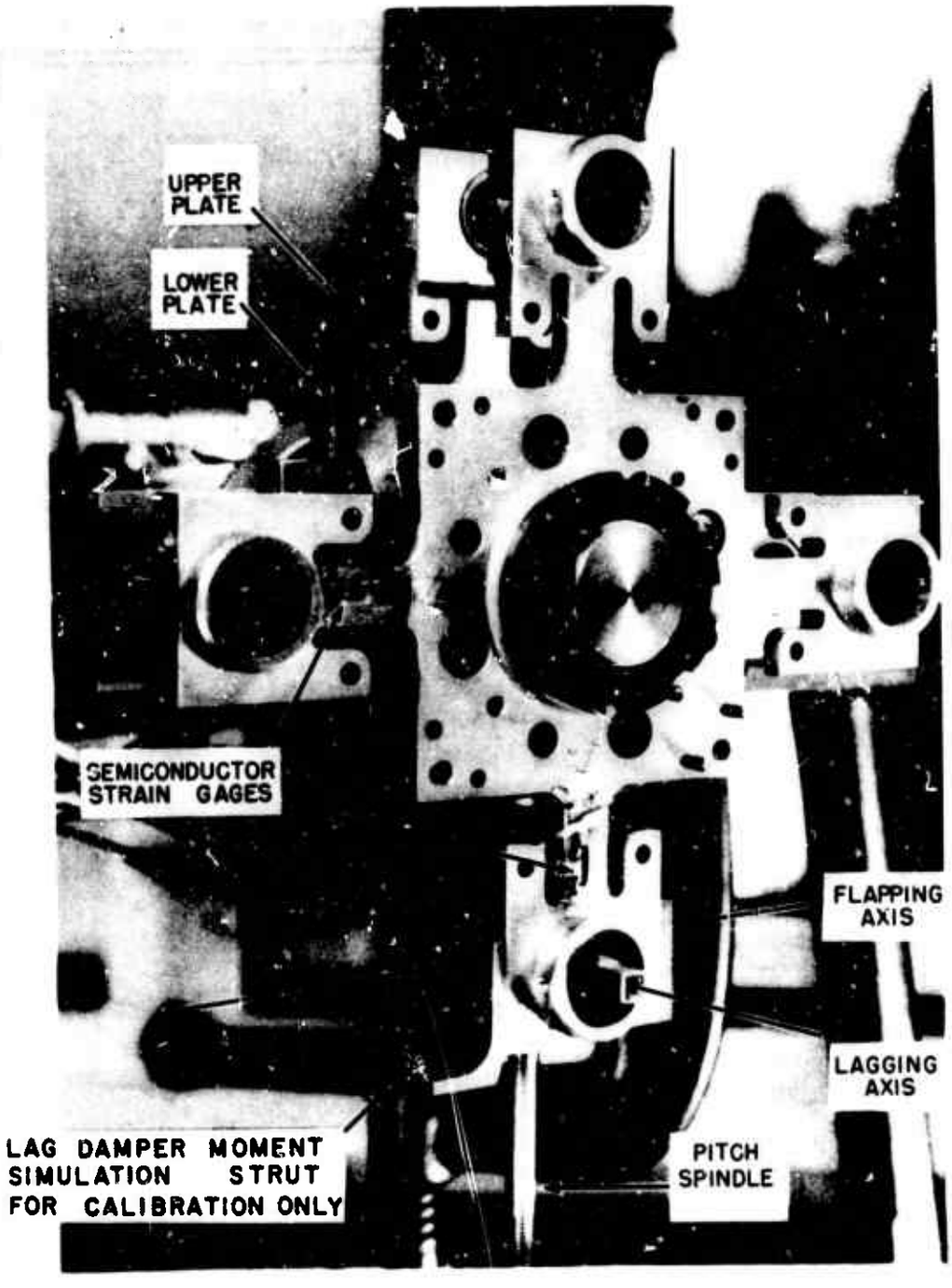

(a) BASIC INSTALLATION

Figure 1. Vibratory Shear Force Rotor Head.

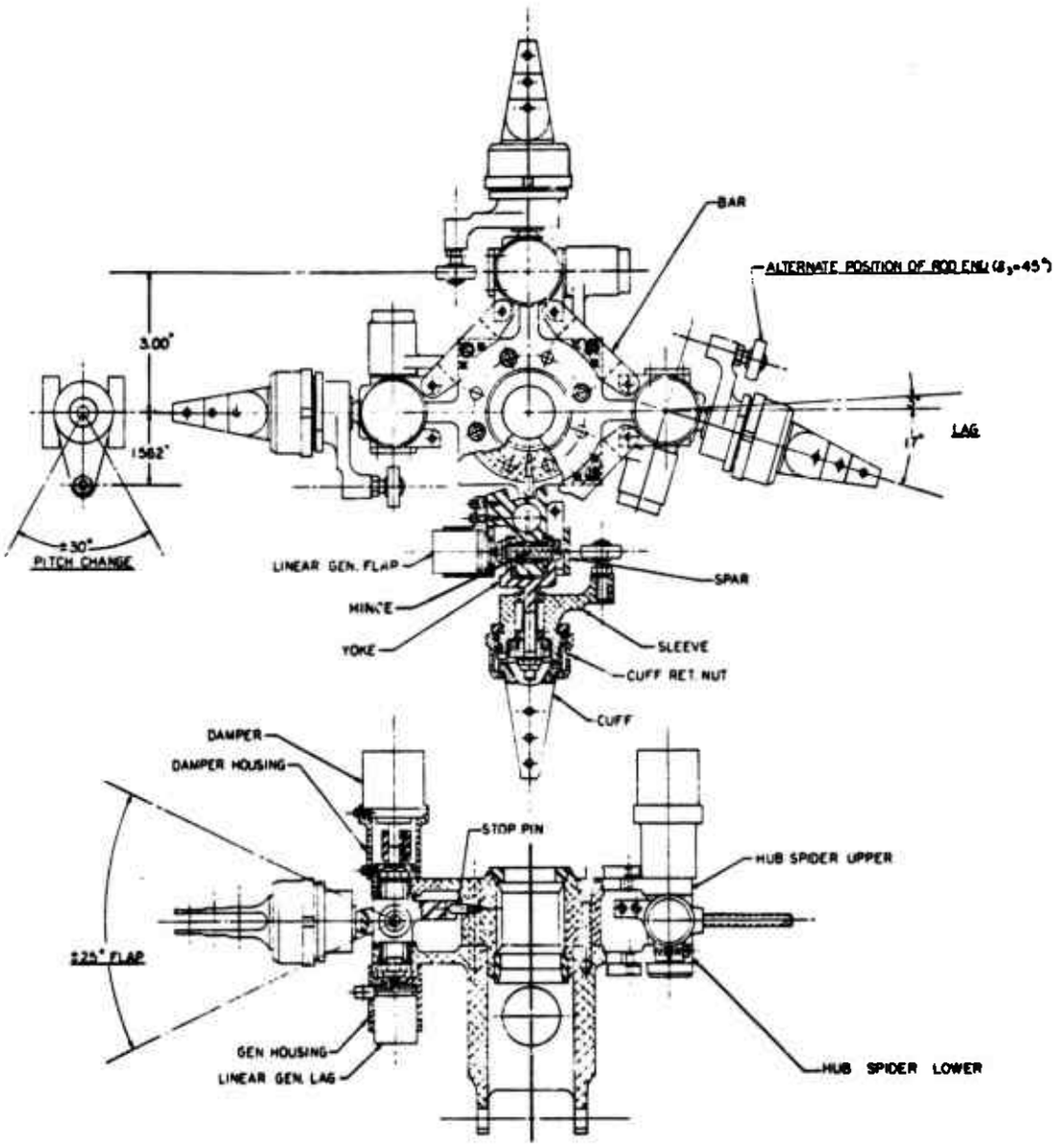

(b) ASSEMBLY DRAWING

Figure 1. Concluded.

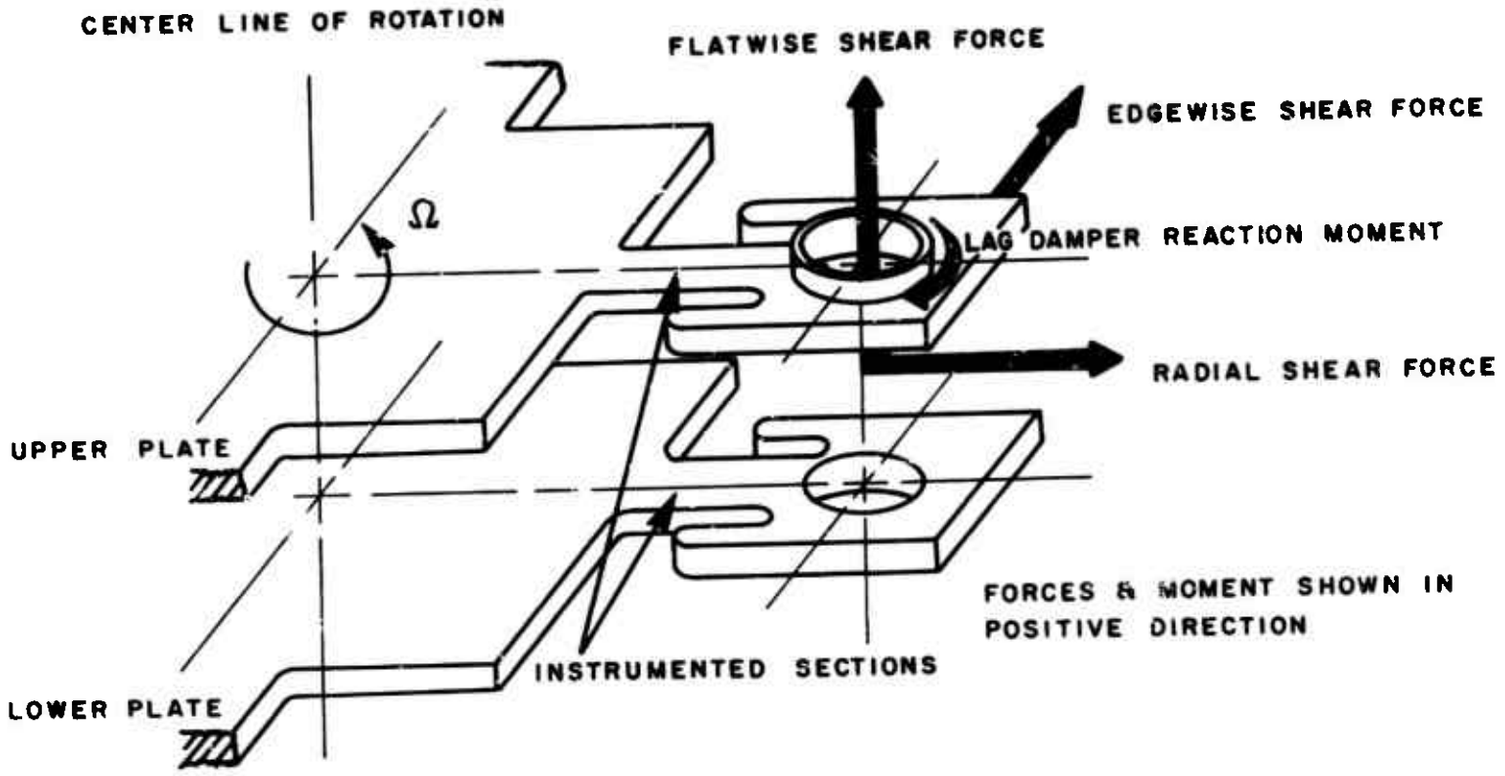

(a) DEFINITION OF SHEAR FORCES AND LAG DAMPER REACTION MOMENT

Figure 2. Vibratory Shear Force Rotor Head Details.

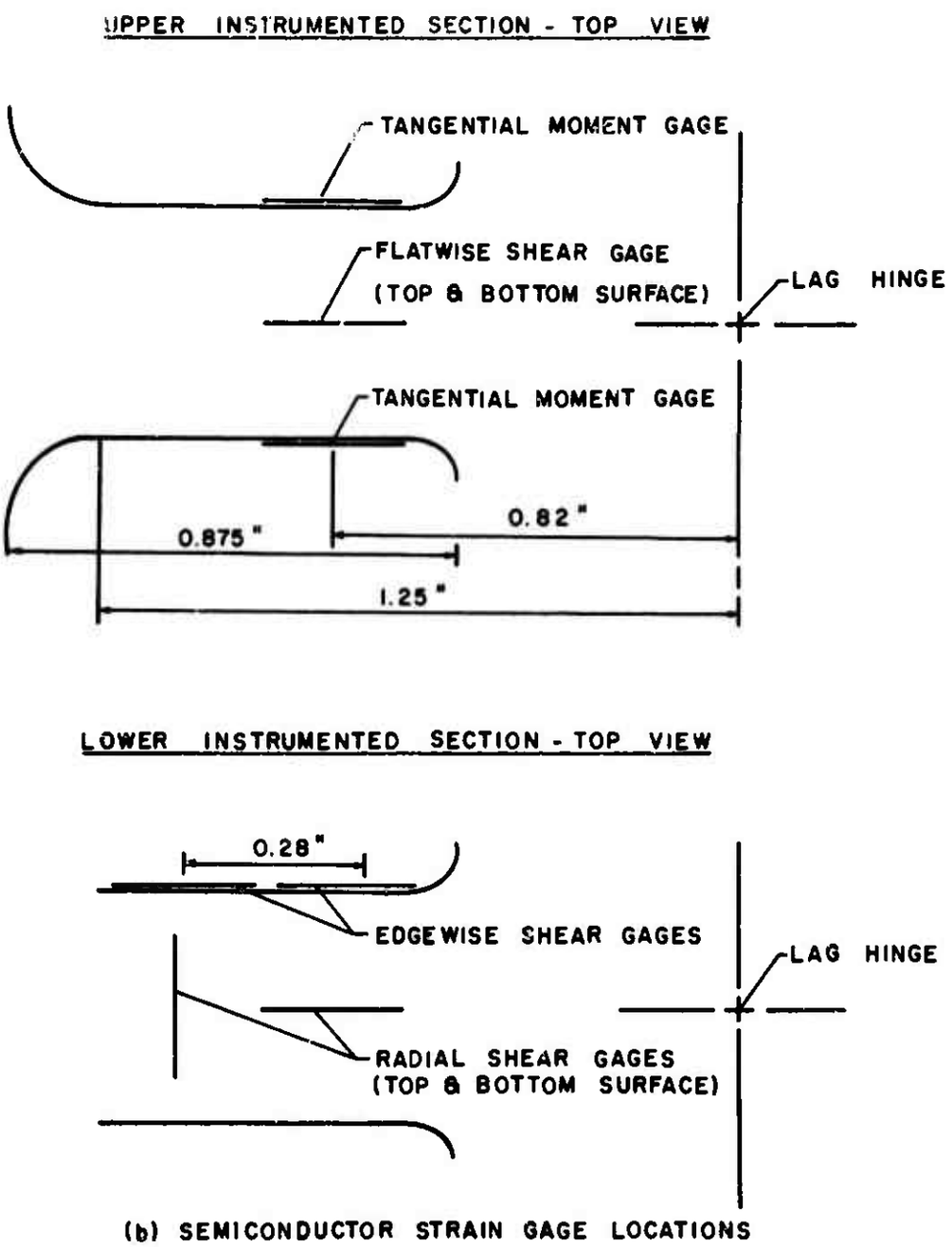

Figure 2. Concluded.

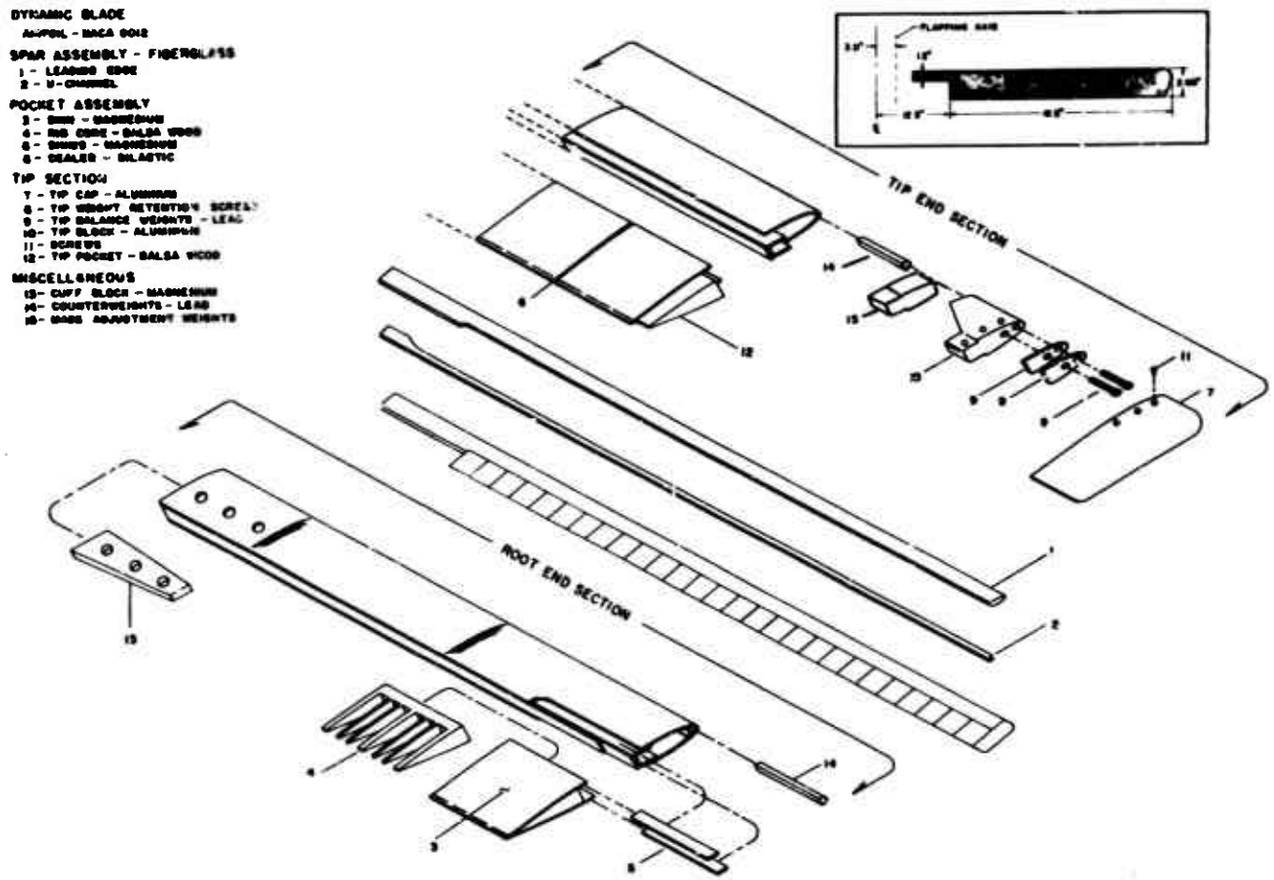

Figure 3. Dynamically Scaled Blade-Exploded View.

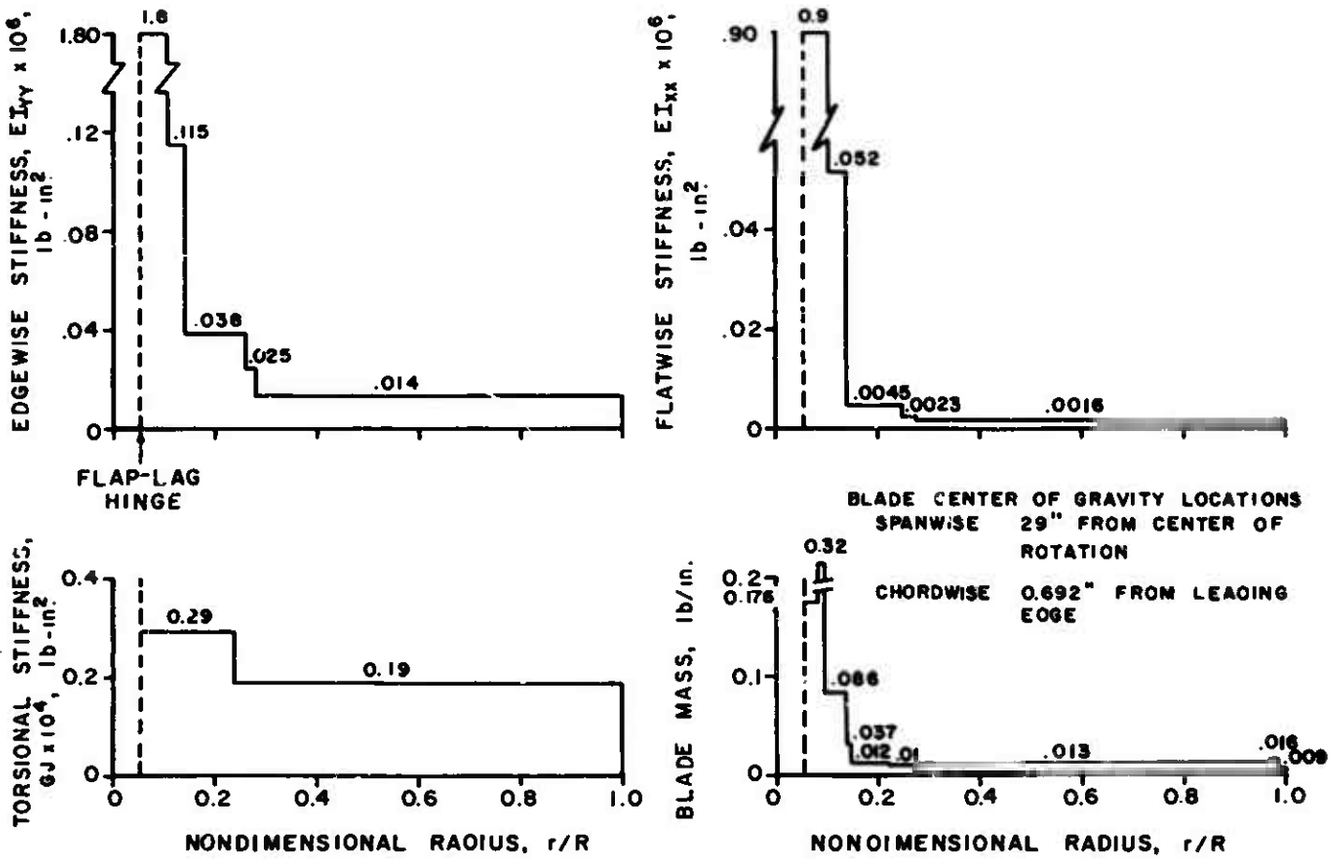

Figure 4. Dynamic Blade Physical Properties.

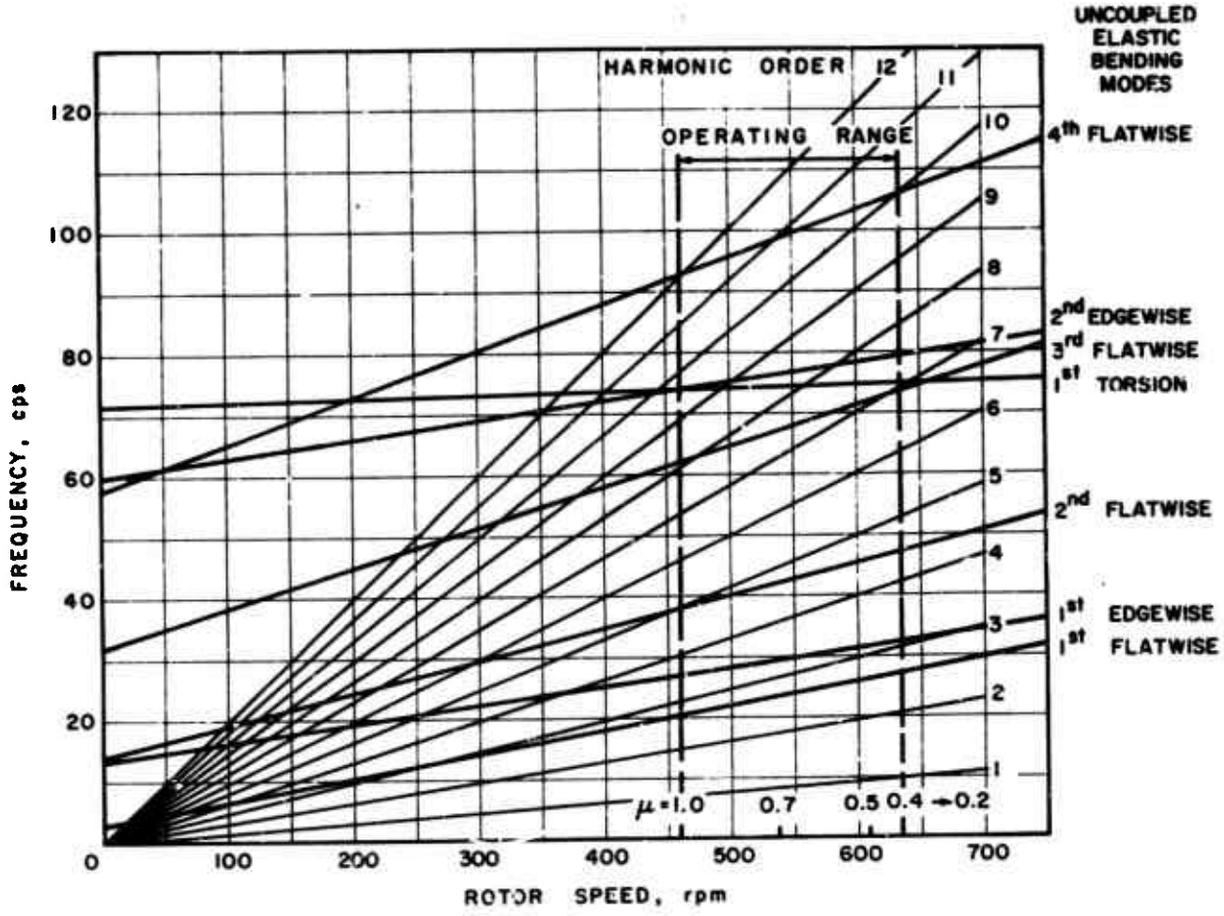

Figure 5. Model Rotor Blade Calculated Natural Frequencies.

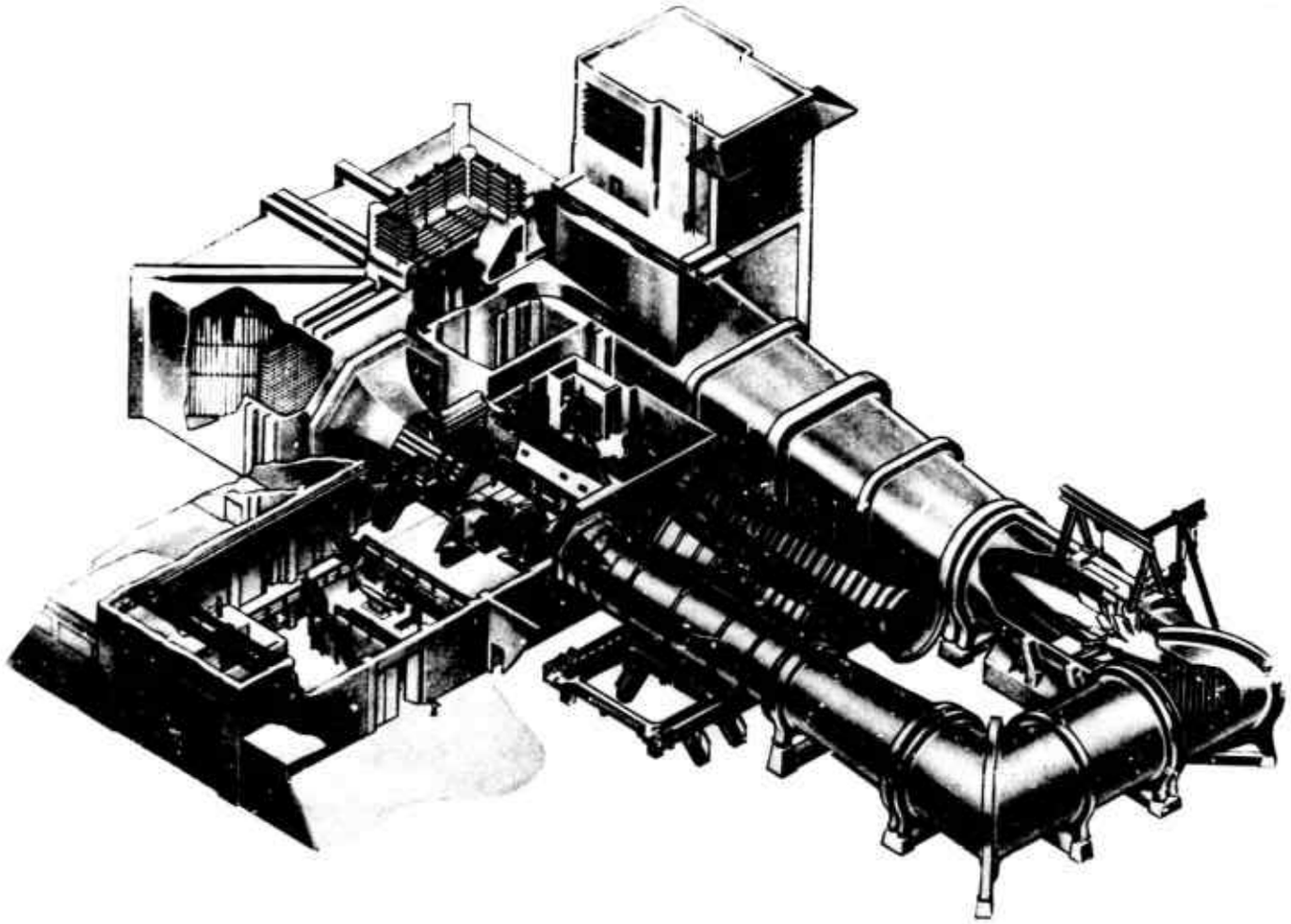

Figure 6. United Aircraft's Subsonic Wind Tunnel.

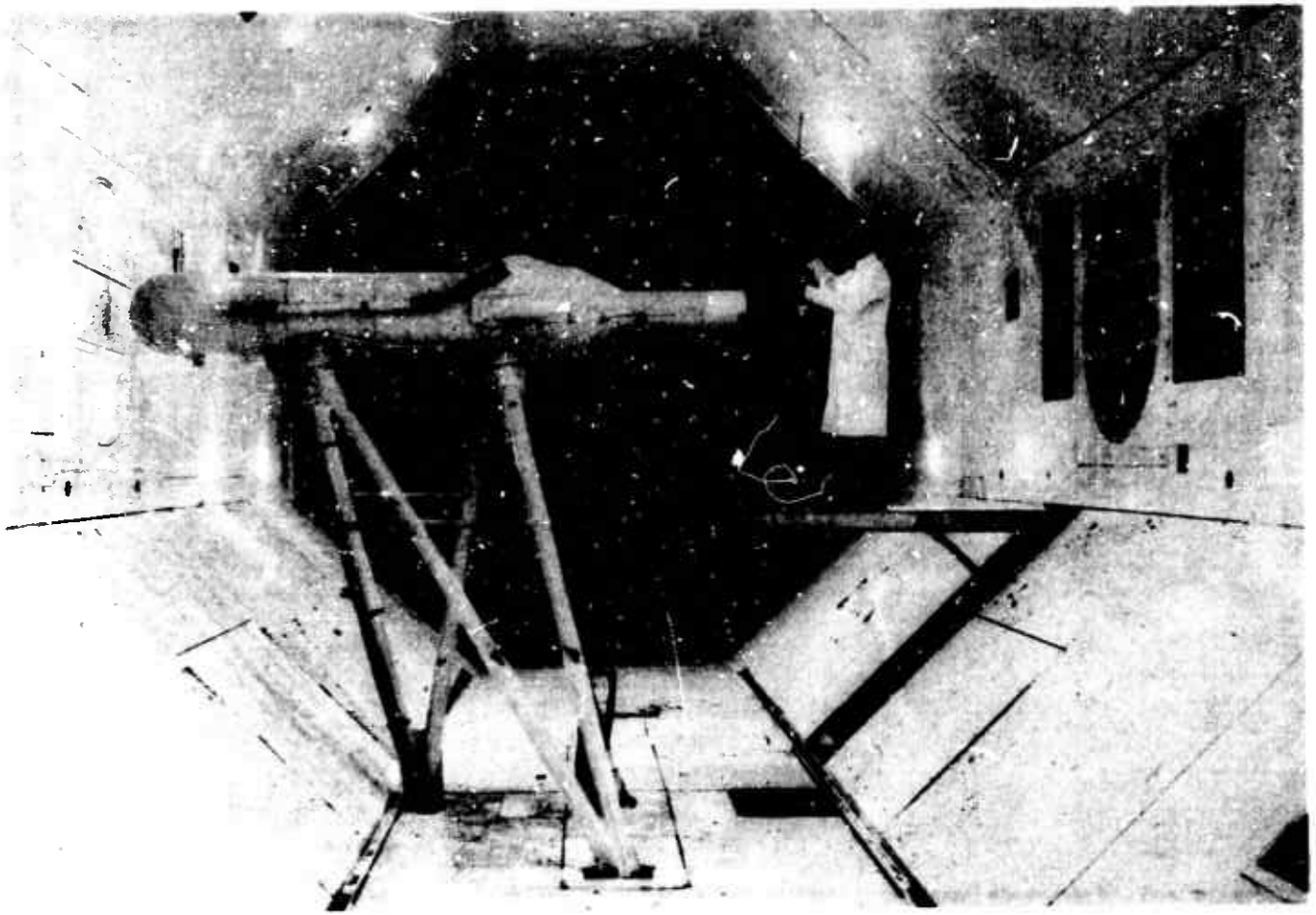

(a) GENERAL VIEW OF MODEL INSTALLATION IN WIND TUNNEL

Figure 7. Sikorsky Helicopter Rotor Test Rig.

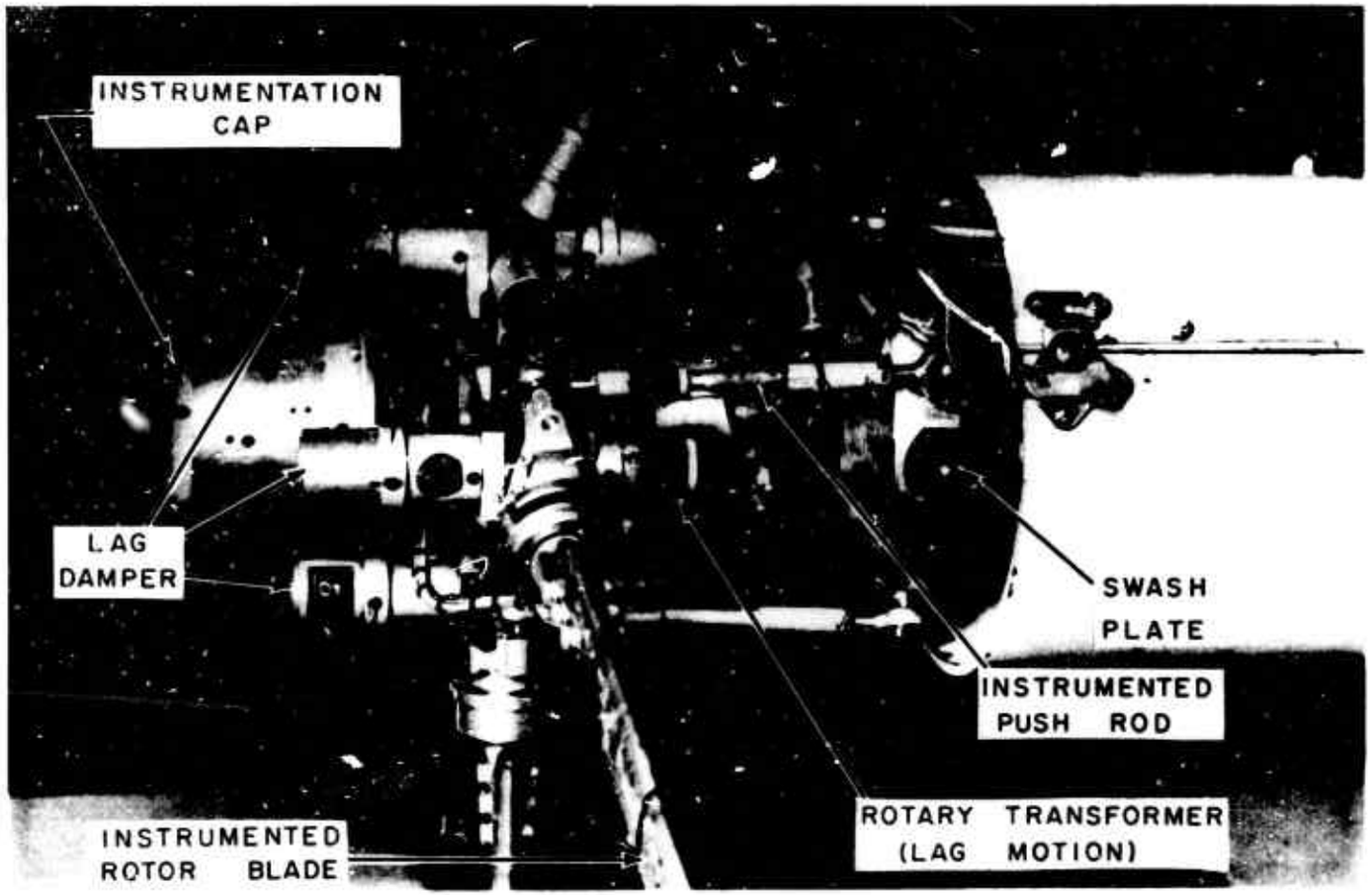

(b) DETAILS OF HUB AND SWASH PLATE AREA

Figure 7. Concluded.

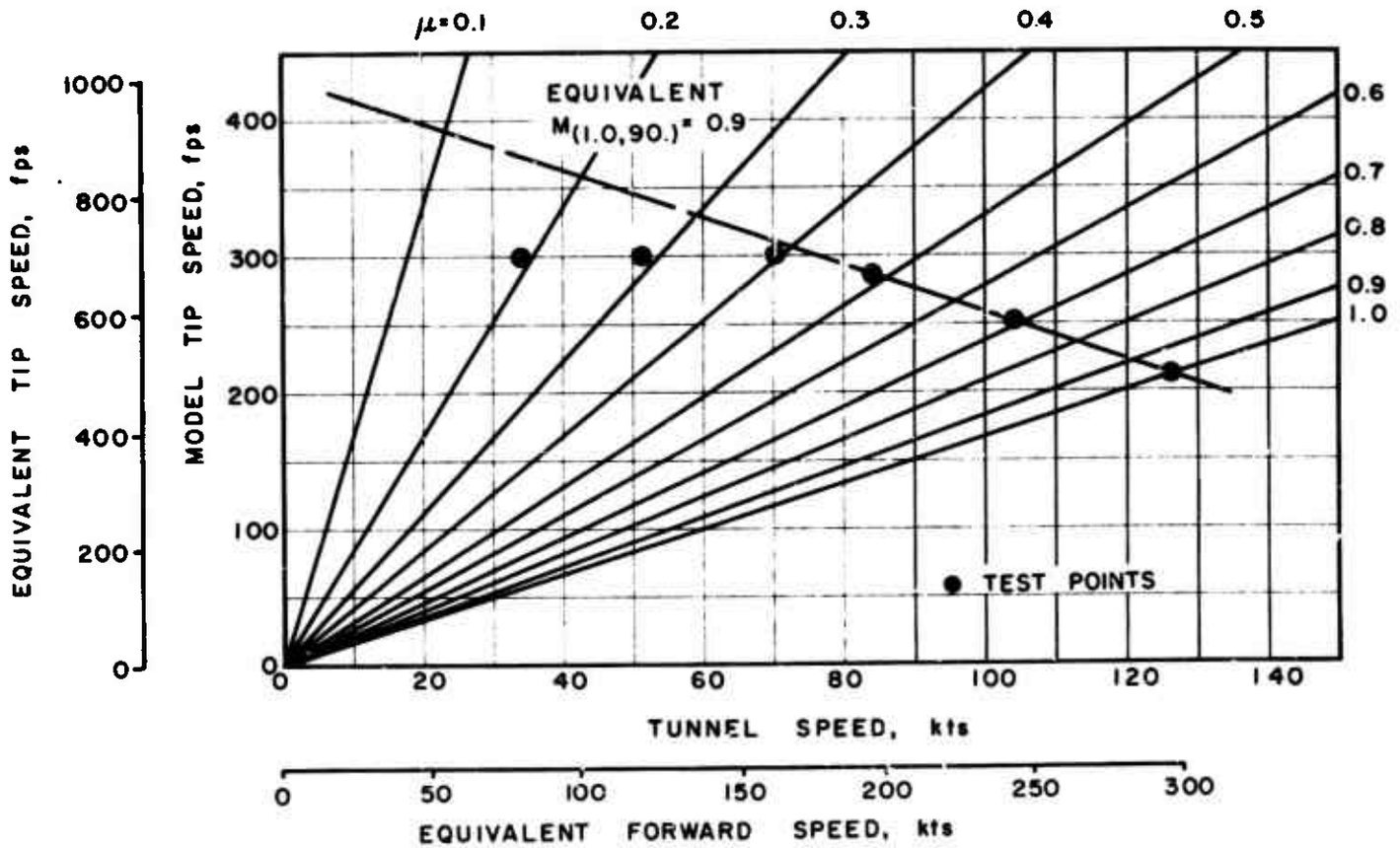

Figure 8. Wind Tunnel Test Conditions.

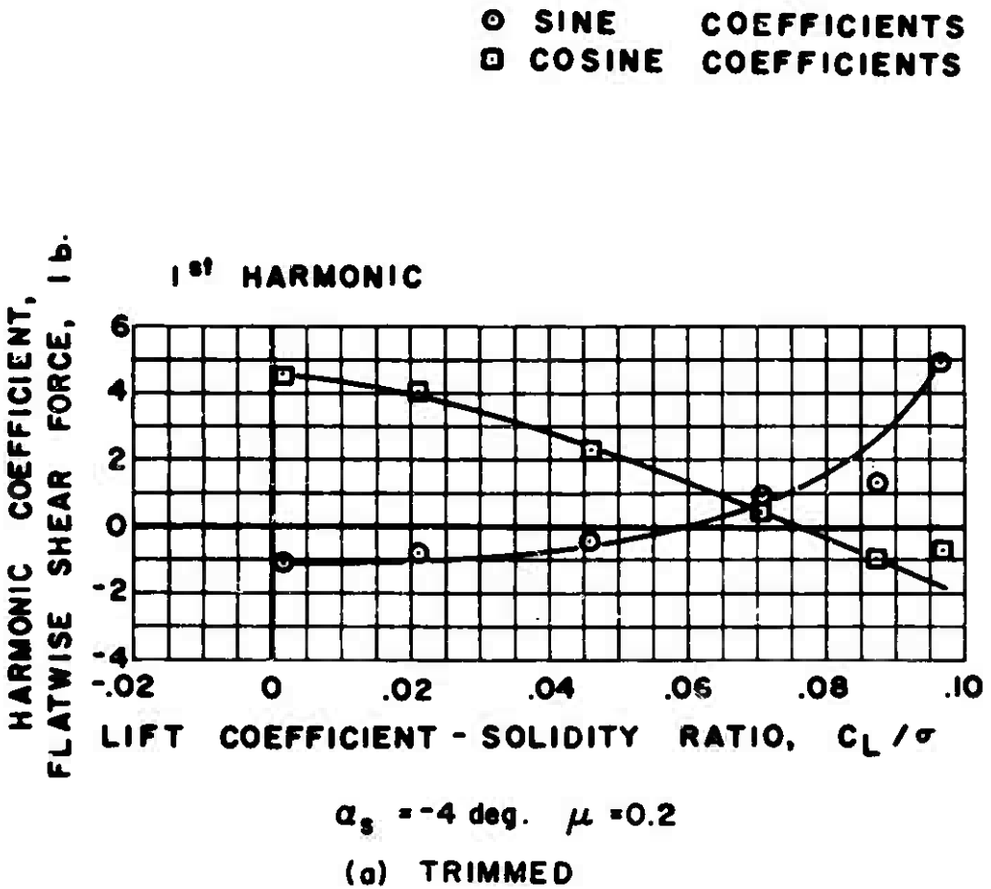

Figure 9. Effect of Trim Condition on Shear Forces.

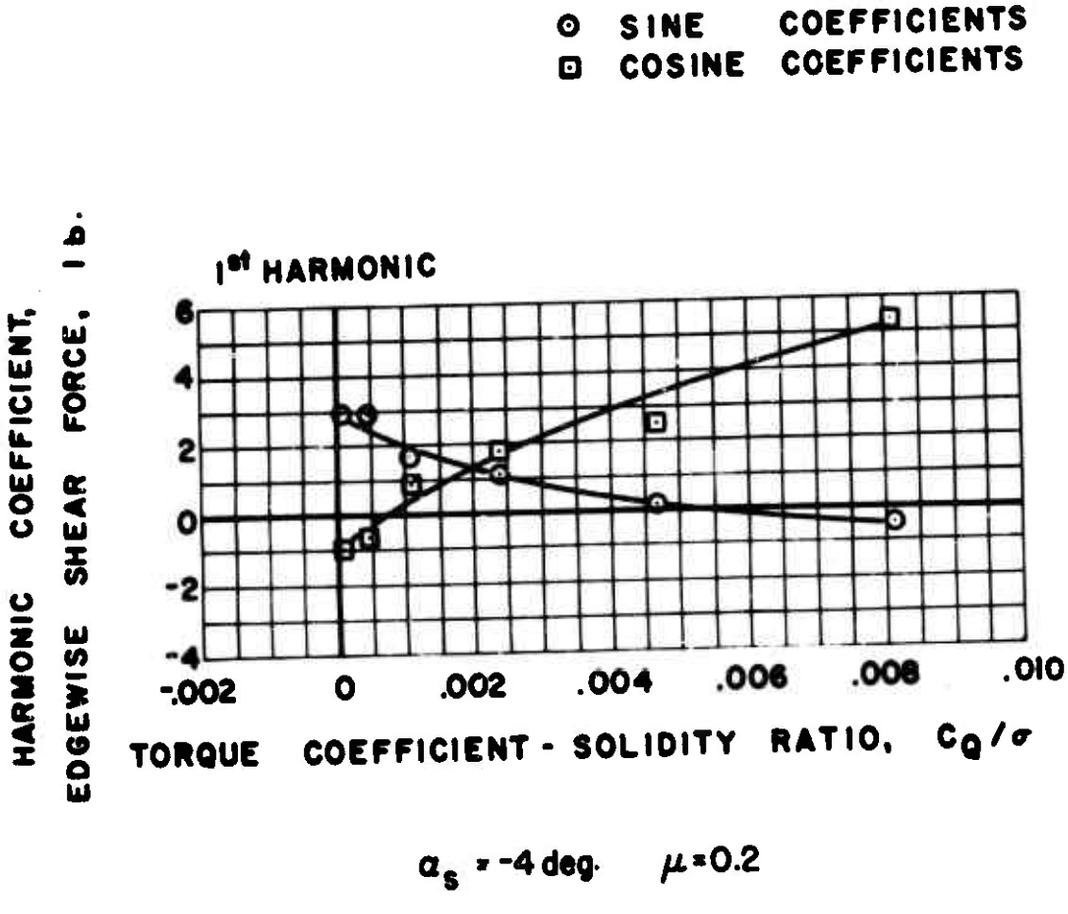

Figure 9(a) Continued.

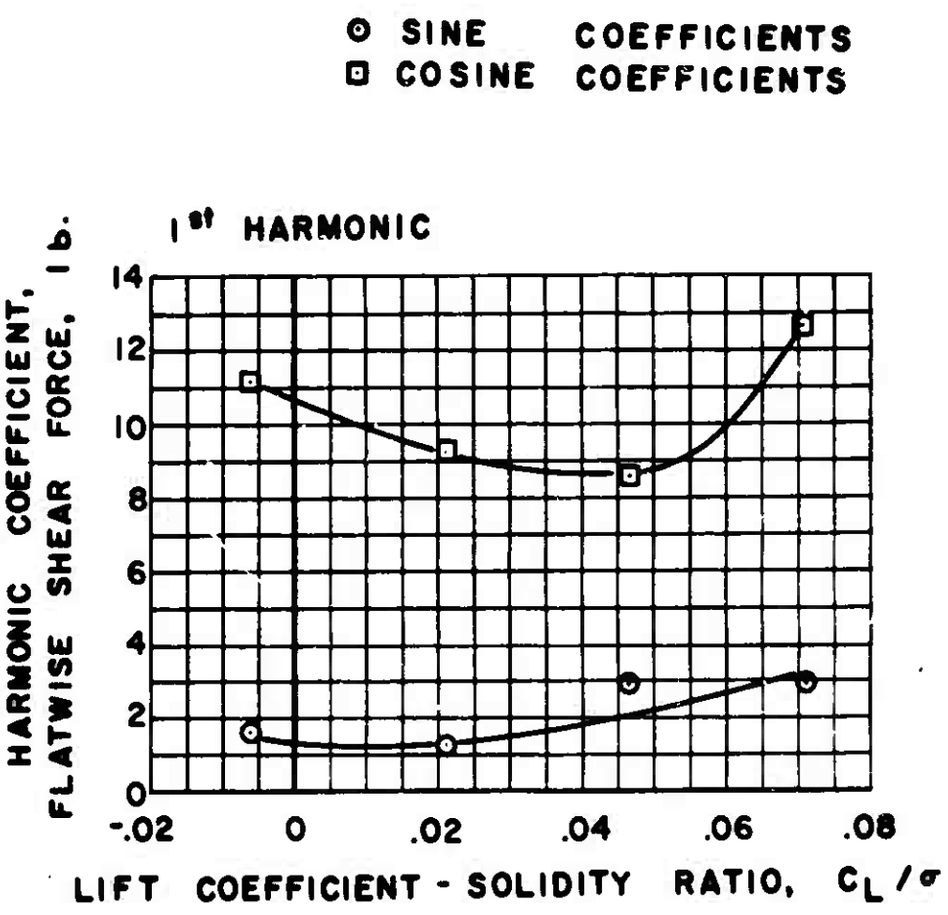

$\alpha_s = 0$ deg. $\mu = 0.2$

-4 deg. FIRST HARMONIC LONGITUDINAL FLAPPING

(b) OUT-OF-TRIM

Figure 9. Continued.

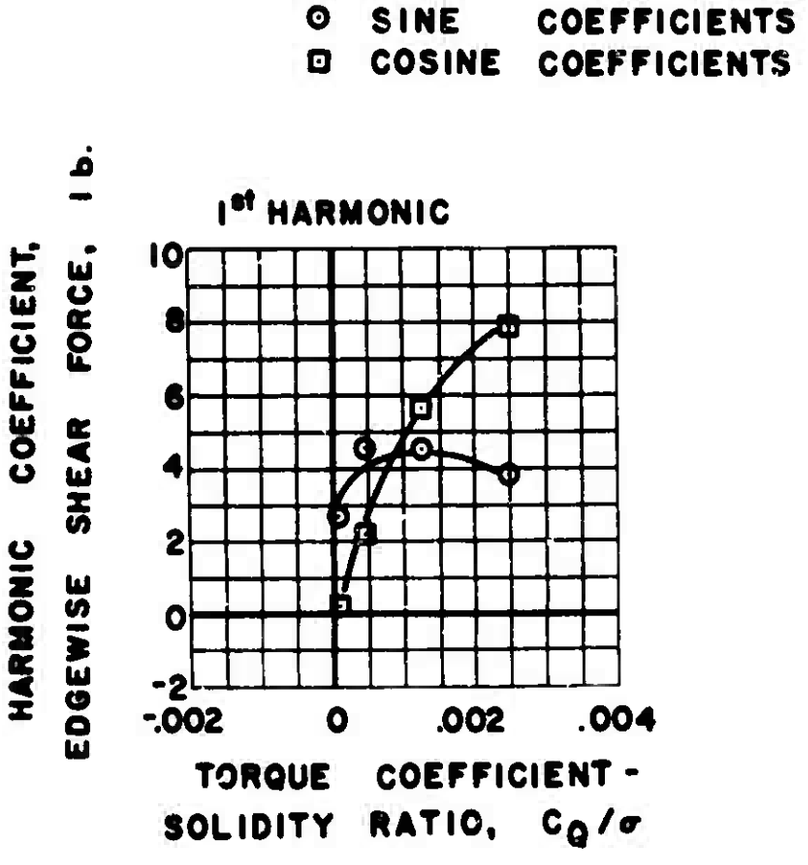

$\alpha_s = 0$ deg. $\mu = 0.2$

Figure 9(b) Concluded.

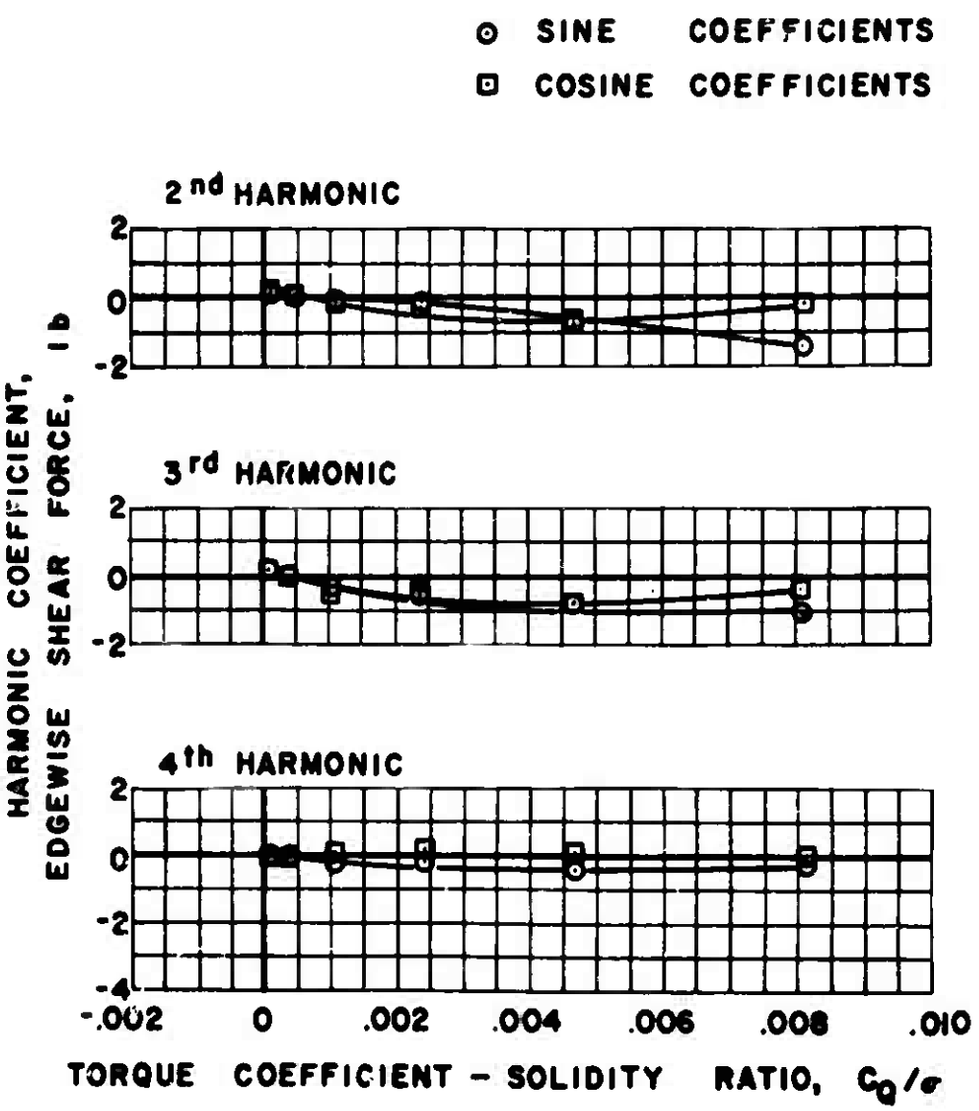

α_s =-4 deg. μ =0.2

(a) FULL LAG DAMPING

Figure 10. Effect of Lag Damping on Shear Forces.

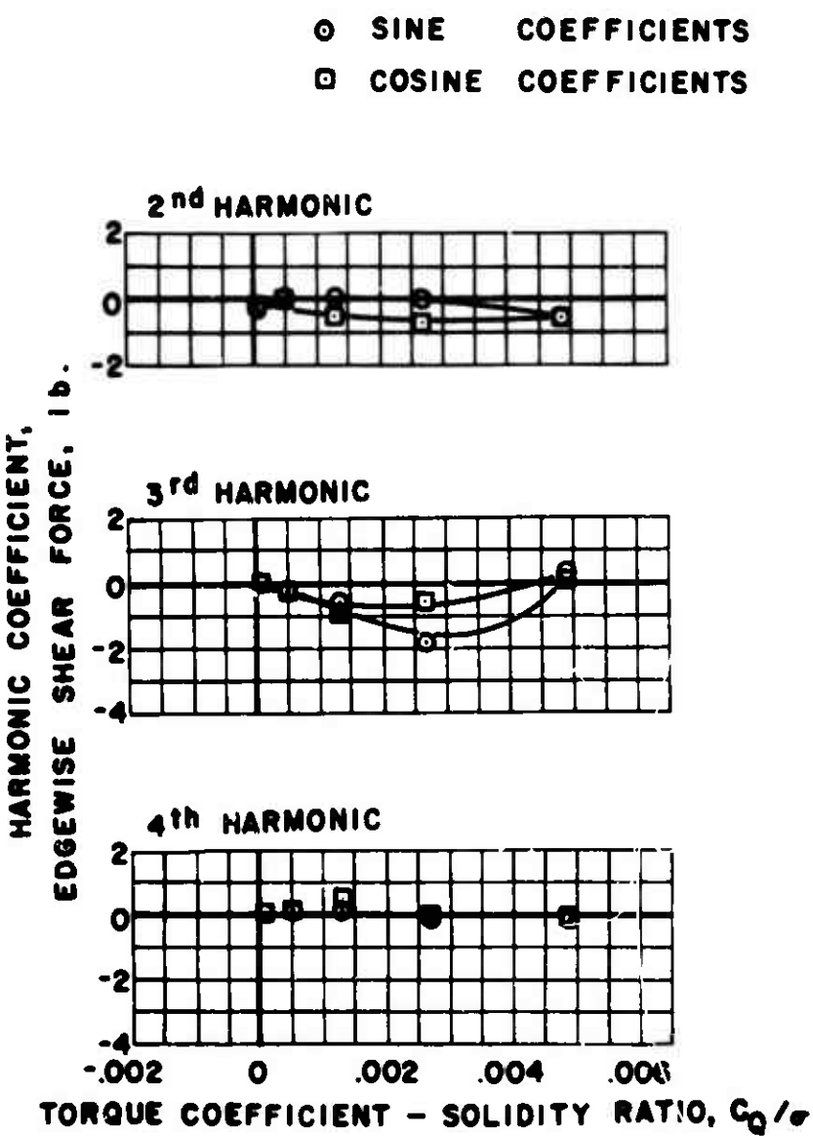

α_s =-4 deg. μ=0.2

(b) ZERO LAG DAMPING

Figure 10. Concluded.

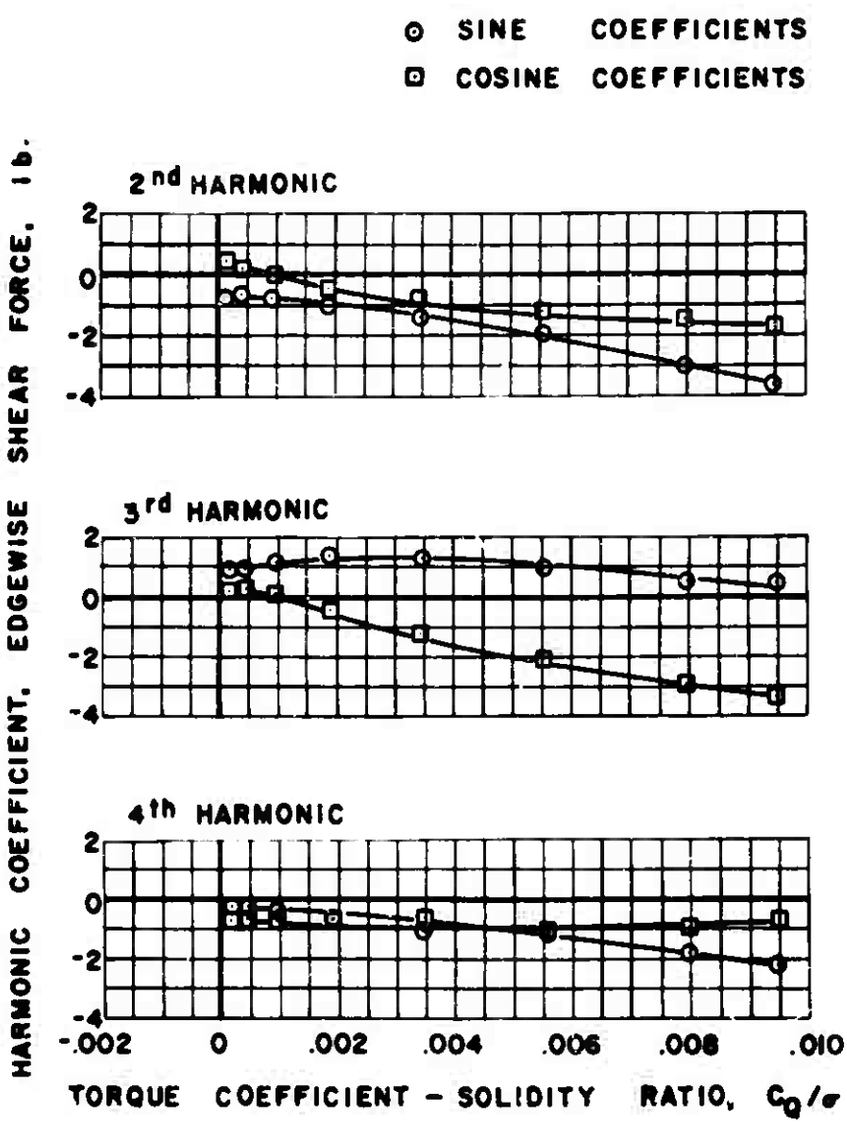

α_s = -4deg. μ = 0.5

(a) FULL LAG DAMPING

Figure 11. Effect of Lag Damping on Shear Forces.

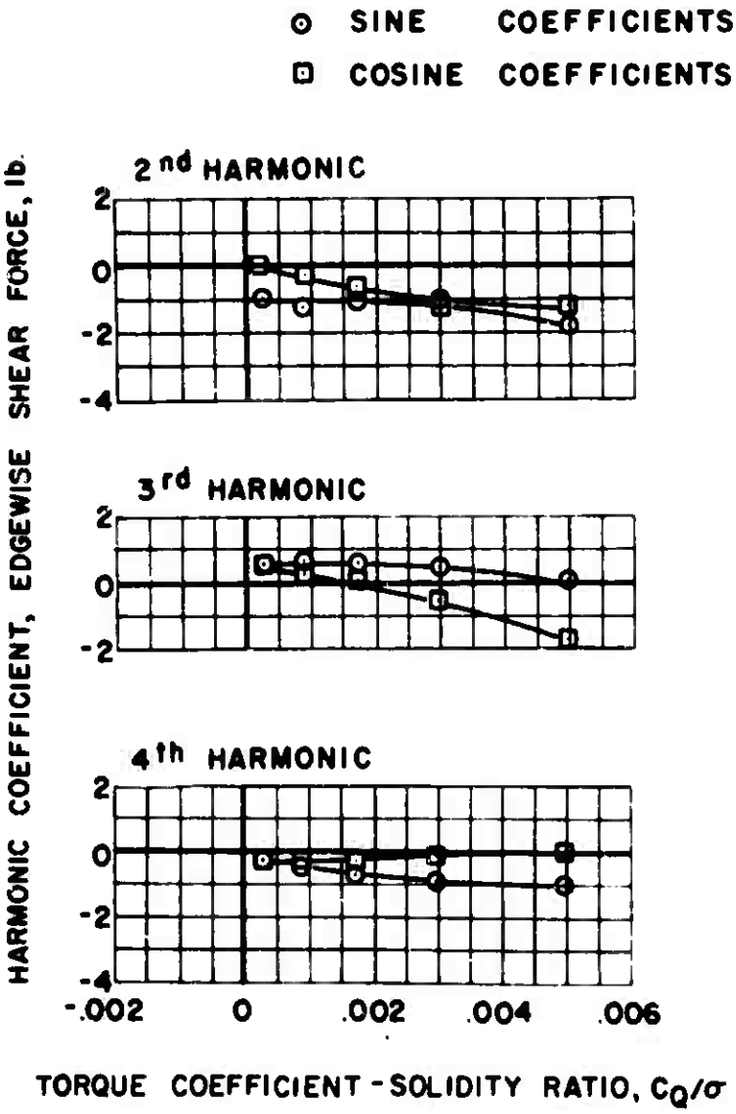

$\alpha_s = -4$ deg. $\mu = 0.5$

(b) ZERO LAG DAMPING

Figure 11. Concluded.

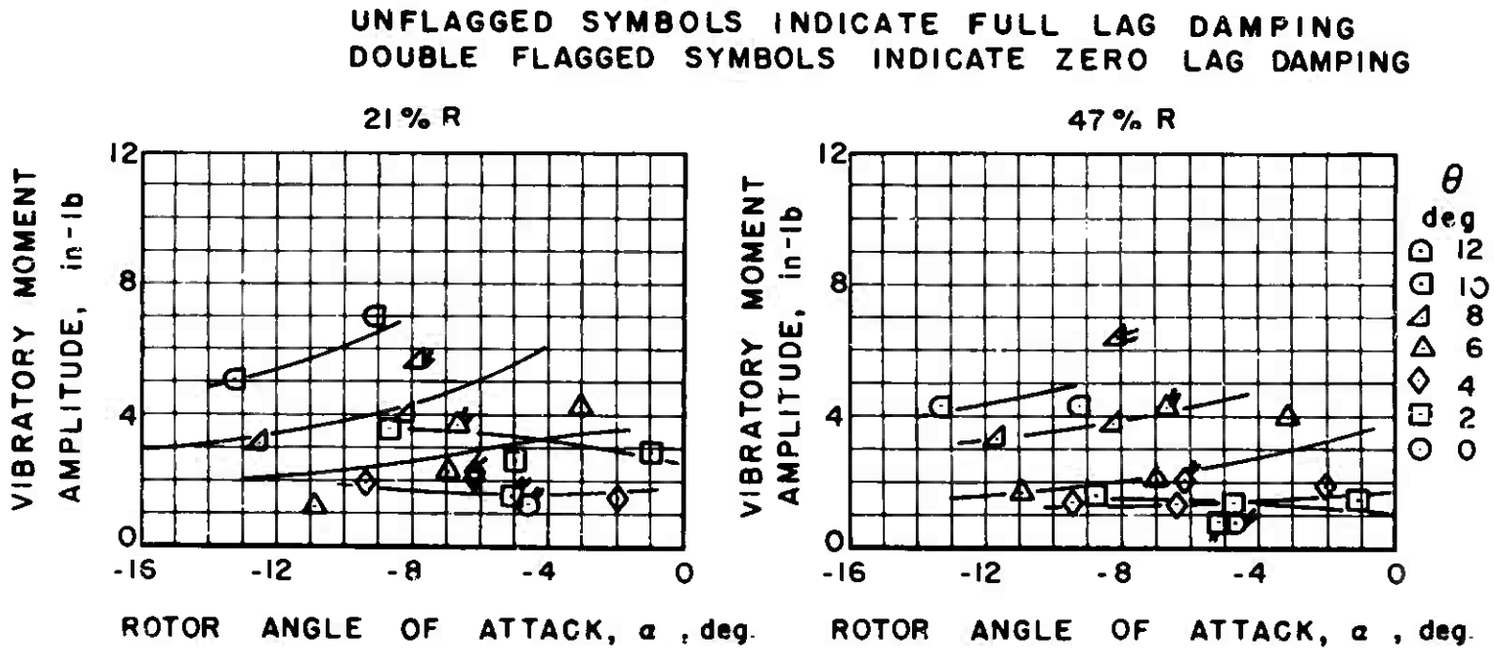

(a) $\mu = 0.2$

Figure 12. Effect of Lag Damping on Edgewise Blade Bending Moment.

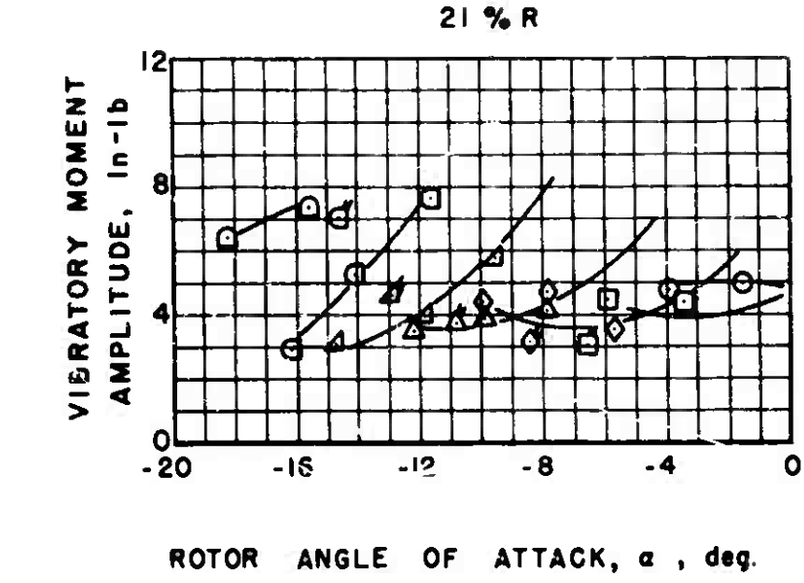

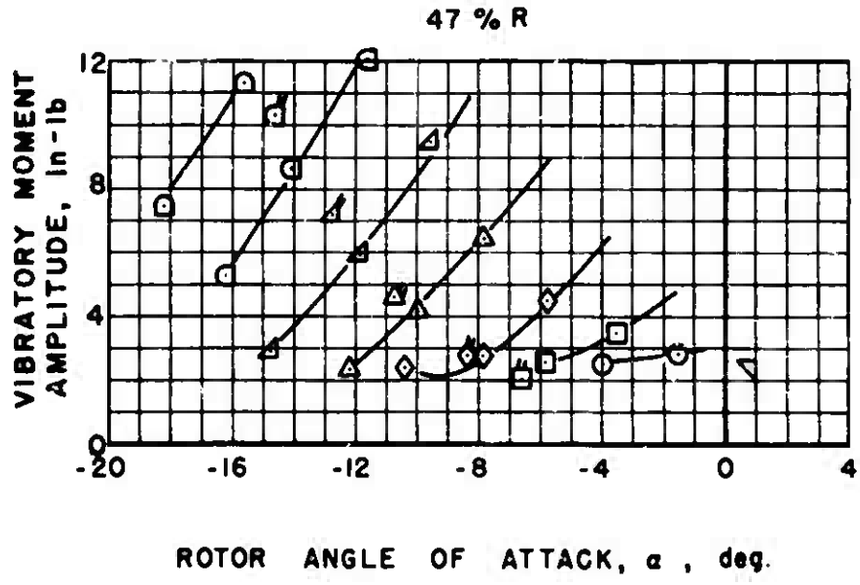

(b) $\mu = 0.5$

Figure 12. Continued.

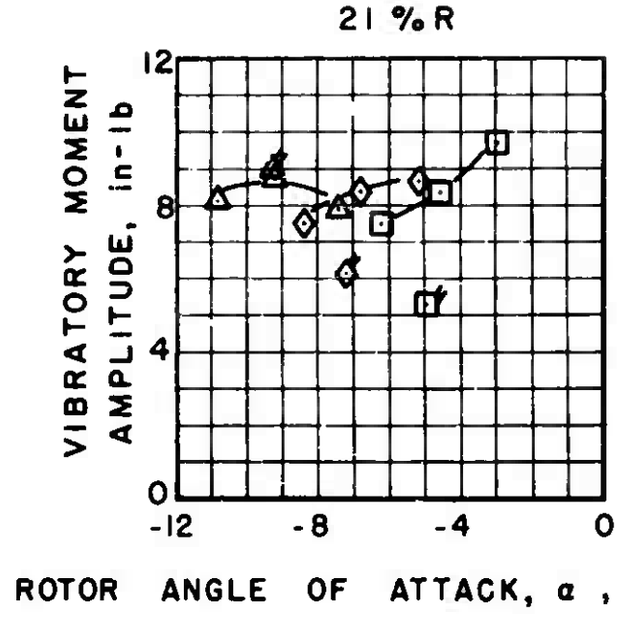

(c) $\mu = 0.7$

Figure 12. Concluded.

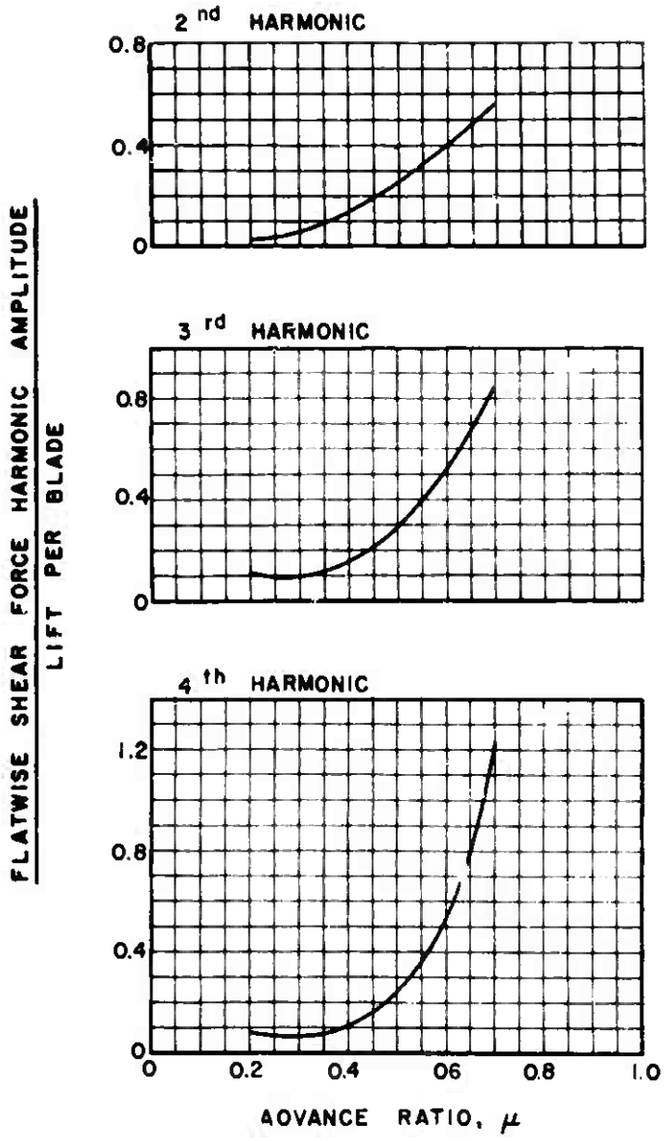

Figure 13. Effect of Advance Ratio on Nondimensional Shear Forces.

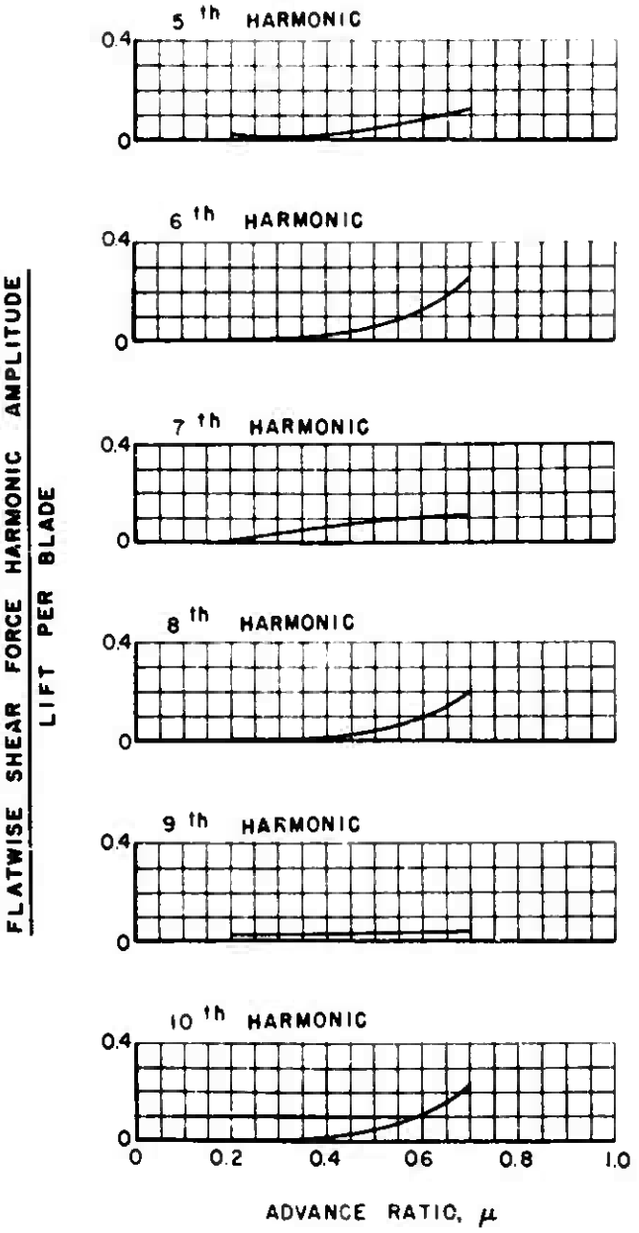

Figure 13(a). Continued.

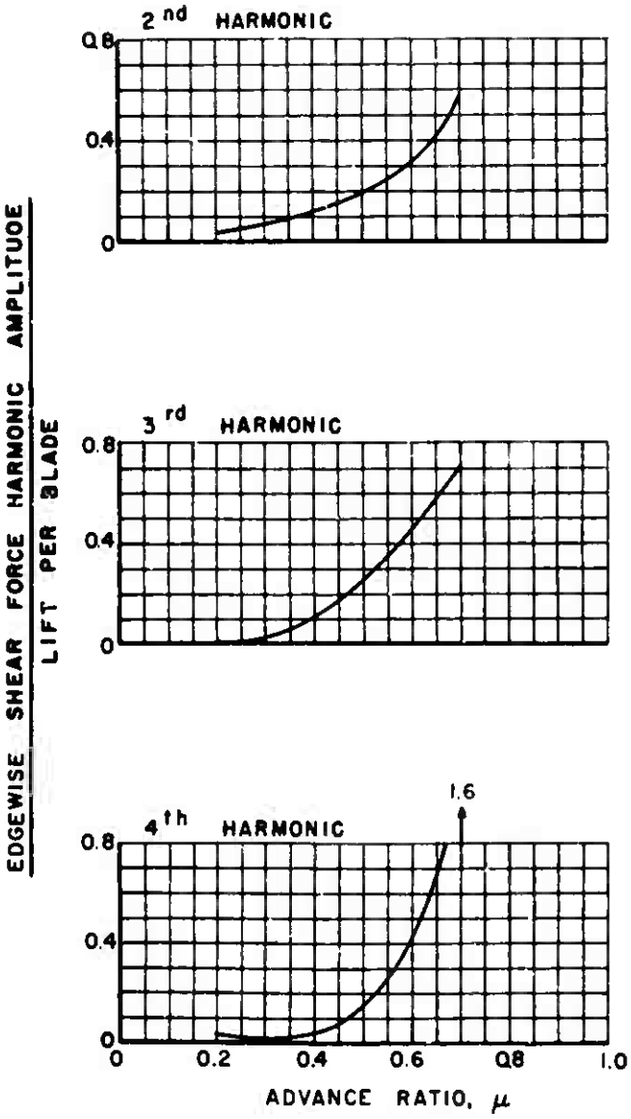

$C_L/\sigma = 0.035$, $\alpha_s = -4$ deg.

(b) EDGEWISE SHEAR

Figure 13. Continued.

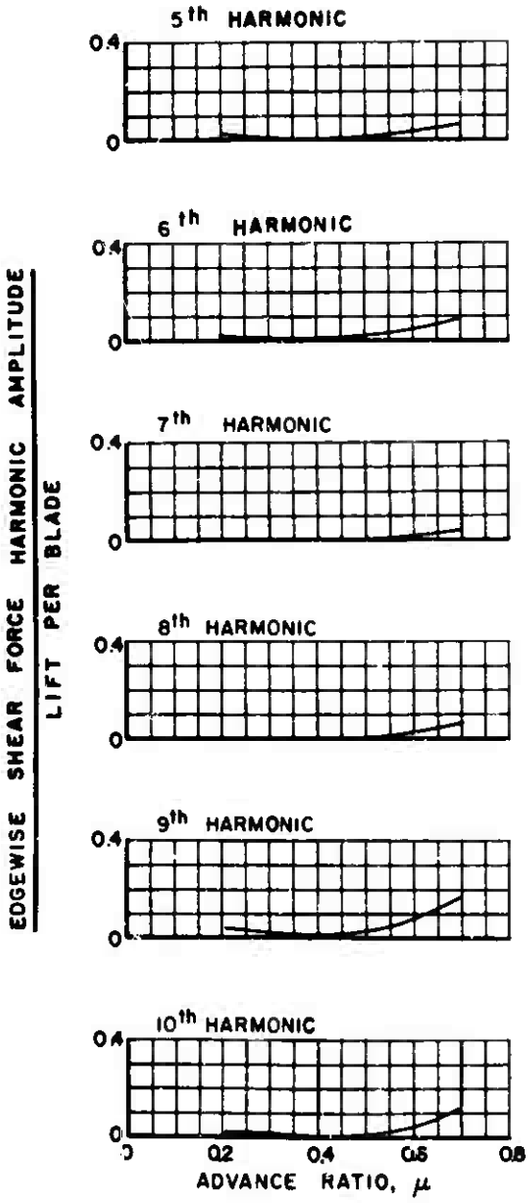

Figure 13(b). Concluded.

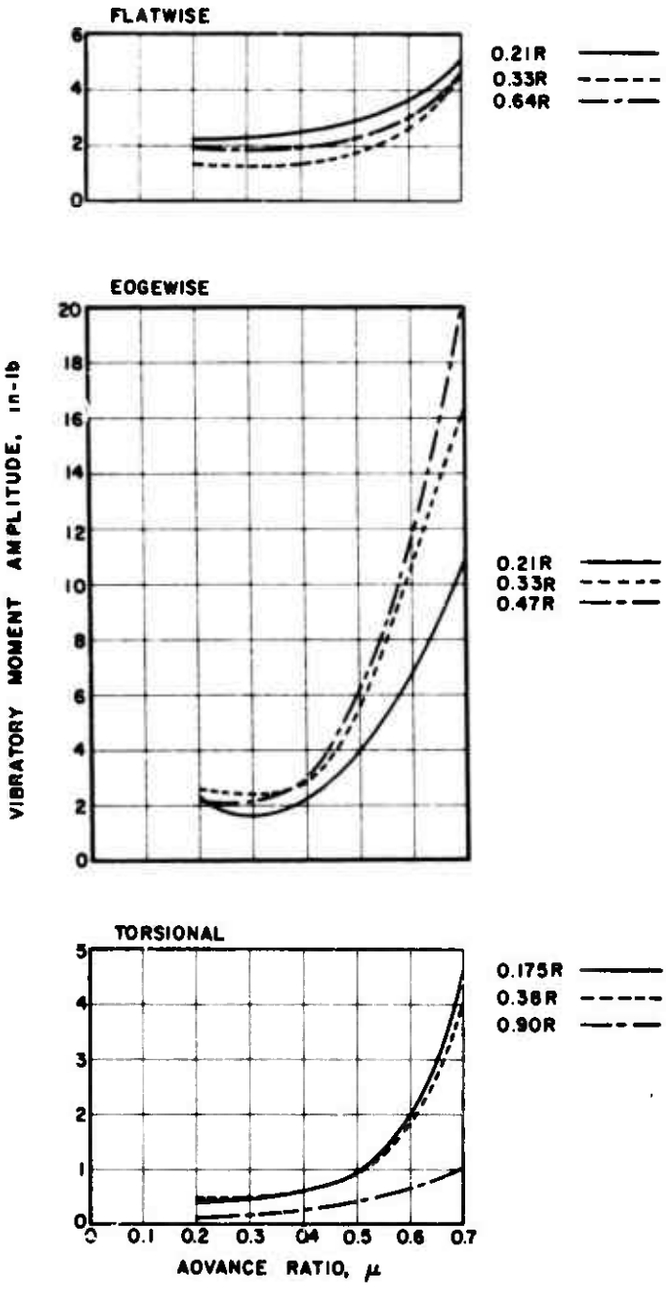

Figure 14. Effect of Advance Ratio on Rotor Blade Vibratory Moments.

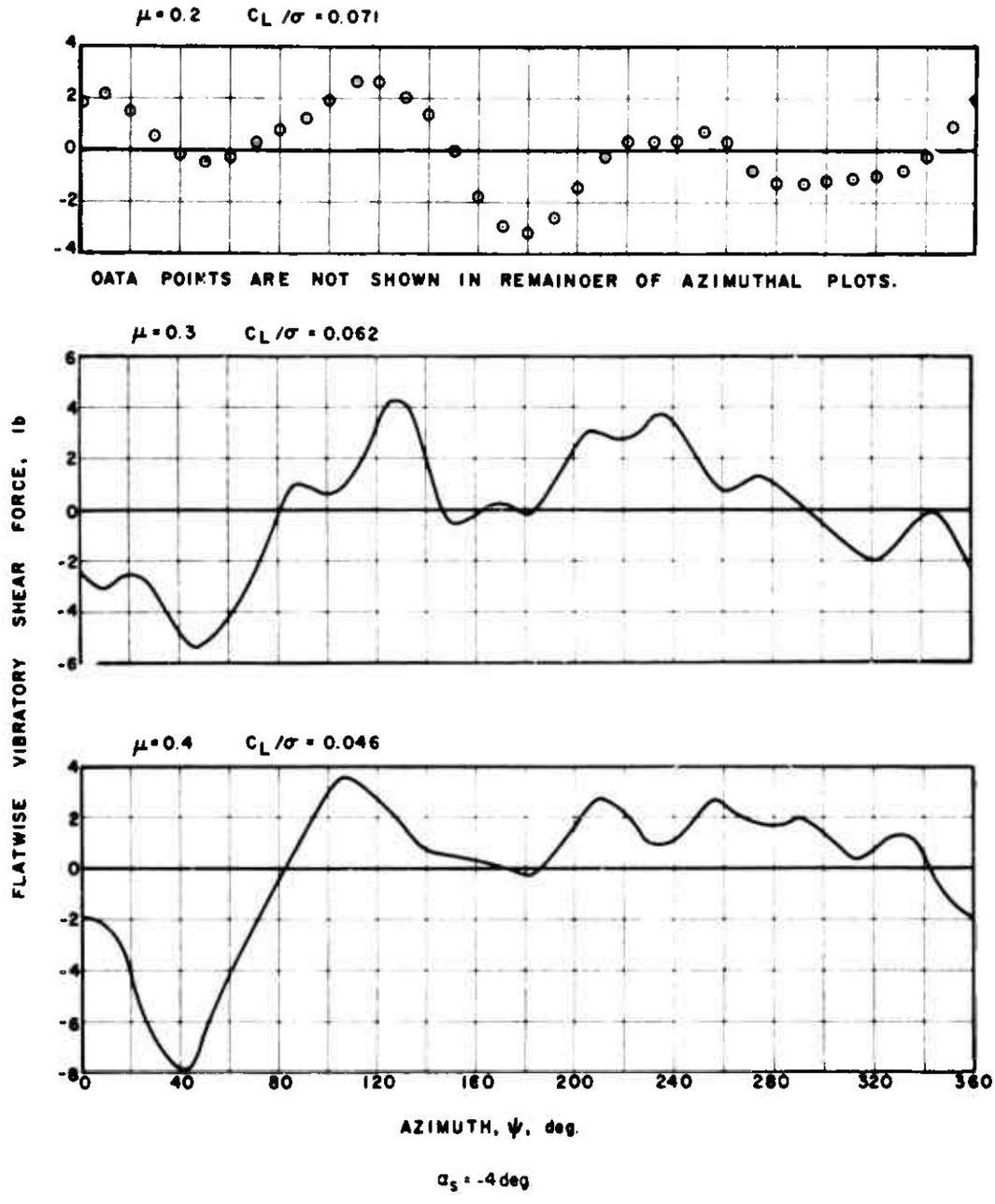

Figure 15. Experimental Flatwise Vibratory Shear Force.

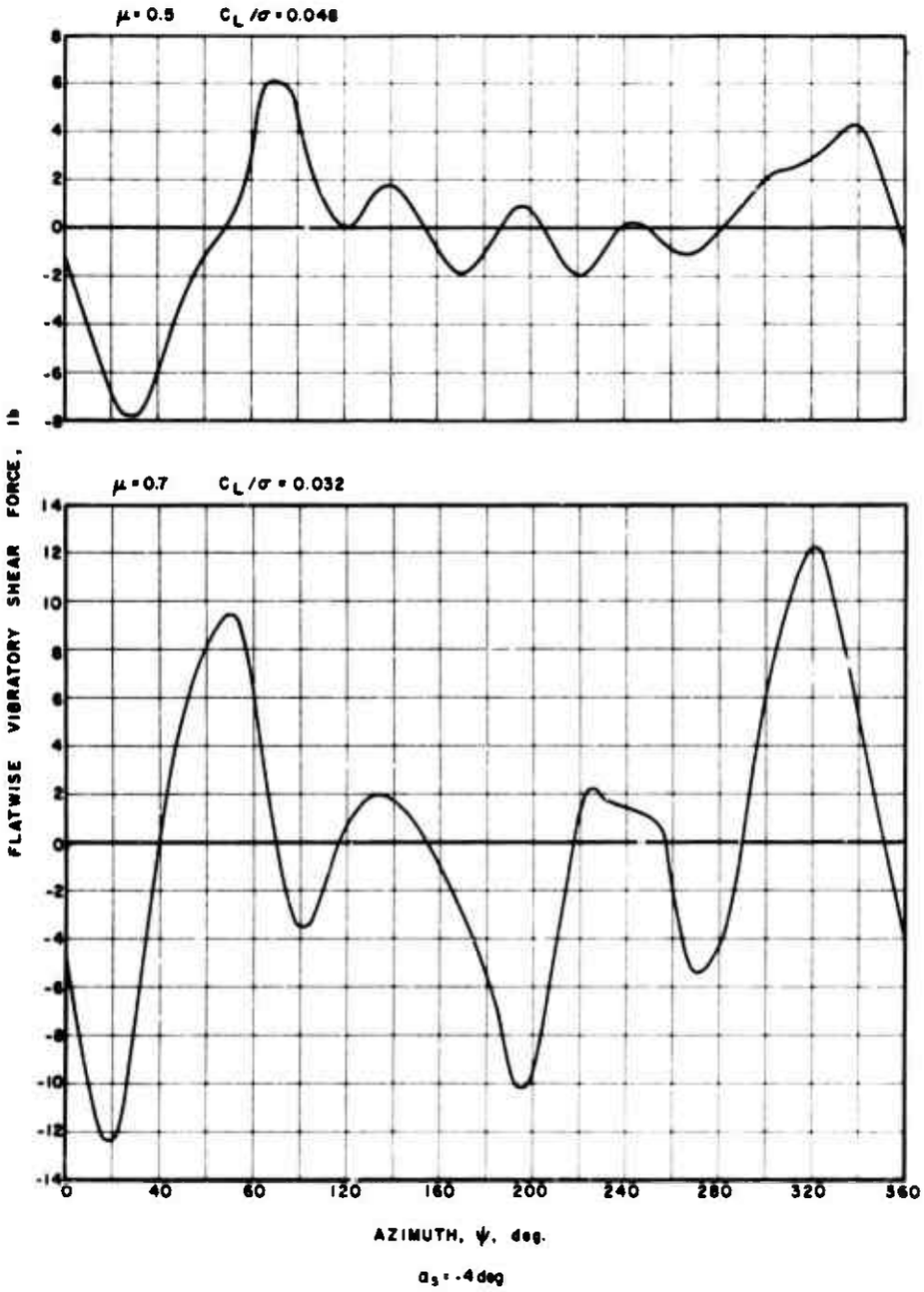

Figure 15. Concluded.

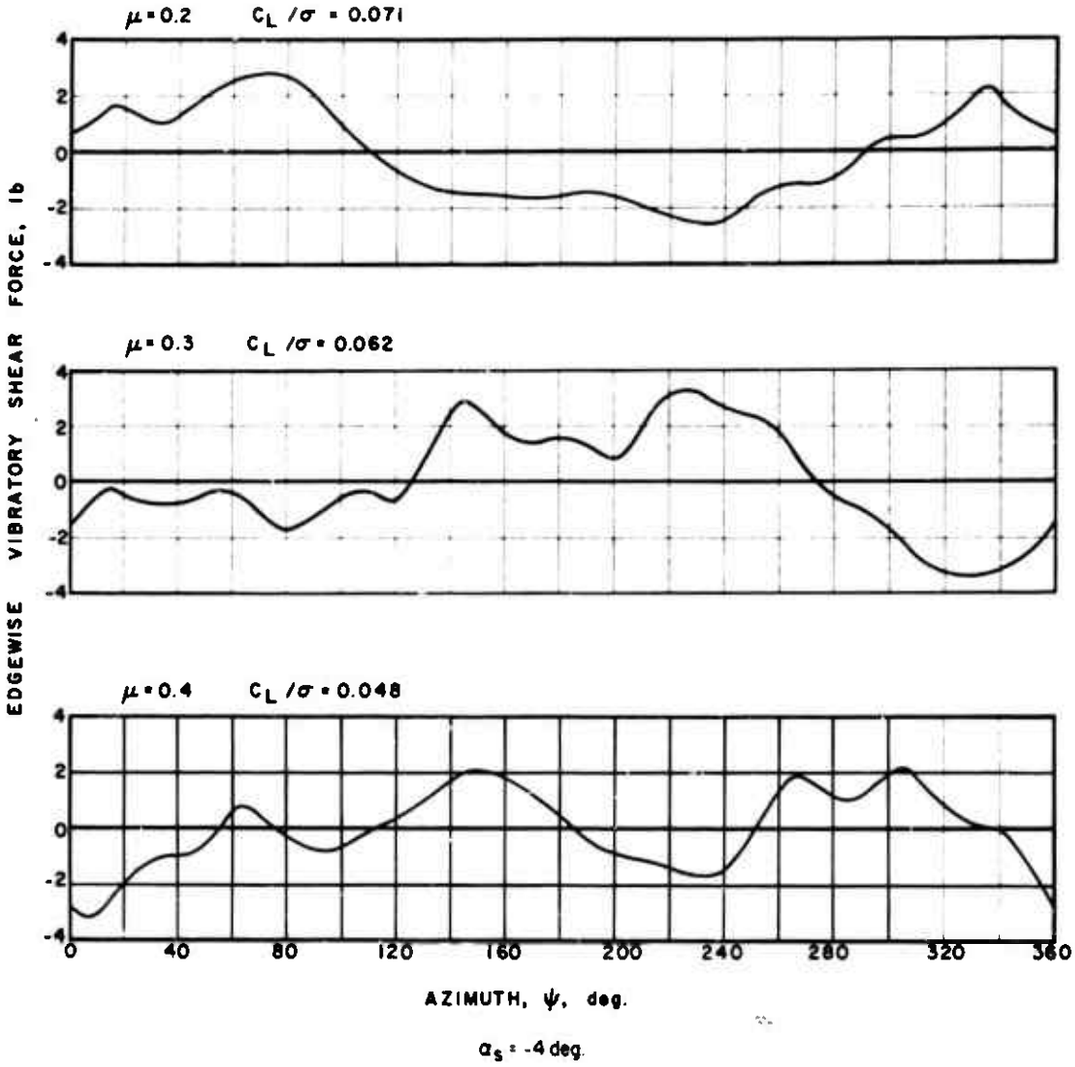

Figure 16. Experimental Edgewise Vibratory Shear Force.

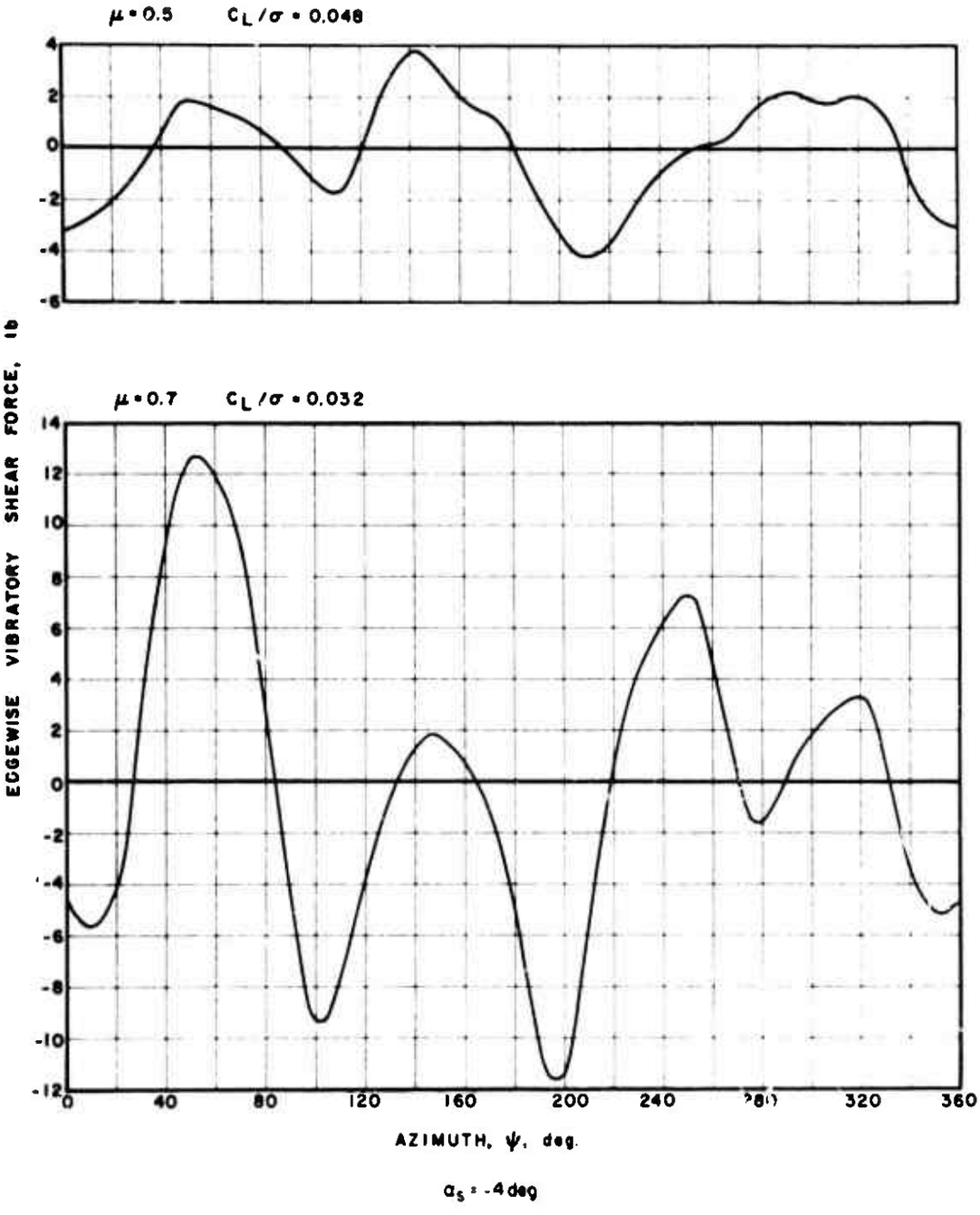

Figure 16. Concluded.

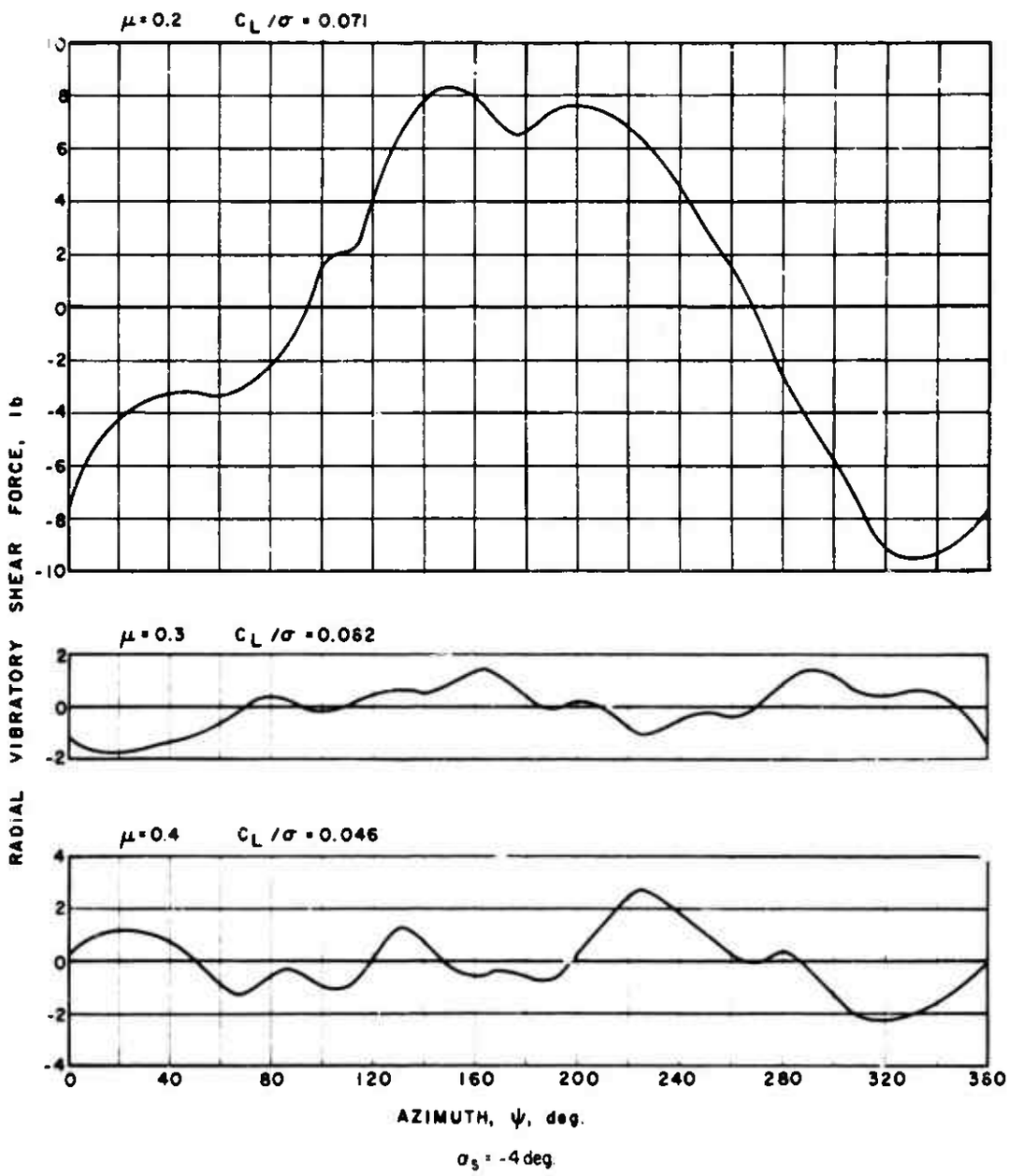

Figure 17. Experimental Radial Vibratory Shear Force.

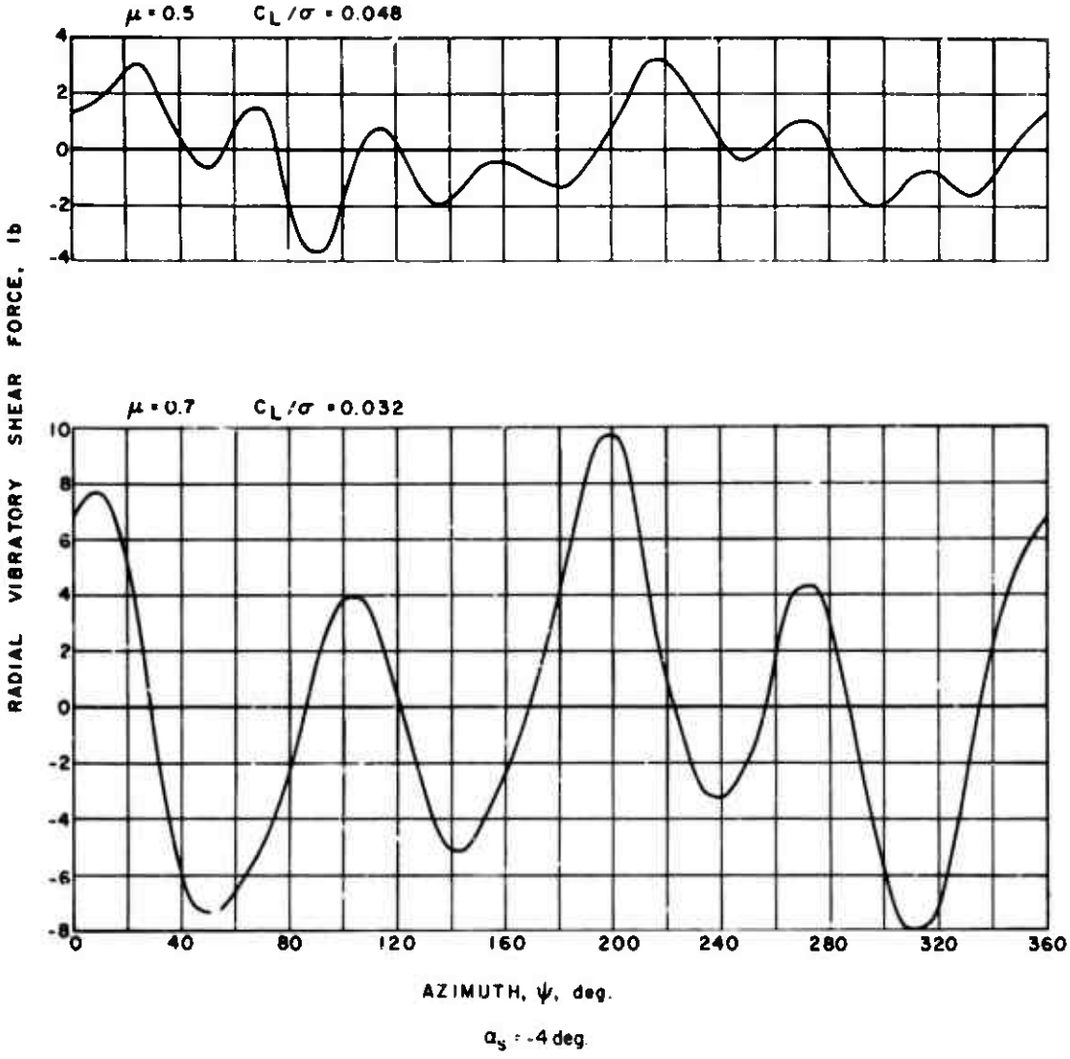

Figure 17. Concluded.

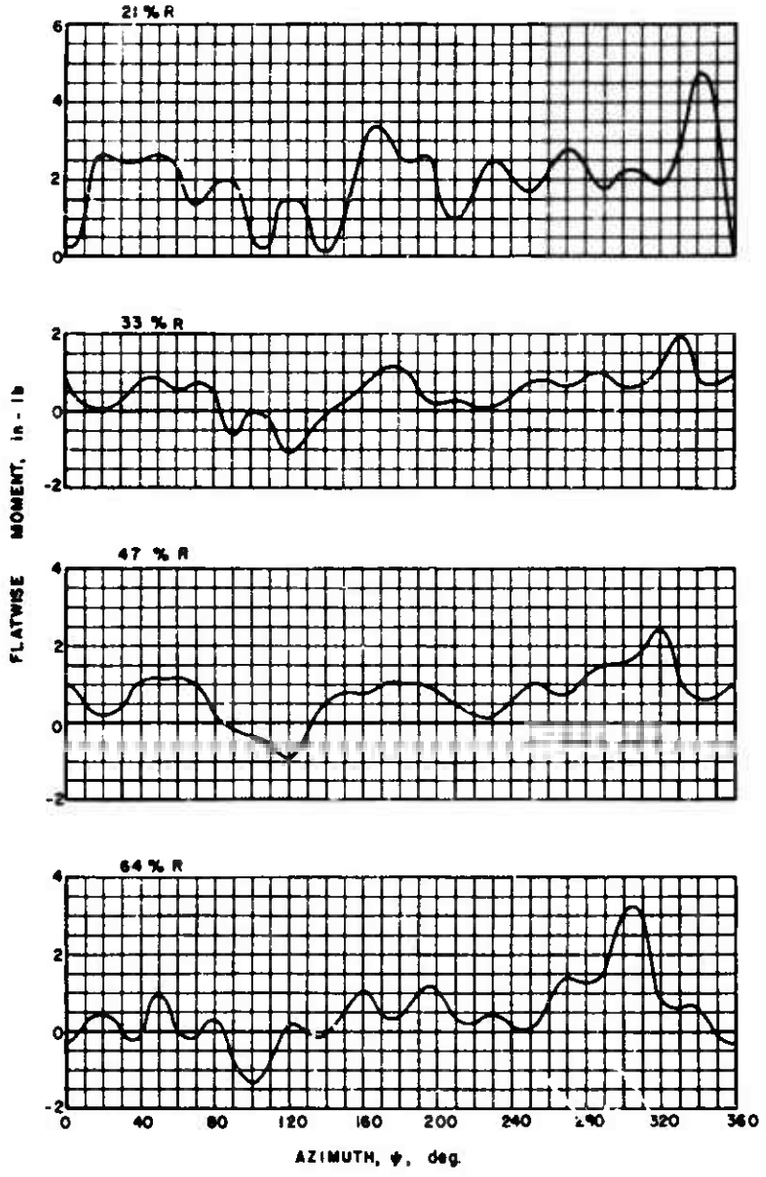

(a) FLATWISE MOMENTS

Figure 18. Experimental Blade Moments.

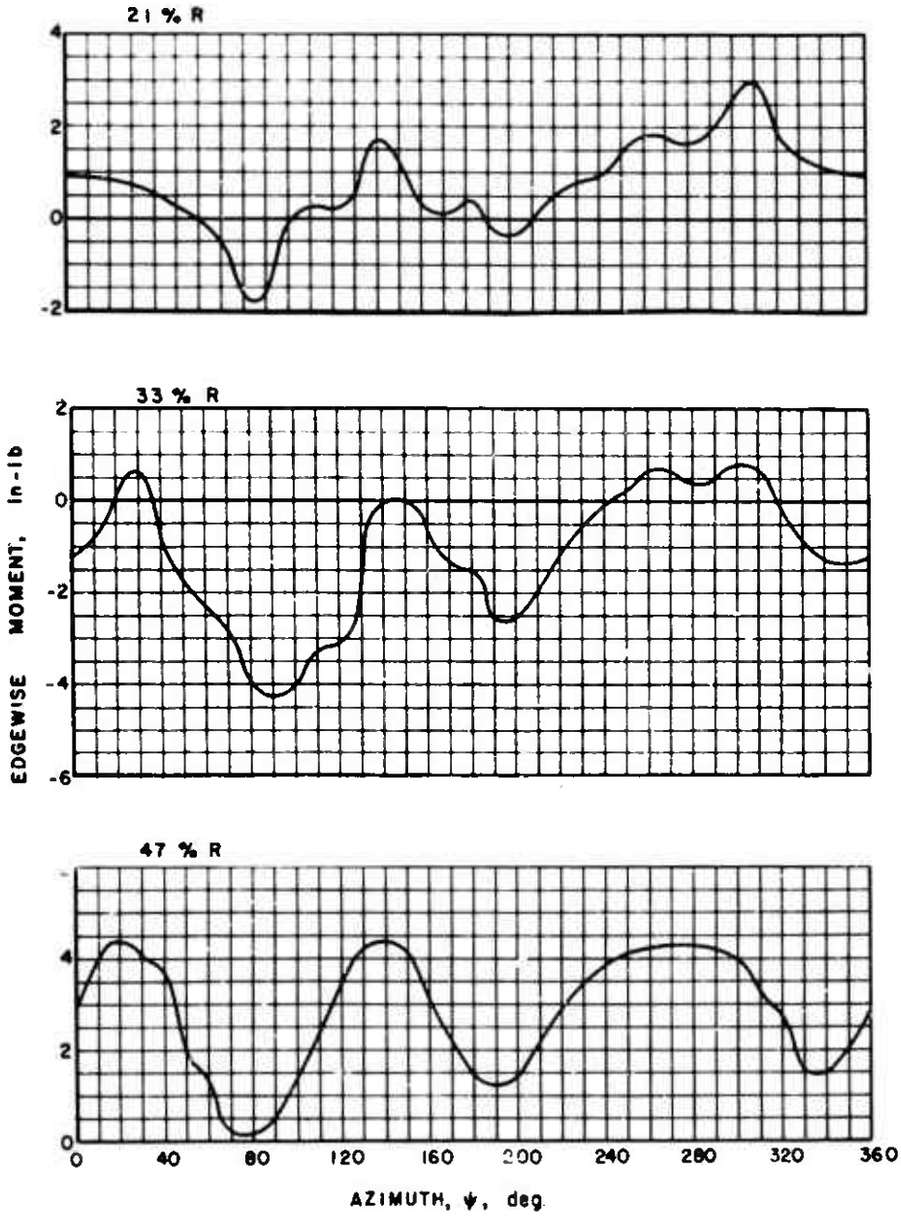

(b) EDGEWISE MOMENTS

Figure 18. Continued.

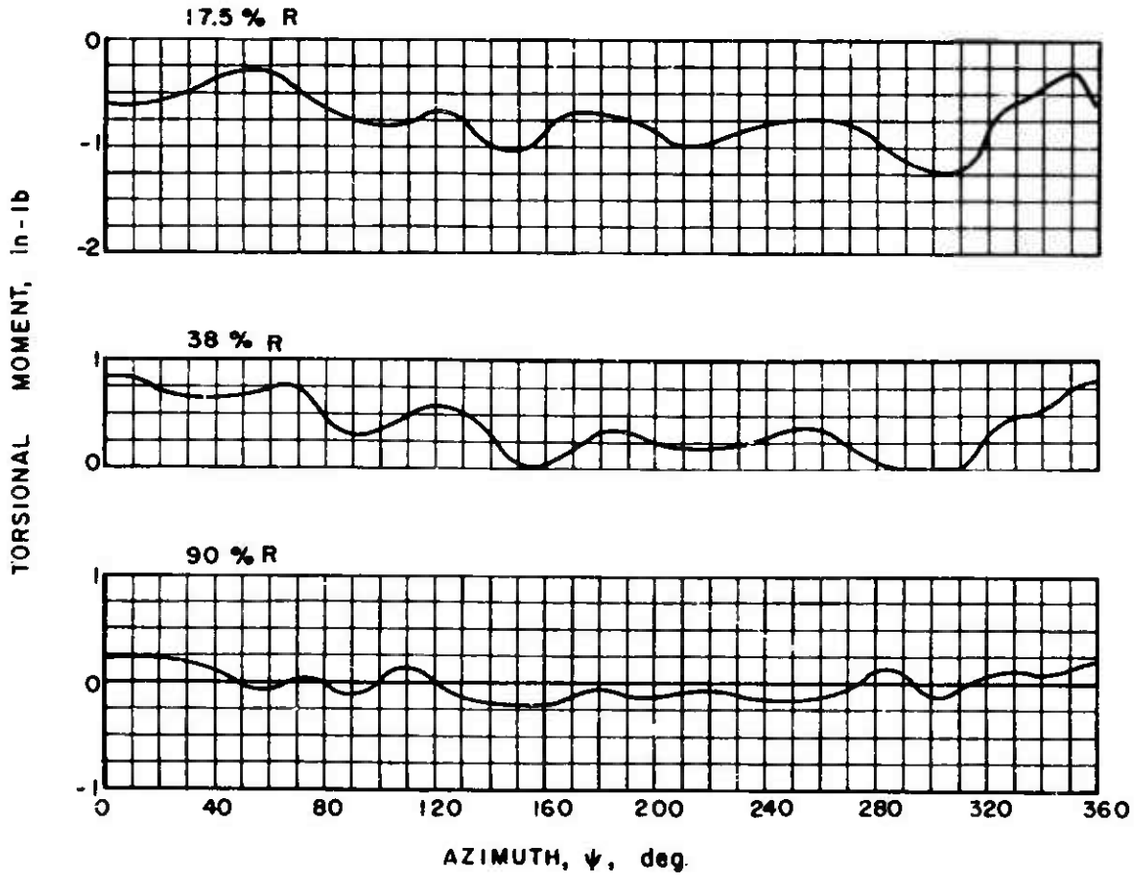

(c) TORSIONAL MOMENTS

Figure 18. Concluded.

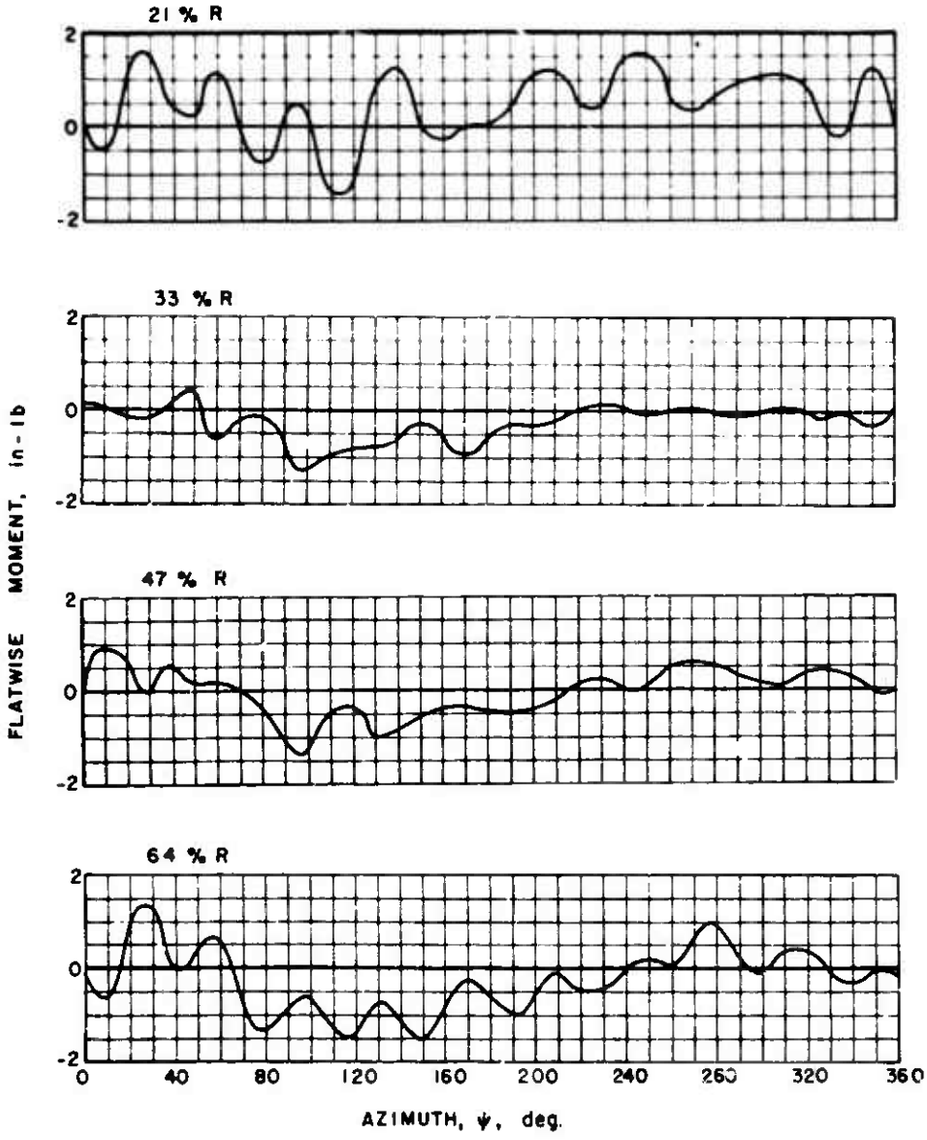

(a) FLATWISE MOMENTS

Figure 19. Experimental Blade Moments.

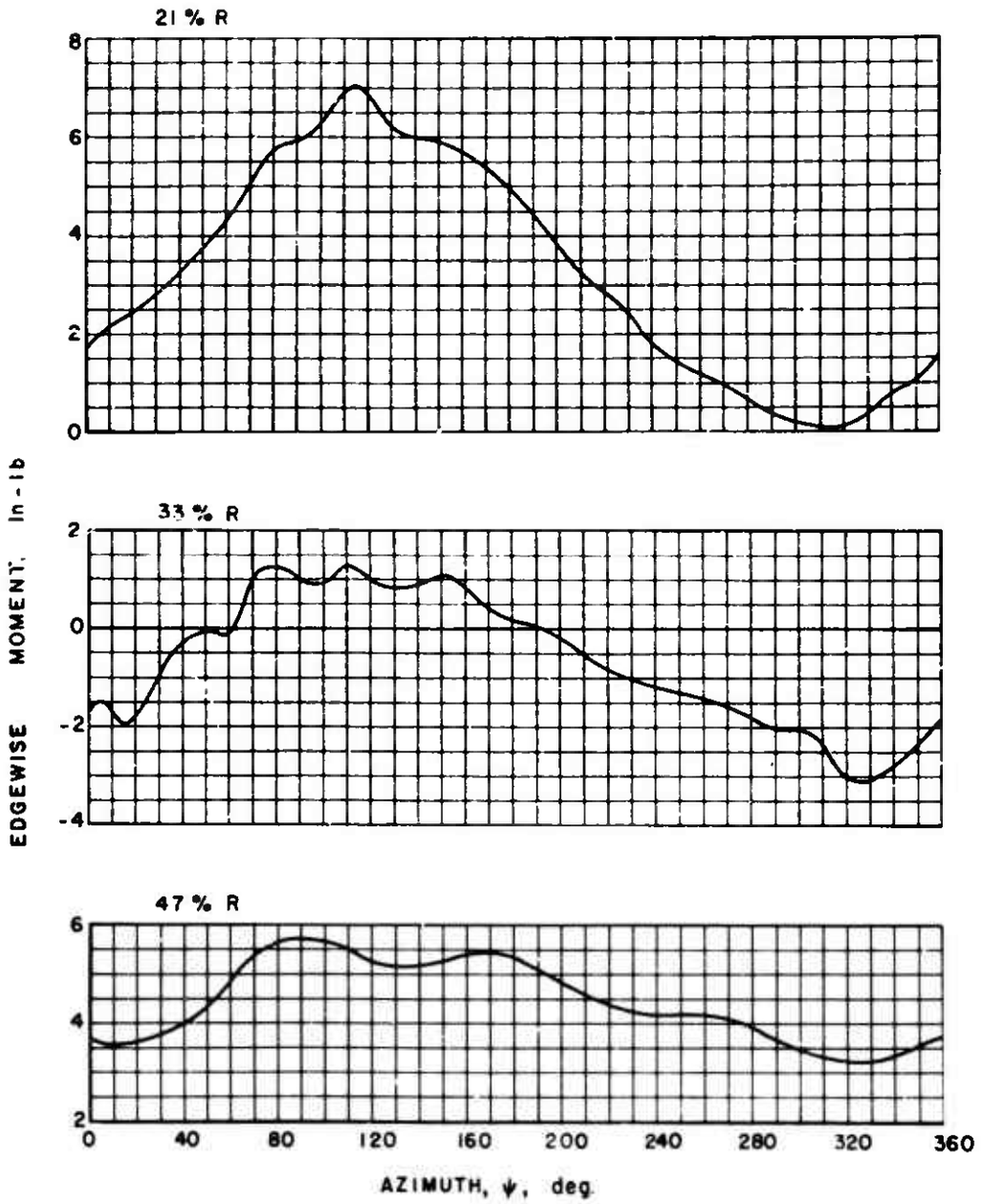

(b) EDGEWISE MOMENTS

Figure 19. Continued.

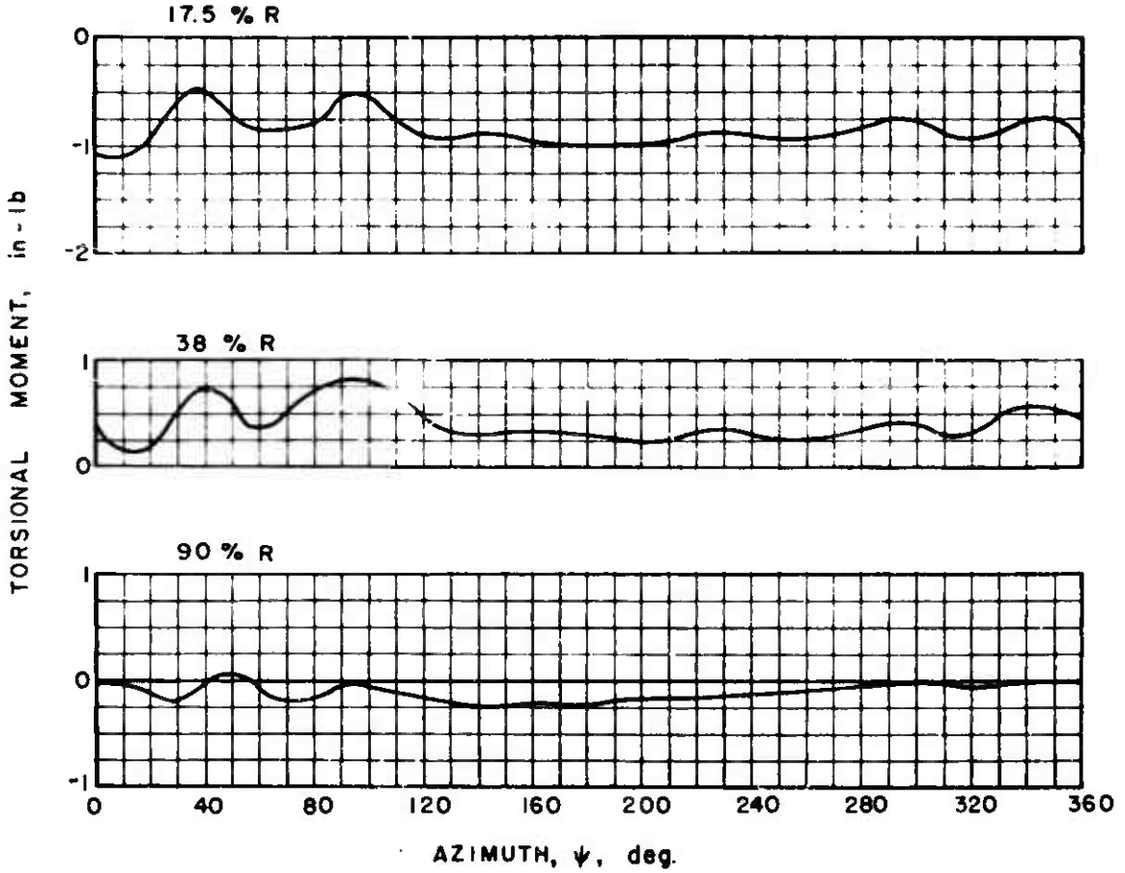

(c) TORSIONAL MOMENTS

Figure 19. Concluded.

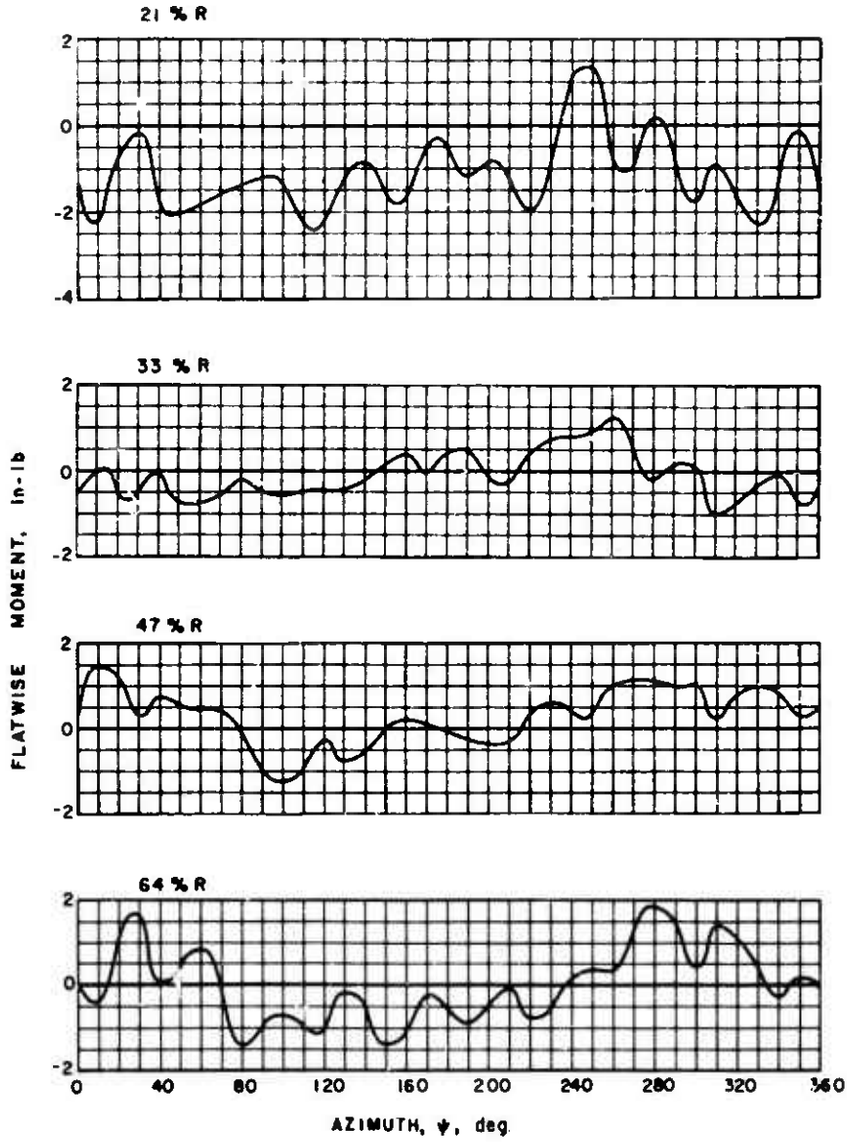

(a) FLATWISE MOMENTS

Figure 20. Experimental Blade Moments.

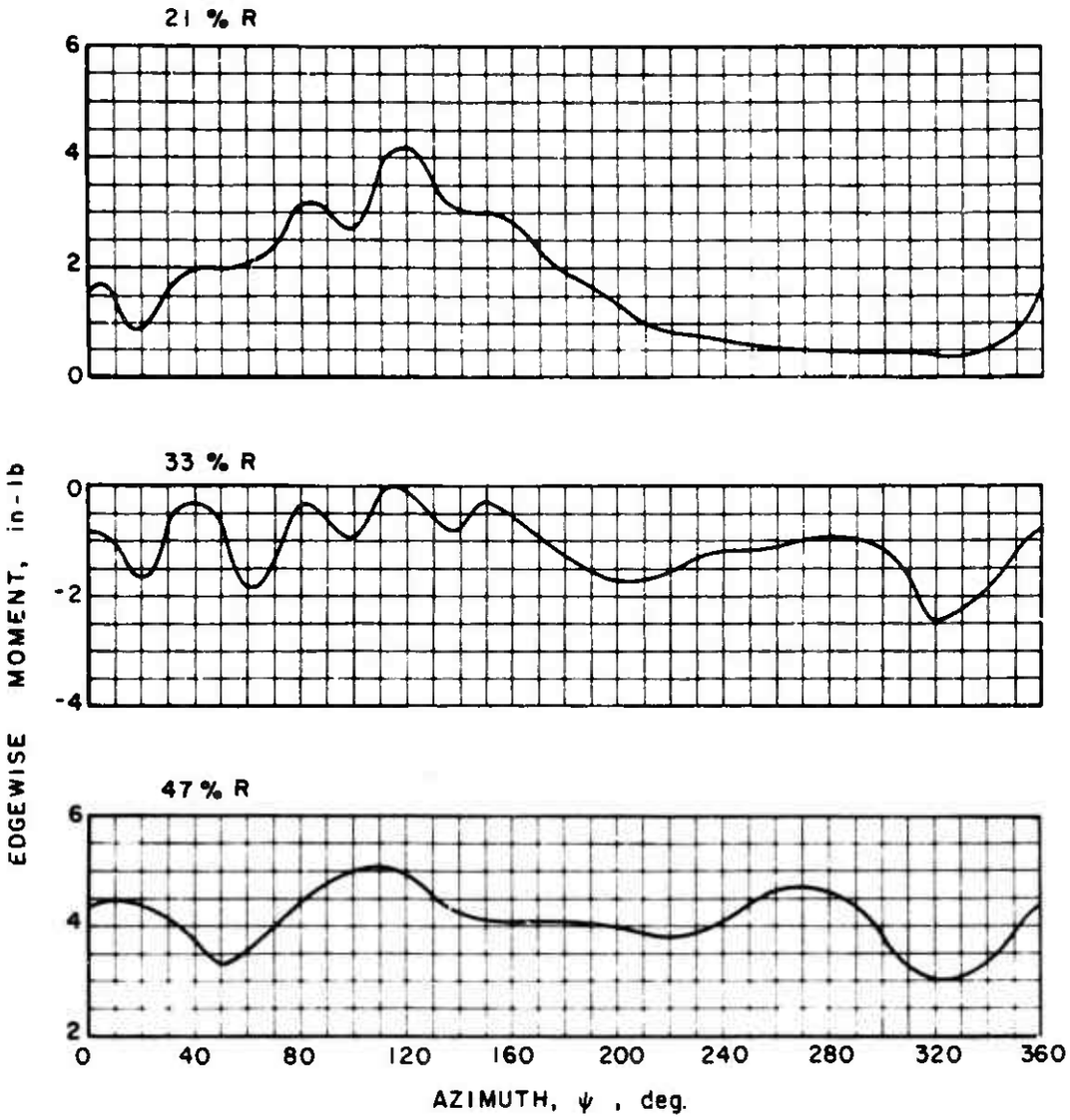

(b) EDGEWISE MOMENTS

Figure 20. Continued.

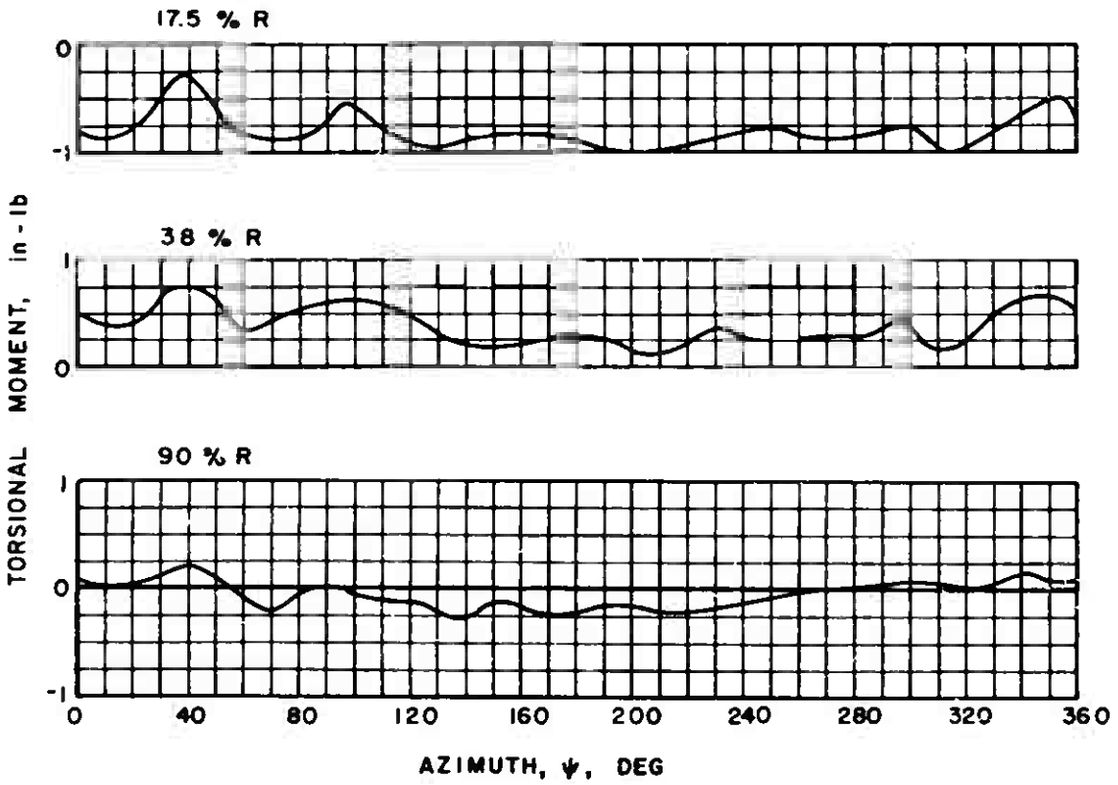

(c) TORSIONAL MOMENTS

Figure 20. Concluded.

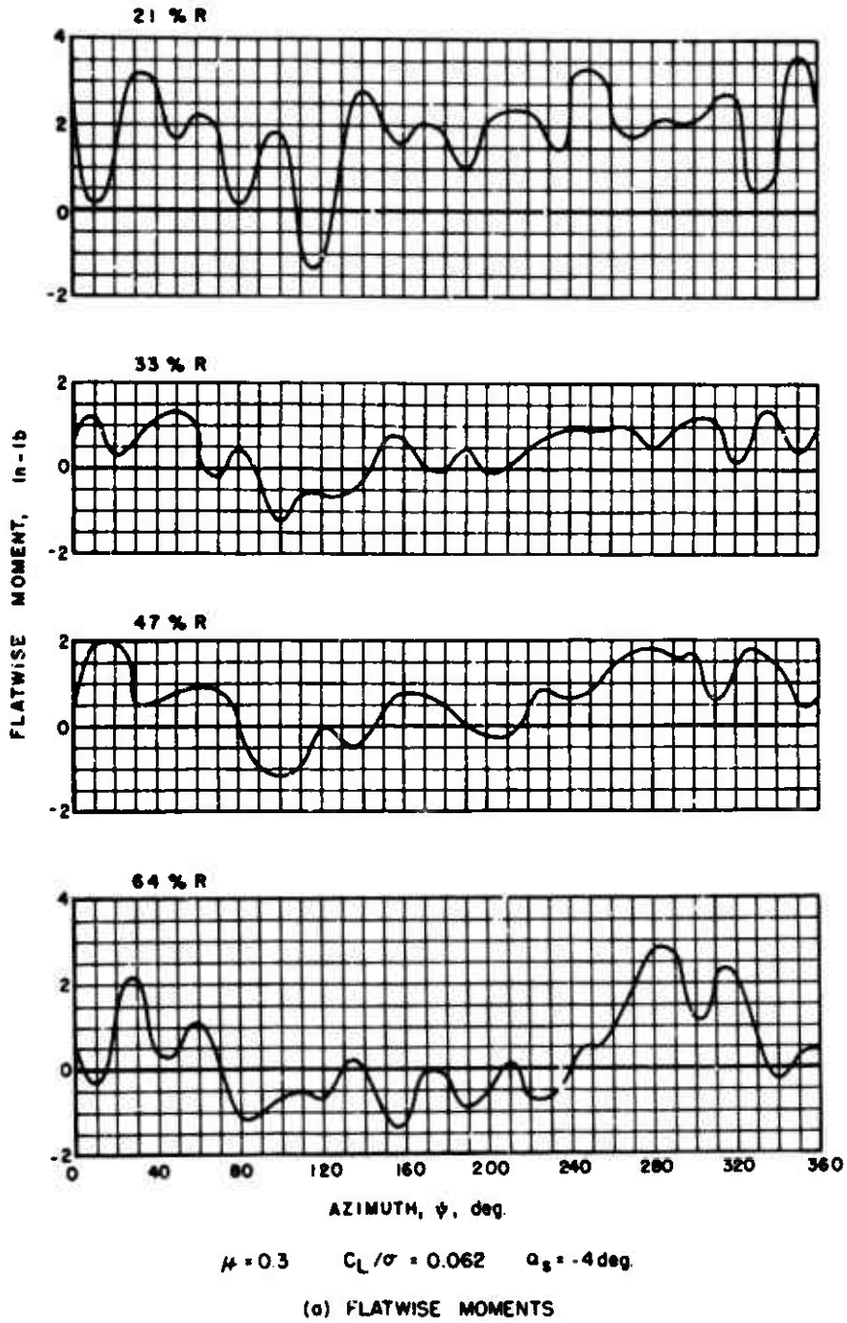

Figure 21. Experimental Blade Moments.

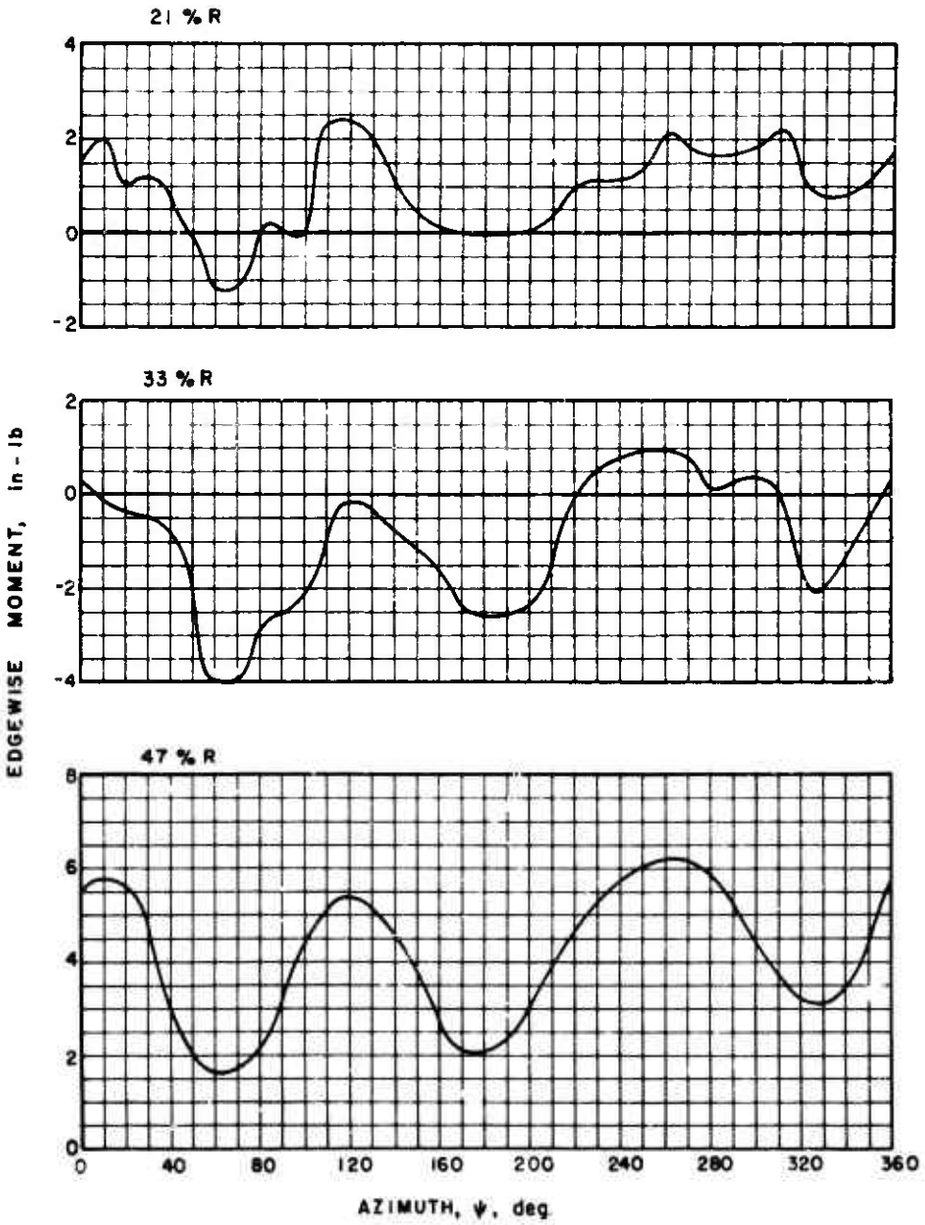

(b) EDGEWISE MOMENTS

Figure 21. Continued.

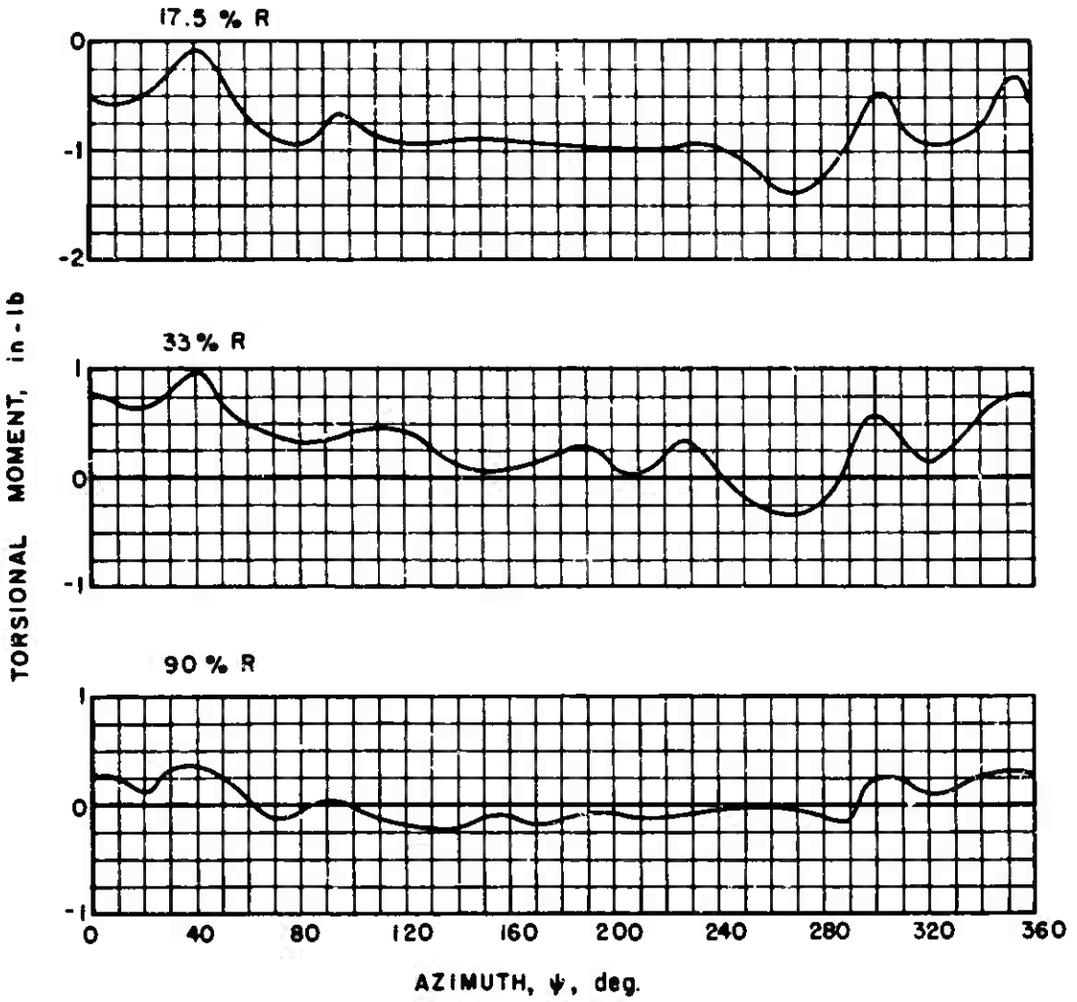

(c) TORSIONAL MOMENTS

Figure 21. Concluded.

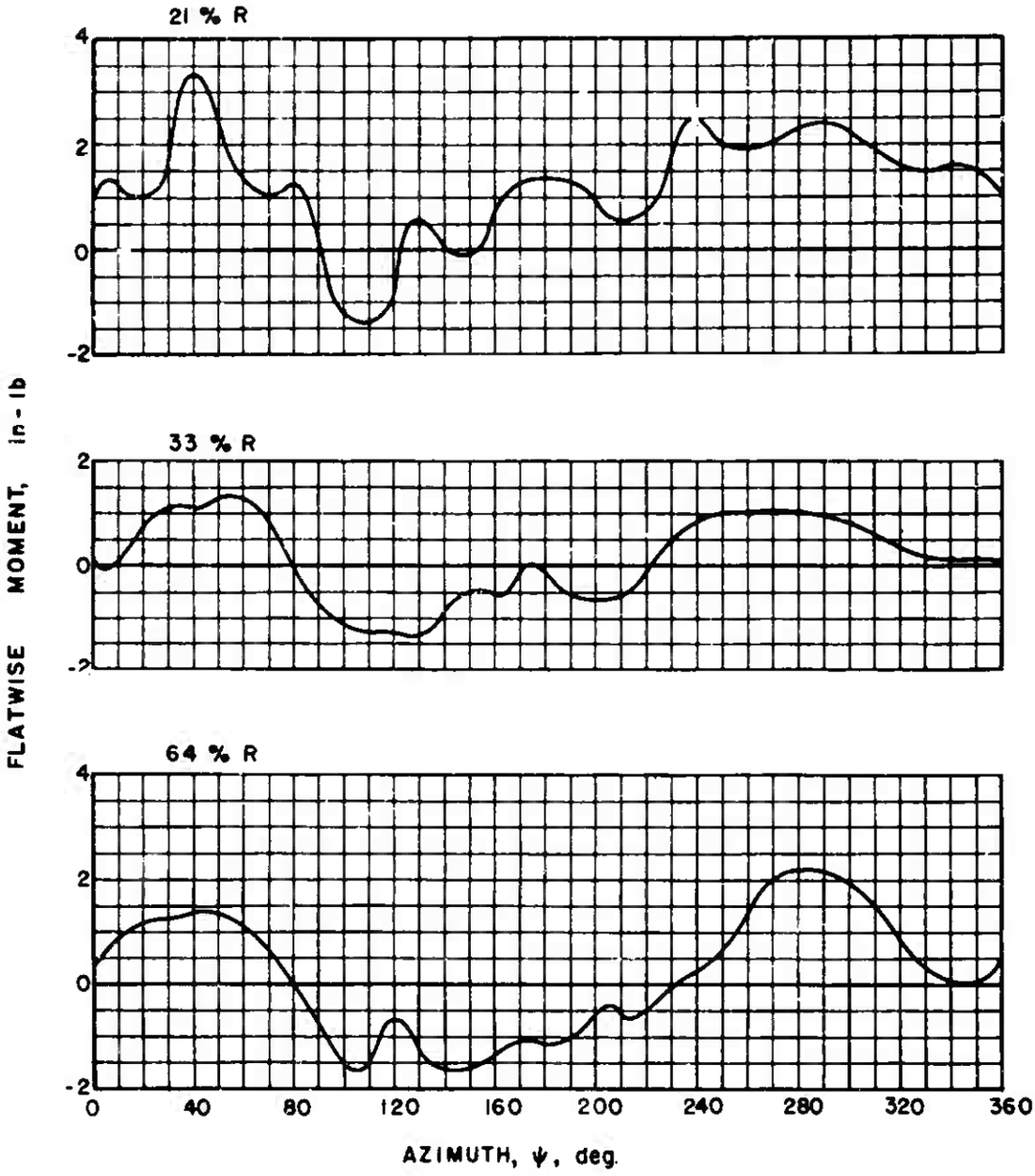

$\mu = 0.4$ $C_L/\sigma = 0.046$ $\alpha_s = -4$ deg.

(a) FLATWISE MOMENTS

Figure 22. Experimental Blade Moments.

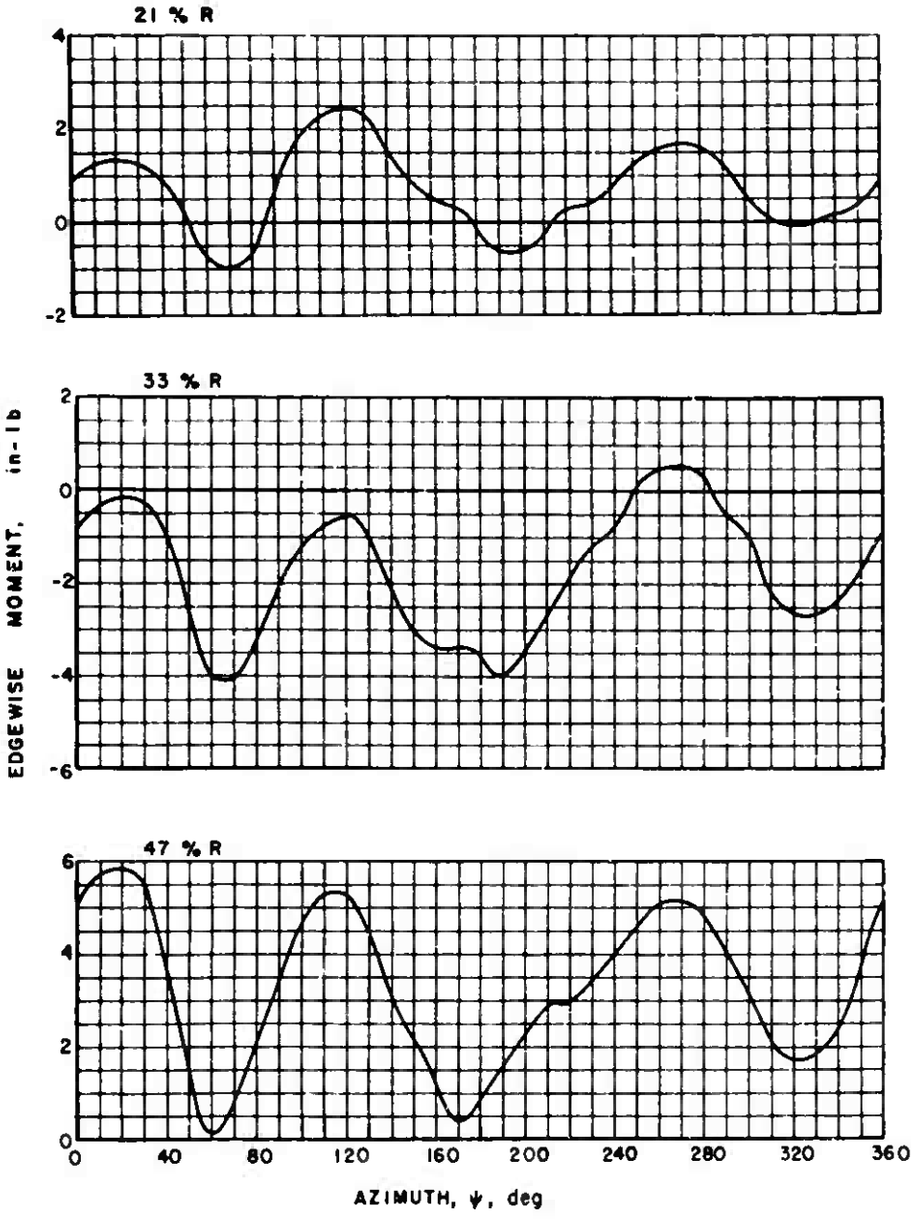

(b) EDGEWISE MOMENTS

Figure 22. Continued.

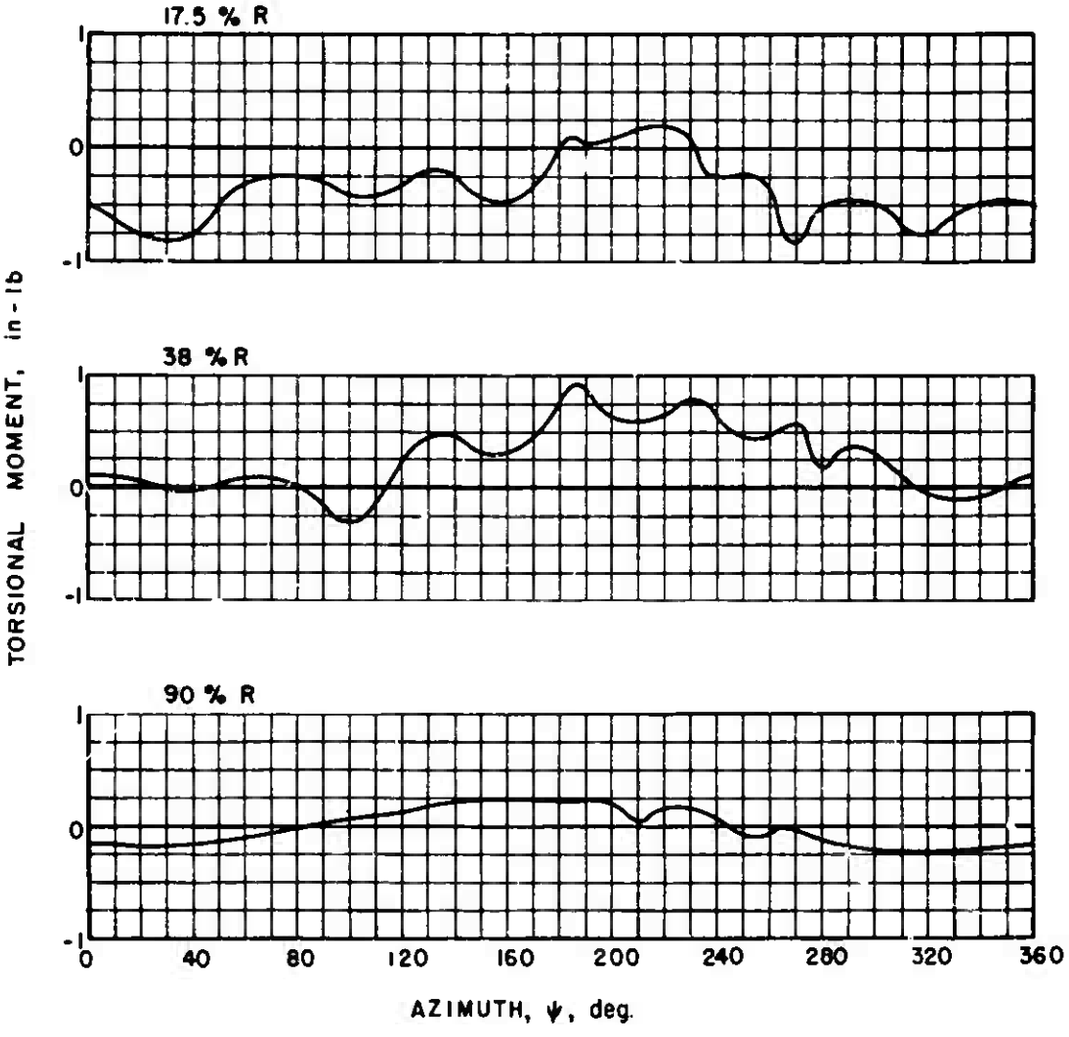

(c) TORSIONAL MOMENTS

Figure 22. Concluded.

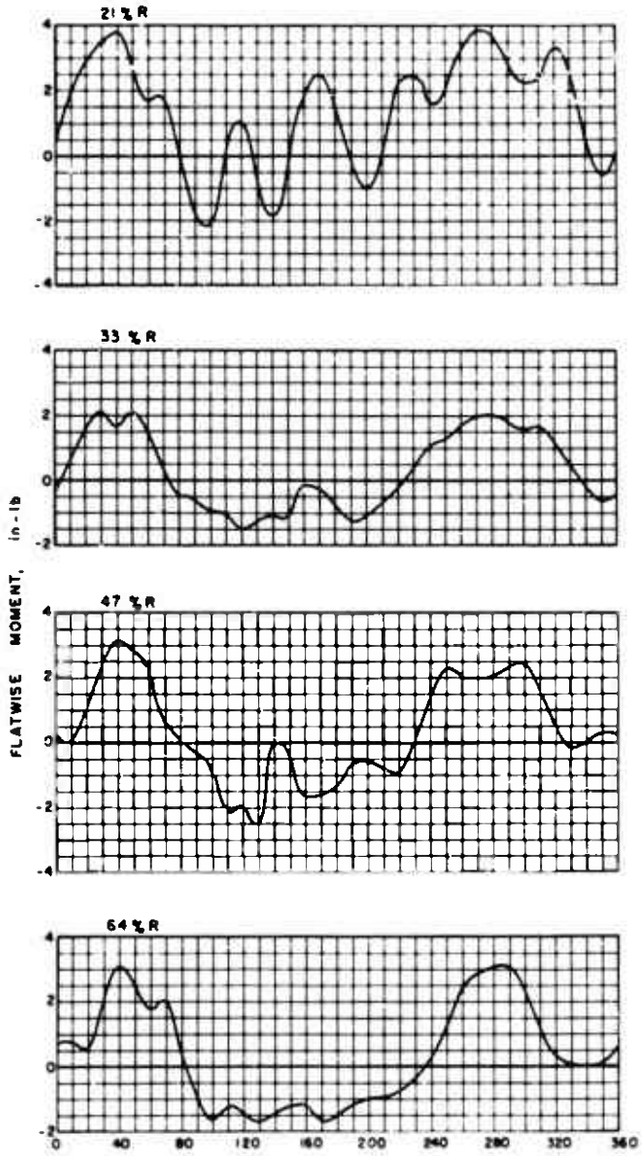

$\mu = 0.5 \quad C_L/\sigma = 0.048 \quad \alpha_s = -4 \text{ deg}$

(a) FLATWISE MOMENTS

Figure 23. Experimental Blade Moments.

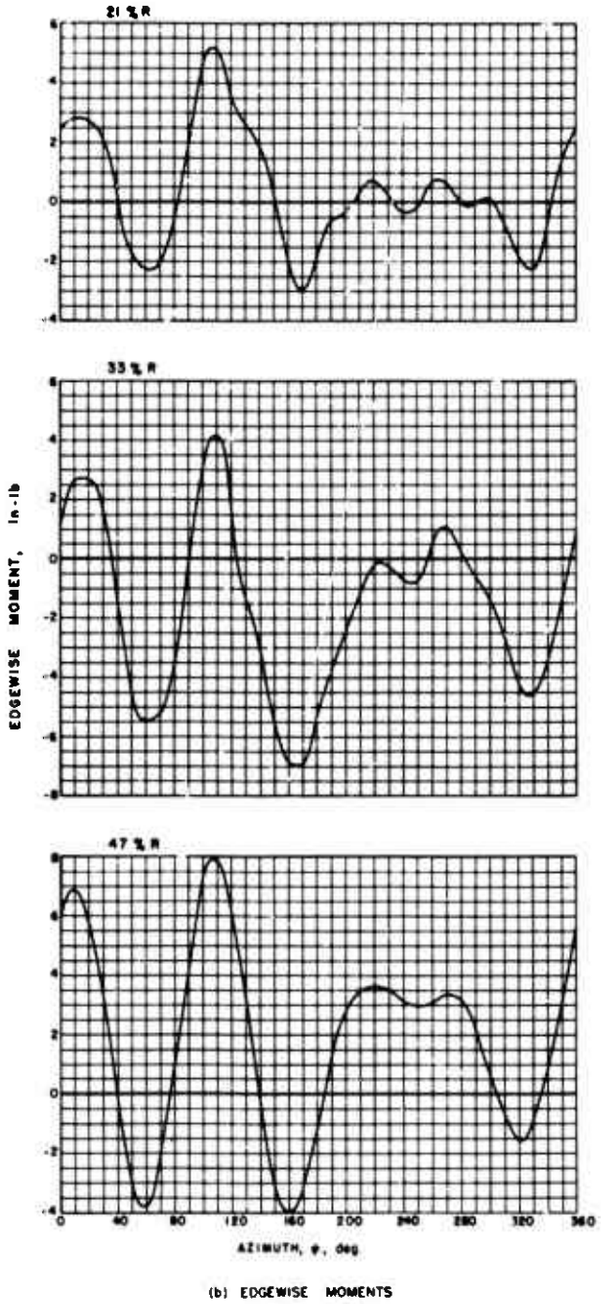

(b) EDGEWISE MOMENTS

Figure 23. Continued.

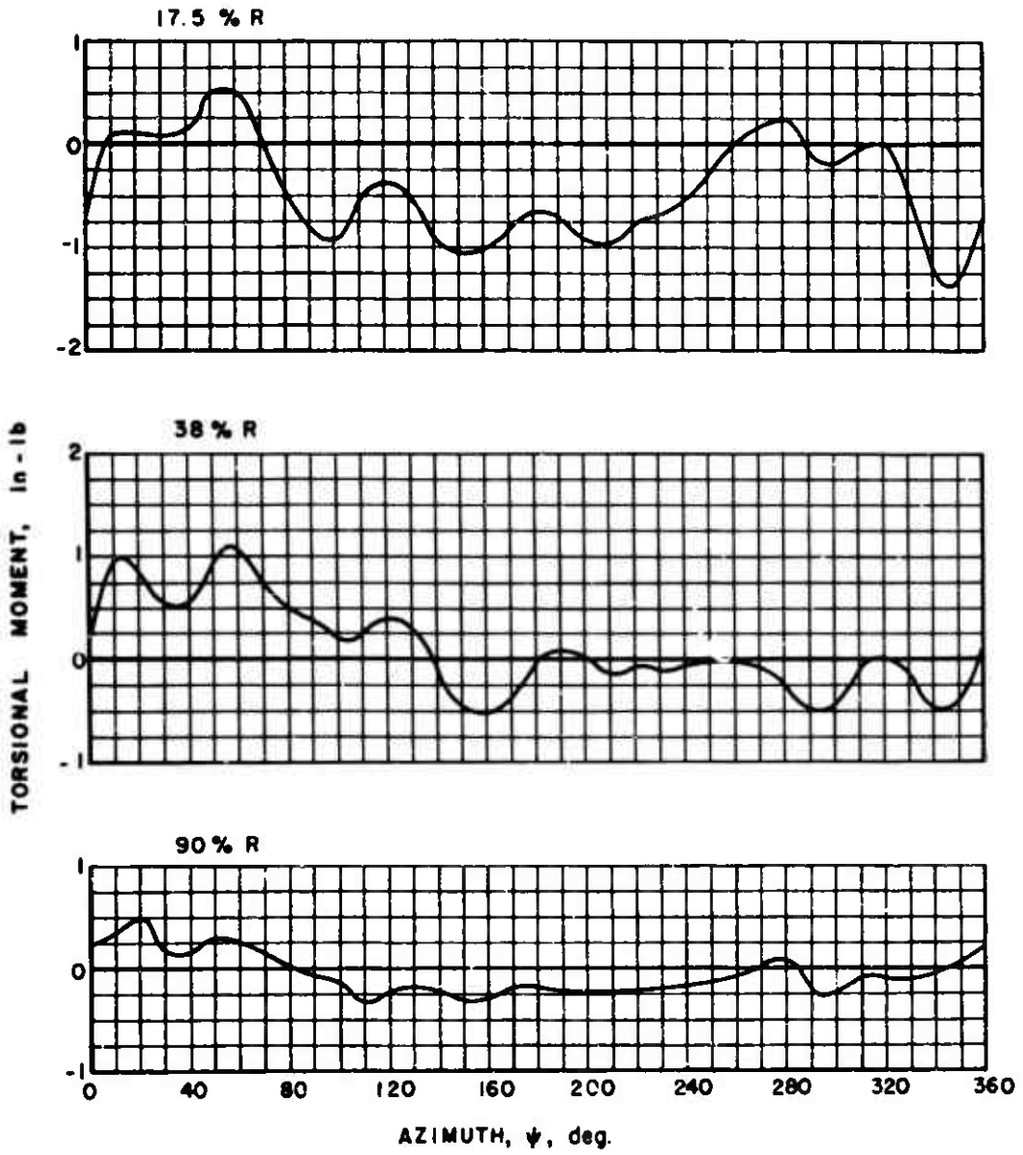

(c) TORSIONAL MOMENTS

Figure 23. Concluded.

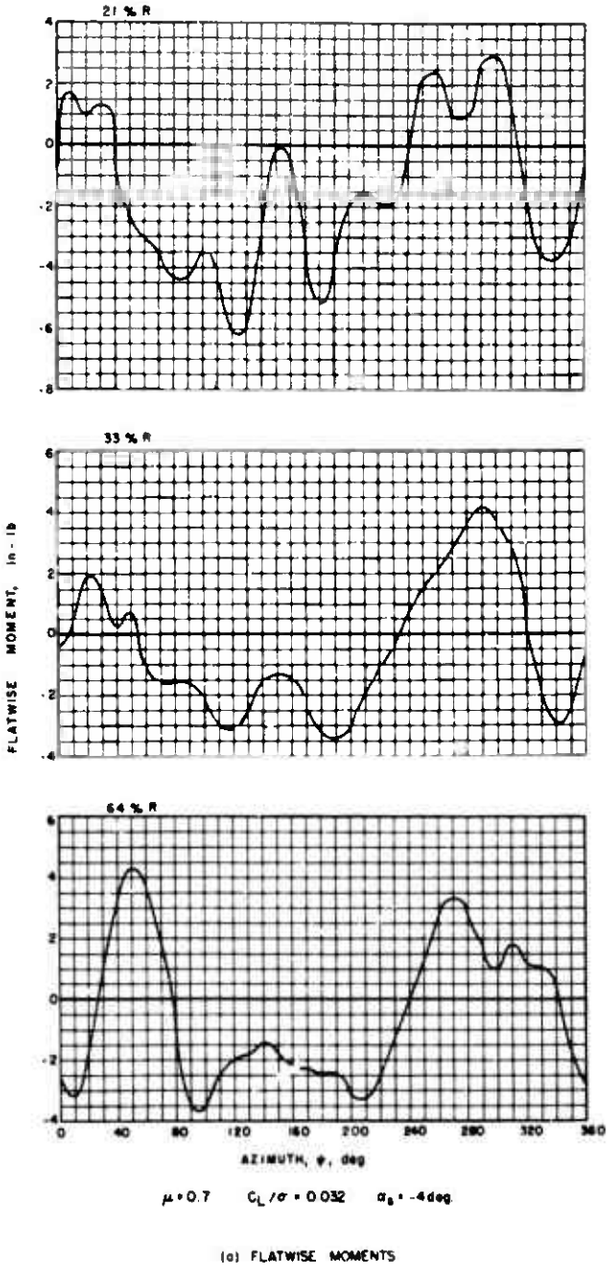

$\mu = 0.7$ $C_L/\sigma = 0.032$ $\alpha_s = -4$ deg

(a) FLATWISE MOMENTS

Figure 24. Experimental Blade Moments.

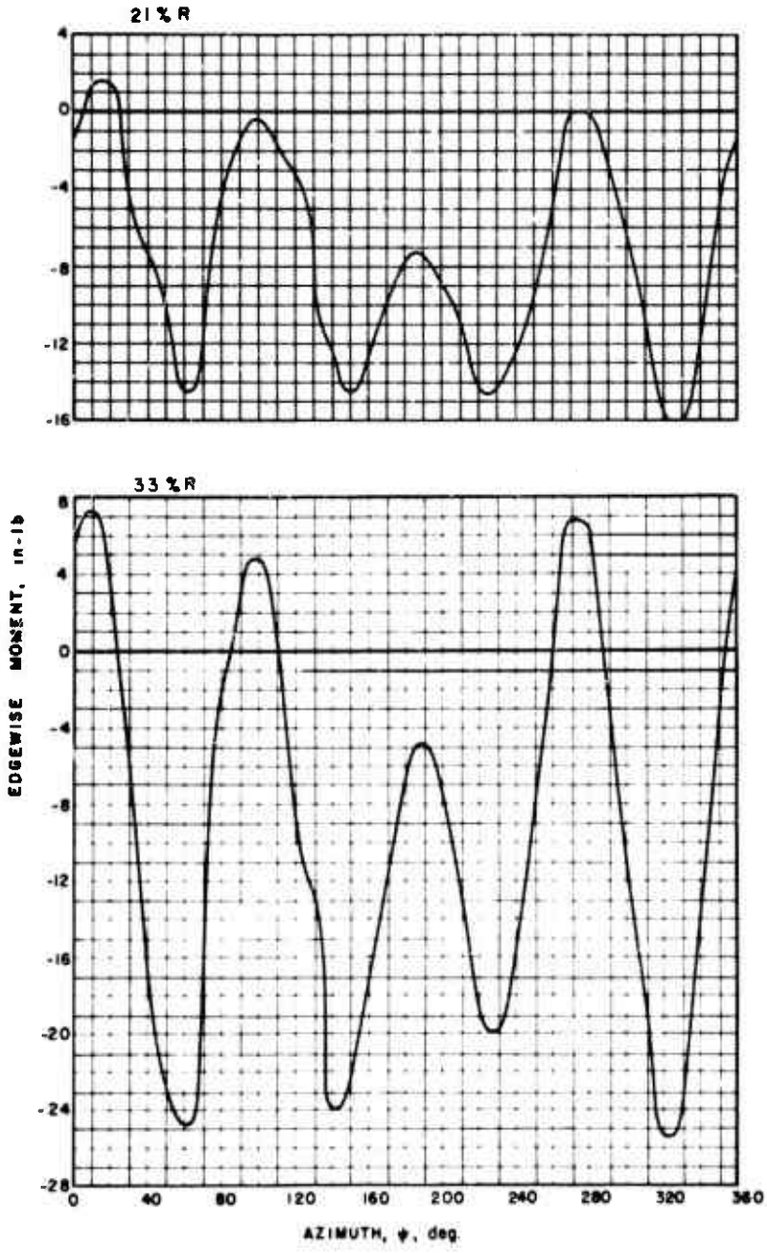

(b) EDGEWISE MOMENTS

Figure 24. Continued.

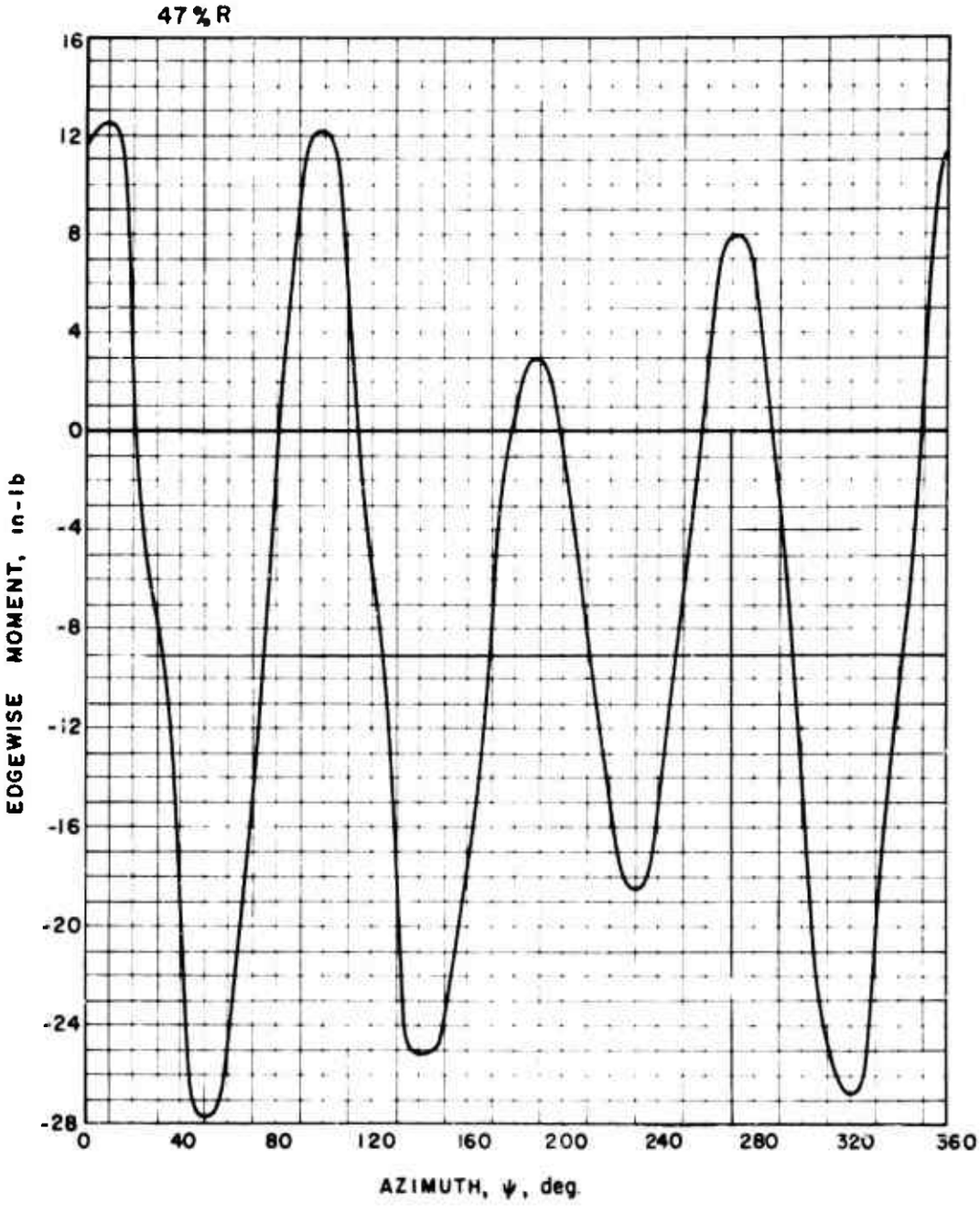

Figure 24(b). Continued.

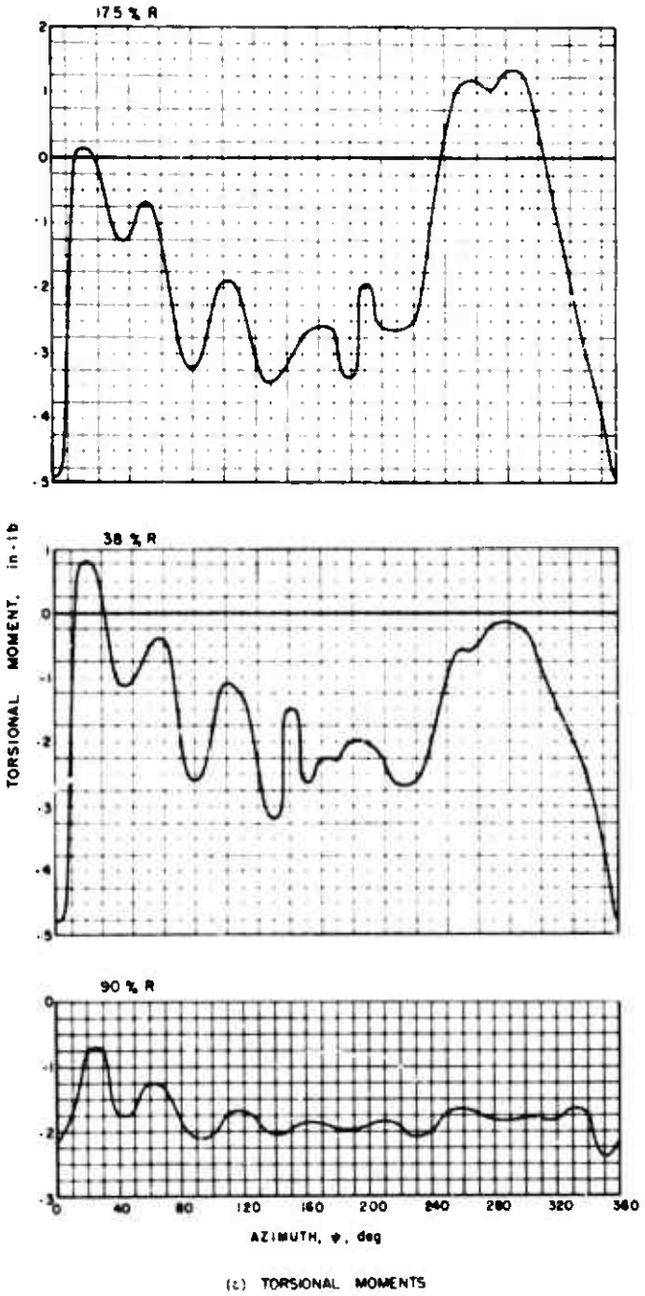

Figure 24. Concluded.

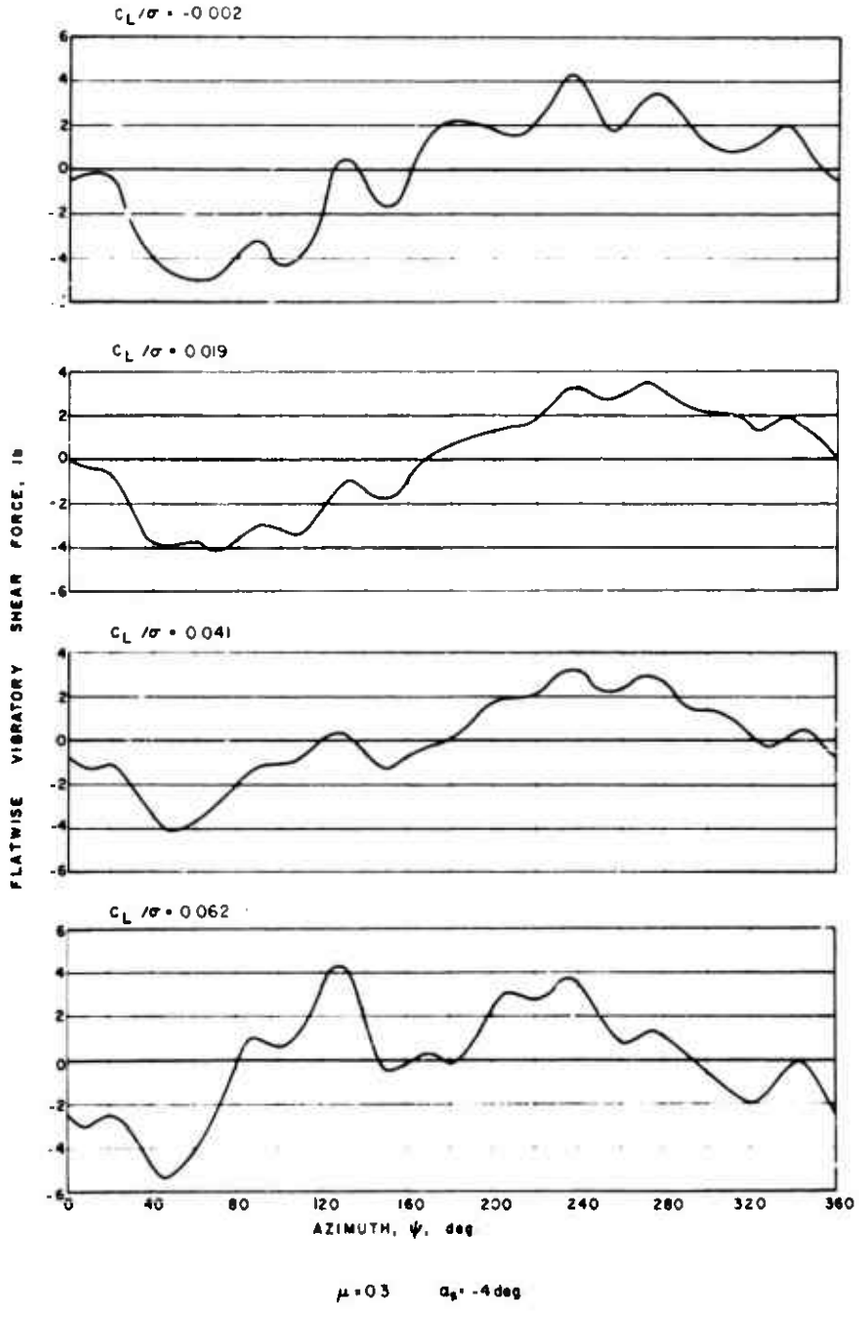

Figure 25. Effect of Rotor Lift on Flatwise Vibratory Shear Force.

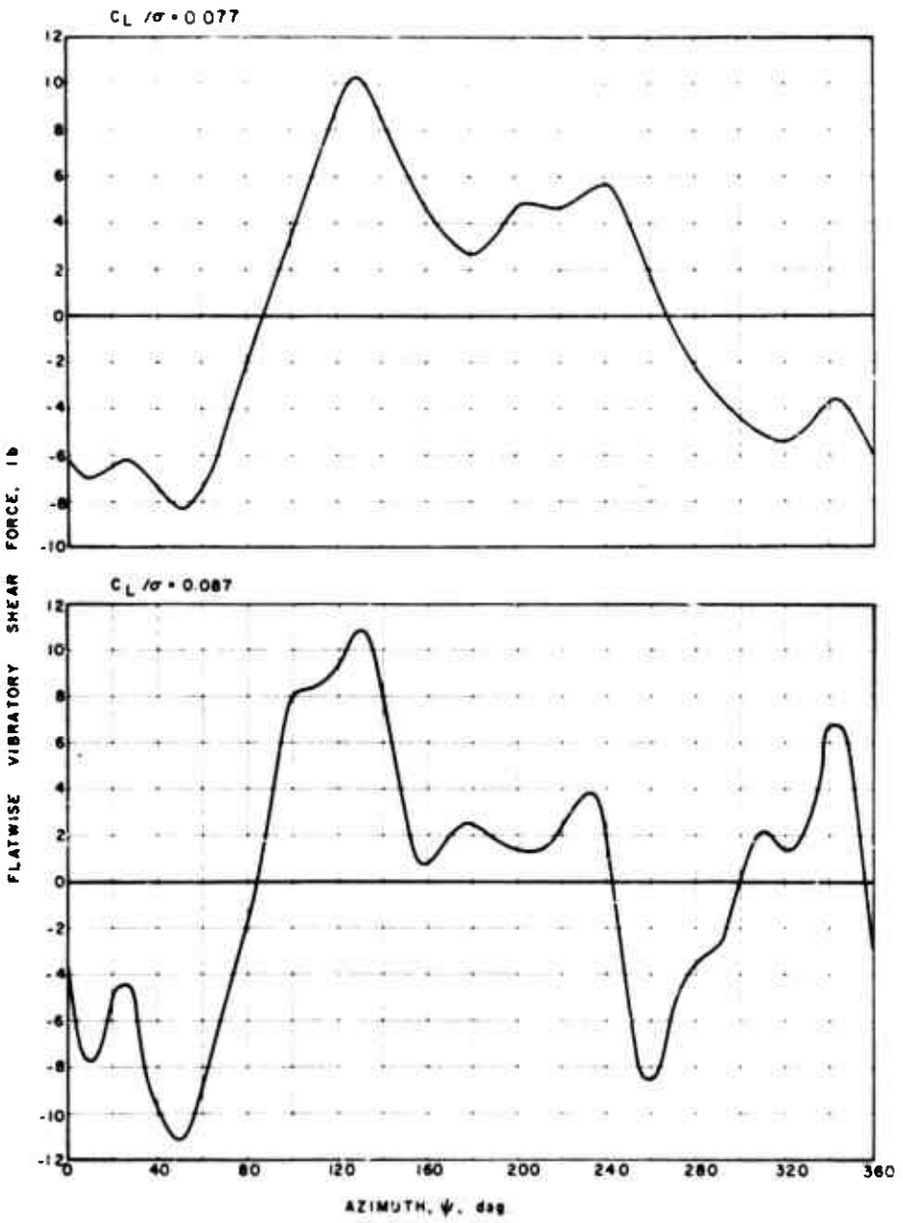

Figure 25. Concluded.

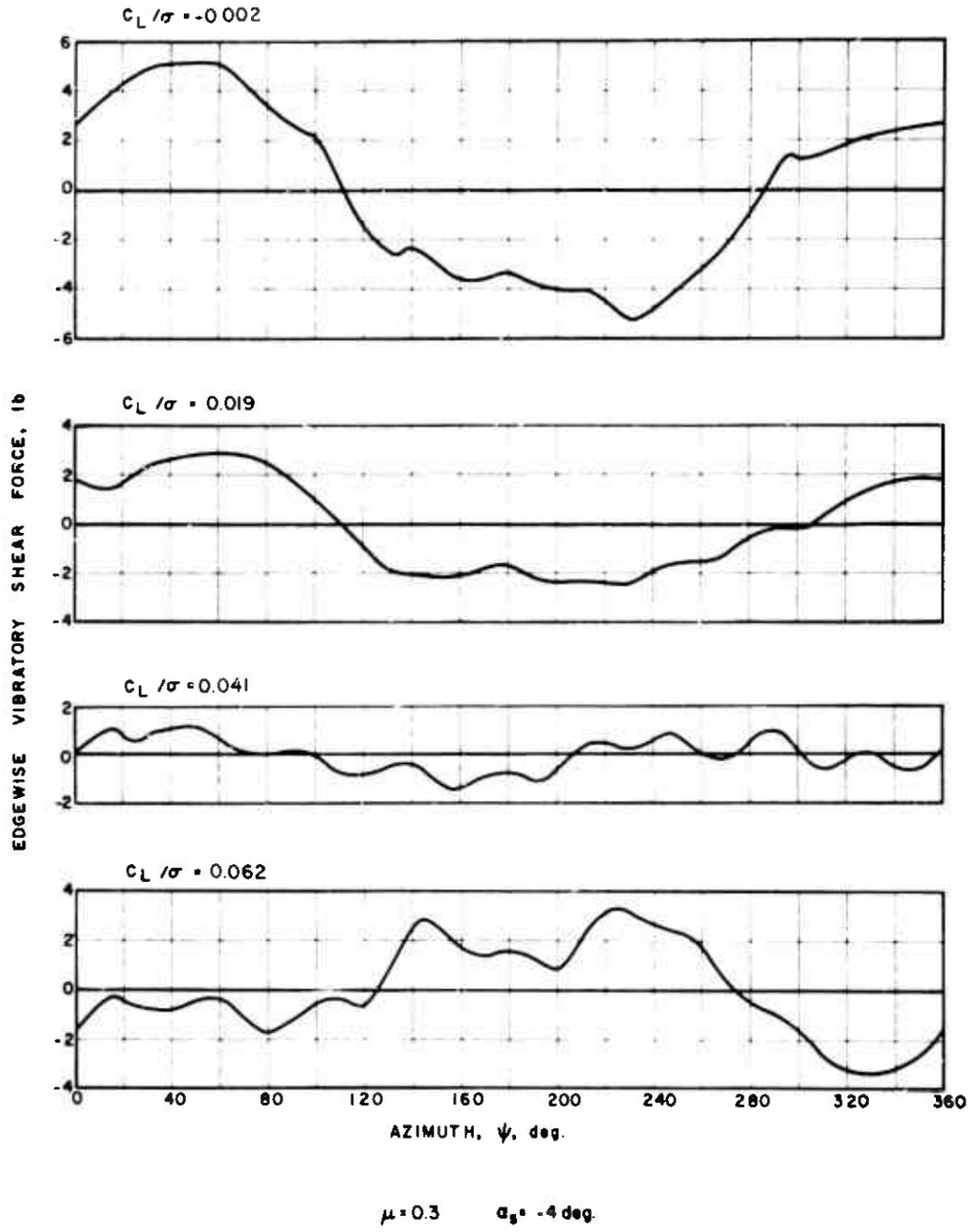

Figure 26. Effect of Rotor Lift on Edgewise Vibratory Shear Force.

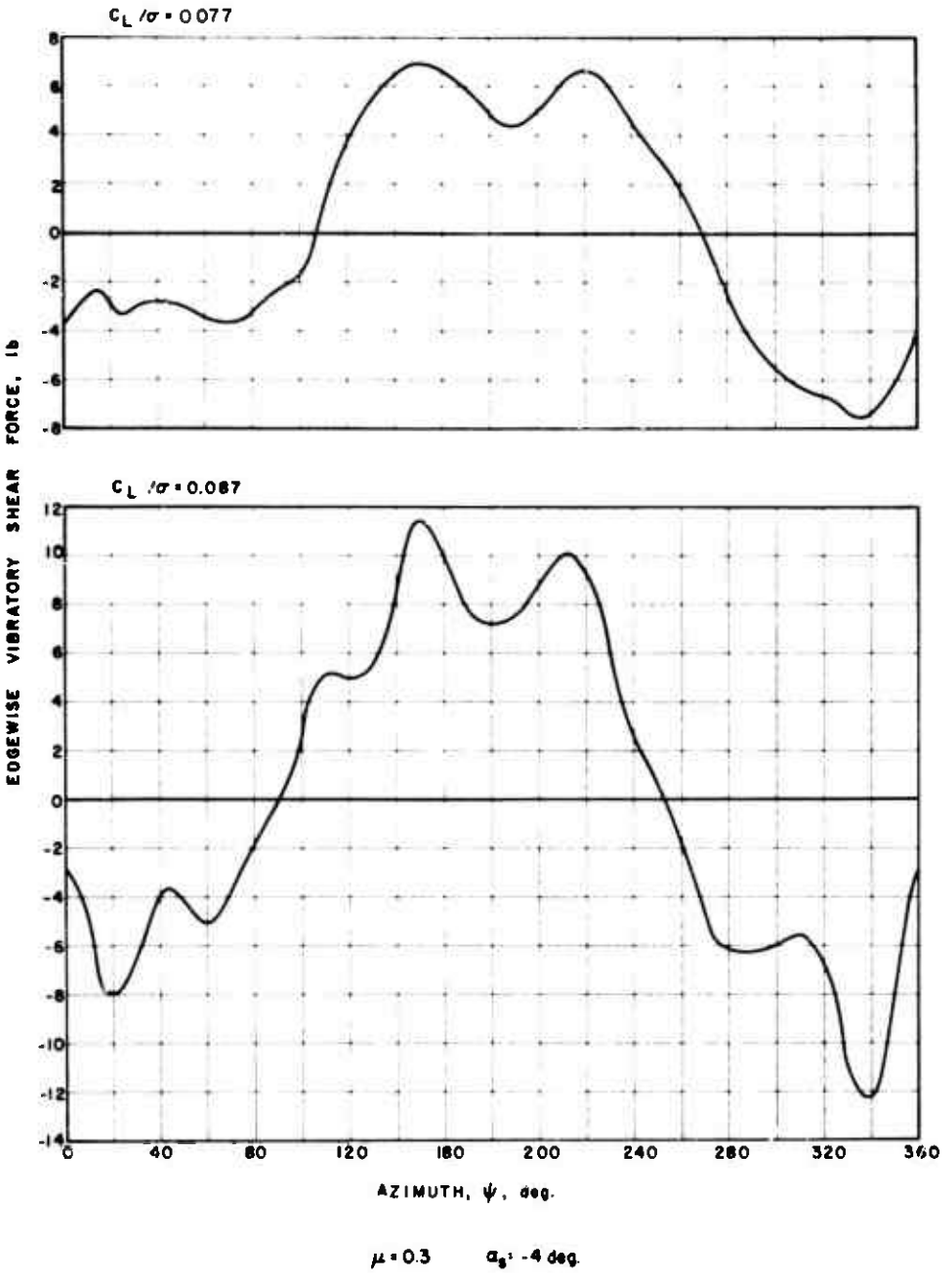

Figure 26. Concluded.

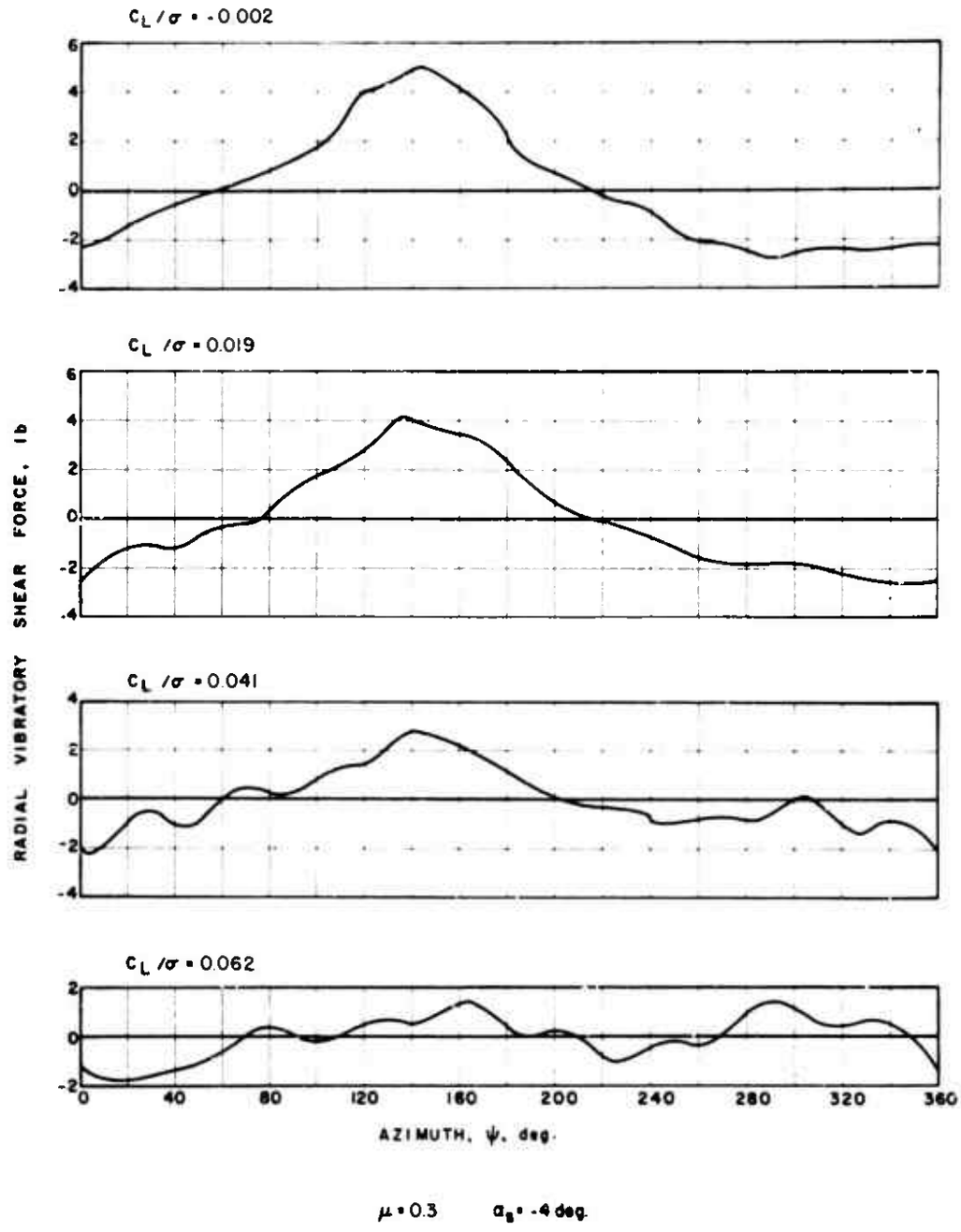

Figure 27. Effect of Rotor Lift on Radial Vibratory Shear Force.

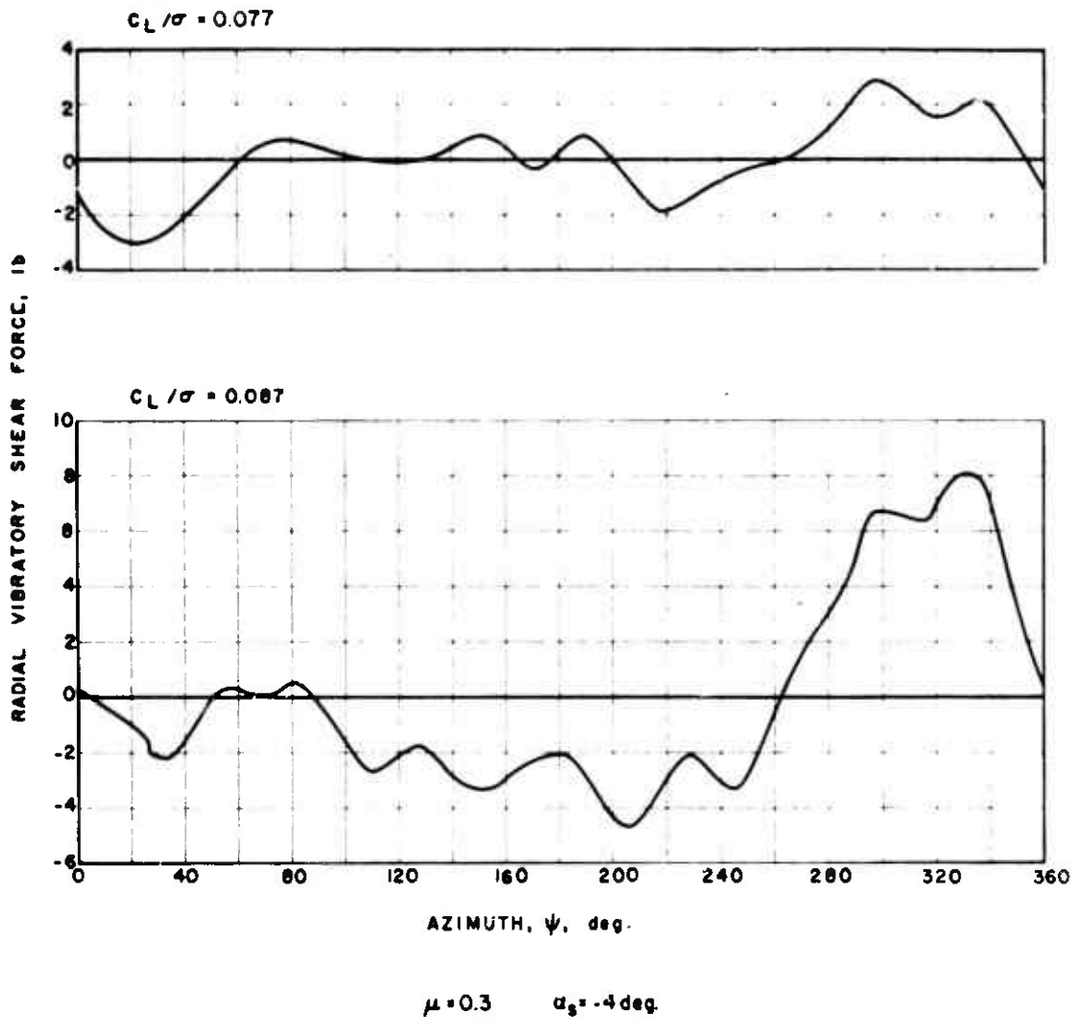

Figure 27. Concluded.

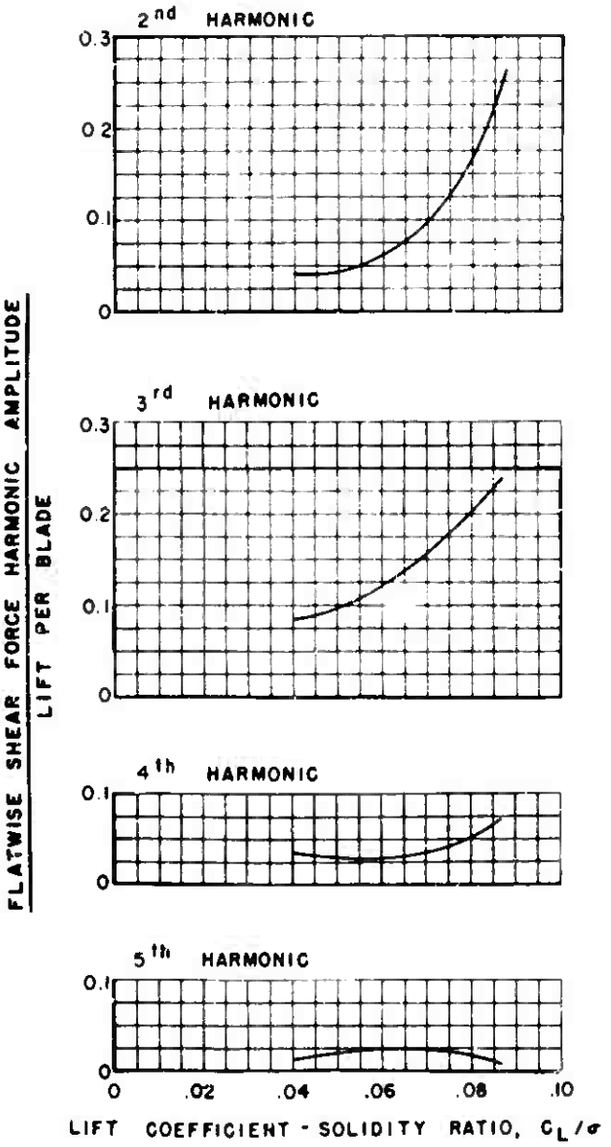

$\mu = 0.3$, $\alpha_s = -4$ deg

(a) FLATWISE

Figure 28. Effect of Rotor Lift on Nondimensional Shear Forces.

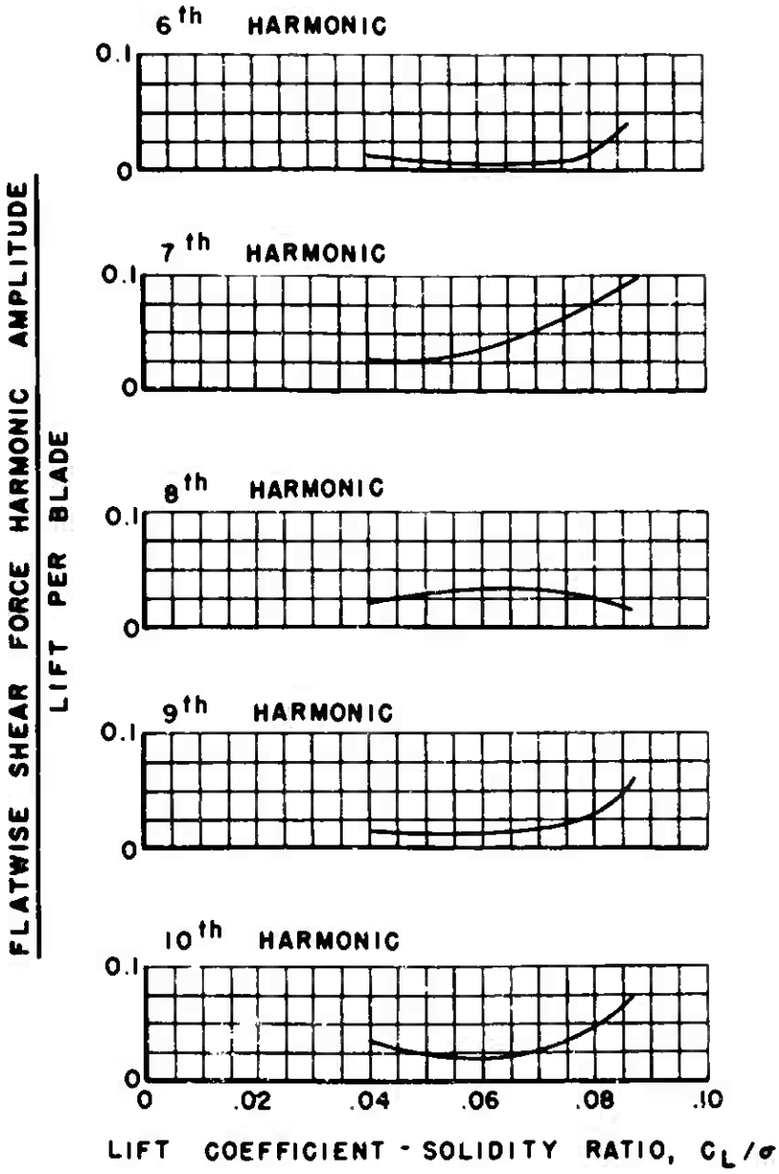

$\mu = 0.3$, $\alpha_s = -4$ deg.

Figure 28(a). Continued.

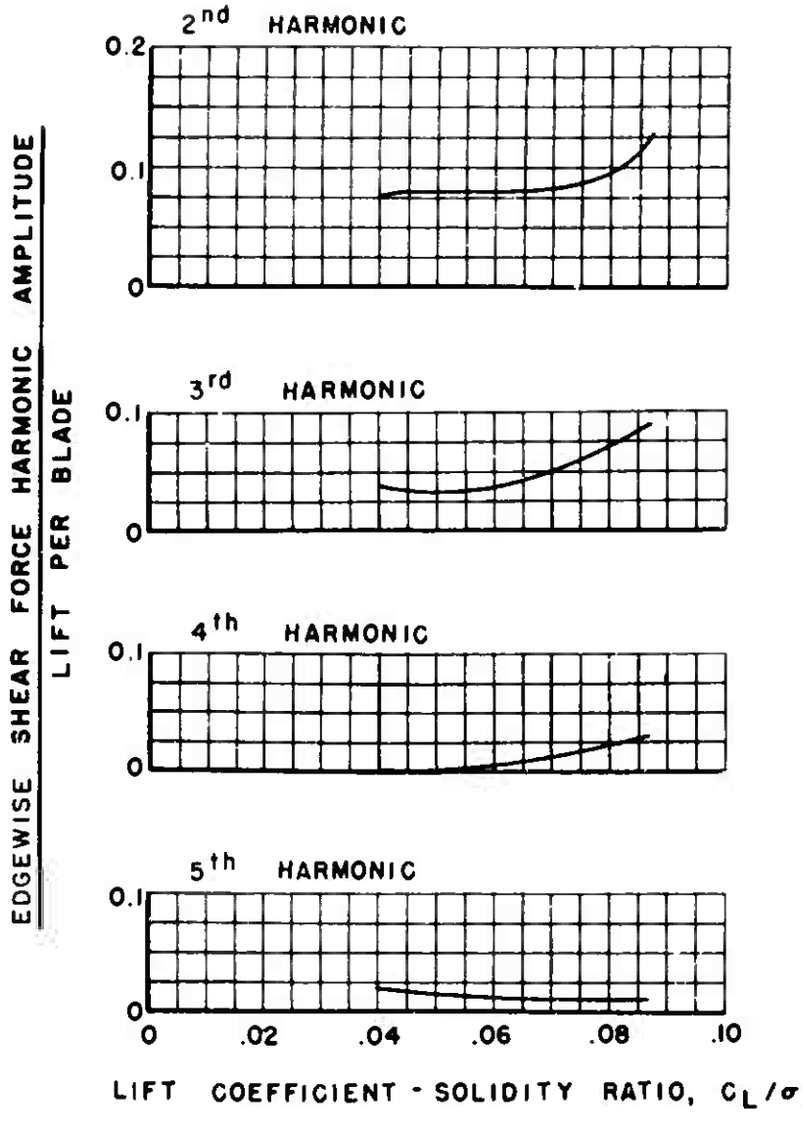

$\mu = 0.3$ $\alpha_s = -4$ deg.

(b) EDGEWISE

Figure 28. Continued.

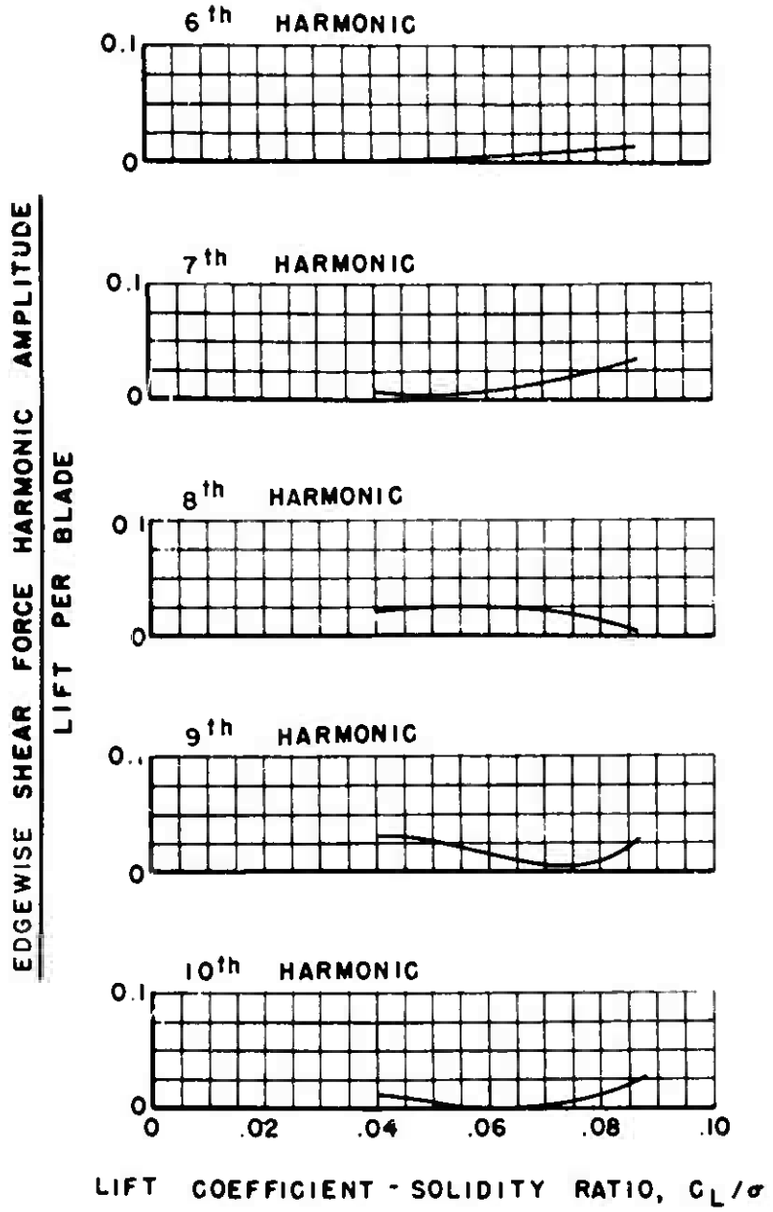

$\mu = 0.3$ $\alpha_s = -4$ deg

Figure 28(b). Concluded.

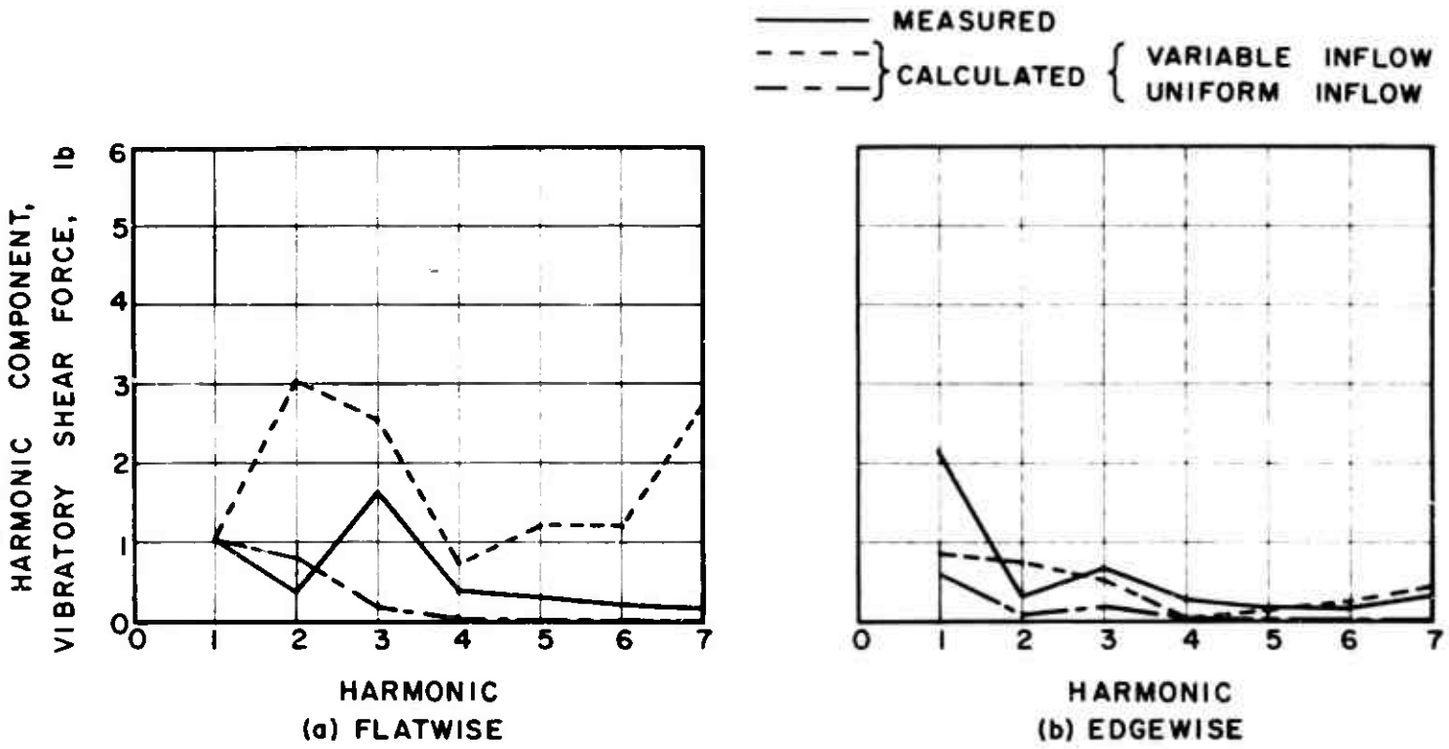

$\mu = 0.2$ $C_L/\sigma = 0.071$ $\alpha_s = -4$ deg.

Figure 29. Comparison of Theoretical and Experimental Vibratory Shear Force Harmonic Amplitudes.

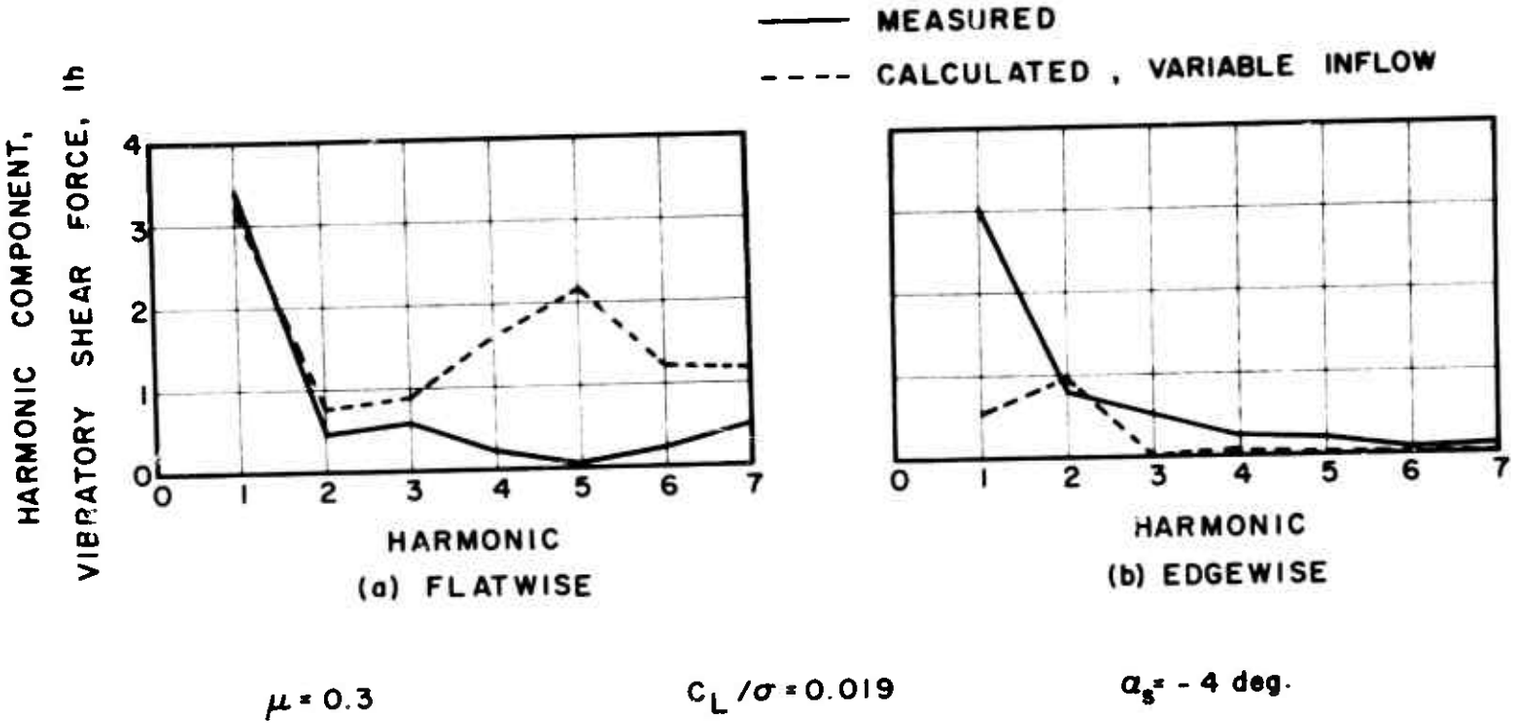

Figure 30. Comparison of Theoretical and Experimental Vibratory Shear Force Harmonic Amplitudes.

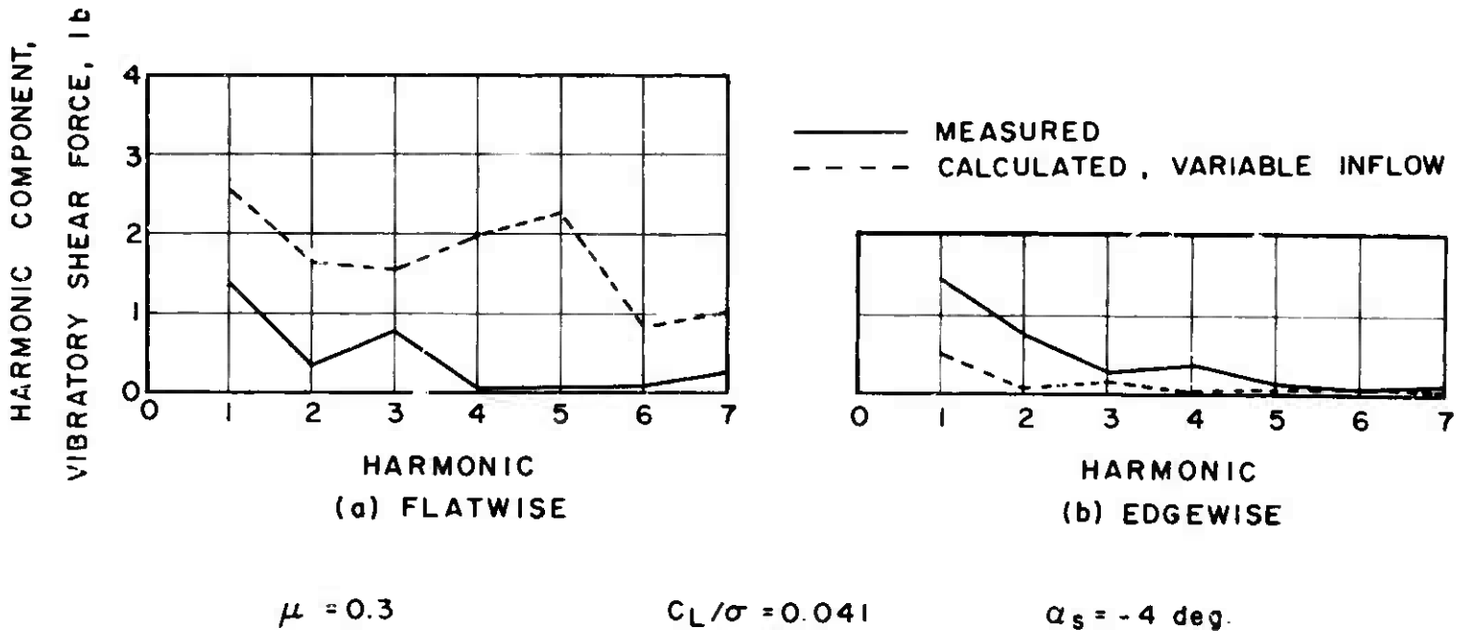

$\mu = 0.3$ $C_L/\sigma = 0.041$ $\alpha_s = -4$ deg.

Figure 31. Comparison of Theoretical and Experimental Vibratory Shear Force Harmonic Amplitudes.

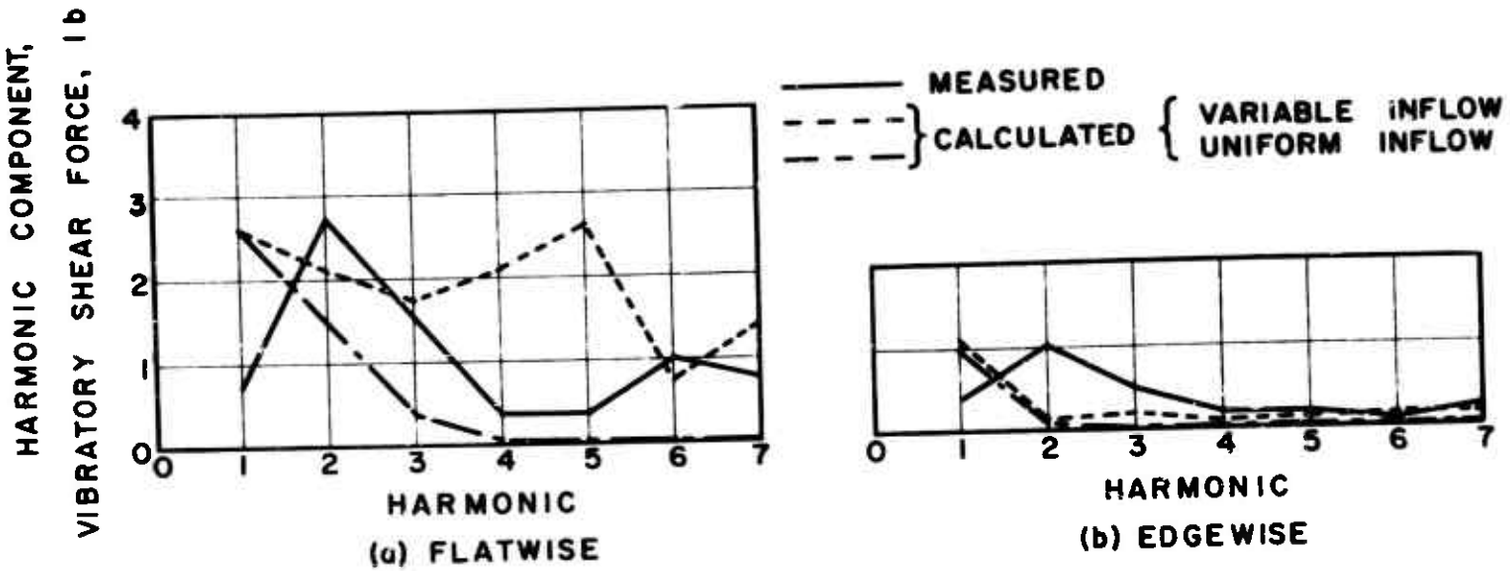

μ =0.3 C_L/σ = 0.062 α_s = -4 deg.

Figure 32. Comparison of Theoretical and Experimental Vibratory Shear Force Harmonic Amplitudes.

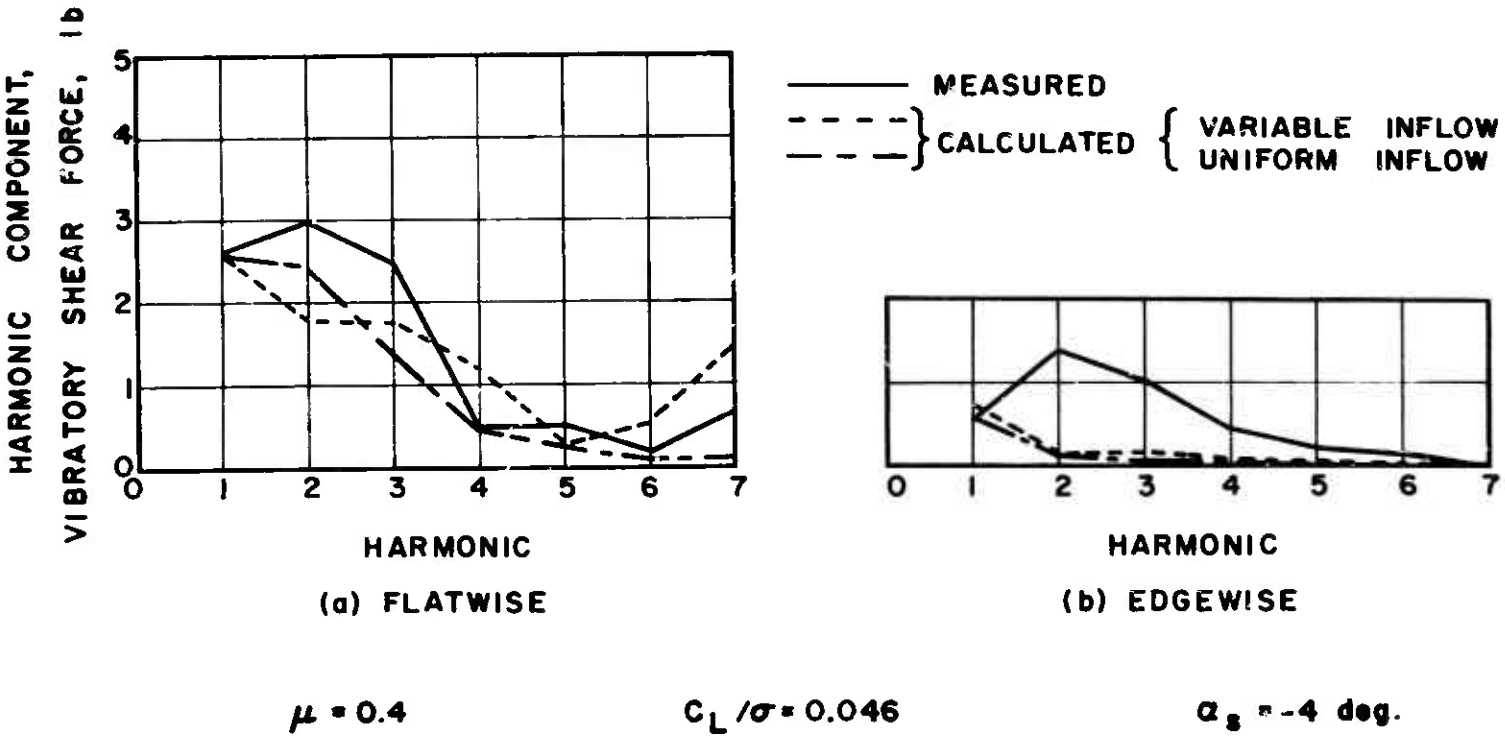

Figure 33. Comparison of Theoretical and Experimental Vibratory Shear Force Harmonic Amplitudes.

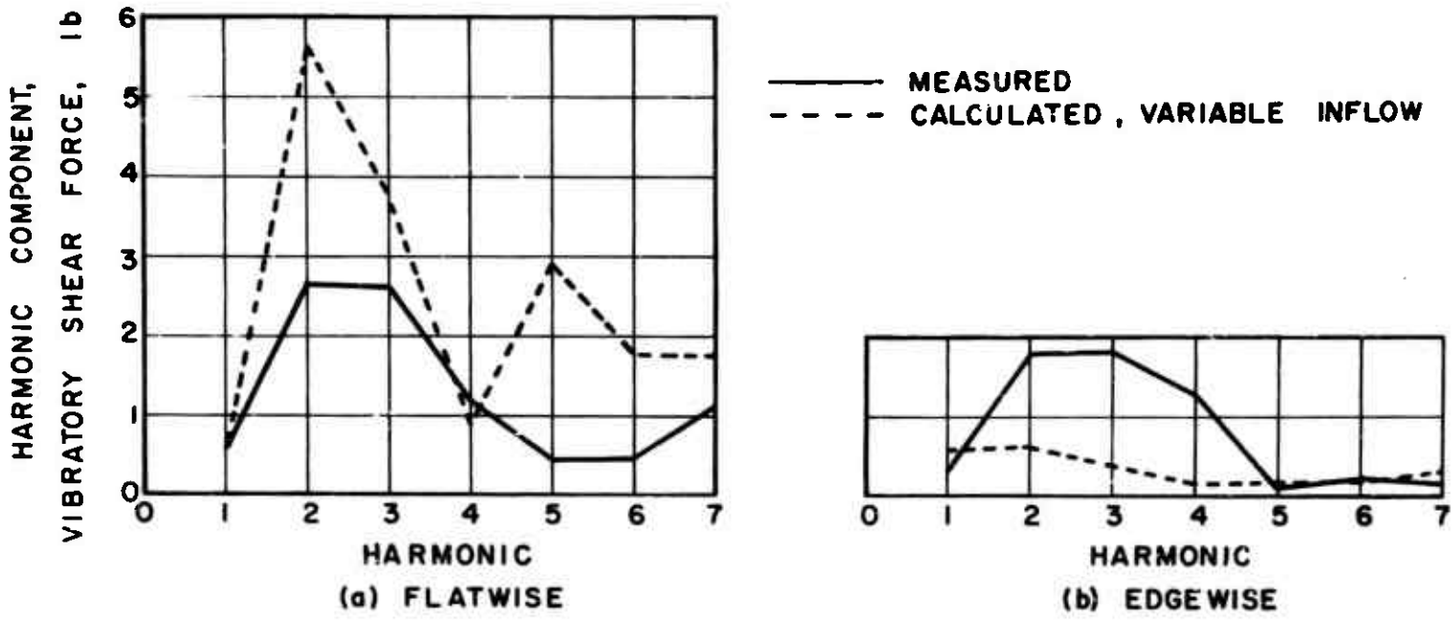

$\mu = 0.5$ $C_L/\sigma = 0.048$ $\alpha_s = -4$ deg.

Figure 34. Comparison of Theoretical and Experimental Vibratory Shear Force Harmonic Amplitudes.

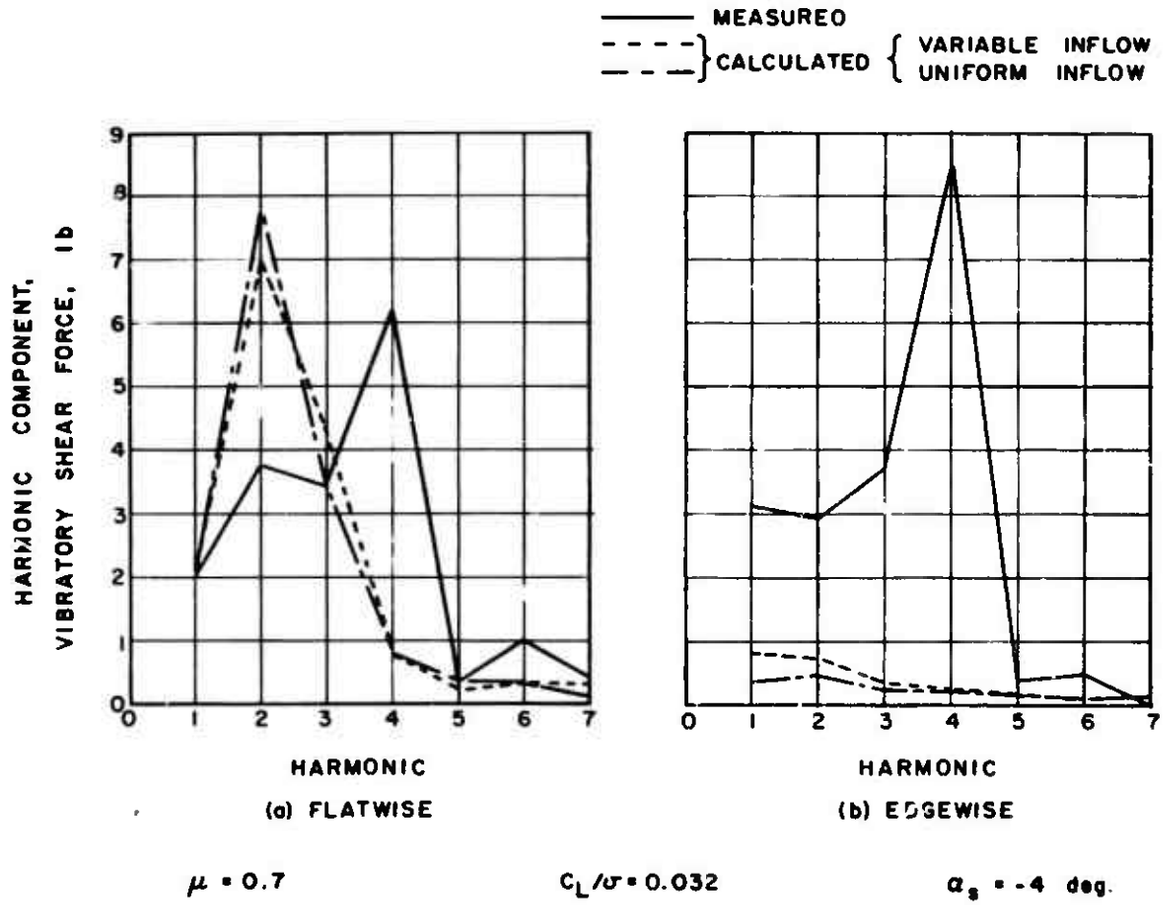

Figure 35. Comparison of Theoretical and Experimental Vibratory Shear Force Harmonic Amplitudes.

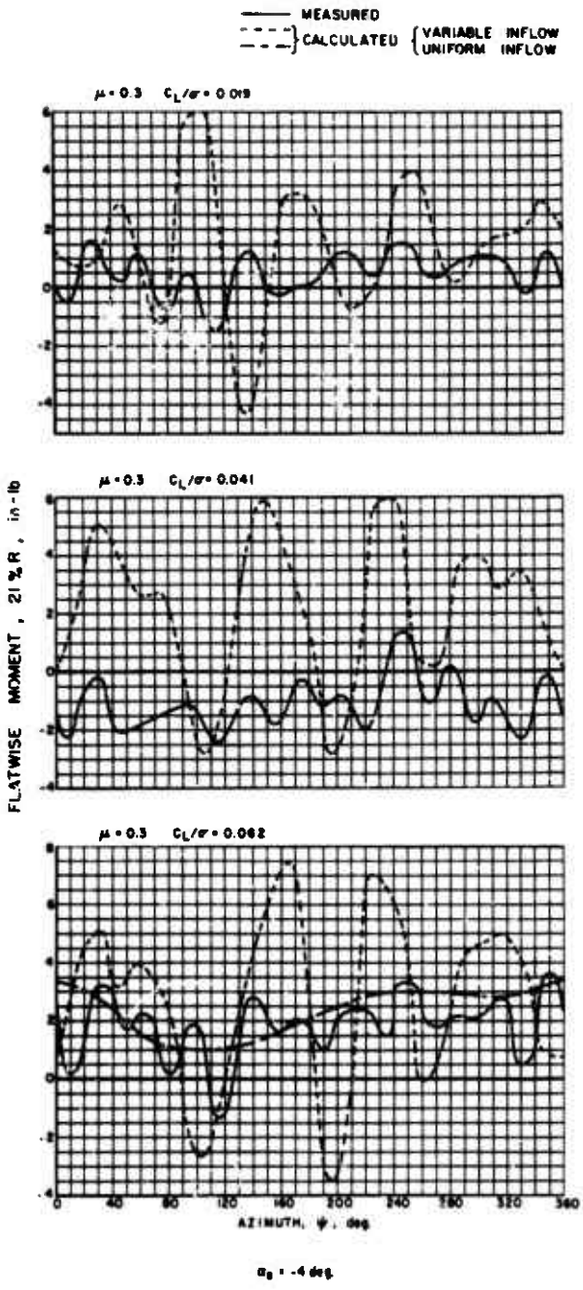

Figure 36. Comparison of Theoretical and Experimental Flatwise Rotor Blade Bending Moments.

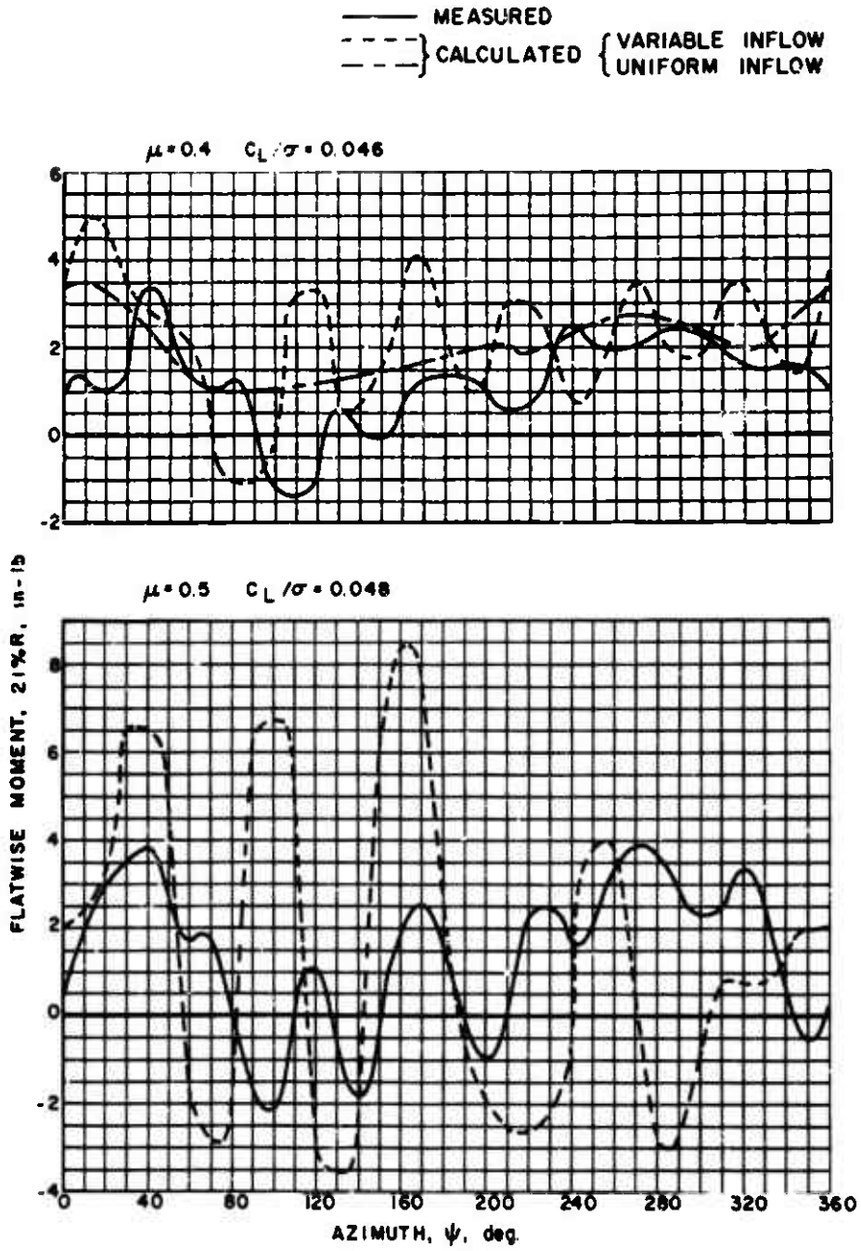

Figure 36. Concluded.

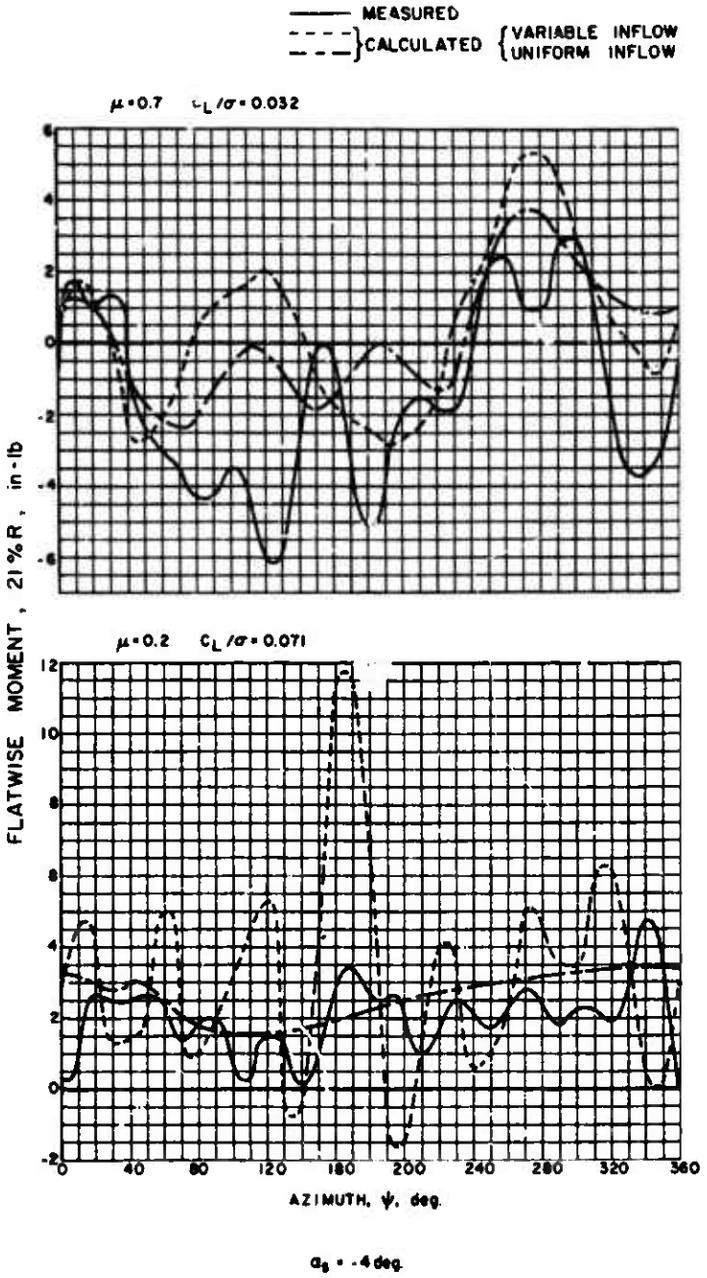

Figure 37. Comparison of Theoretical and Experimental Flatwise Rotor Blade Bending Moments.

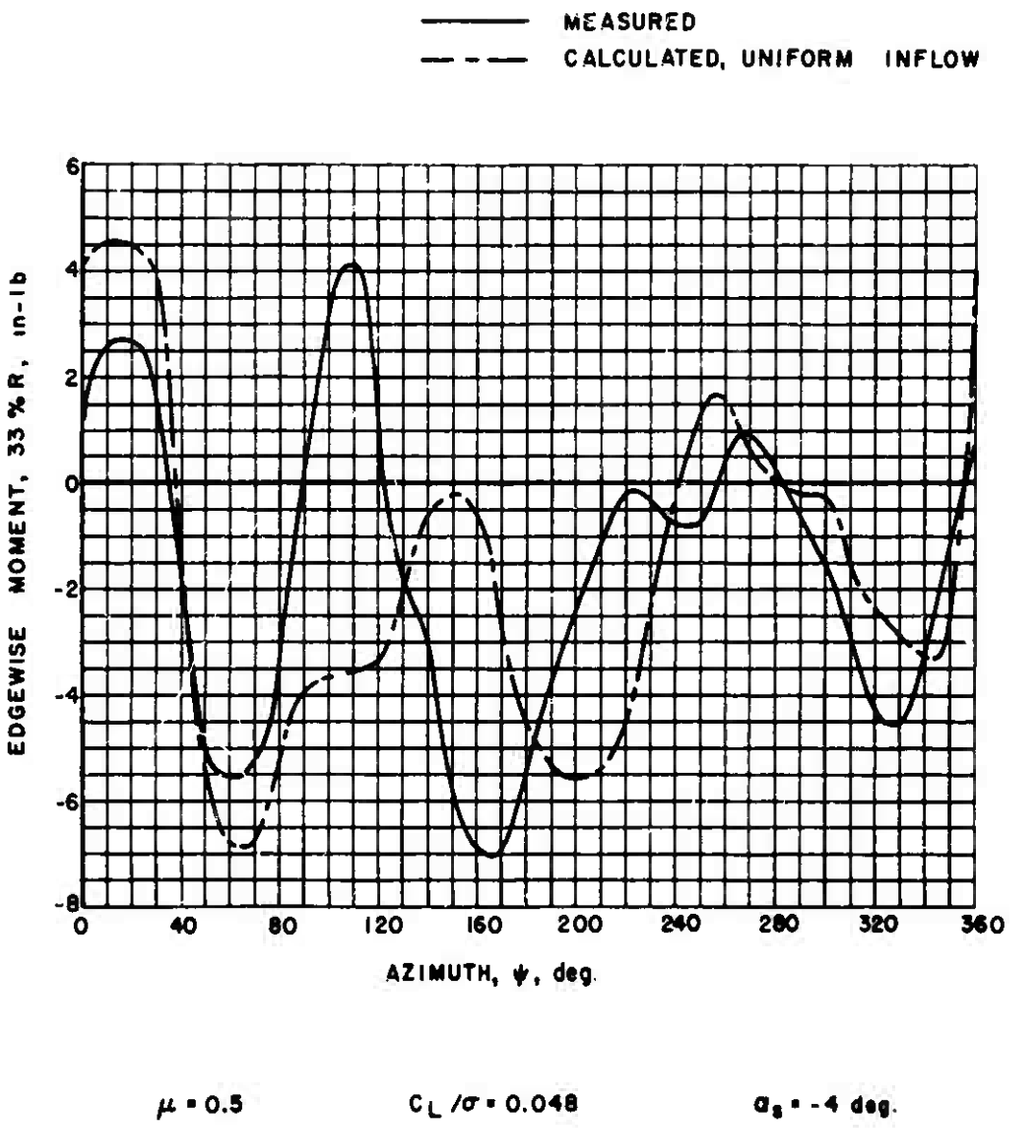

Figure 38. Comparison of Theoretical and Experimental Edgewise Rotor Blade Bending Moments.

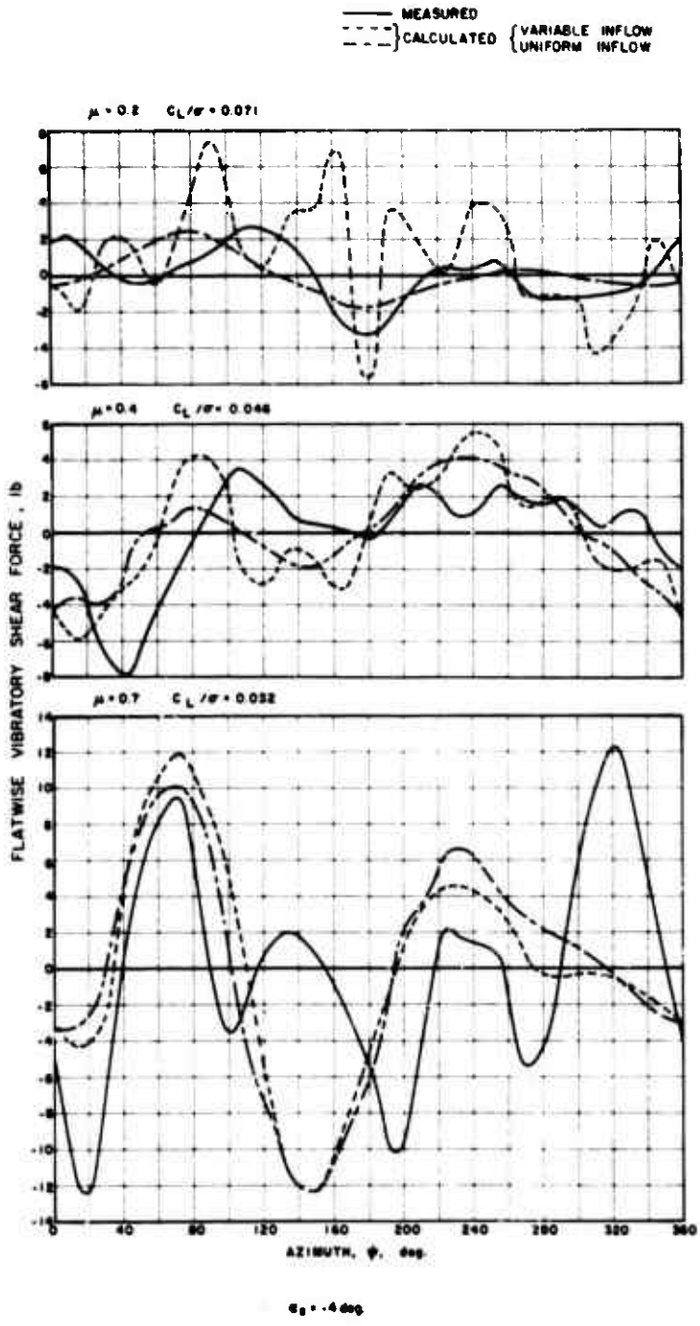

Figure 39. Azimuthal Variation of Vibratory Shear Force.

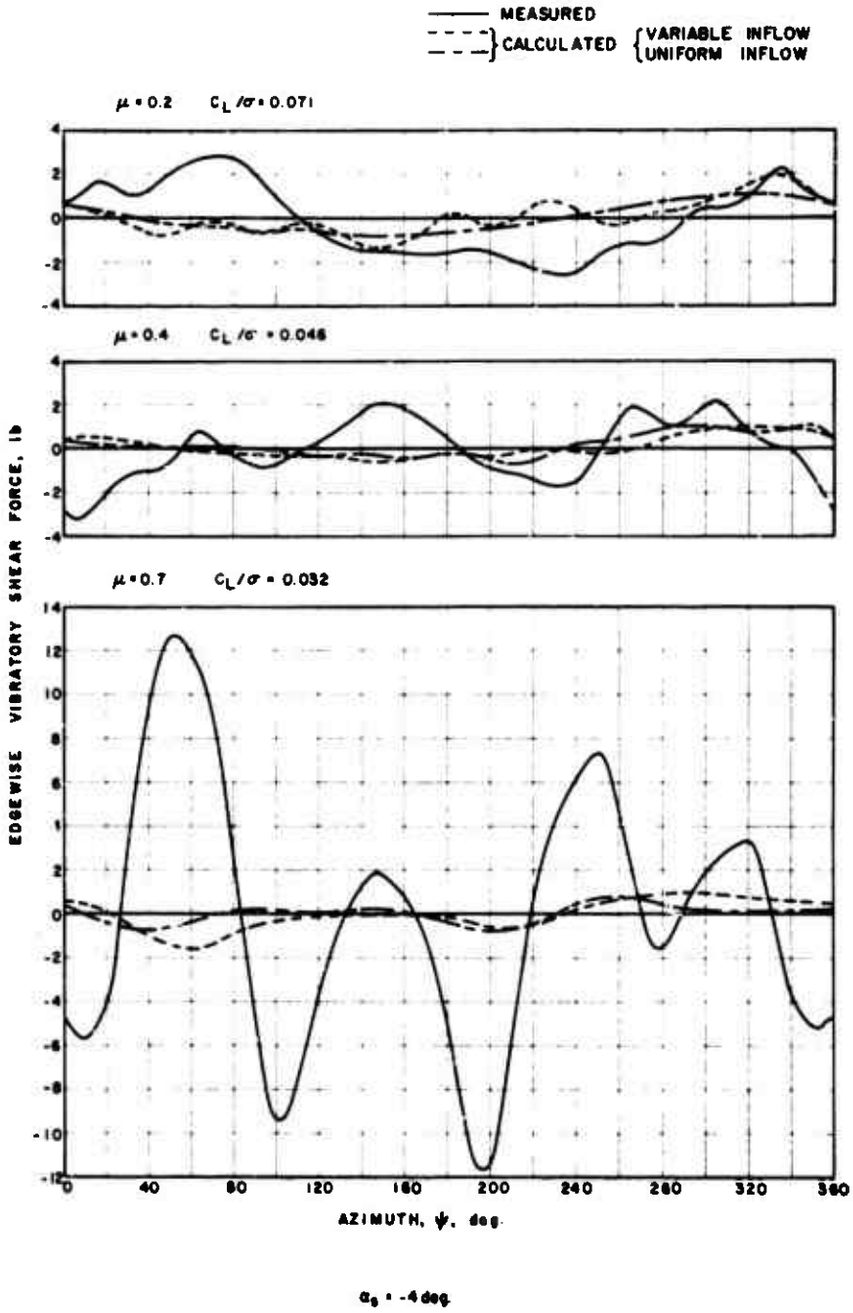

Figure 39. Concluded.

DISTRIBUTION

US Army Materiel Command	3
US Army Aviation Materiel Command	5
United States Army, Pacific	1
Chief of R&D, DA	1
Director of Defense Research and Engineering	1
US Army R&D Group (Europe)	2
US Army Aviation Materiel Laboratories	28
Army Aeronautical Research Laboratory, Ames Research Center	1
US Army Research Office-Durham	1
Plastics Technical Evaluation Center	1
US Army Engineer Waterways Experiment Station	1
US Army Test and Evaluation Command	1
US Army Electronics Command	2
US Army Combat Developments Command Experimentation Command	1
US Army Aviation School	1
US Army Aviation Test Activity	2
Air Force Flight Test Center, Edwards AFB	2
Air Proving Ground Center, Eglin AFB	1
US Army Field Office, AFSC, Andrews AFB	1
Systems Engineering Group, Wright-Patterson AFB	1
Naval Air Systems Command, DN	7

Office of Naval Research	1
Commandant of the Marine Corps	1
Marine Corps Liaison Officer, US Army Transportation School	1
Lewis Research Center, NASA	1
Manned Spacecraft Center, NASA	1
NASA Scientific and Technical Information Facility	2
NAFEC Library (FAA)	2
US Army Board for Aviation Accident Research	1
Bureau of Safety, Civil Acronautics Board	2
US Naval Aviation Safety Center	1
Federal Aviation Agency, Washington, DC	2
US Army Medical R&D Command	1
US Government Printing Office	1
Defense Documentation Center	20

APPENDIX I

EXPERIMENTAL FLATWISE AND EDGEWISE SHEAR FORCE FIGURES

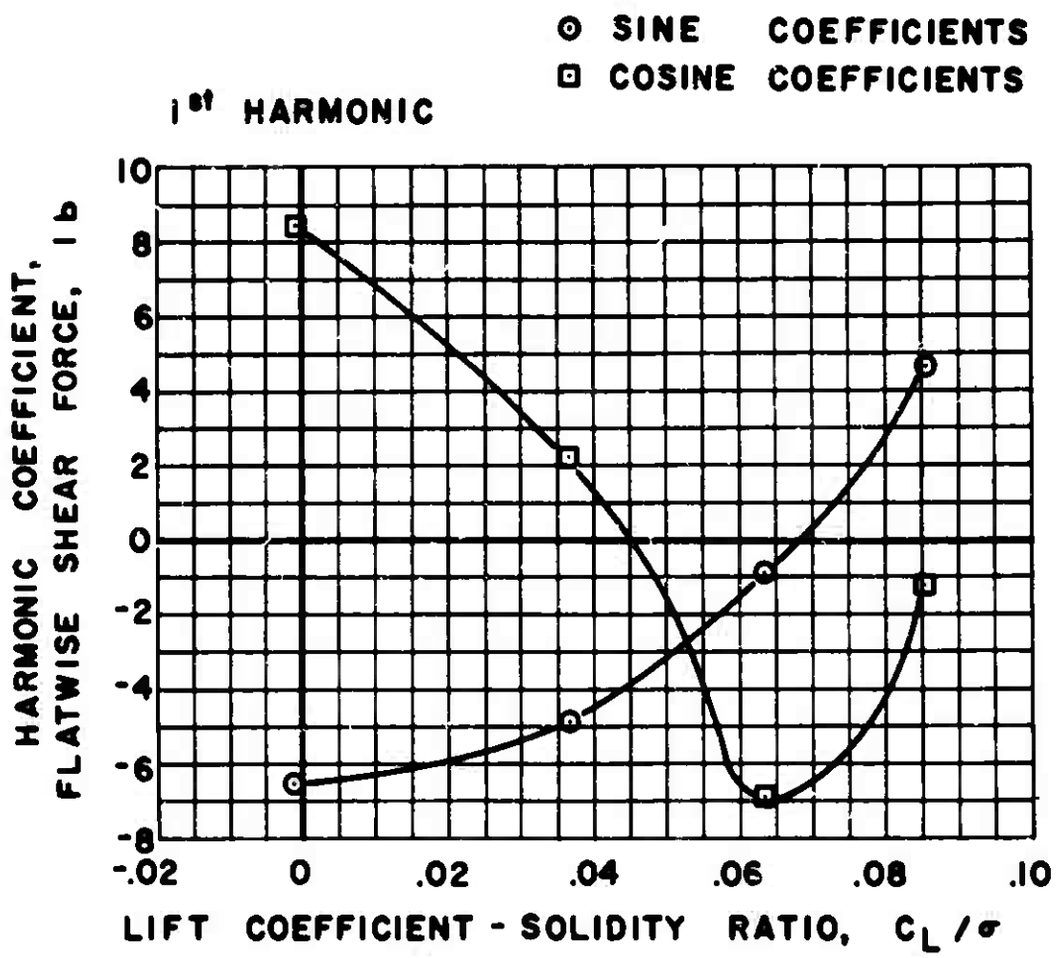

$\mu = 0.2$ $\alpha_s = 0$ deg.

(a) FLATWISE

Figure 40. Experimental Shear Force.

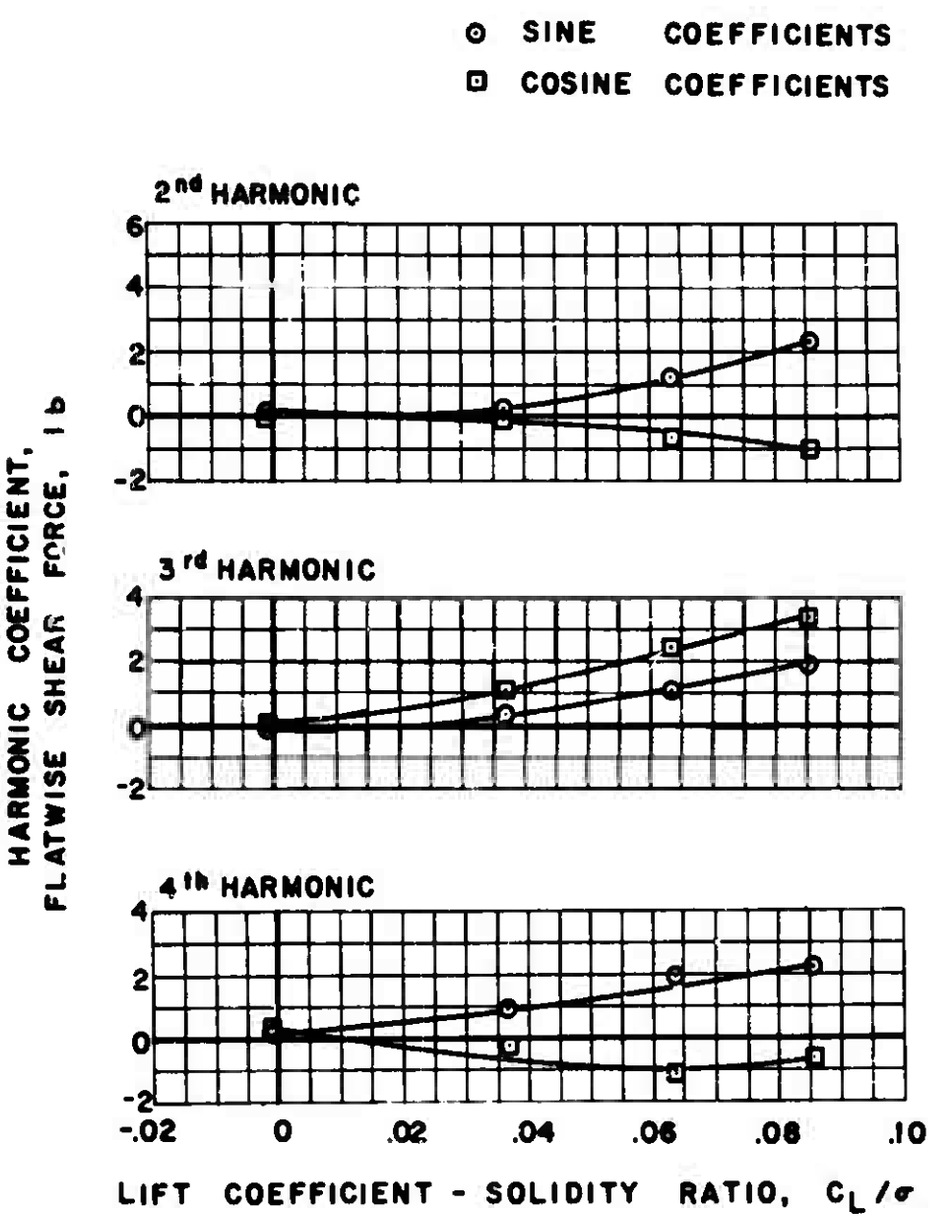

$\mu = 0.2$ $\alpha_s = 0$ deg.

Figure 40(a). Continued.

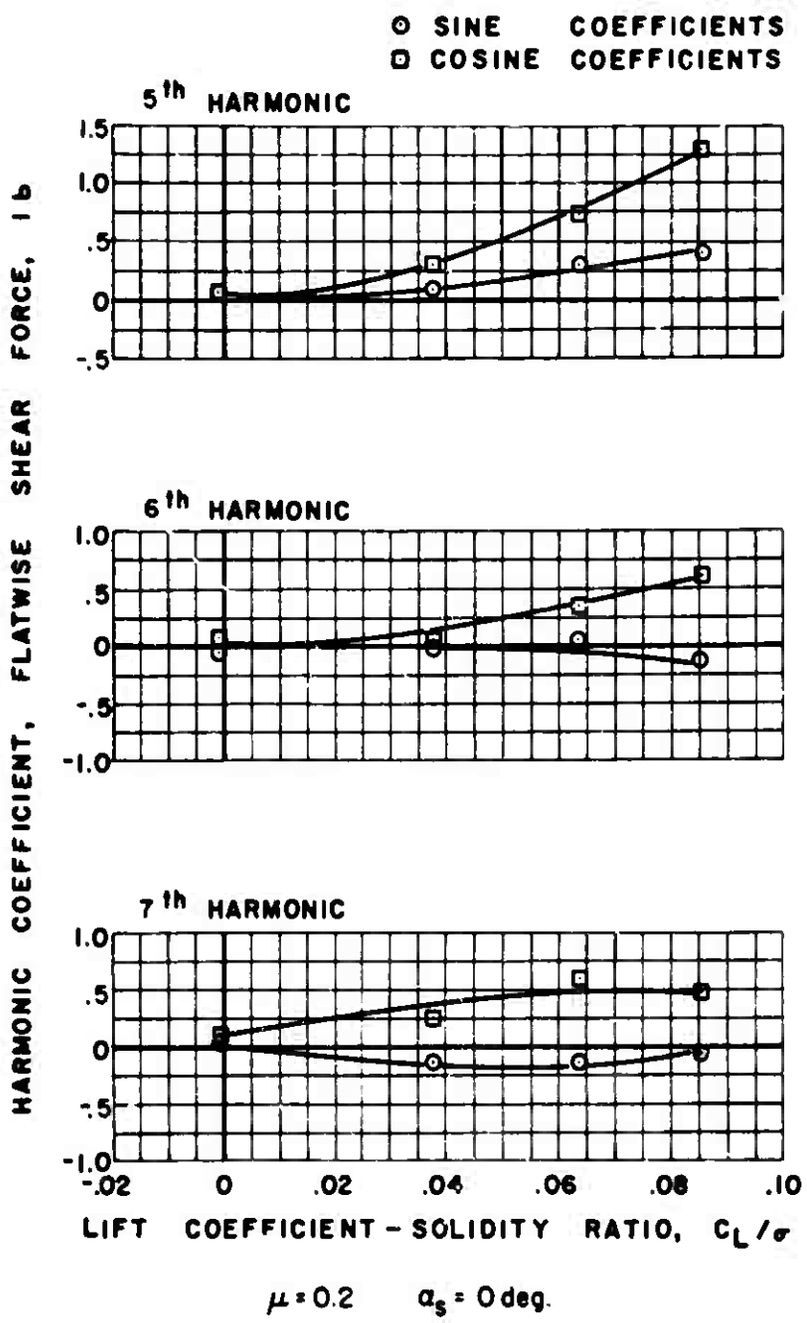

Figure 40(a). Continued.

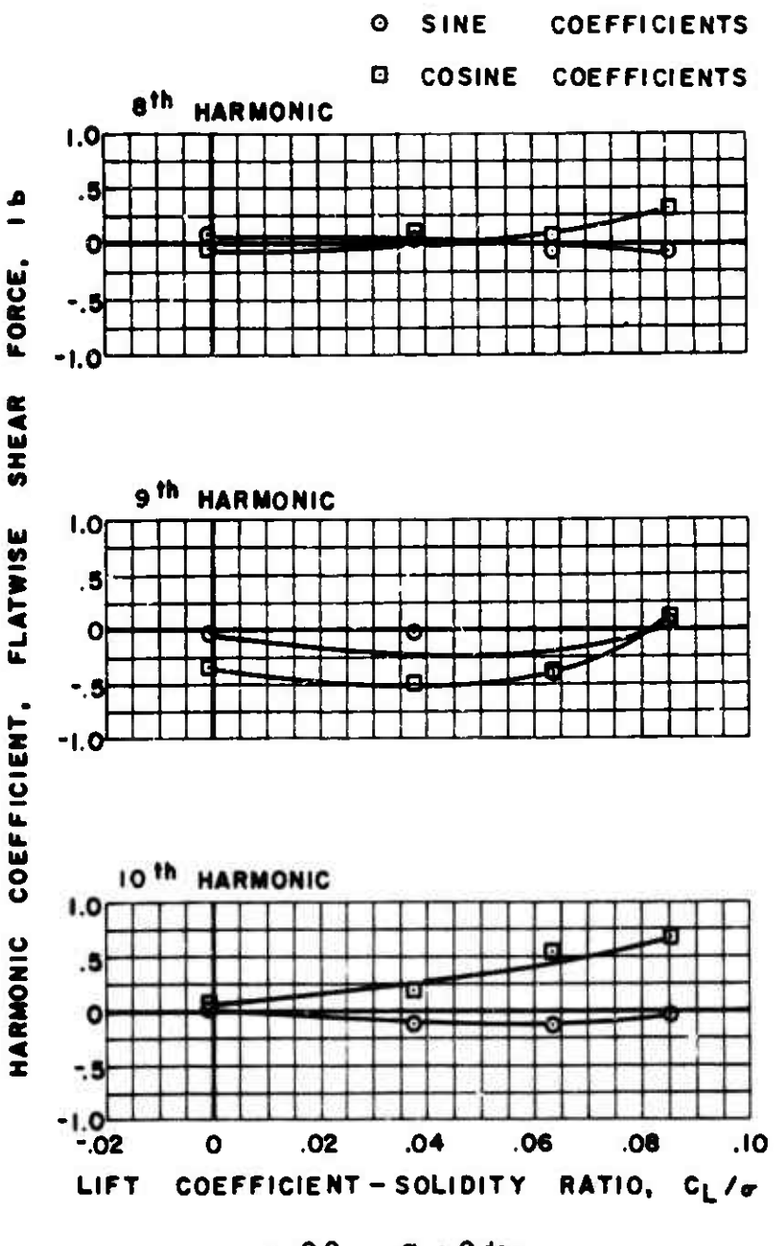

Figure 40(a). Continued.

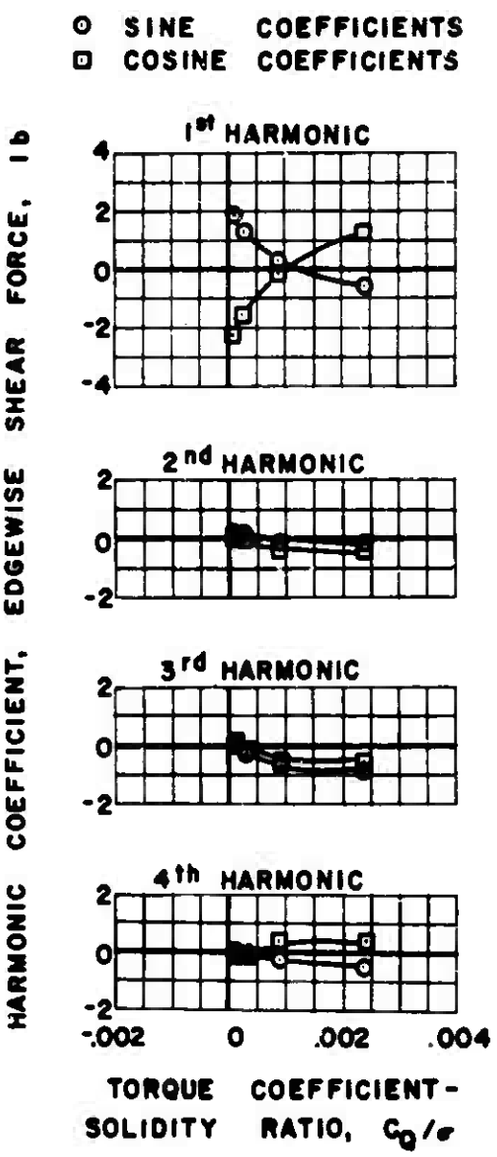

$\mu = 0.2$ $\alpha_s = 0$ deg.

(b) EDGEWISE

Figure 40. Continued.

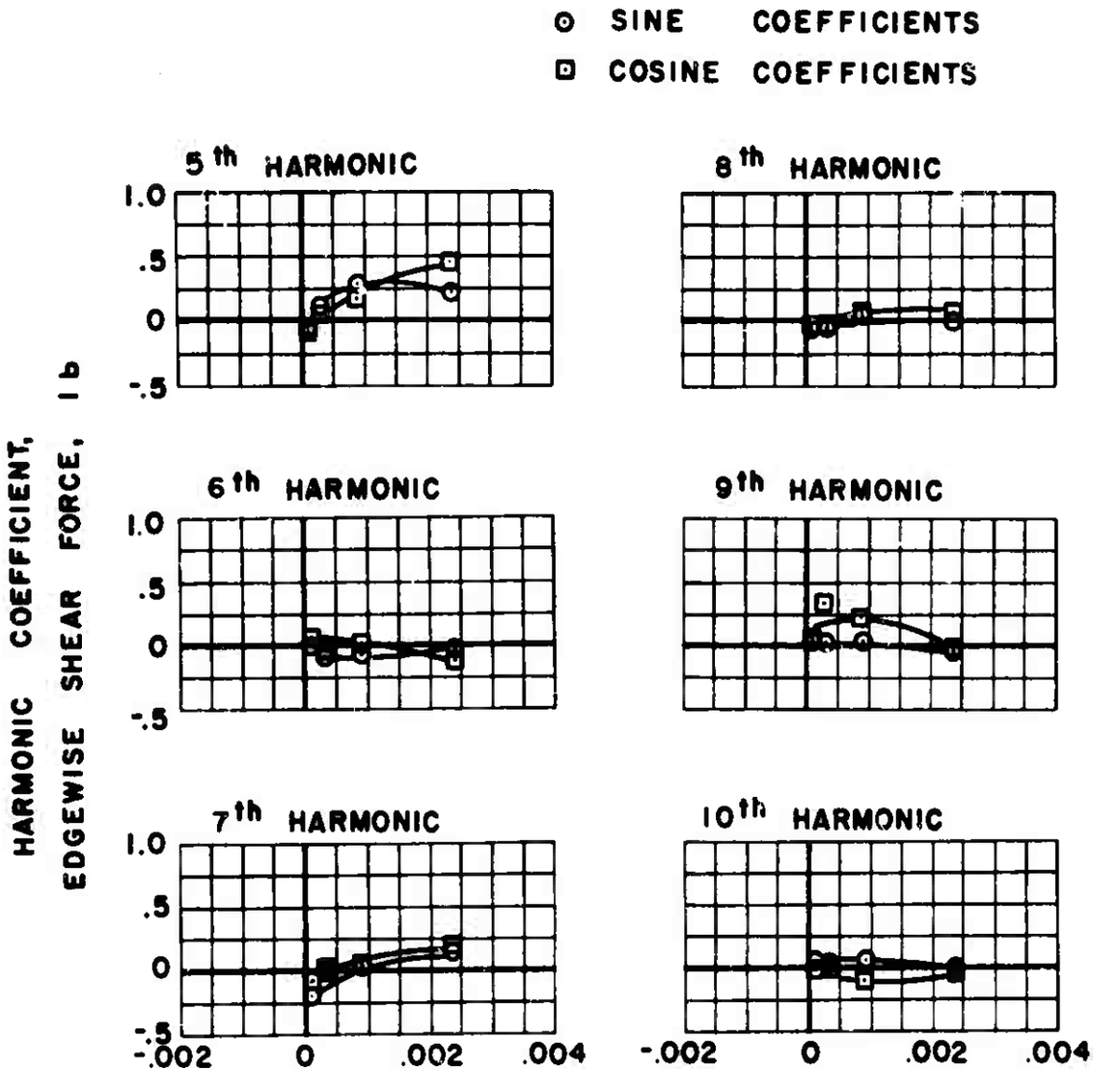

Figure 40(b). Concluded.

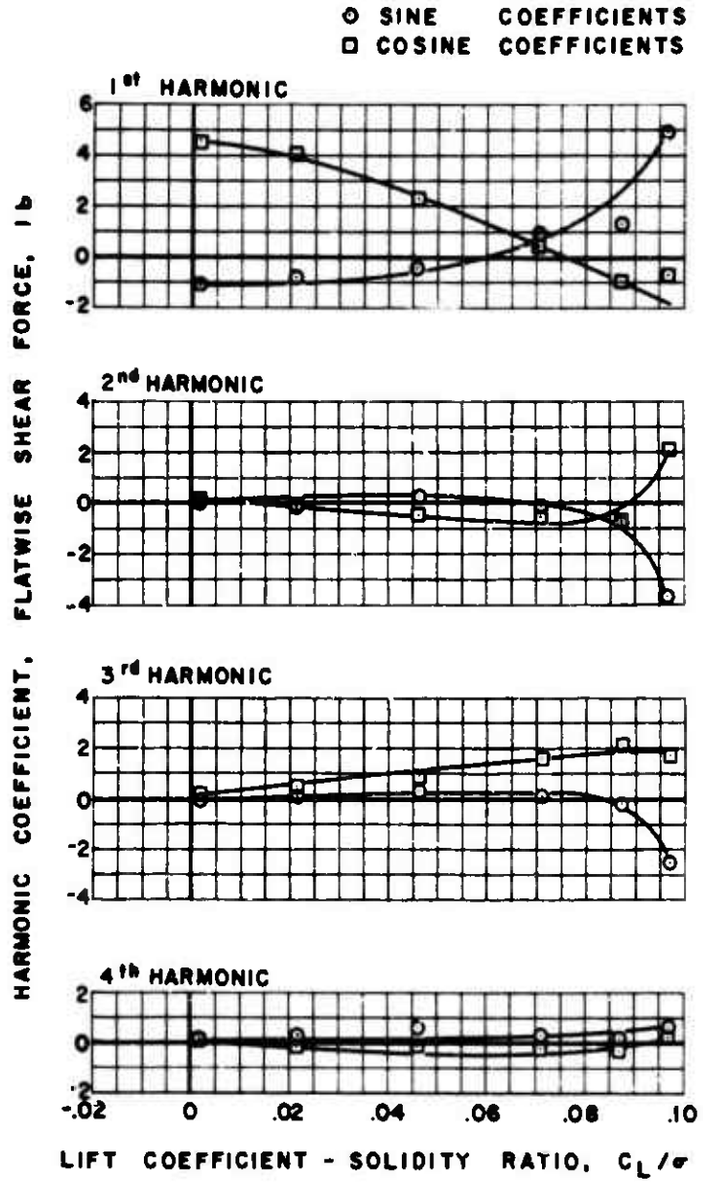

Figure 41. Experimental Shear Force.

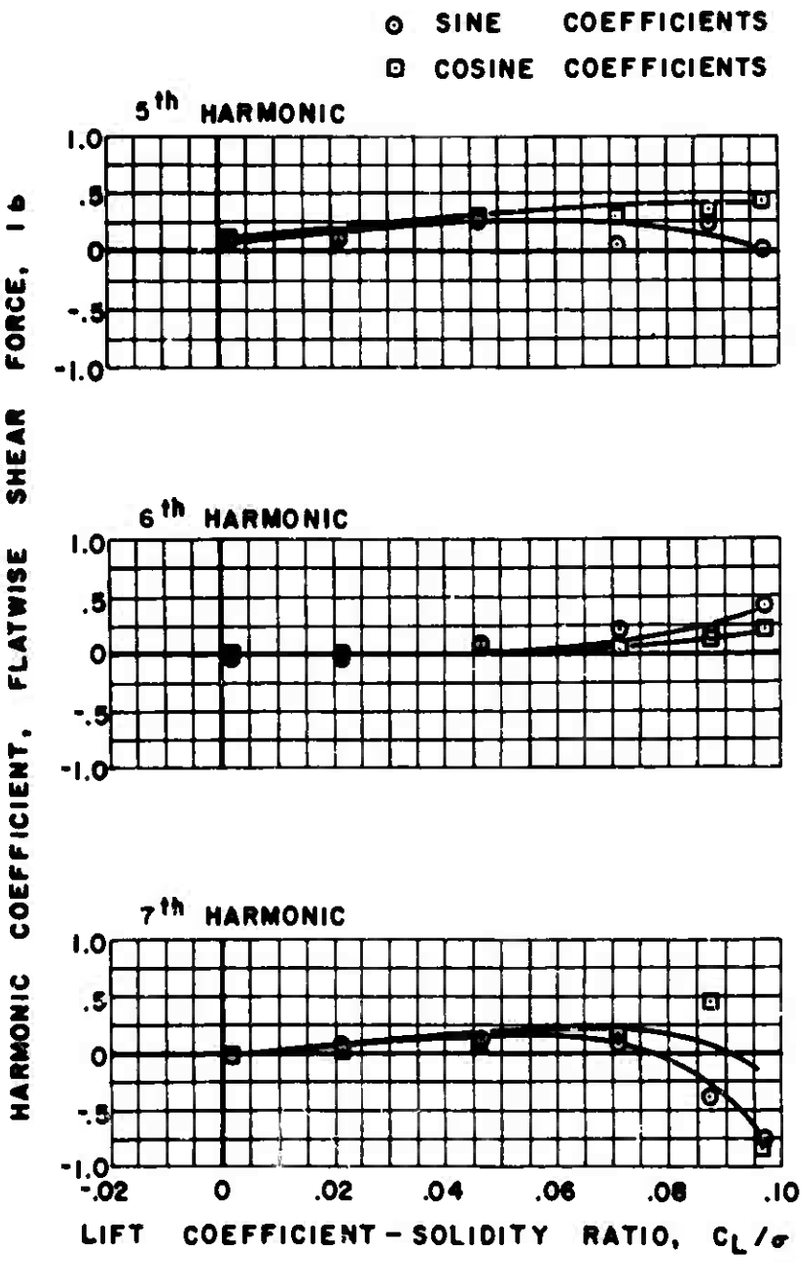

Figure 41(a). Continued.

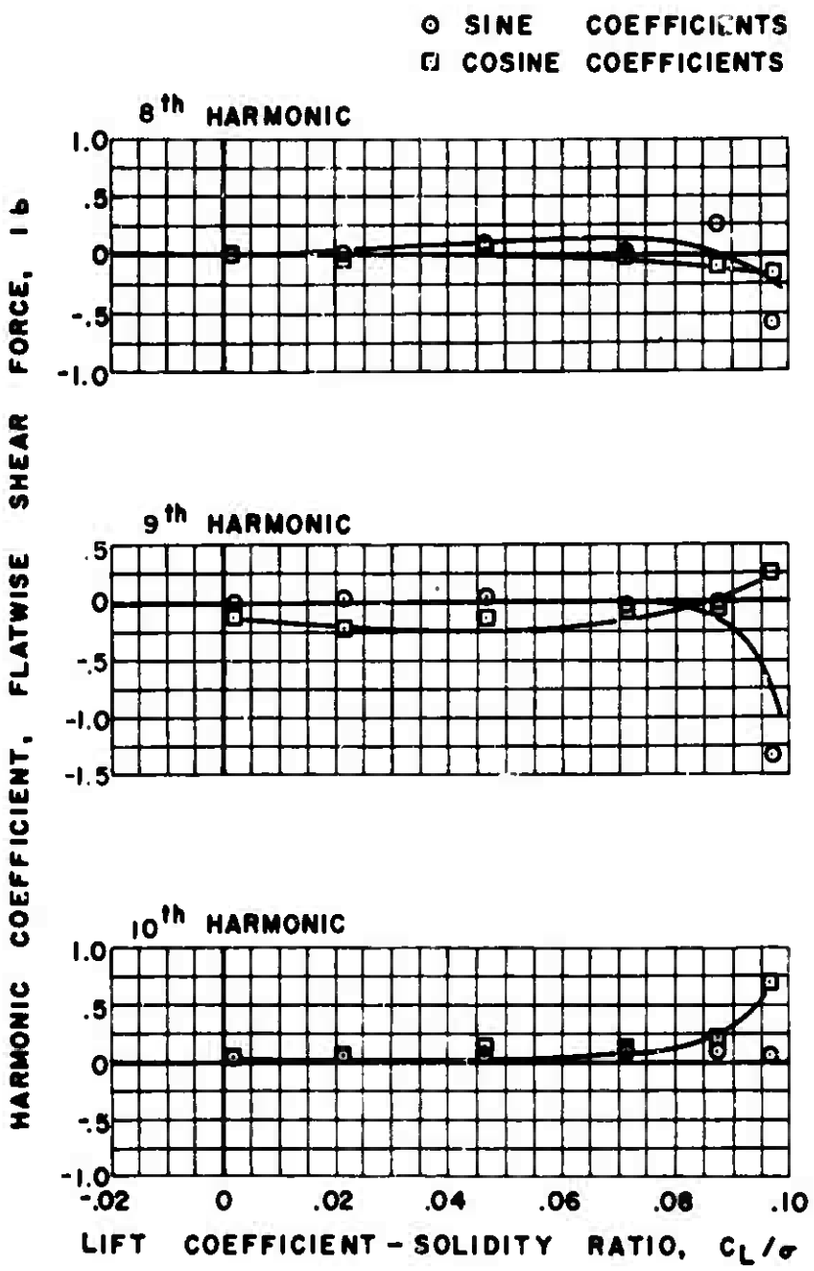

Figure 41(a). Continued.

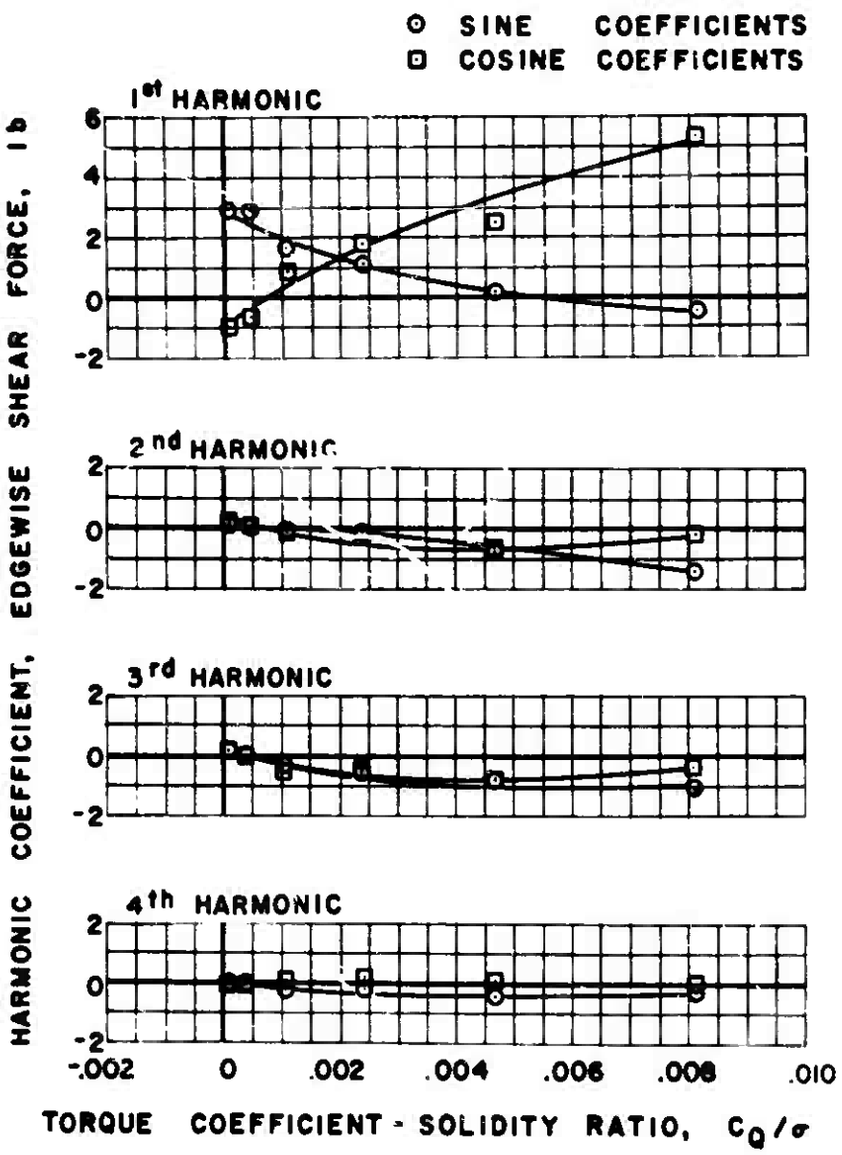

$\mu = 0.2$ $\alpha_s = -4$ deg.

(b) EDGEWISE

Figure 41. Continued.

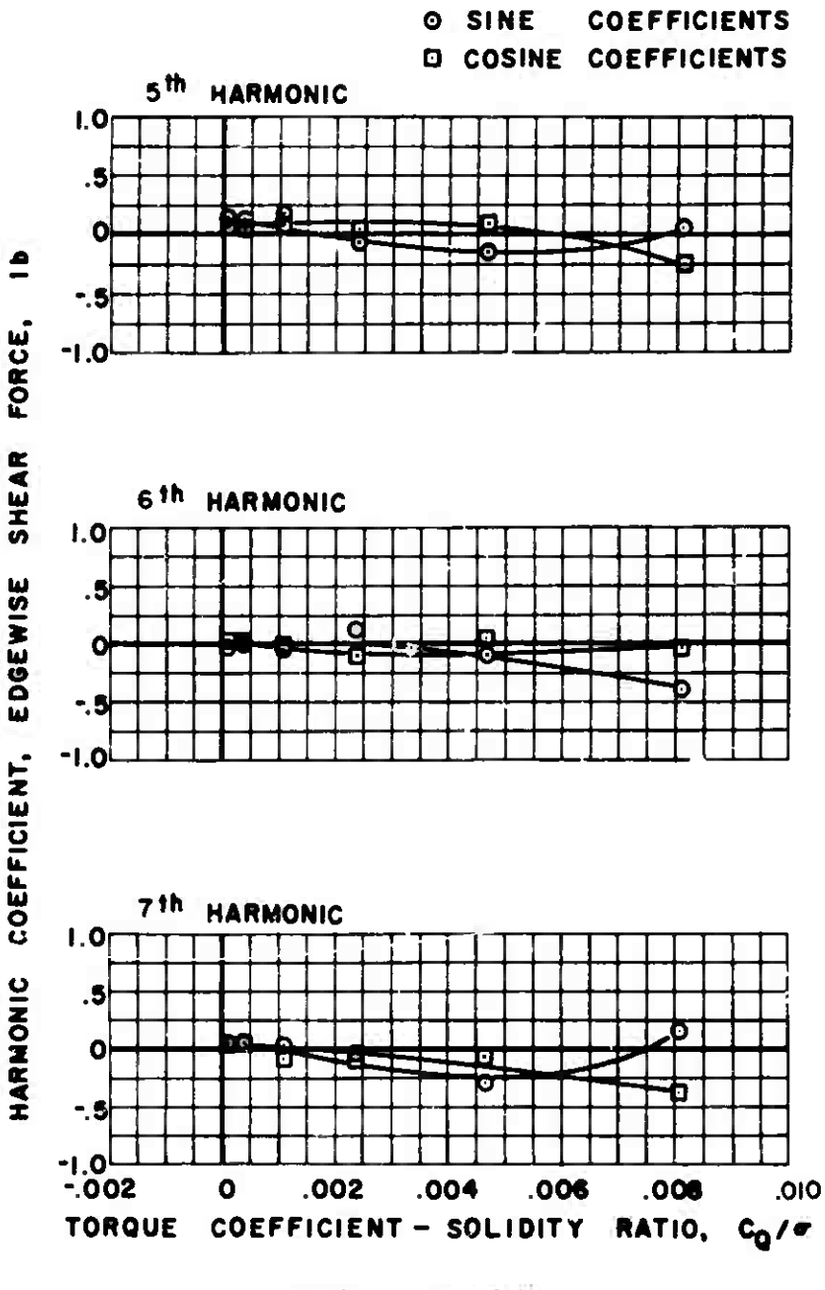

Figure 41(b). Continued.

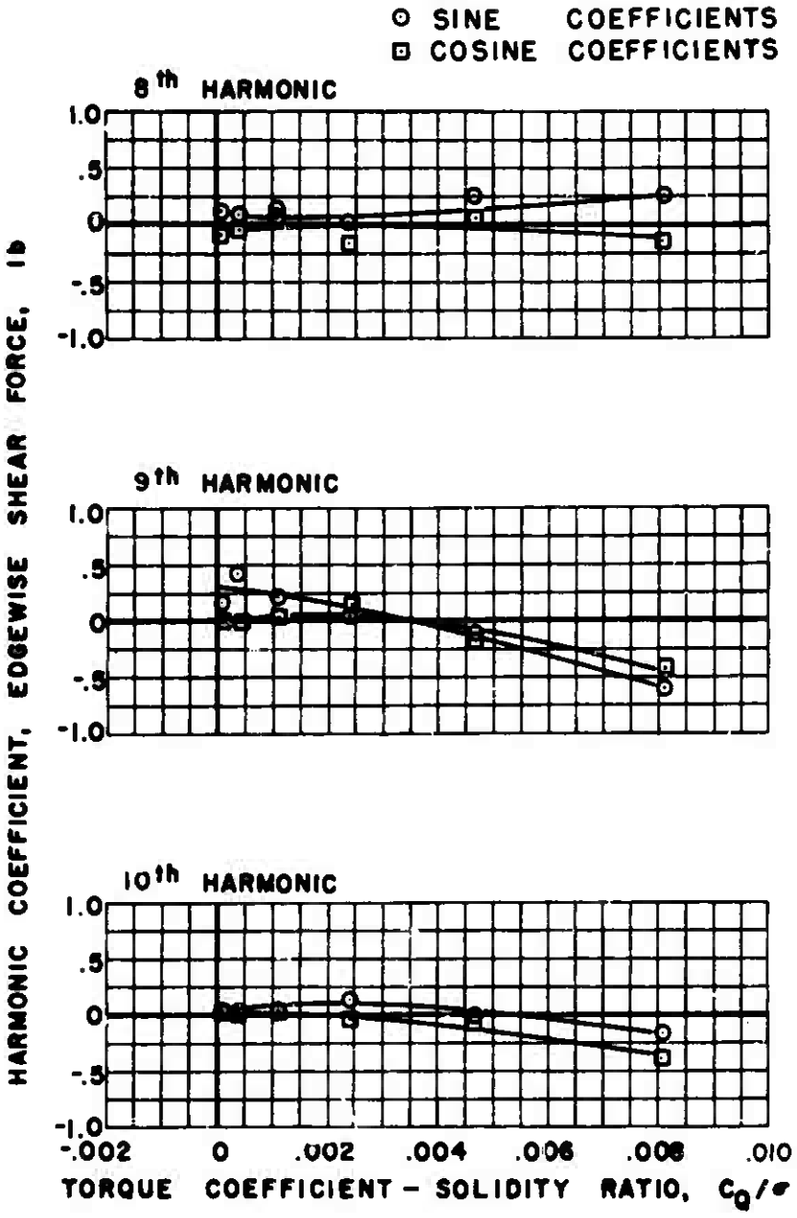

Figure 41(b). Concluded.

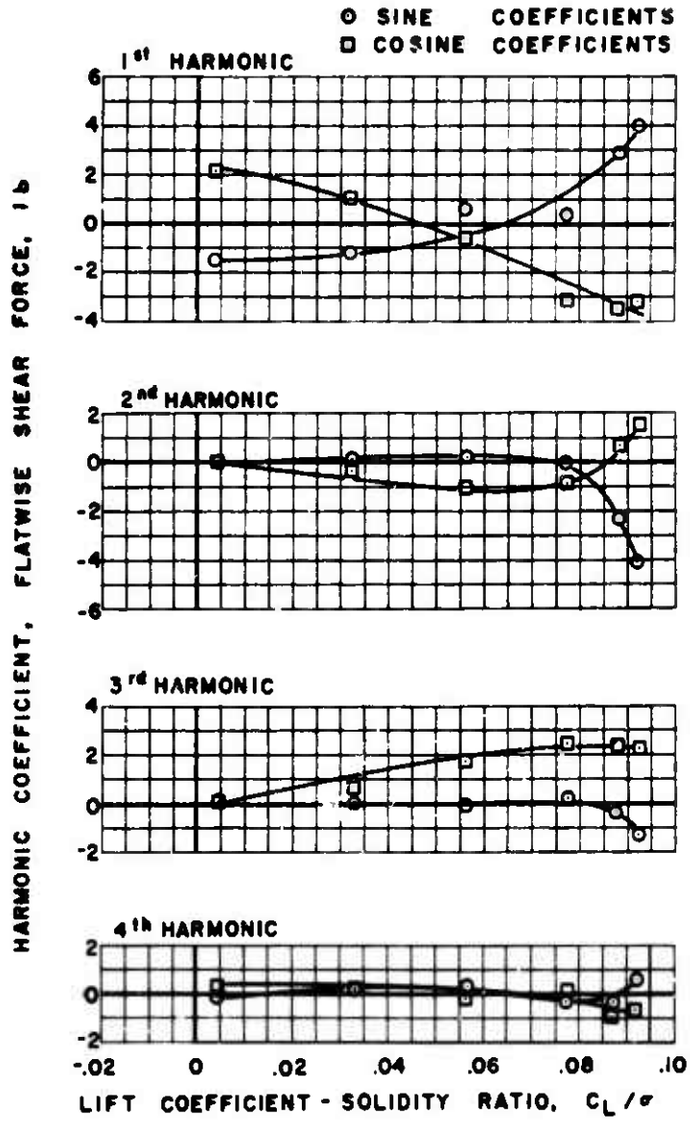

Figure 42. Experimental Shear Force.

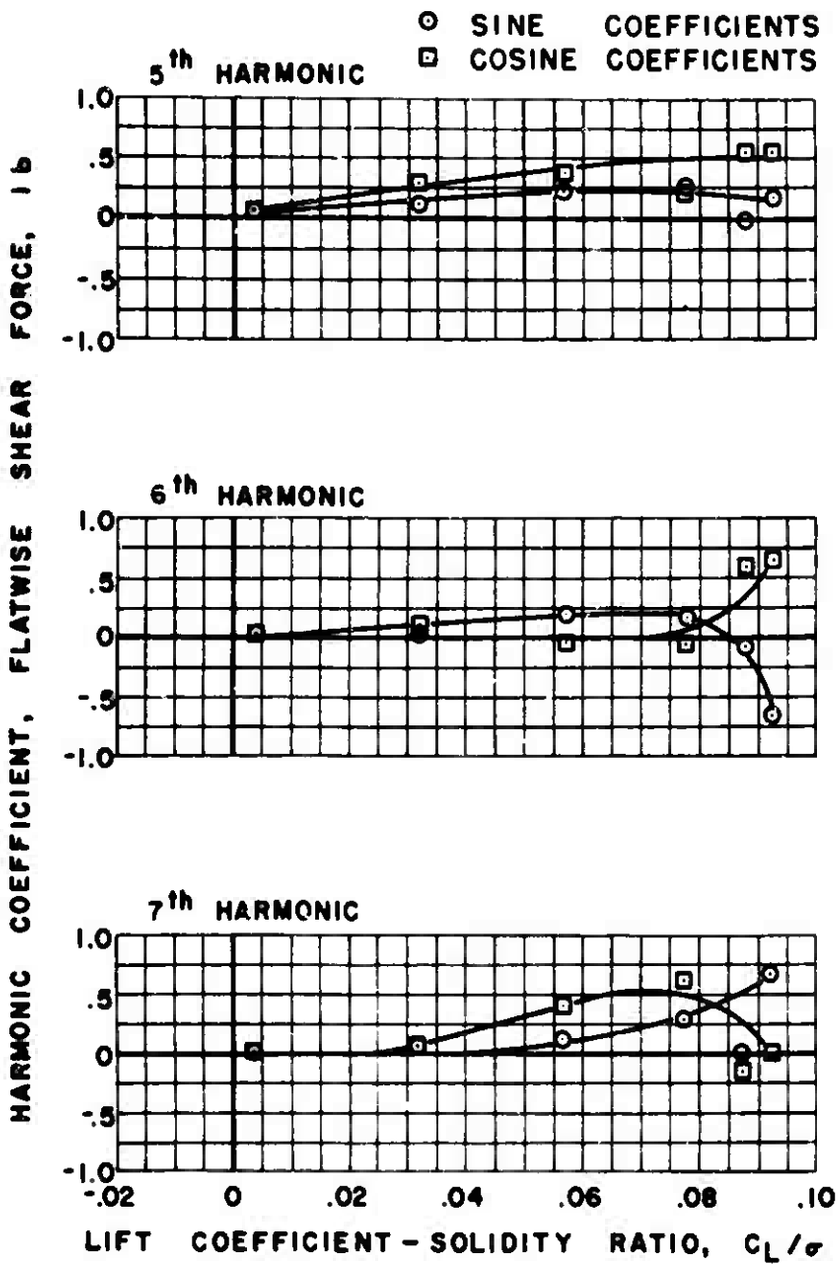

Figure 42(a). Continued.

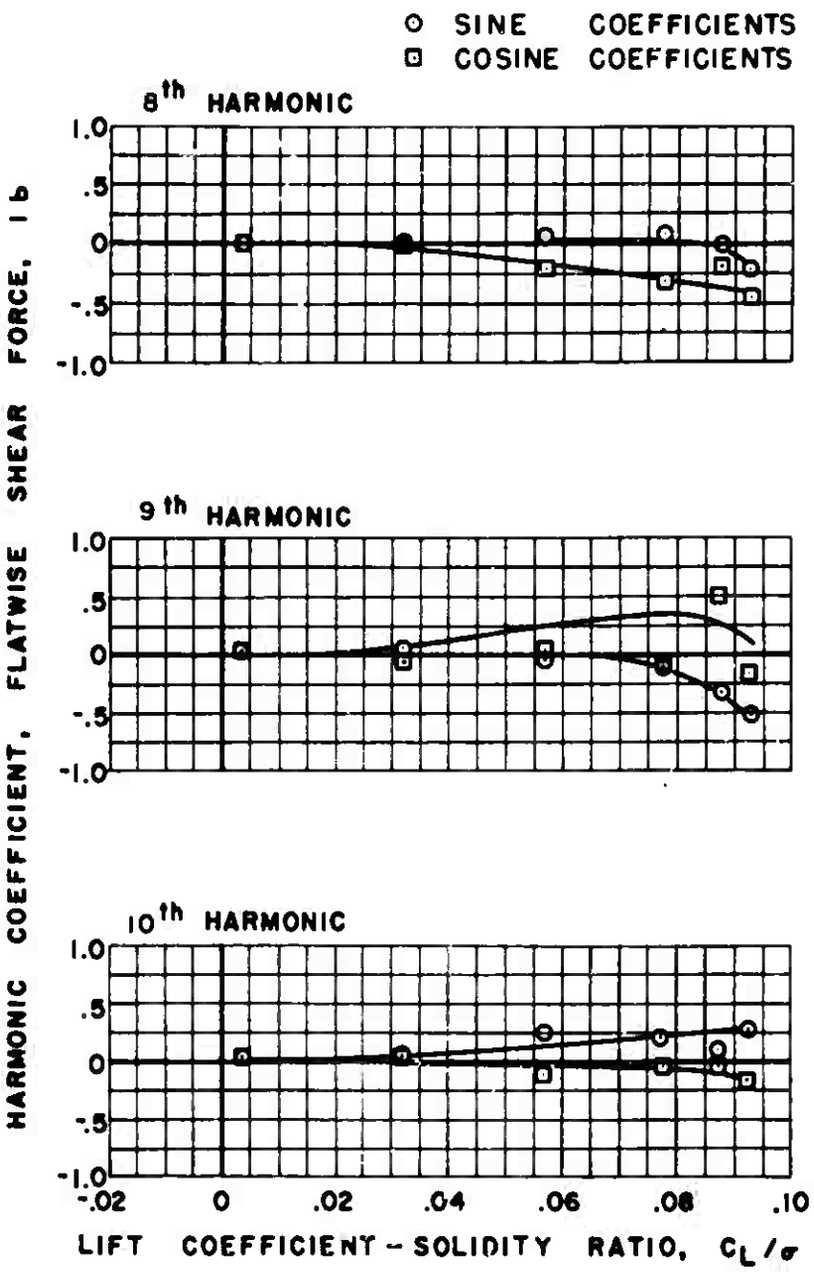

Figure 42(a). Continued.

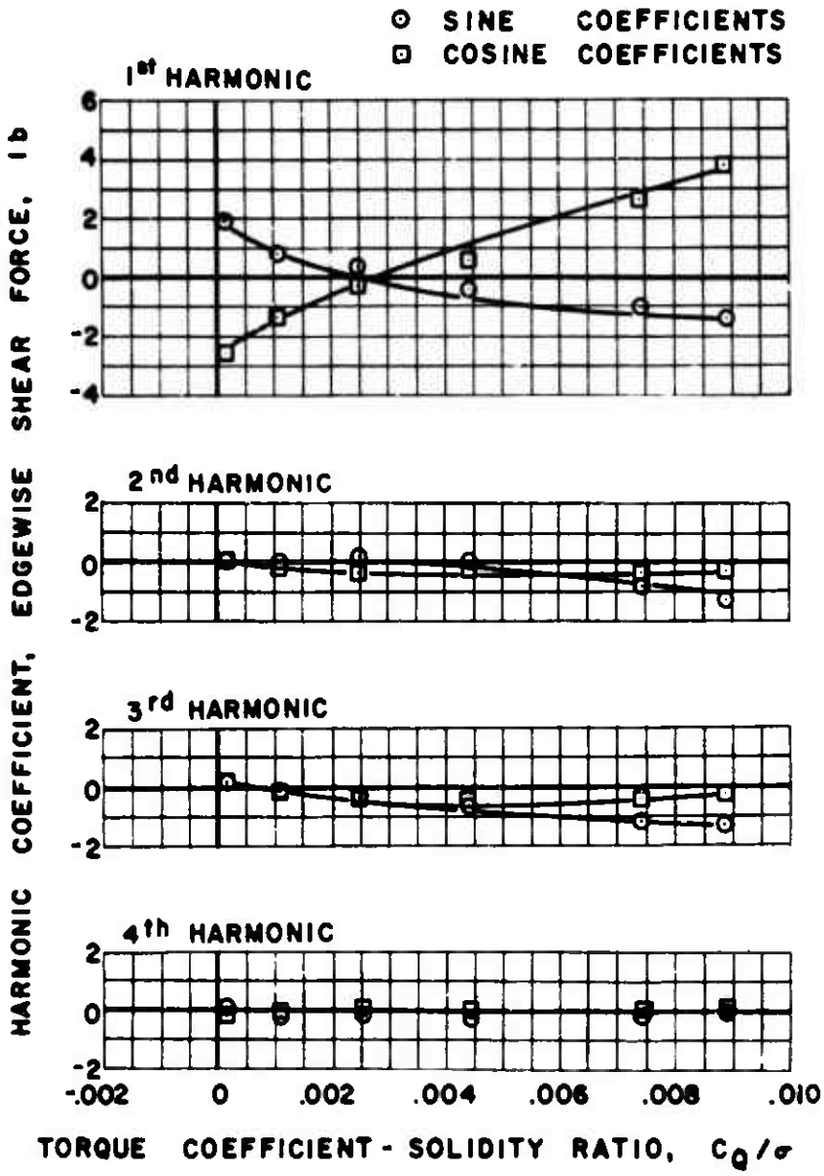

$\mu = 0.2$ $\alpha_s = -8$ deg.

(b) EDGEWISE

Figure 42. Continued.

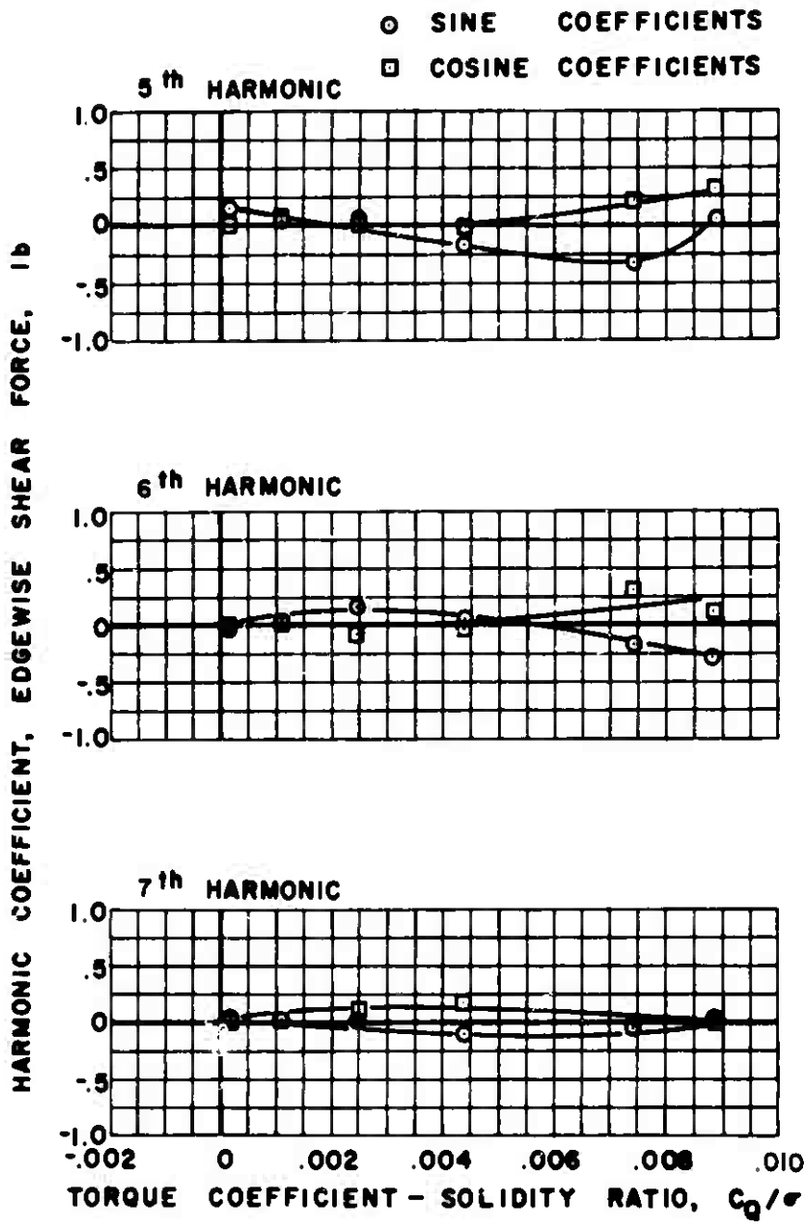

Figure 42(b). Continued.

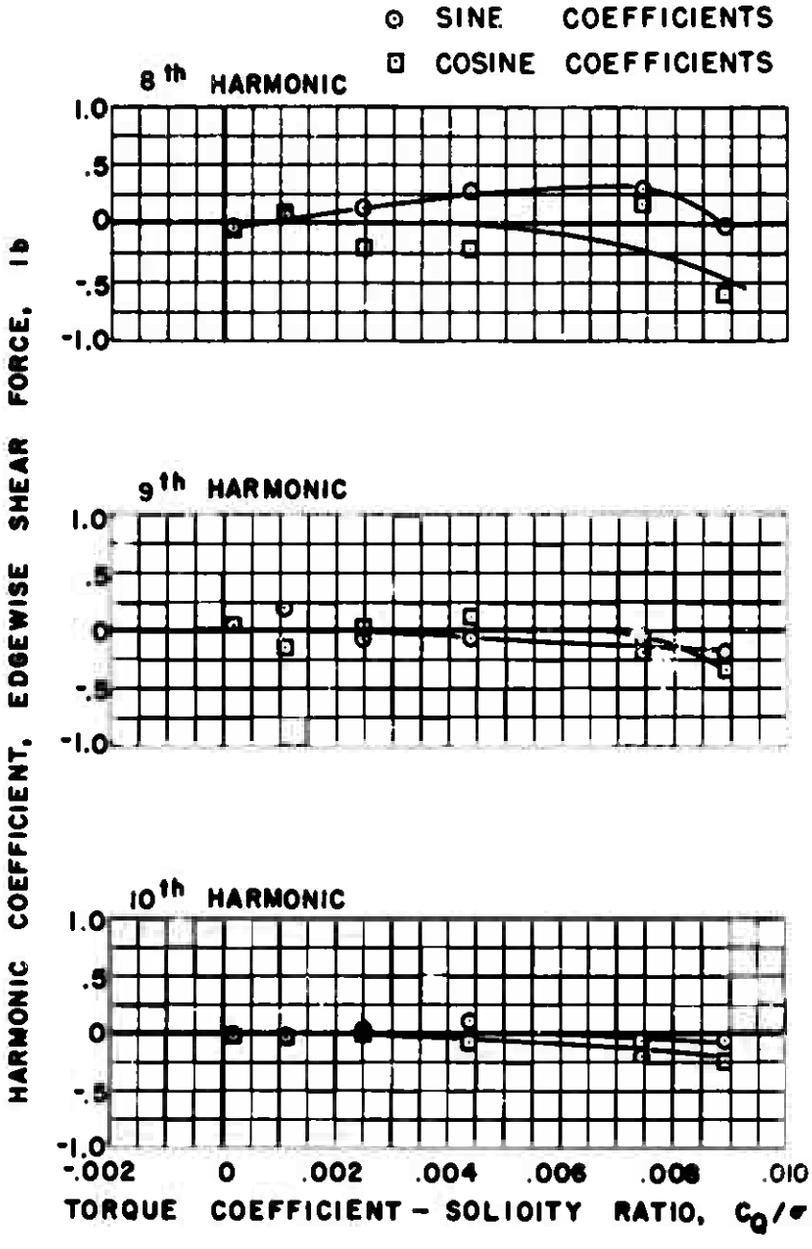

Figure 42(b). Concluded.

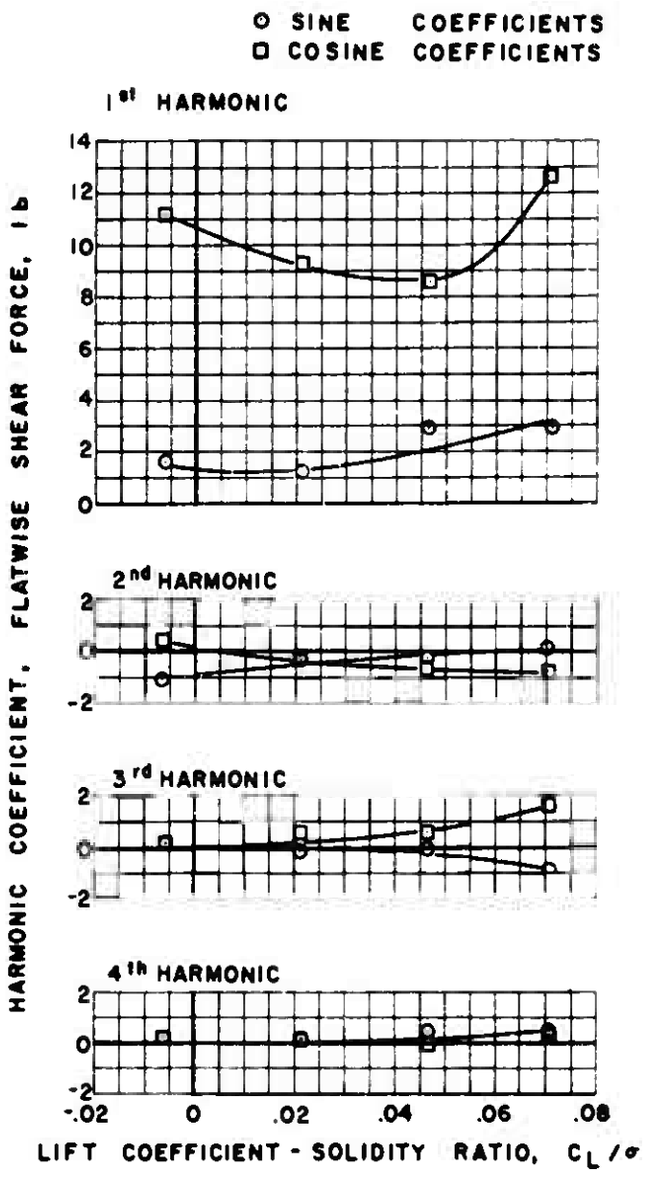

Figure 43. Experimental Shear Force, Out of Trim, -4 Degree Longitudinal Flapping.

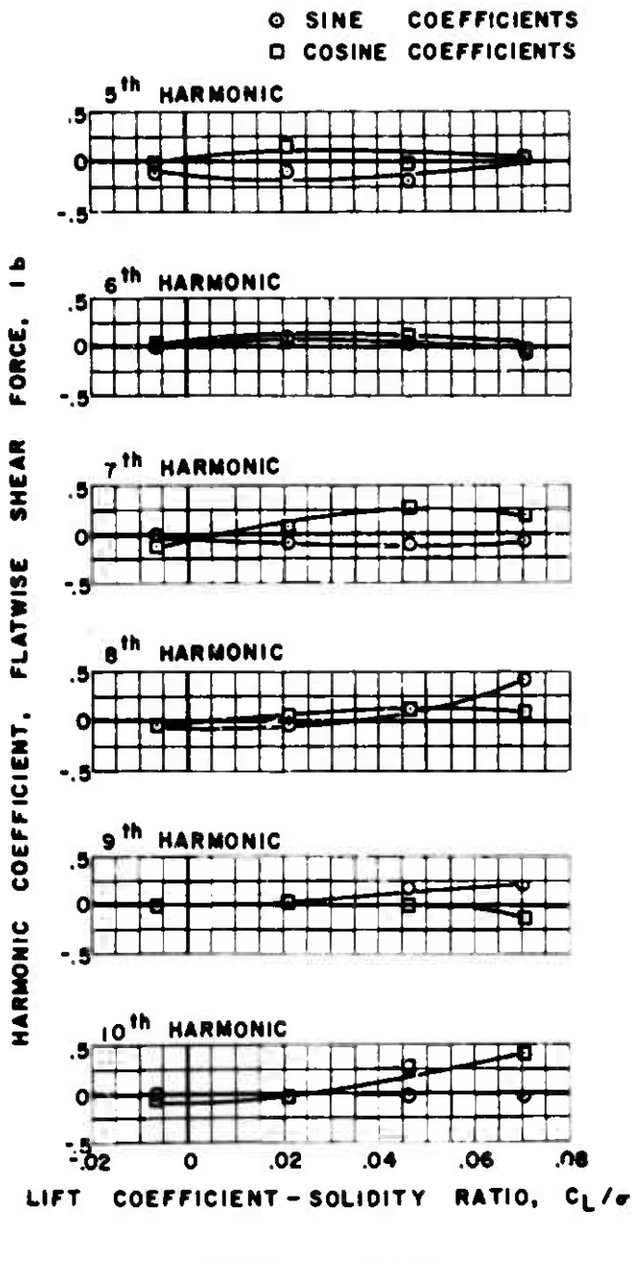

Figure 43(a). Continued

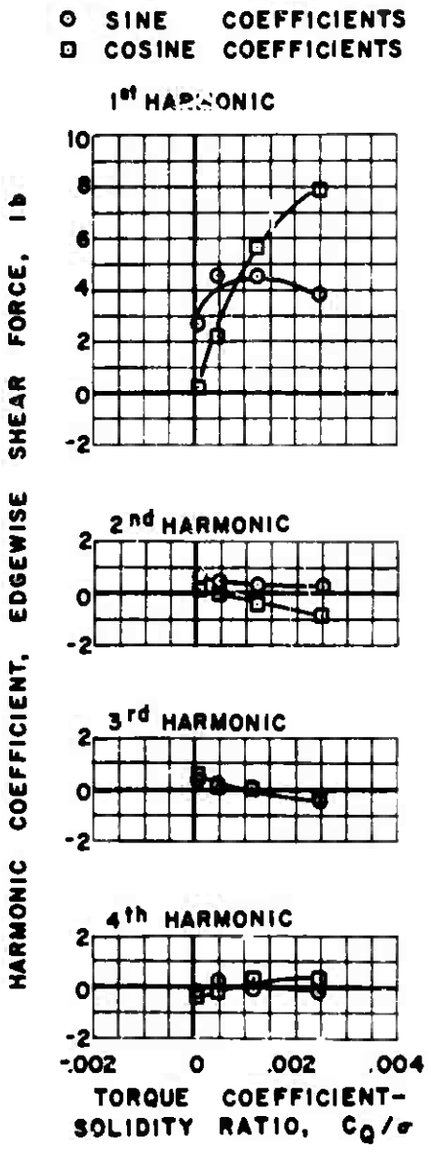

$\mu = 0.2$ $\alpha_s = 0$deg.

(b) EDGEWISE

Figure 43. Continued.

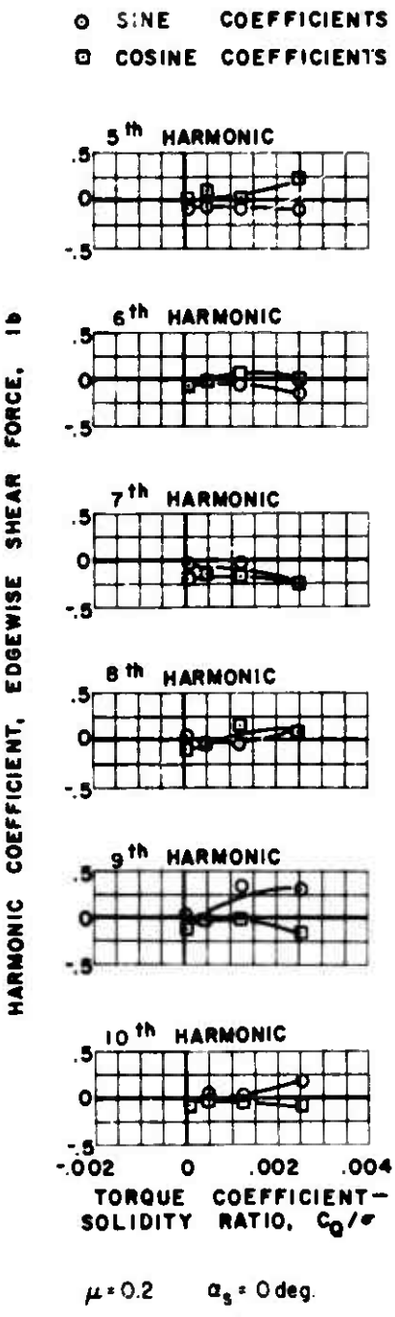

Figure 43(b). Concluded.

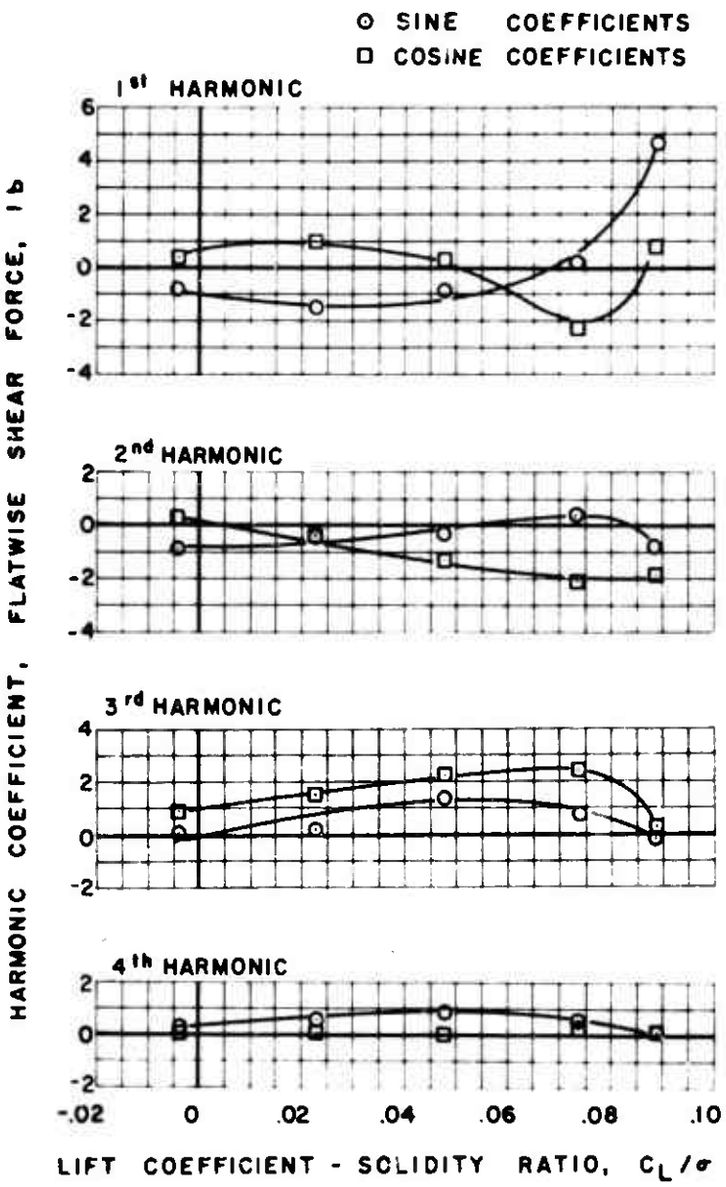

Figure 44. Experimental Shear Force, Zero Lag Damping.

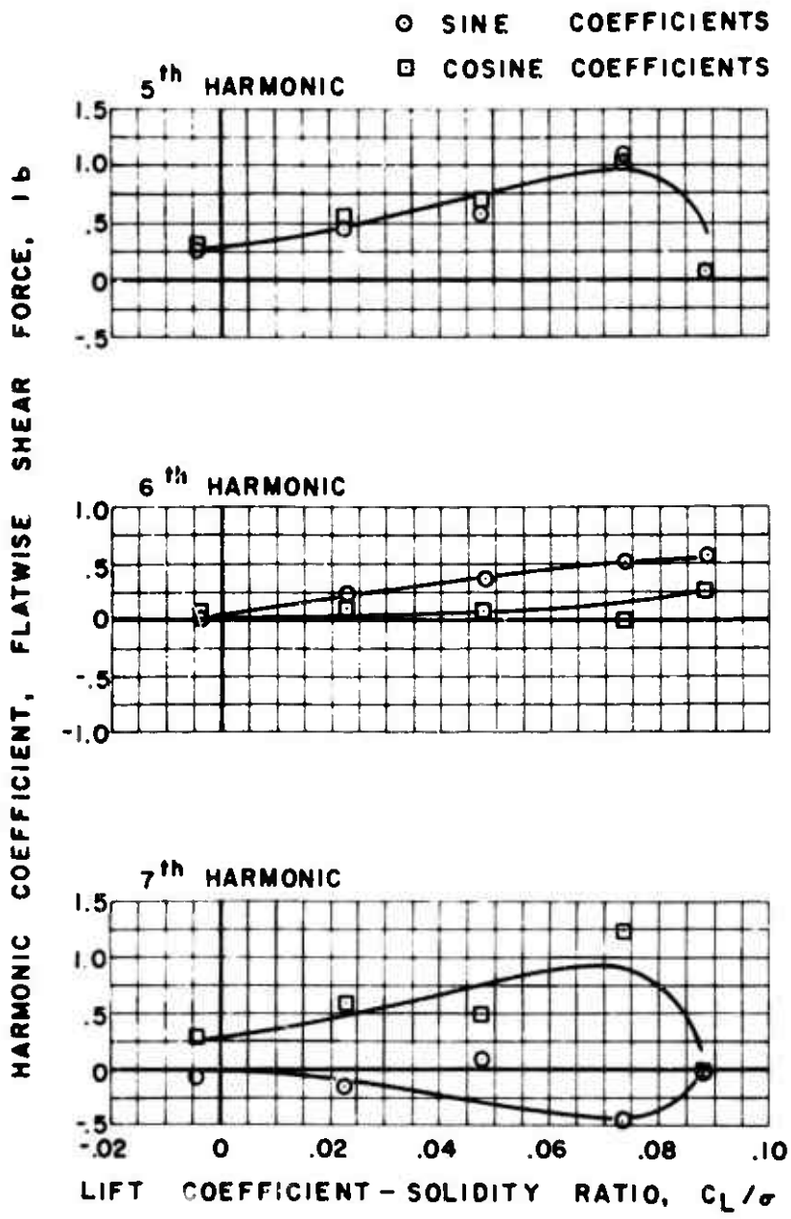

Figure 44(a). Continued.

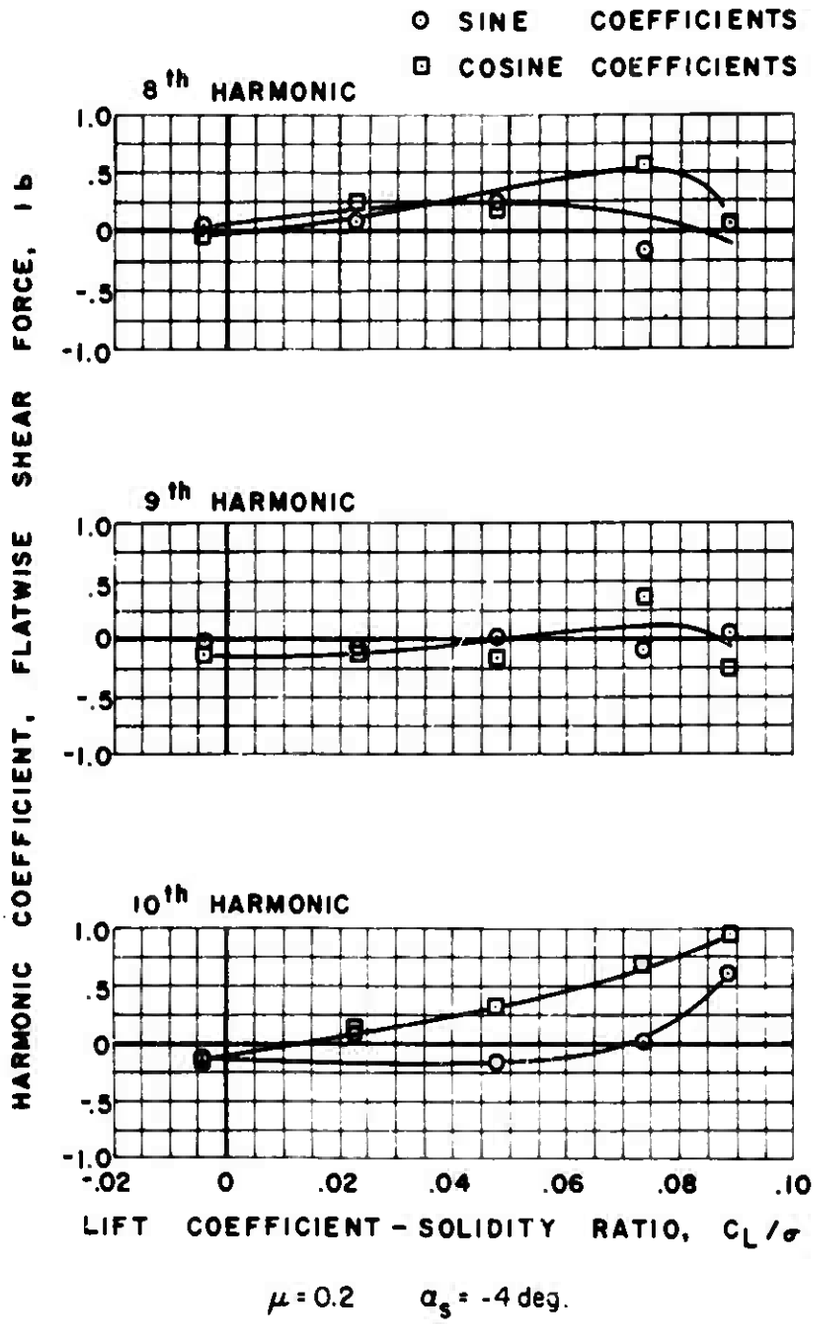

Figure 44(a). Continued.

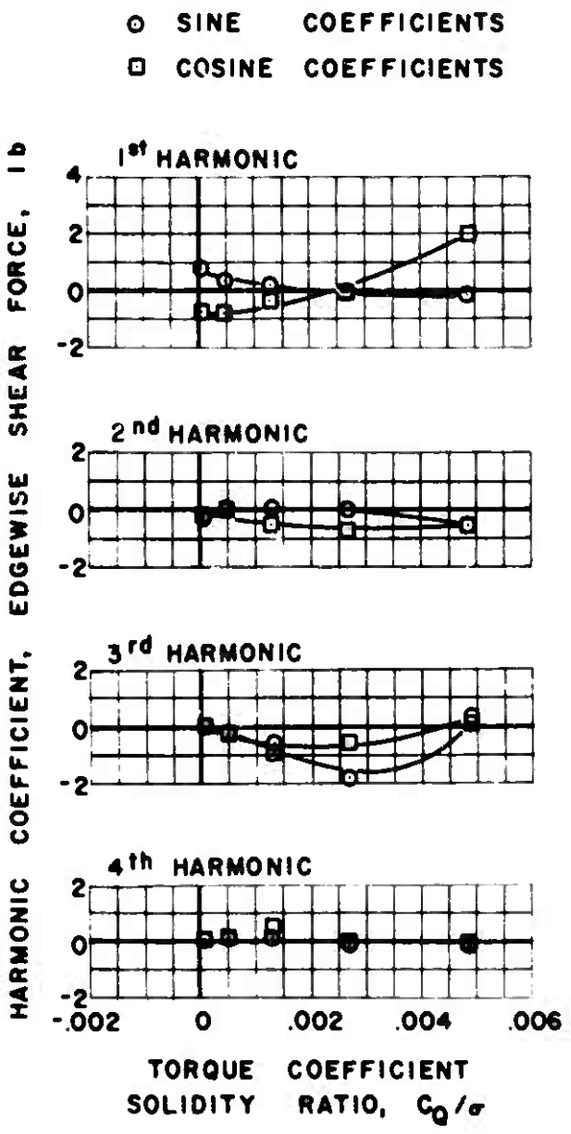

$\mu = 0.2$ $\alpha_s = -4$ deg.

(b) EDGEWISE

Figure 44. Continued.

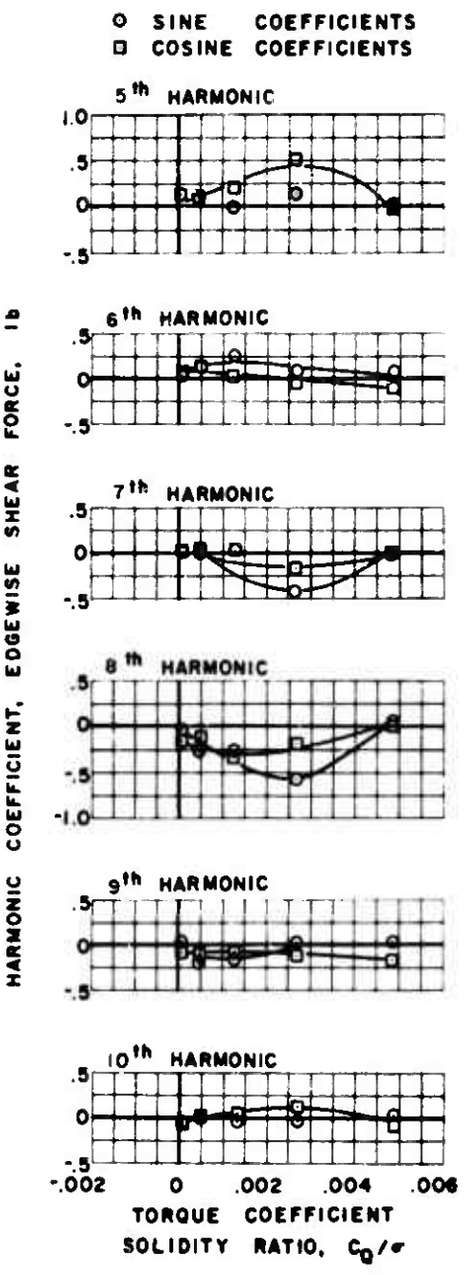

Figure 44(b). Concluded.

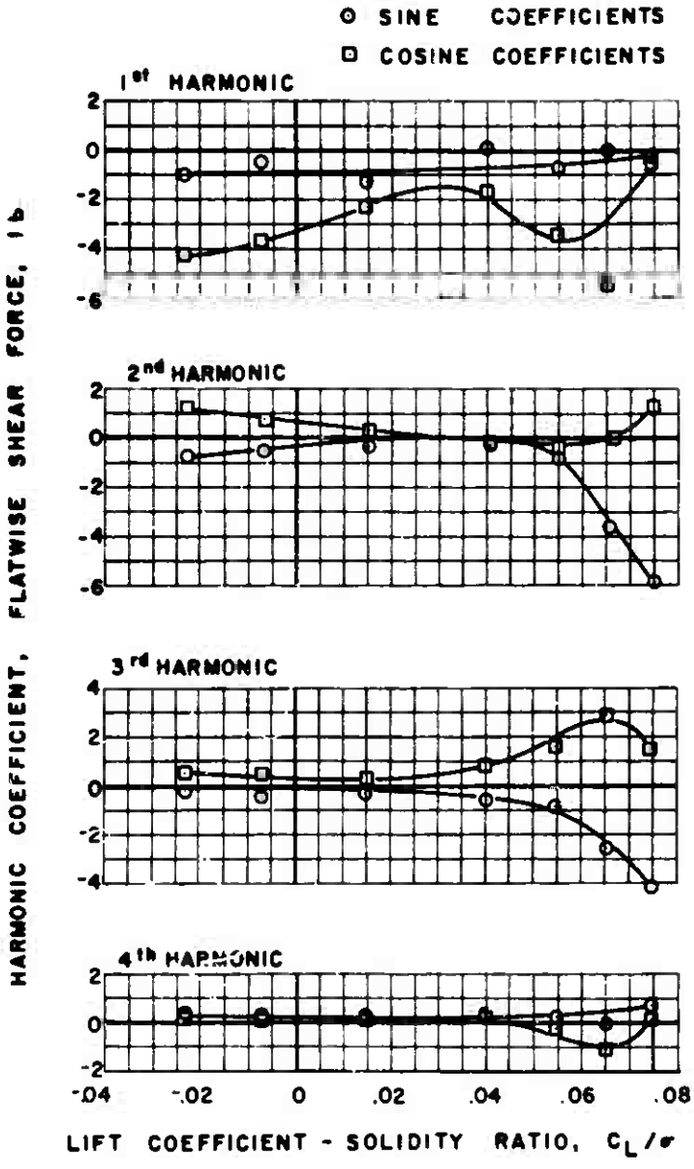

Figure 45. Experimental Shear Force.

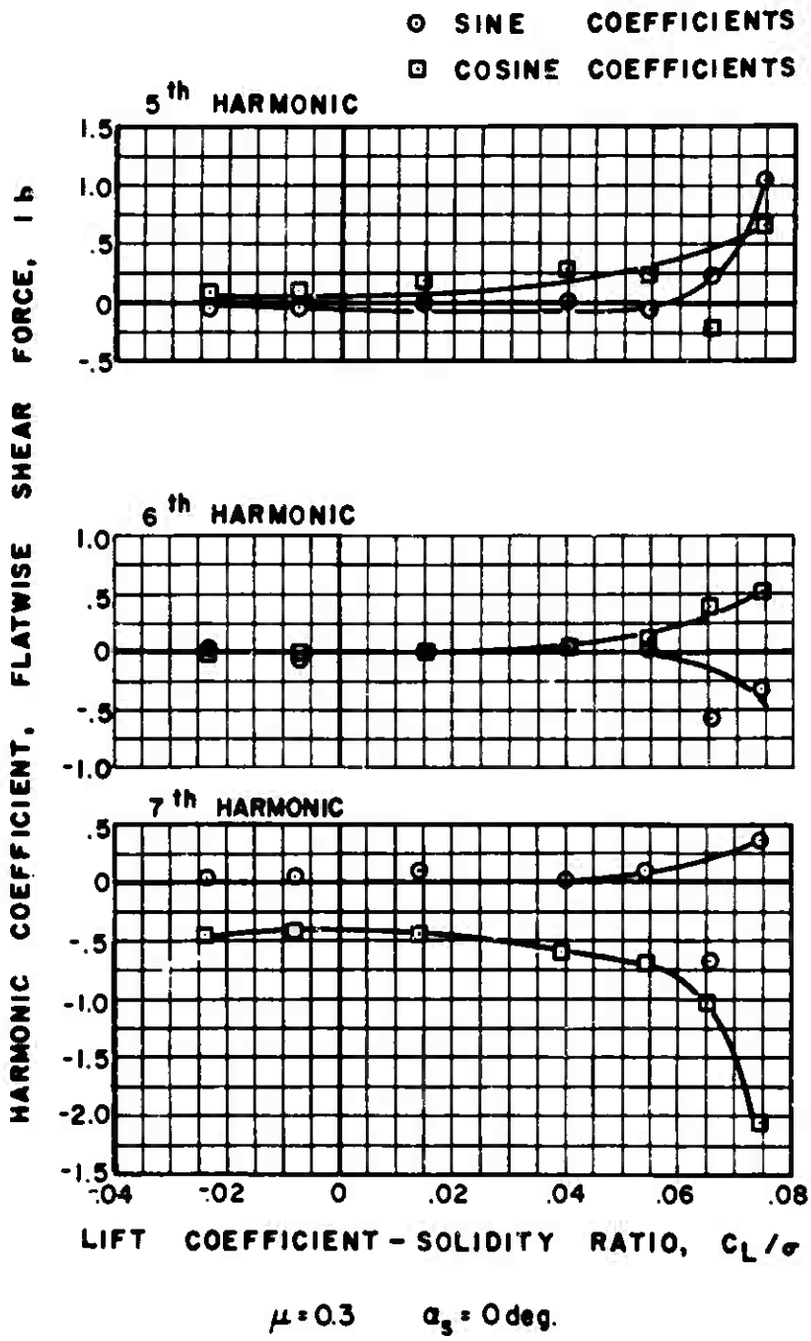

Figure 45(a). Continued.

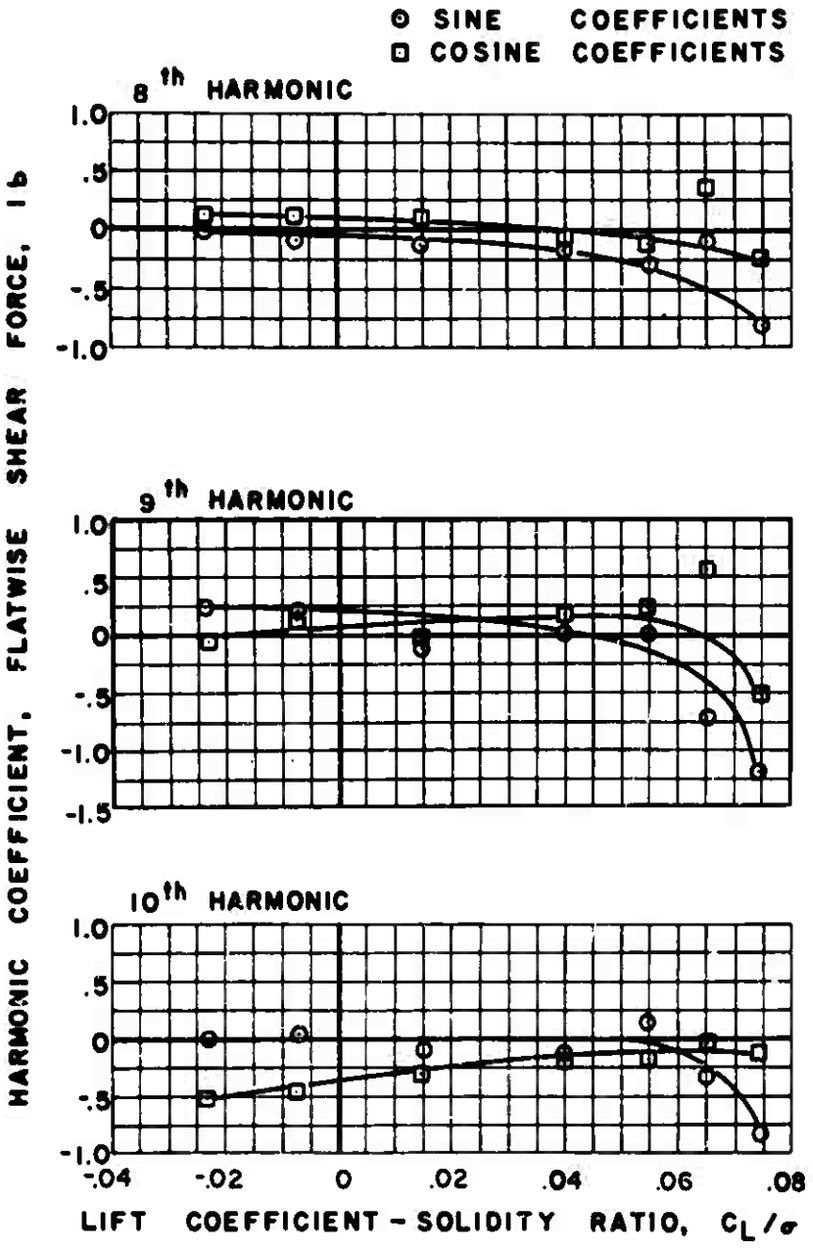

Figure 45(a). Continued.

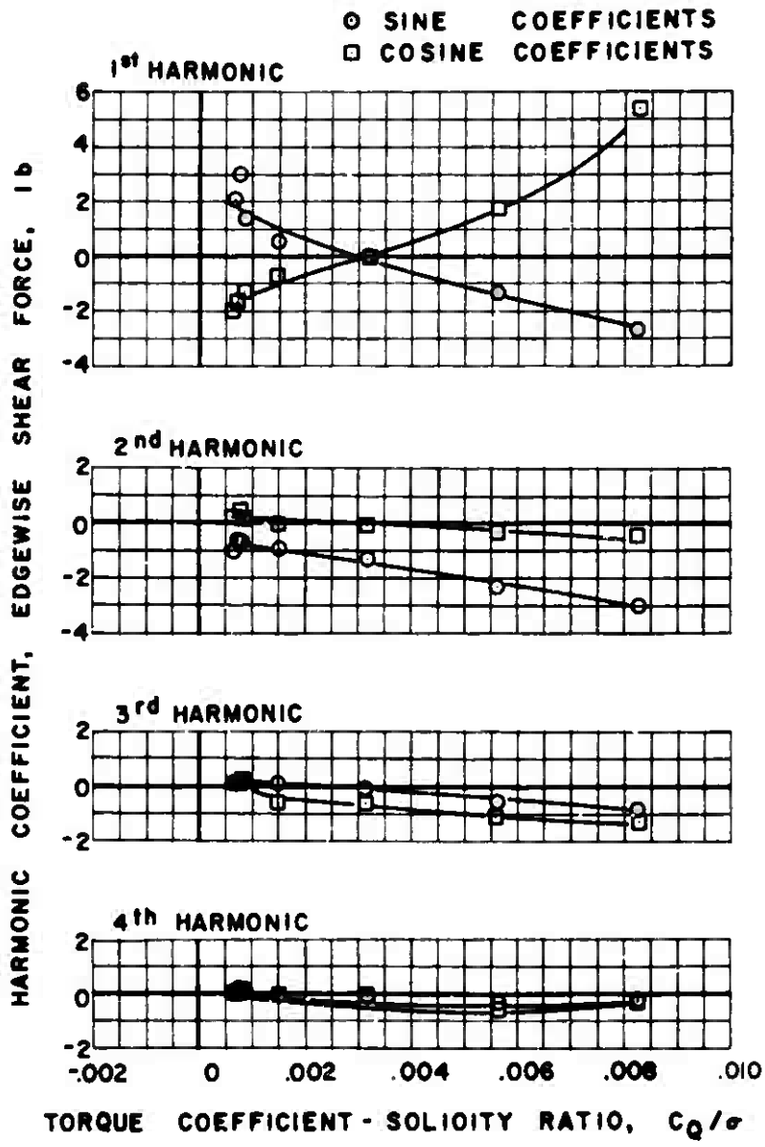

$\mu = 0.3$ $\alpha_s = 0$ deg.

(b) EDGEWISE

Figure 45. Continued.

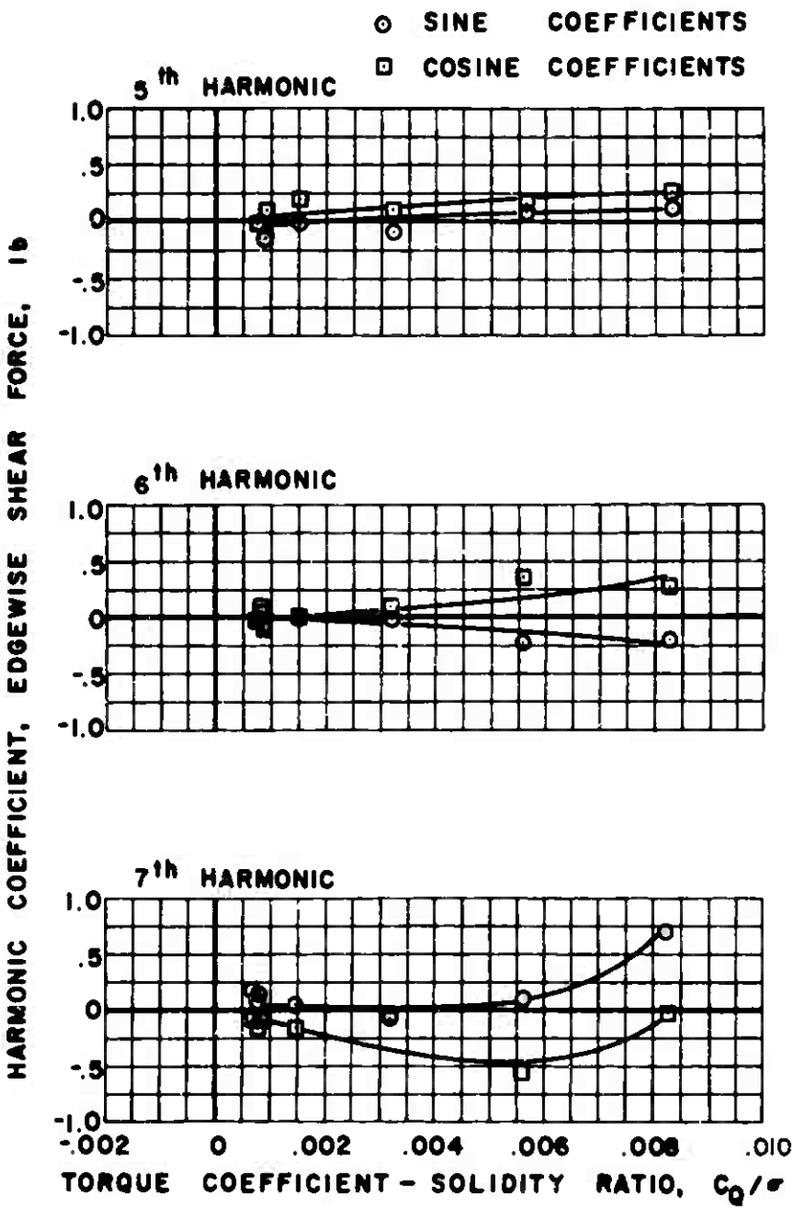

Figure 45(b). Continued.

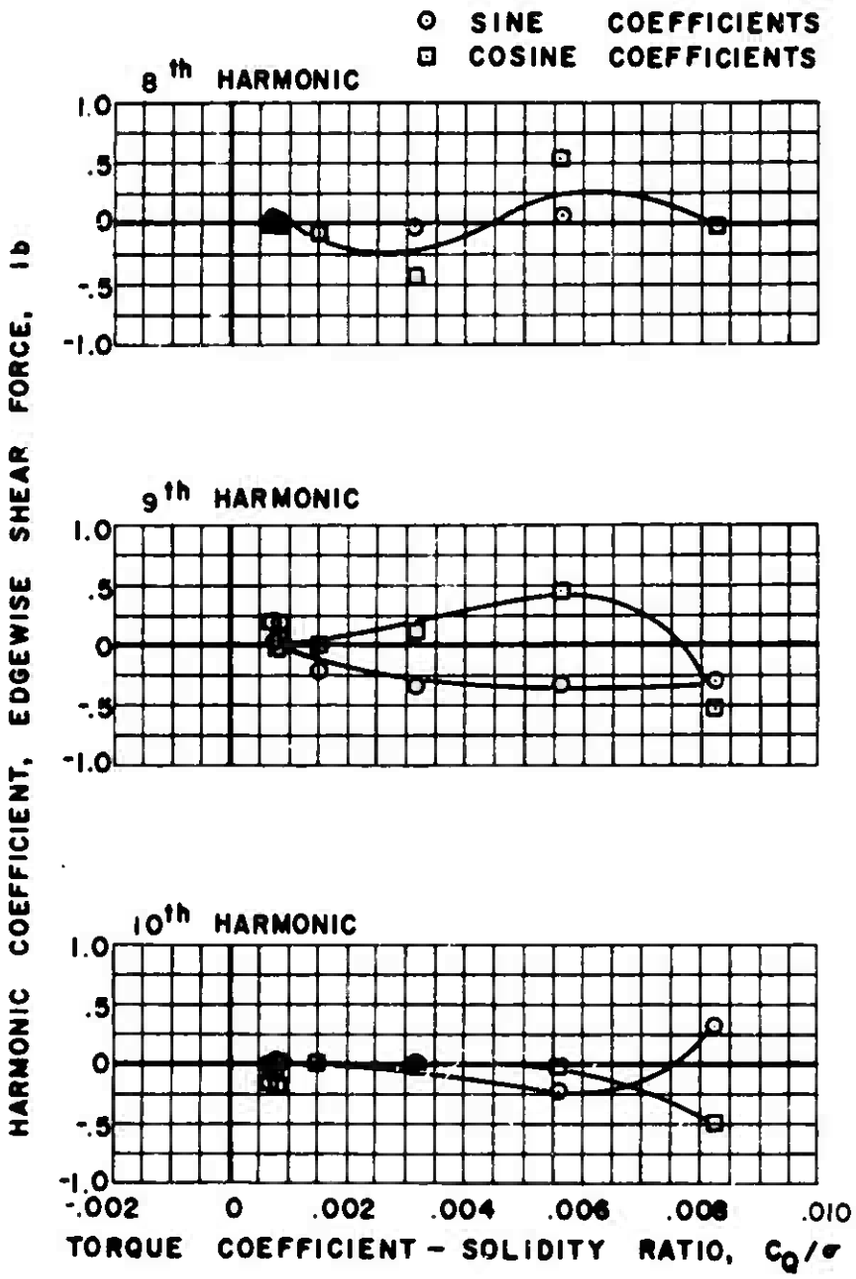

Figure 45(b). Concluded.

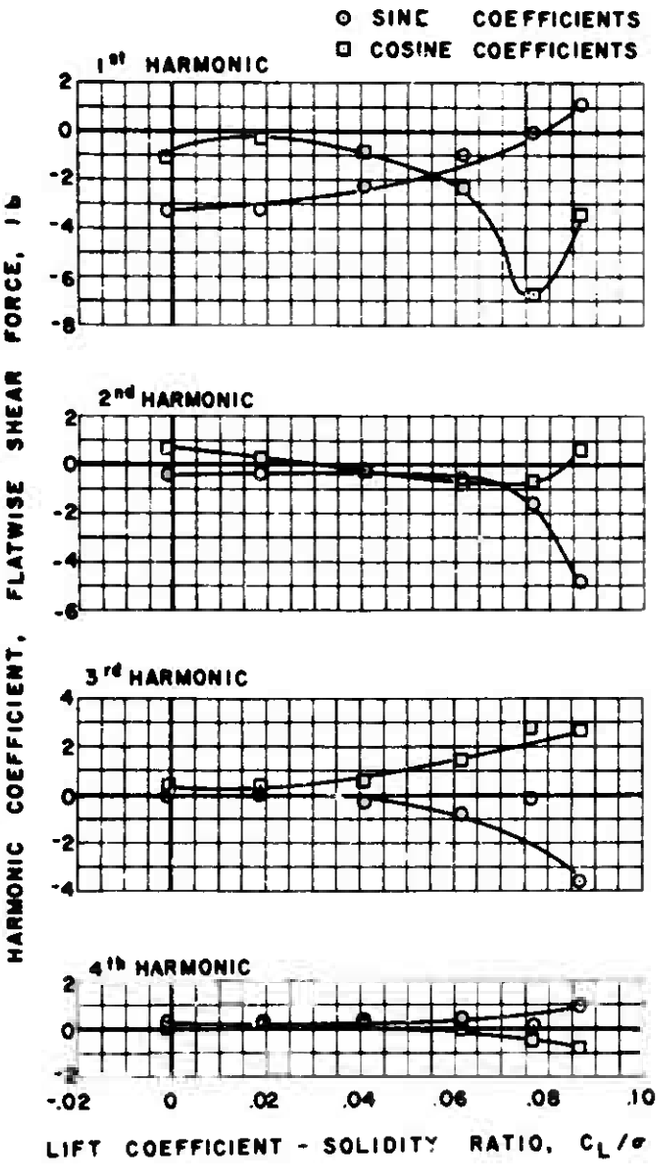

Figure 46. Experimental Shear Force.

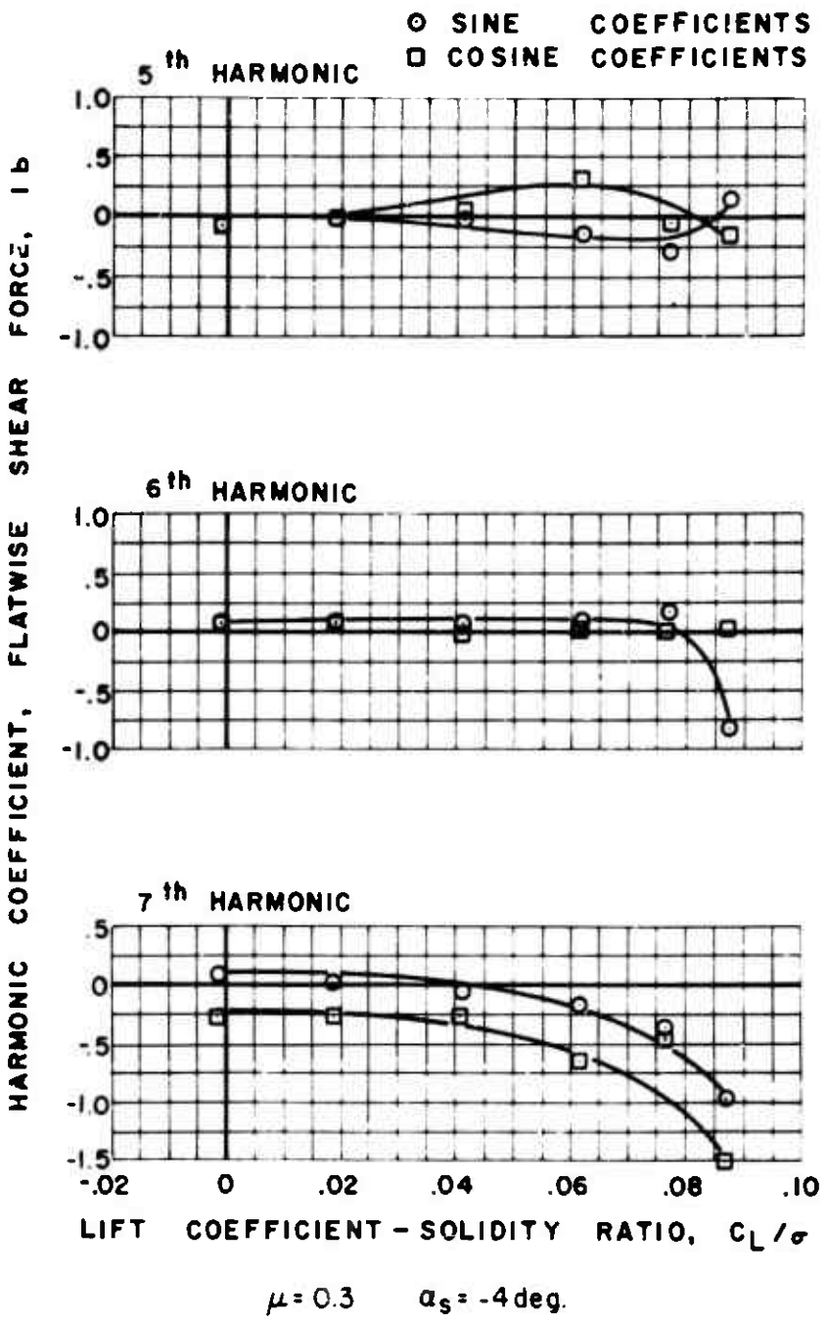

Figure 46(a). Continued.

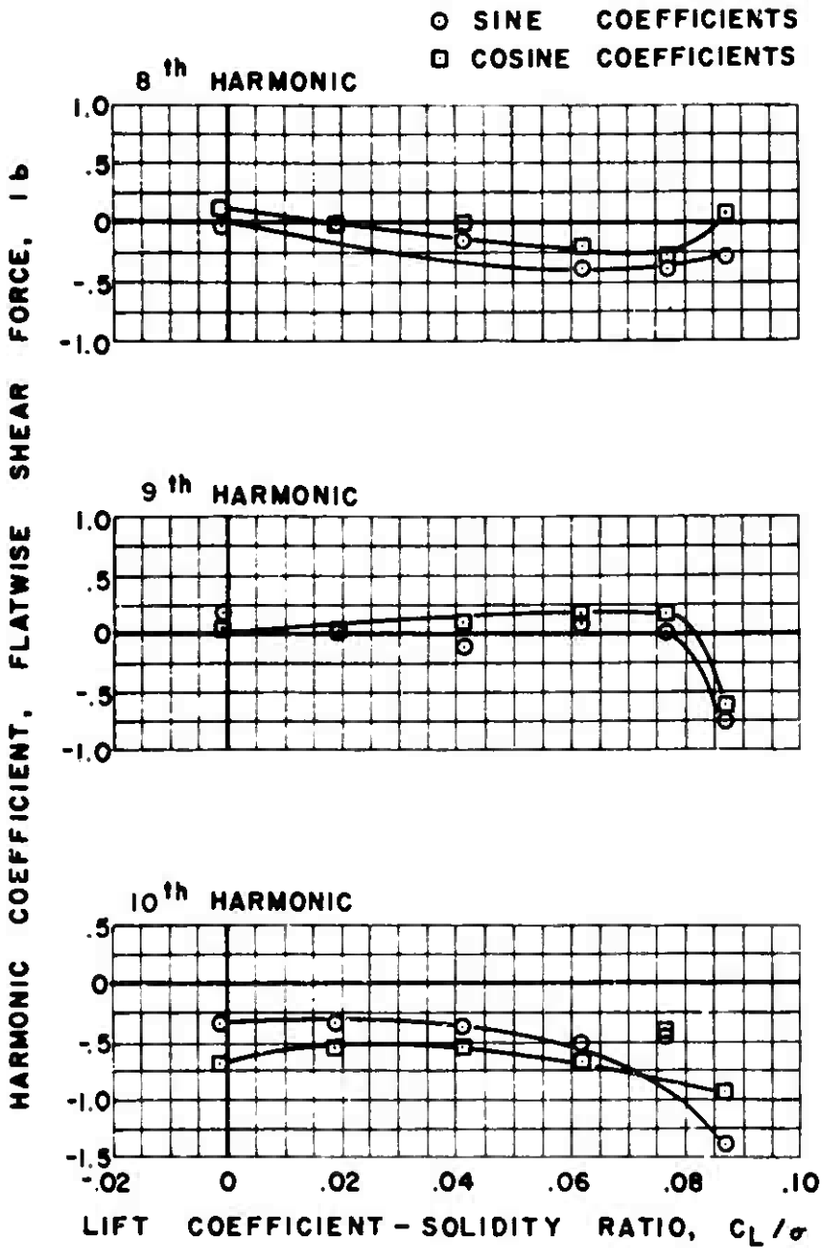

Figure 46(a). Continued.

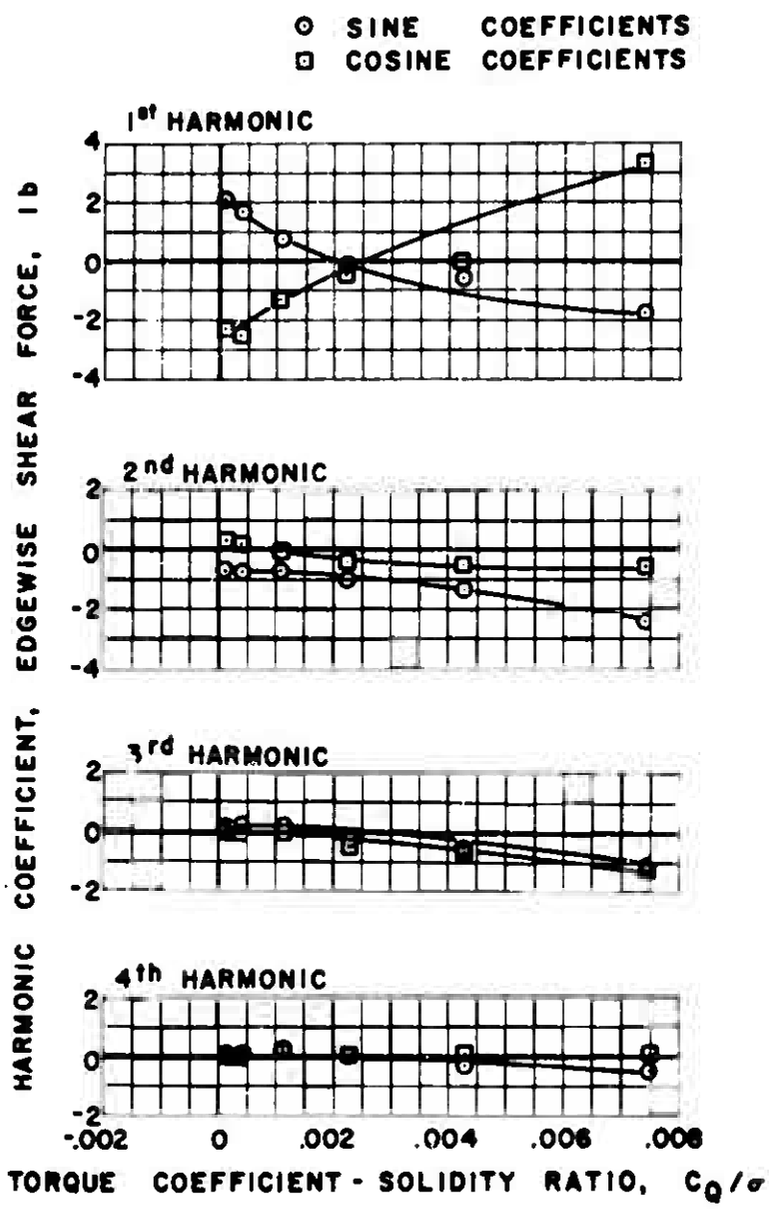

$\mu = 0.3$ $\alpha_s = -4$deg.

(b) EDGEWISE

Figure 46. Continued.

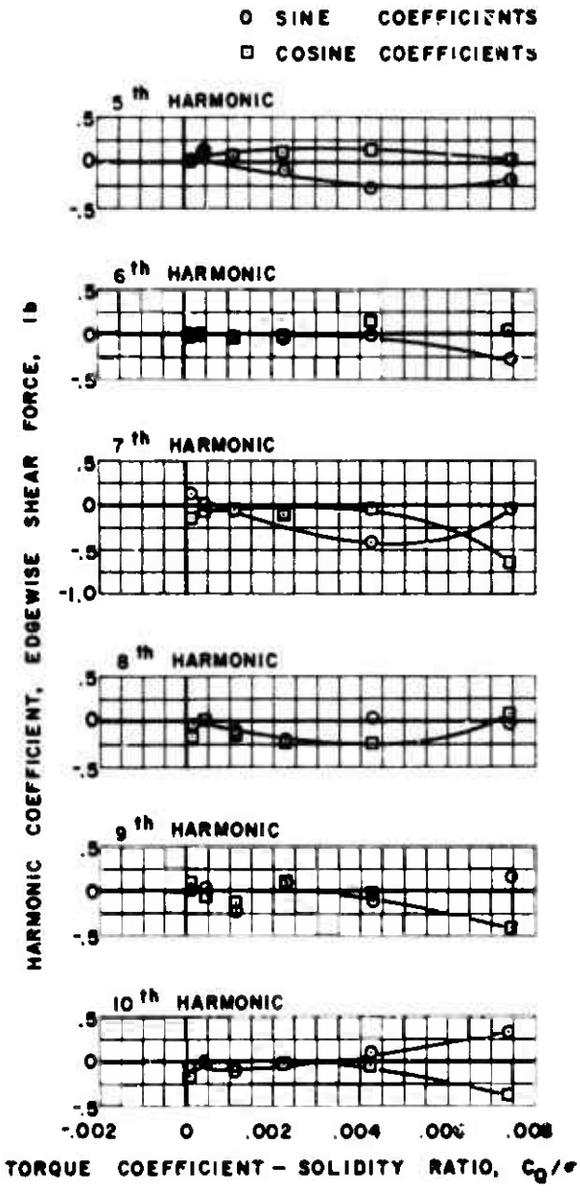

Figure 46(b). Concluded.

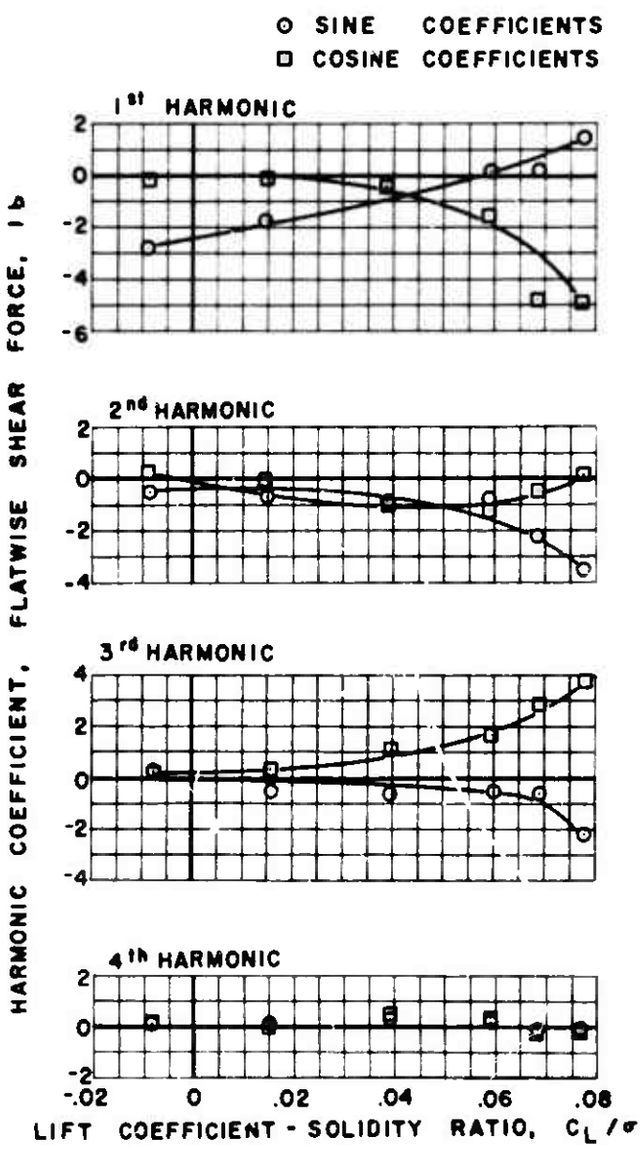

$\mu = 0.3$ $\alpha_s = -8$ deg.

(a) FLATWISE

Figure 47. Experimental Shear Force.

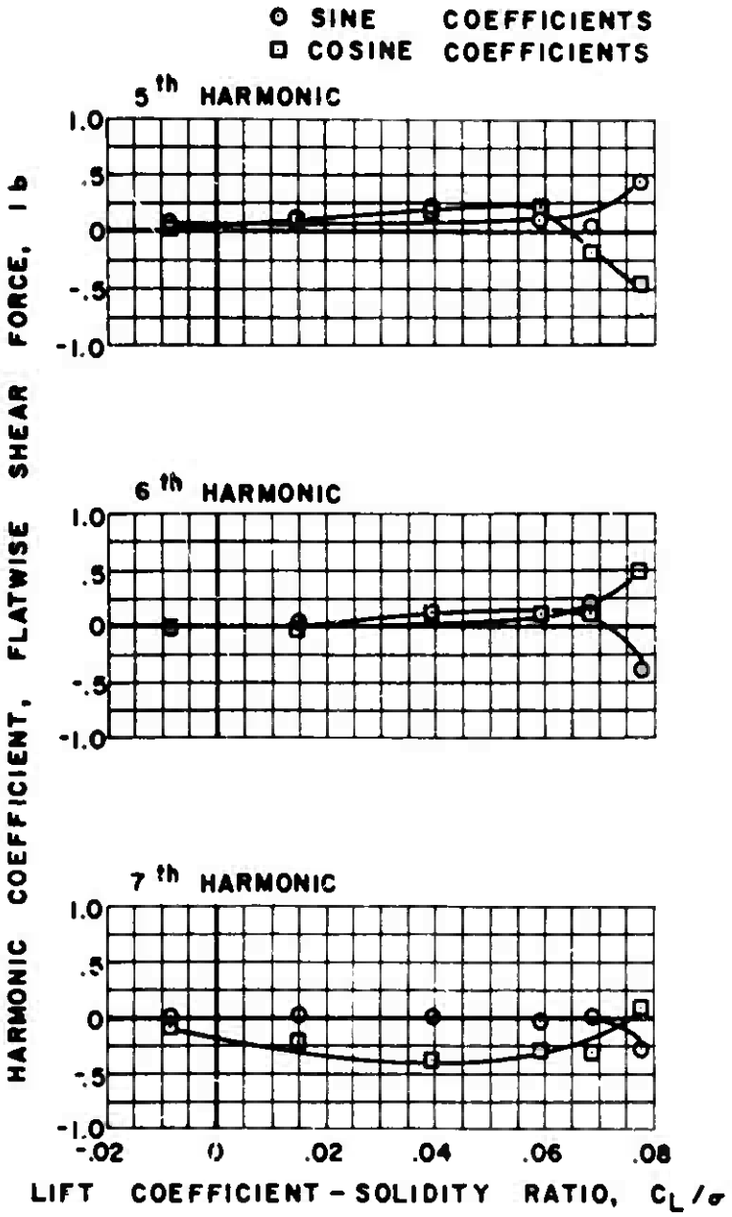

Figure 47(a). Continued.

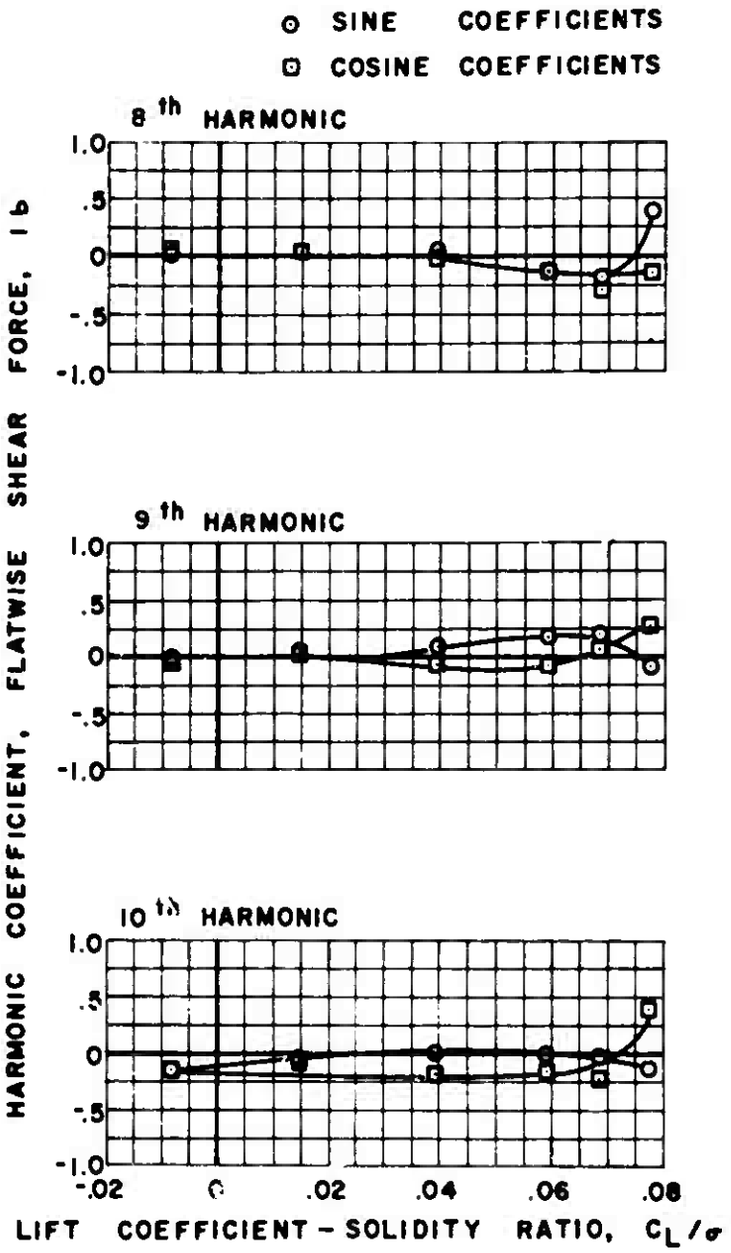

$\mu = 0.3$ $\alpha_s = -8$ deg.

Figure 47(a). Continued.

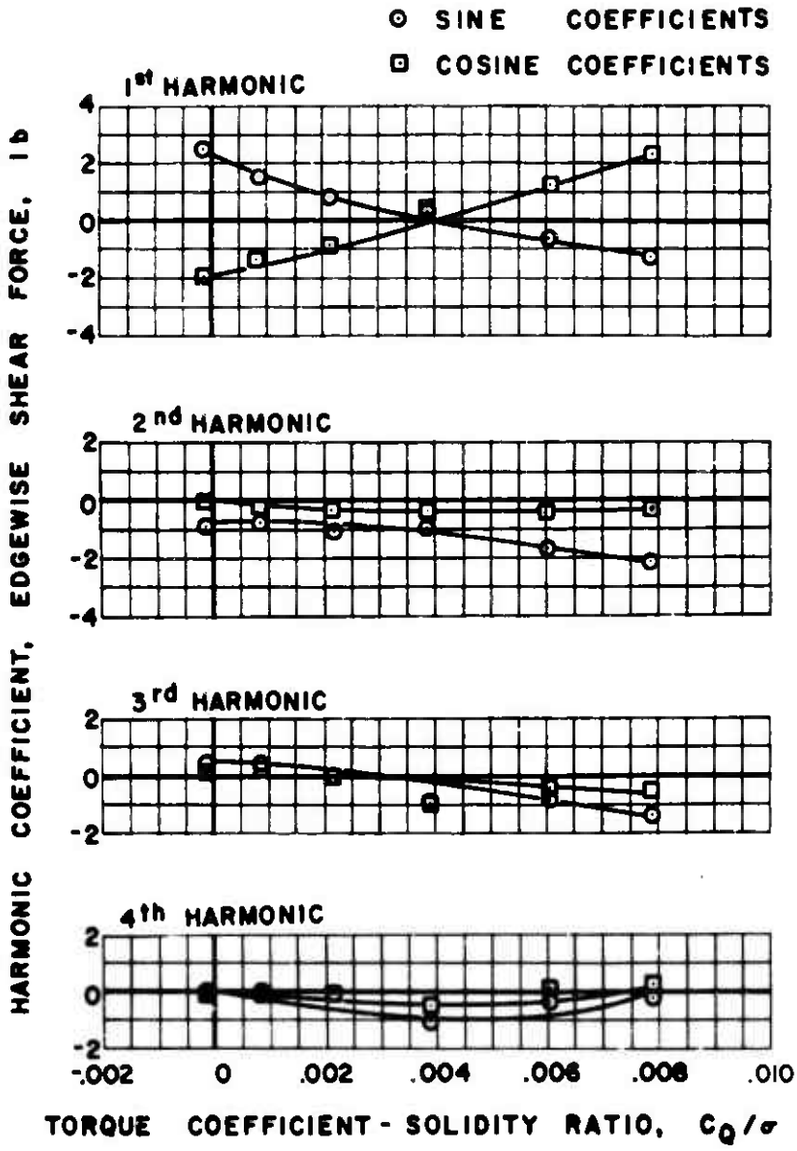

$\mu = 0.3$ $\alpha_s = -8$ deg.

(b) EDGEWISE

Figure 47. Continued.

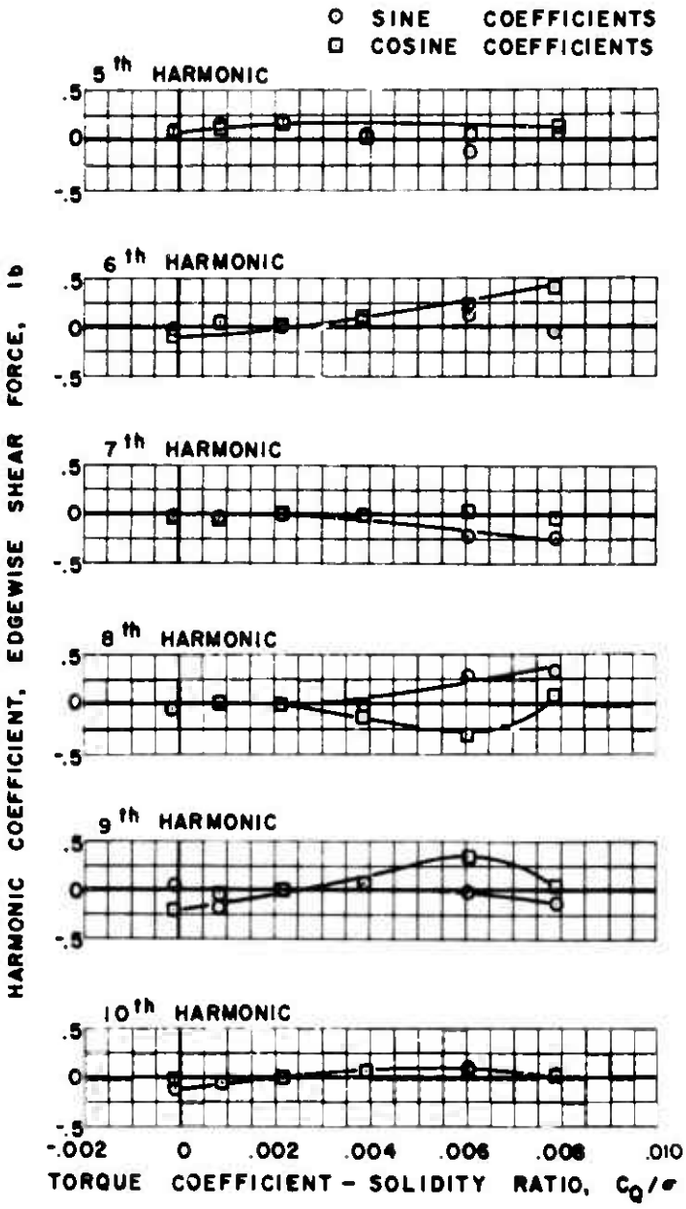

Figure 47(b). Concluded.

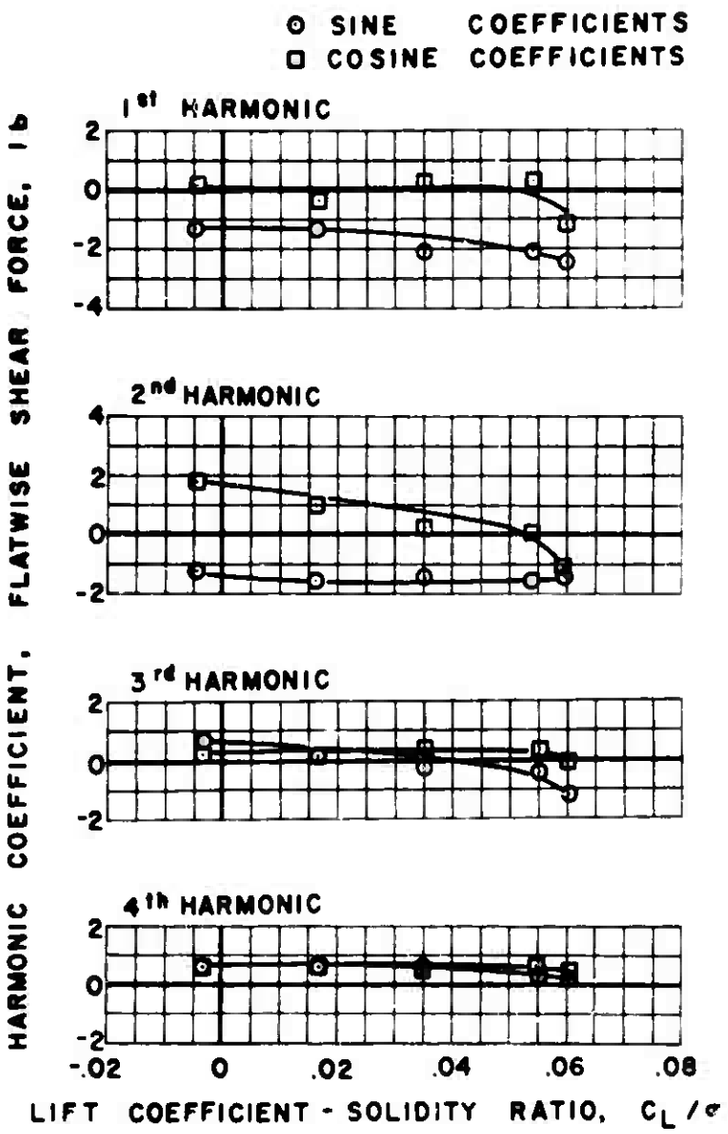

$\mu = 0.4$ $\alpha_s = 4$ deg.

(a) FLATWISE

Figure 48. Experimental Shear Force.

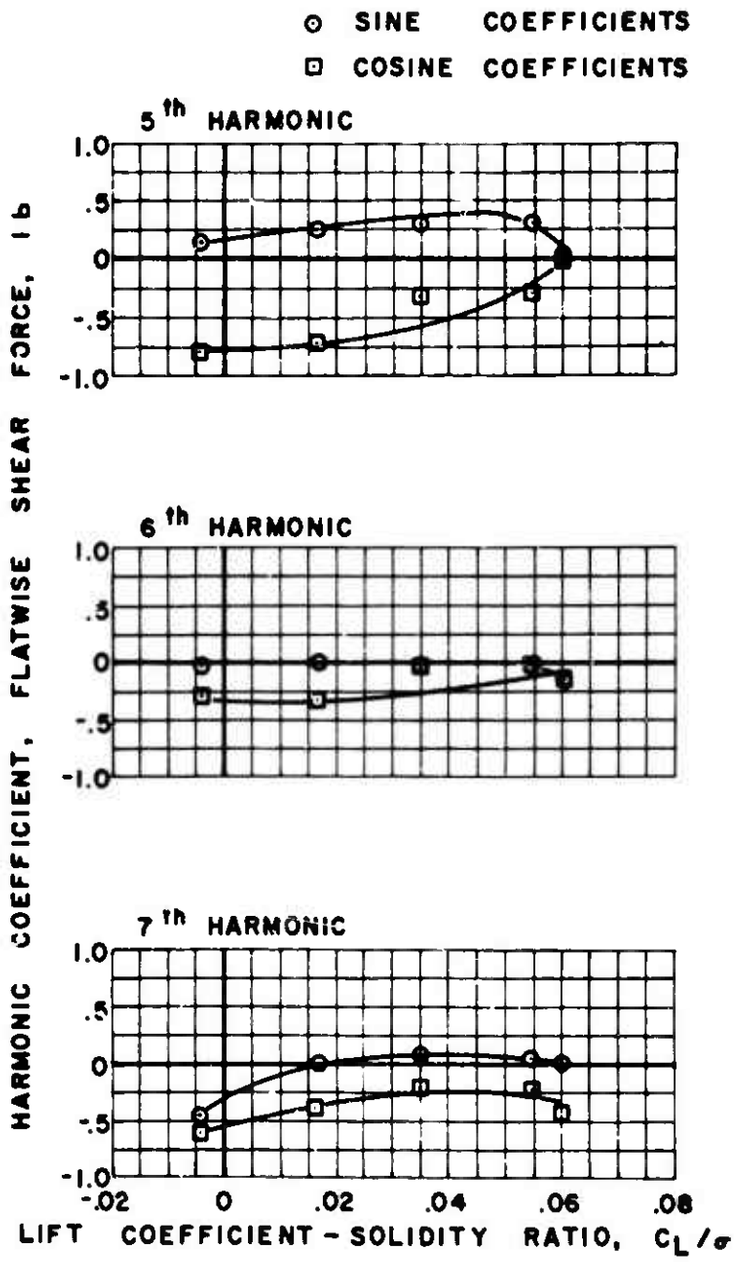

Figure 48(a). Continued.

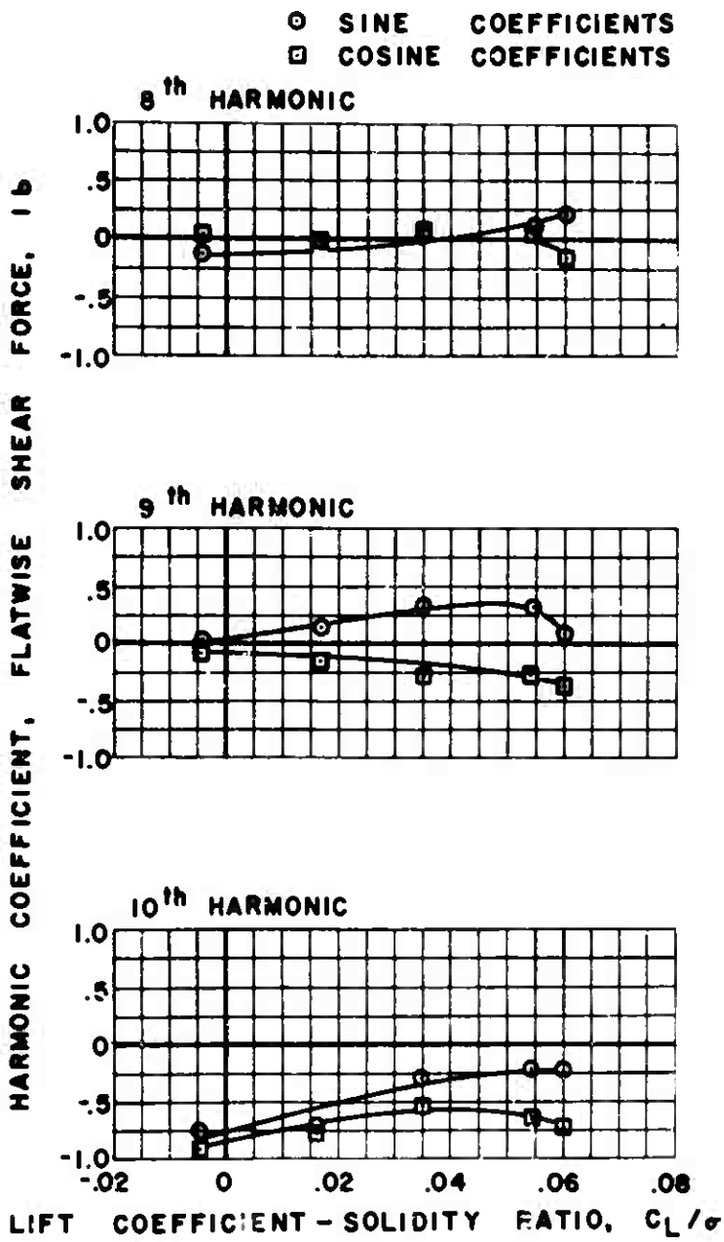

Figure 48(a). Continued.

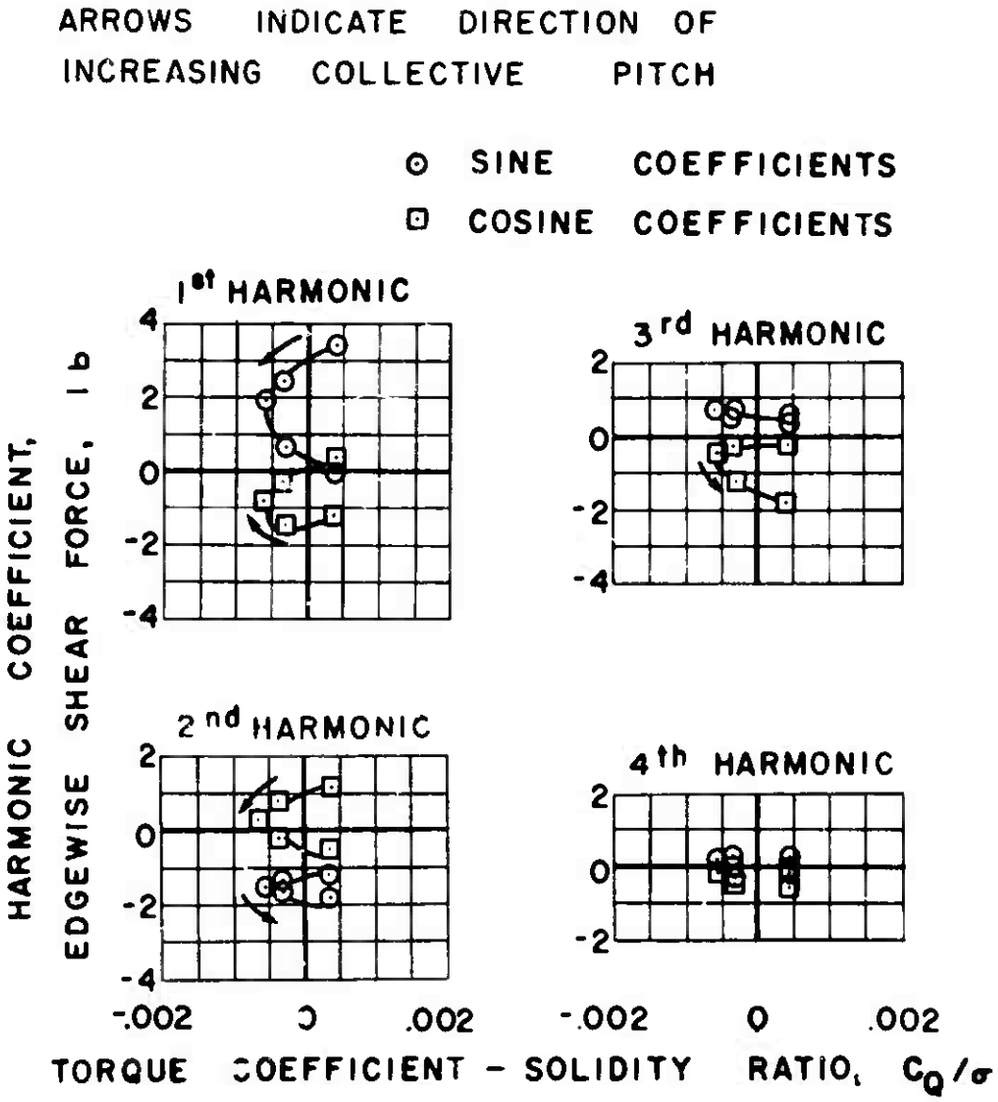

$\mu = 0.4$ $\alpha_s = 4$ deg.

(b) EDGEWISE

Figure 48. Continued.

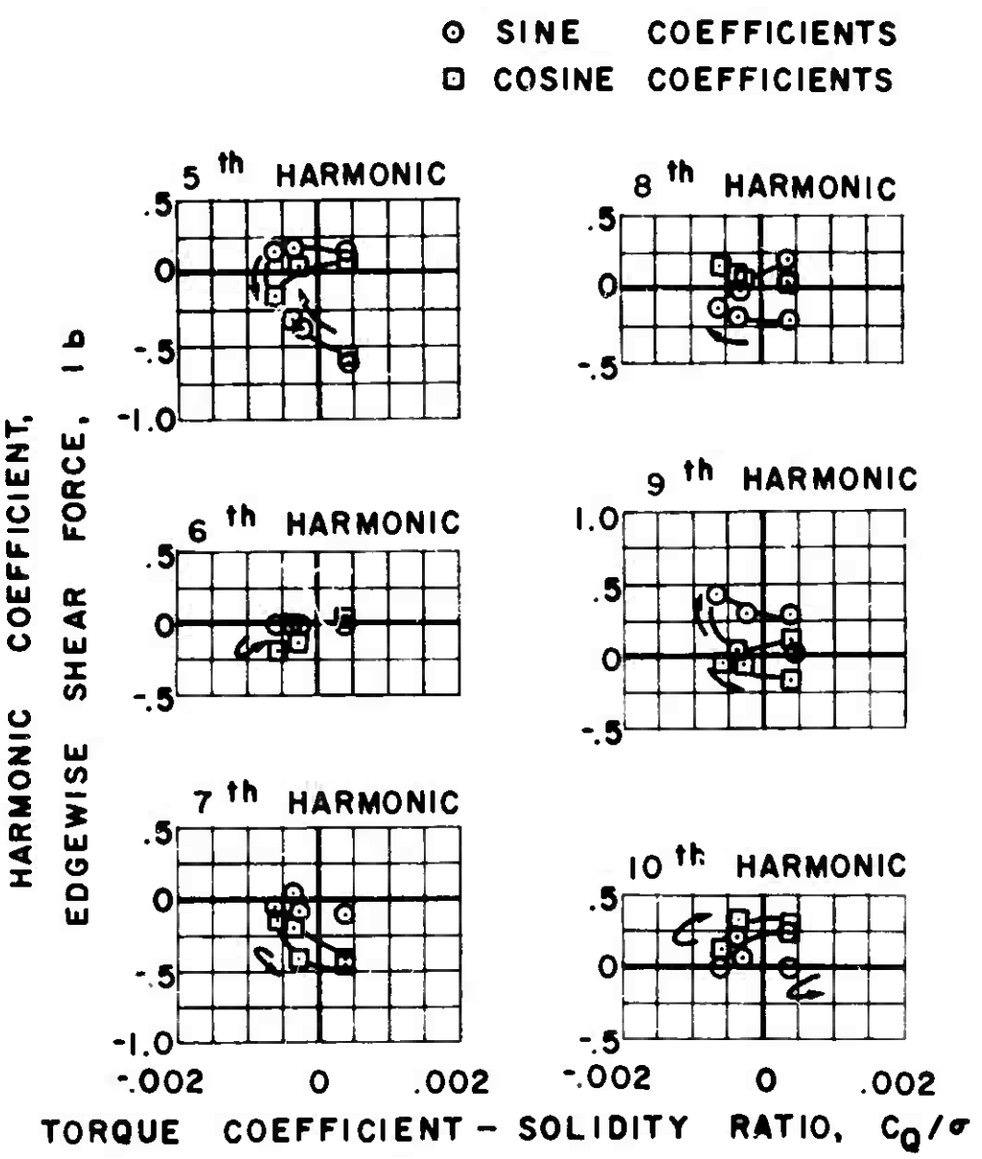

$\mu = 0.4$ $\alpha_s = 4$ deg.

Figure 48(b). Concluded.

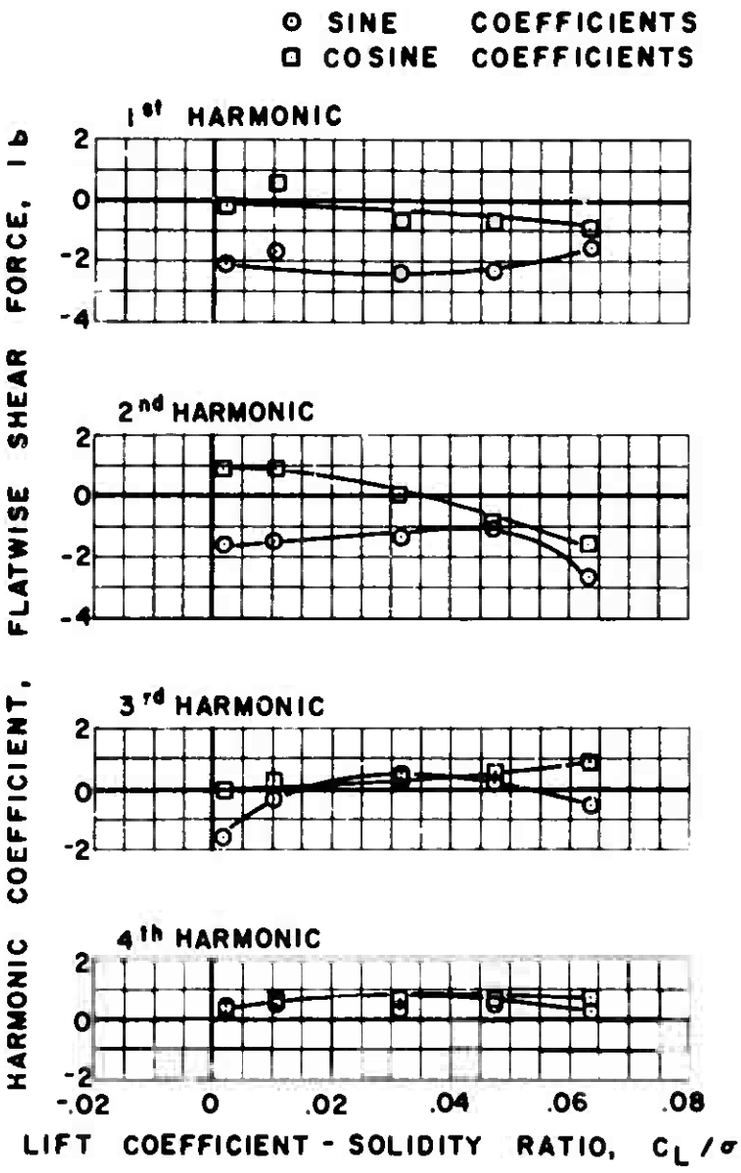

$\mu = 0.4$ $\alpha_s = 0$ deg.

(a) FLATWISE

Figure 49. Experimental Shear Force.

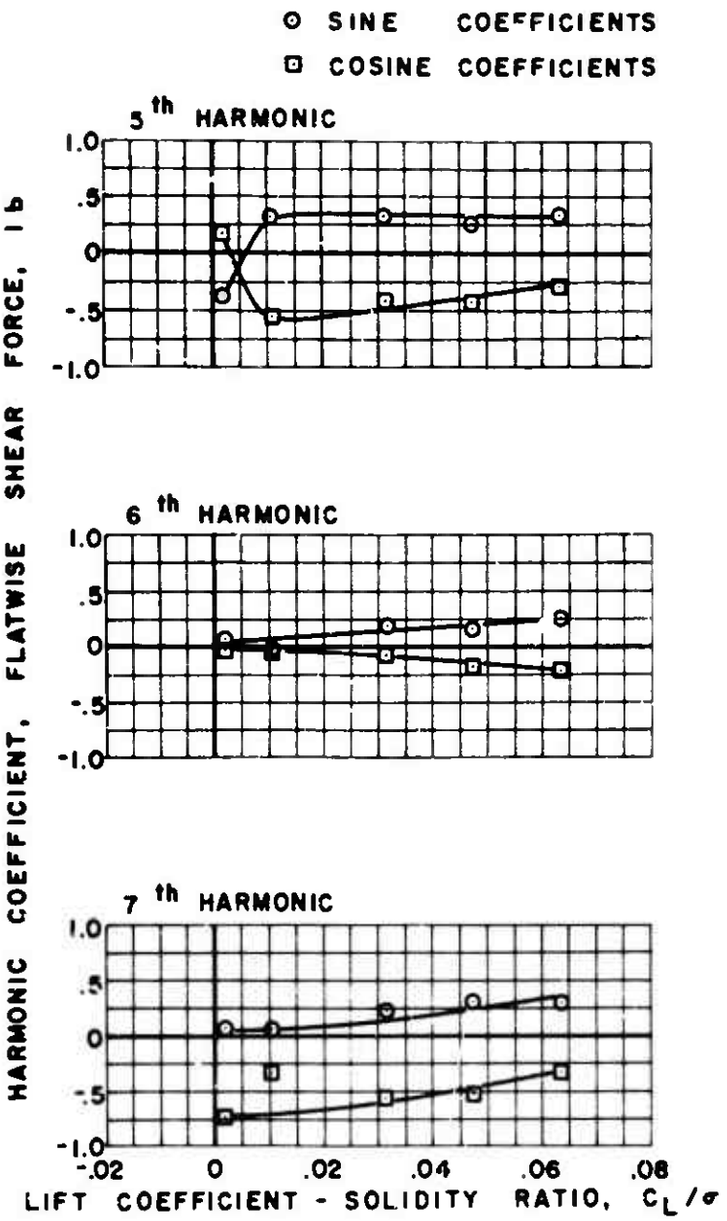

Figure 49(a). Continued.

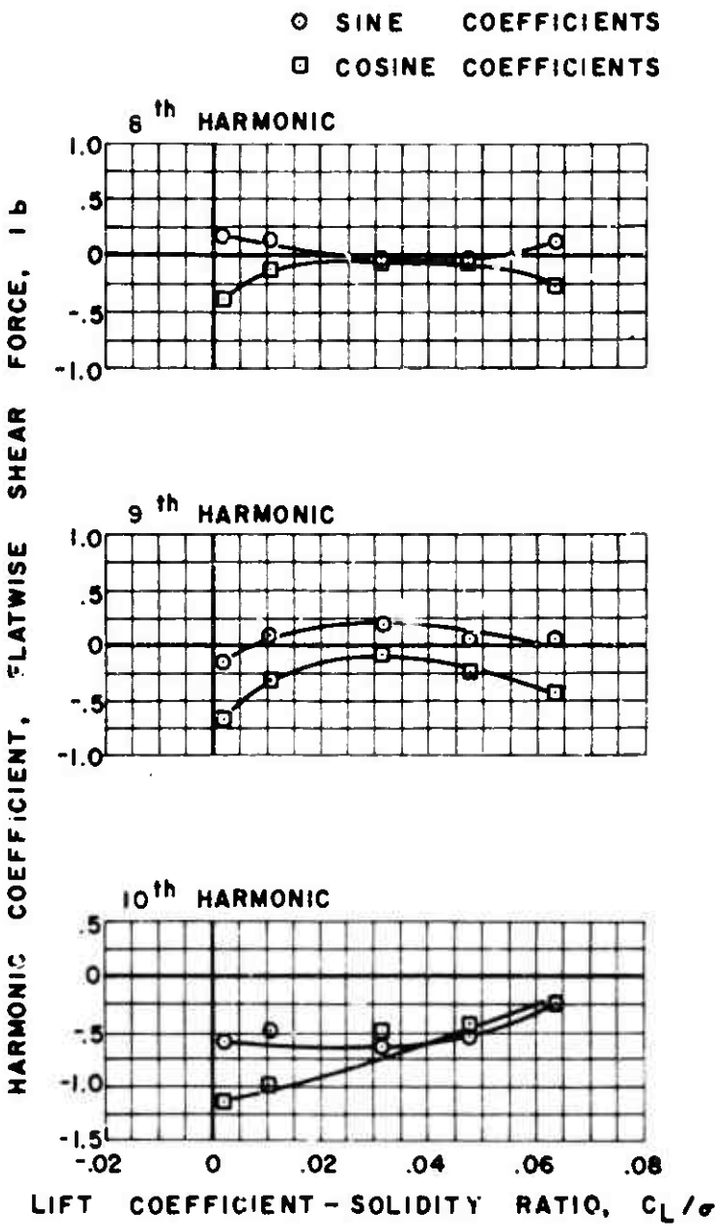

Figure 49(a). Continued.

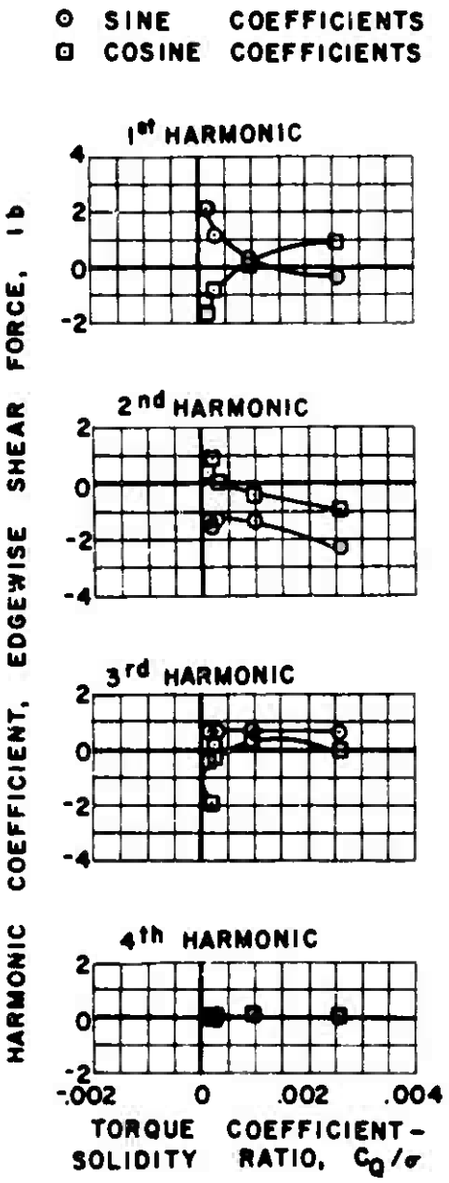

(b) EDGEWISE

Figure 49. Continued.

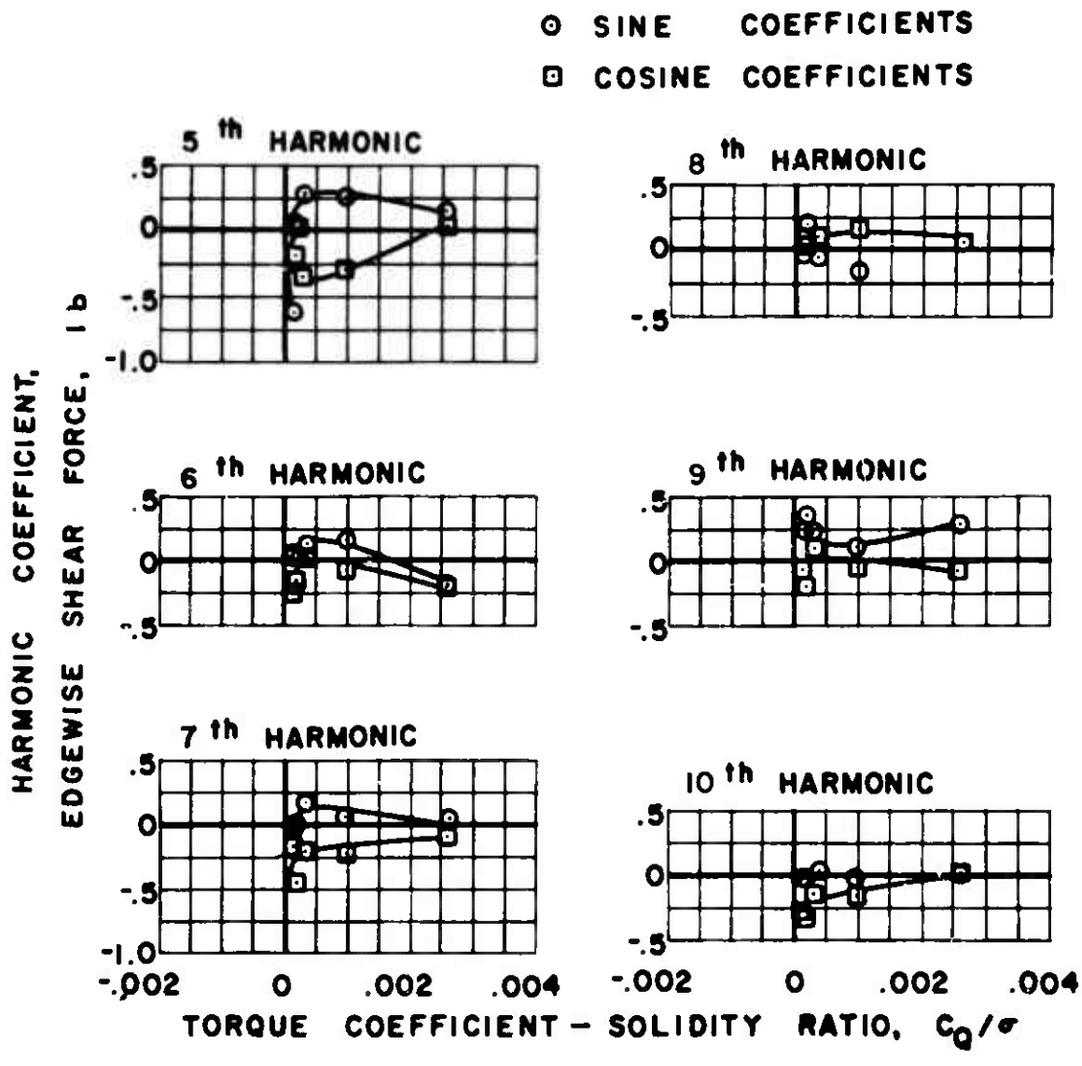

Figure 49(b). Concluded.

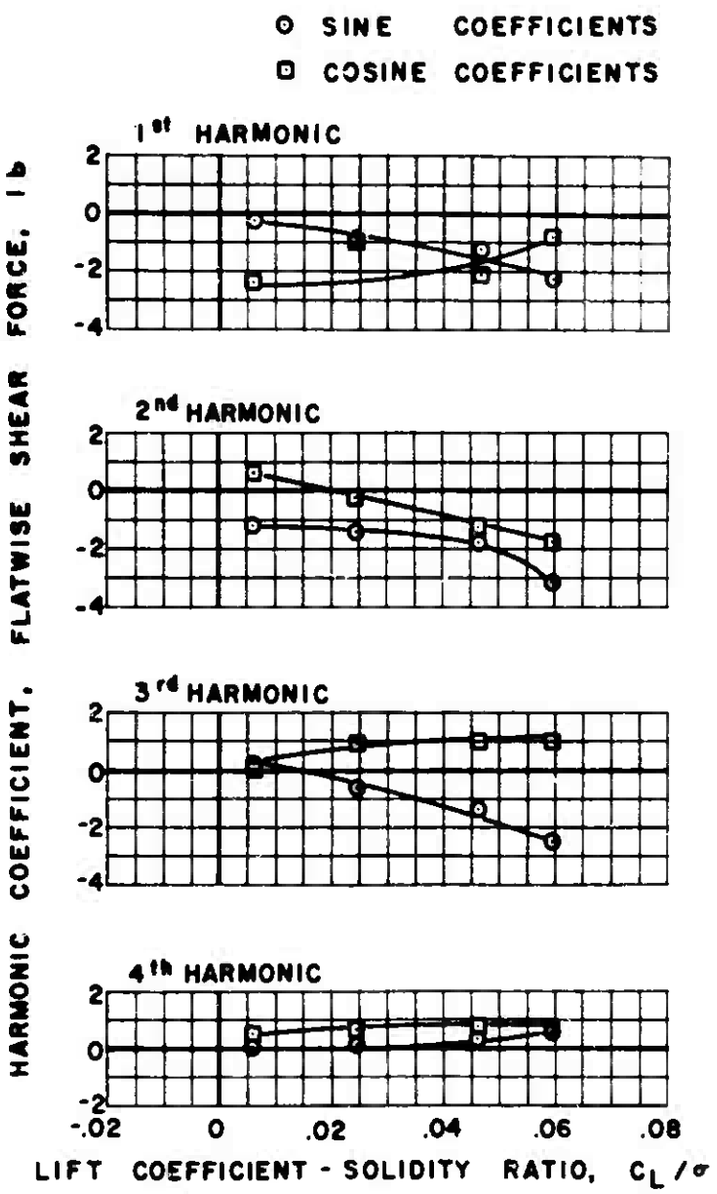

Figure 50. Experimental Shear Force.

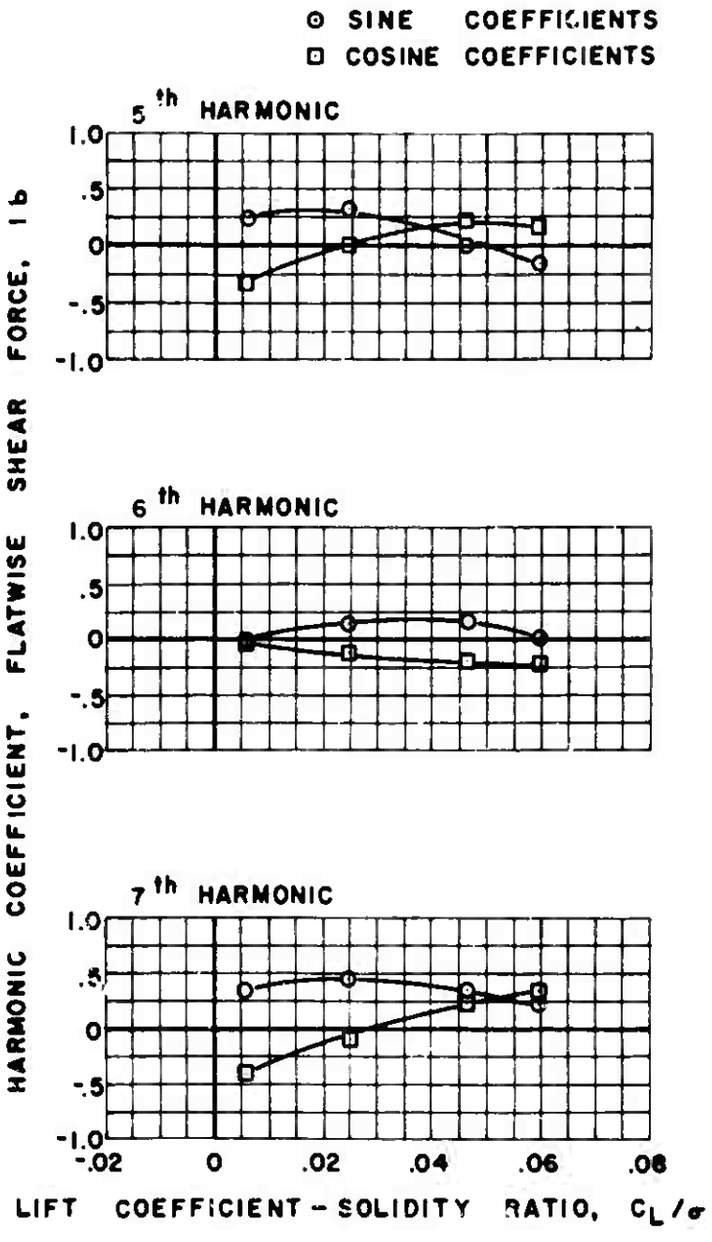

Figure 50(a). Continued.

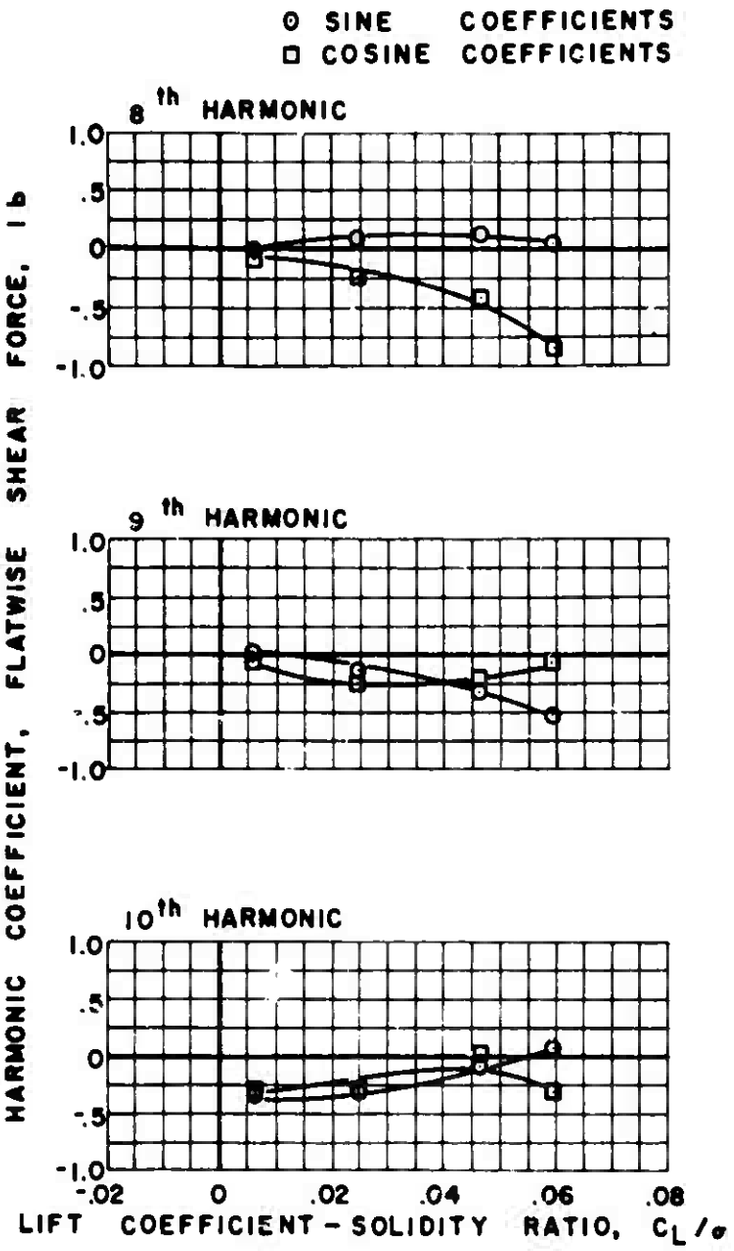

Figure 50(a). Continued.

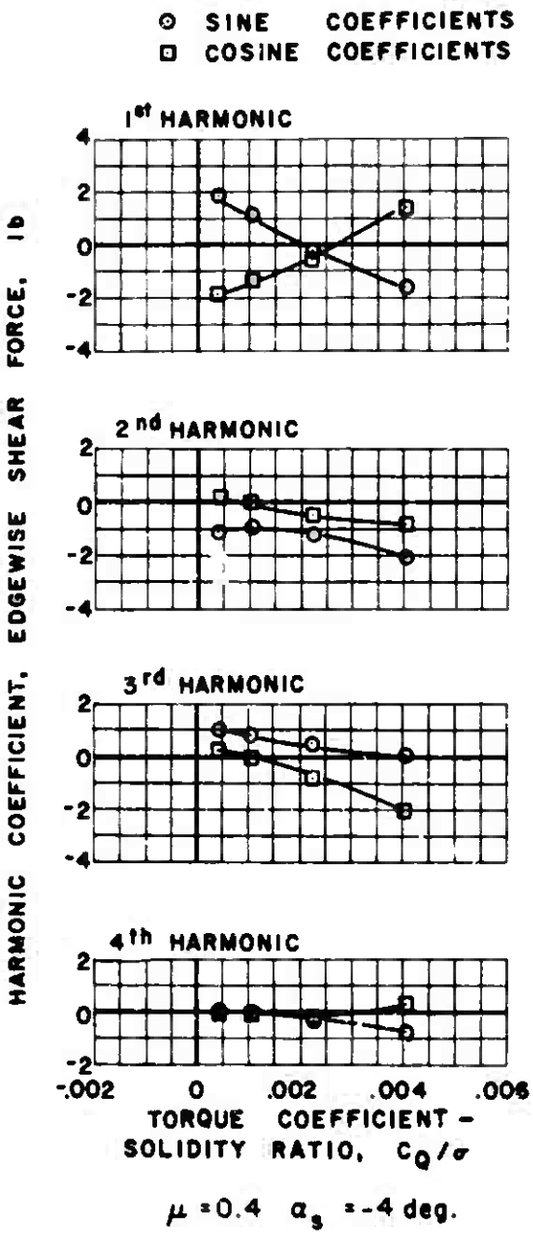

(b) EDGEWISE

Figure 50. Continued.

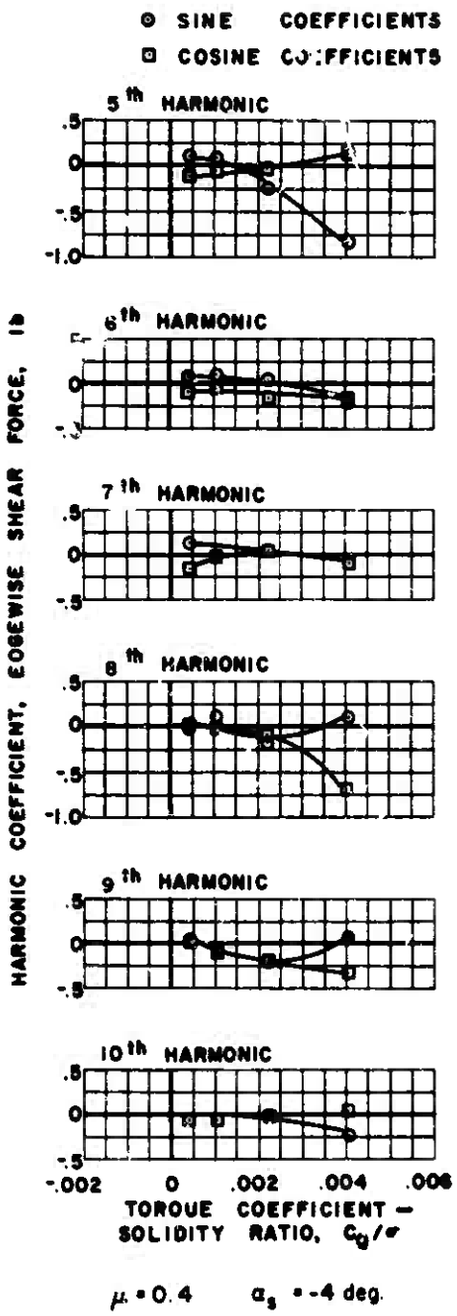

Figure 50(b). Concluded.

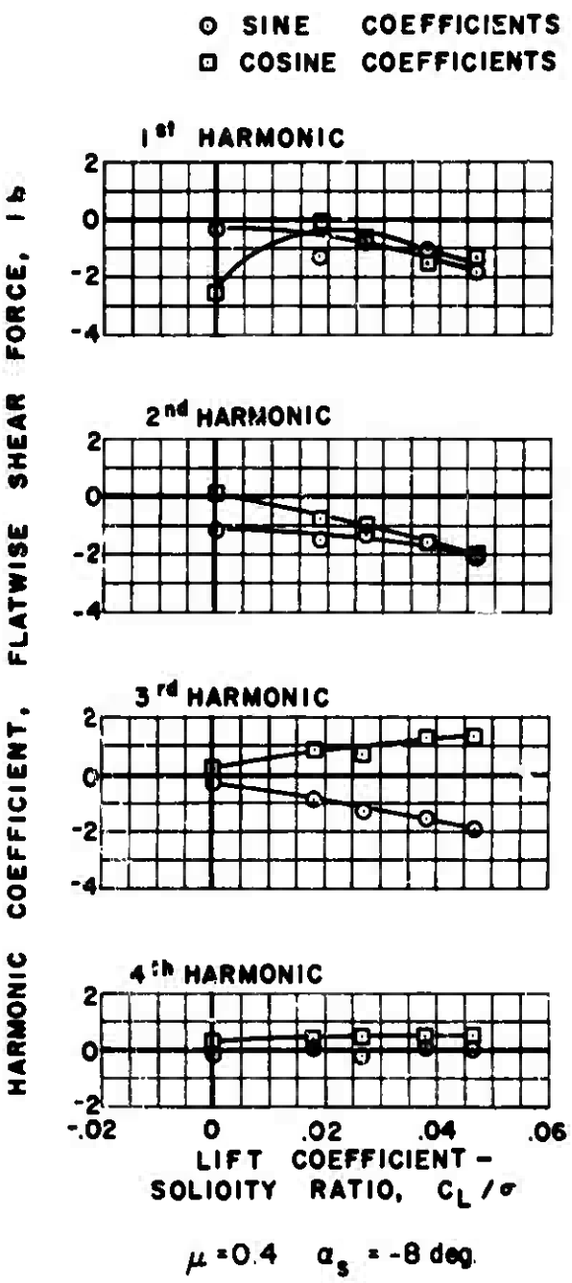

Figure 51. Experimental Shear Force.

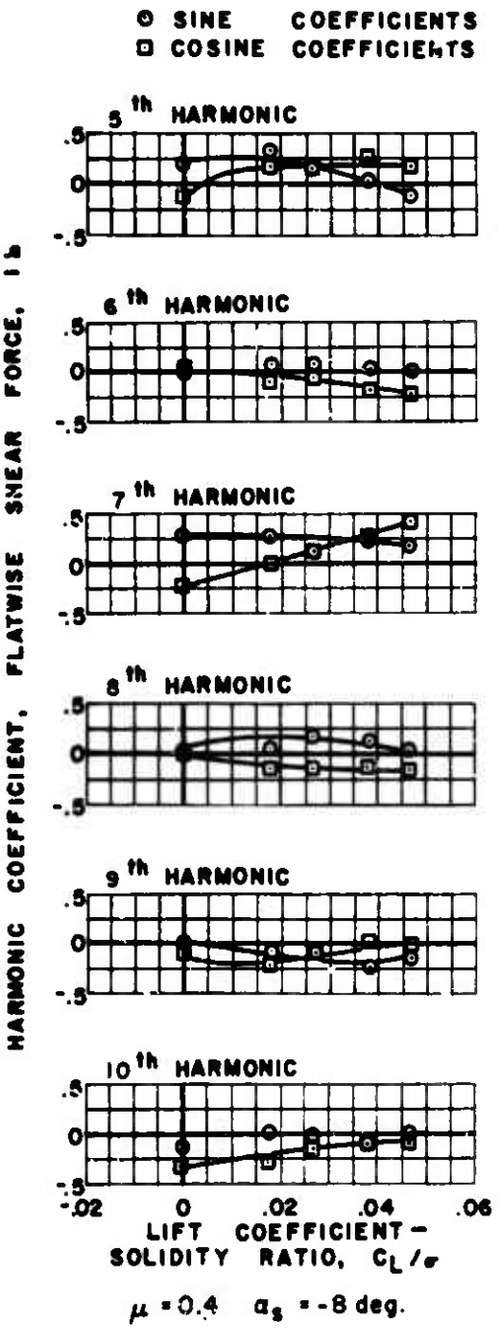

Figure 51(a). Continued.

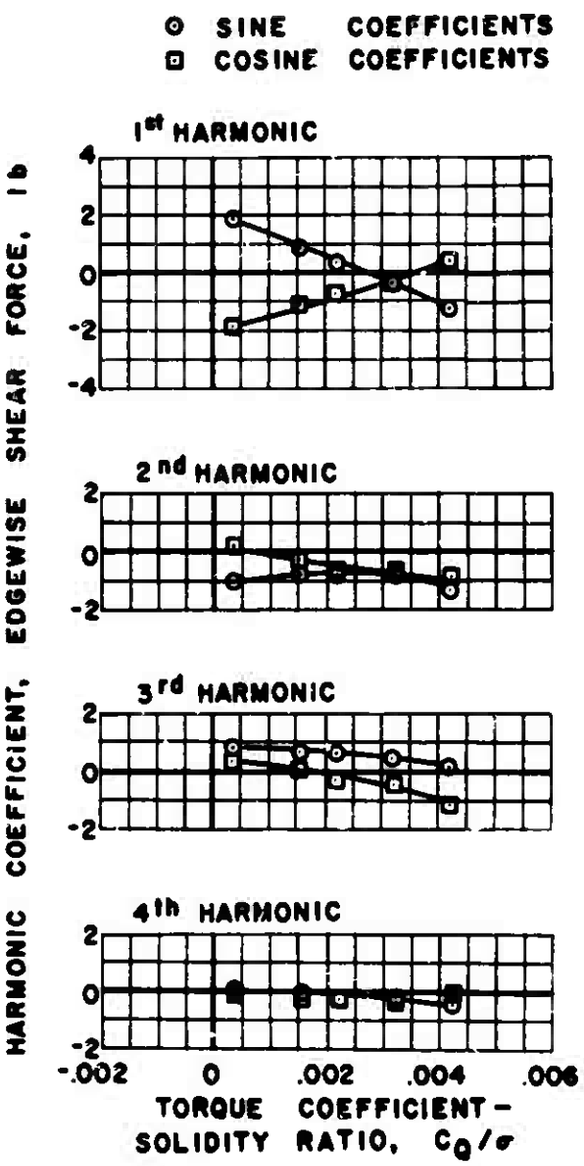

(b) EDGEWISE

Figure 51. Continued.

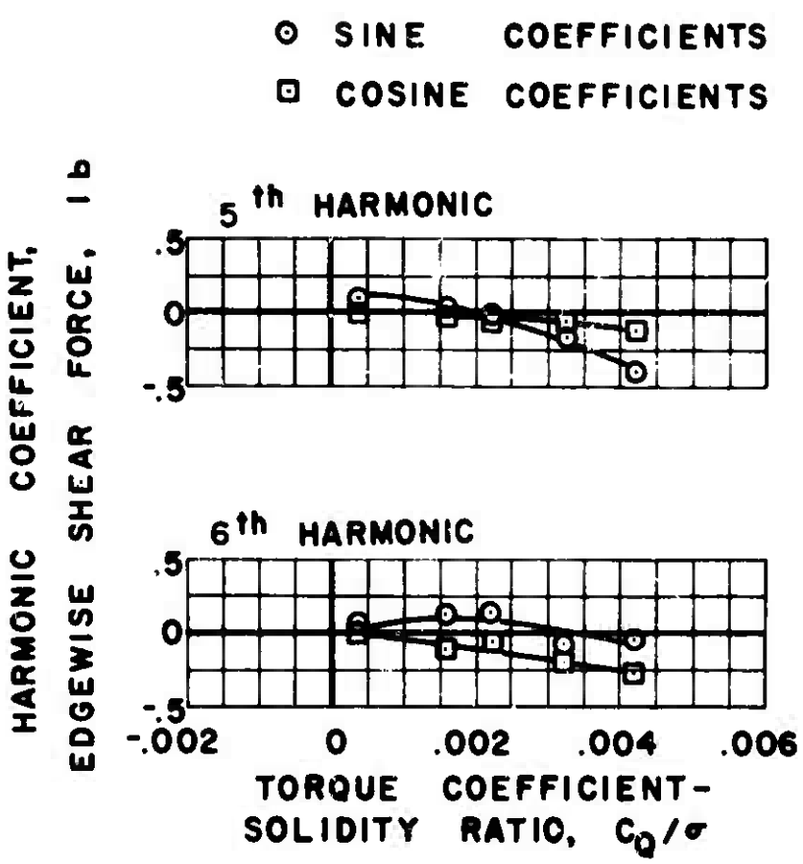

IN THIS TEST CONDITION THE MAGNITUDE OF THE EDGEWISE HARMONICS ABOVE THE SIXTH DID NOT EXCEED THE REPEATABILITY OF THE SYSTEM AND ARE NOT PRESENTED.

$\mu = 0.4$ $\alpha_s = -8$ deg.

Figure 51(b). Concluded.

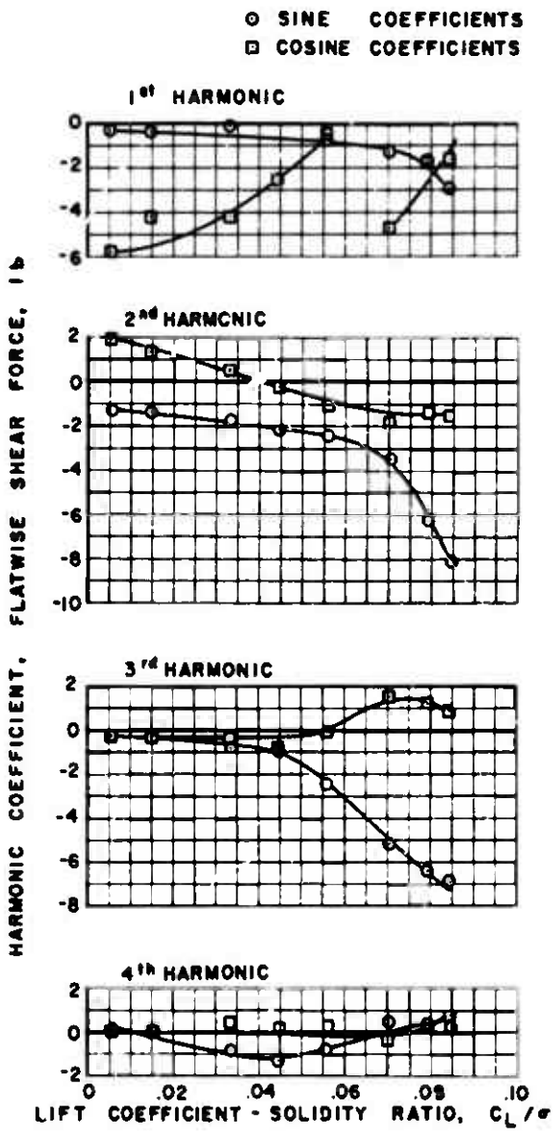

$\mu = 0.5$ $\alpha_s = 0$ deg.

(a) FLATWISE

Figure 52. Experimental Shear Force.

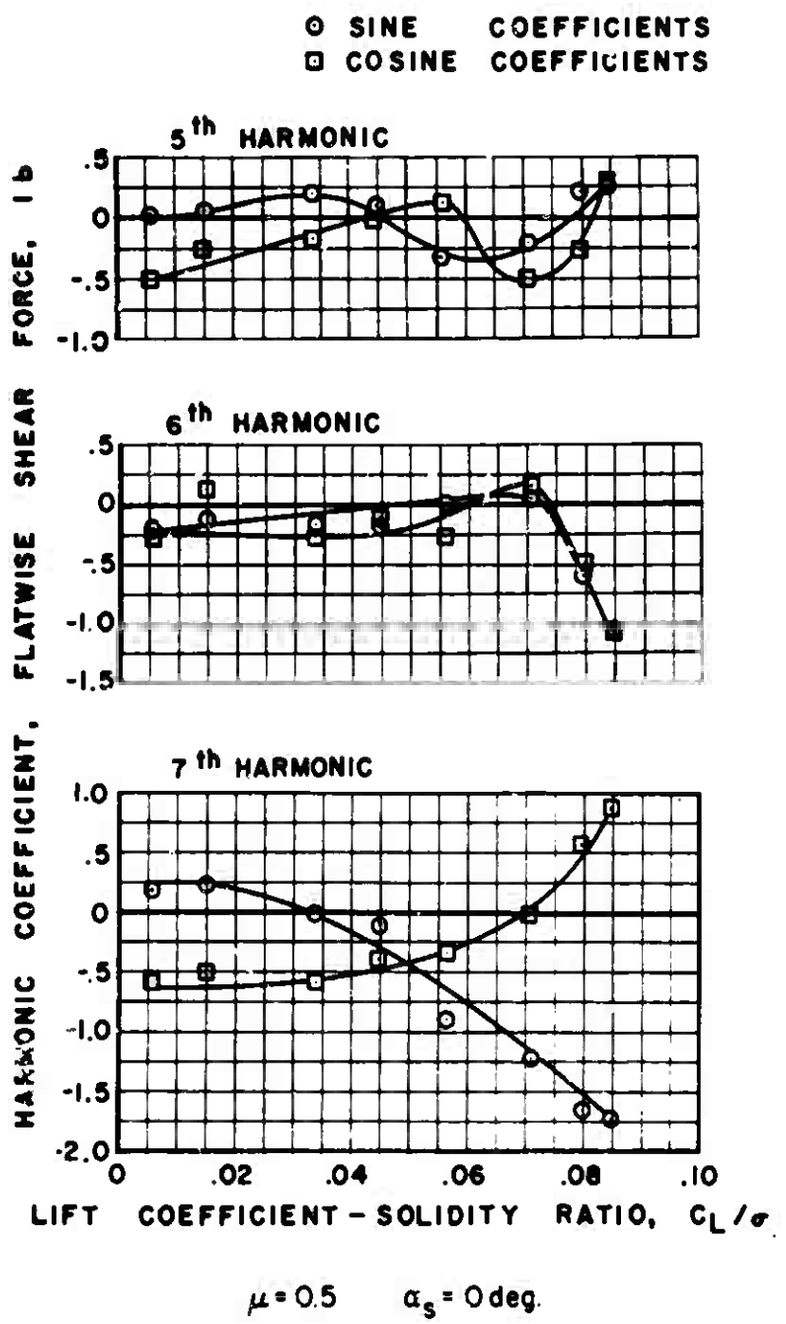

Figure 52(a). Continued.

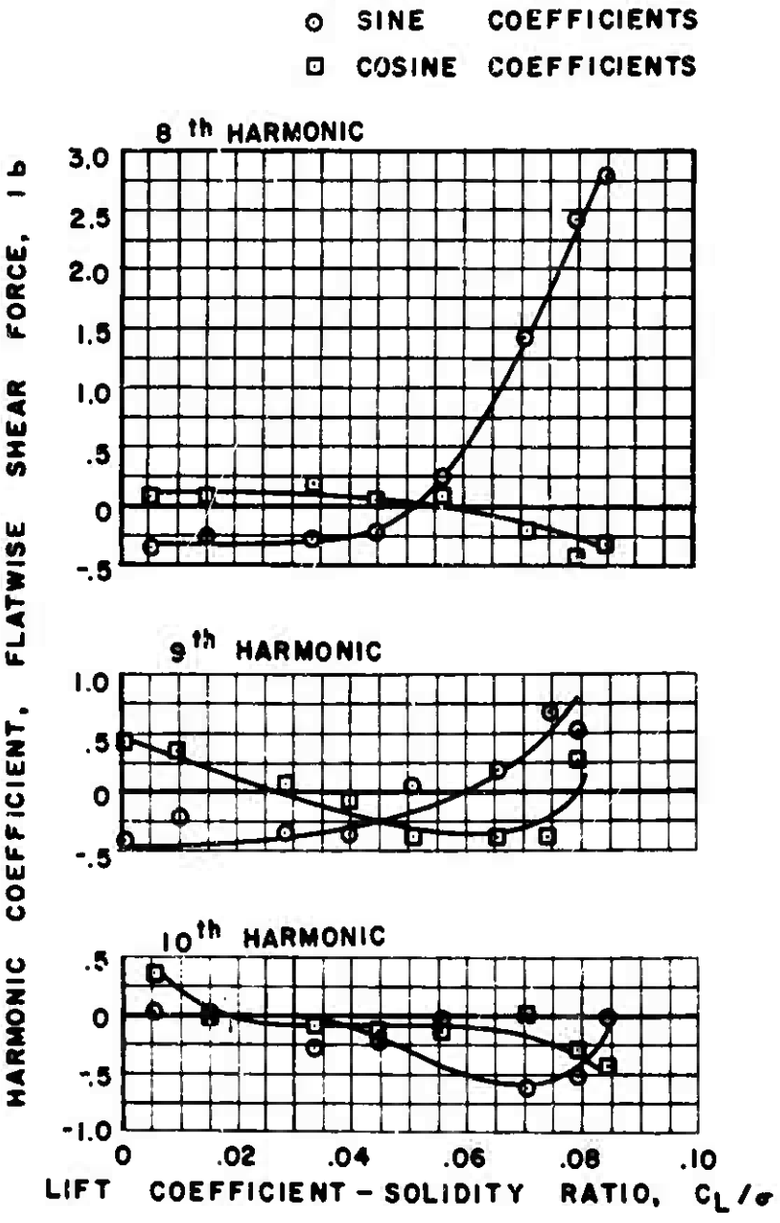

$\mu = 0.5$ $\alpha_s = 0$ deg.

Figure 52(a). Continued.

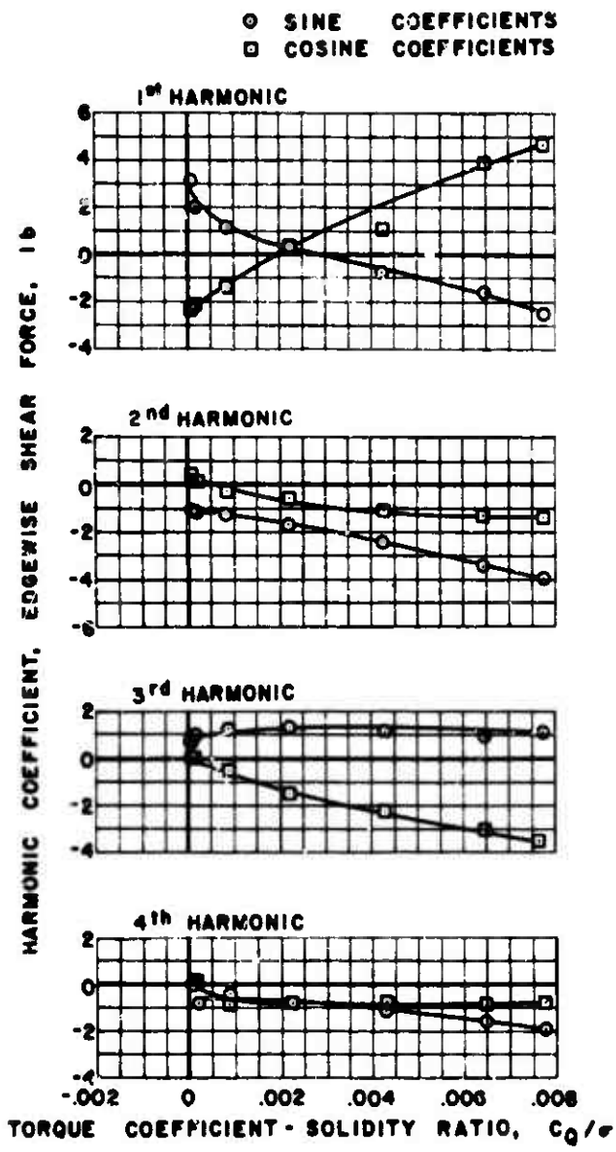

$\mu = 0.5$ $\alpha_s = 0$ deg.

(b) EDGEWISE

Figure 52. Continued.

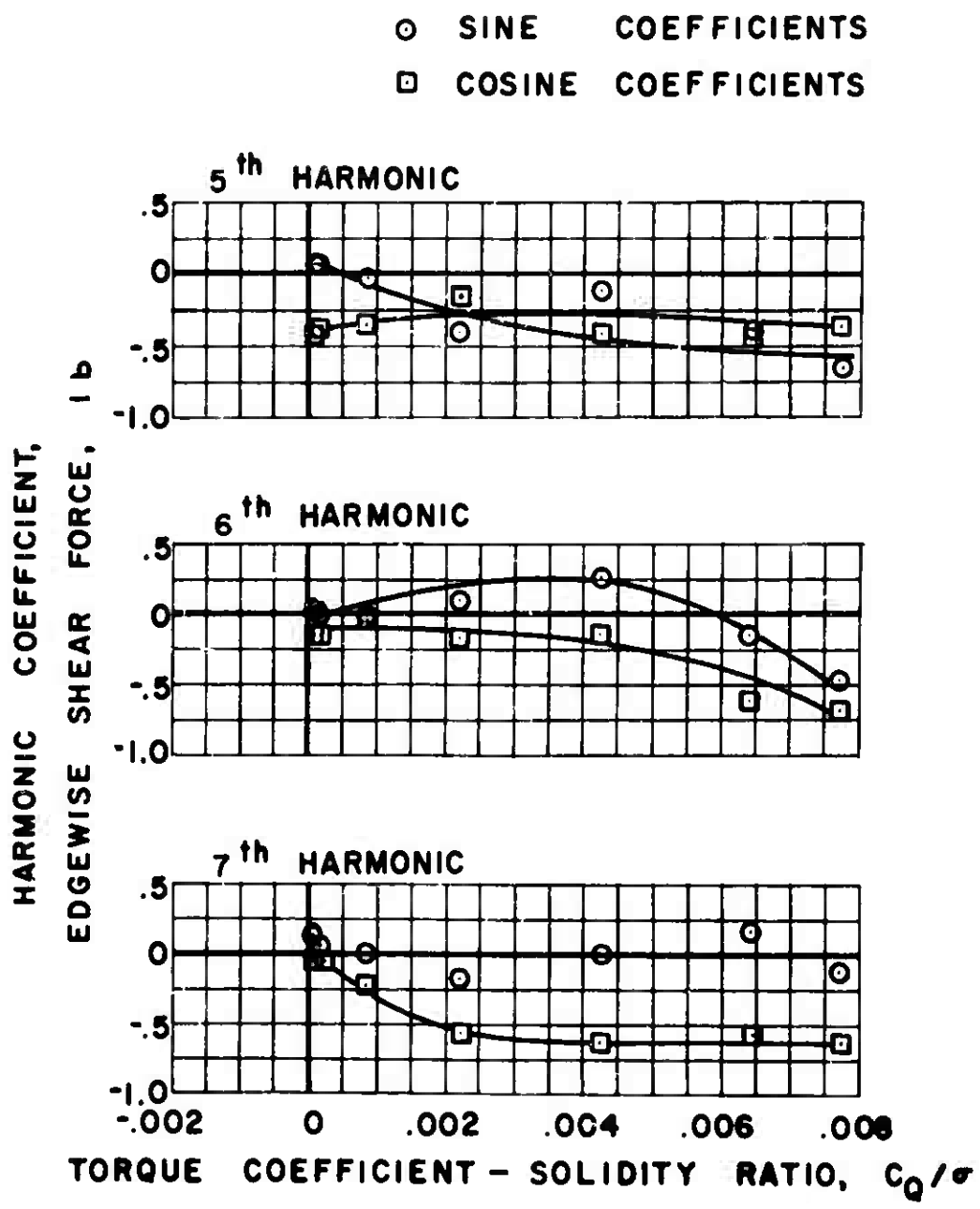

Figure 52(b). Continued.

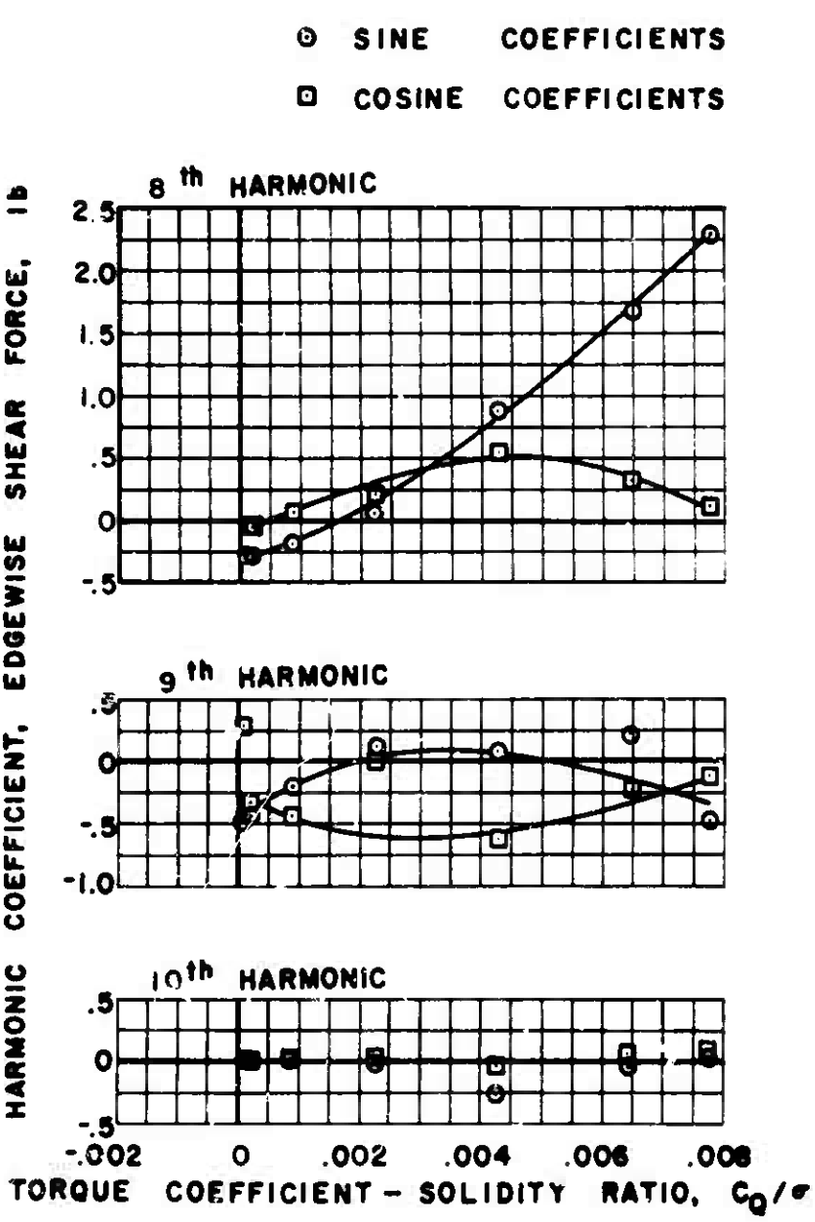

$\mu = 0.5$ $\alpha_s = 0$ deg.

Figure 52(b). Concluded.

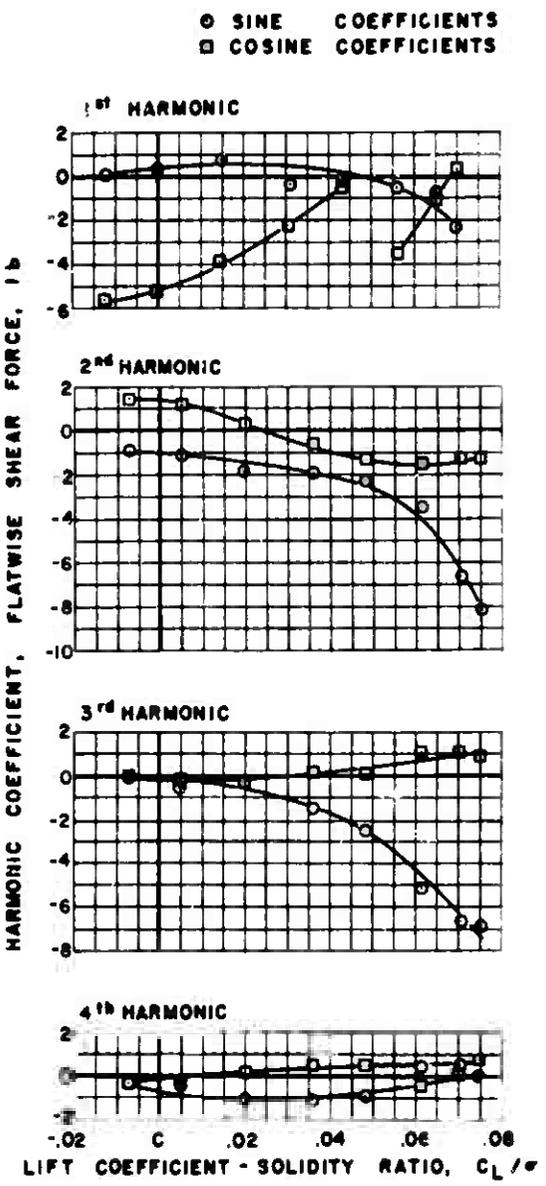

Figure 53. Experimental Shear Force.

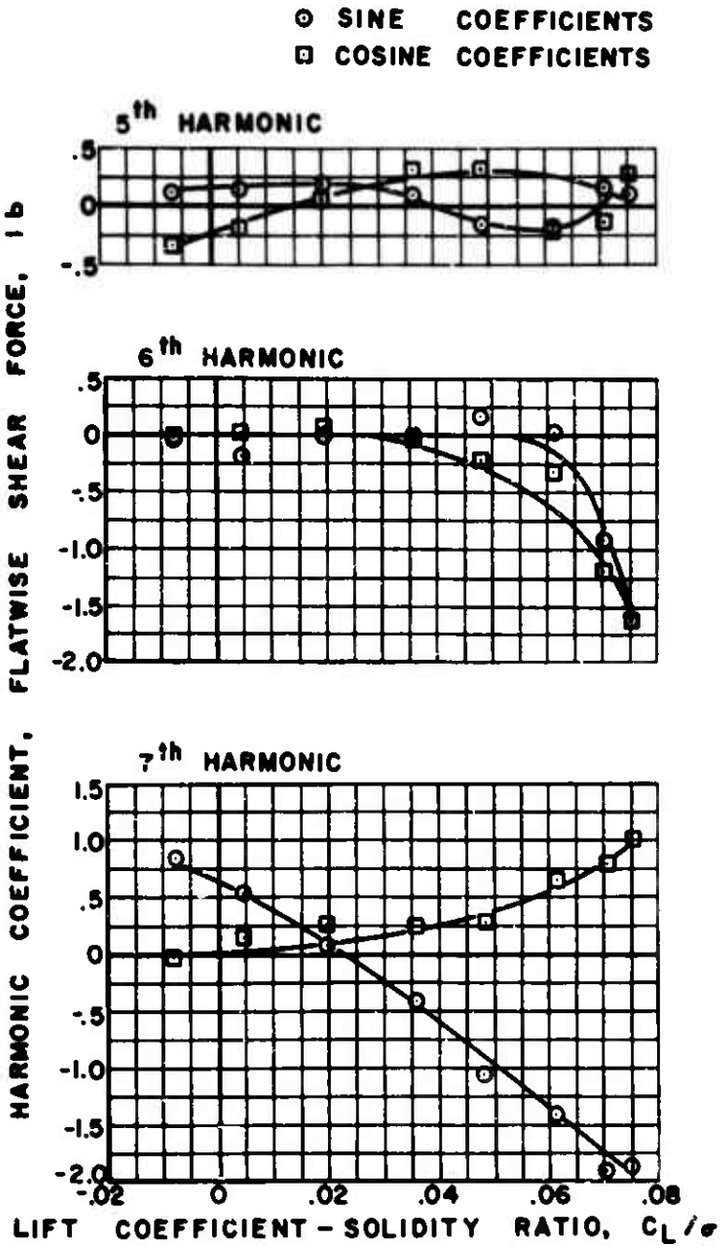

$\mu = 0.5$ $\alpha_s = -4$deg.

Figure 53(a). Continued.

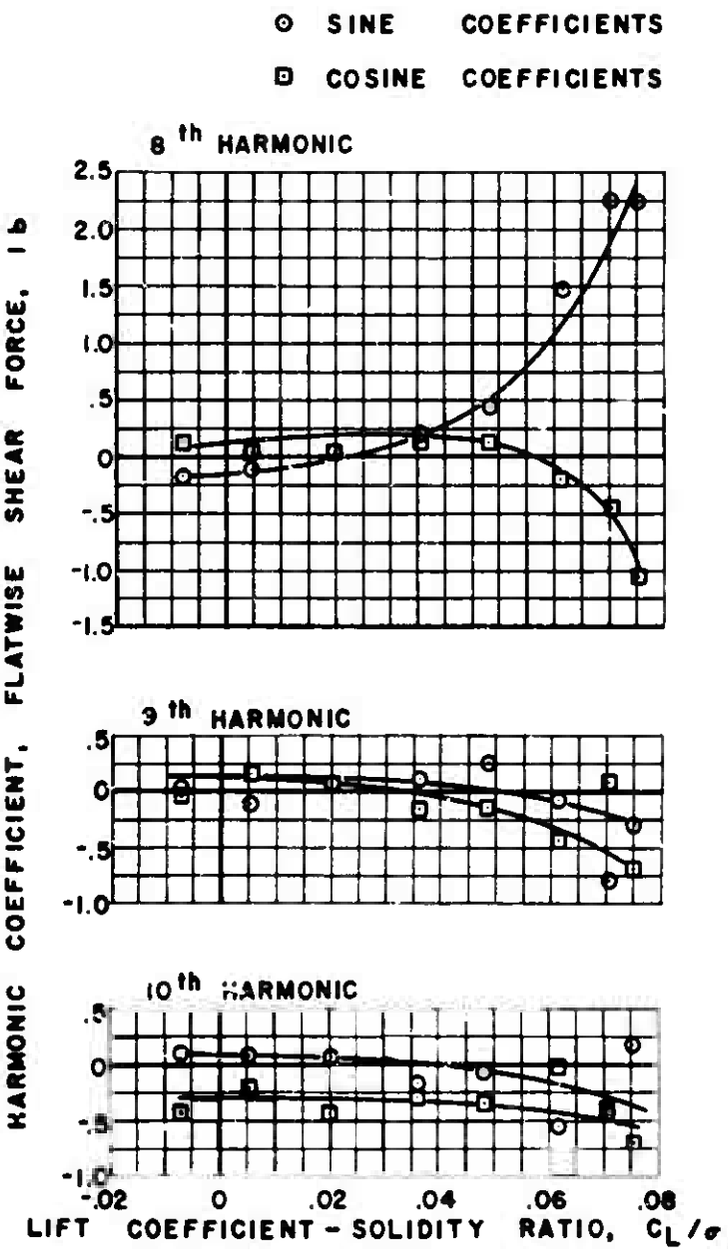

$\mu = 0.5$ $\alpha_s = -4$ deg.

Figure 53(a). Continued.

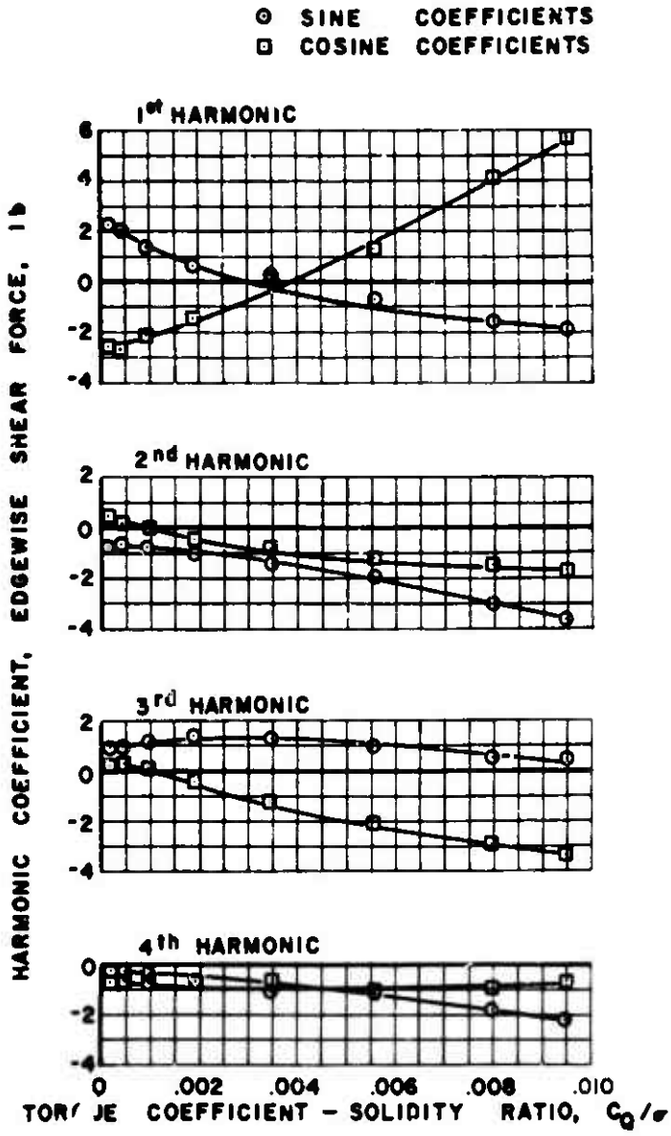

$\mu = 0.5$ $\alpha_s = -4$ deg.

(b) EDGEWISE

Figure 53. Continued.

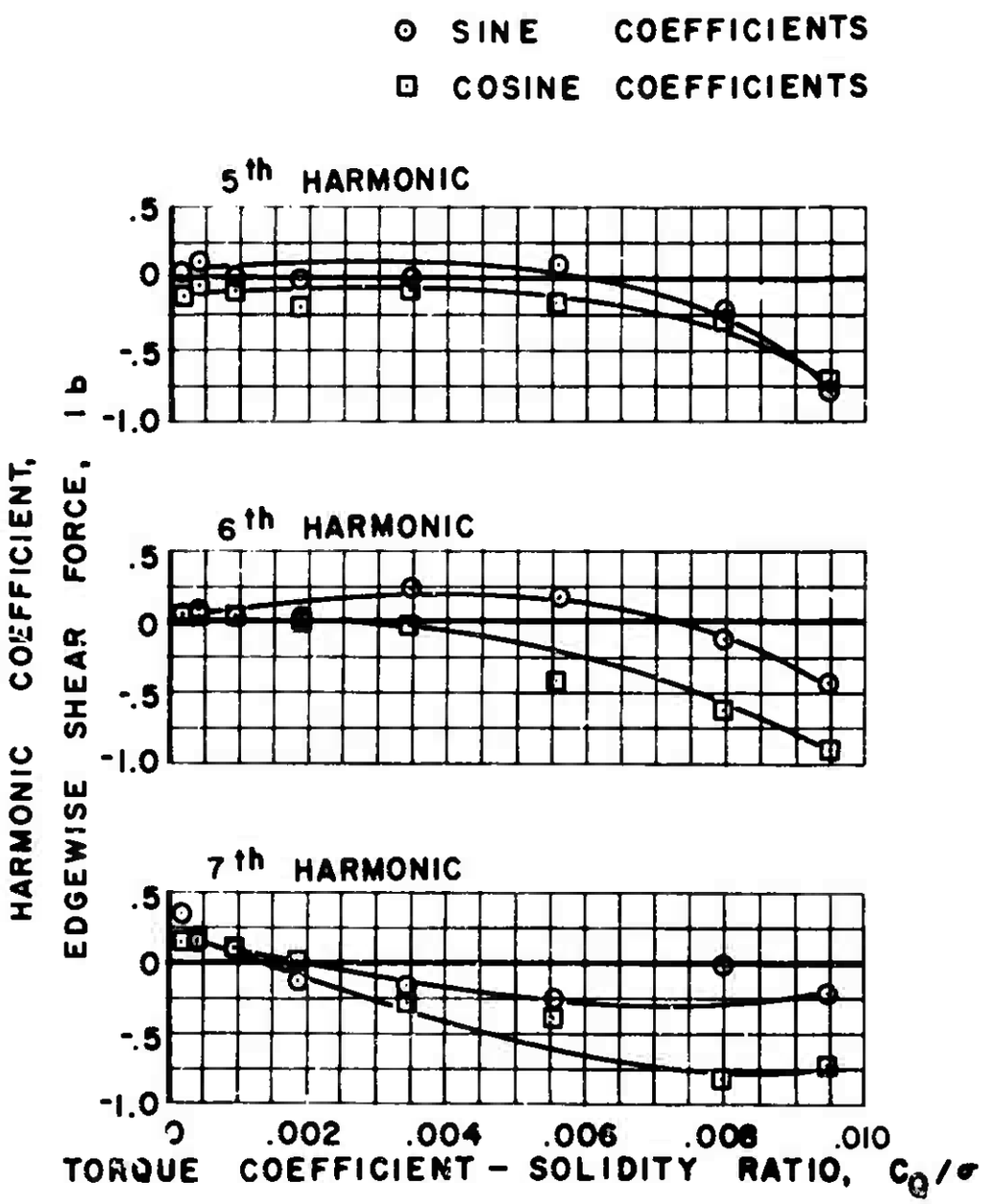

$\mu = 0.5$ $\alpha_s = -4$ deg.

Figure 53(b). Continued.

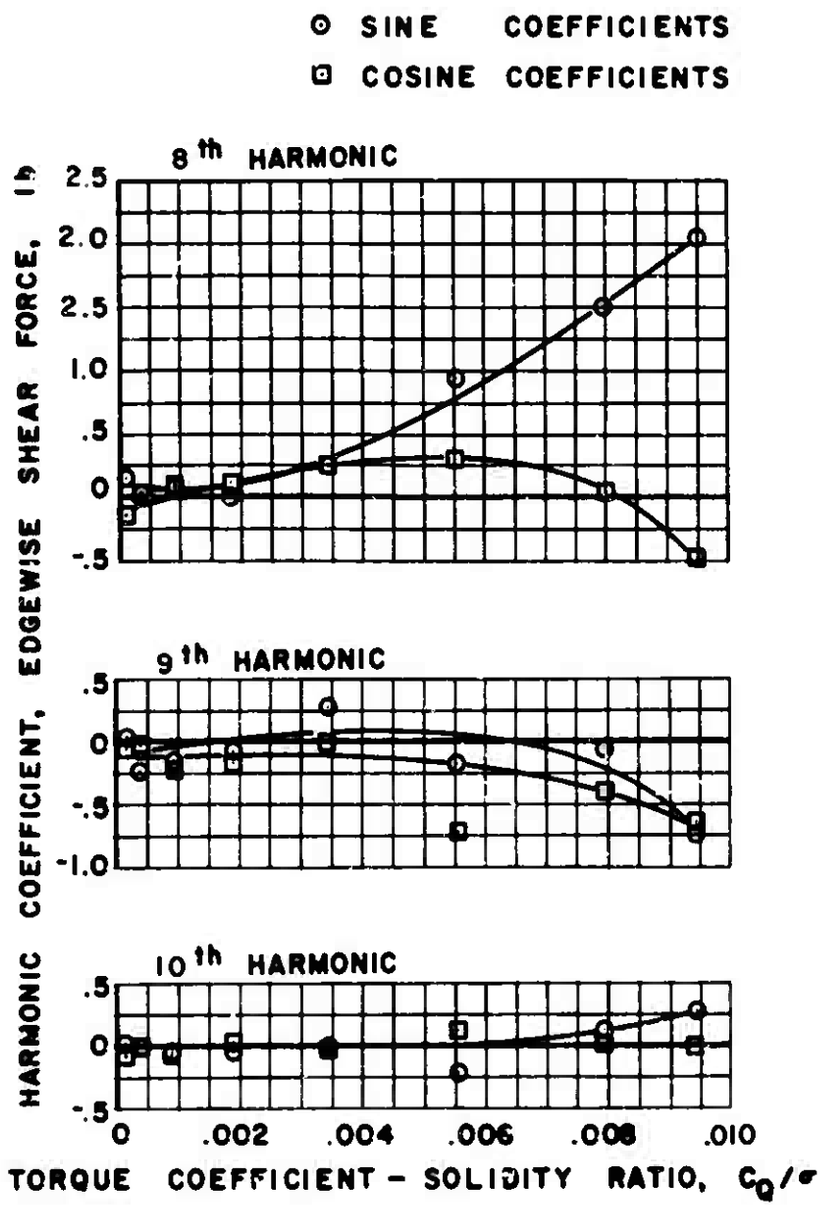

$\mu = 0.5$ $\alpha_s = -4$deg.

Figure 53(b). Concluded.

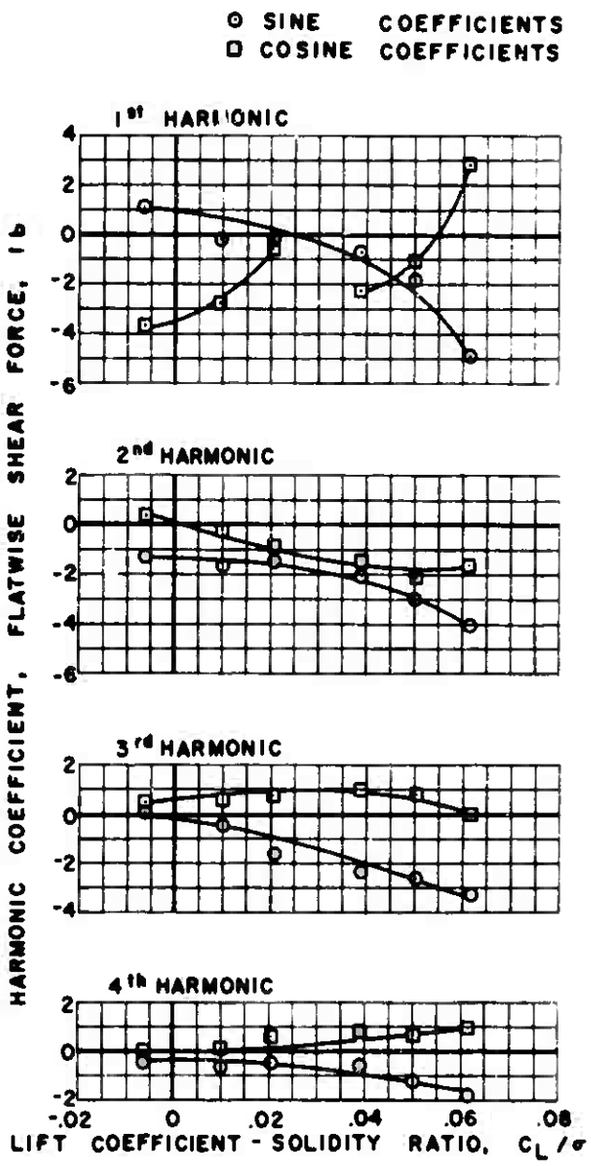

$\mu = 0.5$ $\alpha_s = -8$ deg.

(a) FLATWISE

Figure 54. Experimental Shear Force.

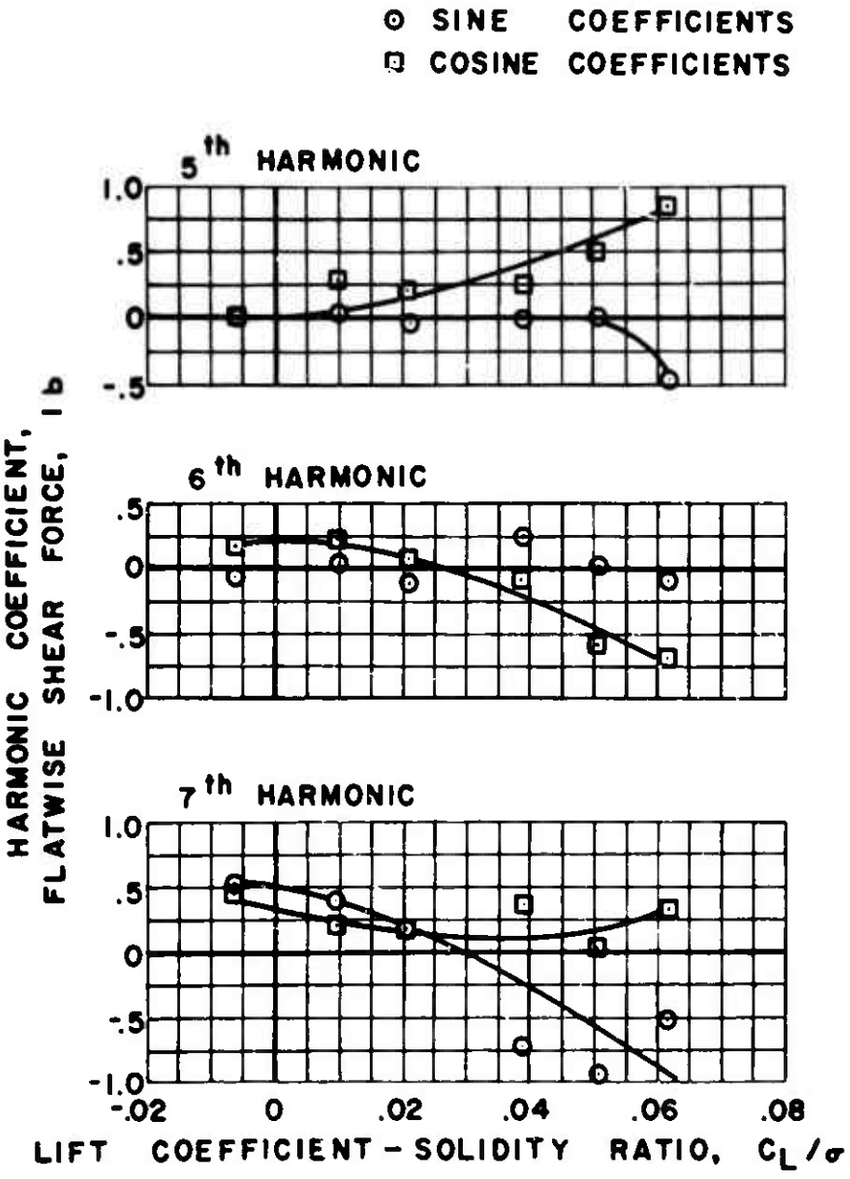

$\mu = 0.5$ $\alpha_s = -8$ deg.

Figure 54(a). Continued.

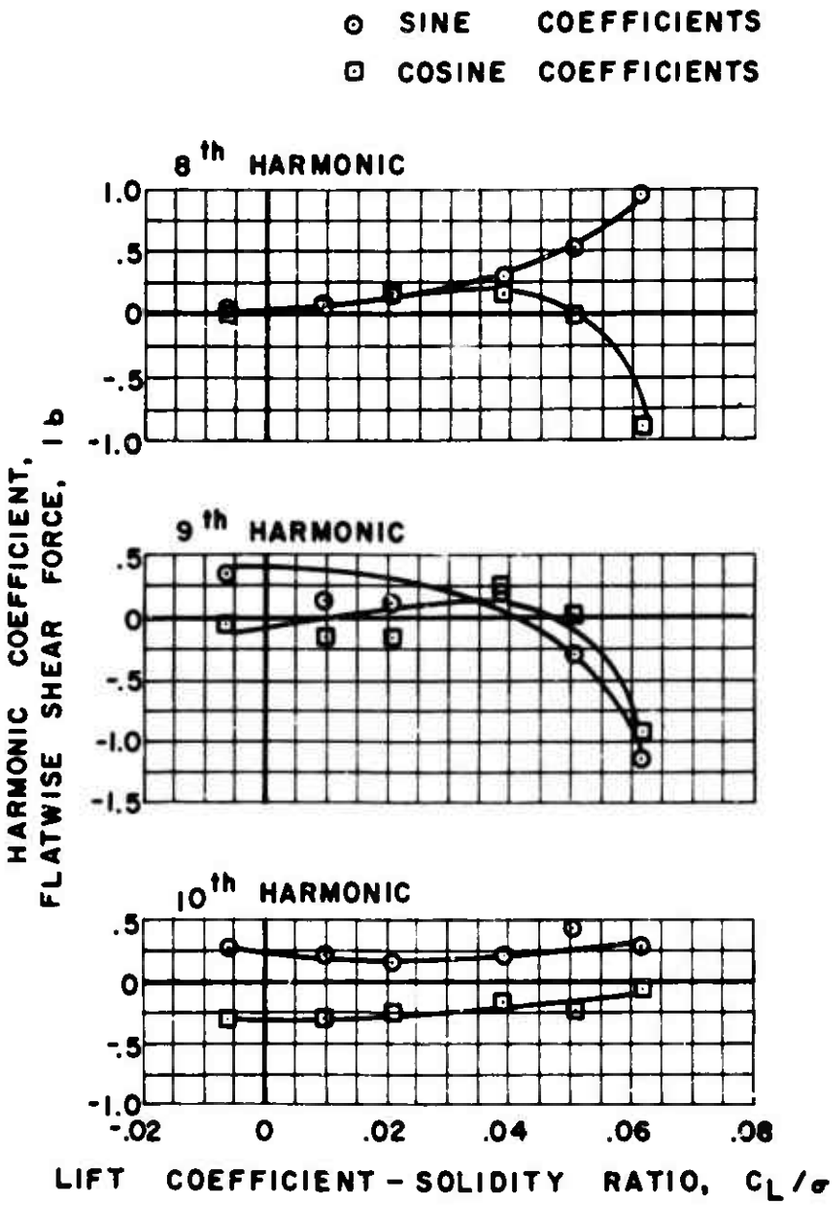

Figure 54(a). Continued.

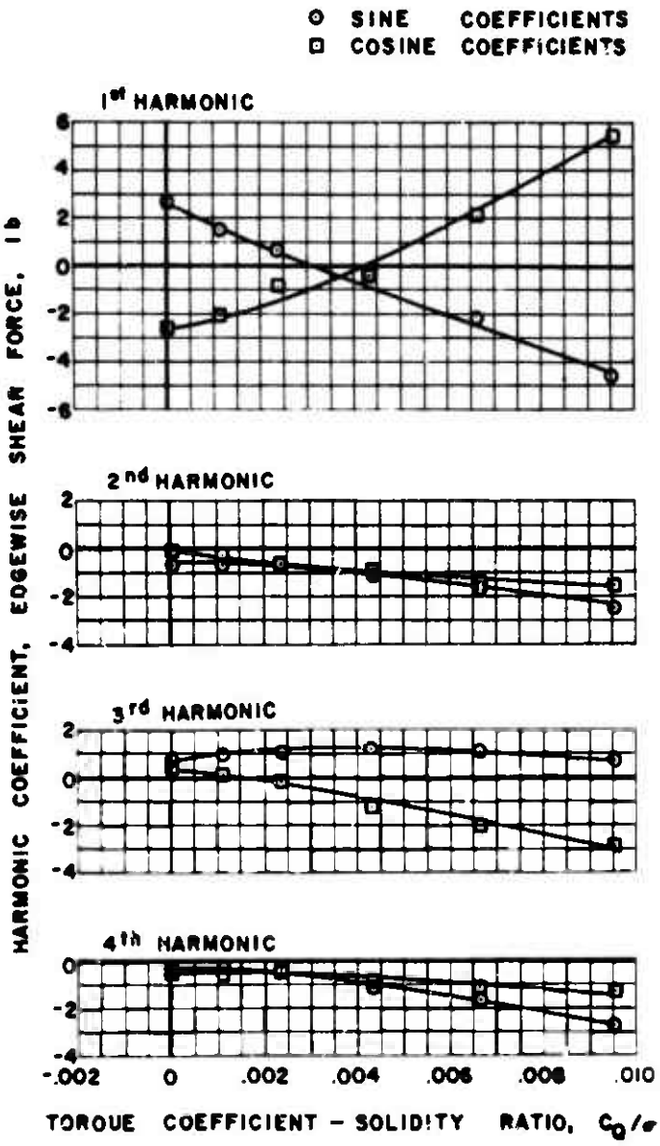

(b) EDGEWISE

Figure 54. Continued.

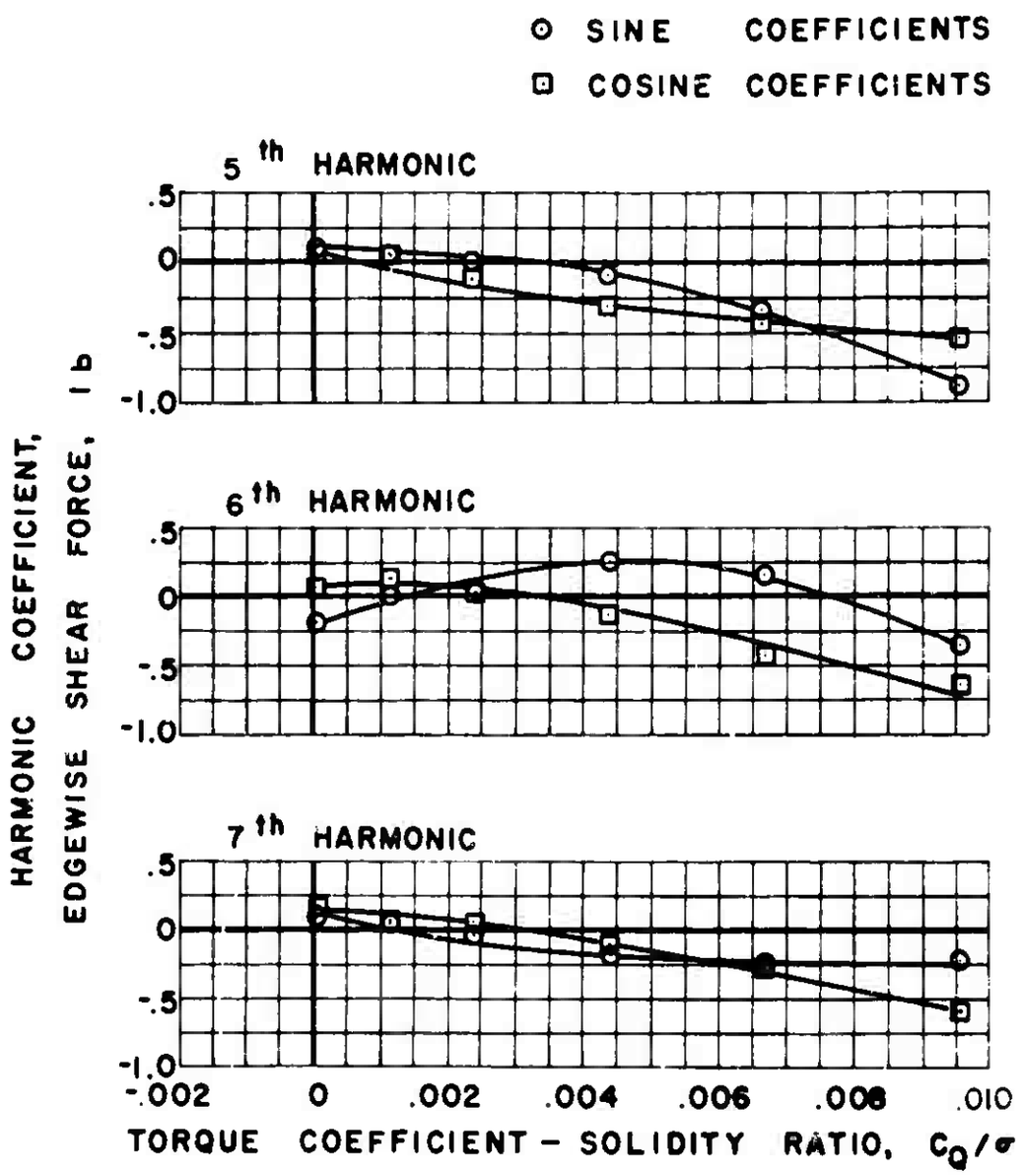

$\mu = 0.5$ $\alpha_s = -8$ deg.

Figure 54(b). Continued.

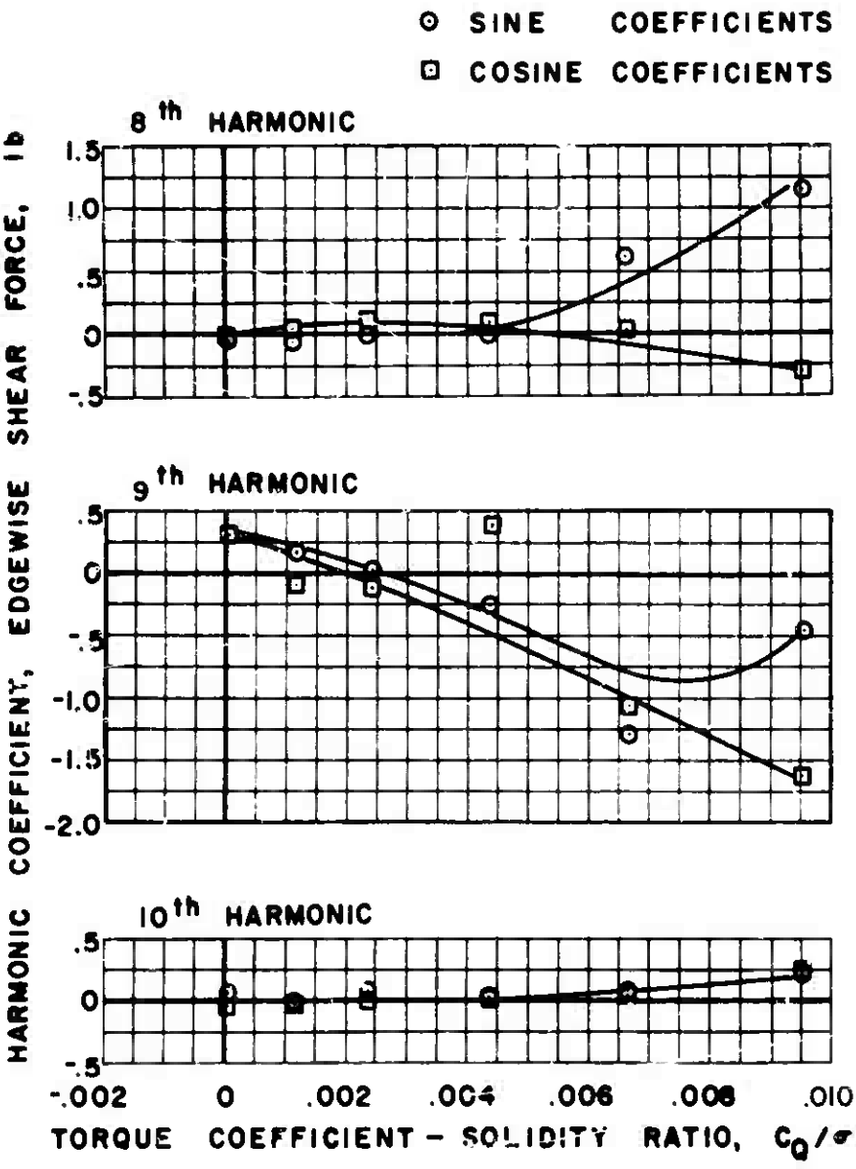

Figure 54(b). Concluded.

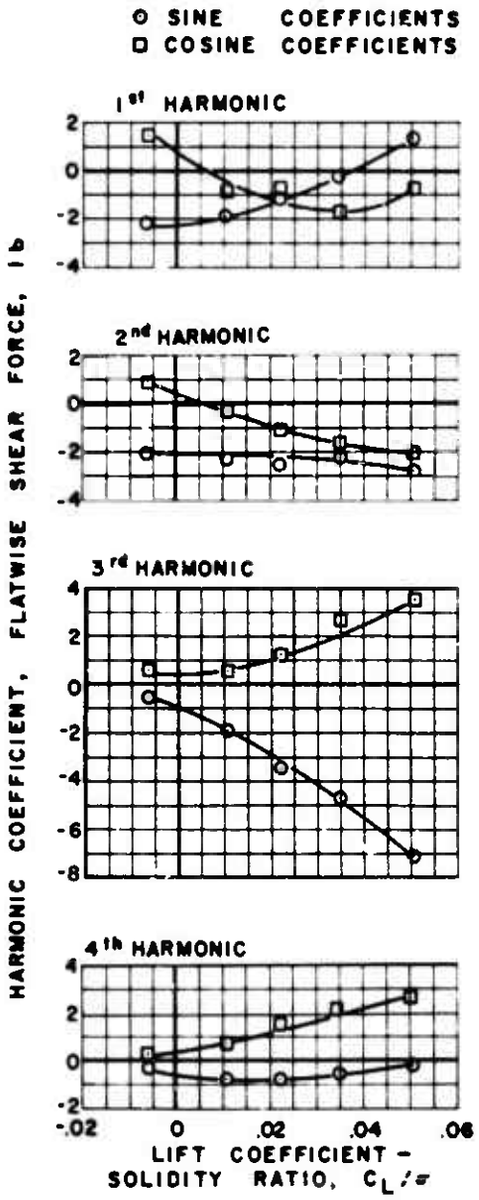

Figure 55. Experimental Shear Force, Zero Lag Damping.

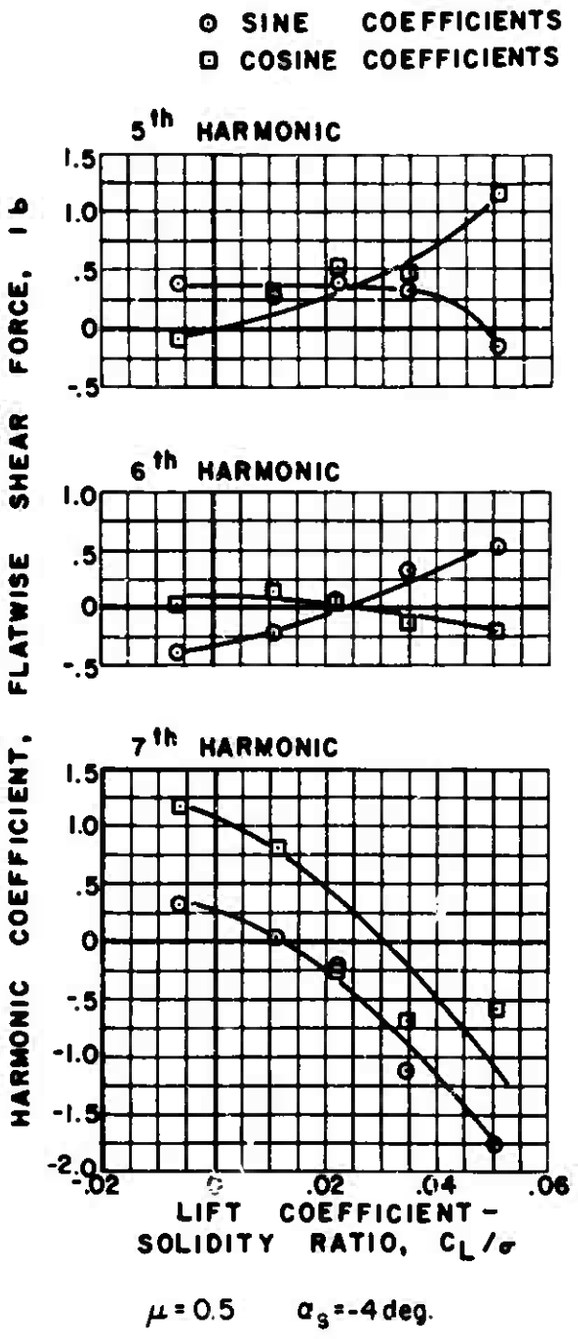

Figure 55(a). Continued.

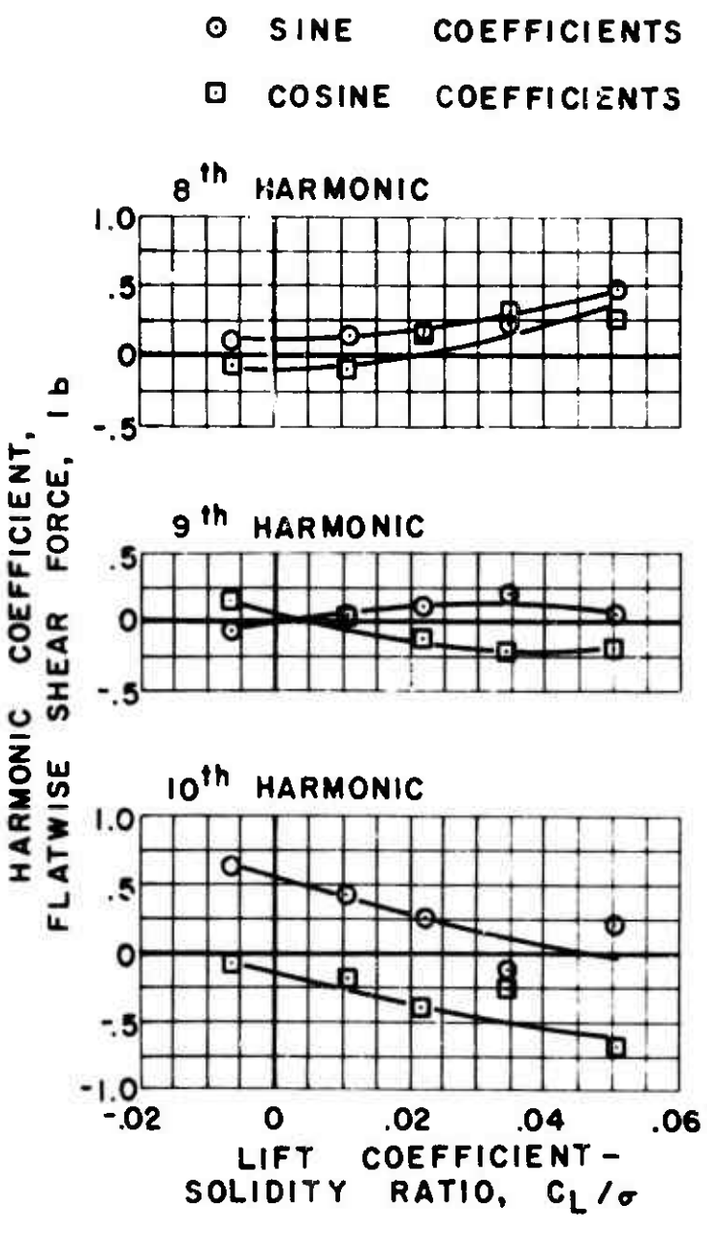

Figure 55(a). Continued.

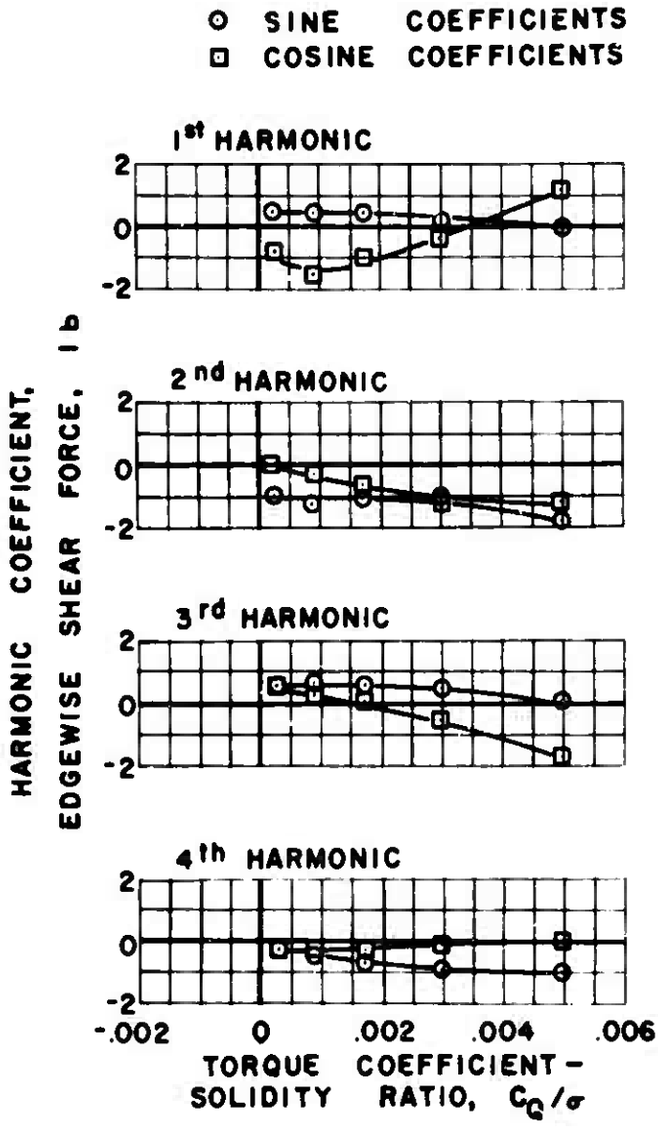

$\mu = 0.5$ $\alpha_s = -4$deg.

(b) EDGEWISE

Figure 55. Continued.

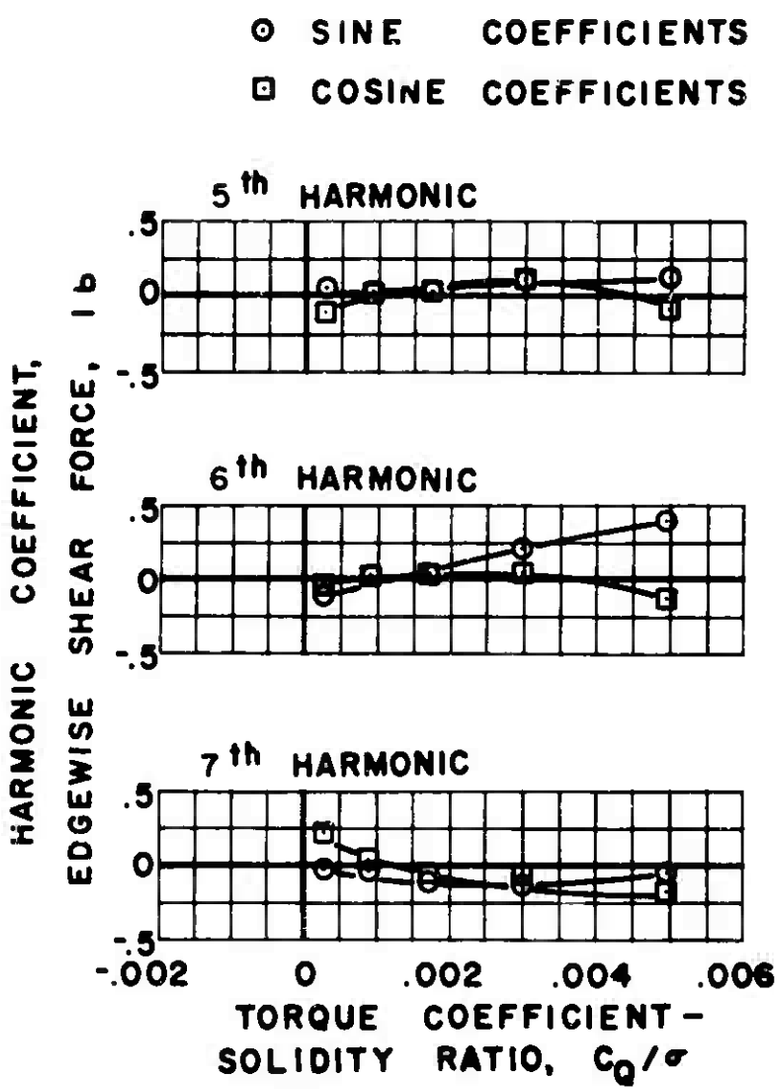

Figure 55(b). Continued.

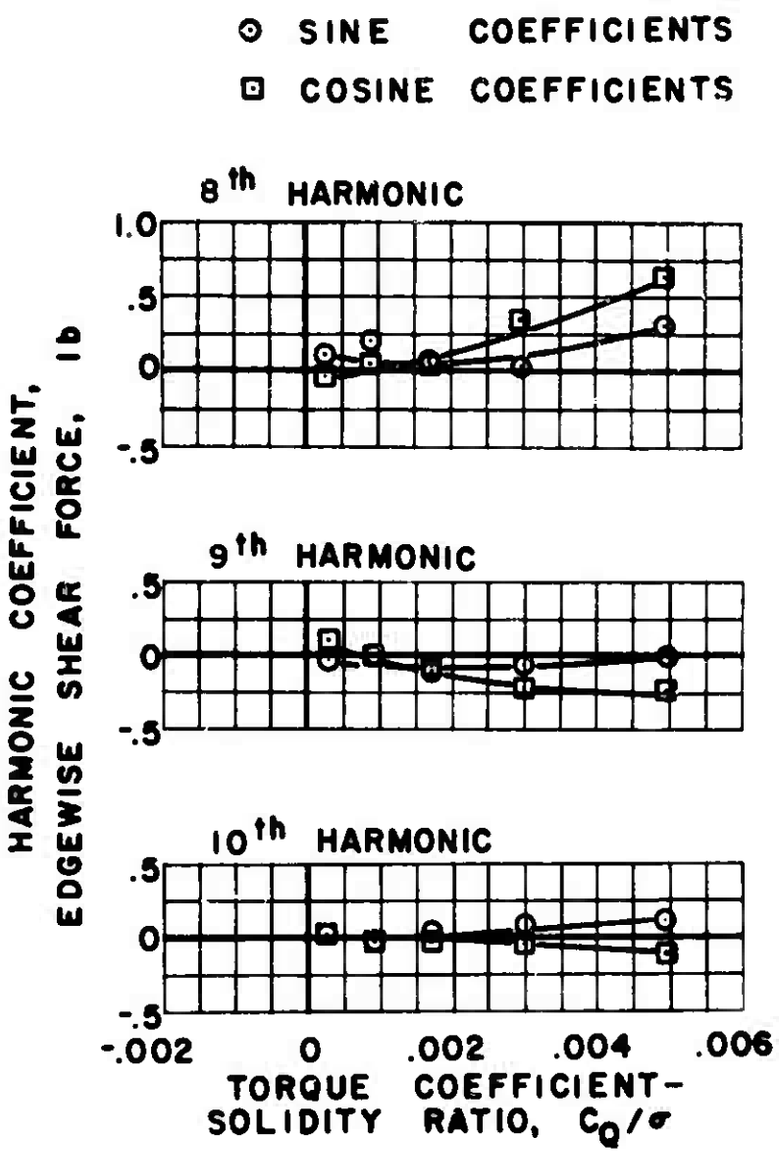

$\mu = 0.5$ $\alpha_s = -4$ deg.

Figure 55(b). Concluded.

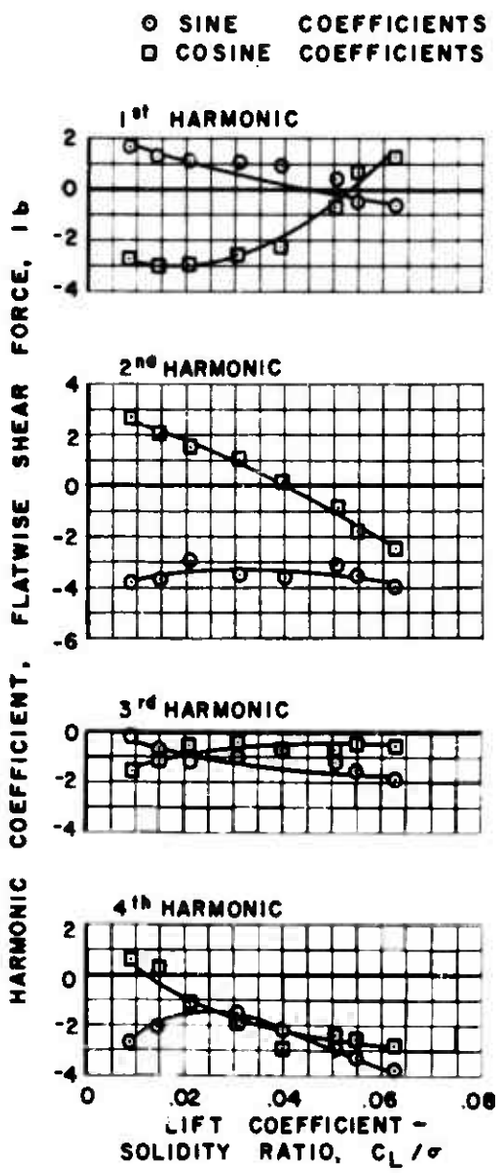

Figure 56. Experimental Shear Force.

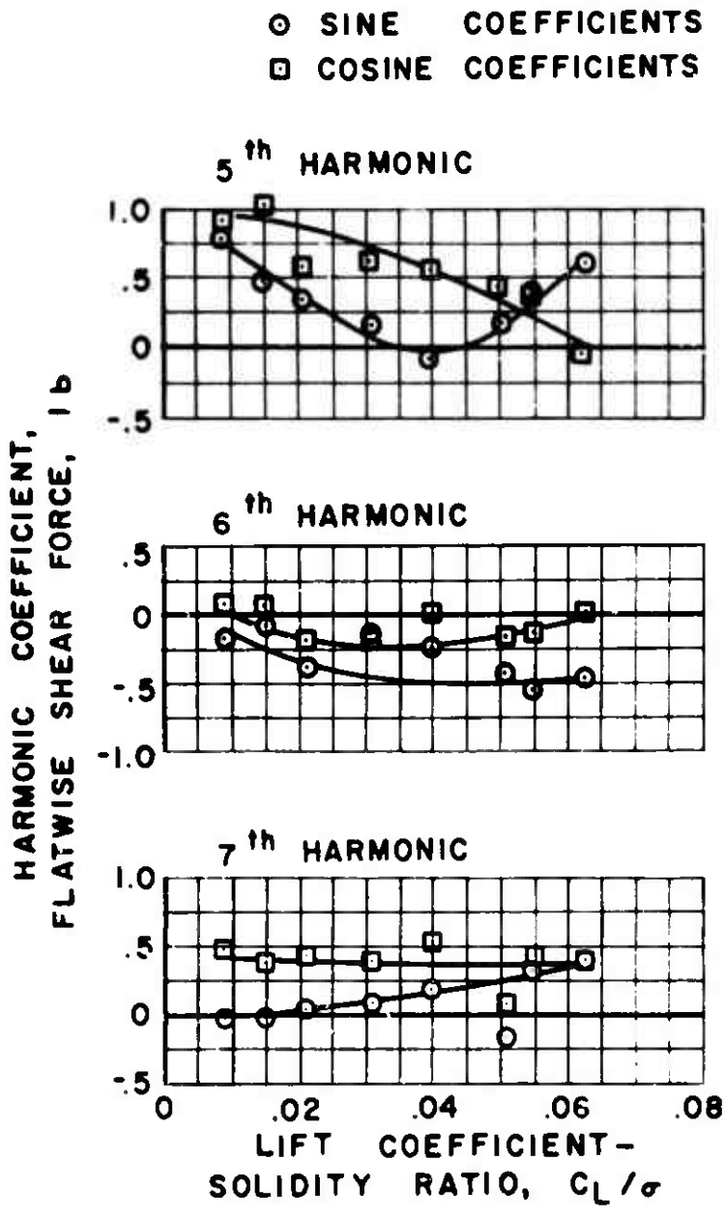

Figure 56(a). Continued.

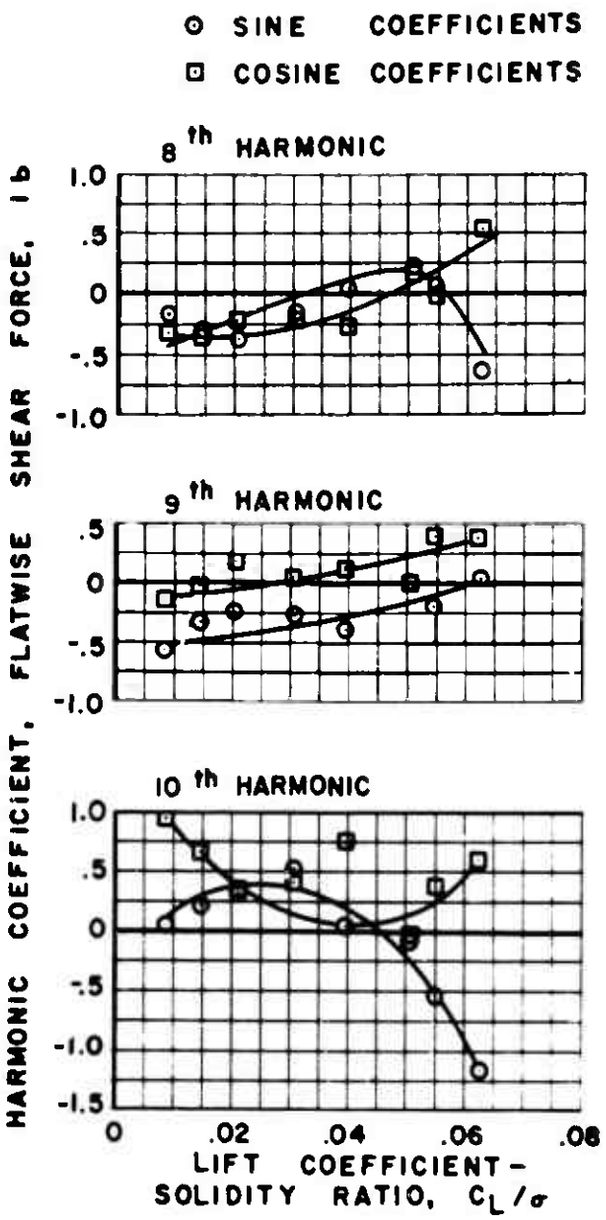

$\mu = 0.7$ $\alpha_s = 4$ deg.

Figure 56(a). Continued.

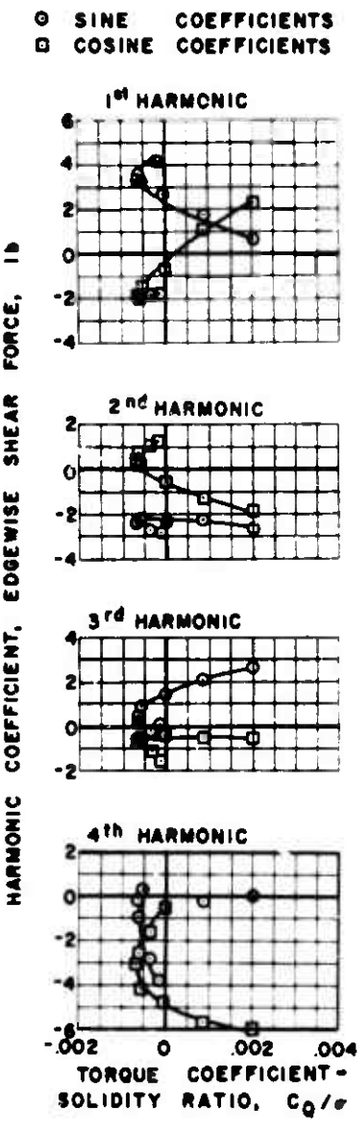

$\mu = 0.7$ $\alpha_s = 4$ deg.

(b) EDGEWISE

Figure 56. Continued.

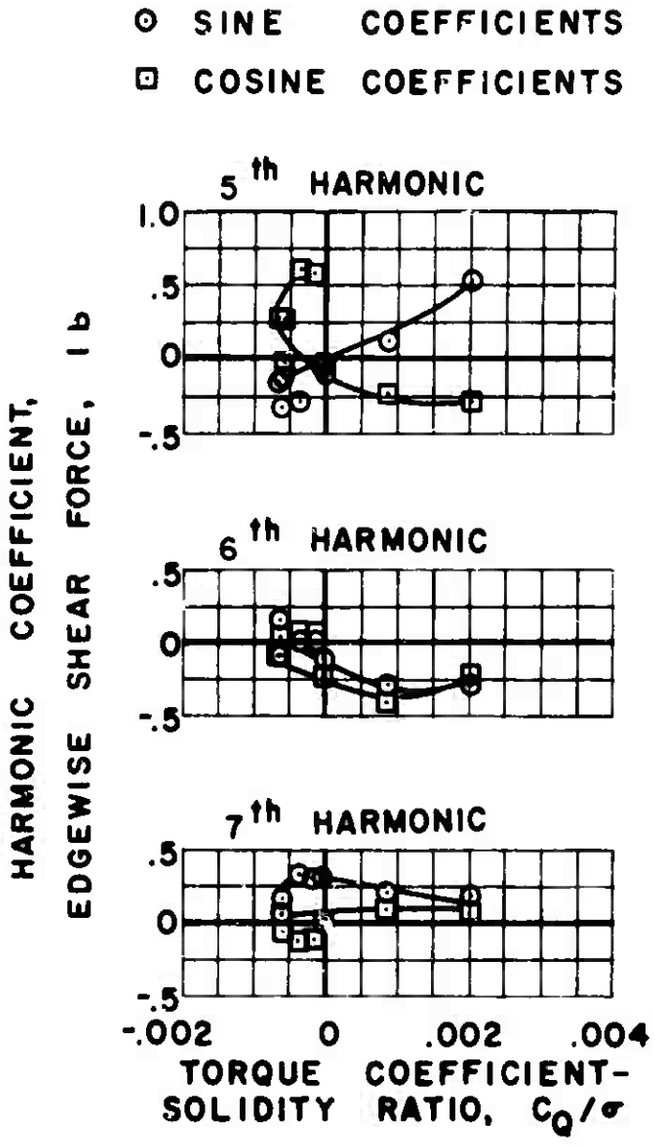

$\mu = 0.7$ $\alpha_s = 4$ deg.

Figure 56(b). Continued.

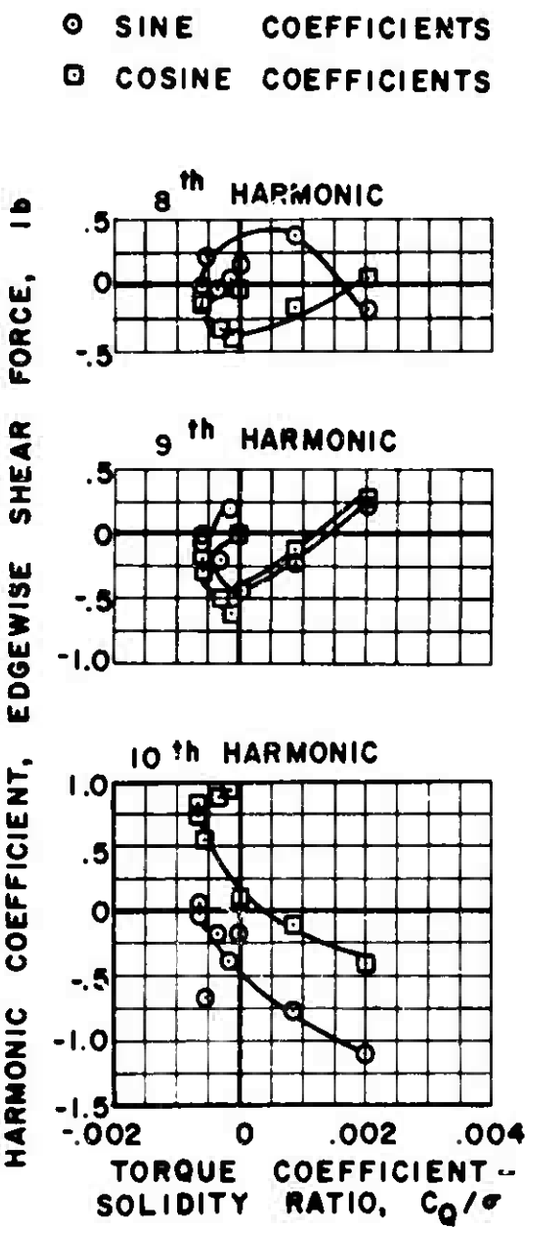

Figure 56(b). Concluded.

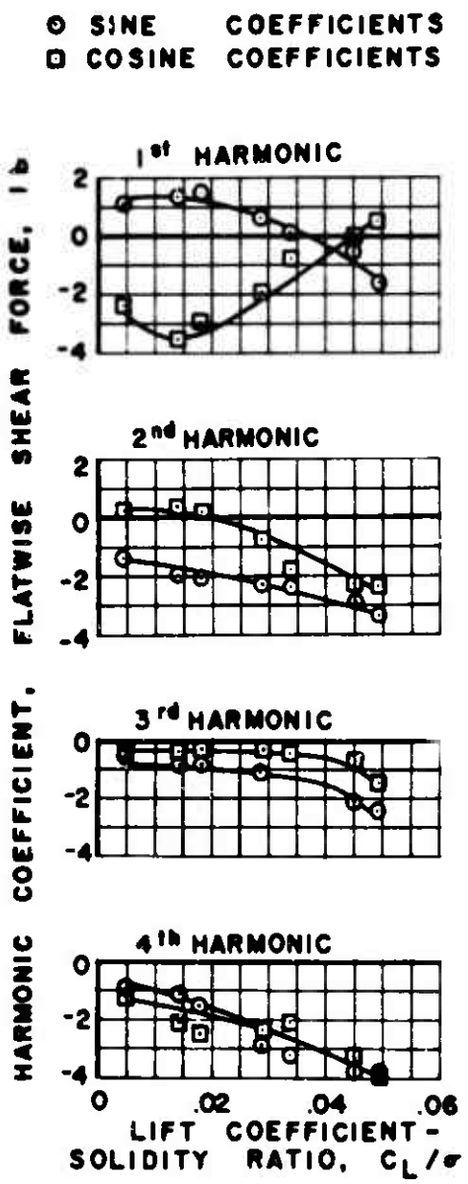

$\mu = 0.7$ $\alpha_s = 0$ deg.

(a) FLATWISE

Figure 57. Experimental Shear Force.

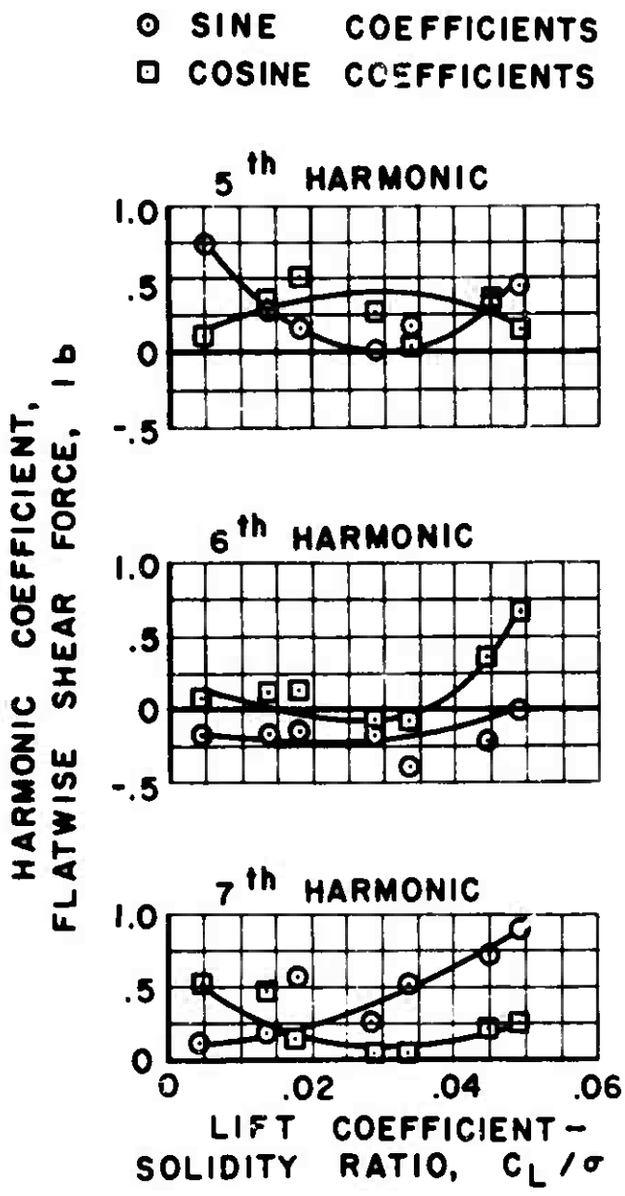

Figure 57(a). Continued.

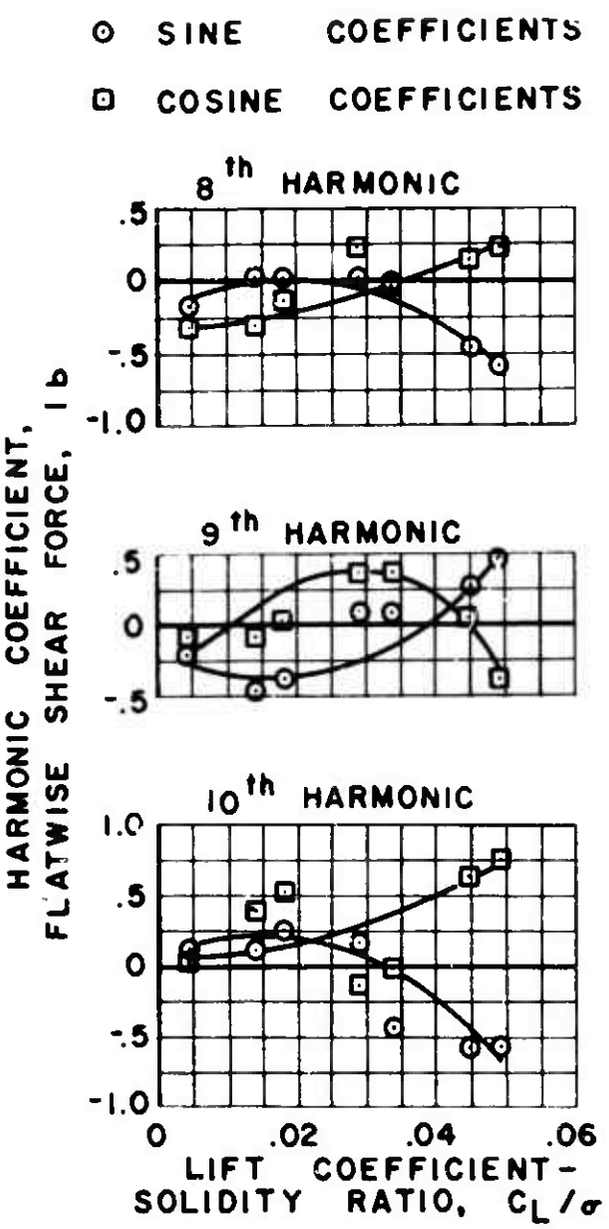

Figure 57(a). Continued.

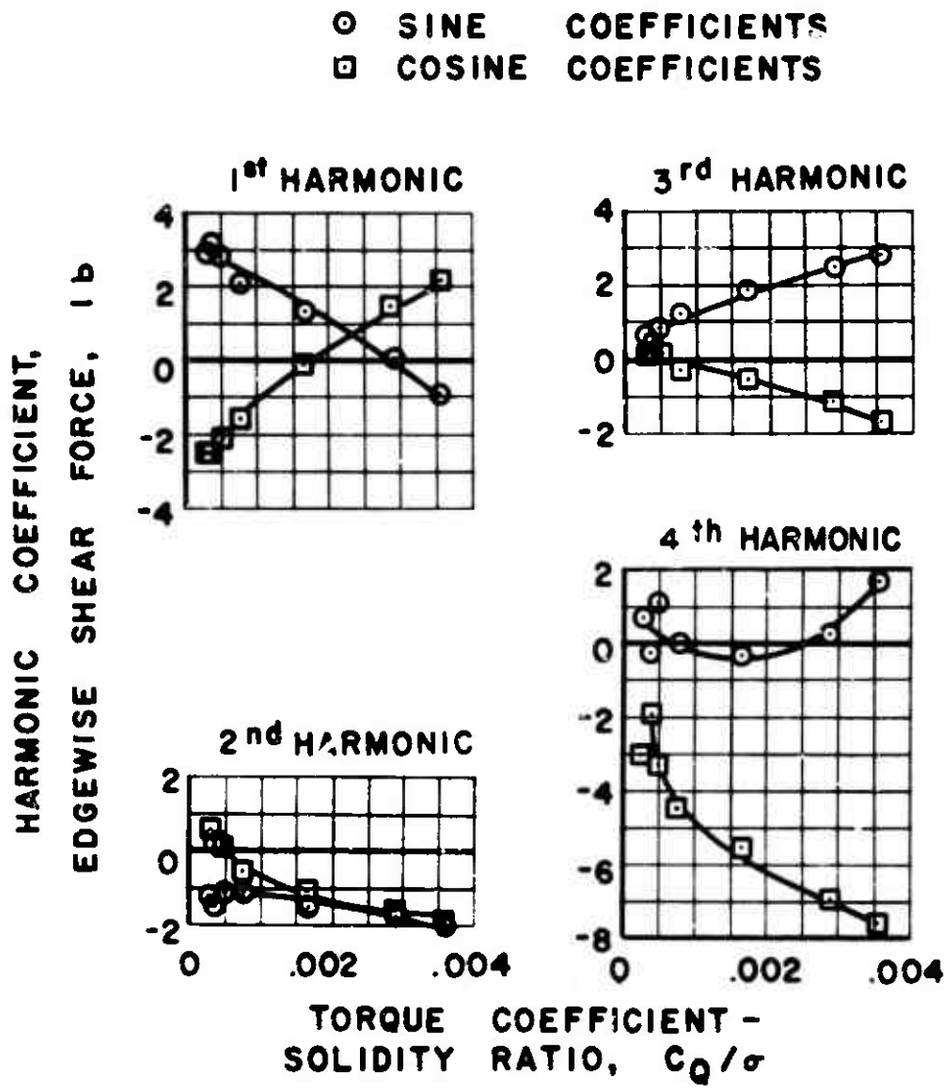

$\mu = 0.7$ $\alpha_s = 0$ deg.

(b) EDGEWISE

Figure 57. Continued.

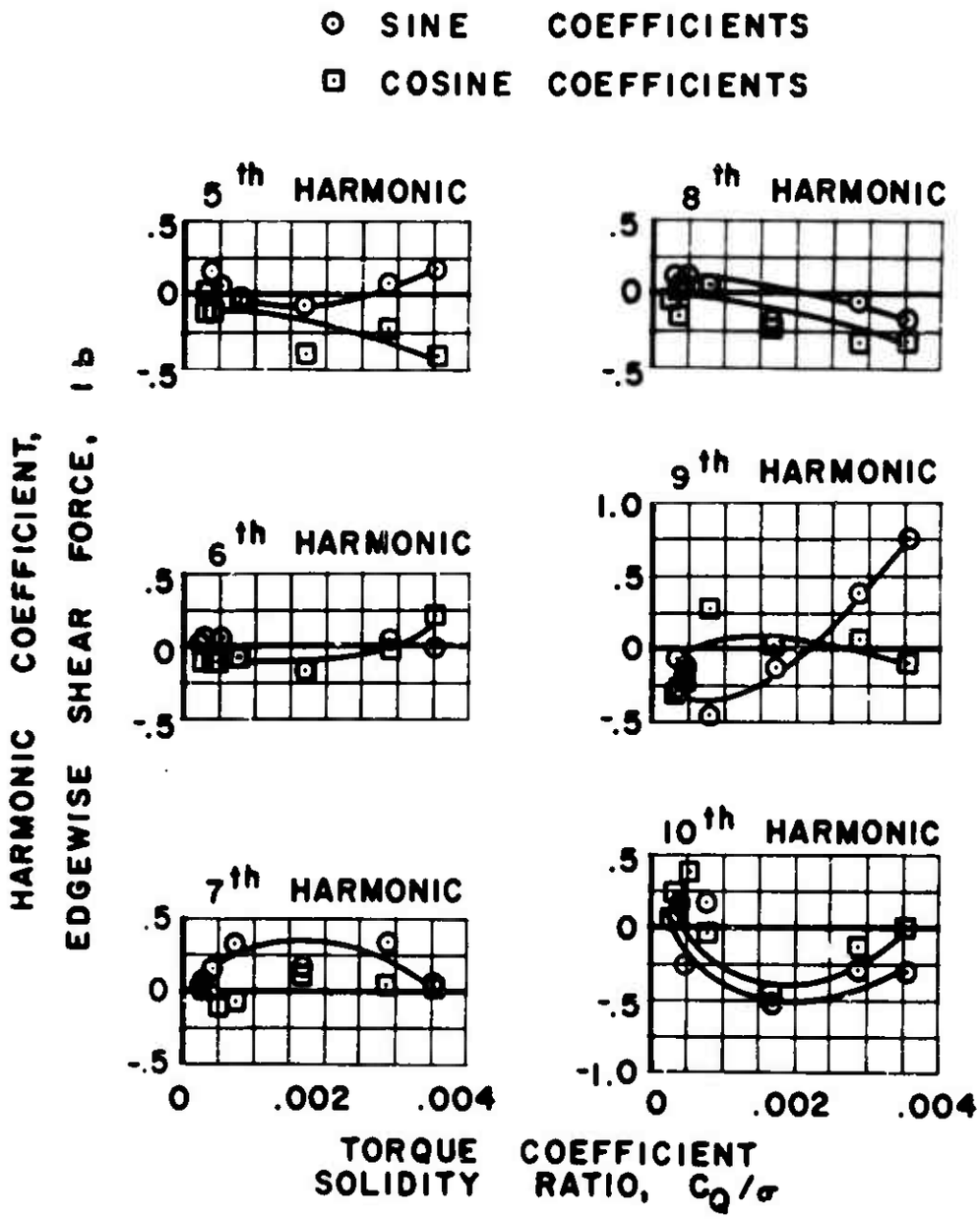

Figure 57(b). Concluded.

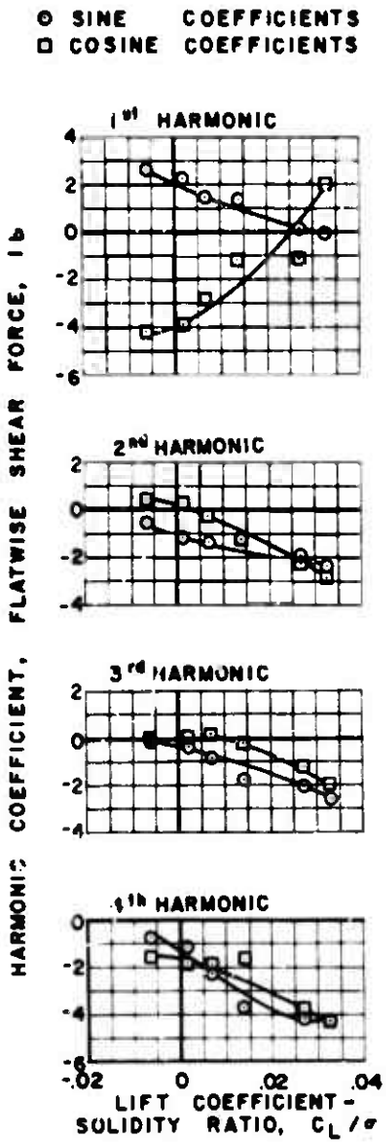

Figure 58. Experimental Shear Force.

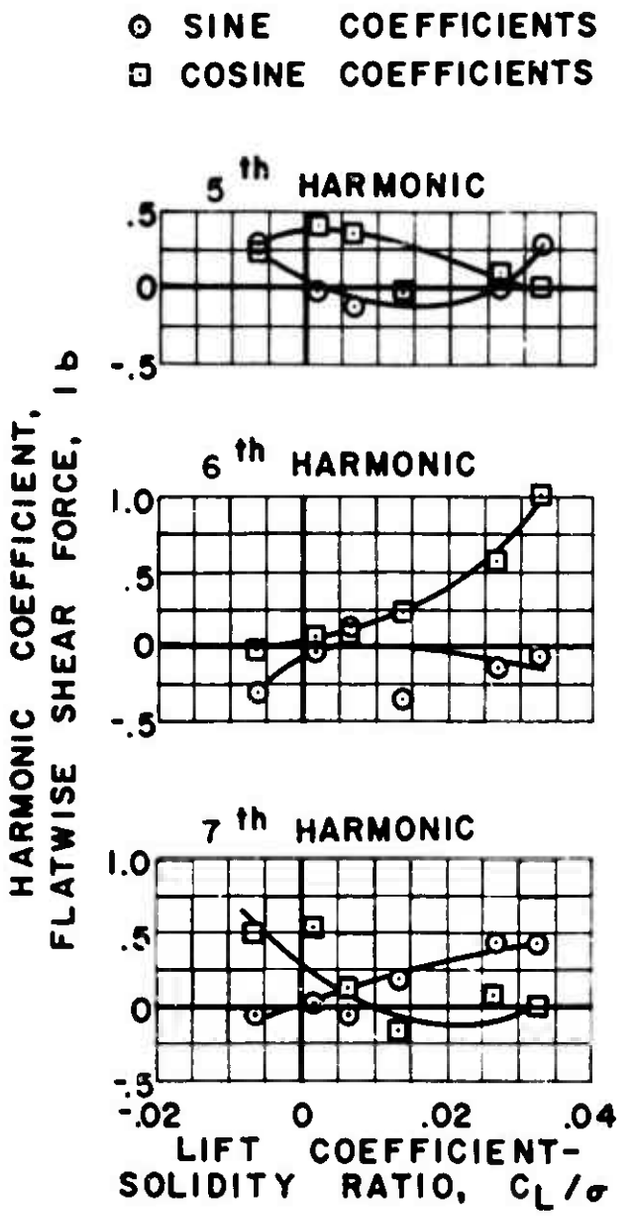

Figure 58(a). Continued.

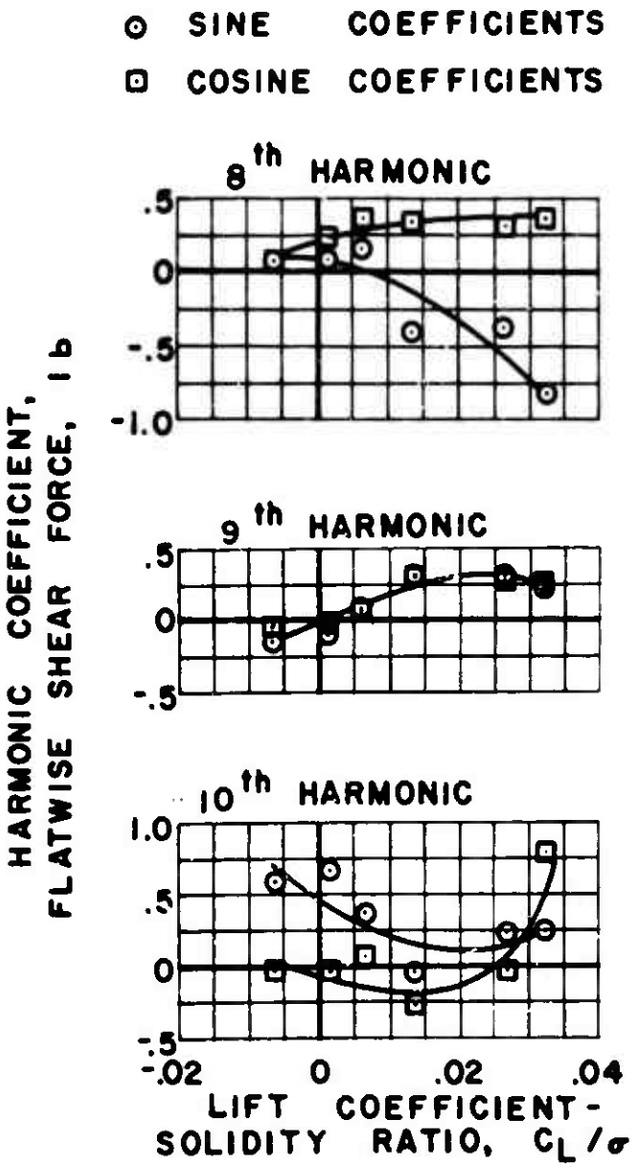

Figure 58(a). Continued.

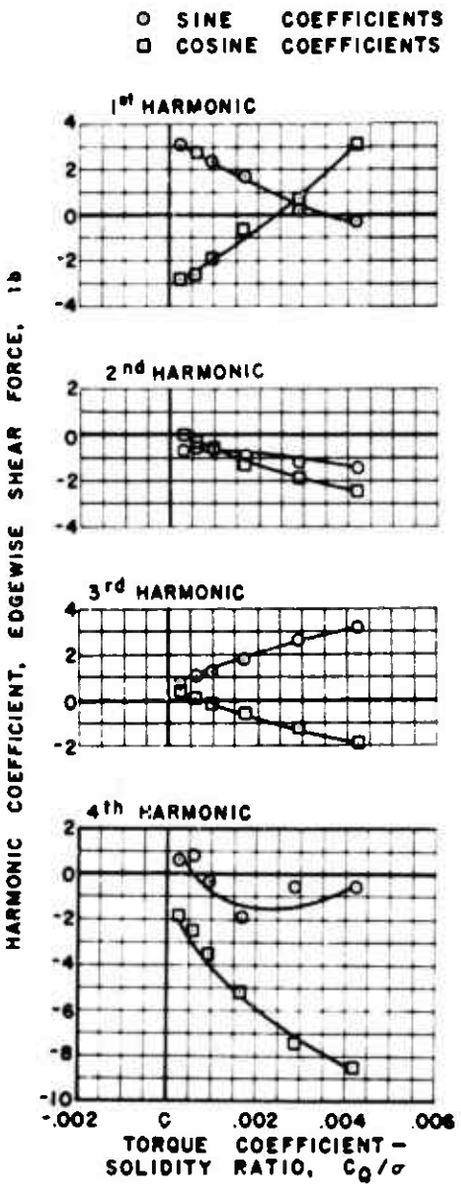

$\mu = 0.7$ $\alpha_s = -4$ deg.

(b) EDGEWISE

Figure 58. Continued.

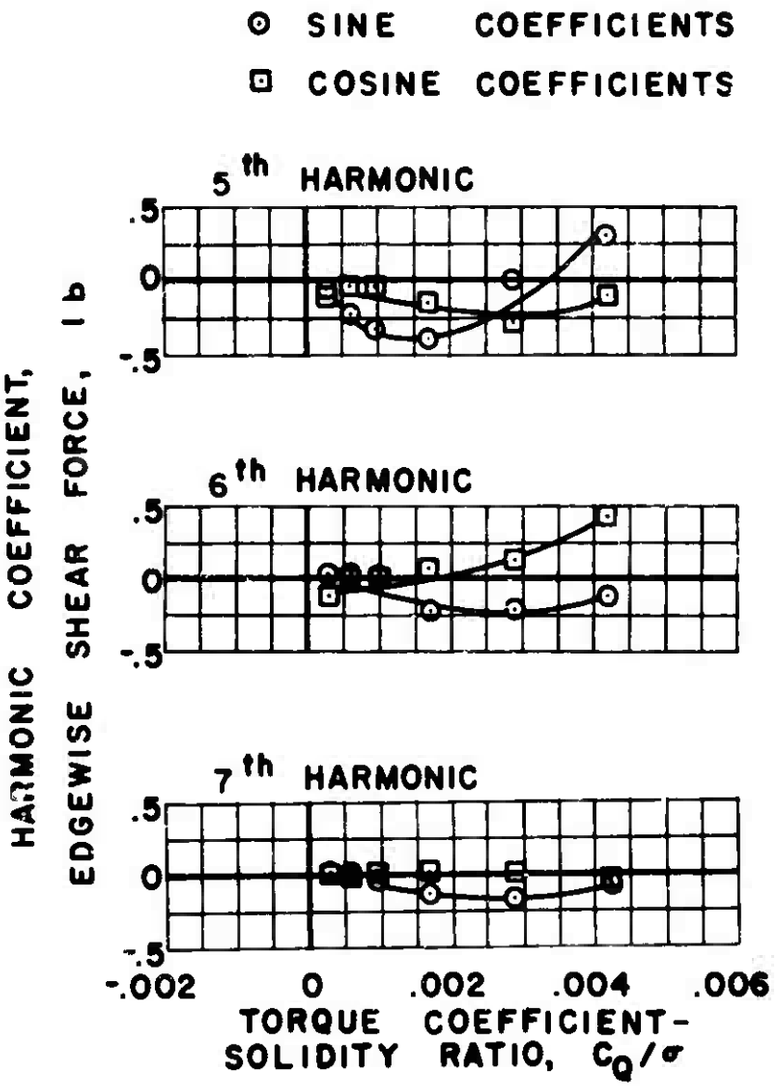

$\mu = 0.7$ $\alpha_s = -4$ deg.

Figure 58(b). Continued.

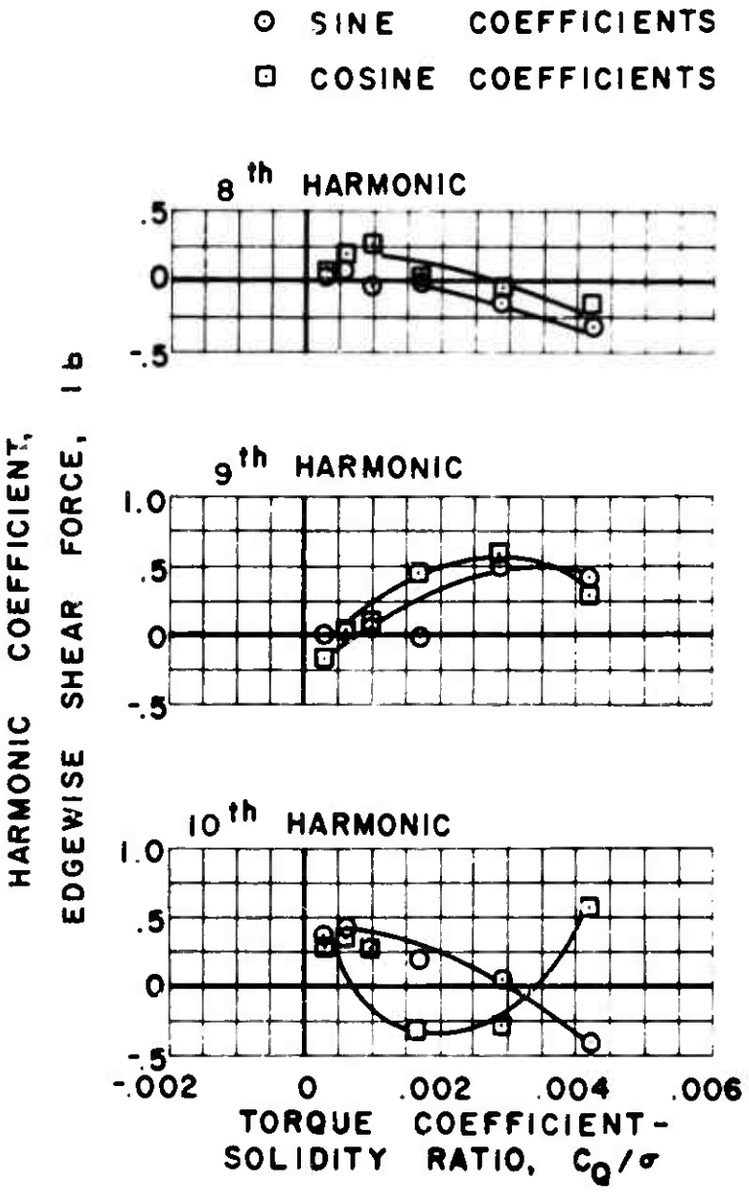

Figure 58(b). Concluded.

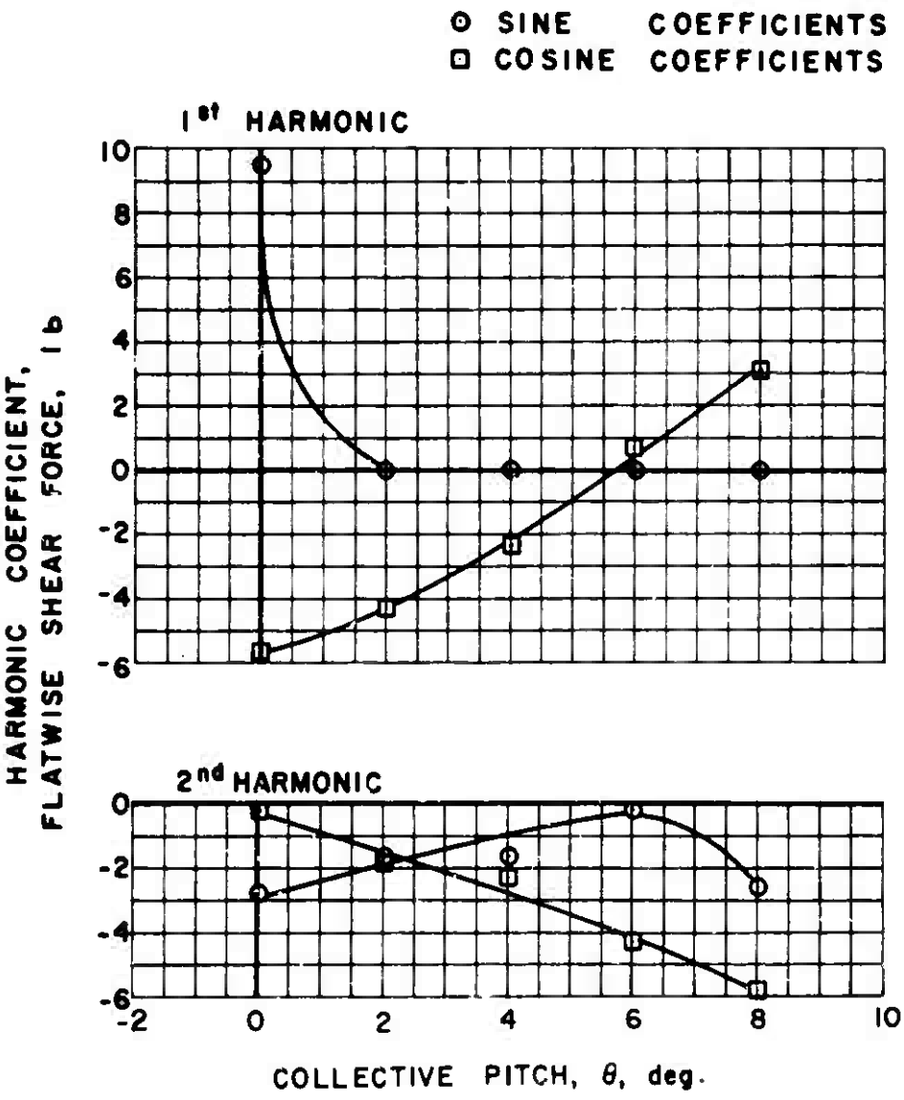

Figure 59. Experimental Shear Force.

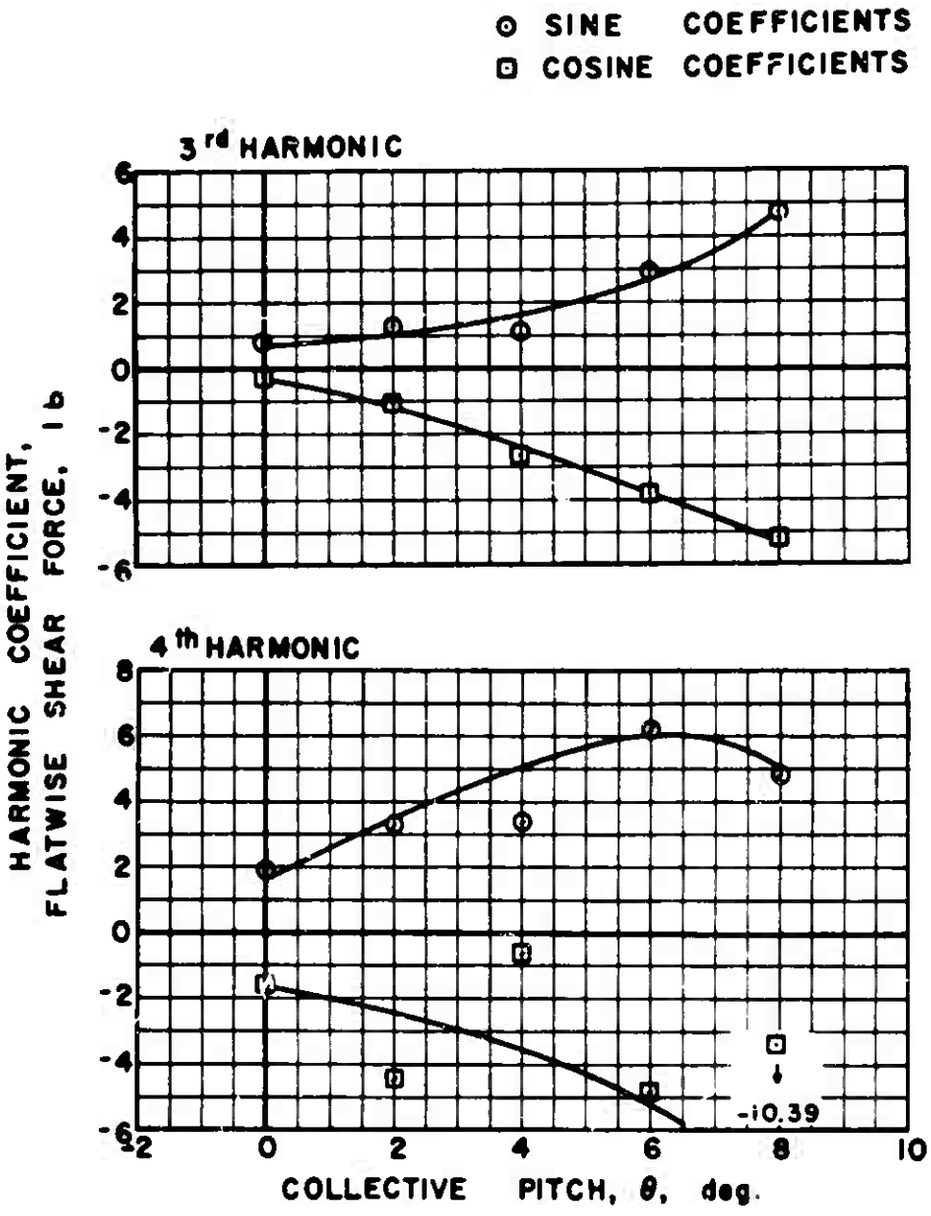

$\mu = 1.0$ $\alpha_s = 0$ deg.

Figure 59(a). Continued.

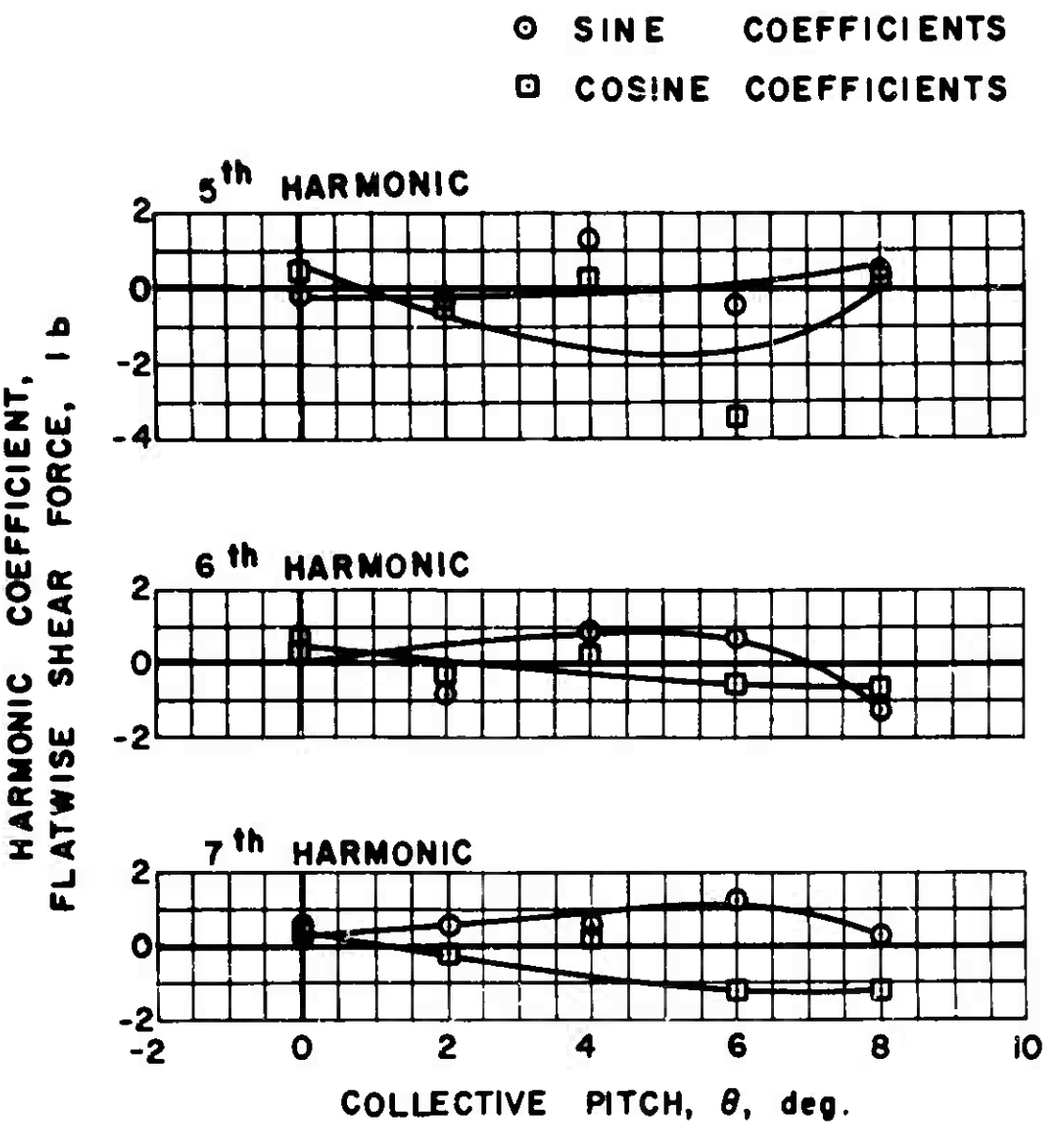

$\mu = 1.0$ $\alpha_s = 0$ deg.

Figure 59(a). Continued.

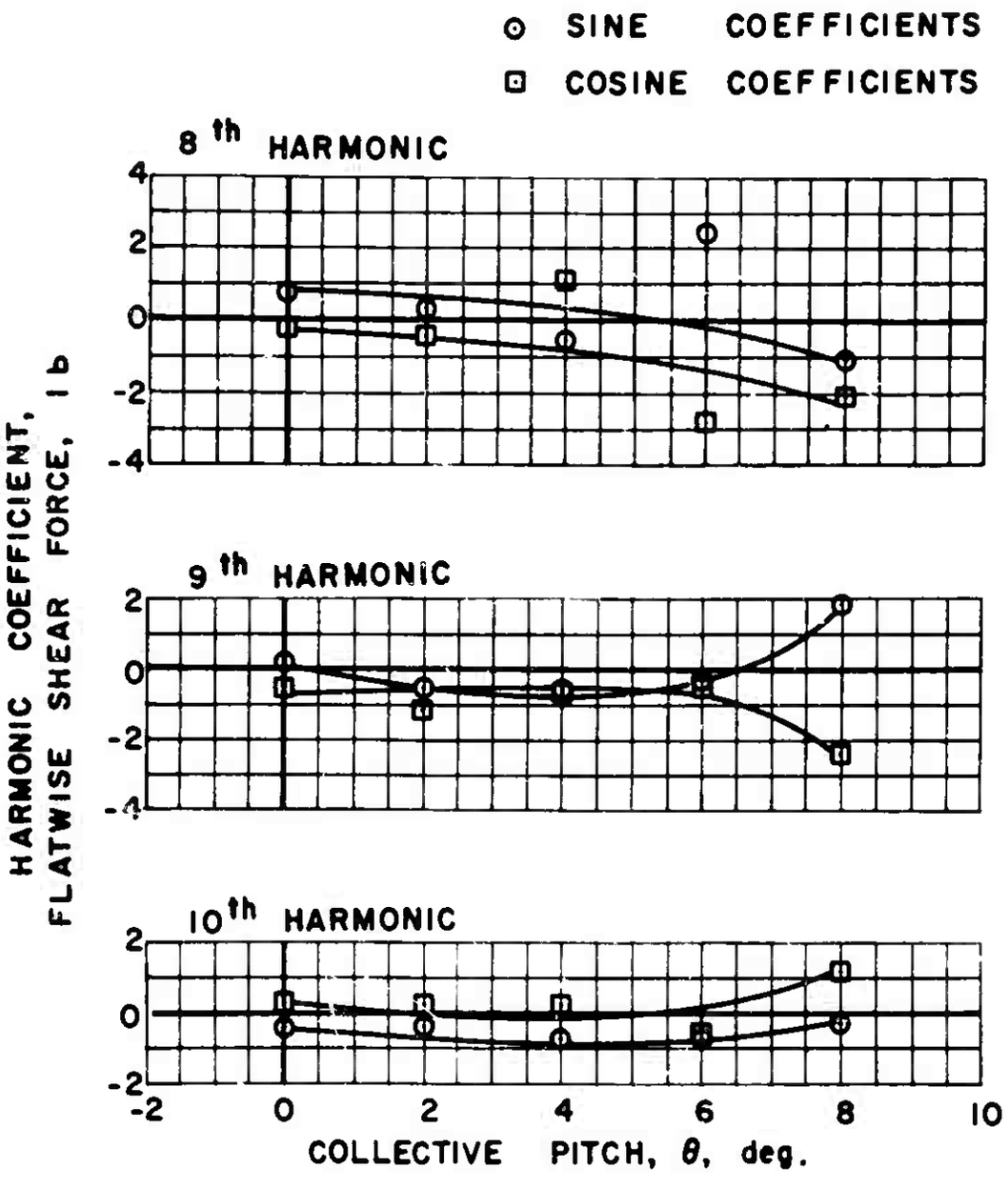

Figure 59(a). Continued.

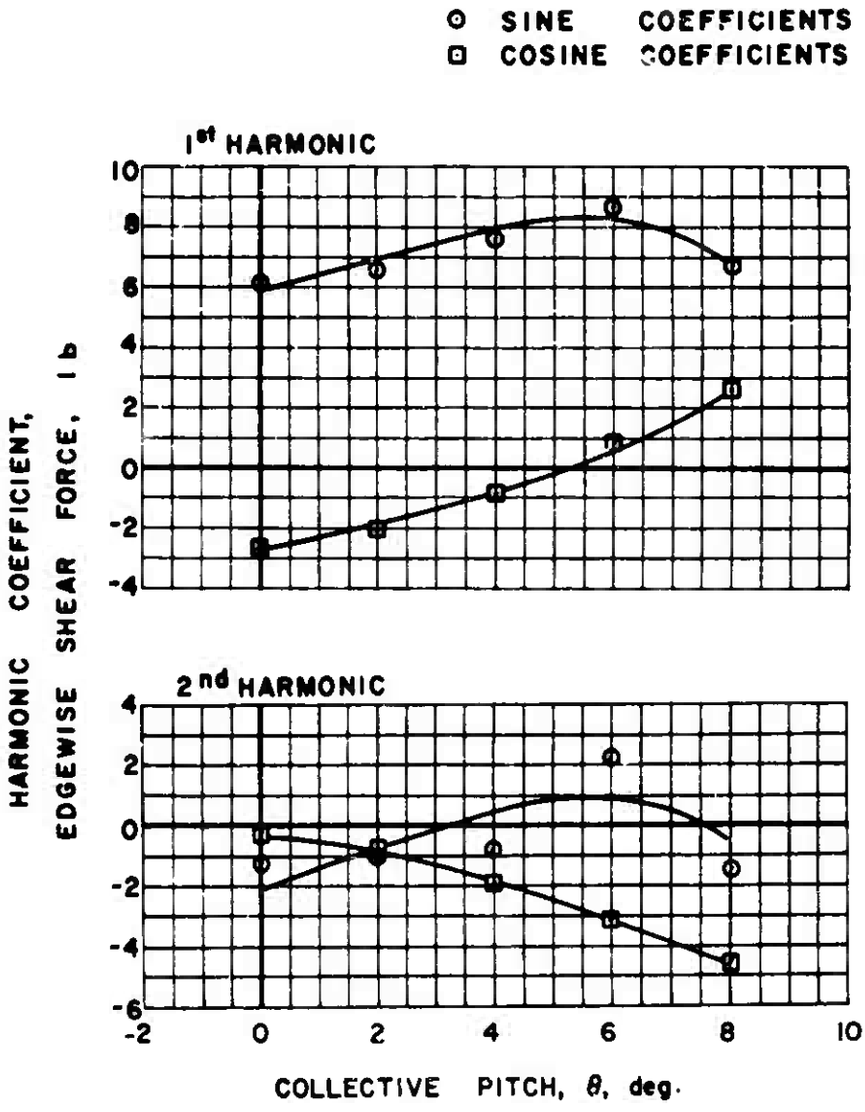

$\mu = 1.0$ $\alpha_s = 0$ deg.

(b) EDGEWISE

Figure 59. Continued.

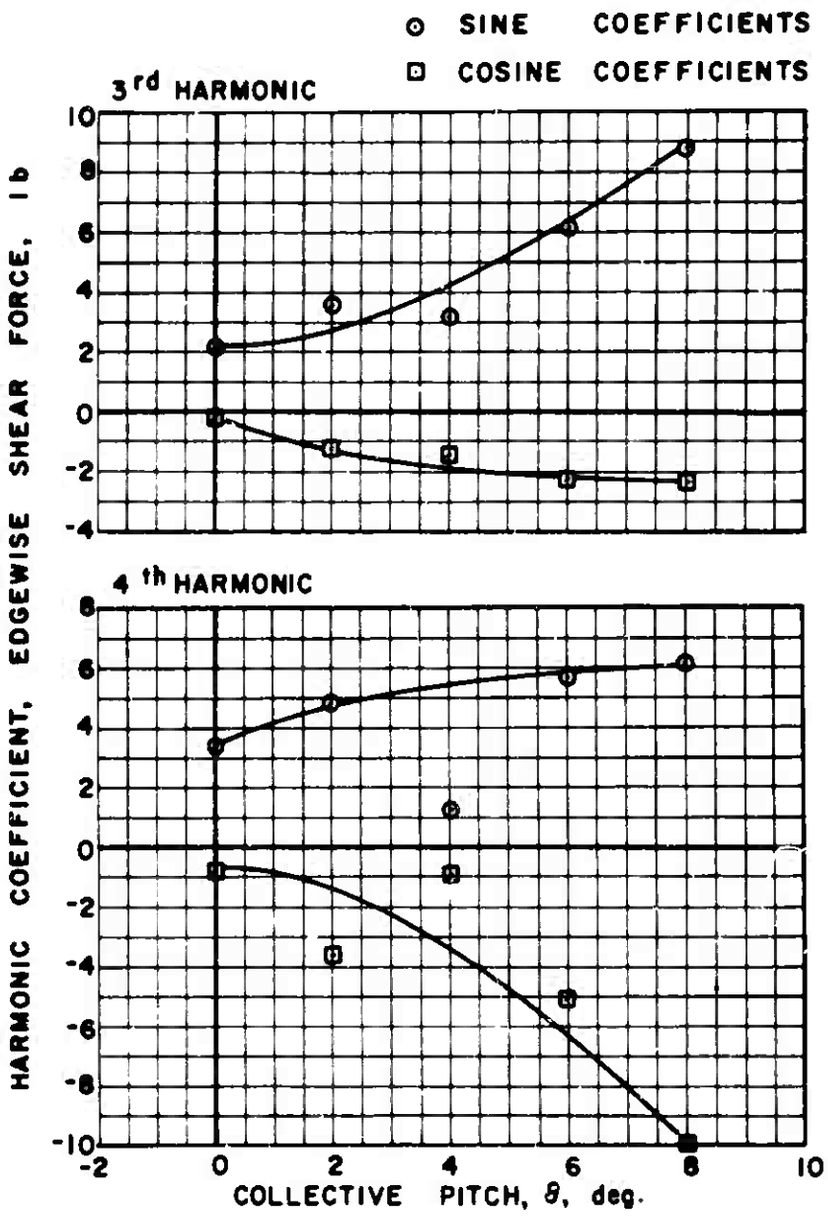

$\mu = 1.0$ $\alpha_s = 0$ deg.

Figure 59(b). Continued.

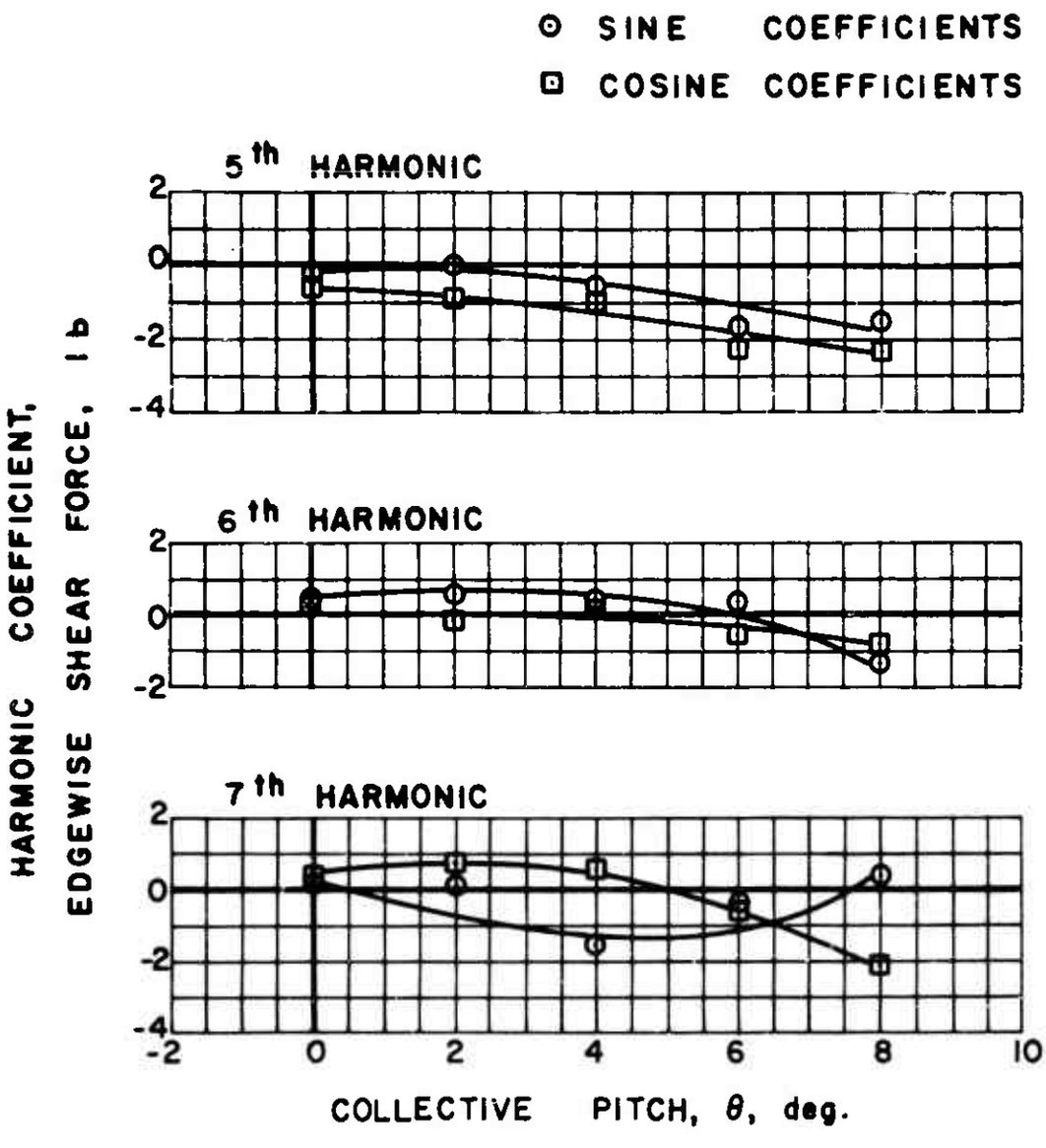

$\mu = 1.0$ $\alpha_s = 0$ deg.

Figure 59(b). Continued.

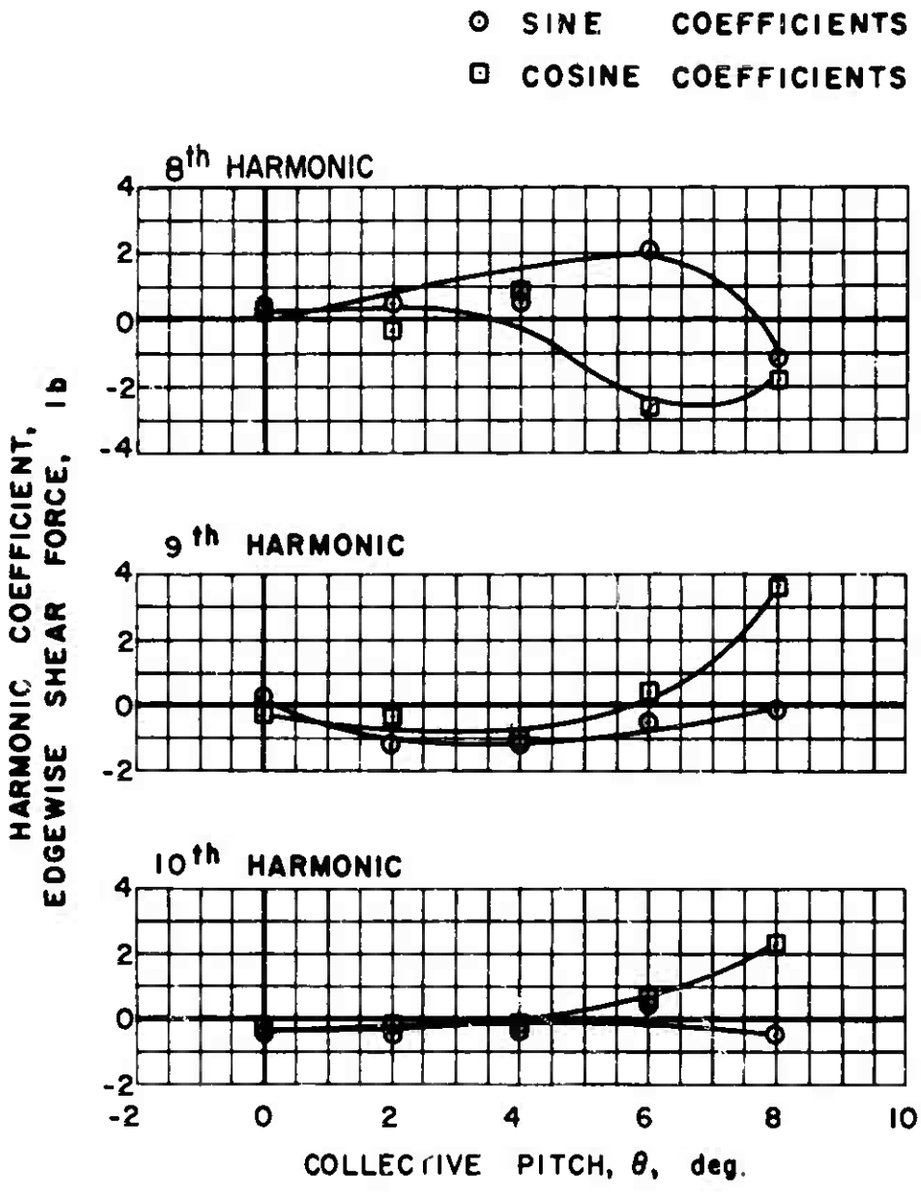

Figure 59(b). Concluded.

APPENDIX II
EXPERIMENTAL RADIAL SHEAR FORCE FIGURES

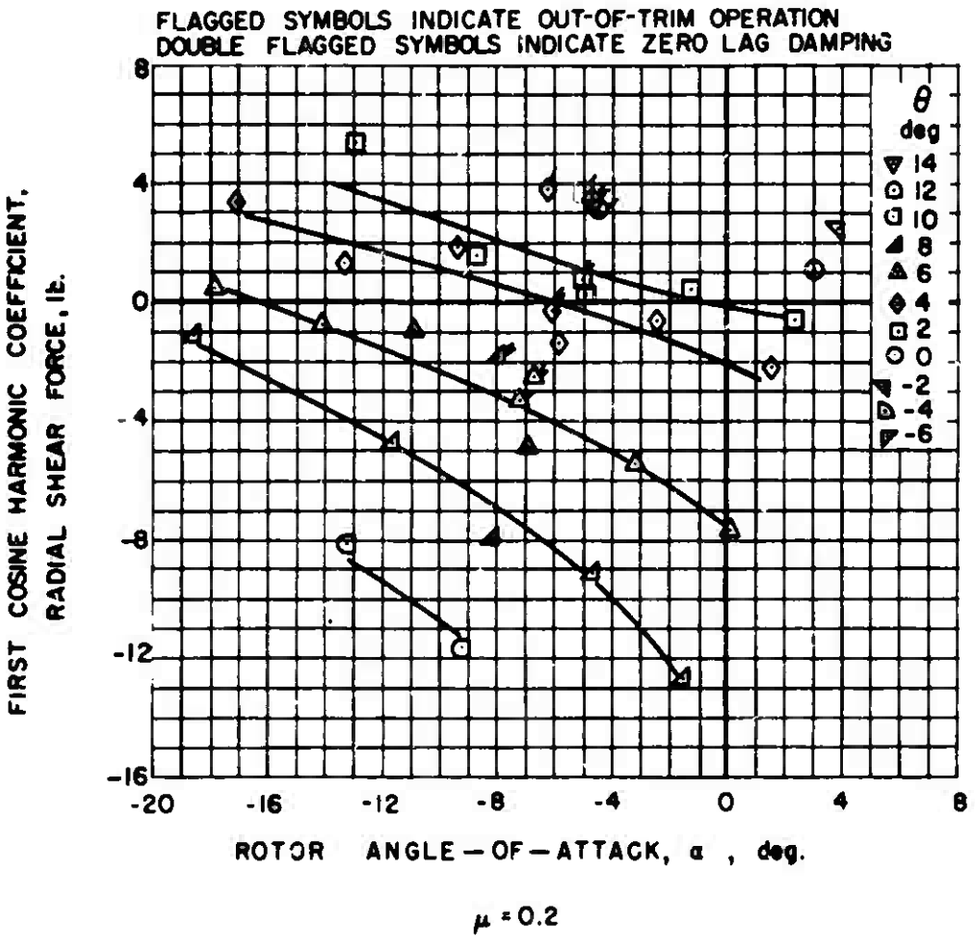

Figure 60. Experimental Radial Shear Force.

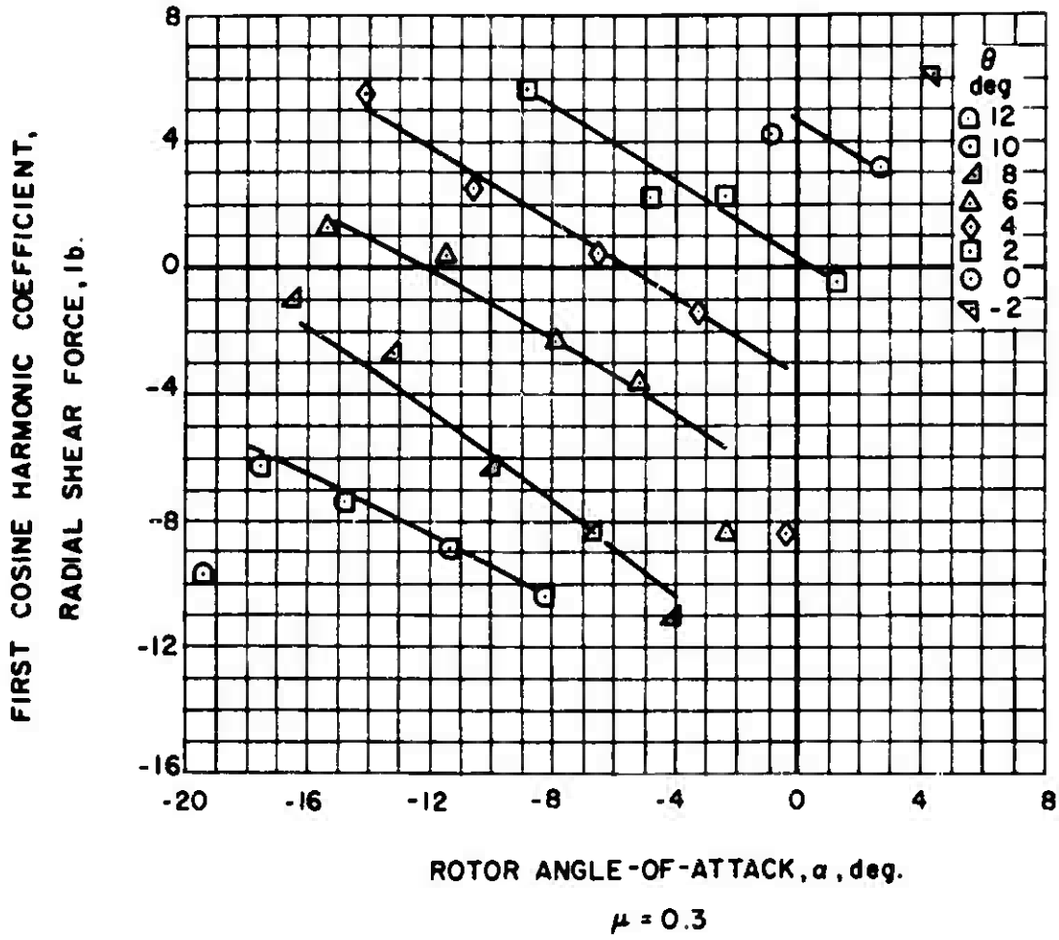

Figure 61. Experimental Radial Shear Force.

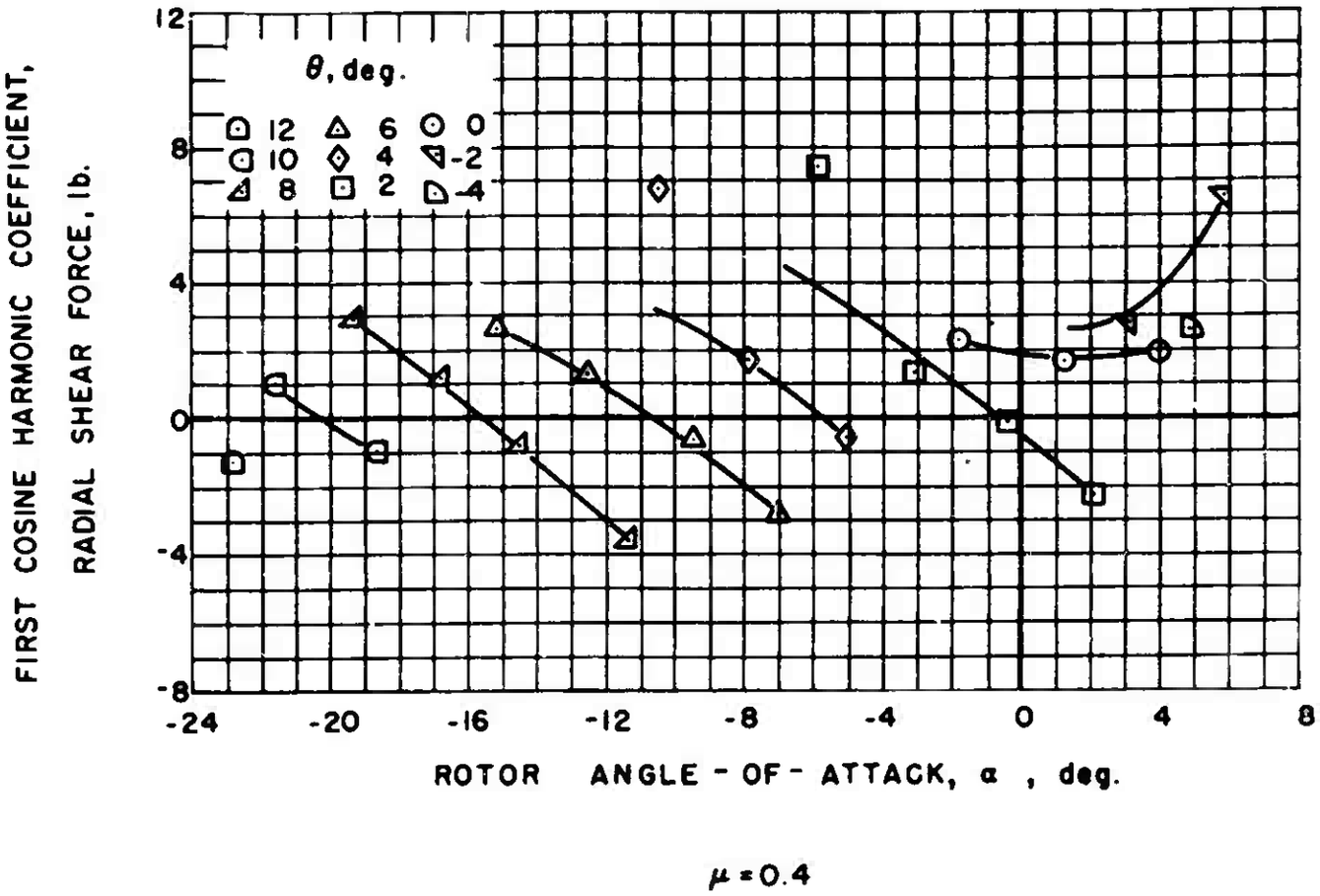

Figure 62. Experimental Radial Shear Force.

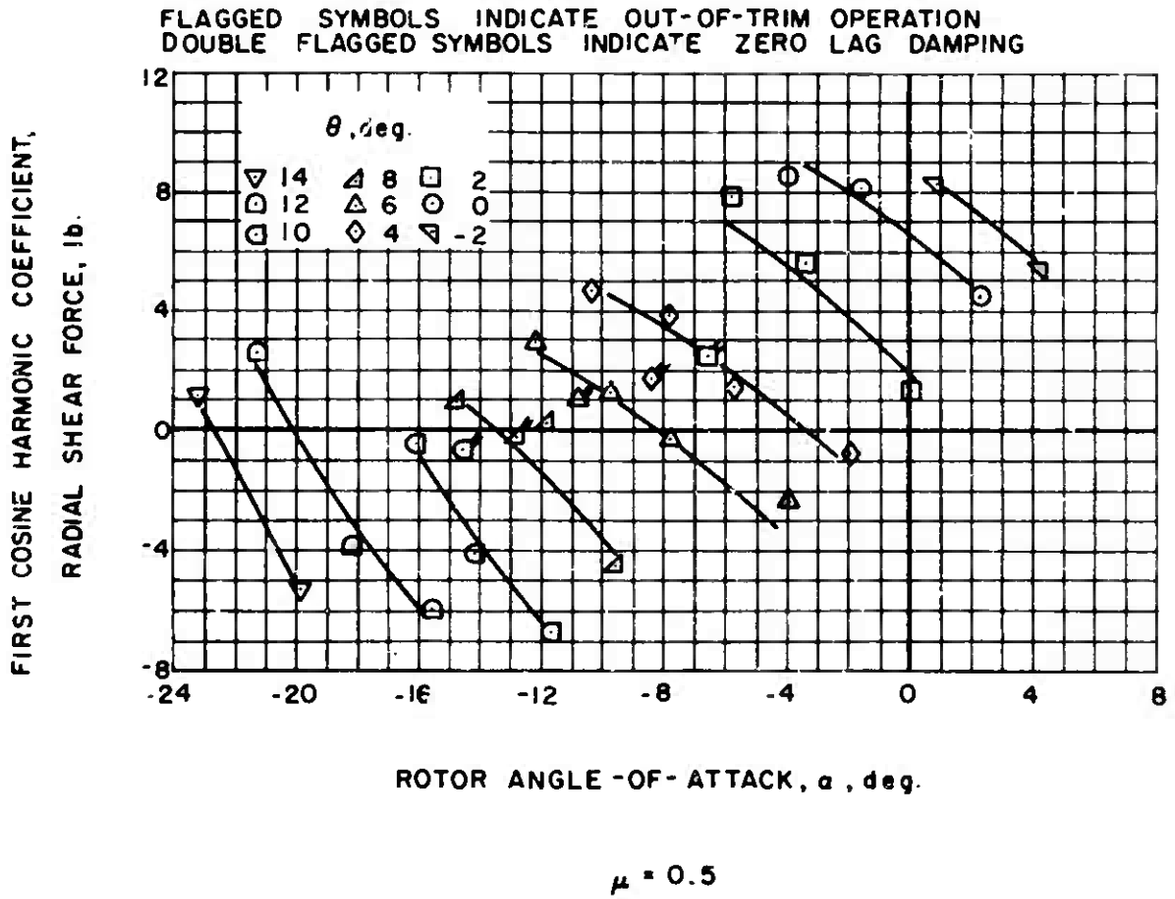

Figure 63. Experimental Radial Shear Force.

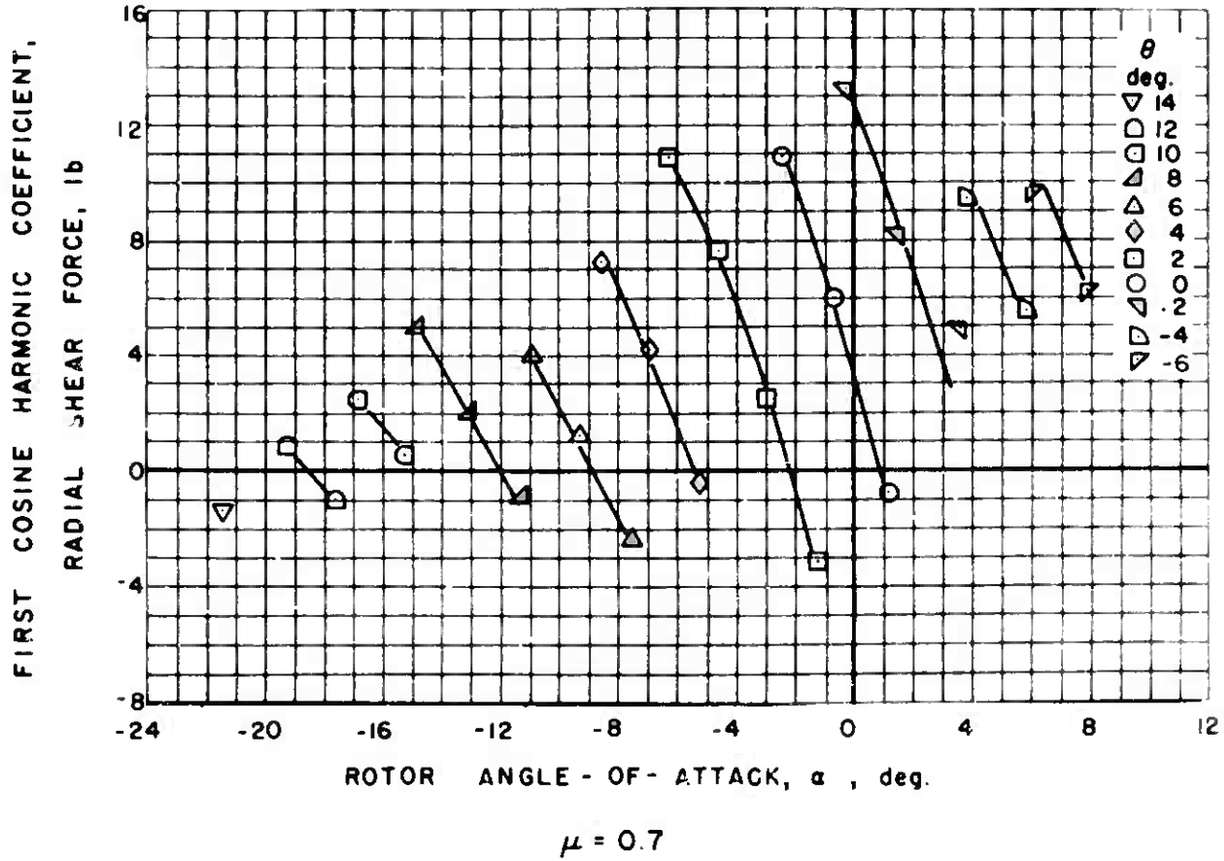

Figure 64. Experimental Radial Shear Force.

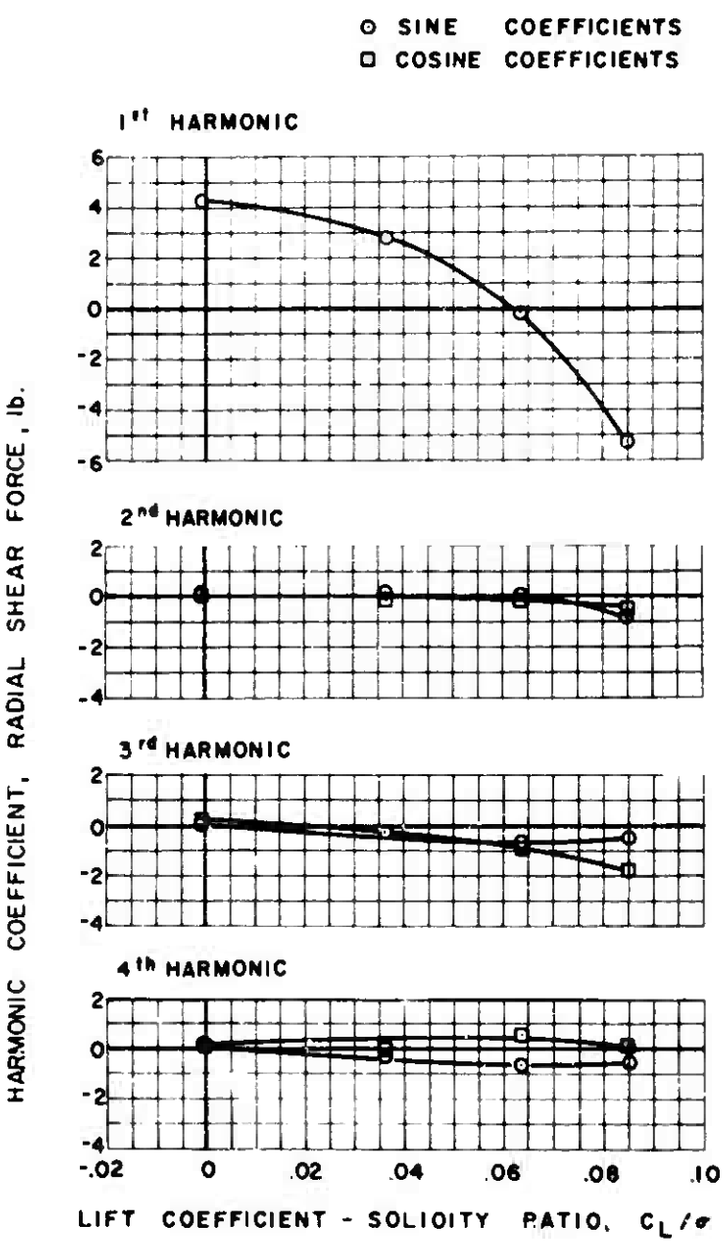

Figure 65. Experimental Radial Shear Force.

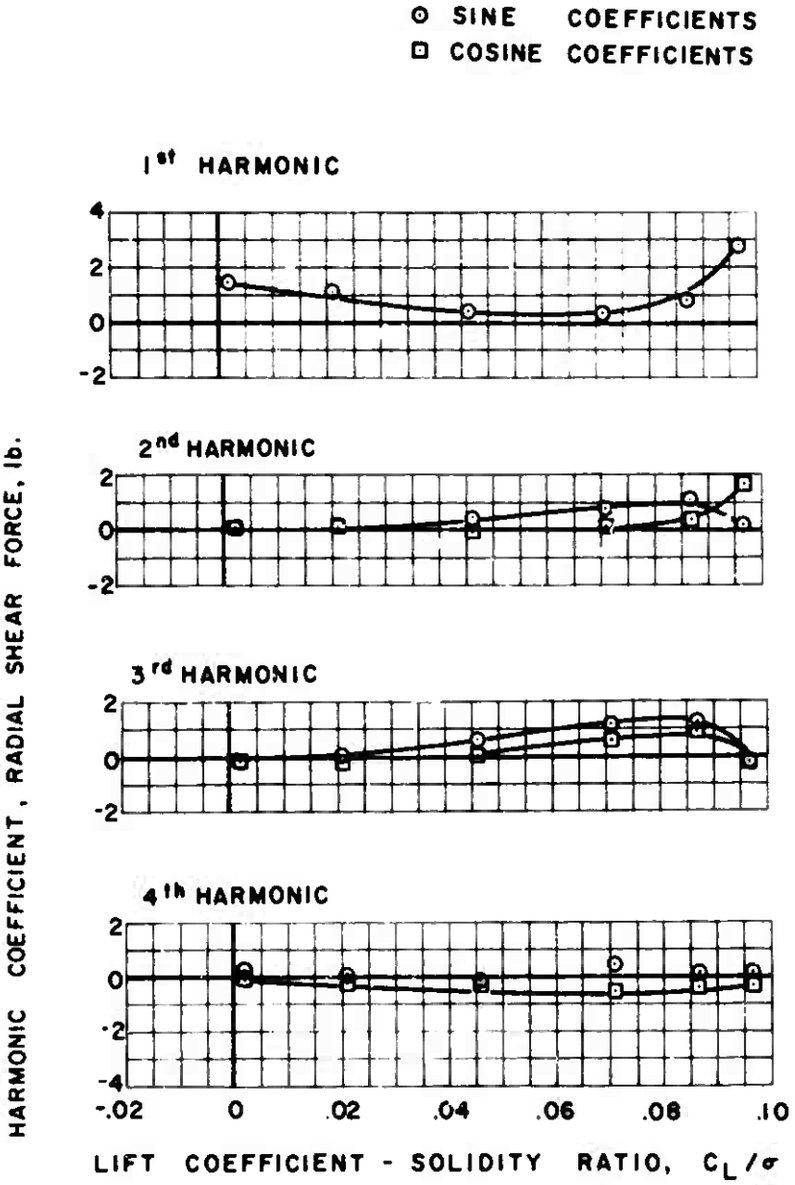

Figure 66. Experimental Radial Shear Force.

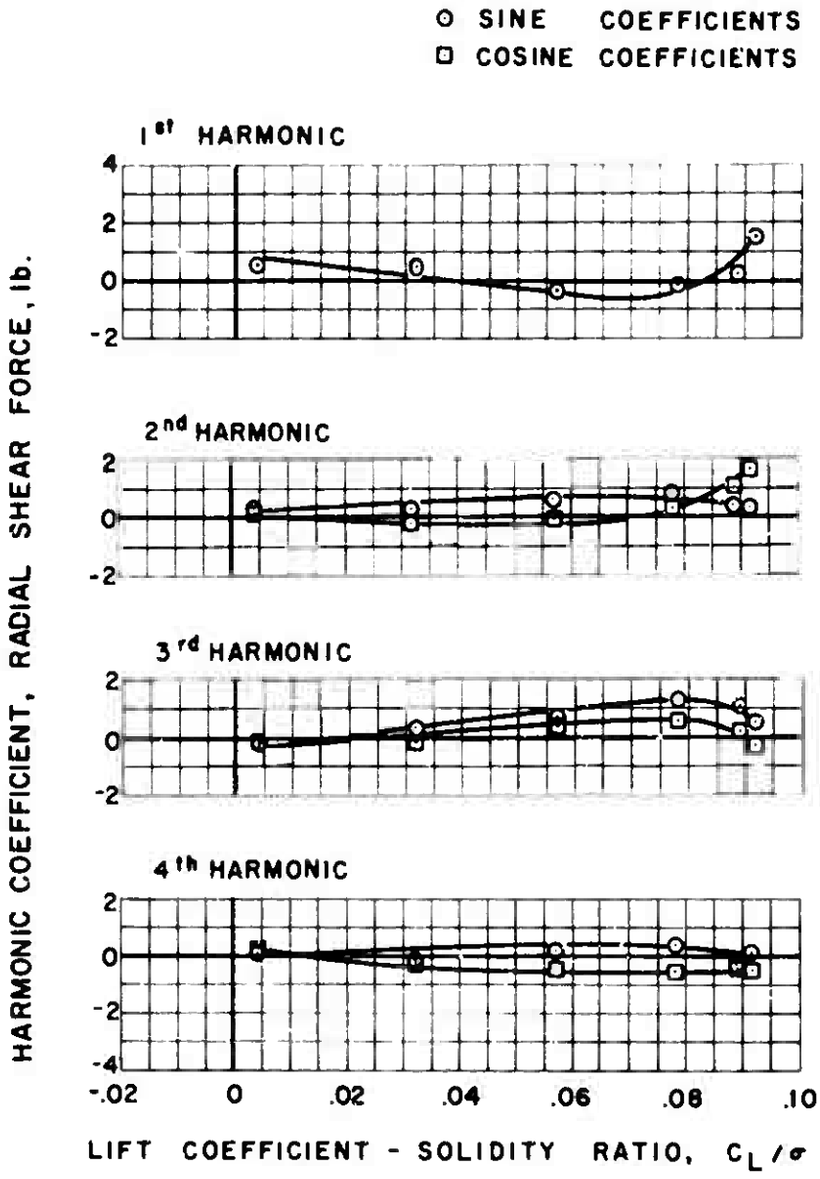

Figure 67. Experimental Radial Shear Force.

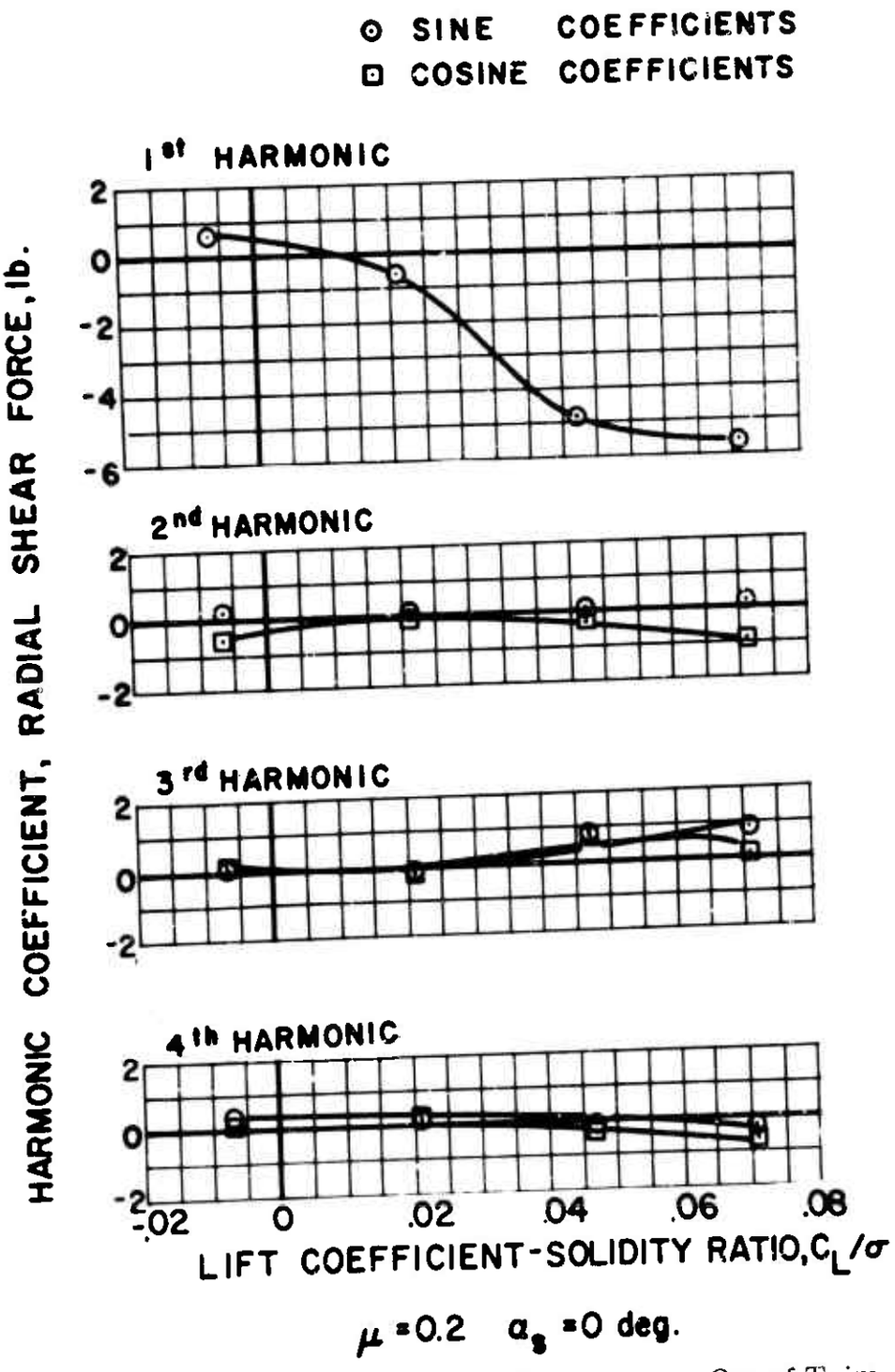

Figure 68. Experimental Radial Shear Force, Out of Trim, -4 Degree Longitudinal Flapping.

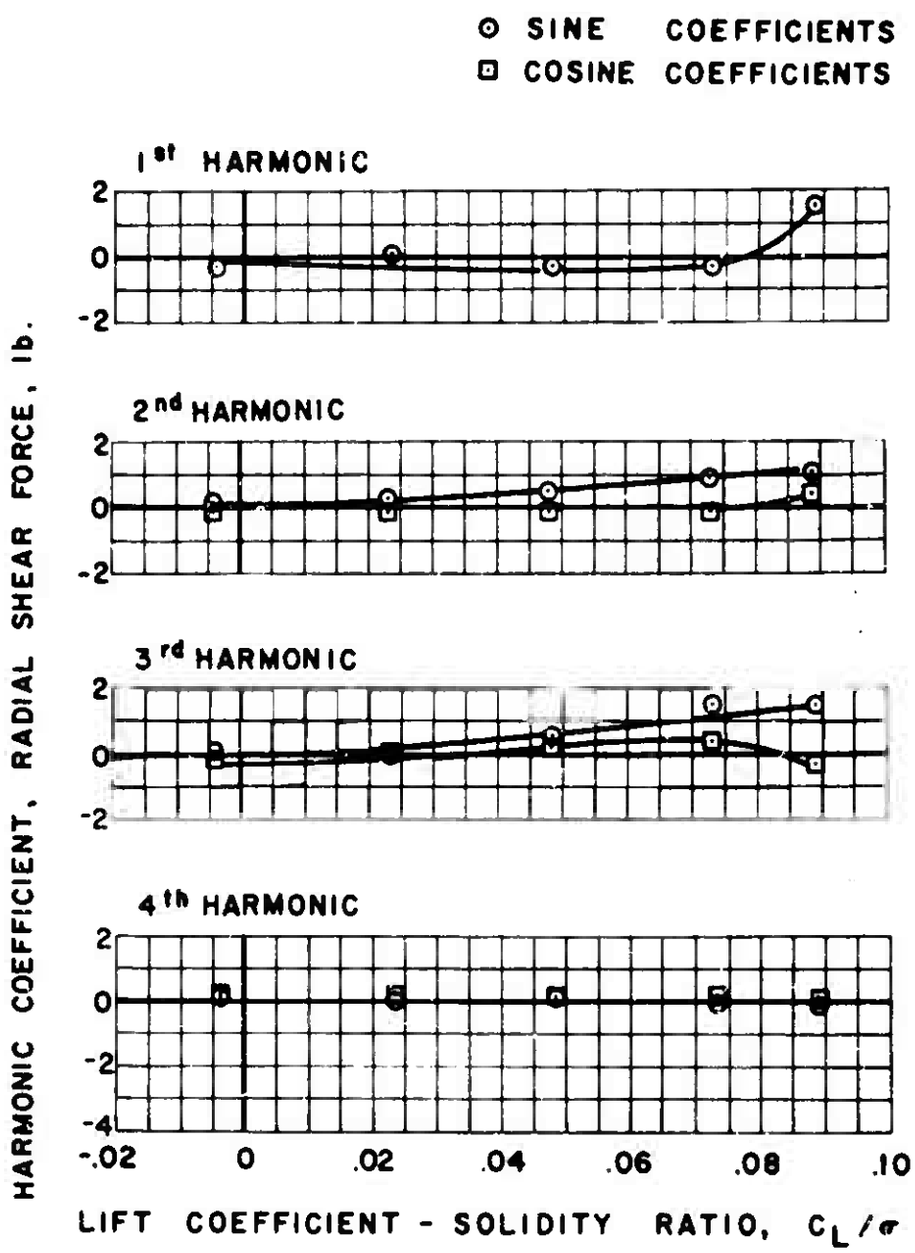

Figure 69. Experimental Radial Shear Force, Zero Lag Damping.

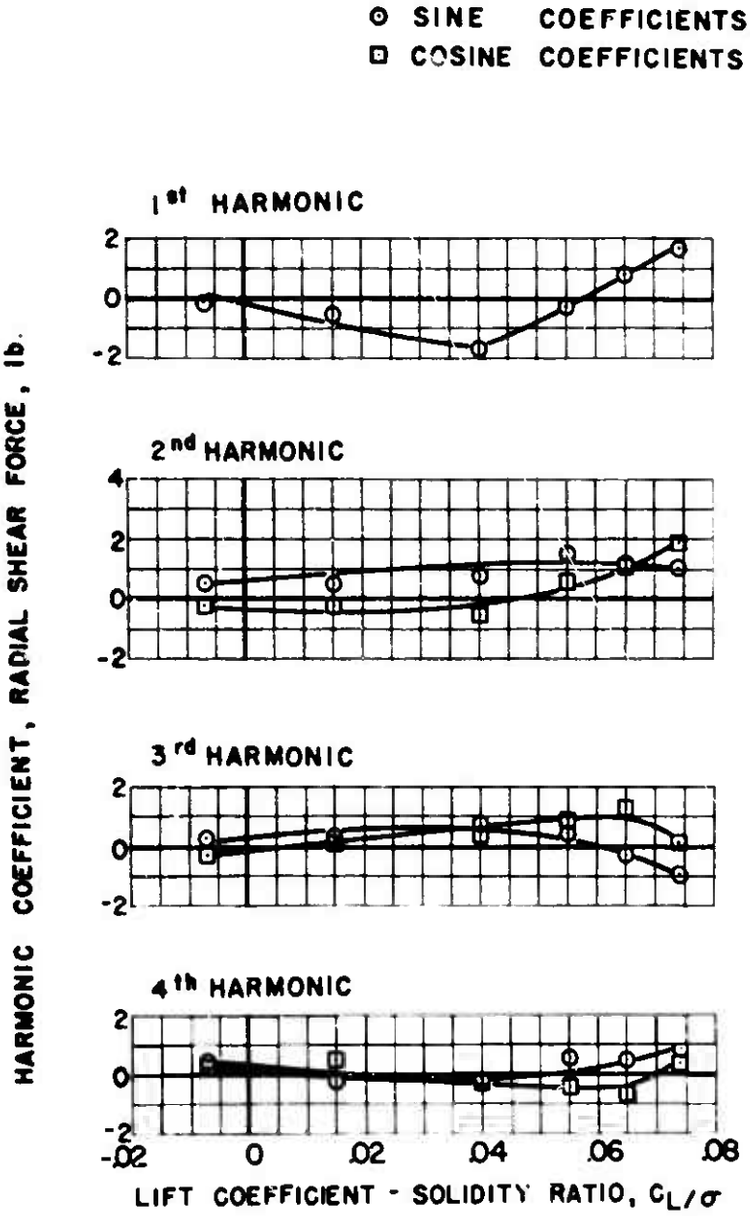

Figure 70. Experimental Radial Shear Force.

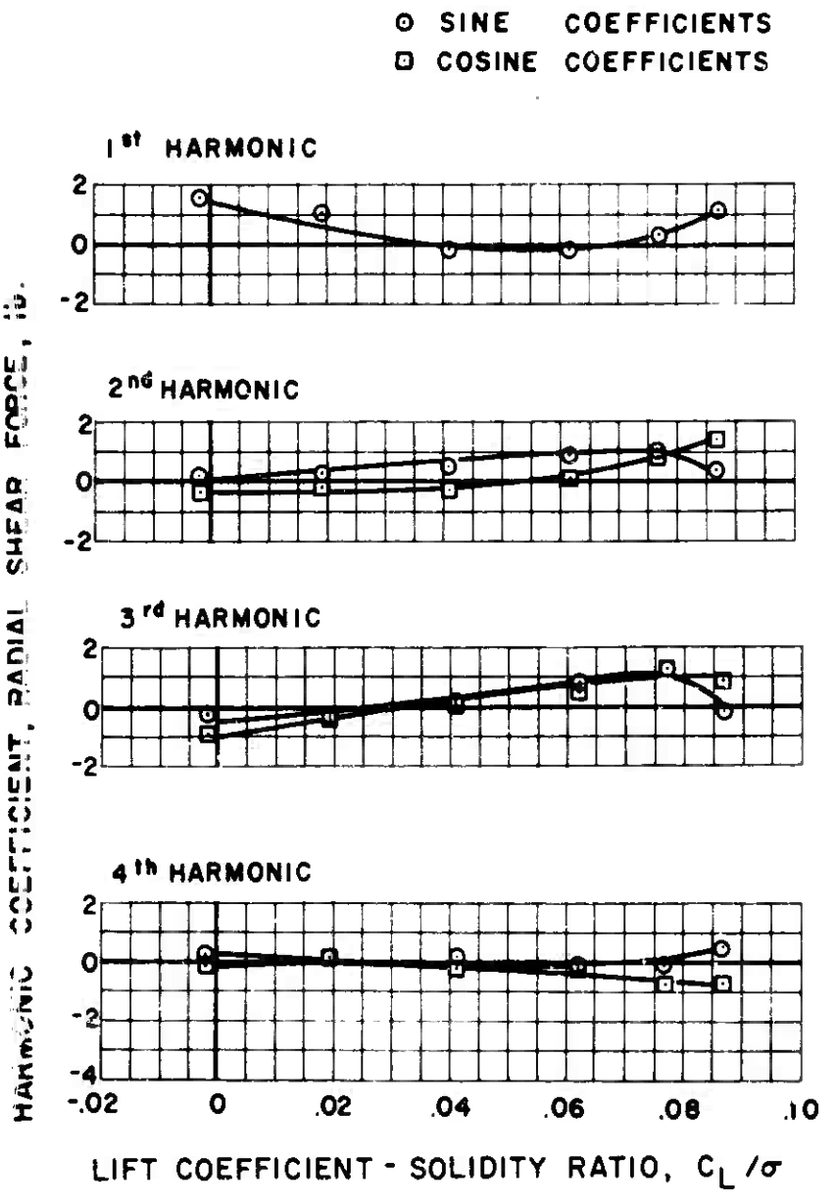

Figure 71. Experimental Radial Shear Force.

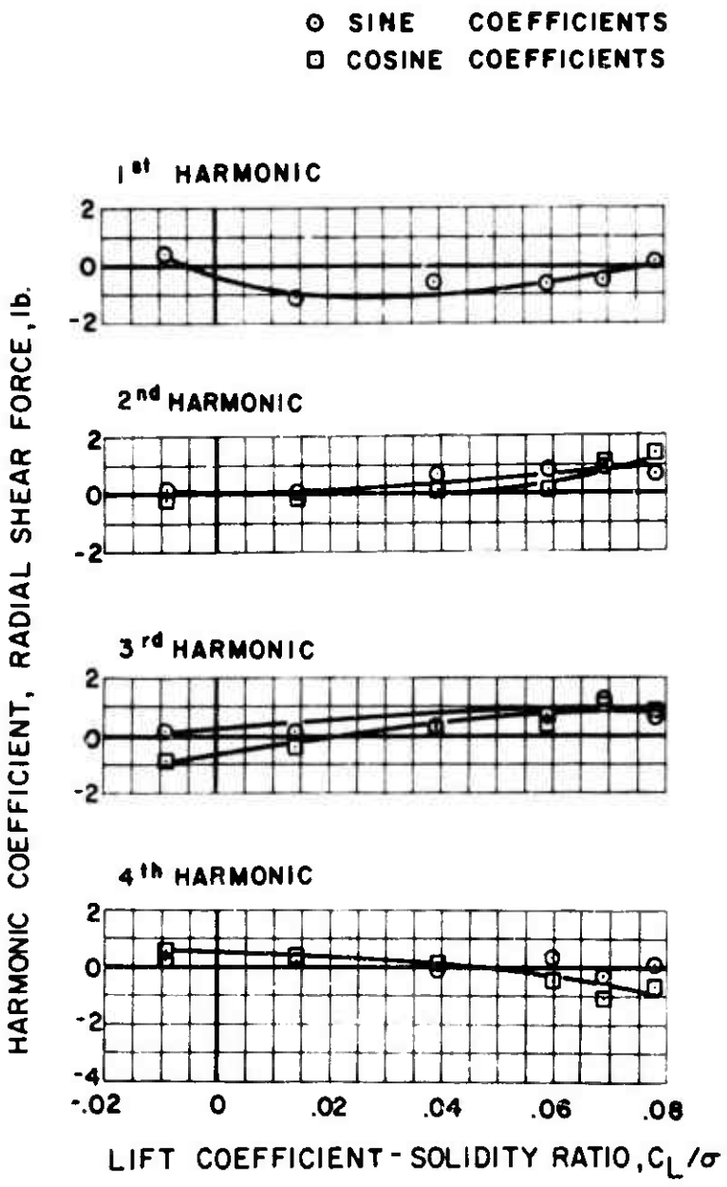

Figure 72. Experimental Radial Shear Force.

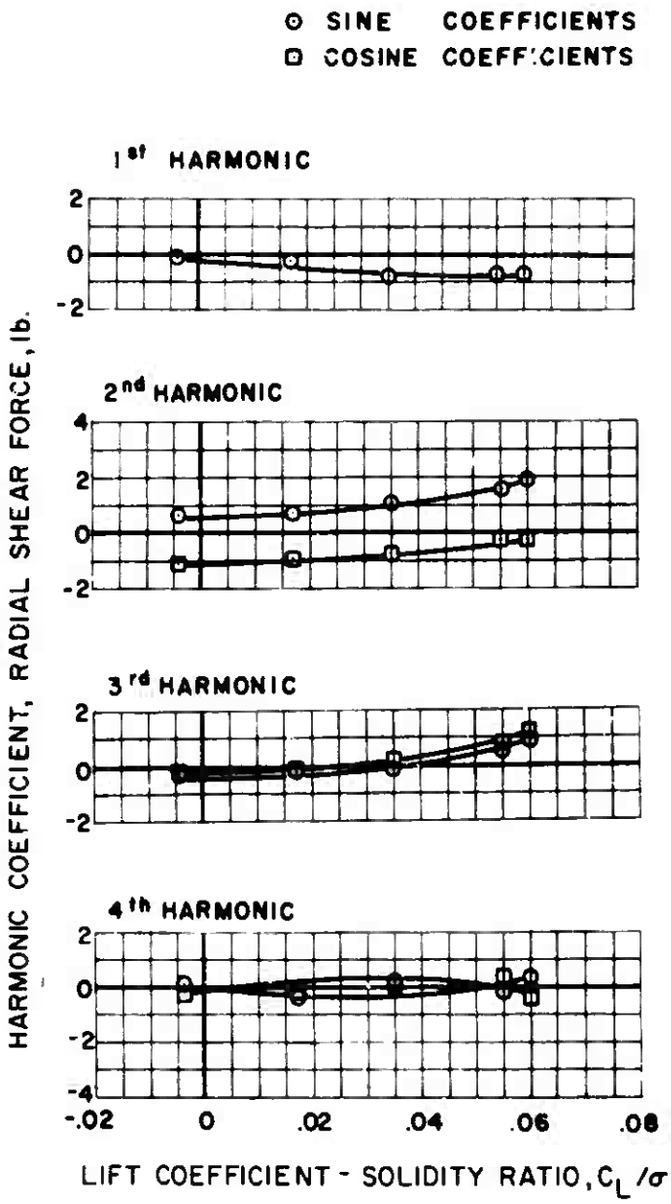

Figure 73. Experimental Radial Shear Force.

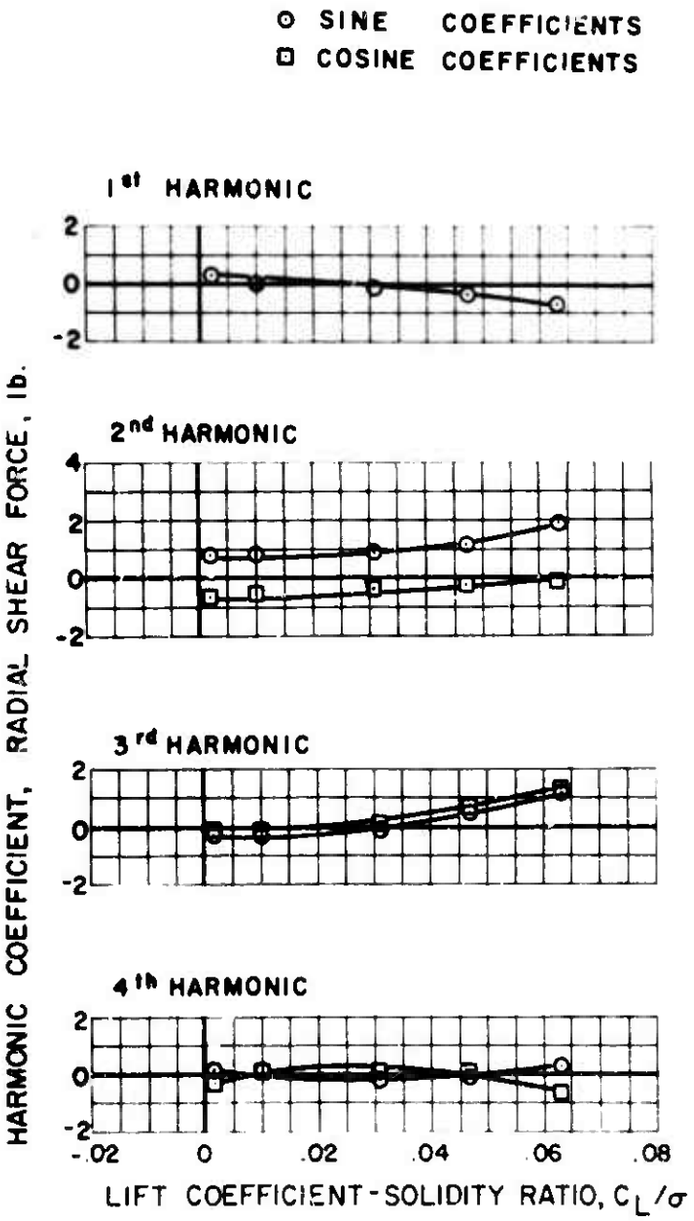

$\mu = 0.4$ $\alpha_s = 0$ deg.

Figure 74. Experimental Radial Shear Force.

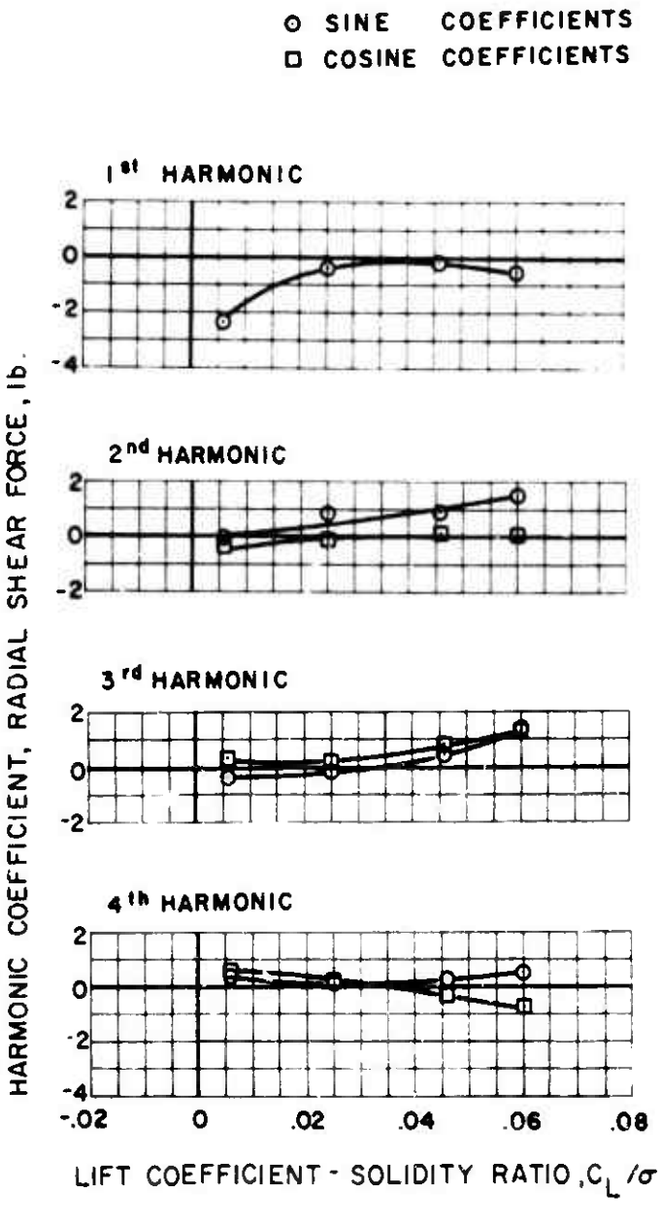

Figure 75. Experimental Radial Shear Force.

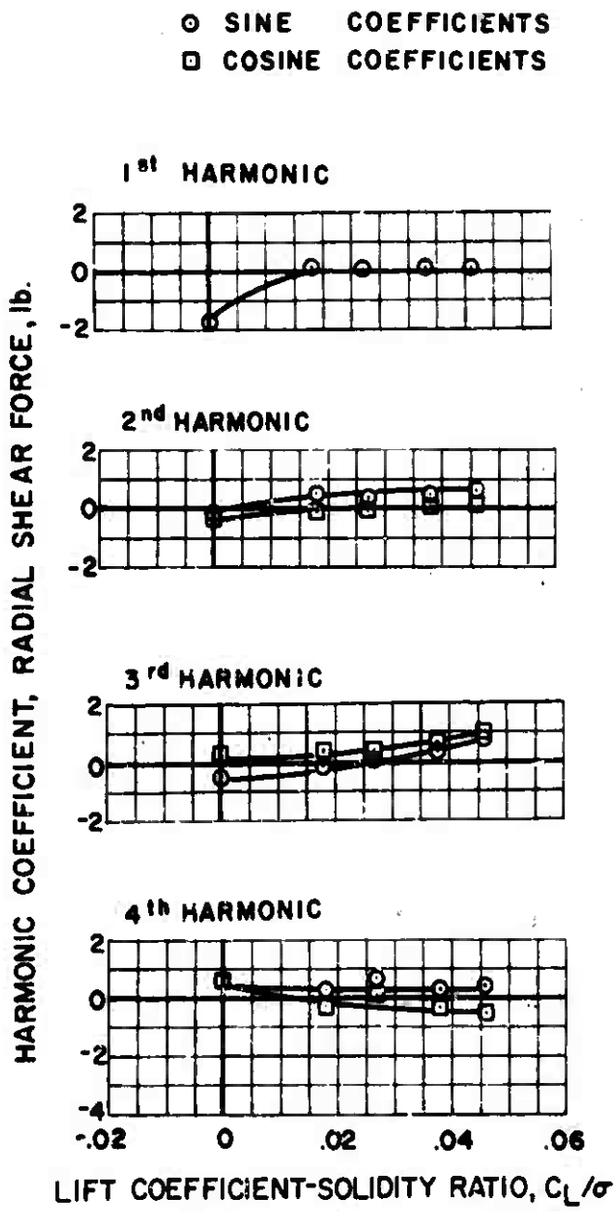

$\mu = 0.4$ $\alpha_s = -8$ deg.

Figure 76. Experimental Radial Shear Force.

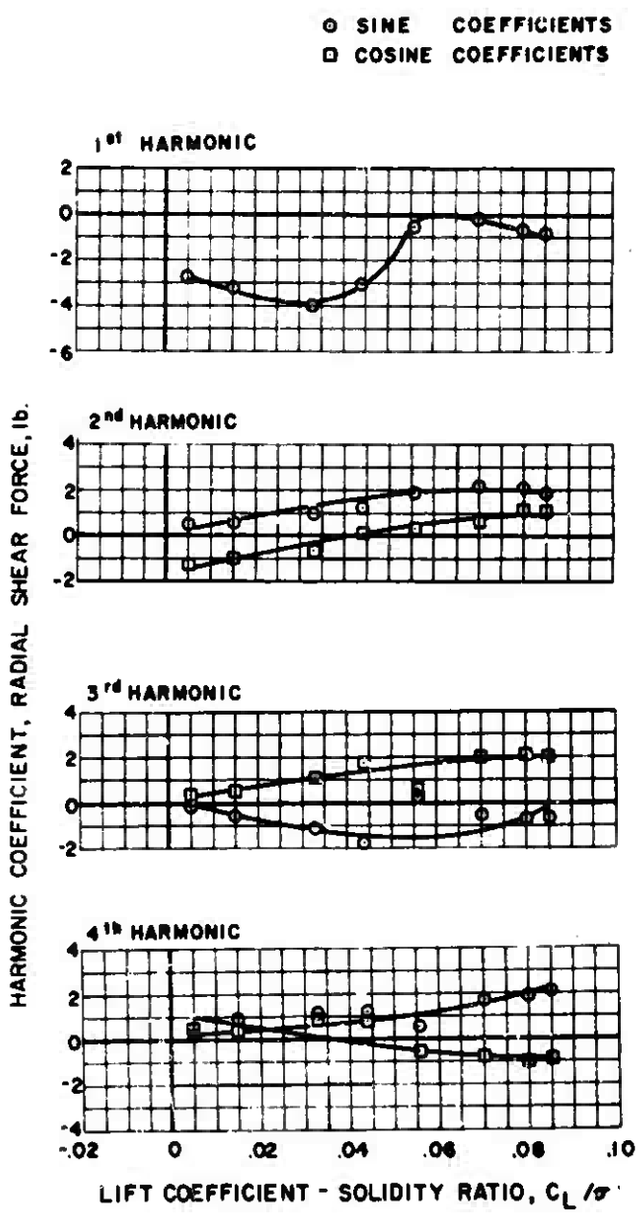

Figure 77. Experimental Radial Shear Force.

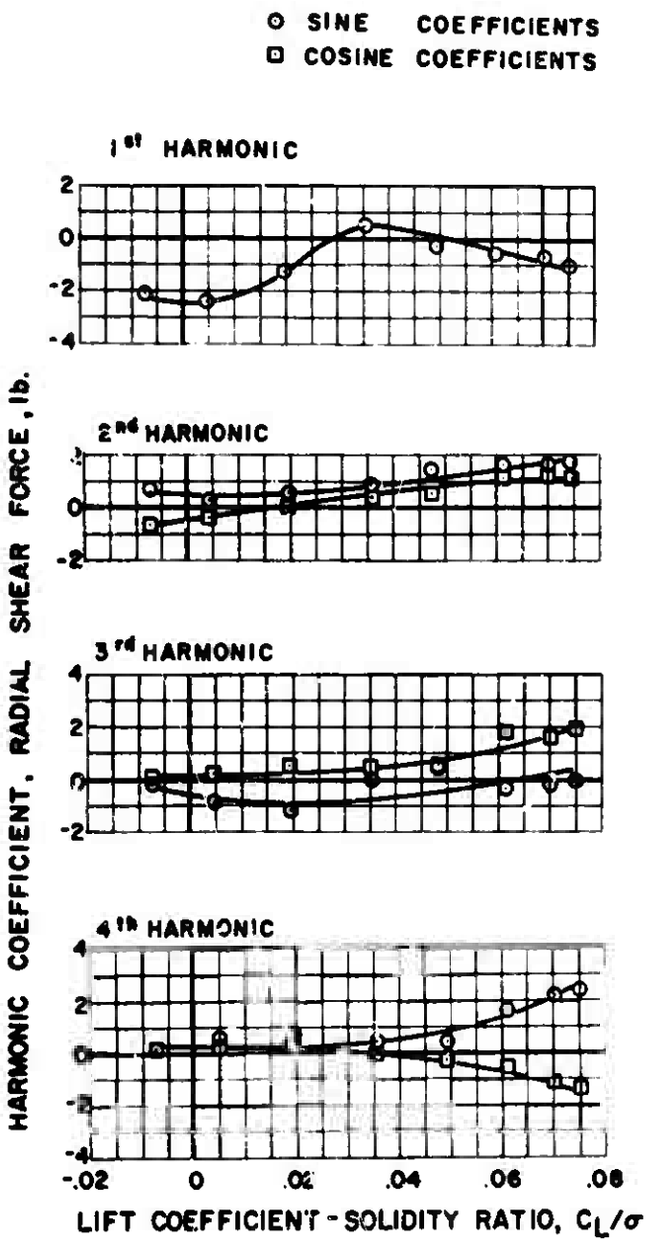

Figure 78. Experimental Radial Shear Force.

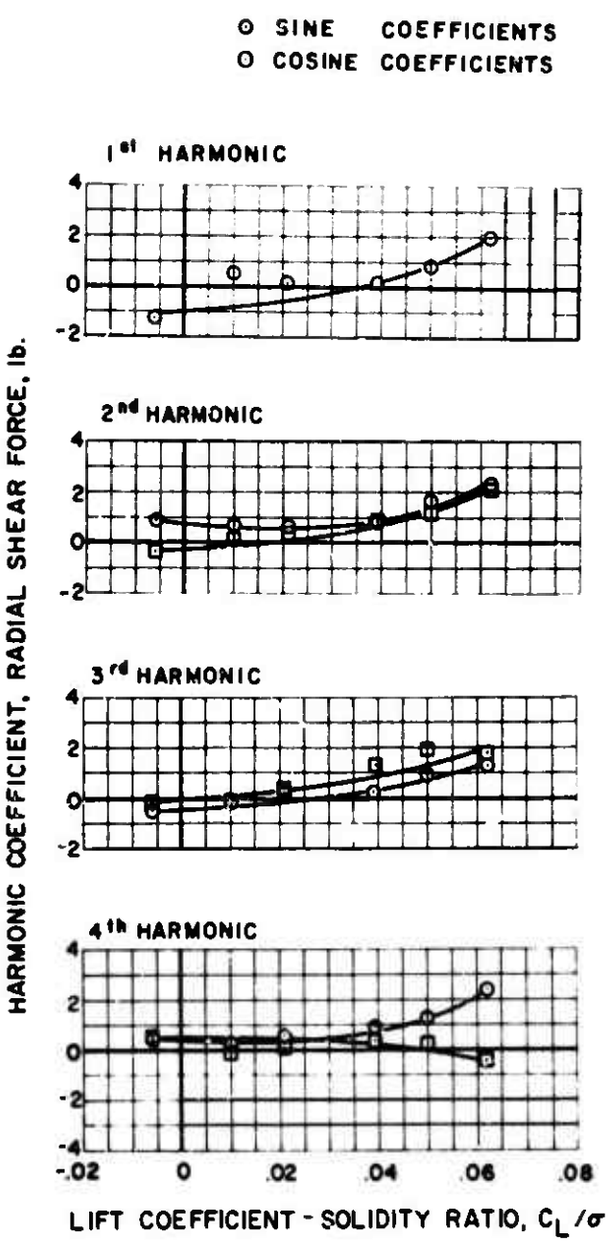

Figure 79. Experimental Radial Shear Force.

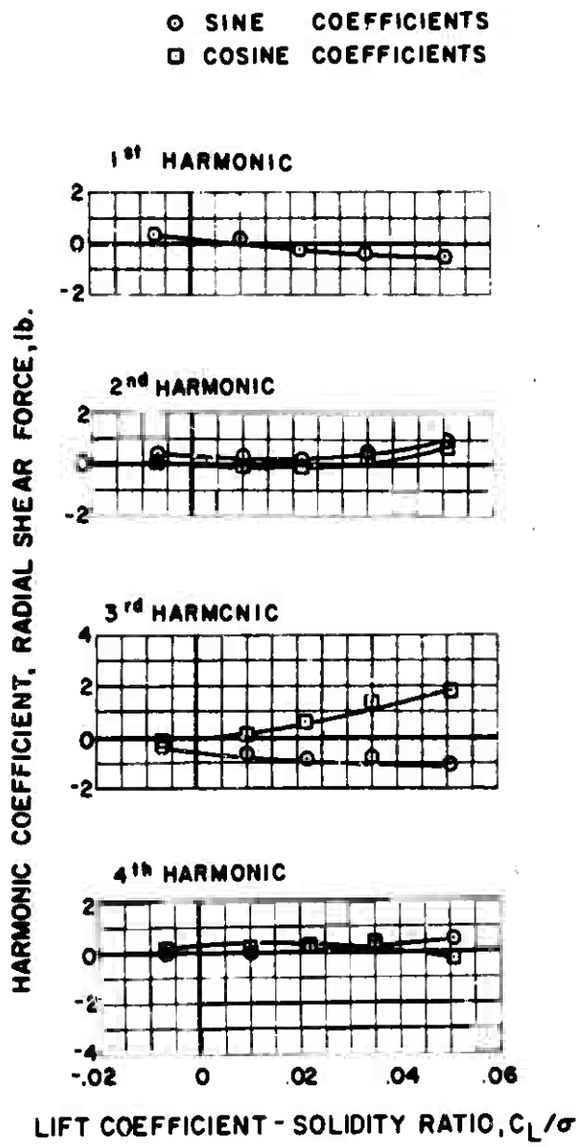

Figure 80. Experimental Radial Shear Force, Zero Lag Damping.

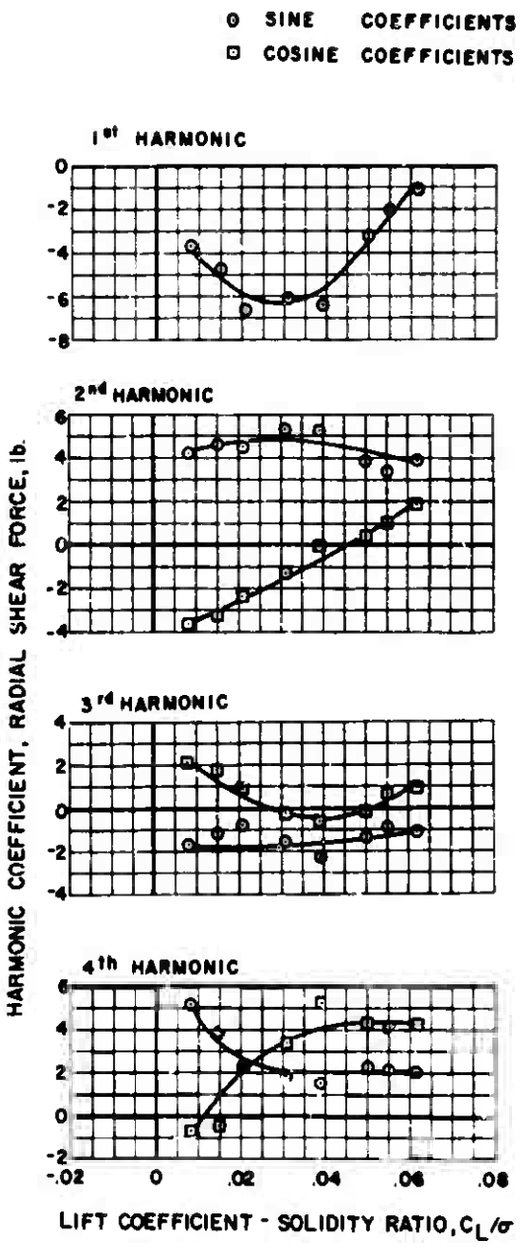

Figure 81. Experimental Radial Shear Force.

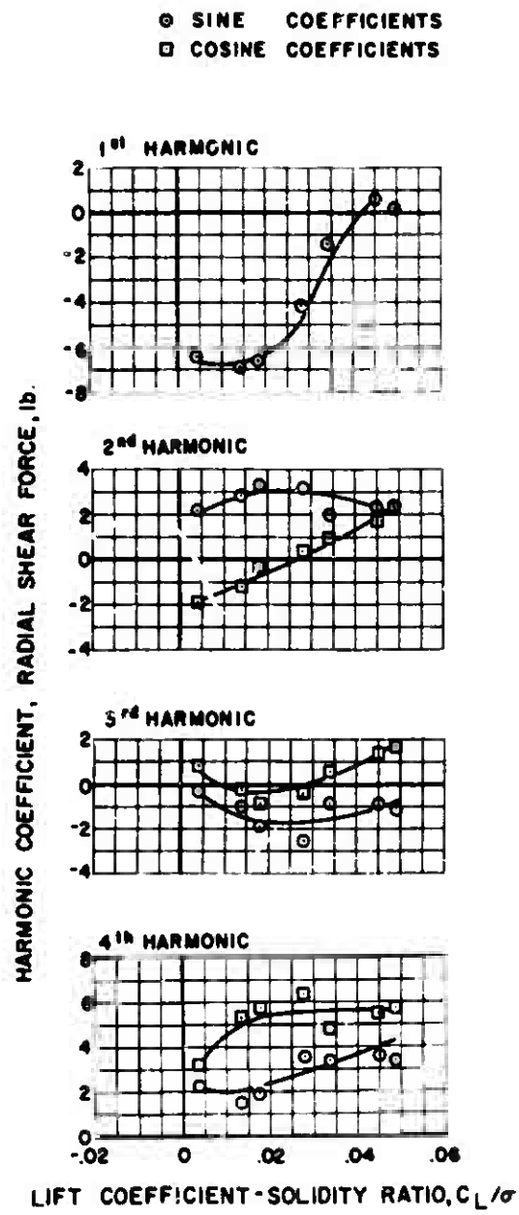

Figure 82. Experimental Radial Shear Force.

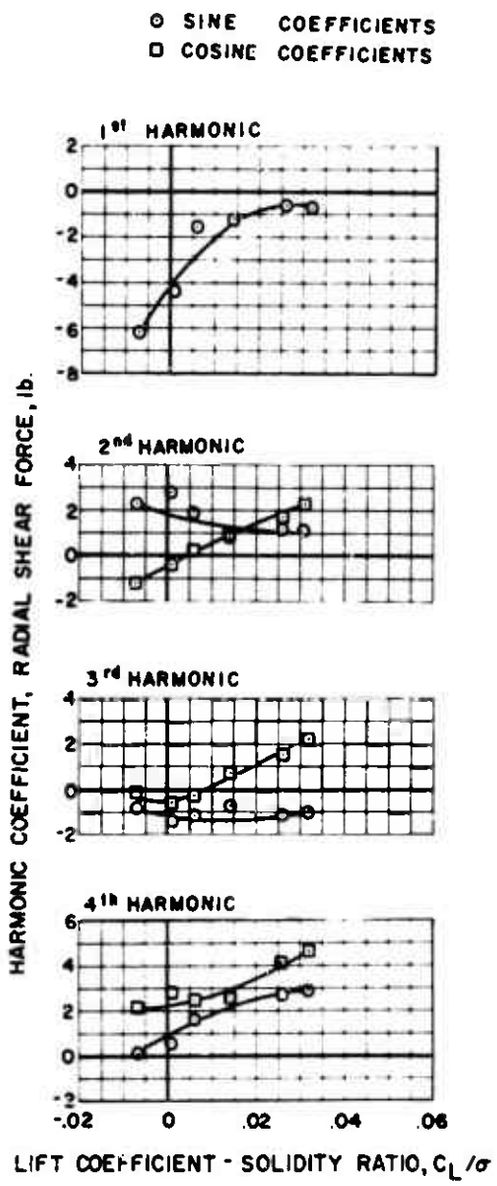

Figure 83. Experimental Radial Shear Force.

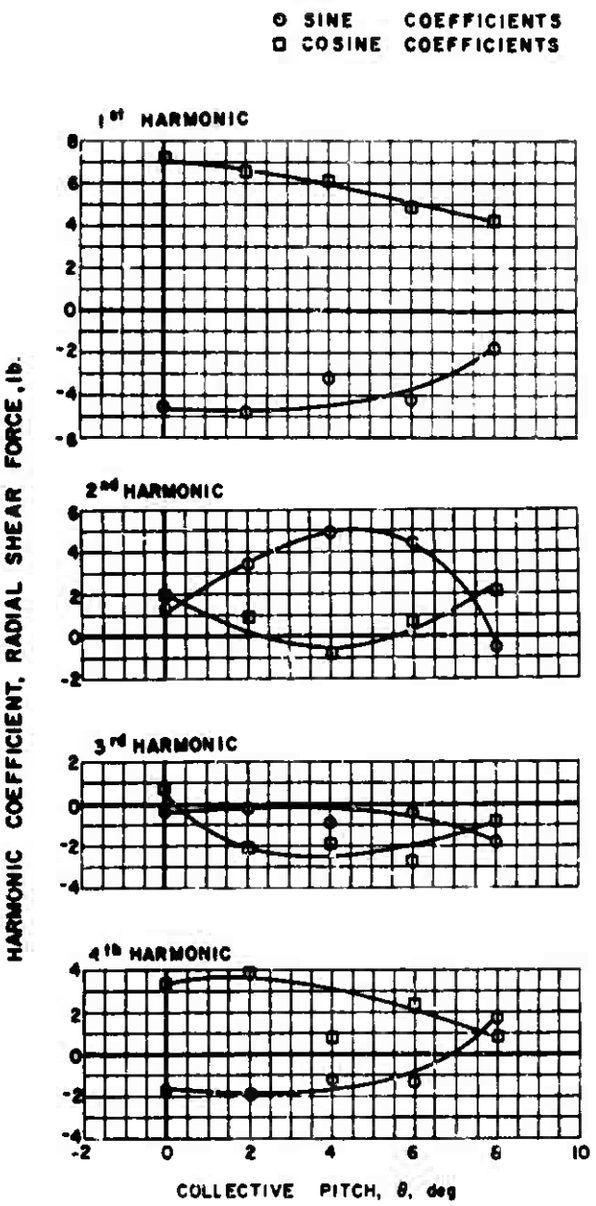

Figure 84. Experimental Radial Shear Force.

APPENDIX III

EXPERIMENTAL VIBRATORY MOMENT AMPLITUDE FIGURES

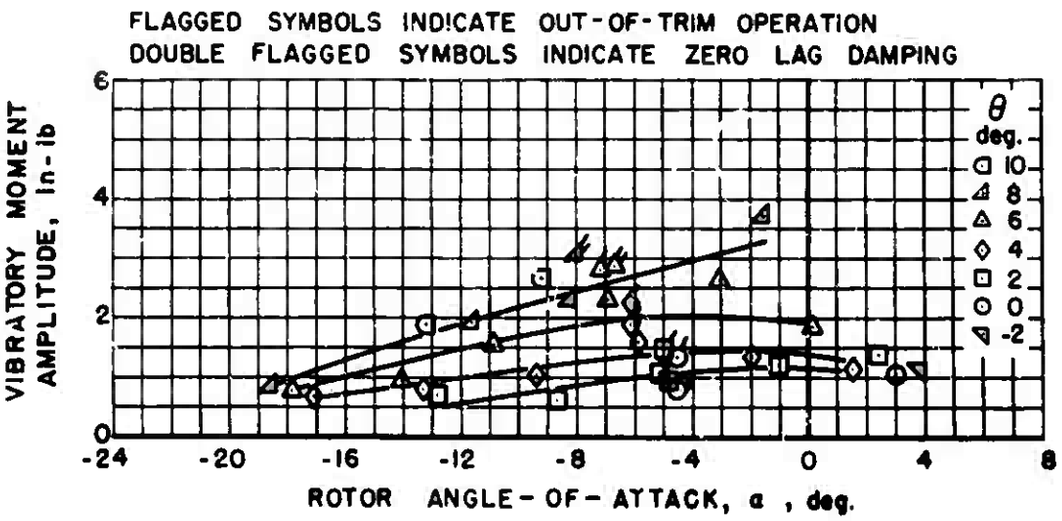

(a) FLATWISE BENDING MOMENT, 21 %R

Figure 85. Experimental Vibratory Moment Amplitude, $\mu = 0.2$.

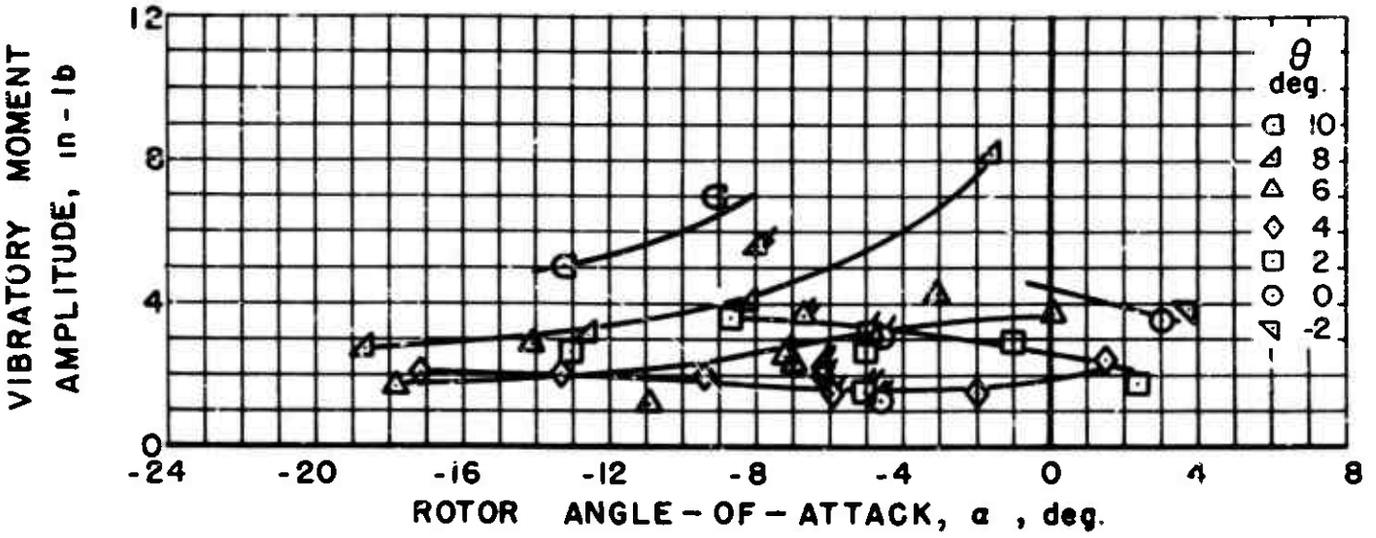

(b) EDGEWISE BENDING MOMENT, 21% R

Figure 85. Continued.

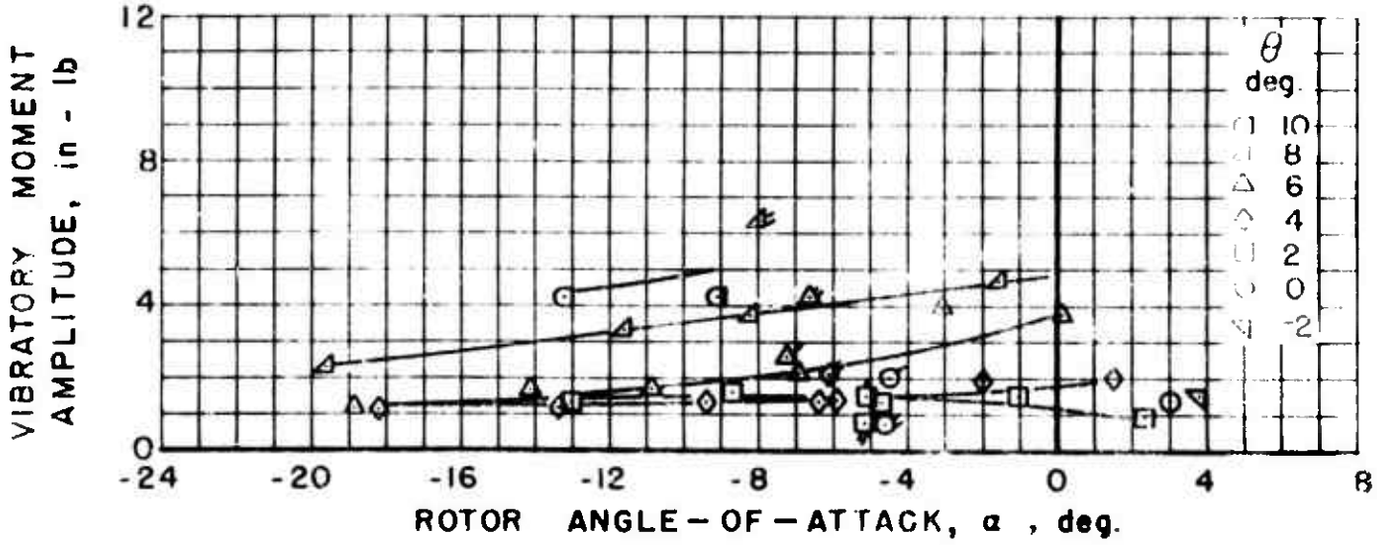

(c) EDGEWISE BENDING MOMENT, 47 % R

Figure 85. Continued.

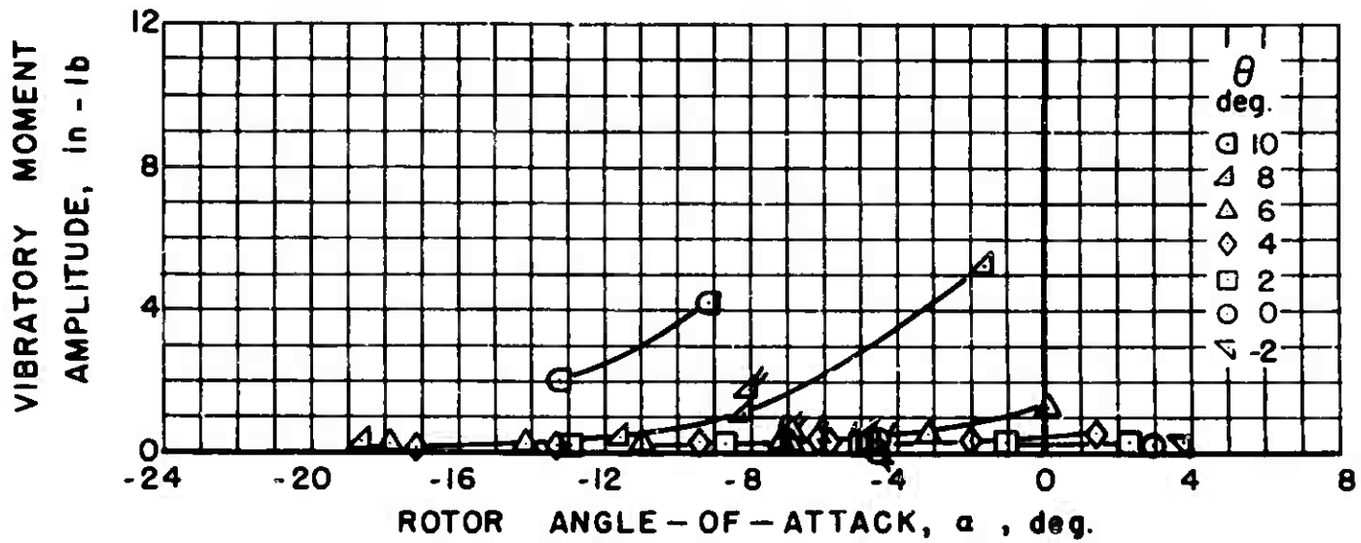

(d) TORSIONAL MOMENT, 17.5 % R

Figure 85. Concluded.

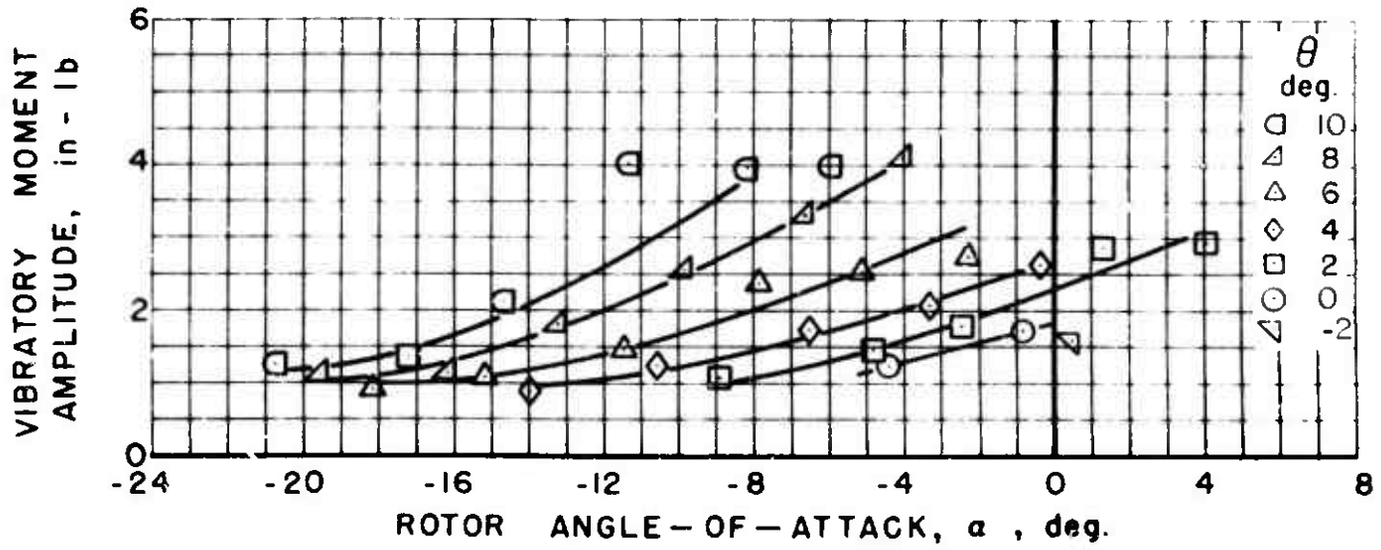

(a) FLATWISE BENDING MOMENT, 21 % R

Figure 86. Experimental Vibratory Moment Amplitude, $\mu = 0.3$.

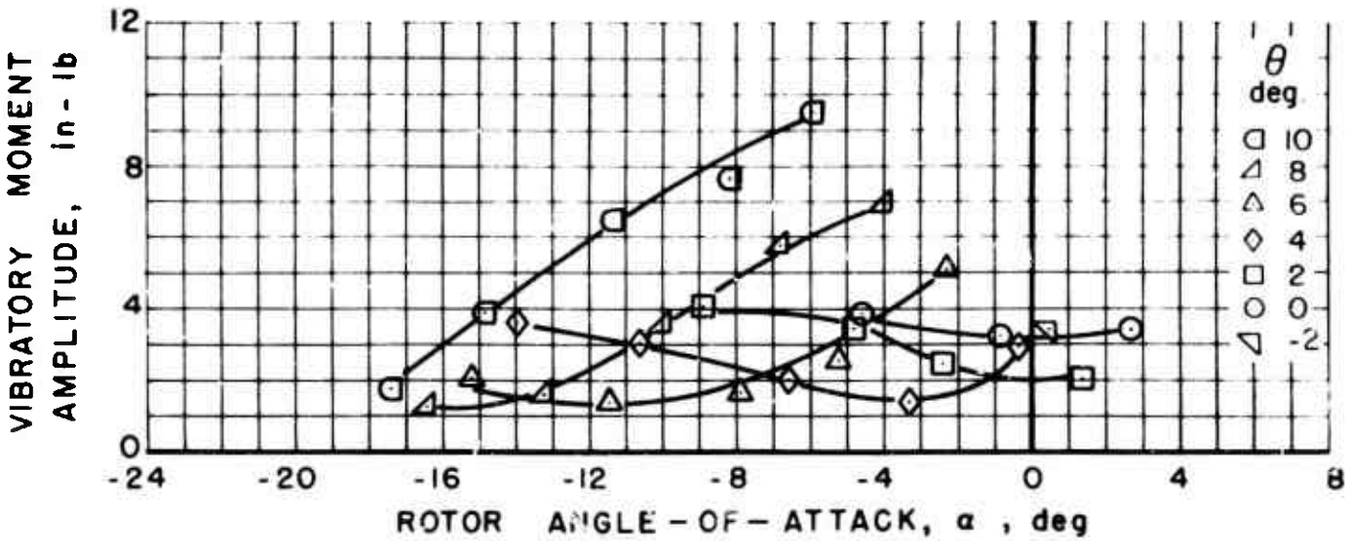

(b) EDGEWISE BENDING MOMENT, 21 % R

Figure 86. Continued.

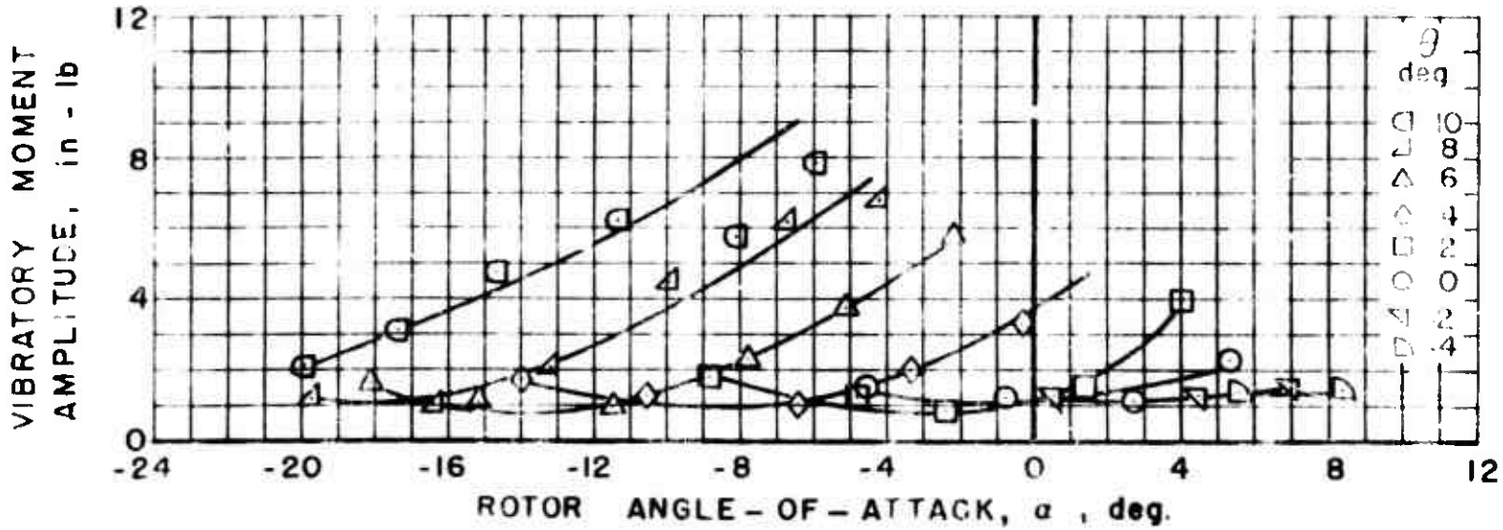

(c) EDGEWISE BENDING MOMENT, 47 % R

Figure 86. Continued.

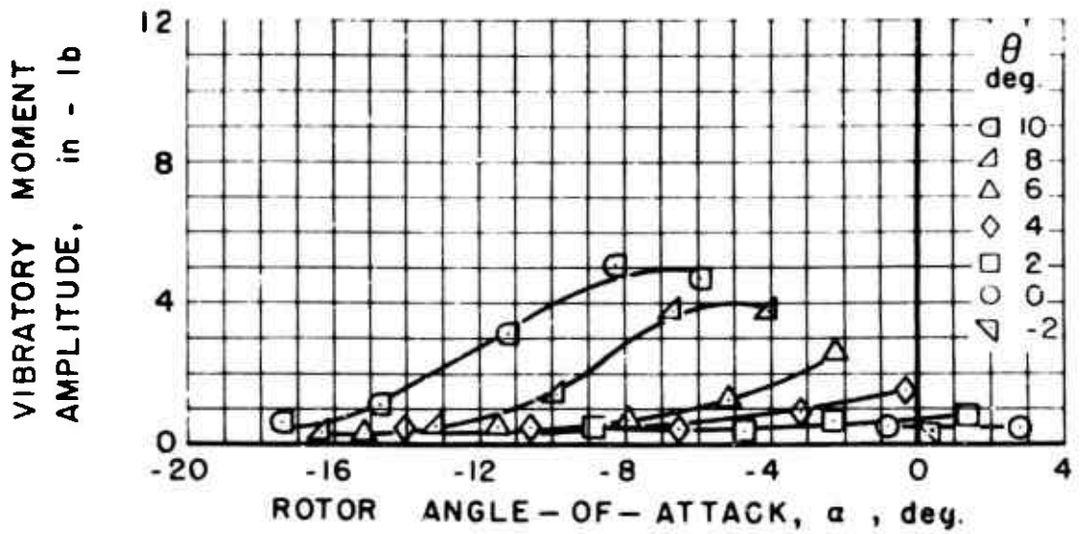

(d) TORSIONAL MOMENT, 17.5 % R

Figure 86. Concluded.

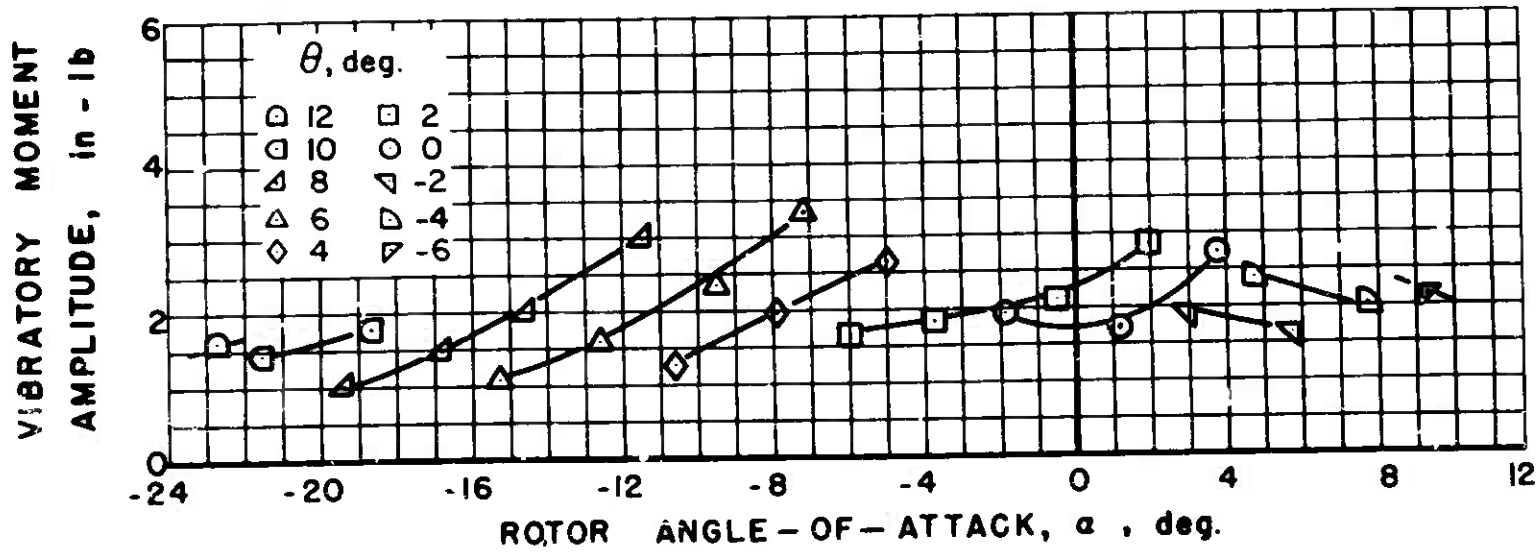

(a) FLATWISE BENDING MOMENT, 21 % R

Figure 87. Experimental Vibratory Moment Amplitude, $\mu = 0.4$.

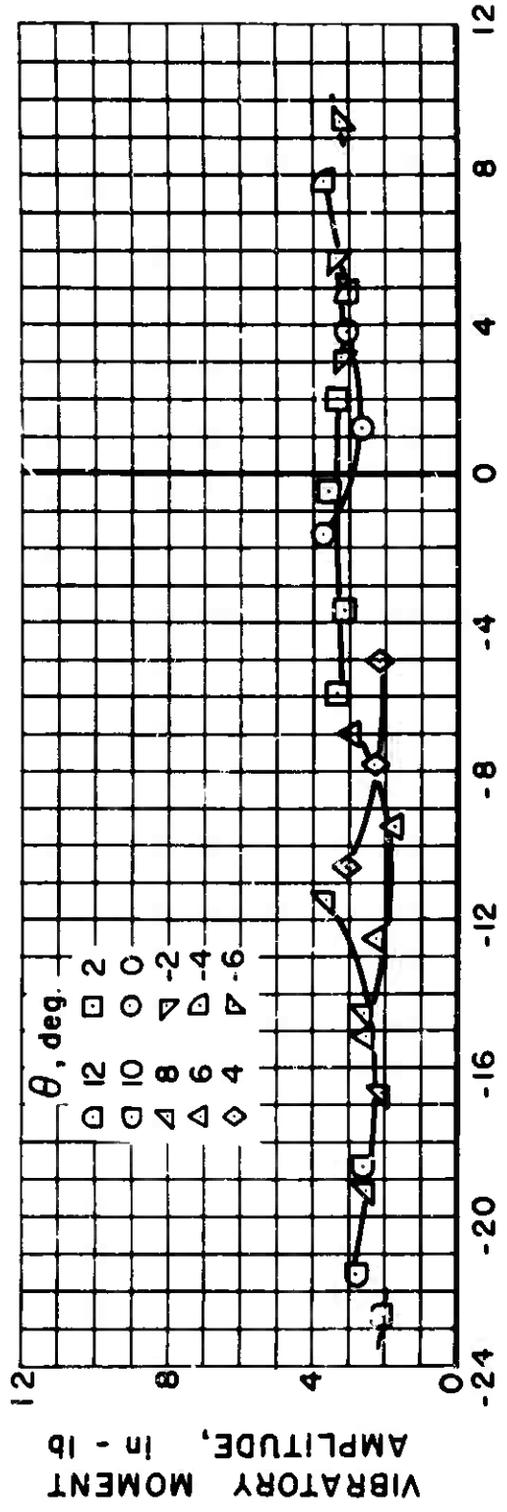

(b) EDGEWISE BENDING MOMENT, 21 %

Figure 87. Continued.

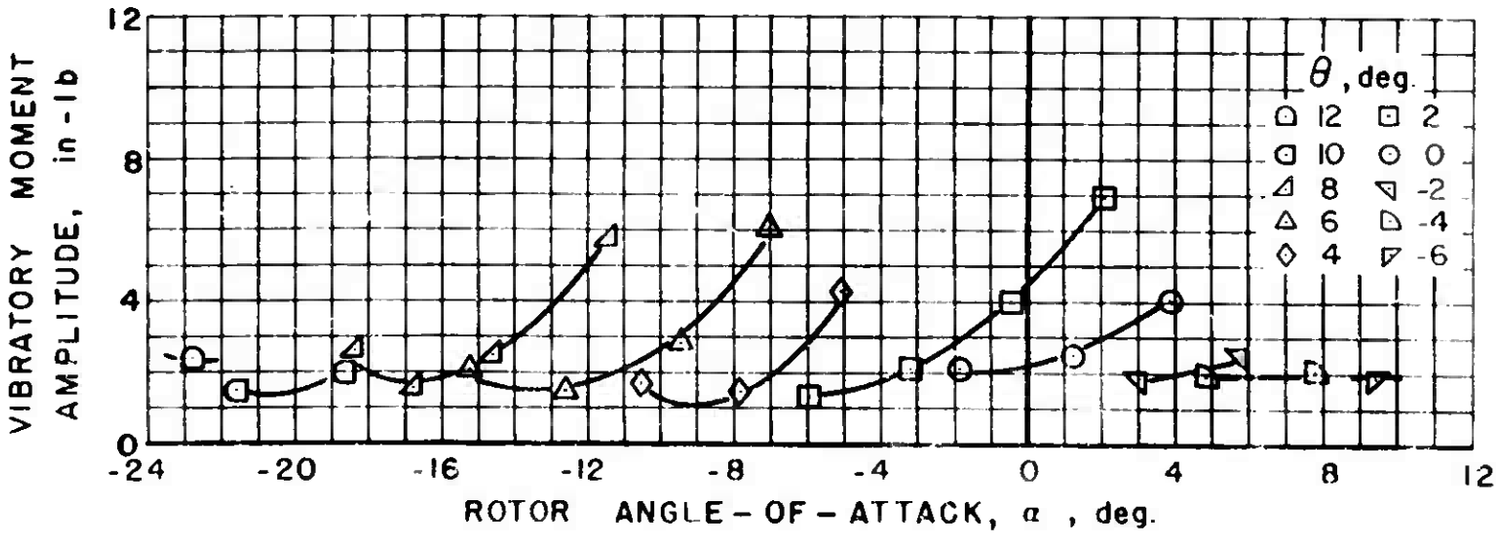

(c) EDGEWISE BENDING MOMENT, 47 % R

Figure 87. Continued.

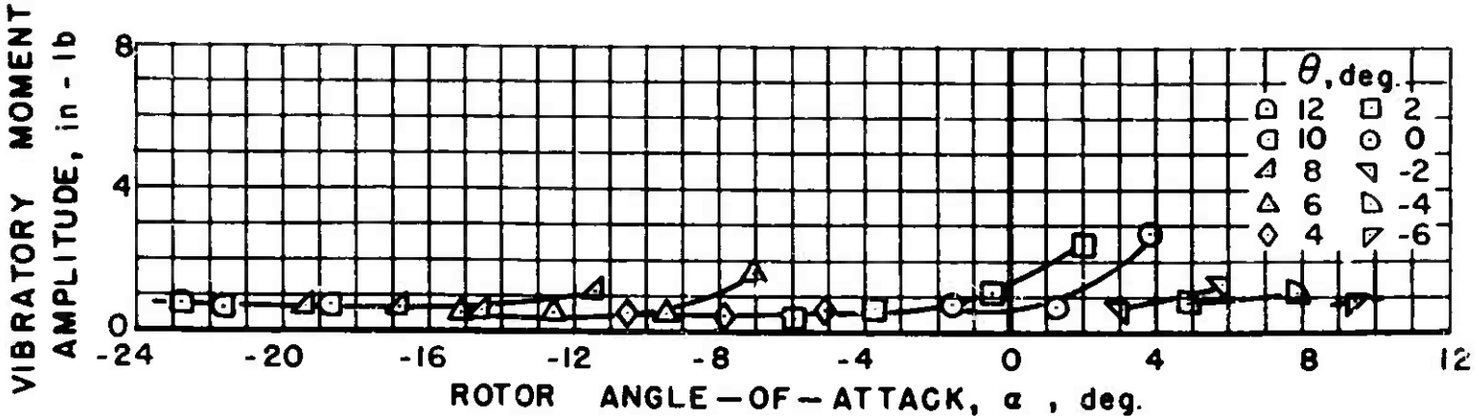

(d) TORSIONAL MOMENT, 17.5 % R

Figure 87. Concluded.

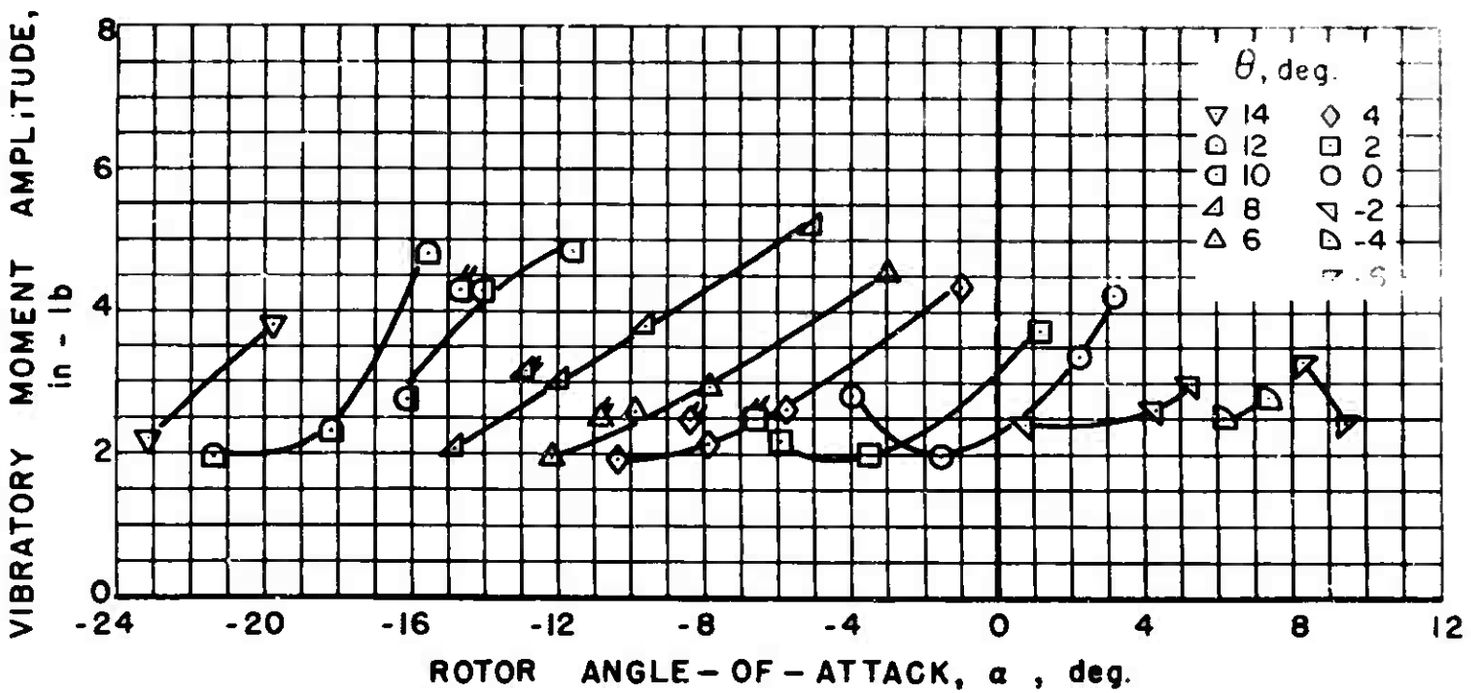

(a) FLATWISE BENDING MOMENT, 21 % R

Figure 88. Experimental Vibratory Moment Amplitude, $\mu = 0.5$.

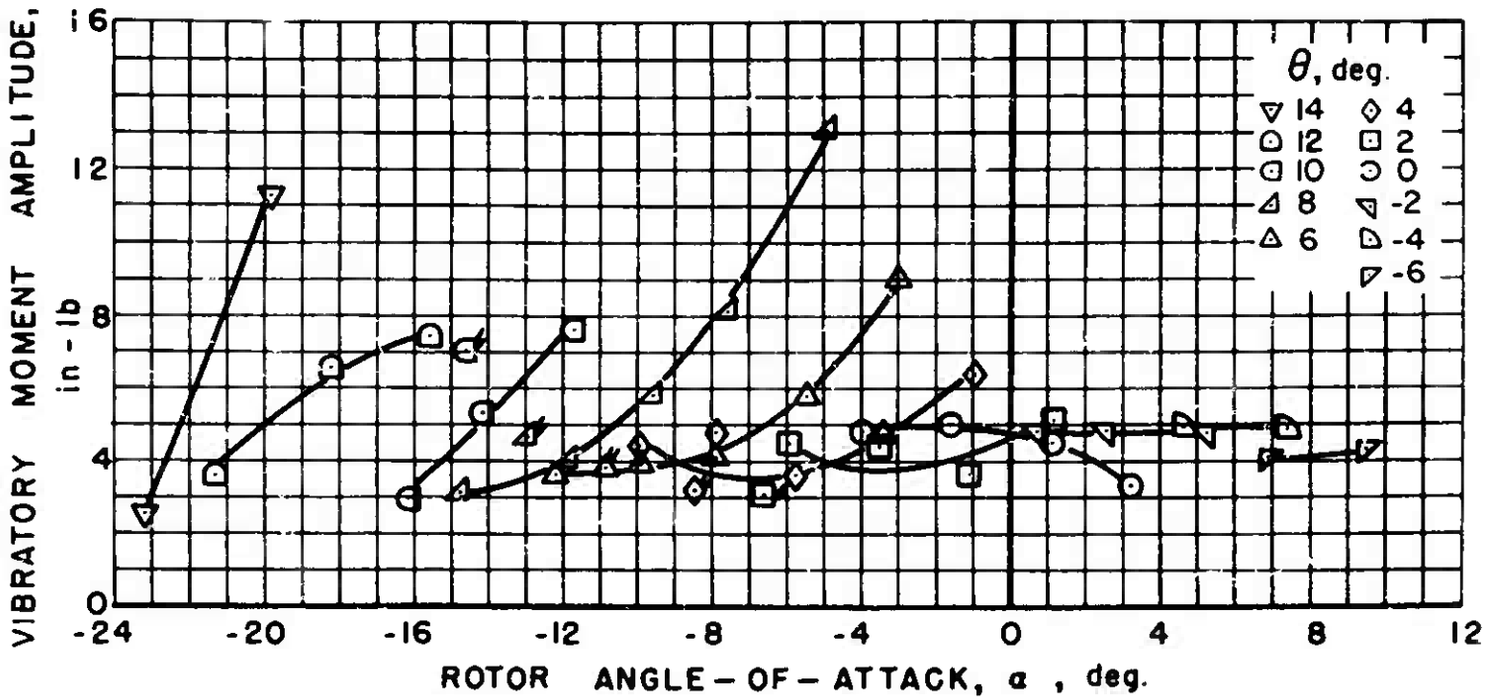

(b) EDGEWISE BENDING MOMENT, 21 % R

Figure 88. Continued.

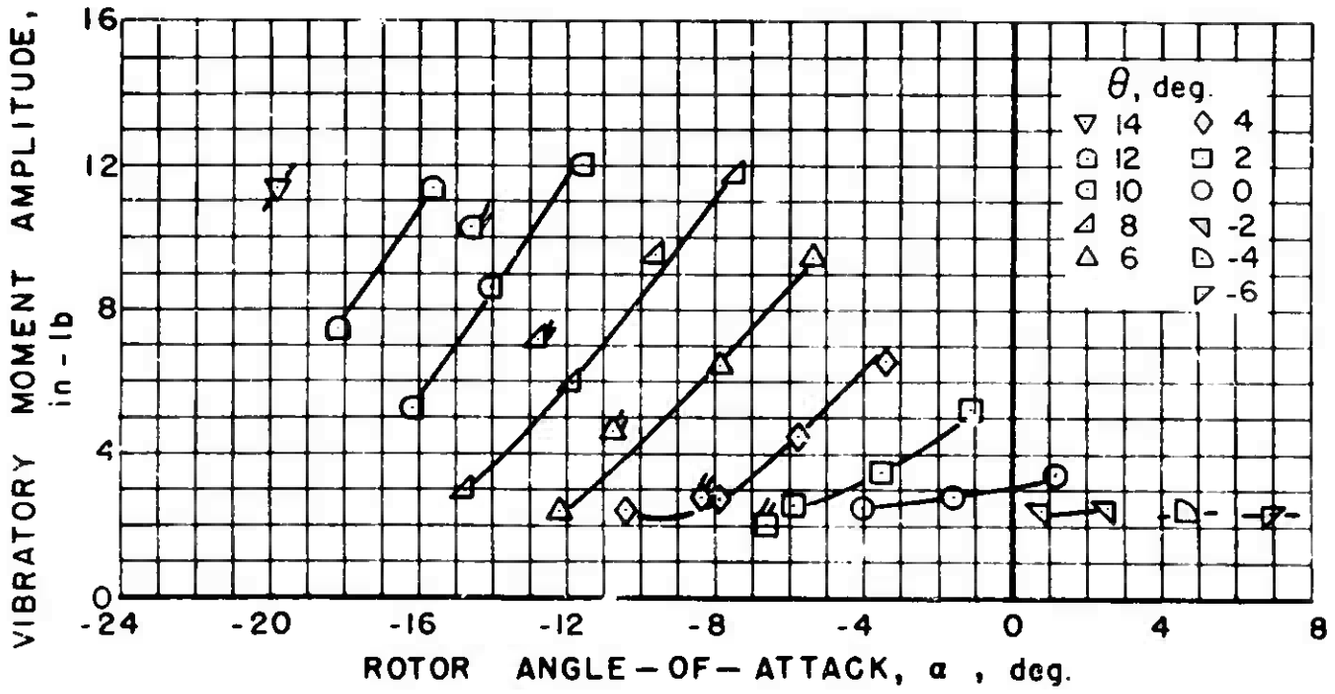

(c) EDGEWISE BENDING MOMENT, 47 % R

Figure 88. Continued.

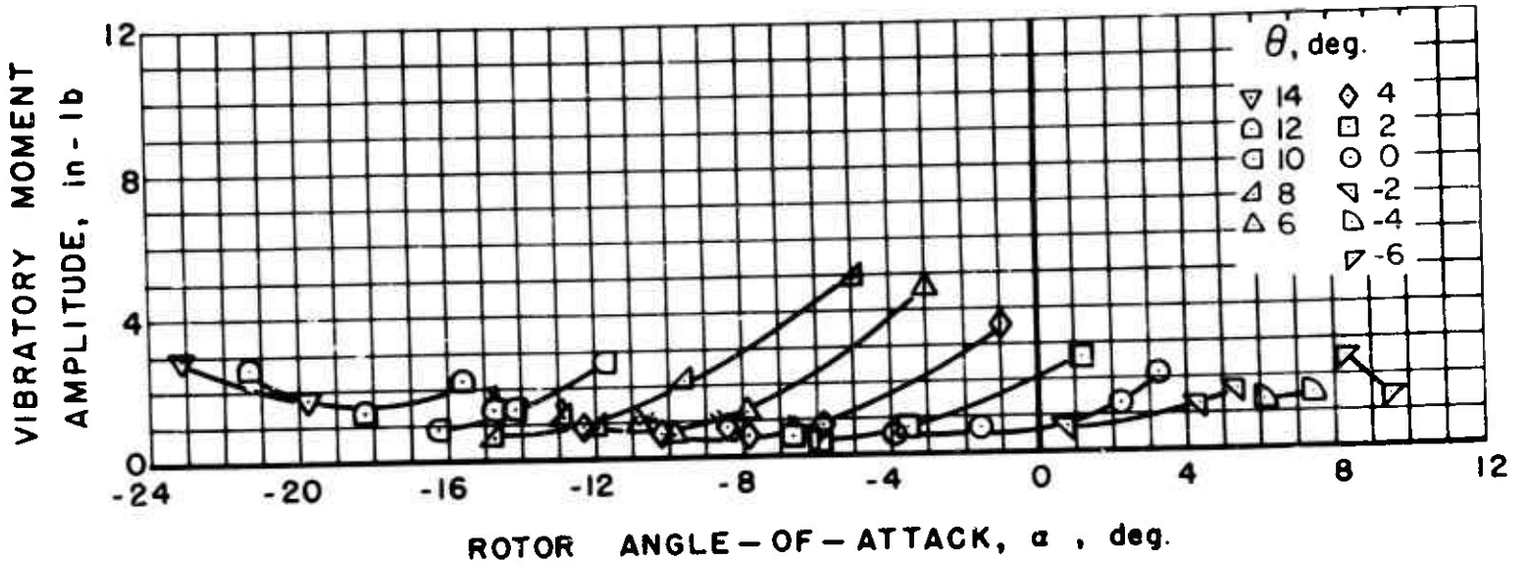

(d) TORSIONAL MOMENT, 17.5 % R

Figure 88. Concluded.

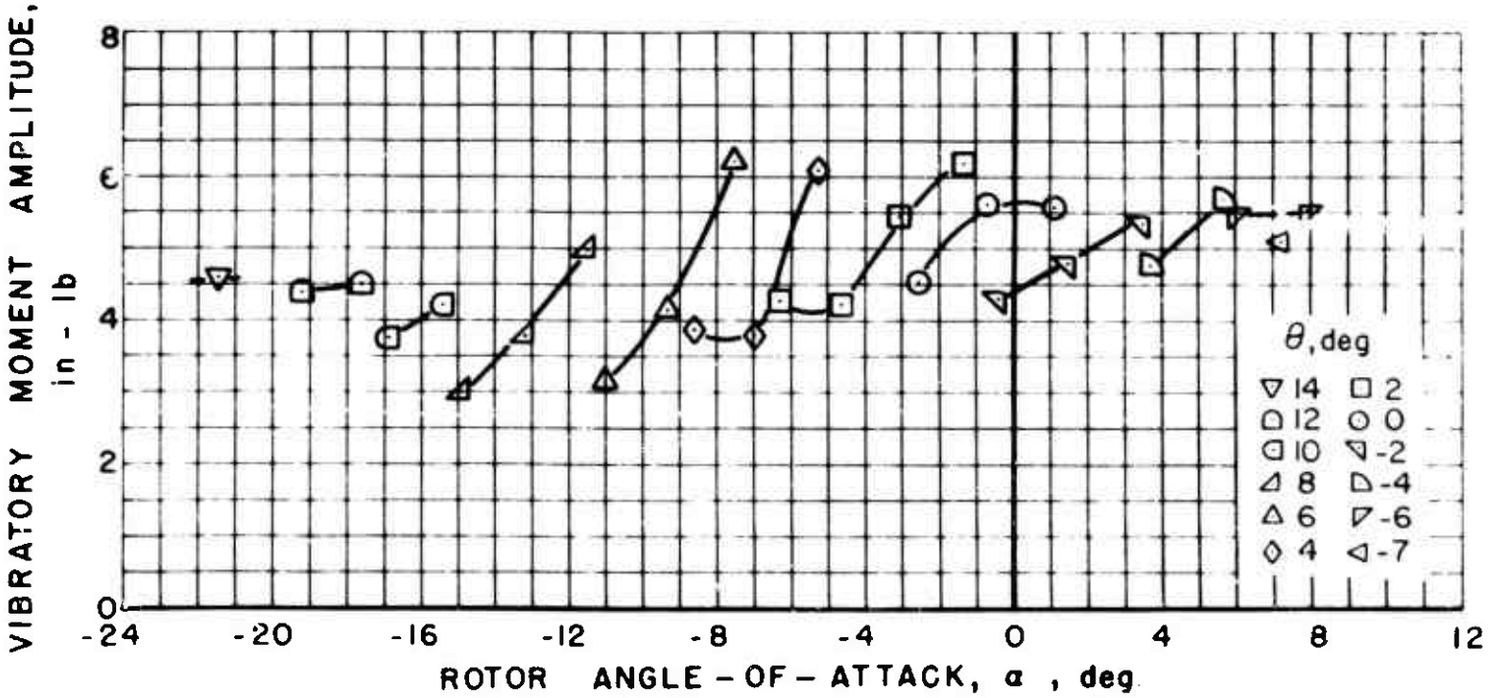

(a) FLATWISE BENDING MOMENT, 21 % R

Figure 89. Experimental Vibratory Moment Amplitude, $\mu = 0.7$.

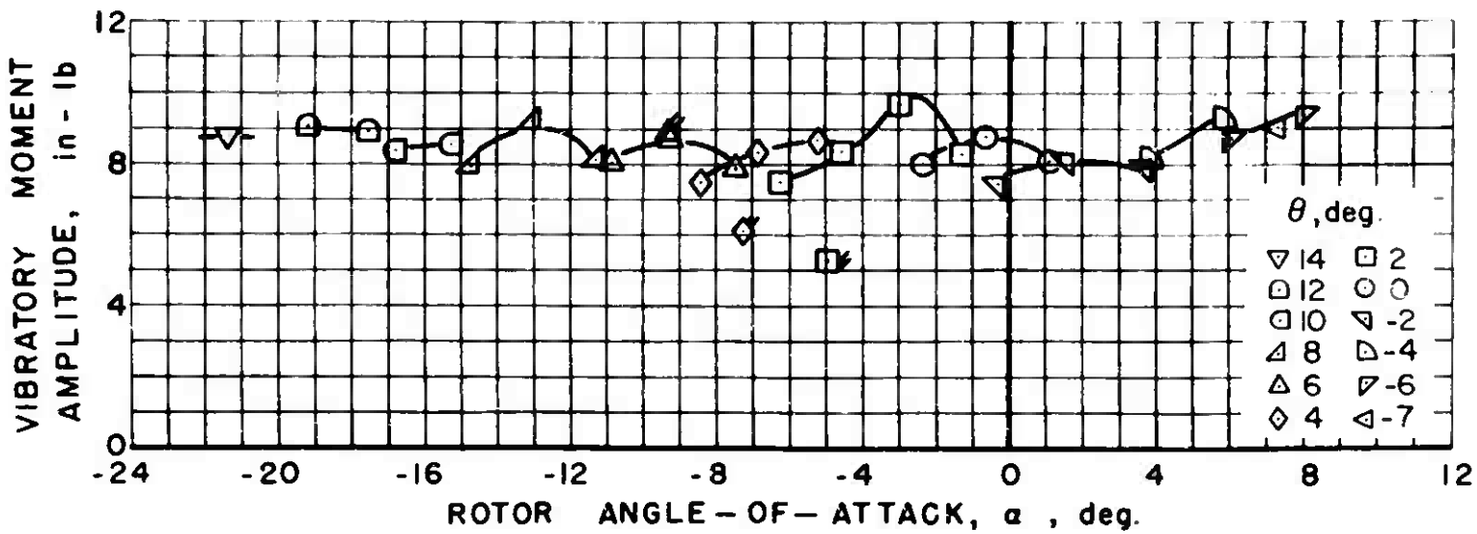

(b) EDGEWISE BENDING MOMENT, 21 % R

Figure 89. Continued.

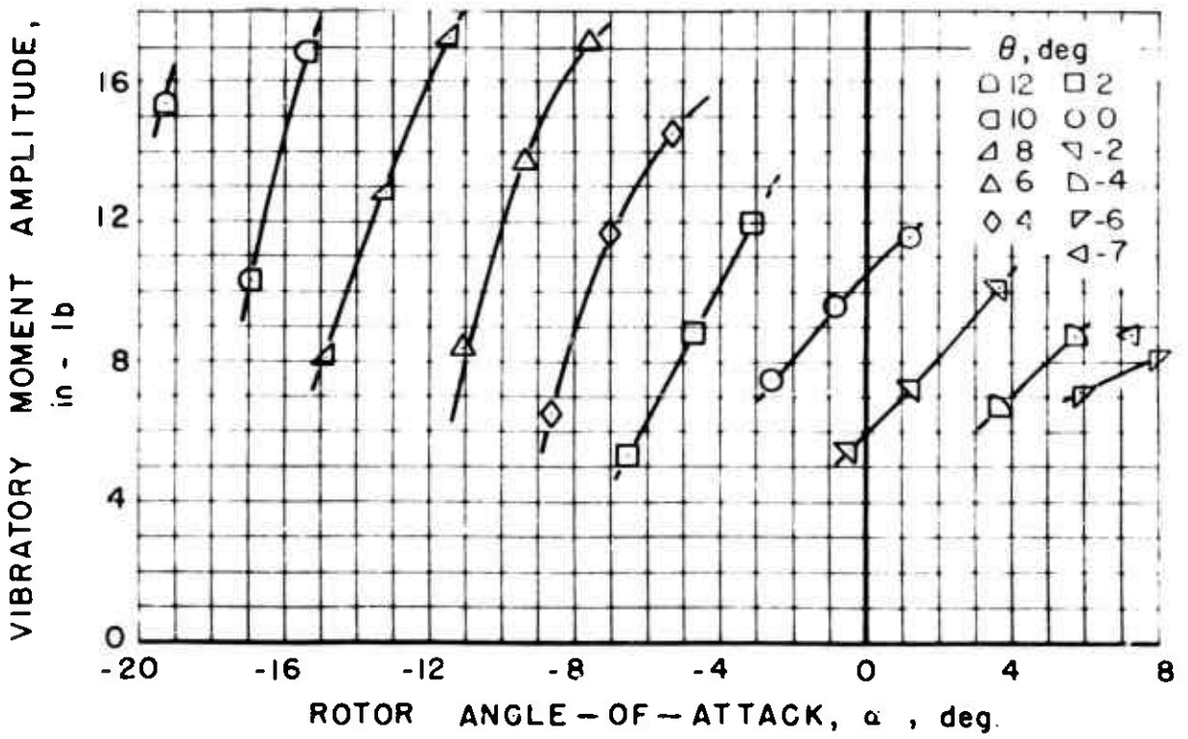

(c) EDGEWISE BENDING MOMENT, 47 % R

Figure 89. Continued.

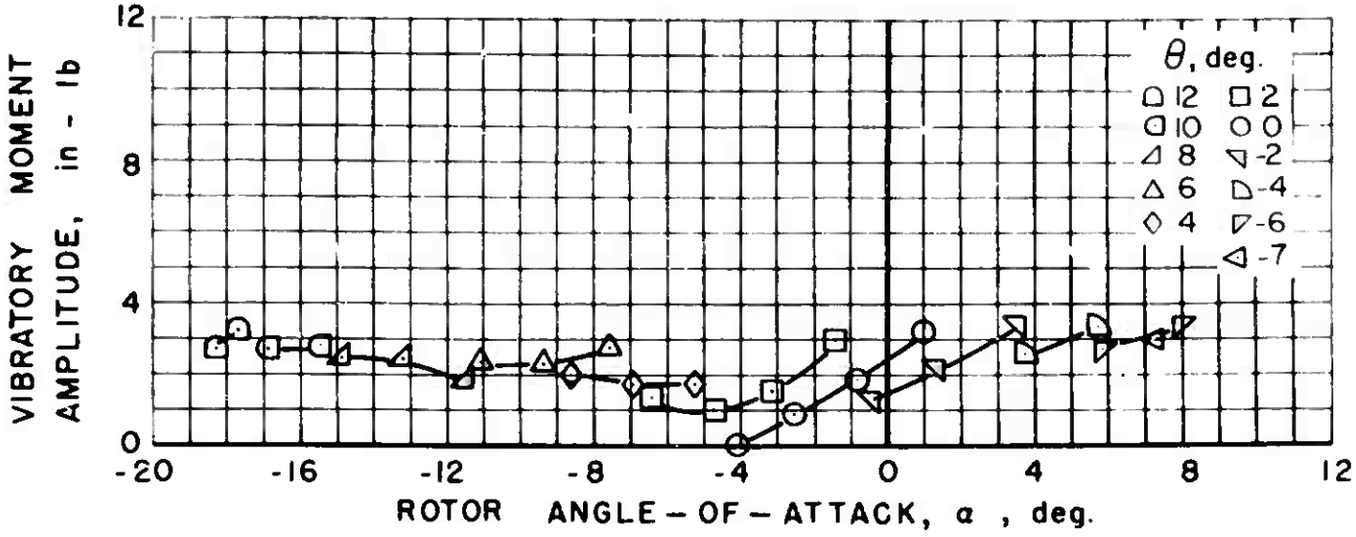

(d) TORSIONAL MOMENT, 17.5 % R

Figure 89. Concluded.

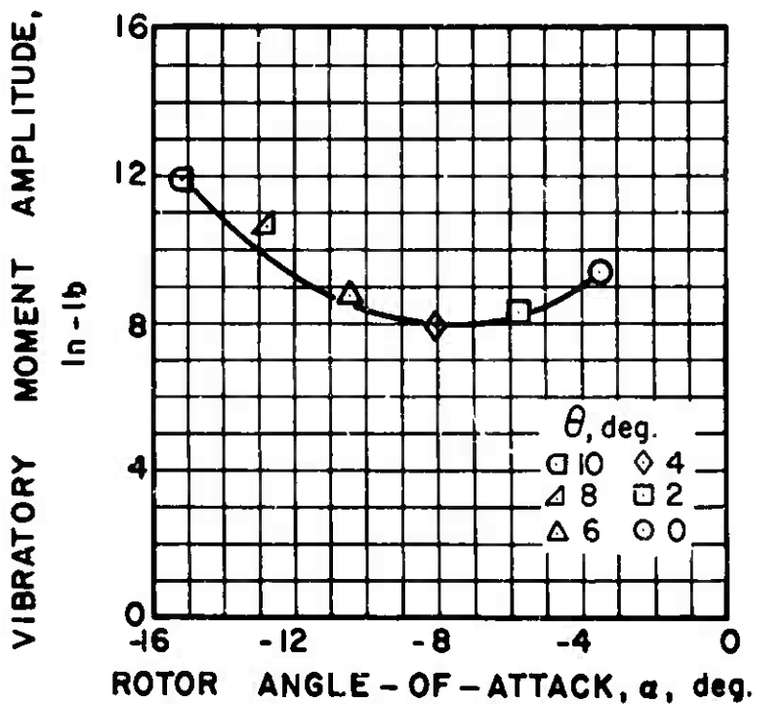

(a) FLATWISE BENDING MOMENT, 21 % R

Figure 90. Experimental Vibratory Moment Amplitude, $\mu = 1.0$.

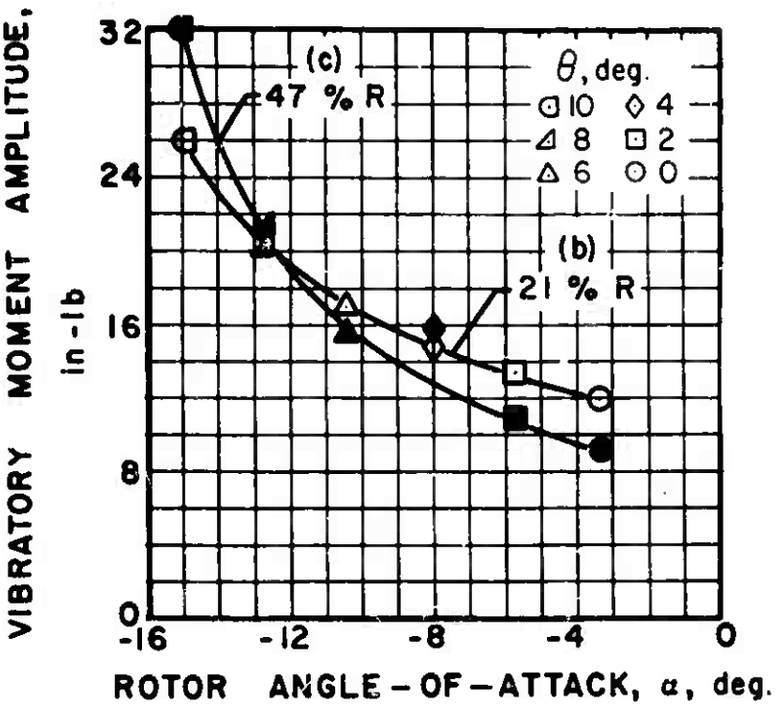

(b) & (c) EDGEWISE BENDING MOMENT

Figure 90. Continued.

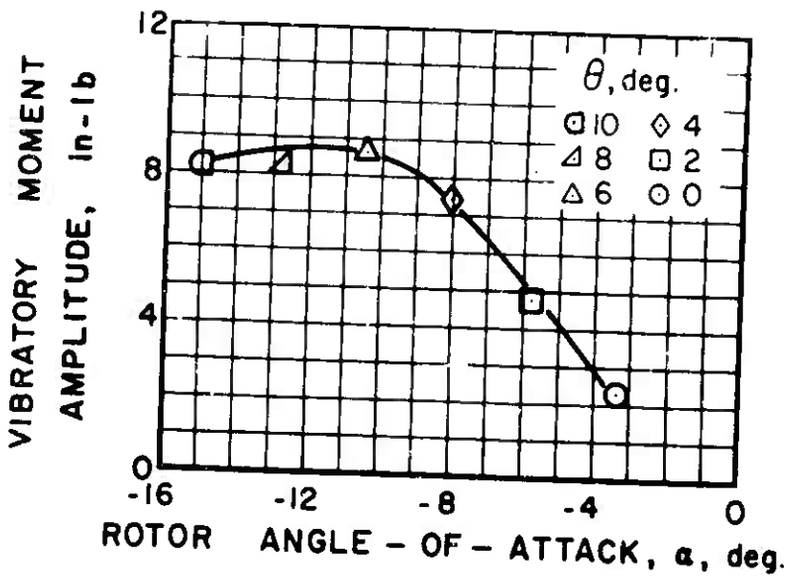

(d) TORSIONAL MOMENT, 17.5 % R

Figure 90. Concluded.

APPENDIX IV

EXPERIMENTAL VIBRATORY CONTROL LOAD AMPLITUDE FIGURES

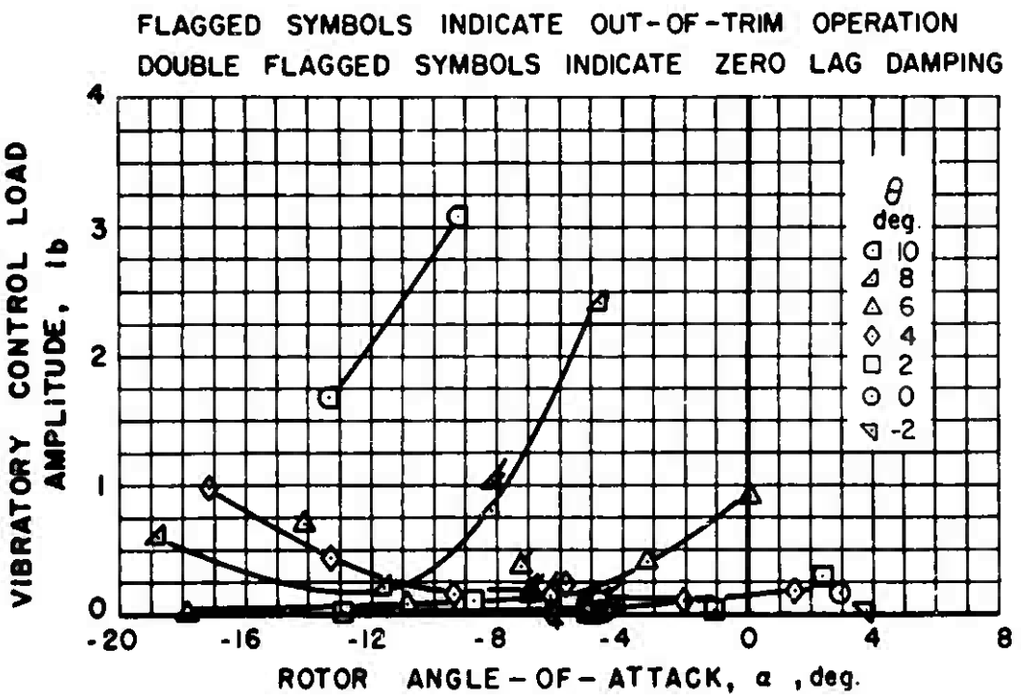

Figure 91. Experimental Vibratory Control Load Amplitude, $\mu = 0.2$.

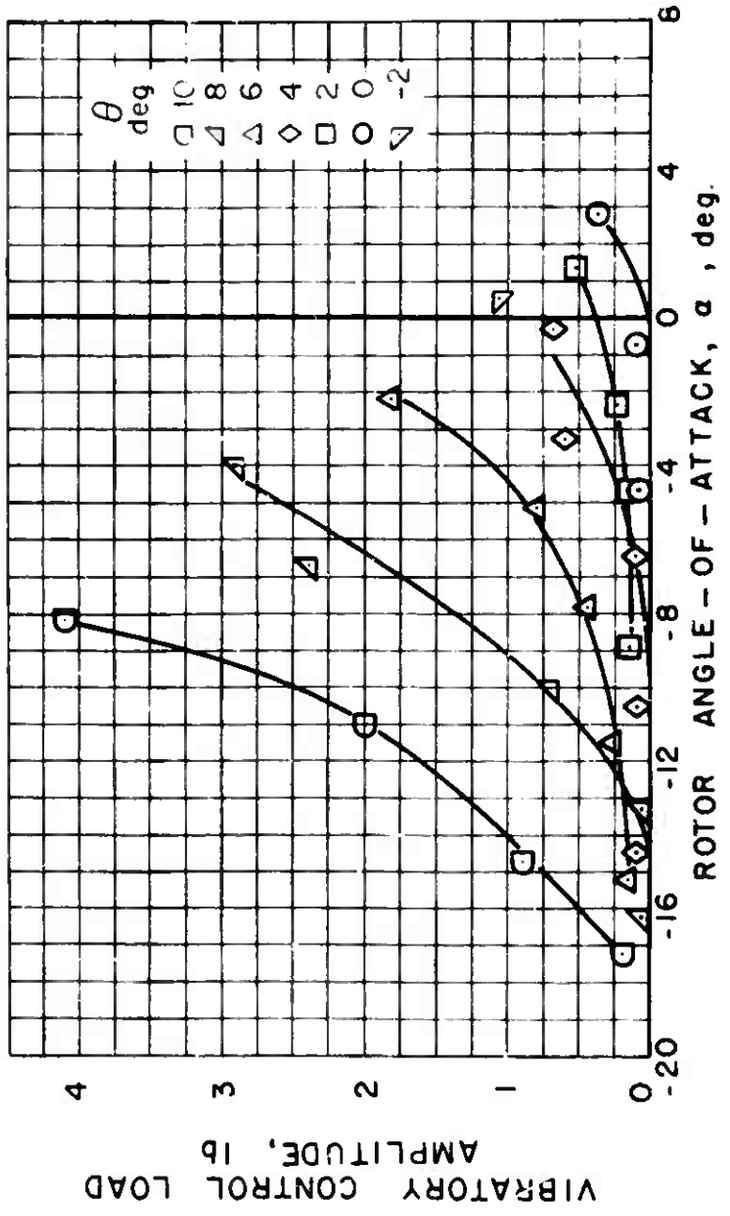

Figure 92. Experimental Vibratory Control Load Amplitude, $\mu = 0.3$.

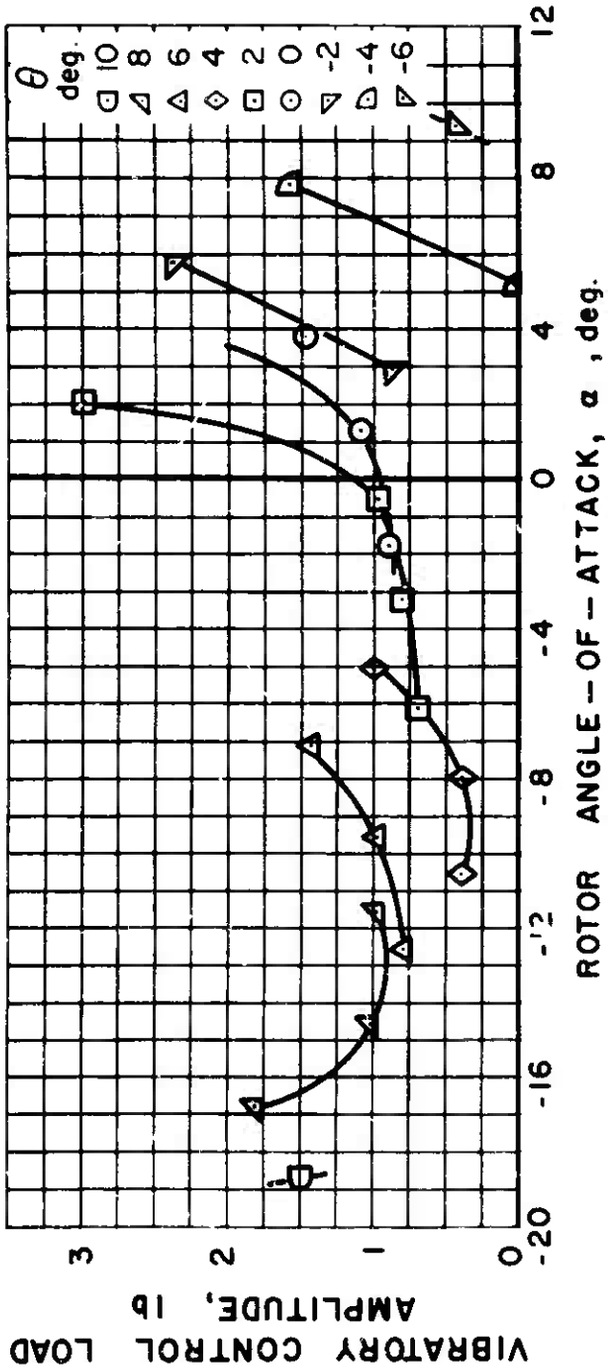

Figure 93. Experimental Vibratory Control Load Amplitude, $\mu = 0.4$.

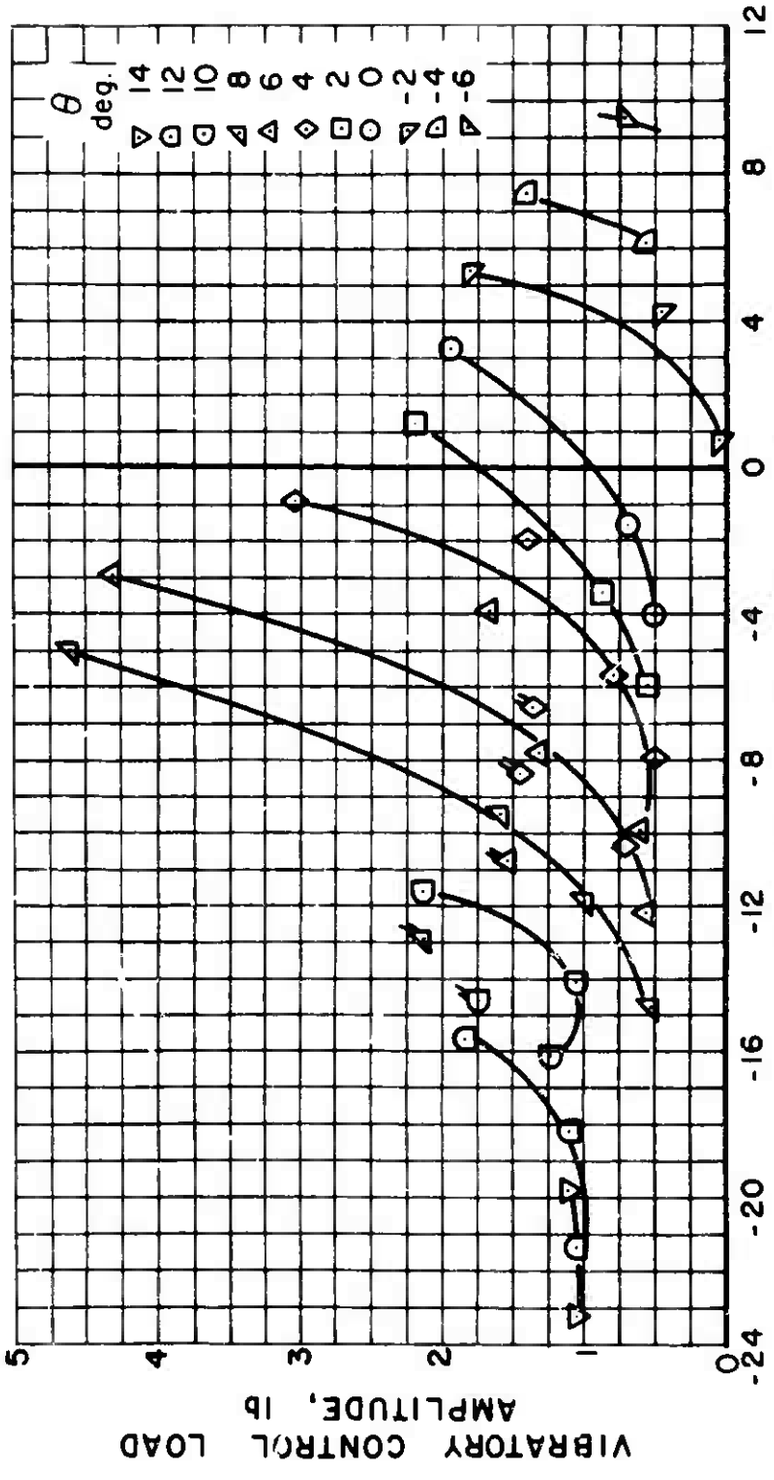

Figure 94. Experimental Vibratory Control Load Amplitude, $\mu = 0.5$.

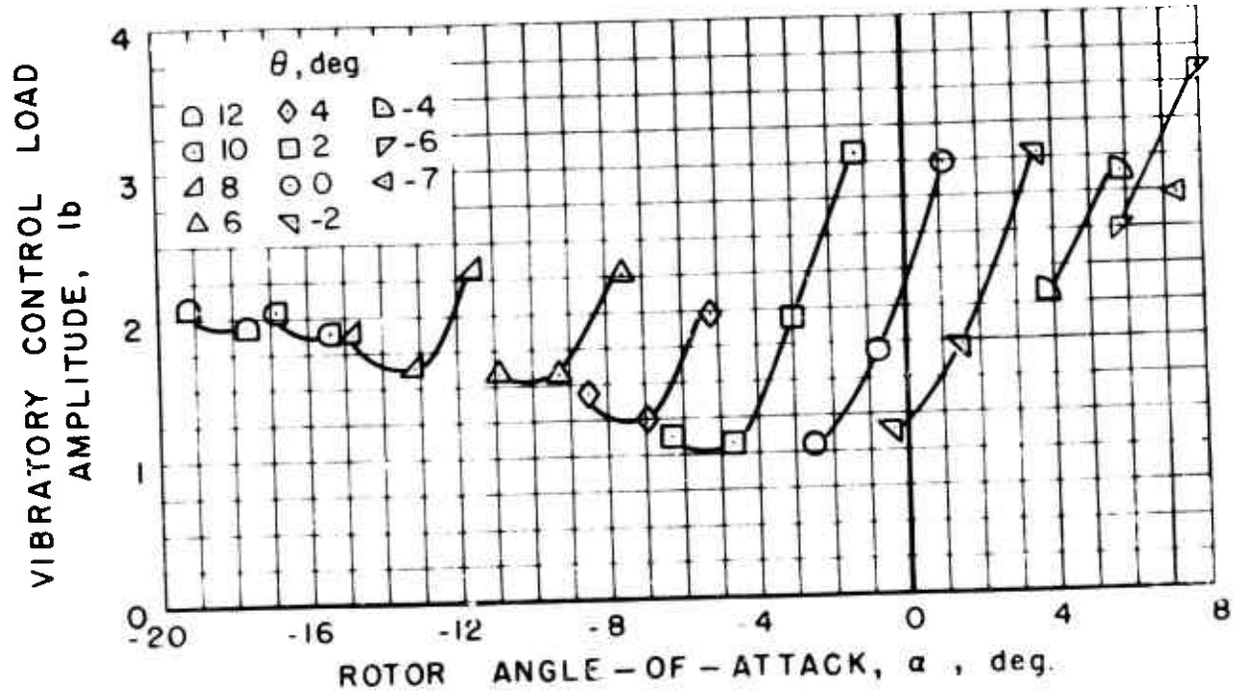

Figure 95. Experimental Vibratory Control Load Amplitude, $\mu = 0.7$.

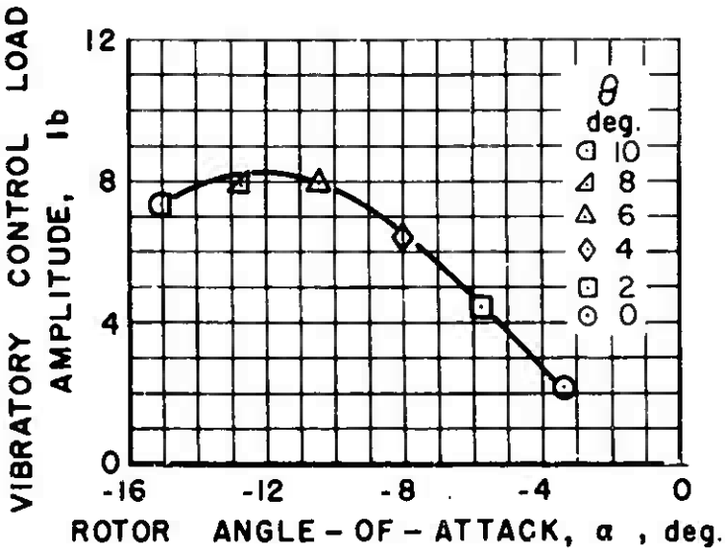

Figure 96. Experimental Vibratory Control Load Amplitude, $\mu = 1.0$.

UNCLASSIFIED

Security Classification

DOCUMENT CONTROL DATA - R & D

(Security classification of title, body of abstract and indexing annotation must be entered when the overall report is classified)

1. ORIGINATING ACTIVITY (Corporate author) Sikorsky Aircraft Division of United Aircraft Corp. Stratford, Connecticut	2a. REPORT SECURITY CLASSIFICATION Unclassified 2b. GROUP

3. REPORT TITLE

"Comparison of Theoretical and Experimental Model Rotor Blade Vibratory Shear Forces"

4. DESCRIPTIVE NOTES (Type of report and inclusive dates)

5. AUTHOR(S) (First name, middle initial, last name)

Lawrence J. Bain

6. REPORT DATE October 1967	7a. TOTAL NO. OF PAGES 305	7b. NO. OF REFS 6
8a. CONTRACT OR GRANT NO. DA 44-177-AMC-136(T) b. PROJECT NO. Task 1D 121401A 14203 c. d.	9a. ORIGINATOR'S REPORT NUMBER(S) USAAVLABS Technical Report 66-77 9b. OTHER REPORT NO(S) (Any other numbers that may be assigned this report) SER-50419	

10. DISTRIBUTION STATEMENT

This document has been approved for public release and sale; its distribution is unlimited.

11. SUPPLEMENTARY NOTES	12. SPONSORING MILITARY ACTIVITY U. S. Army Aviation Material Laboratories Fort Eustis, Virginia

13. ABSTRACT

An investigation was undertaken to obtain quantitative measurements of the vibratory forcing functions from the blades of rotary wing aircraft in the flight speed range encompassing both pure and compound helicopter operation. These measurements were made using dynamically scaled model rotor blades mounted on a specially instrumented rotor head. Testing was accomplished over a range of equivalent forward speeds from 75 to 300 knots and over a range of full-scale rotor lifts from zero to 40,000 lb. In addition to rotor performance, the final data include ten harmonics of the orthogonal blade root shear forces, rotor blade bending moments, and rotor control loads.

A portion of the experimental results were correlated with a fully coupled aeroelastic analysis which included the effects of wake induced velocities. It was found that the inclusion of these effects improved the correlation of the flatwise shear forces over that obtained assuming uniform inflow.

DD FORM 1 NOV 68 1473 (PAGE 1)

S/N 0101-807-6801

UNCLASSIFIED

Security Classification

14 KEY WORDS	LINK A		LINK B		LINK C	
	ROLE	WT	ROLE	WT	ROLE	WT
Helicopter Rotor Blade Vibratory Shear Force Tests Correlations						